THE TULKS VOLCANIC BELT, VICTORIA LAKE SUPERGROUP, CENTRAL NEWFOUNDLAND - GEOLOGY, TECTONIC SETTING AND VOLCANOGENIC MASSIVE SULPHIDE MINERALIZATION

J.G. Hinchey

Report 2011-02

St. John's, Newfoundland
2011

Newfoundland Labrador

Natural Resources

Geological Survey

COVER

A view of the Tulks Hill volcanogenic massive sulphide system from the Tulks River valley (looking east).

Newfoundland Labrador

Natural Resources
Geological Survey

THE TULKS VOLCANIC BELT, VICTORIA LAKE SUPERGROUP, CENTRAL NEWFOUNDLAND – GEOLOGY, TECTONIC SETTING AND VOLCANOGENIC MASSIVE SULPHIDE MINERALIZATION

J.G. Hinchey

Report 2011-02

St. John's, Newfoundland
2011

EDITING, LAYOUT AND CARTOGRAPHY

Senior Geologist	S.J. O'BRIEN
Editor	C.P.G. PEREIRA
Copy Editor	D.G. WALSH
Graphic design, layout and typesetting	J. ROONEY B. STRICKLAND
Cartography	D. LEONARD T. PALTANAVAGE T. SEARS N. STAPLETON

Publications of the Geological Survey are available through the Geoscience Publications and Information Section, Geological Survey, Department of Natural Resources, P.O. Box 8700, St. John's, NL, Canada, A1B 4J6.

This publication is also available through the departmental website.

Telephone:	(709) 729-3159
Fax:	(709) 729-4491 Geoscience Publications and Information Section (709) 729-3493 Geological Survey - Administration (709) 729-4270 Geological Survey
E-mail:	pub@gov.nl.ca
Website:	http://www.nr.gov.nl.ca/nr/mines/Geoscience/index.html

Author's Address: J.G. Hinchey
Department of Natural Resources
P.O. Box 8700
St. John's, NL
Canada
A1B 4J6

ISBN: 978-1-55146-465-7

NOTE

The purchaser agrees not to provide a digital reproduction or copy of this product to a third party. Derivative products should acknowledge the source of the data.

DISCLAIMER

Recommended citation
Hinchey, J.G.
2011: The Tulks Volcanic Belt, Victoria Lake Supergroup, Central Newfoundland – Geology, Tectonic Setting and Volcanogenic Massive Sulphide Mineralization. Government of Newfoundland and Labrador, Department of Natural Resources, Geological Survey, St. John's, Report 2011-02, 167 pages.

CONTENTS

Page

Page

FIGURES

Page

Page

Page

PLATES

Page

Page

Page

TABLES

Page

ABSTRACT

The Tulks Volcanic Belt (TVB), of the Victoria Lake supergroup, central Newfoundland, is dominated by quartz ± feldspar porphyritic felsic volcaniclastic rocks and lesser amounts of mafic volcanic rocks and intercalated sedimentary rocks. The belt has traditionally been viewed as a single stratigraphic sequence of ca. *498 Ma age, but recent geochronological studies imply that it may be composite and include rocks as young as 453 Ma. These rocks developed in volcano-sedimentary basins developed in active volcanic arcs on the peri-Gondwanan margin of the Iapetus Ocean.*

The belt is host to five important clusters of VMS deposits. From south to north, these include the Boomerang, Tulks Hill, Tulks East, Daniels Pond and Bobbys Pond deposits, and a number of smaller sulphide prospects. The major VMS deposits are hosted by felsic volcanic, pyroclastic and volcaniclastic rocks. Mineralizing styles vary from 'classic' exhalative-type mineralization developed on the seafloor, to 'replacement' style mineralization developed in a sub-seafloor environment. There are also mineralized debris flow breccias, suggesting potential for transported ores. As such, the TVB contains a continuum of VMS deposit types.

*Volcanogenic massive sulphide deposits in the TVB are interpreted to have formed in volcanic, volcaniclastic and sediment-rich basins as tectonomagmatic conditions changed from convergent (*e.g.*, active-arc environment) to extensional (*e.g.*, back-arc or arc-rift) environments. The change from compressional to extensional regimes would allow for active rifting, conduit formation, and high levels of focused heat flow, which are ideal conditions for the development of large and productive hydrothermal systems. The deposits display mineralization, alteration, and textural characteristics indicative of both bimodal-siliciclastic type deposits, and deposits classified as 'hybrid bimodal felsic VMS-epithermal' deposits. These two types of deposits dominate the southern and northern parts of the belt, respectively. The latter are intermediate to 'classic' VMS-type deposits and epithermal-type mineralization of the type generally associated with subaerial volcanism. It is suggested that VMS deposits in the northern part of the belt formed in a higher standing portion of the basin in relatively shallow-water conditions, proximal to vents and active magmatic systems that may have supplied some fluid input. This is in contrast to a deeper water, more distal environment envisioned for the deposits in the southern part of the belt.*

To clarify their tectonostratigraphic affinity within the Victoria Lake supergroup and to better understand these mineralizing environments, U–Pb geochronology, trace-element lithogeochemistry and Sm/Nd isotopic geochemistry have been applied to the host rocks of all of the major VMS deposits in the TVB. However, the absence of zircon in many sampled volcanic rocks complicated these geochronological studies, and the exact age of host sequences to some deposits remains unknown. A subvolcanic porphyry from the Tulks Hill deposit, dated previously at 498 +6/-4 Ma, provides a minimum age for the nearby Tulks Hill and Tulks East deposits; and was interpreted to be the age of all the TVB rocks. Two new U–Pb zircon ages were obtained; one from the felsic tuff that hosts mineralization at the Boomerang deposit and the other from a felsic dyke interpreted to be broadly synvolcanic. The combined TIMS and SHRIMP data for these two samples indicate an identical U–Pb age of 491 ± 3 Ma. This date is younger than the 498 +6/-4 age from Tulks Hill, although the errors do overlap at their older and younger limits, respectively. Inheritance patterns in the Boomerang samples suggest the presence of older crustal material having Cambrian (514–510 Ma) ages, akin to those reported from the Tally Pond group, an

older sequence within the Victoria Lake supergroup. The new geochronological results suggest that VMS mineralization in the Tulks area and at Boomerang may represent temporally discrete events, despite some apparent similarities. The age determined for the Boomerang deposit is closer to (but not identical with) a U–Pb date of 488 ± 3 Ma, obtained some 30 km to the southwest of the Boomerang deposit, from the Pats Pond group. This suggests that the younger sequence of rocks may be regionally extensive, as proposed by other workers, and implies that it may have potential elsewhere for VMS mineralization similar to the Boomerang deposit.

The comparison of lithogeochemical patterns from the major deposits is complicated by the effects of hydrothermal alteration near the VMS mineralizing environments. Nevertheless, examination of immobile trace-element signatures suggests that the host sequences to the deposits, with the exception of the Daniels Pond deposit, cannot be easily distinguished on the basis of their geochemistry. The volcanic and pyroclastic rocks are all broadly arc-related, and show a mixture of calc-alkaline and tholeiitic signatures that perhaps record the construction and later rifting of individual arc sequences. Nd-isotope signatures from felsic rocks in the Boomerang area, the Pats Pond group, and one sample from the Bobbys Pond deposit are higher (εNd of +3.8 to +5.5) than those from the Tulks Hill, Tulks East, and Daniels Pond areas (εNd of around +2 to +3). Although not a straightforward correlation, as the volcanic rocks that host the Tulks East and Tulks Hill deposits also locally contain higher εNd values of between +4 to +5, the data may support a link between the Boomerang deposit area and the Pats Pond group; representing a possibly younger package of mineralized rocks. The new results, when taken with the results to date, suggest that the tract of rocks known as the TVB includes rocks of more than one age, but of generally similar geochemistry and tectonic setting.

INTRODUCTION

PURPOSE AND SCOPE

The Victoria Lake supergroup (VLSG) in central Newfoundland has long been the focus of exploration activity aimed at the discovery of volcanogenic massive sulphide (VMS) deposits. The main areas of interest over the years have been the Tally Pond Volcanic Belt (TPVB) and the Tulks Volcanic Belt (TVB) as defined originally by Kean and Jayasinghe (1980). In the TVB alone, exploration since the 1960s has resulted in the discovery of six major VMS occurrences, with the latest being the 2004 discovery of the Boomerang deposit cluster by Messina Minerals Incorporated.

In response to renewed interest in the VLSG for base-metal exploration, generated, in part, by the advancement of the Duck Pond Mine project, the Geological Survey of Newfoundland and Labrador initiated a metallogenic study in 2002 aimed at documenting the nature and setting of the known VMS occurrences throughout the VLSG. Early studies focused on the TPVB (*e.g.*, *see* Moore, 2003; Squires and Moore 2004), which hosts the Duck Pond Mine, whereas the present study (2006–2008) was restricted to the TVB and focused on deposit-level studies, relying heavily on diamond-drill core for lithologic, metallogenic, geochemical, and alteration studies, in addition to detailed mapping.

Field work in 2006 focused on the southern portion of the TVB, extending from the southern tip of Red Indian Lake south to the Pats Pond area (Figure 1). This portion of the belt is host to significant VMS mineralization at the Tulks East and Tulks Hill deposits, and the Boomerang deposit cluster (Boomerang–Domino–Hurricane sulphide lenses), as well as numerous VMS occurrences. The 2007 field season focused on the northern portion of the TVB, with emphasis on well-defined VMS deposits, including the Jacks Pond, Daniels Pond, and the Bobbys Pond deposits, as well as several smaller prospects that have exploration potential. Preliminary results from these investigations were presented in a series of papers (Hinchey, 2007, 2008; Hinchey and McNicoll, 2009) in addition to numerous oral and poster displays that collectively form the basis for this report. Significant outputs of this study include:

1) a detailed documentation of the six major VMS deposits as well as minor occurrences in the TVB;
2) a revised classification scheme for these mineral occurrences;
3) documentation of the tectonostratigraphic settings of the deposits and occurrences and host rocks;
4) documentation of alteration halos associated with the VMS deposits;
5) radiogenic isotopic studies of the VMS deposits; and
6) geochronological data from the recently discovered Boomerang deposit.

All areas of the TVB, including the mineral deposits hosted therein are readily accessible by seasonally maintained logging roads from the towns of Millertown and Buchans, with well-maintained gravel roads passing on both sides of Red Indian Lake. Networks of abandoned forestry roads crisscross the area giving excellent access by pickup truck and all-terrain vehicles.

PREVIOUS WORK

The following is a brief summary of some of the more pertinent work conducted in the TVB (Figures 1, 2, and 3) since the late 1950s. It is not intended to represent a complete history of work and studies in the area. For more complete references to previous work the reader is directed to Evans and Kean (2002) as well as to the numerous company assessment reports that have been completed for the area.

The first regional mapping in the area was conducted by Riley (1957), followed by Williams (1970) for the Geological Survey of Canada. More detailed mapping by the Newfoundland Department of Mines and Energy followed (Kean, 1977, 1979a, b, 1982, 1983; Kean and Jayasinghe, 1980, 1982; Kean and Mercer, 1981; Evans *et al*., 1994a, b, c). The area was the subject of recent investigations by the Geological Survey of Canada as part of the Targeted Geoscience Initiative (TGI) Red Indian Line project (*e.g.*, Rogers and van Staal, 2002; Rogers *et al.*, 2005, 2006; van Staal *et al.*, 2005; Lissenberg *et al.*, 2005; and Zagorevski *et al.*, 2007a, b). The metallogeny of the VLSG was the subject of several studies (Evans and Kean, 2002; Moore, 2003; Squires and Moore, 2004). The Victoria Lake Group was defined by Kean (1977) and Kean *et al.* (1981), and subsequently elevated to supergroup status by Evans and Kean (2002), who summarized the geology, geochemistry, tectonic setting, and VMS mineralization of the VLSG.

Much of the TVB occurs within the 1905 Anglo-Newfoundland Development Company (A.N.D.) charter lands, in which the Newfoundland Government effectively granted the Anglo-Newfoundland Development Company a 99 year lease on exclusive timber, water and mineral rights to the area. As such, the TVB was not under competitive staking during this time interval. Numerous exploration projects have been conducted in the area, many of which were brought to the advanced exploration stage with diamond-drilling programs. The earliest known exploration in the

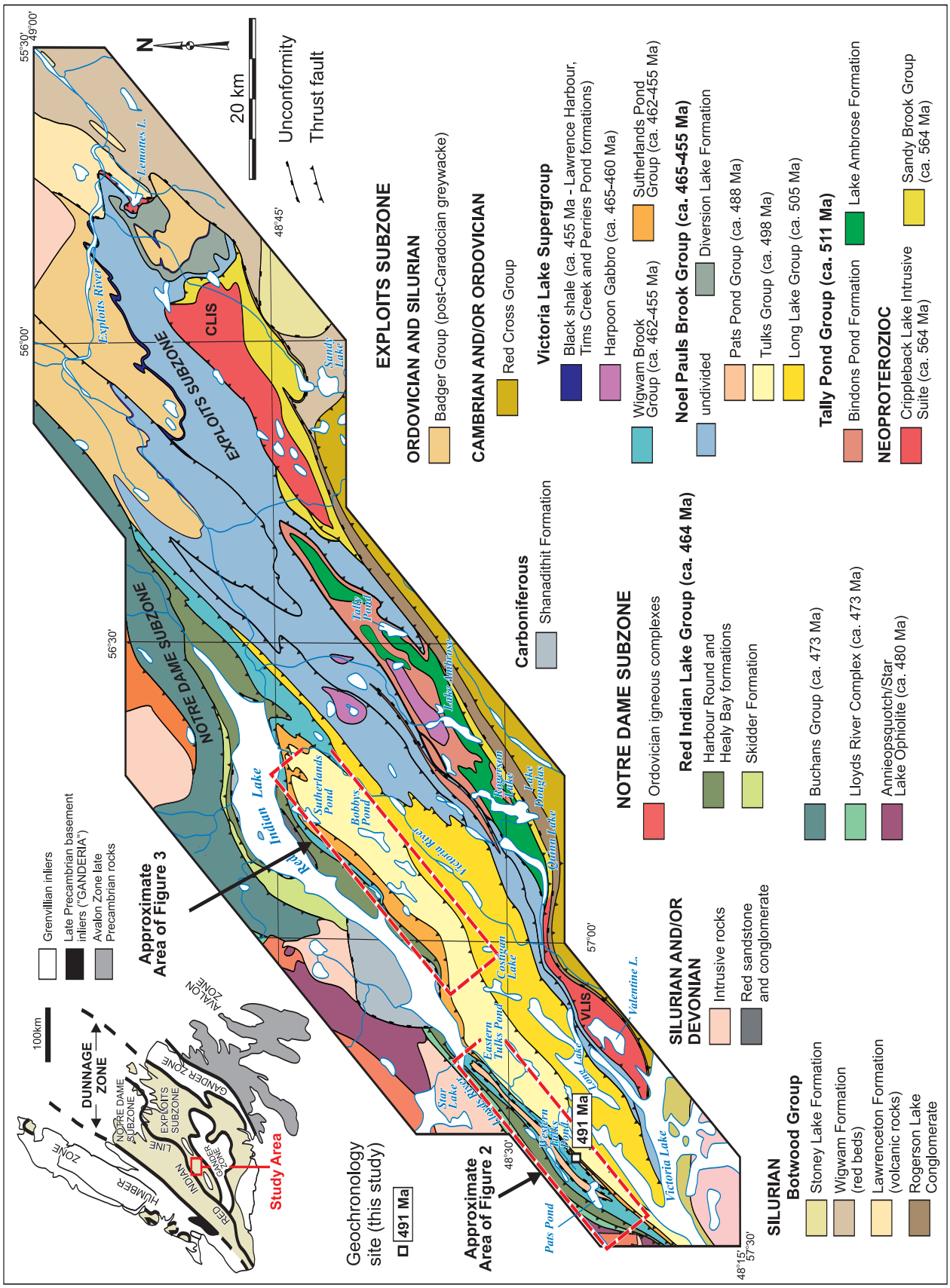

Figure 1. *Location and geology of the area surrounding Red Indian Lake, including rocks of the Victoria Lake supergroup. CLIS–Crippleback Lake intrusive suite; VLIS–Valentine Lake intrusive suite. Geological map from a compilation by N. Rogers based, in part, on GSC mapping as indicated in the text.*

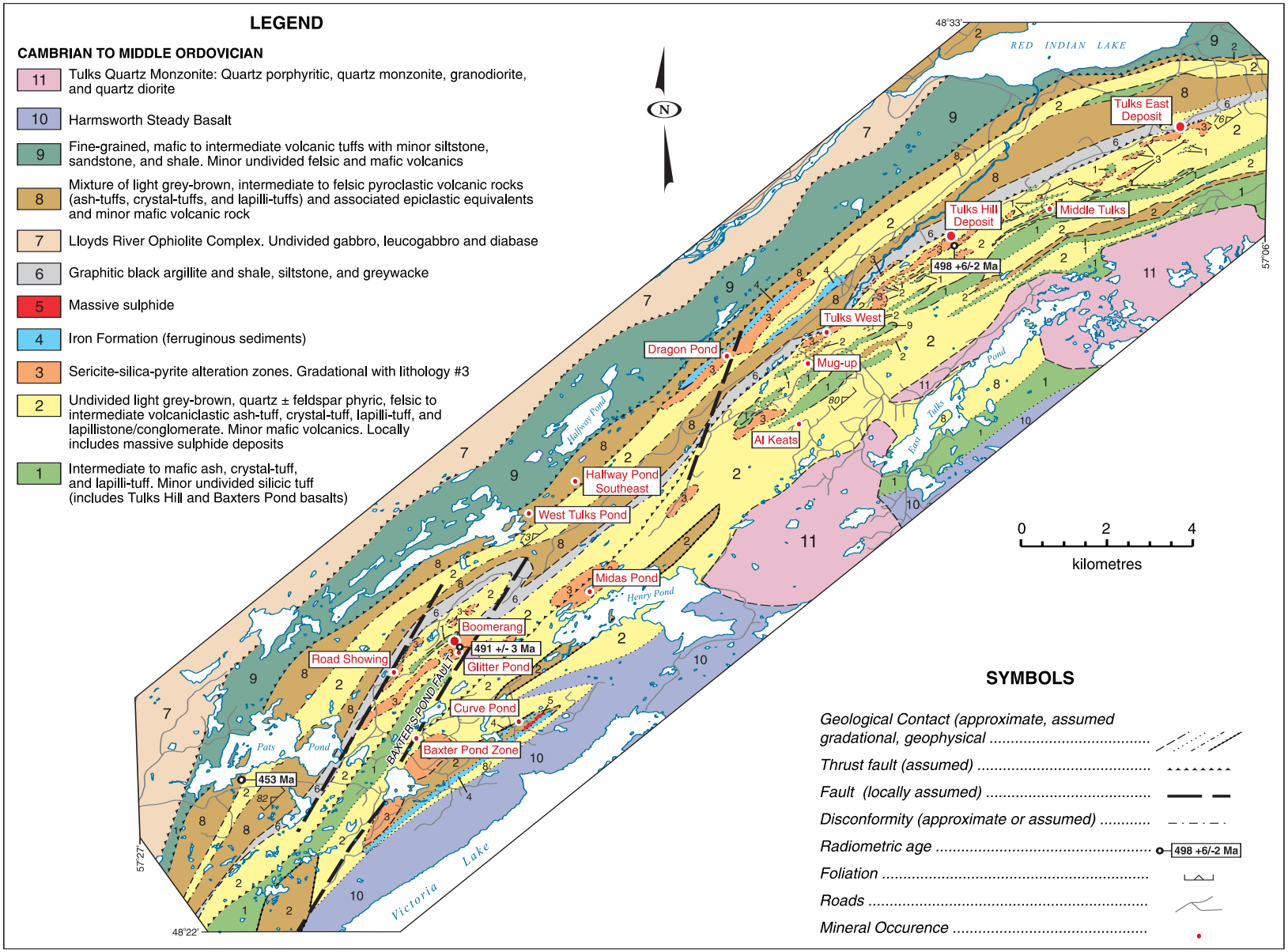

Figure 2. *Geology map of the southern Tulks Volcanic Belt illustrating the various rock types and the VMS deposits, prospects, and showings. Note that the map is not intended to distinguish the various groupings defined by van Staal* et al.*, (2005), but is rather meant to represent a lithological map. Partly modified and compiled from industry sources (*e.g.*, Noranda, 1998) and government publications (*e.g.*, Kean, 1982; Evans* et al.*, 1994c; Evans and Kean, 2002; van Staal* et al.*, 2005*).

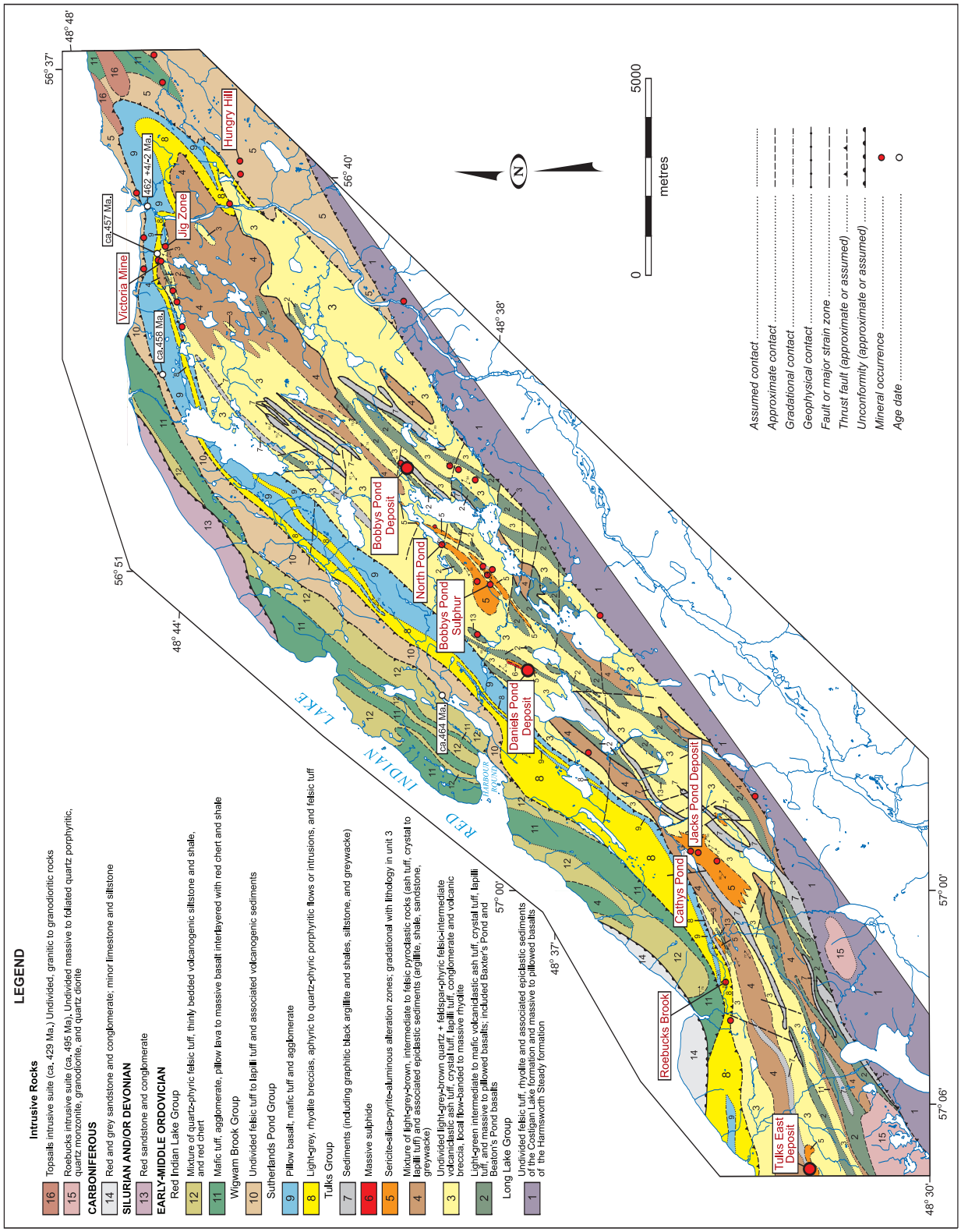

Figure 3. *Geology map of the northern Tulks Volcanic Belt illustrating the various rock types and the VMS deposits, prospects, and showings. Note that for clarity purposes not all of the mineral occurrences are labelled. Geology partly modified and compiled from industry sources* (e.g., *Noranda, 1998 and Greene* et al., *2001) and government publications* (e.g., *Kean, 1979a; Evans* et al., *1994c; Evans and Kean, 2002; Rogers* et al., *2005; Lissenberg* et al., *2005).*

area occurred in 1905 at the Victoria Mine, where three shallow exploration development shafts were sunk on high-grade chalcopyrite–pyrite outcrops. Several small stockpiles of massive chalcopyrite–pyrite were extracted; portions of which remain on site. It was not until the 1930s that the prospect was drilled, with 38 diamond-drill holes being completed as part of exploration programs prior to 1980, resulting in the discovery of ore-grade material (Desnoyers, 1991). However, tonnage proved to be low and the massive sulphides had poor continuity, thereby downgrading the economic potential of the prospect. Another early exploration program, by Asarco, consisting of prospecting, stream and soil sampling, led to the discovery of the Tulks Hill deposit in 1961 (Evans and Kean, 2002). Asarco conducted detailed evaluation work on the prospect, eventually outlining a geological resource for the deposit. Abitibi-Price commenced exploration near the southern end of Red Indian Lake in the 1970s, that led to the discovery of the Tulks East and the Jacks Pond prospects in 1977 and 1980, respectively; ultimately delineating three massive sulphide lenses at the Tulks East deposit (Barbour and Thurlow, 1982). Following up on lake-sediment geochemical surveys and detailed airborne EM surveys, Abitibi-Price discovered a large zone with anomalous gold at the Midas Pond–Glitter Pond location (Evans and Wilton, 2000). In 1985, BP Resources Canada Ltd. acquired Abitibi-Price's land holdings and mineral rights to the TVB (excluding the area around the Bobbys Pond deposit), and in 1989, following additional systematic compilation, geophysical and geochemical surveys, and diamond drilling, discovered the 'Green Zone' (*i.e.*, the Curve Pond showing) at the southern end of the TVB and the Daniels Pond deposit in the northern TVB. However, BP Resources Canada Ltd. suspended exploration activities in the area in 1991 and put the property assets up for sale. In 1985, the Canadian Nickel Company Ltd. (Canico; a subsidiary of INCO) optioned the 'Victoria Property', consisting of the northern portion of the TVB including land between the A.N.D. charter to the southwest and the Victoria River to the northeast, encompassing the area around Bobbys Pond. After a systematic exploration program, Canico defined the Bobbys Pond VMS deposit. Noranda Mining and Exploration acquired the mineral rights to the TVB in 1993 and continued work, including additional geophysical surveys, mapping, surficial geochemistry and lithogeochemistry. This work resulted in several new discoveries including the Roebucks, Cathys Pond, Parking Lot, Daniels Pond extension, Bobbys Pond south and Sutherlands Pond prospects in the northern TVB. Also, Noranda further evaluated the Tulks East deposit and the Curve Pond prospect in the southern part of the belt with diamond drilling and defined additional massive sulphides at Tulks East. Interestingly, Noranda also examined the Boomerang alteration zone (*see* below) and drilled several holes in this area. After discovering alteration zones and stringer sulphides, they intersected massive sulphides grading 0.46% Cu, 2.63% Pb, 7.4% Zn, 76.5 g/t Ag, and 0.67 g/t Au over 1.8 m (true thickness) in hole GA-97-05 (Banville *et al*., 1998; Noranda, 1998). This intersection forms part of the Domino VMS deposit subsequently discovered by Messina Minerals in 2006 (Messina Minerals Inc. Press Release, February 27, 2006). In 1998, Noranda Inc. decided to put its central Newfoundland properties up for sale. From 1999 to 2006, the southern TVB was explored by several companies, including Tulks Resources (1999–2000), Windarra Resources (2001), Mishibishu Gold Corporation (2002–2003), and finally Messina Minerals Inc. (2004–present). During this period, significant work was completed on the Tulks East and Curve Pond prospects, in addition to the Midas Pond gold prospect. In December, 2004, Messina Minerals Inc. discovered the Boomerang VMS deposit. Subsequent work has delineated two associated VMS deposits termed Domino and Hurricane. Messina Minerals Inc. presently continues to explore the area in search of additional resources. Subsequent to 1998, Kelmet Resources Ltd. took possession of the northern part of the belt and began exploration activities. In 2002, Royal Roads Corporation (now Buchans Minerals Corp.) merged with Kelmet Resources and took over the direction of the exploration program in the area. Buchans Minerals Corp. continues to explore the area, with a focus on expanding the resource at the Daniels Pond deposit. The Bobbys Pond deposit in the northern part of the belt was acquired by Mountain Lake Resources from INCO, and Mountain Lake Resources has conducted resource definition work.

The numerous industry reports prepared over the years on the TVB were invaluable sources of information for this project. It should be noted that the reference to Noranda (1998) includes data derived from many of the earlier company assessment reports. Recent NI 43-101 technical reports on the Boomerang deposit (Dearin, 2006), the Bobbys Pond deposit (Agnerian, 2008), and the Daniels Pond deposit (Webster *et al.*, 2008) also provide valuable overviews of the geology and mineralization in the belt.

REGIONAL GEOLOGY

SETTING WITHIN THE APPALACHIAN OROGEN

The Dunnage Zone of the Newfoundland Appalachians (Figure 1, inset) represents the vestiges of Cambro-Ordovician continental and intra-oceanic arcs, back-arc basins, and ophiolites that formed in the Iapetus Ocean (Kean *et al*., 1981; Swinden, 1990; Williams, 1995). The zone is bisected by an extensive fault system (the Red Indian Line, RIL) into a western peri-Laurentian segment (Notre Dame and Dashwoods subzones), and an eastern peri-Gondwanan segment (Exploits Subzone). The two main segments of the Dunnage Zone are differentiated on stratigraphic, structural, faunal, and isotopic characteristics (Williams *et al*., 1988). The RIL separates the Buchans Group, and locally the Red Indian Lake group (Rogers *et al.*, 2005), which formed on the Laurentian side of the Iapetus Ocean, from the VLSG, which formed on the Gondwanan side of the Iapetus Ocean. Both the Buchans Group and the VLSG are composite terranes that include rocks of different ages and tectonic settings.The deformation associated with final closure of the Iapetus Ocean during the Silurian (dated directly as syn- to post-432 ± 1.4 Ma; Zagorevski *et al.*, 2007b), included thrusting and folding that ultimately juxtaposed these originally geographically seperate volcanic belts.

Mapping by the Geological Survey of Newfoundland and Labrador (GSNL) in the 1970s and 1980s (*e.g.*, Kean, 1977; Kean *et al.*, 1981; Evans and Kean, 2002 and references therein) indicated that the TVB (*see* Figures 1, 2, and 3) represents the remnants of at least one of several bimodal Cambrian to Ordovician volcanic-arc sequences. Together with adjacent volcanic and sedimentary belts of variable tectonic affinities, it belongs to the VLSG (Evans and Kean, 2002); broadly divided into the TVB (*ca.* 498 Ma), the Long Lake Volcanic/Volcano-clastic Belt (*ca.* 505 Ma), and the Tally Pond Volcanic Belt (*ca.* 515 Ma), with further subdivisions resulting from more recent work (*see* below). In addition to the Cambro-Ordovician volcanic and volcaniclastic rocks of the VLSG, there are also large areas of late Precambrian (565–563 Ma) plutonic rocks (Evans *et al.*, 1990), which represent inliers of old basement, most likely representing the Ganderia crustal block (*e.g.*, van Staal *et al.*, 1998). Previous lithogeochemical studies, based largely on subordinate mafic volcanic rocks, indicate that the VLSG contains rocks of several distinct geochemical types representing different tectonic environments, *e.g*., active arc, arc-rift, back-arc, and mature arc (*see* Swinden *et al.*, 1989; Evans and Kean, 2002).

Evans and Kean (2002) divide the VLSG into the northern and southern terrains, separated by the Rogerson Lake Conglomerate. The TVB, comprising part of the northern terrain, is bounded to the north by the RIL and the sedimentary and volcaniclastic rocks of the Harbour Round Belt (*e.g.*, Red Indian Lake group of Rogers *et al.*, 2005), and to the south by a regionally extensive magnetic high anomaly, representing the Roebuck's Intrusive Suite and the mafic volcanic rocks of the Long Lake belt.

The TVB covers an area of approximately 65 by 8 km, trending from the northeast to southwest. It is broadly defined as a bimodal volcano-sedimentary belt dominated by felsic compositions and variable amounts of mafic volcanic rocks, and volcaniclastic and sedimentary rocks derived from both felsic and mafic volcanic rocks. The most common rock types of the TVB are light-grey to white, quartz ± feldspar porphyritic felsic to intermediate pyroclastic rocks, massive rhyolite, and felsic to intermediate ash tuffs, crystal tuffs, and lapilli tuffs, local bimodal breccias, and minor subvolcanic porphyritic intrusions. Mafic volcanic rocks are subordinate and are dominated by fine ash tuff, lapilli tuff, breccias, local pillow lavas, flows and hypabyssal intrusions. Black shales, argillites and greywackes are also locally abundant.

REGIONAL ALTERATION

The TVB experienced lower to middle, greenschist-grade metamorphism and moderate to strong deformation. The presence of well-developed, bedding-parallel regional foliations, defined by the alignment of chlorite and sericite, commonly obliterates primary textures. The stratigraphy typically strikes northeast and dips steeply to the northwest, and the belt is transected by shear zones and faults.

Alteration throughout the TVB can be divided into three types, namely:

1) alteration associated with regional metamorphism,
2) regionally extensive, semiconformable, hydrothermal alteration, and
3) hydrothermal alteration directly associated with the massive sulphide lenses. Although the mineral assemblages for these overlap to some extent, their variable intensities and distribution allow them to be differentiated.

Alteration associated with regional metamorphism is dominated by sericite–feldspar–silica–carbonate mineral

assemblages. This regional alteration, although pervasive, is typically only weakly developed. Fine-grained muscovite or sericite is the most abundant alteration mineral and is associated with all felsic to intermediate rock types throughout the TVB, occurring as both a regional and local hydrothermal alteration product. Sericite occurs as fine dustings on phenocrysts (particularly plagioclase) as well as fine-grained wisps and disseminations in the matrix of the felsic to intermediate tuffaceous rocks, and as rims or mantles on plagioclase and quartz phenocrysts. Secondary feldspars resulting from regional-scale alteration are dominated by Na feldspar (albite) with lesser K-feldspar. The secondary feldspars form overgrowths on, and also replace primary plagioclase feldspar. Sericite commonly occurs as internal flecks on secondary albite crystals and as alteration haloes around the secondary feldspars. Quartz occurs as fine-grained (μm scale), locally polycrystalline, recrystallized grains in the groundmass displaying undulose extinction, whereas carbonate occurs as fine-grained (~0.1-0.5 mm) porphyroblasts. Weak to moderate chlorite–sericite–quartz alteration spatially associated with the bimodal sills is also attributed to regional-scale alteration processes. Although the regional alteration products are pervasive, and easily identified in the relatively un-altered hangingwall rocks, their identification in the footwall, and the immediate hangingwall is much more difficult.

RADIOMETRIC AGES

All rocks within the TVB were originally considered to be of similar age based on a 498 +6/-4 Ma U–Pb date of a subvolcanic porphyritic intrusion, located close to the Tulks Hill VMS deposit (Evans *et al*., 1990). This age was recently re-interpreted by using a weighted average of the $^{207}Pb/^{206}Pb$ ages, versus the original linear regression technique, resulting in a slightly younger age of 496.5 ± 1 Ma (G.R. Dunning, personal communication, 2008).

Recent mapping and geochronological studies through the GSC TGI program (*e.g.*, Rogers *et al.*, 2005; van Staal *et al.*, 2005) interpret the TVB as a series of generally westward-younging (with local complications) tectonostratigraphic units including the Tulks group (*ca.* 498 Ma), the Pats Pond group (*ca.* 488 Ma), the Sutherlands Pond group (*ca.* 462–457 Ma; Zagorevski *et al.*, 2008; Dunning *et al*., 1987), and the Wigwam Brook group (*ca.* 453 Ma; van Staal *et al*., 2005; Zagorevski *et al*., 2007a). Although these geochronological data have provided additional constraints on the distribution of various units, some of the proposed map patterns and tectonostratigraphic interpretations of the TVB geology (*e.g.*, Rogers *et al.*, 2005; van Staal *et al.*, 2005; Zagorevski *et al*., 2007a) are different than those inferred from the data otained during this study (*see* case study on the Boomerang area below). Additionally, geochronological data obtained from this study dated the Boomerang VMS deposit at 491 Ma, which pose questions as to which tectonostratigraphic package of rocks it occurs in (*see* details in the U–Pb Section and discussion below).

COMPLICATIONS IN MAP PATTERNS ARISING FROM LIMITED OUTCROP

The TVB has been the subject of numerous mapping programs, both from an industry perspective (*e.g.*, Noranda, 1998; Delaney *et al.*, 2001; Greene *et al.*, 2001; Dadson, 2002) and a (provincial and federal) geological survey perspective (*e.g.*, Kean, 1977, 1979a, b, 1982, 1983; Kean and Jayasinghe, 1980, 1982; Kean and Mercer, 1981; Evans *et al*., 1994a, b, c; Lissenberg *et al.*, 2005; Rogers *et al.*, 2005). The paucity of outcrop in the TVB accounts for the numerous and varied interpretations of distribution of geological units. The lack of outcrop in the area demands a great deal of interpretation and interpolation, and these variable map patterns reflect different individual interpretations of the same data.

Industry mapping has commonly been conducted at a property scale and incorporates local-scale geophysical data to assist interpretations. As such, these maps (*e.g.*, Noranda, 1998 and references therein) provide excellent lithological regional maps, effectively illustrating that the TVB consists of a series of northeast–southwest-striking rock packages dominated by felsic-intermediate, with lesser mafic, volcanic rocks, and variable amounts of intercalated graphitic sedimentary rocks. Electromagnetic surveys have proven to be very efficient in delineating graphitic sedimentary rocks in the belt, and their presence is confirmed through field mapping and diamond drilling. As such, industry maps serve as excellent detailed lithological maps for the area. However, they do not so readily portray the temporal relationships because the TVB is dominated by felsic-intermediate volcanic rocks of essentially identical appearance at the macro scale, which can only be unravelled by detailed, systematic geochemical and geochronological studies.

Some of the earliest detailed regional mapping in the TVB was conducted through the Newfoundland and Labrador Department of Mines and Energy by Kean (1977, 1979a, b, 1982, 1983), Kean and Jayasinghe (1980, 1982), and Kean and Mercer (1981), followed by Evans *et al*. (1994a, b, c). This mapping outlined the distribution of northeast–southwest-trending felsic volcanic rocks with minor mafic volcanic rocks and sedimentary rocks. The results of these earlier mapping projects have been commonly used as a starting point for industry surveys. Results indicated that the TVB was composite, with young (*ca.* 463

Ma) rocks identified in the Victoria River area of the northern TVB (*e.g.*, Dunning *et al.,* 1987; *see* below), and older rocks (*ca.* 498 Ma) in the Tulks Hill area.

The most recent regional mapping in the area was conducted by the Geological Survey of Canada (GSC) as part of the larger Targeted Geoscience Initiative (TGI) program (*e.g.*, Lissenberg *et al.,* 2005; Rogers *et al.,* 2005; and van Staal *et al*., 2005). This program was successful in identifying and outlining additional, informally defined, tectonostratigraphic units within the TVB, largely based on U–Pb geochronological ages obtained from the southern TVB. This work, in conjunction with geochemical correlations, demonstrated that the TVB is composed of composite terraines (*i.e.*, it consists of generally westward-younging fault-bound volcano-sedimentary belts) with localized complexities. Some of the complexities associated with map patterns are not necessarily supported by the data (*see* case study on map patterns in the Boomerang area of the southern TVB below for details). The map patterns portrayed through the GSC's TGI program (*e.g.*, Lissenberg *et al.,* 2005; Rogers *et al.,* 2005; and van Staal *et al*., 2005) build upon, and broadly agree with, the distribution of rock types and groupings proposed by earlier workers (Evans and Kean, 2002 and references therein). However, the map patterns locally vary significantly from the earlier works, especially with respect to the indication of regional-scale folds defined by mafic volcanic rocks throughout the belt, as well as with the positioning of Caradoc age volcanic units in the middle of Tremadoc age volcanic rocks in the vicinity of Pats Pond in the southern extent of the TVB and in the area around the southern end of Red Indian Lake (*e.g.*, Lissenberg *et al.*. 2005; Rogers *et al.,* 2005; and van Staal *et al*., 2005). This interpretation differs from the simpler, more linear northeast–southwest map patterns suggested by earlier mapping. This variation in map patterns, representing a variation from a homoclinal model to a model requiring more structurally complex (*via* thust stacks and folding/faulting) stratigraphy, is discussed in more detail below and reflects the difficulty in extrapolation from the few isolated outcrops (especially in the case of the mafic volcanic rocks) to a regional scale. It should be noted that the GSC's TGI mapping program took more of a regional-scale tectonostratigraphic approach compared to the more localized lithological-based approach outlined above.

Maps presented in Figures 2 and 3 of this paper, are based on lithological rather than tectonostratigraphic relationships and were produced using site visits together with data compiled from previous mapping and geophysical surveys. From a tectonostratigraphic perspective, the subdivisions defined by the recent GSC mapping have been mostly maintained; however, in some cases the distribution of rock types and local interpretation of units have been incorporated from more detailed mapping (*e.g.*, Kean 1977, 1979a, b, 1982, 1983; Kean and Jayasinghe 1980, 1982; Kean and Mercer 1981; Evans *et al*. 1994a, b, c; and others). The most obvious differences between these maps and those of Lissenberg *et al.* (2005); Rogers *et al.* (2005); and van Staal *et al.* (2005) are that they indicate linear rather than folded map patterns for the mafic volcanics of the TVB, and they map out and indicate the graphitic sedimentary rocks interpreted to be Cambro-Ordovician to Caradoc in age.

Although Figures 2 and 3 use the detailed property-scale mapping and associated regional linear interpolations, there is also local evidence supporting some of the folded map patterns outlined by Lissenberg *et al.* (2005); Rogers *et al.* (2005), and van Staal *et al.* (2005). These include locally northwest-facing overturned stratigraphy at Daniels Pond (*see* below), which is distinct from the regional southwest-dipping stratigraphy, and the location of fold interference patterns in the northern Victoria River area (*e.g.*, Rogers *et al.,* 2005).

VOLCANOGENIC MASSIVE SULPHIDE MINERALIZATION, TULKS VOLCANIC BELT

INTRODUCTION AND DEPOSIT CLASSIFICATION

All of the major mineral occurrences examined as part of this study are included in the volcanogenic massive sulphide class of mineralization; however, there are significant differences in settings and styles of formation.

Volcanogenic massive sulphide mineralization occurs as polymetallic massive sulphide, lens-shaped accumulations, which form from the focused discharge of metal-ladden fluids ommiting from submarine hydrothermal vents. The fluids, dominated by sea water with variable magmatic fluid components, are circulated by sub-seafloor hydrothermal convection cells through faulted country rocks, fueled by high-heat flow regimes associated with subvolcanic intrusions. Most VMS deposits form in extensional tectonic settings associated with ocean spreading centres or volcanic-arc, rifted-arc and back-arc systems (*e.g.*, *see* Franklin *et al.*, 2005; Galley *et al.*, 2007 and references therein). These tectonic regimes lead to fracturing and faulting of the host rocks, that lead to enhanced permeability, which is essential to focused fluid flow. The circulating oceanic waters, heated by subvolcanic intrusion heat sources, effectively leach metals and other components from the country rocks, producing metal-enriched buoyant brines that are carried up from deep-reaching syn-volcanic faults to the water-seafloor interface, or in some cases just below the seafloor interface. If prospective conditions exist, such as hydrothermal venting into a reduced, anoxic stratified water column, or the presence of permeable strata that would allow for shallow sub-seafloor metal replacement to occur as infillings of primary pore space in autoclastic, volcaniclastic or epiclastic successions below an impermeable cap rock, the potential exists to form either an 'exhalative'-type VMS deposit or a sub-seafloor replacement type VMS deposit, respectively (*e.g.*, *see* Doyle and Allen, 2003; Franklin *et al.*, 2005; Galley *et al.*, 2007).

In addition to exhalative and replacement styles of formation, VMS deposits have also been classified under several different schemes (*i.e.*, *see* Swinden, 1991; Barrie and Hannington, 1999; Hannington *et al.*, 1999; Franklin *et al.*, 2005; and Galley *et al.*, 2007). Most of the more-recent classification schemes divide VMS deposits on the basis of host rock types and associated alteration assemblages. The most commonly used classification scheme was proposed by Barrie and Hannington (1999) with modifications by Galley *et al.* (2007). The classification scheme, from the chemically most primitive to the most evolved, is illustrated in Figure 4 (from Galley *et al.*, 2007) and includes: 1) mafic, 2) bimodal mafic, 3) siliclastic mafic, 4) bimodal felsic, 5) bimodal siliclastic, and 6) high sulphidation bimodal felsic dominated deposit types. Only the last three types are interpreted to be present in the TVB, and these will be briefly explained herein.

Bimodal-felsic Type

This deposit type is defined as having either >50% felsic volcanic rocks, and/or 35 to 70% felsic volcaniclastic rocks, and <15% siliclastic rocks in the host stratigraphic succession; mafic volcanic rocks and intrusive rocks make up the remainder. The felsic rocks are principally calc-alkalic, although transitional high-silica rhyolites to calc-alkalic compositions are also common. The bimodal-felsic deposits occur in compositionally more mature volcanic arcs, or rifted volcanic arc settings compared to the bimodal mafic deposits. These deposits are usually more Ag- and Zn-rich than the other VMS types, and may contain barite.

Siliciclastic-felsic Type

This deposit type contains approximately equal proportions of volcanic and siliciclastic rocks. Felsic volcanic rocks are generally calc-alkalic, and mafic rocks typically comprise less than 10 volume percent of the host rock sequence. These deposits occur within continental arcs, rifted arcs and back-arcs, and typically have the lowest Cu content and the highest Pb content of all the VMS deposit types.

High-sulphidation Bimodal-felsic Type

This deposit type is very similar to the bimodal-felsic deposits in that the stratigraphy is dominated by felsic volcanic rocks with abundant volcaniclastic and sedimentary rocks. The distinguishing characteristic of this deposit type is that it contains alteration products that are typical of both traditional high-sulphidation epithermal deposits as well as typical VMS deposits. Aluminous alteration (*e.g.*, kaolinite group minerals, illite, pyrophyllite) are common and indicate acidic conditions of formation.

In terms of the above described VMS classification schemes, the TVB predominantly contains deposits of the siliclastic felsic deposit type, although local examples of bimodal-felsic and high-sulphidation bimodal felsic deposits also exist. Volcanogenic massive sulphide accumu-

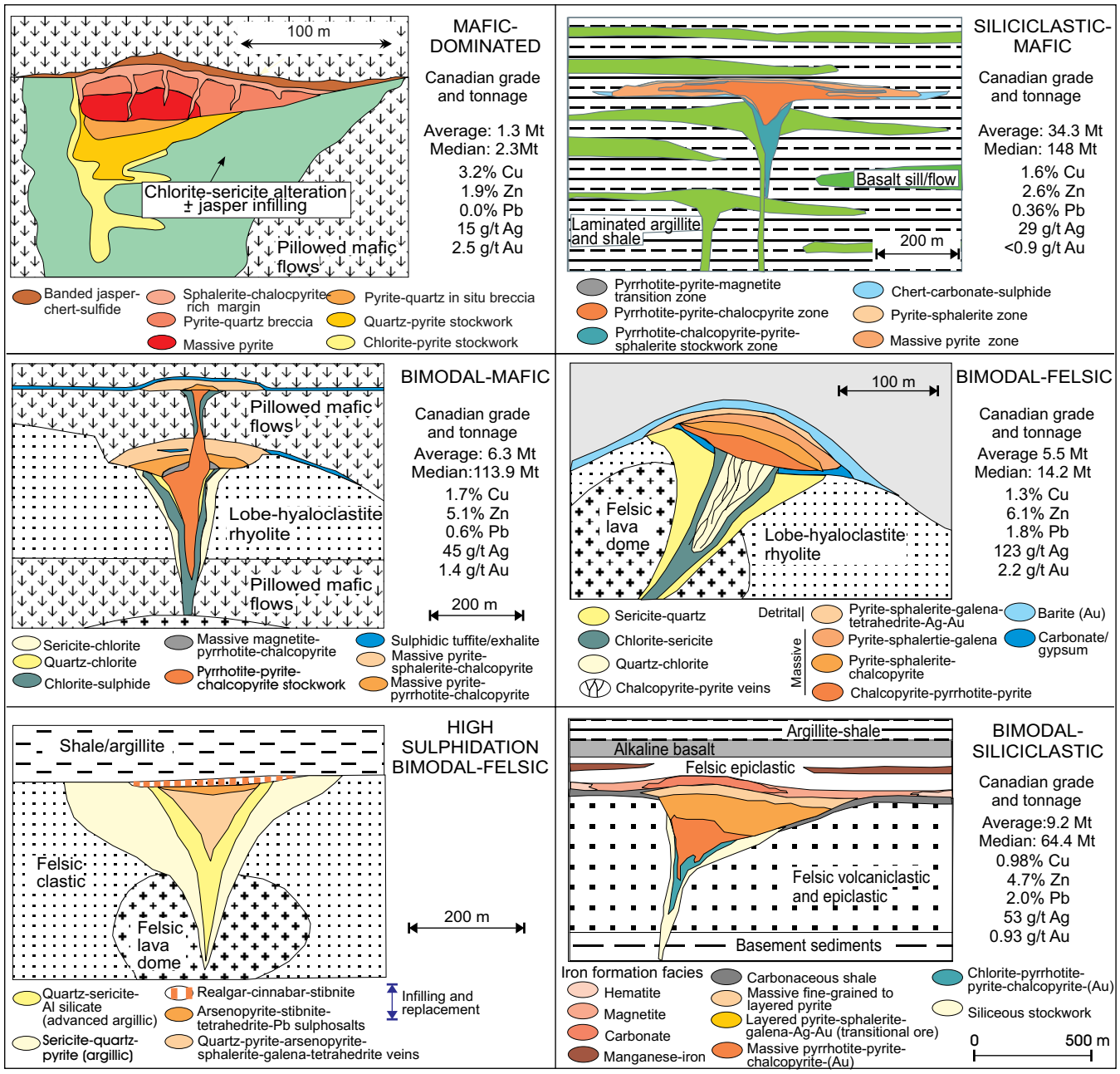

Figure 4. *Classification of VMS deposits on the basis of host-rock and alteration assemblages (after Barrie and Hannington, 1999; from Galley* et al.*, 2007, Franklin* et al.*, 2005).*

lations in the TVB formed in both the seafloor exhalative type setting, as exemplified by the presence of iron formations with associated sulphides (*e.g.*, Curve Pond, Dragon Pond, and Cathys Pond occurrences), and hangingwall volcaniclastic debris flows with massive sulphide clasts (*e.g.*, Daniels Pond deposit), as well as the sub-seafloor replacement type setting (*e.g.*, Boomerang deposit, Tulks East deposit); with some instances where evidence of both types of emplacement are recorded in single deposit systems (*e.g.*, Boomerang).

GEOLOGY AND VMS MINERALIZATION–SOUTHERN TULKS VOLCANIC BELT

LOCAL GEOLOGY

The southern Tulks Volcanic Belt consists of various felsic, intermediate and mafic volcanic rocks including ash through to lapilli tuff and lapillistone/agglomerates, local rhyolite flows, high-level (commonly amygdaloidal) dykes and sills, sedimentary rocks (black shales, graphitic argillites and greywacke), thin units of sedimentary exhalative chemical sediments (*i.e.*, iron formations), and subvolcanic intrusions (Plate 1). The rocks have experienced subgreenschist-facies metamorphism and moderate to strong deformation. Folding is common at the outcrop and drillcore scale (Plate 2), but the paucity of outcrop makes identification of larger folds difficult. Primary textures are usually obliterated by well-developed, bedding-parallel, foliations (S_1 and S_2: Plate 2). Rock units typically strike steeply to the northeast and dip northwest, and the prominent regional foliation is defined by alignment of chlorite and sericite. The belt is transected by numerous late shear zones and faults.

All of the rocks in the southern TVB were originally considered to be of a similar age, based upon a date of 498 +6/-4 Ma from a subvolcanic intrusion in the vicinity of the Tulks Hill deposit (Evans *et al*., 1990). However, recent mapping and geochronological studies by the GSC have revised the stratigraphic nomenclature to define a series of generally westward-younging tectonostratigraphic units including the Tulks group (*ca.* 498 Ma), the Pats Pond group (*ca.* 487 Ma), the Sutherlands Pond group (*ca.* 462 Ma: Dunning *et al*., 1987), and the Wigwam Brook group (*ca.* 453 Ma: van Staal *et al*., 2005; Zagorevski *et al*., 2007a). According to the maps based on their work, the VMS deposits that are the focus of this report are interpreted to be hosted within the Tulks (*e.g.*, Bobbys Pond, Daniels Pond, Tulks East, and Tuks Hill deposits) and Pats Pond (*e.g.*, Boomerang deposit) groups (*see* section on Geochronology below).

As the Pats Pond group is used later in this report for comparative purposes with the host rocks to VMS deposits, a brief description of the characteristic rock types is given. As described by Zagorevski *et al.* (2007a), the Pats Pond group is dominated by intermediate quartz-phyric and mafic tuffs. The stratigraphically lowest unit within the group consists of calc-alkaline pillow basalt overlain by feldspar ± quartz-phyric ash, crystal and lapilli tuffs. These are, in turn, overlain by quartz-phyric andesitic tuffs, and the stratigraphically highest portion of the group is dominated by basaltic to andesitic ash tuff, lapilli tuff, and rhyolitic tuff. From the base to the top, Zagorevski (2007a) subdivided the group into six informal geochemical units, PP1 through to PP6.

VOLCANOGENIC MASSIVE SULPHIDE DEPOSITS

Massive sulphide deposits in the southern TVB are dominantly associated with felsic volcanic rocks (ash- to quartz ± feldspar crystal tuffs and local rhyolite flows) hosted within sequences dominated by volcaniclastic, epiclastic and sedimentary rocks. Abundant mafic and felsic sills intrude epiclastic sedimentary rocks (argillite/wacke) within the mineralized sequences, with both syn- and post-mineralization varieties observed, suggesting a possible arc-rift or back-arc basin tectonic setting for massive sulphide formation.

Three VMS deposit clusters occur in the southern TVB, as well as numerous prospects and zones of alteration. From south to north, these deposits are the Boomerang-Domino-Hurricane cluster, the Tulks East, and the Tulks Hill deposits. Volcanogenic massive sulphide mineralization is typically associated with intense sericite–silica–pyrite alteration, and less intense chlorite and carbonate alteration, and is interpreted to have formed in sub-seafloor replacement environments (*see* discussion below). Some of the prospects are associated with intense chlorite alteration and chemical sedimentary exhalative horizons (*e.g.*, iron-formations).

A detailed discussion of the lithogeochemical signatures associated with the host rocks of these deposits as well as lithogeochemical signatures of the associated alteration assemblages for each deposit is presented in the geochemistry section. A detailed analysis of the geochemistry of the minor occurrences and outcrop samples collected during this project are not presented in this report; however, all sample descriptions and lithogeochemical data collected is presented in Appendix 1A and 1B. All relevant drillhole locations are given in Appendix 1C.

Boomerang–Domino–Hurricane Deposit Cluster

Location

The Boomerang–Domino–Hurricane deposit cluster is located toward the southern extremity of the Tulks Valley, approximately 3 km northeast of Pats Pond and 17.5 km

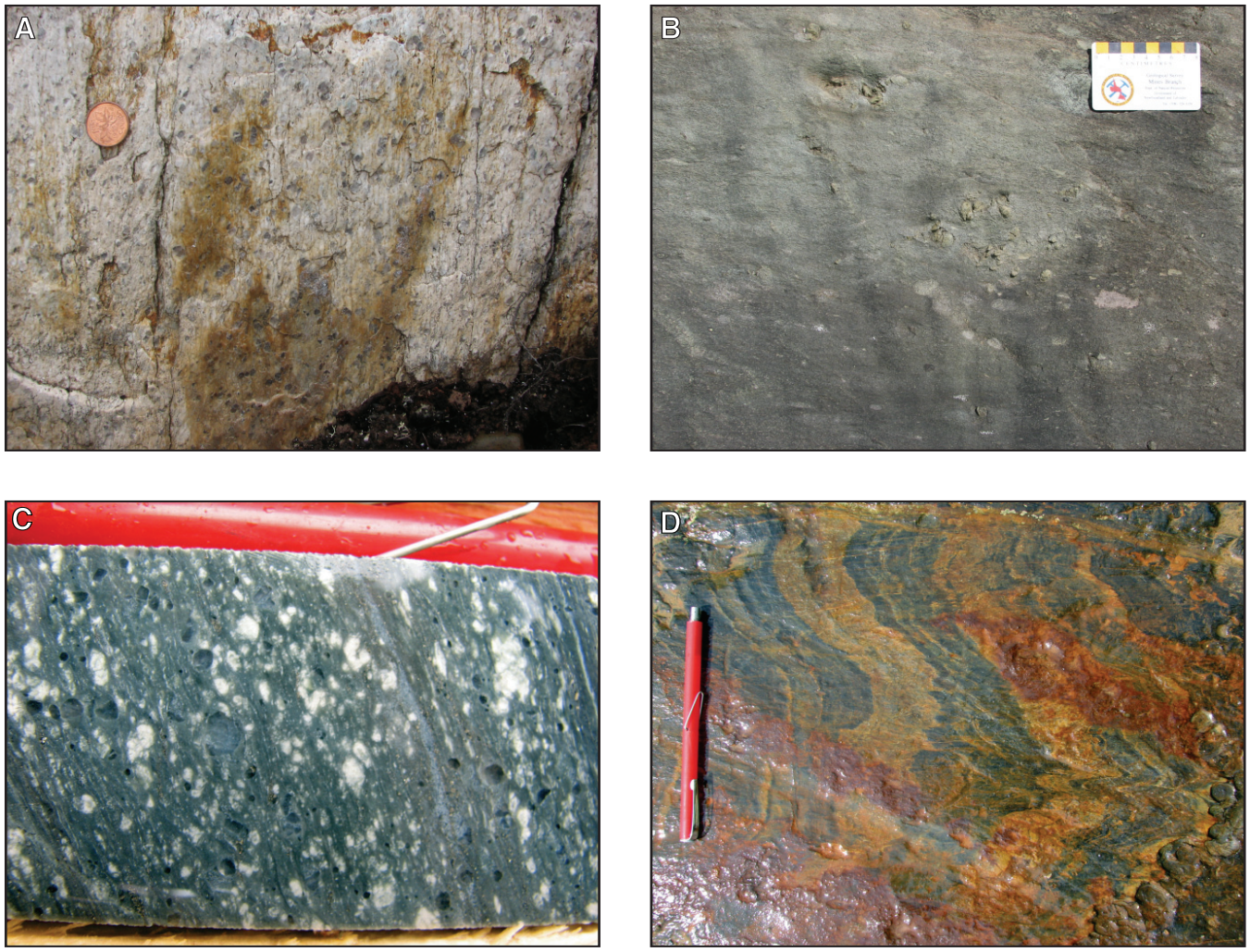

Plate 1. *Common rock types of the southern TVB: A. Quartz porphyritic felsic volcanic; B. amygdaloidal basalt; C. quartz-feldspar porphyritic felsic volcanic; and D. interbedded sediments.*

southwest of the southern tip of Red Indian Lake (Figure 2). The Boomerang–Domino–Hurricane deposit cluster consists of three massive sulphide lenses; namely the Boomerang, Domino, and Hurricane lenses. However, for the purposes of this report, all of the massive sulphide lenses will be grouped together under the name "Boomerang deposit" to simplify discussion.

Local Geology and Mineralization

The stratigraphic succession hosting the Boomerang deposit consists of a series of felsic to intermediate volcanic rocks (ash- and quartz ± feldspar crystal tuff, lapilli tuff, coarse-grained volcaniclastic conglomerate and breccia, black argillite, siltstone, chert and black shale, felsic and amygdaloidal mafic sills, and intermediate dykes (Plate 3)). Massive, coherent rhyolite lavas are not recoginized at the Boomerang deposit, which contrasts with the local abundance of rhyolitic flows at the Tulks Hill and Tulks East deposits (*see* below).

Based on observed inter-fingering and 'soft-sediment' textures, and results from geochronology (*see* section on U–Pb Geochronology below), most of the bimodal sills are considered to be synchronous with the volcano-sedimentary rocks (Plate 4); however, others are interpreted to be post-deposition *(e.g.*, *see* Figure 6). Well-defined fining-upward sedimentary sequences (*e.g.*, turbiditic sequences) are commonly seen in drillcore, and along with the bimodal sills may suggest an arc-rift type environment (Plates 3 and 4; Figure 5A). All these rock types, with the exception of some of the late sills, are overprinted by strong northwest-dipping foliations. The observation that some of the sills are foliated, whereas others are massive with little to no obvious foliation, implies different ages for the sills, or alternatively contrasting competences between sills. Although the lack of

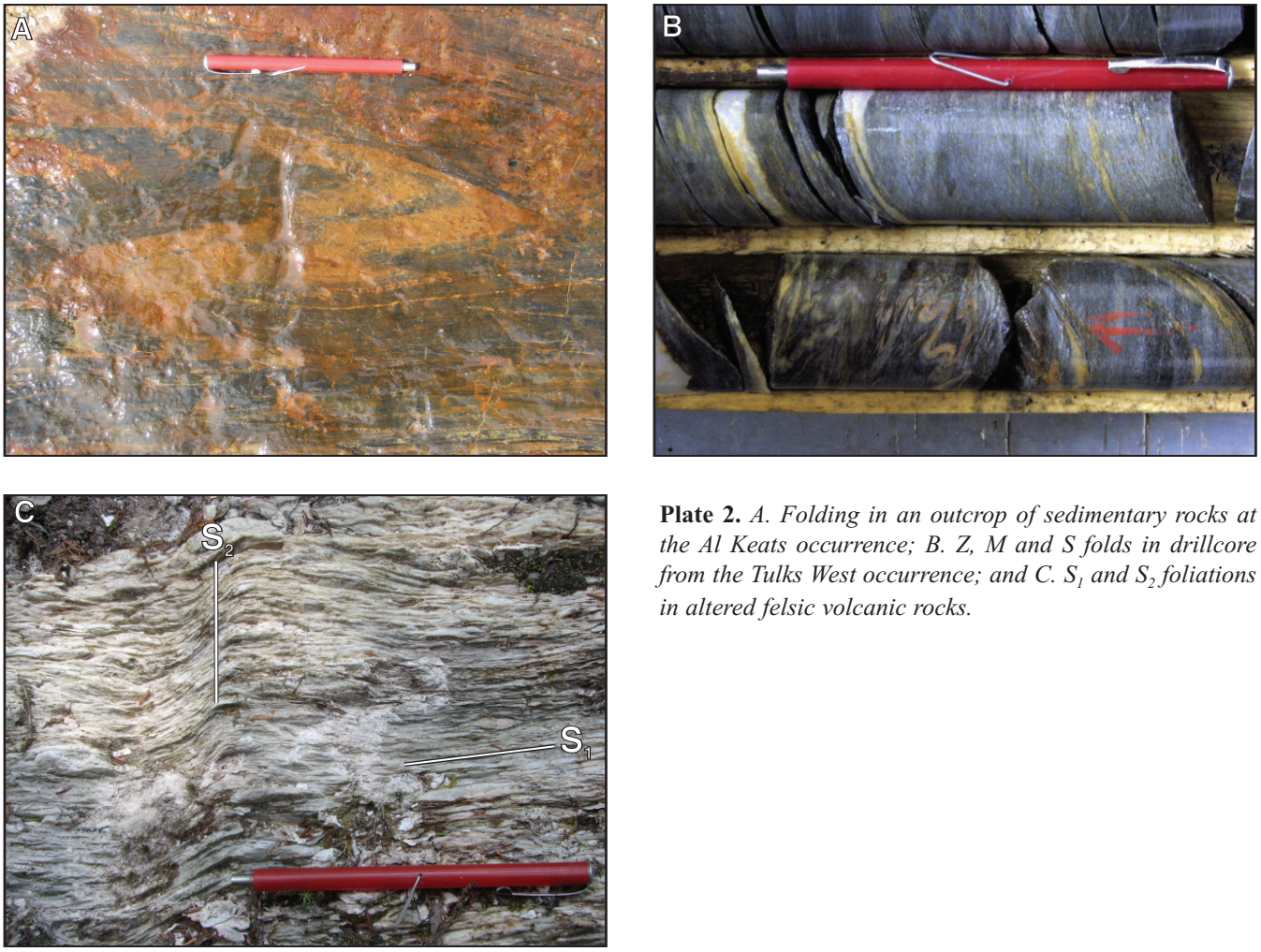

Plate 2. *A. Folding in an outcrop of sedimentary rocks at the Al Keats occurrence; B. Z, M and S folds in drillcore from the Tulks West occurrence; and C. S_1 and S_2 foliations in altered felsic volcanic rocks.*

available outcrop hinders observation of regional-scale folding, local-scale isoclinal folding is commonly observed in drillcore (Plate 3O) and may provide an explanation for some of the pinching and swelling recognized in the massive sulphides, as indicated by varying thicknesses of massive sulphide intersections.

The stratigraphy of the deposit is divided into a stratigraphic hangingwall sequence, the mineralized horizon, and the stratigraphic footwall sequence, as shown in Figures 5A and 6 and described by Squires *et al*. (2006) and Dearin (2006). The geological interpretation depicted in Figure 6 is the most current interpretation proposed by G. Squires (Messina Minerals Inc. and P. Tallman (personal communication, 2008). The decametre-scale folding depicted in the hangingwall is a new concept, and may prove very useful for the future exploration of structurally thickened massive sulphide horizons.

The hangingwall sequence consists of undifferentiated, locally fining upward, felsic to intermediate volcaniclastic and epiclastic rocks dominated by ash- and quartz ± feldspar crystal tuff, black shale, argillite, greywacke, chert, volcaniclastic conglomerate/breccia, and bimodal, locally amygdaloidal, sills (Plate 3, Figure 5). Most of the sills contain a weak to moderate foliation, suggesting that they are pre- to syntectonic in origin, and geochronological evidence indicates that at least some of the felsic sills are synvolcanic, and hence syn-mineralization with the replacement-style ore bodies at the Boomerang deposit. The tuffaceous rocks are commonly capped by fine-grained black argillite and/or shales. Geological interpretations of G. Squires (Messina Minerals Inc.), suggest that large decameter-scale folding has affected the hangingwall rocks. In this geological interpretation, some of the felsic dykes in the hangingwall are illustrated as linear bodies paralleling axial planal cleavage in the hinges of folds, and as such must be post-deformational. Petrographically, the felsic to intermediate tuffs that

Plate 3. *Photographs of rock types, stratigraphy, mineralization and alteration from the Boomerang deposit; A. Intercalated felsic tuffs and black argillite (locally sulphide bearing). Note the rip-up clasts of the argillite in the tuffs (DDH GA-05-021 @ ~420 m); B. Finely inter-laminated black argillite/greywacke and felsic ash-tuff. Note abundant overprinting pyrite (DDH GA-05-021 @ ~370 m); C. Pyroclastic felsic tuff with rip-up clasts of black argillite (DDH GA-05-021 @ ~420 m); D. Heterolithic volcaniclastic breccia/conglomerate. This lithology is common and typically displays fining-upward relationships where it grades into felsic tuff (DDH GA-04-011 @ ~25 m); E. Light-grey, medium-grained felsic sill. The sills occur in both the hangingwall and footwall to the deposit and locally cut the massive sulphides (DDH GA-05-079 @ ~255 m); F. Amygdaloidal basaltic sill. Amygdules (filled with calcite) occur toward the tops of the sills suggesting a high-level of emplacement. The sills have chilled lower contacts (DDH GA-97-05 @ ~285 m); G. Intercalated felsic tuff and black argillite immediately overlying the ore horizon (DDH GA-05-021 @ ~510 m) and H. Mineralized black argillite (DDH GA-05-021 @ ~510 m). Note that all diamond-drill core is NQ size (~47 mm in diameter).*

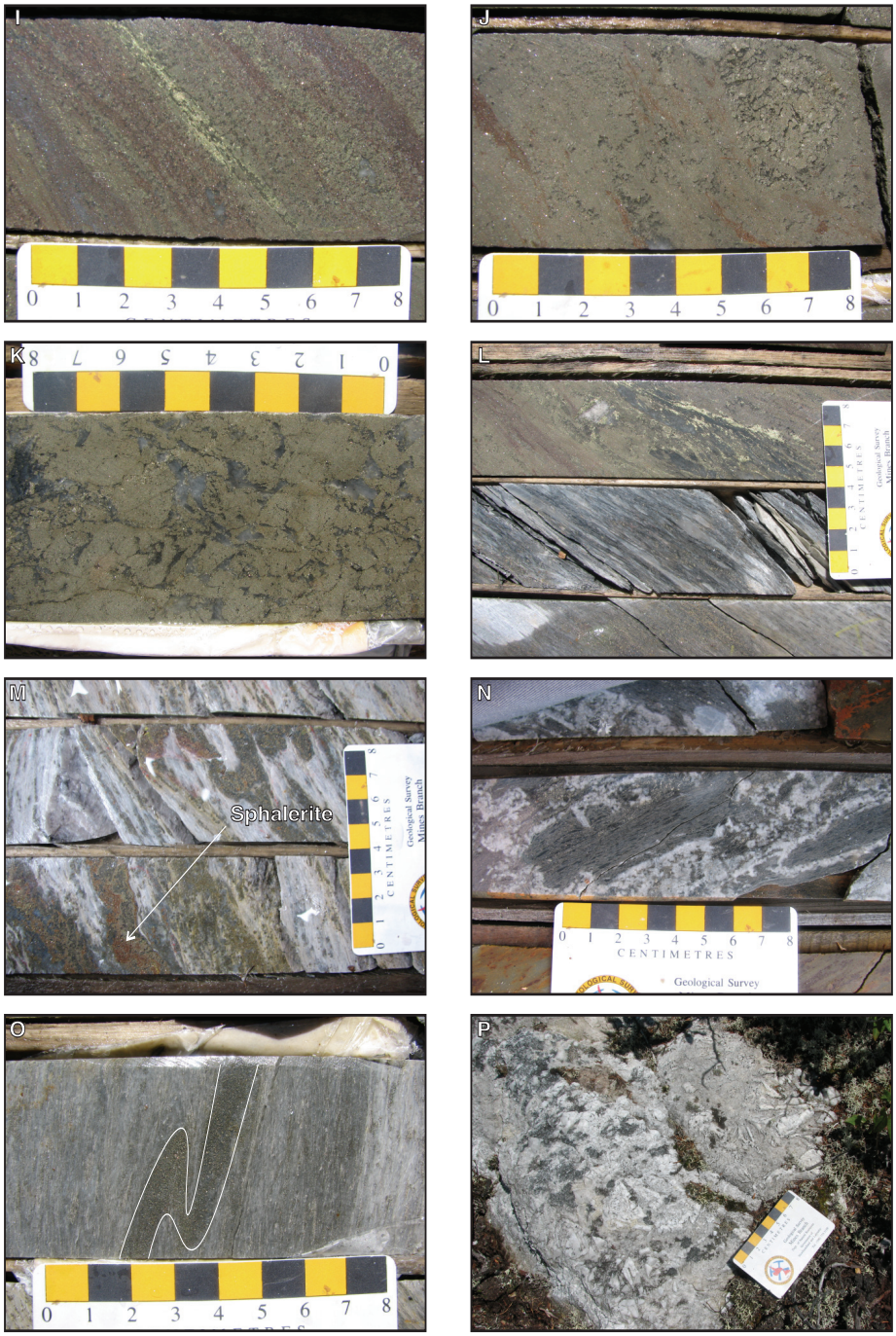

Plate 3. (Continued) *Photographs of rock types, stratigraphy, mineralization and alteration from the Boomerang deposit: I. High-grade, massive sulphides (Zn–Pb–Cu). Note the abundant relic quartz crystals and preserved layering suggesting that the sulphides invaded and replaced a crystal-rich tuff (DDH GA-04-011 @ ~279 m); J. Massive sulphides with coarse-grained blebby pyrite porphyroblasts (DDH GA-04-011 @ ~278.5 m); K. Pyritic massive sulphides with quartz, the sulphides are interpreted to have totally replaced the protolith (DDH GA-05-021 @ ~501 m); L. Massive sulphide replacing the heterolitic felsic lapilli tuff footwall (DDH GA-04-011 @ ~288.5 m); M. Intensely sericitized felsic tuff in a stringer zone beneath the massive sulphide horizon. Note the base-metal-rich composition of the stringers (DDH GA-04-011 @ ~305 m); N. Chaotic carbonate alteration in footwall rocks (DDH GA-97-05 @ ~625 m); O. Sericitized and pyritized footwall felsic tuff. Note the isoclinal folding of the pyrite stringer suggesting post-mineralization structural overprinting (DDH GA-04-011 @ ~310 m); and P. Outcrop of massive barite (locally replaced by silica) in the footwall. Note that all diamond-drill core is NQ size (~47 mm in diameter).*

Plate 4. *A. Interfingering contact relationship between felsic volcanic (left hand side) and an intermediate to mafic dyke (right hand side) suggesting that both were emplaced synchronously (DDH GA-97-05 @ ~79 m); and B. Soft-sediment deformation texture between a mafic sill (left) and an ash tuff (right) (DDH GA-04-11 @ ~205 m). Note that the diamond-drill core is NQ size (~47 mm in diameter).*

dominate the hangingwall sequence consist of 0.5–2 mm fractured and broken plagioclase crystals (~ 0-40 vol. %), and <0.5–1 mm quartz crystals (~5-20 vol. %) in a very-fine grained quartz and feldspar groundmass (Plate 5A and B). Albite locally occurs as small (~0.5 mm), partially resorbed and altered porphyroblastic crystals; interpreted to be related to regional, low-grade greenschist alteration (Plate 5E). All of the hangingwall samples collected are altered to some degree with varying proportions of sericite–silica–chlorite–carbonate alteration. The sericite, silica, and chlorite typically occur as very fine-grained accumulations in the groundmass, whereas the carbonate commonly occurs as 0.5–1 mm overprinting glomeroporphyrocrysts and euhedral rhombohedral crystals. Intense alteration and base-metal sulphide, as stringers and disseminations, are locally present in the immediate hangingwall (*see* section below).

Footwall rocks consist of fine-grained, pyroclastic crystal-ash tuffs with common base-metal stringer sulphides (Plate 3L–O), with local lapilli tuffs and fine-grained sedimentary rocks. As with the hangingwall stratigraphy, the footwall sequence contains bimodal sills. The sills have been affected by hydrothermal alteration and are interpreted to be synvolcanic. The tuffs are extremely sericitized and display an intense foliation and a local crenulation cleavage. Isoclinal folding is manifest in the footwall tuffs as folded sulphide stringers (Plate 3O). This folding may be indicative of regional-scale structural folding, as suggested for the hangingwall rocks by G. Squires (Messina Minerals, personal communication, 2008). An outcrop of massive barite, known from the early days of exploration, has been included in the 'footwall' sequence (*e.g.*, *see* Figure 6). However, its location below the main ore zone, which is replacement in nature, is peculiar as barite is commonly inferred to represent an exhalative process. The data suggests that the barite outcrop is either structurally juxtaposed, or it represents another favourable exploration horizon at a lower stratigraphic level. The co-existence of black shales, that typically denote a reduced anoxic environment, with barite, that denotes an oxidized environment, are difficult to reconcile. Petrographically, the tuffaceous rocks that dominate the footwall stratigraphy are very similar to those in the hangingwall, but they have experienced more intense hydrothermal alteration and typically contain up to 10 vol. % disseminated pyrite and massive sulphide stringers (Plate 6).

The mineralized horizon of the Boomerang deposit consists of strongly altered pyroclastic felsic ash and crystal tuff, as well as black shales, chert and argillite, all of which are intimately associated with massive sulphide mineralization (Plate 3G–L). The high temperature alteration predominantly consists of sericite with lesser chlorite, carbonate and silica alteration. The massive sulphides occur as several lenses within the fine-grained tuffaceous and sedimentary rocks, with the sedimentary rocks consisting of argillite, shales and chert. Geometrically, the sulphide lenses dip approximately 85° to the northwest and have slight plunges from 0 to 15° southwest. The sulphides consist of fine- to medium-grained banded and wispy intergrowths of red and yellow sphalerite, chalcopyrite, galena, and pyrite (Plate 3I). Silicate gangue, dominanted by relict quartz crystals, commonly occur in the massive sulphides. Metal zonation is apparent whereby the margins of the massive sulphide lenses are dominated by pyrite, the bases of the sulphide lenses are enriched in Zn and Cu, Pb and Ag occur toward the core of the lenses, and the tops of the lenses contain gold

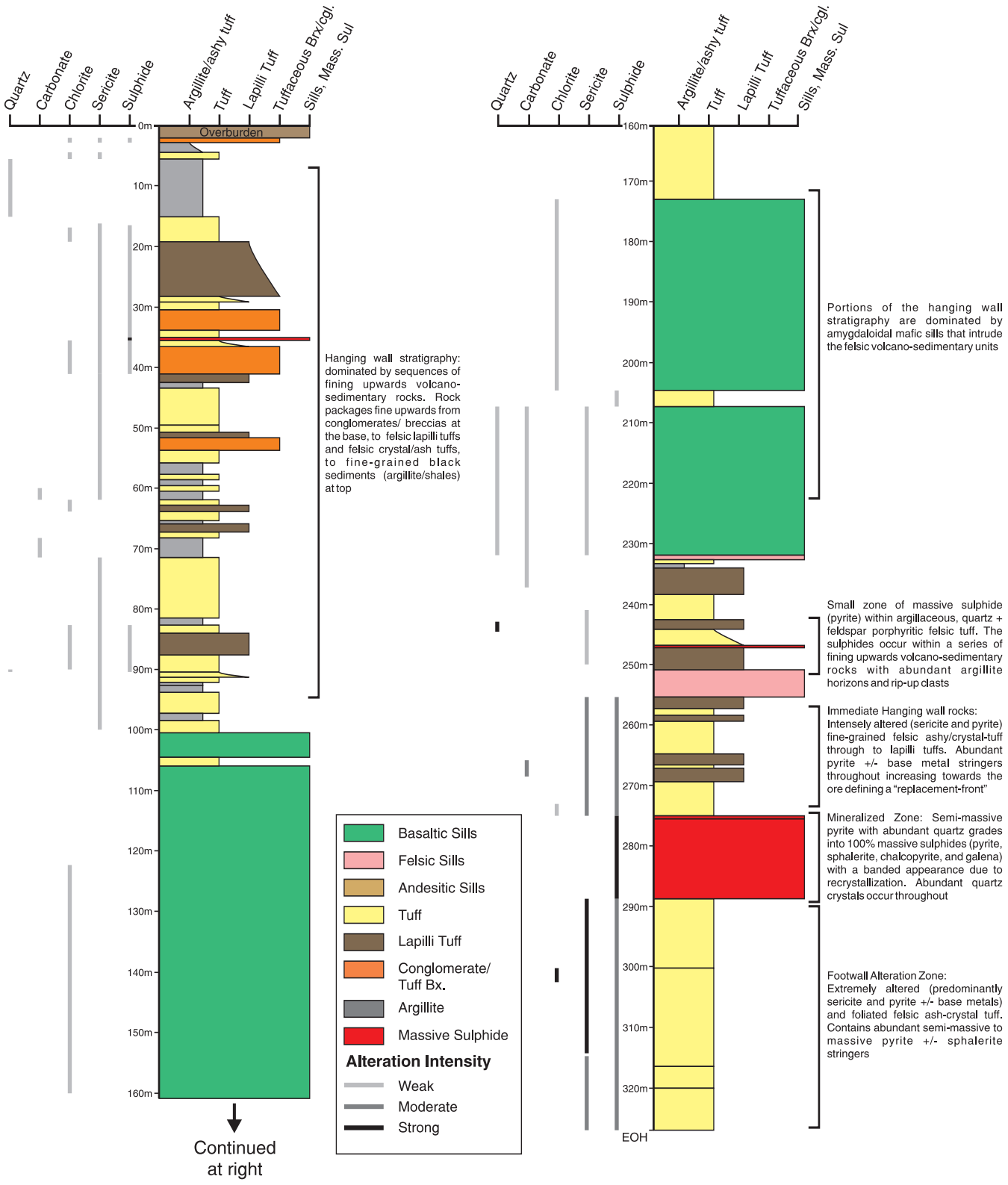

Figure 5. *A. Schematic drillhole stratigraphic column for DDH GA-04-11 (discovery hole) from the Boomerang deposit illustrating rock types and relations and alteration patterns.*

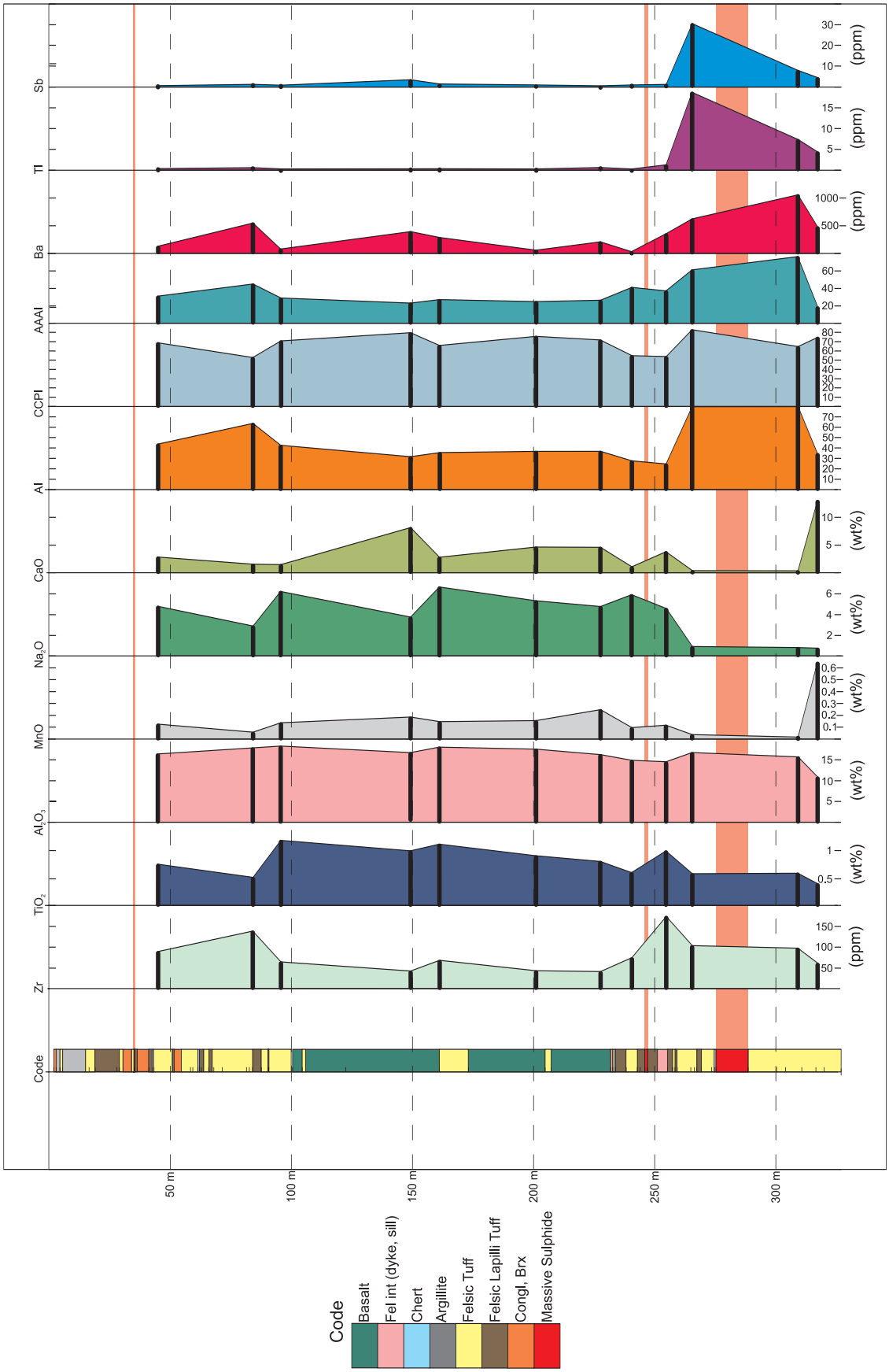

Figure 5. *B. Geochemical strip log for GA-04-011 (Boomerang) illustrating elemental variation in relation to the ore horizons.*

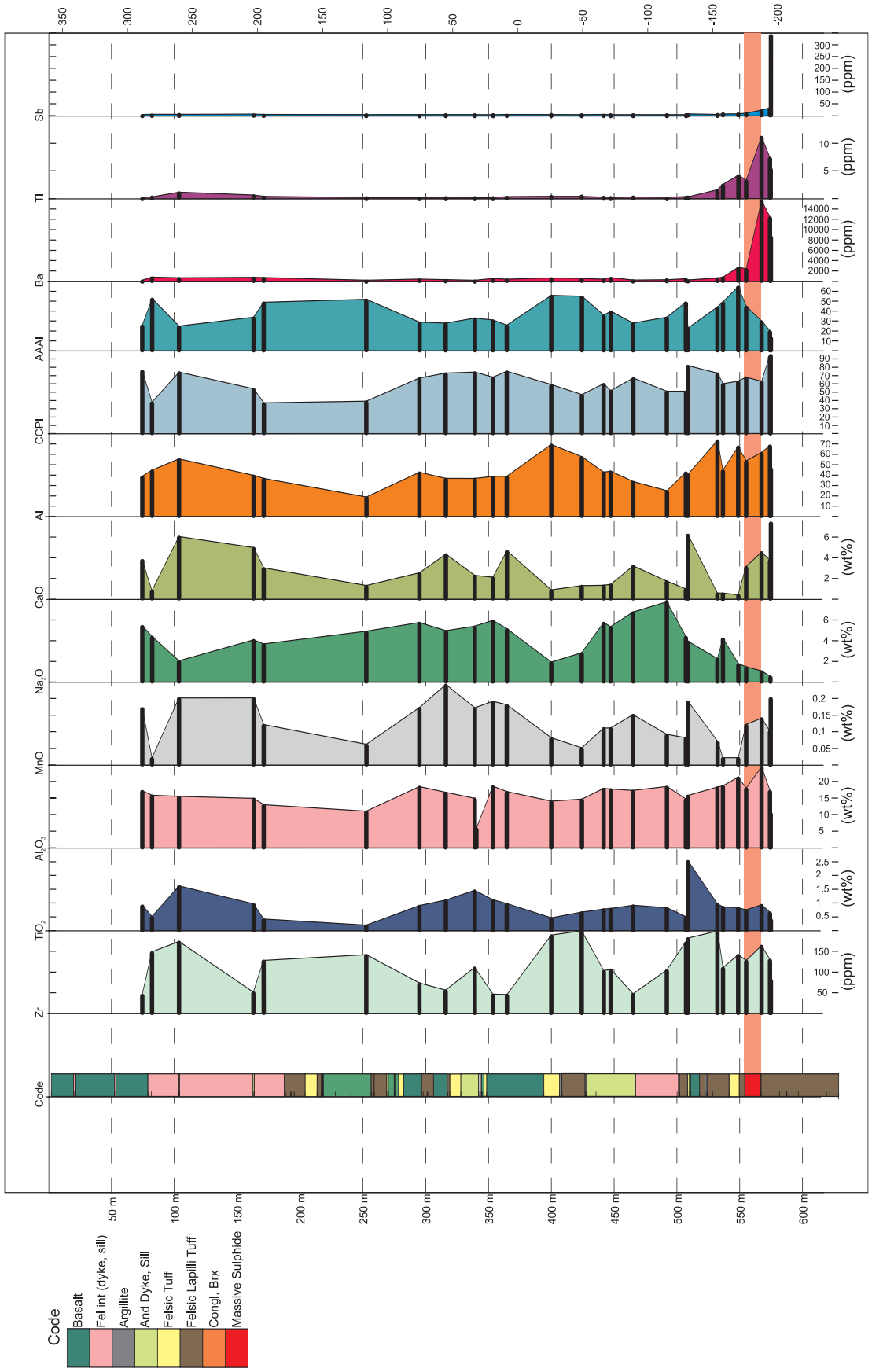

Figure 5. *C. Geochemical strip log for and GA-97-05 (Domino) illustrating elemental variation in relation to the ore horizons.*

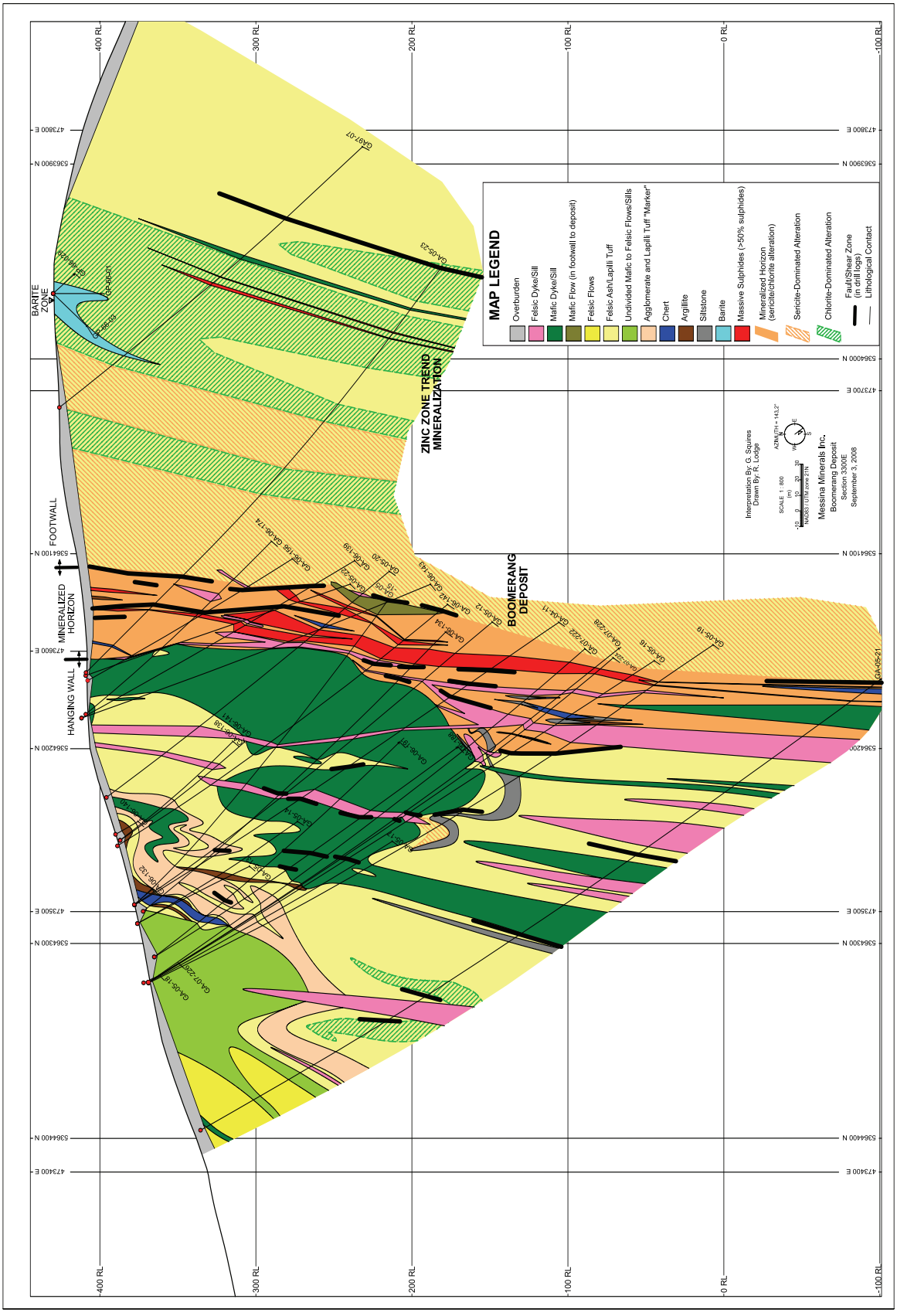

Figure 6. *Cross-section from the Boomerang deposit illustrating the positioning and relationships between the hangingwall, footwall and mineralized horizon. Note the presence of large-scale isoclinal folding in the hangingwall stratigraphy. Note also the location of the barite zone deep in the footwall rocks (from Messina Minerals Inc.; G. Squires, personal communication, 2008). Section azimuth is 143°.*

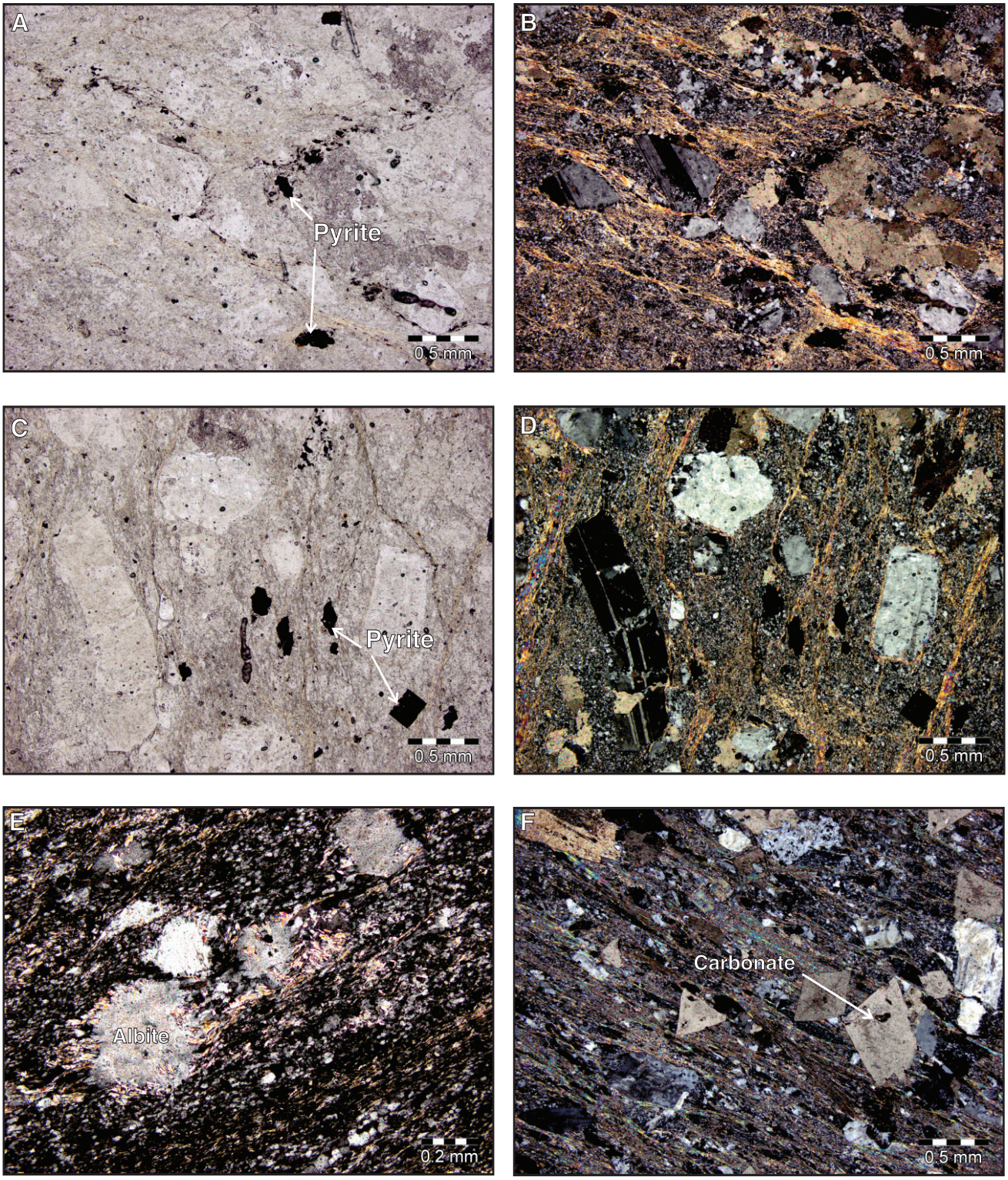

Plate 5. *Photomicrographs of typical Boomerang hangingwall tuffaceous rocks. A and B. from sample JHC-06-172 illustrate a quartz and feldspar phyric, crystal tuff with moderate sericite–quartz–carbonate alteration; C, D and E. From sample JHC-06-179 and also illustrate quartz and feldspar phyric, crystal volcaniclastic tuff with moderate sericite–quartz–carbonate alteration, in addition to relict albite alteration attributed to regional metamorphism; F is from sample JHC-06-202 in the immediate hangingwall and illustrates an intensely altered felsic tuff with sericite–carbonate–quartz alteration assemblages. See Appendix 1A for sample location.*

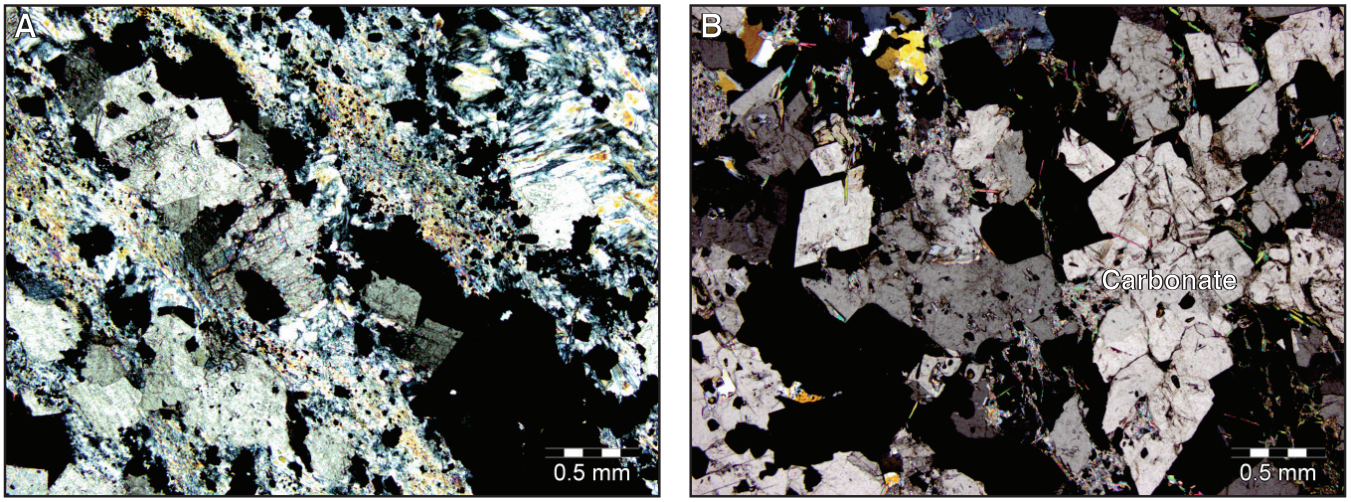

Plate 6. *Microscopic features of typical Boomerang footwall tuffaceous rocks displaying intense carbonate–sericite–silica–chlorite alteration with disseminated to stringer-style sulphides. Samples JHC-06-184 (A) and JHC-06-185 (B).* See *Appendix 1A for sample location.*

enriched pyritic caps (Dearin, 2006; Tallman, 2006). Coarse-grained porphyroblastic aggregates of pyrite occur locally and are interpreted to represent re-crystallization products (Plate 3J and K). Local concentrations of arsenopyrite and tetrahedrite (*see* Page *et al.*, 2008) are associated with some of the high-grade silver and gold intervals; an association originally observed at the Domino massive sulphide lens.

A recent NI43-101 compliant mineral resource estimate for the Boomerang deposit returned an indicated resource of 1.36 Mt grading 7.09% Zn, 3.00% Pb, 0.51% Cu, 110.43 g/t Ag, and 1.66 g/t Au (Messina Minerals Inc., Press Release, June 21, 2007). An additional 0.7 Mt of inferred resources is estimated for the Boomerang and Domino lenses.

Alteration

Distinguishing between regional, semiconformable alteration, and local hydrothermal alteration related to VMS mineralizing processes, is based upon the relative intensities and extents of alteration. Regional hydrothermal alteration, driven by the large-scale convection of seawater by the emplacement of subvolcanic intrusions, is represented by stratabound, weakly to moderately developed sericite–carbonate–silica–chlorite–pyrite alteration. There are a number of examples of this type of alteration associated with the known VMS occurences (*see* Unit 7 on Figure 2 and Unit 10 on Figure 3), and all are gradational with the felsic volcanic dominated stratigraphies hosting VMS mineralization. In the vicinity of the Boomerang deposit, this type of regional hydrothermal alteration is developed over a strike length of 3–3.5 km. It should also be noted that the prospective altered horizon associated with the Boomerang deposit is cut off by the Baxters Pond fault to the northeast (Figure 2). Hangingwall rocks at Boomerang commonly display evidence of regional sub-greenschist to greenschist-facies alteration as well as local hydrothermal alteration related to VMS formation. In contrast, the footwall rocks and mineralized horizon rocks are dominanted by VMS-related alteration minerals. The regional hydrothermal alteration in the hangingwall tuffaceous rocks occurs as fine-grained wisps of sericite and chlorite in the groundmass and as rims on feldspar and quartz phenocrysts and resorbed albite, as fine-grained silicified matrix, and ubiquitius overprinting carbonate alteration. The hangingwall stratigraphy also displays minor intervals of sulphide-bearing exhalative (?) sedimentary rocks with alteration that is more intense than typical for the hangingwall.

At Boomerang, VMS-related hydrothermal alteration is recoginized in the footwall, hangingwall, and mineralized horizon rocks. The distribution and extent of this alteration is related to the geometry of the fault and fracture systems along which the mineralizing fluids migrated as well as permeability and porosity contrasts within the volcanic succession. The immediate hangingwall rocks, dominated by ash to felsic to intermediate crystal tuffs, display intense sericite–carbonate–silica alteration (Plate 5F) with local sulphide stringer mineralization. The carbonate alteration occurs both as a late-stage euhedral overprinting alteration product (*e.g.*, related to regional metamorphism) as well as amorphous masses associated with silica alteration. The intensity of the alteration in the hangingwall is one piece of evidence supporting a sub-seafloor replacement style of mineralization (*see* discussion below). Footwall alteration is dominated by intense sericite alteration with local zones of moderate to strong chlorite–silica–carbonate alteration and

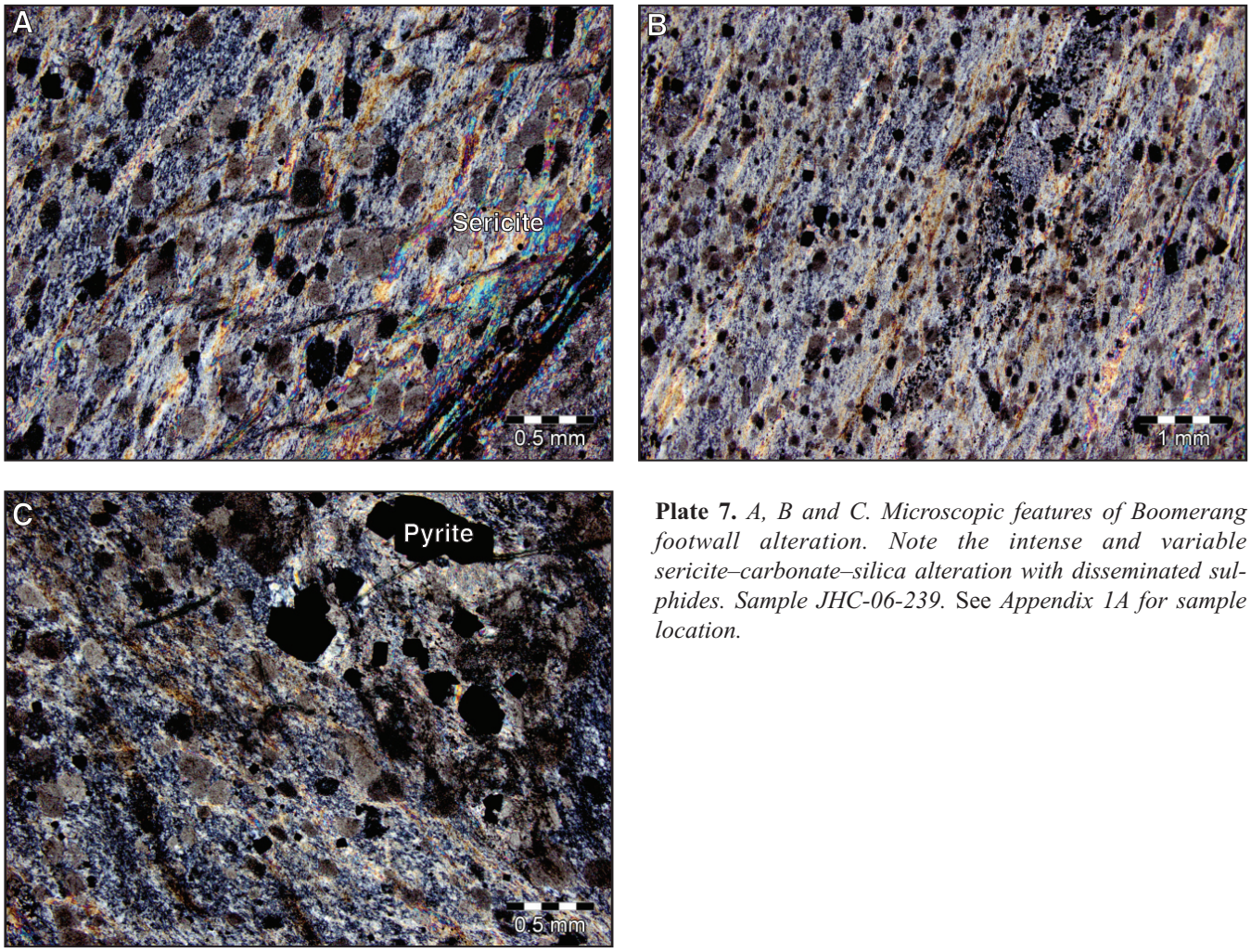

Plate 7. *A, B and C. Microscopic features of Boomerang footwall alteration. Note the intense and variable sericite–carbonate–silica alteration with disseminated sulphides. Sample JHC-06-239.* See *Appendix 1A for sample location.*

locally sulphide stringer zones (Plate 7). Locally, zones of intense hydrothermal carbonate–chlorite–quartz alteration also occur, with carbonate forming 'chaotic' alteration patterns reminiscent to those observed at the Duck Pond deposit (Plate 3N; Squires *et al.*, 2001). The vein-like, or chaotic net-textured appearance of the carbonate suggests that it formed *via* replacement mechanisms rather than by precipitation on the seafloor. Local barite alteration has also been observed in the footwall rocks, particularly in the footwall to the Domino massive sulphide lense, where barium concentrations reach levels greater than 1%. The mineralized horizon displays similar alteration assemblages to the footwall, dominated by sericite–carbonate–chlorite–silica, with abundant base-metal-rich sulphide stringers. Base-metal sulphide mineralization is commonly observed as infillings and replacements within the intense carbonate alteration.

Tulks Hill Deposit

Location

The Tulks Hill deposit is located in the Tulks River valley, approximately 4 km south of the south end of Red Indian Lake (Figure 2). The deposit crops out as a rusty zone on the side of Tulks Hill and is visable from the Tulks River valley (Plate 8), and it was explored through an adit, which extends some 175 m into the hillside for the purposes of bulk sampling.

Local Geology and Mineralization

The Tulks Hill deposit is hosted by quartz-phyric rhyolite (Plate 1) and altered felsic to intermediate volcanic rocks, dominated by blue quartz ± feldspar-phyric crystal

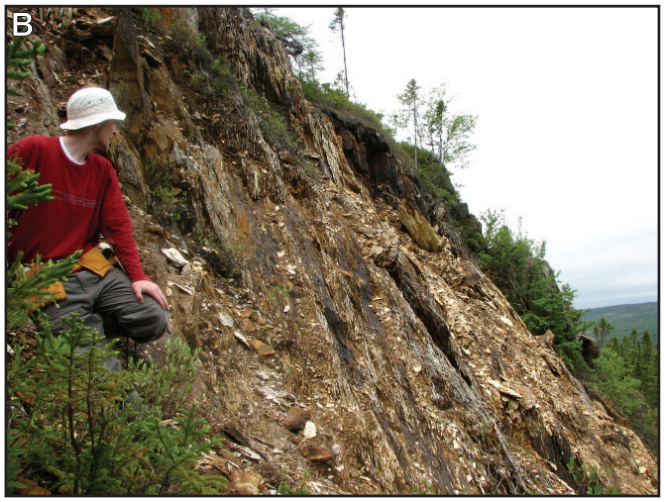

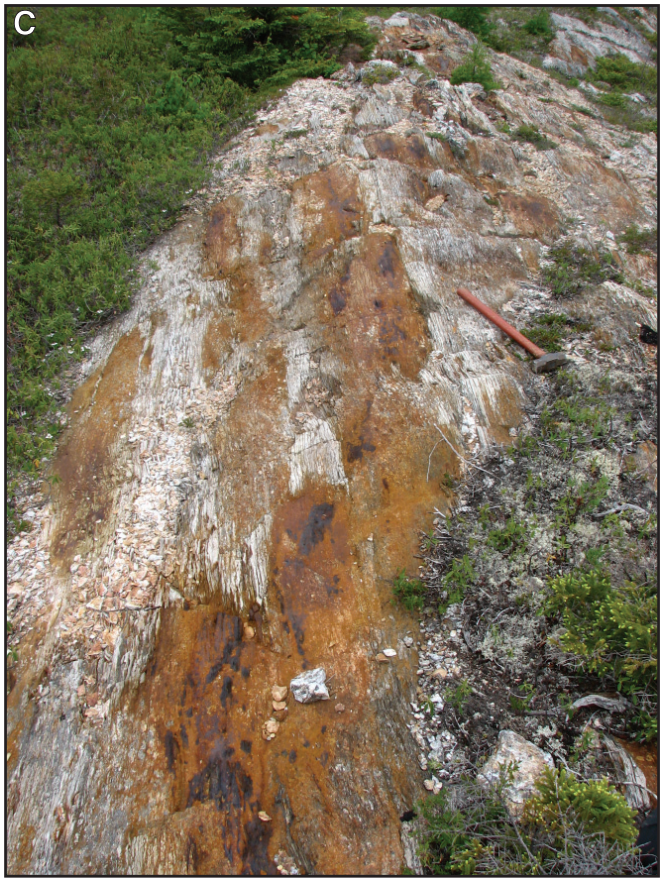

Plate 8. *A. View of the Tulks Hill VMS system from the Tulks River valley (looking east); B. schistose felsic volcanic rocks; and C. footwall alteration in felsic volcanic rocks from the Tulks Hill VMS deposit.*

tuff and crystal lapilli-tuff. In addition to the felsic to intermediate tuff and rhyolite, the stratigraphy also contains mafic sills, black argillite and shale (Figures 7 and 8). Substantial work was conducted on the deposit by Moreton (1984), Jambor and Barbour (1987), and exploration companies.

The quartz-phyric rhyolites display well-preserved primary textures. Quartz crystals are rounded to teardrop-shaped and set in a groundmass dominated by fine-grained recrystallized quartz and sericite (Plate 9), and also as partially resorbed crystals. The felsic tuffaceous rocks contain abundant broken quartz crystals in fine-grained, quartz–sericite groundmass. Abundant overprinting biotite is also commonly present in the tuffaceous rocks.

The deposit consists of four tabular massive sulphide lenses, *i.e.*, T1 to T4 (Figure 7), collectively containing 720

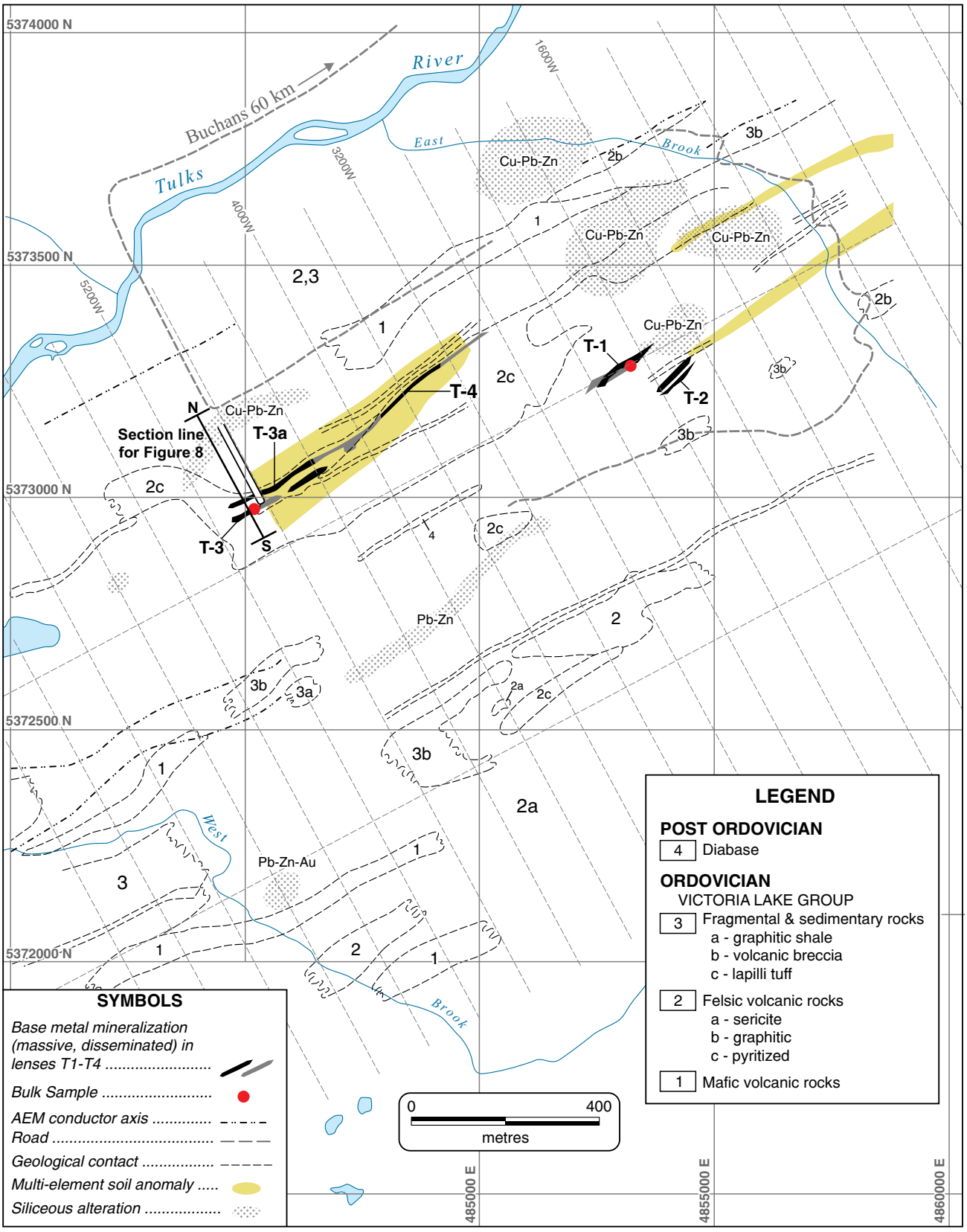

Figure 7. *Simplified geology map of the Tulks Hill deposit area illustrating rock types and alteration patterns (from Prominex Resources Corp. web page; geology compiled from United Bolero).*

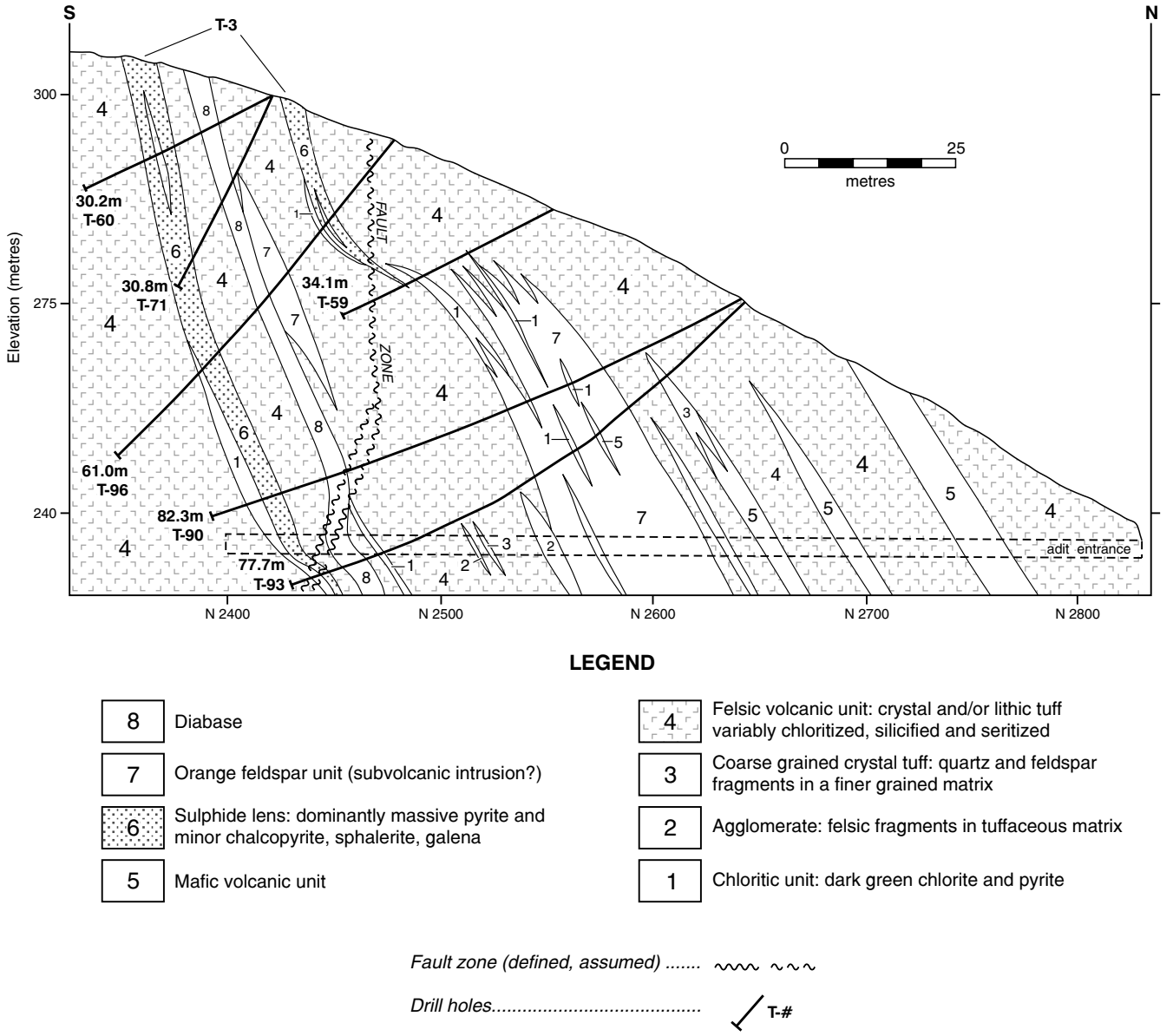

Figure 8. *North – south cross-section of the T-3 Lens, Tulks deposit (from Evans and Kean, 2002; after Moreton, 1984). Section is located on Figure 7.*

000 tonnes of massive sulphide, grading 5.6% Zn, 1.3% Cu, 2.0% Pb, 41 g/t silver and 0.4 g/t gold (Jambor and Barbour, 1987; Figure 7). Lenses T1, T2 and T3 crop out at surface and are marked by gossan development, whereas lens T4 occurs only at depth. Some of the lenses may represent structural repetitions of the same horizons due to isoclinal folding suggested by Moreton (1984) and Saunders (1999). In conjunction with the ubiquitous alteration both above and below the ore horizon, this structural complication makes definitive identification of the stratigraphic footwall versus hangingwall difficult.

The massive sulphides are dominated by pyrite with sphalerite, galena, chalcopyrite, arsenopyrite, tetrahedrite–tennanite and pyrrhotite present as accessory sulphide minerals (*e.g.*, *see* Evans and Kean, 2002). Minor amounts of non-sulphide gangue, including quartz, sericite, chlorite, carbonate, albite and barite occur within the massive sulphides. Significant magnetite also occurs within the T1 and T2 lenses and distinguishes the Tulks Hill sulphides from other massive-sulphide bodies in the area. Although not identified as part of this study, oxidation and supergene alteration minerals, including digenite, covellite and anglesite have been identified at the deposit (*e.g.*, *see* Jambor, 1984).

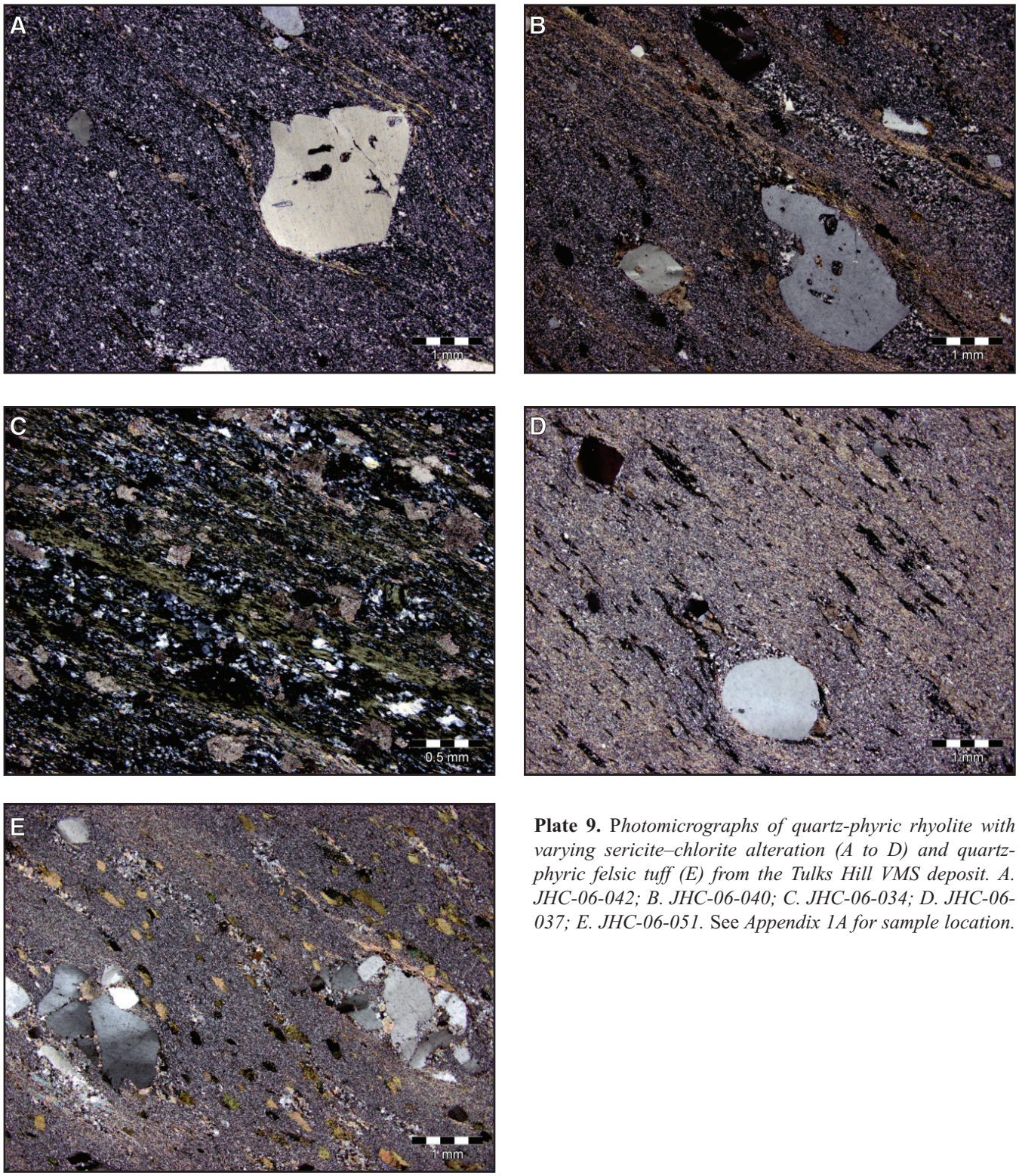

Plate 9. P*hotomicrographs of quartz-phyric rhyolite with varying sericite–chlorite alteration (A to D) and quartz-phyric felsic tuff (E) from the Tulks Hill VMS deposit. A. JHC-06-042; B. JHC-06-040; C. JHC-06-034; D. JHC-06-037; E. JHC-06-051.* See *Appendix 1A for sample location.*

Alteration

Alteration in the vicinity of the Tulks Hill deposit is by local hydrothermal alteration, with little in the way of regional metamorphic products preserved. However, the albite in, and around, the Tulks Hill massive sulphide lenses is interpreted to reflect regional metamorphism. Alteration associated with the sulphide lenses has been observed over a 2000-m-long zone (McKenzie *et al*., 1993). Prominent sericite, chlorite, pyrite and silica alteration occurs within the host felsic quartz-crystal tuff and quartz-phyric rhyolite in proximity to the sulphide lenses. Alteration and related stringer mineralization are present in both the hangingwall and footwall, and suggest emplacement *via* a replacement process (Kean and Evans, 1986).

Tulks East Deposit

Location

The Tulks East deposit is located near the southern tip of Red Indian Lake (Figures 1 and 2), approximately 53 km southwest of the town of Millertown.

Local Geology and Mineralization

The stratigraphy hosting the Tulks East deposit consists of altered felsic to intermediate volcanic rocks including ash- and quartz ± feldspar crystal tuff, lapilli tuff, coarse-grained volcaniclastic conglomerate and breccia, quartz-phyric rhyolite flows and local basaltic sills (Plate 10). Fining-upward sequences are commonly observed within the host volcaniclastic rocks. The footwall stratigraphy consists mainly of felsic crystal and lapilli tuffs with lesser amounts of rhyolite, minor conglomerate and lapillistone, mafic tuffs, and intermediate to mafic amygdaloidal sills (Figures 9A, and 10). Mineralization occurs toward the top of this sequence, and is immediately overlain by felsic tuff and rhyolitic flows, followed by a thick sequence of intercalated graphitic argillite and mafic to intermediate high-level sills and dykes. The Tulks East fault is developed within the argillic sequence, and affects a zone averaging about 20–30 m thick (Figures 9A and 10). In some drillcores, the footwall to hangingwall transition is intact, *i.e.*, not faulted (Plate 10B), and suggests that the footwall and overlying graphitic argillite represent a primary stratigraphic succession (*e.g.*, implication is that the graphitic sediments are Tremadoc in age). This interpretation is indirectly substantiated by the presence of a Tremadoc conodont recovered at the Jacks Pond deposit, approximately 10 km to the northwest of the Tulks East deposit (*cf.* Kean and Evans, 1988). The hangingwall rocks above the graphitic argillite consist predominantly of mafic to intermediate sills and lesser amounts of quartz-phyric felsic volcanic rocks.

Petrographically, the tuffaceous rocks at the Tulks East deposit are similar to those at the Tulks Hill deposit. The crystal tuffs are well foliated and contain 5–25 vol. %, 0.5–5 mm quartz crystals with rare feldspar crystals. The tuffaceous rocks differ from those hosting the Boomerang deposit in that quartz phenocrysts predominate over feldspar at the Tulks East deposit. The quartz-phyric rhyolites display well-preserved primary textures including partially resorbed and embayed quartz crystals within a fine-grained, recrystallized quartz and sericite groundmass (Plate 11). The resorption textures suggest that the quartz phenocrysts were unstable in the melt prior to its solidification, being perhaps related to increased melt temperatures related to mafic magma influx.

To date, this deposit represents the largest accumulation of massive sulphide mineralization in the TVB with three massive sulphide lenses (the A, B, and C zones) totaling ~5.6 million tonnes (Barbour and Thurlow, 1982); all three lenses are tabular and are open at depth. The lenses were originally determined to dip 70° to the northwest and plunge 45° to the north (*e.g*., Barbour and Thurlow, 1982). However, recent diamond drilling by Messina Minerals Inc. suggests that the A Zone actually lies much closer to the surface than would be expected by such geometry (Messina Minerals Inc., Press Release, October 26, 2006).

The massive sulphides consist of medium- to coarse-grained pyrite, intergrown with lesser amounts of pyrrhotite, sphalerite, galena and chalcopyrite (Plate 10E–G). Non-sulphide gangue minerals are dominated by quartz and lesser amounts of sericite, chlorite and carbonate. The A-Zone lens is the largest zone with ~4.5 million tonnes of massive sulphide (~2% base metals (Zn+Cu+Pb)); however, the smaller B Zone (~0.23 million tonnes) has much higher grade (~8.7% Zn, 0.66% Cu, 1.26% Pb, 58.7 g/t Ag, and 0.14 g/t Au; Barbour and Thurlow, 1982). The C Zone contains approximately 1 million tonnes of low-grade pyrite dominant massive sulphide.

Although Tulks East deposit was historically inferred to be dominated by low-grade, un-economic pyritic sulphides, recent work indicates exploration potential for the down-plunge extension of the A-Zone lens (*e.g*., Tallman, 2000; Messina Minerals Inc., Press Releases, October 27, 2005 and August 1, 2006). Structural re-interpretations of the deposit suggest that the B Zone, which typically sits ~15 m above the A Zone, is a fault offset of the down-plunge extension of the A Zone (Messina Minerals Inc., Press Release, October 27, 2005). Additionally, similar hangingwall and footwall stratigraphies of both sulphide lenses, as recoginized through detailed drillhole re-logging during this project, support this interpretation. The A Zone has good potential for higher grade base metals at depth, as indicated

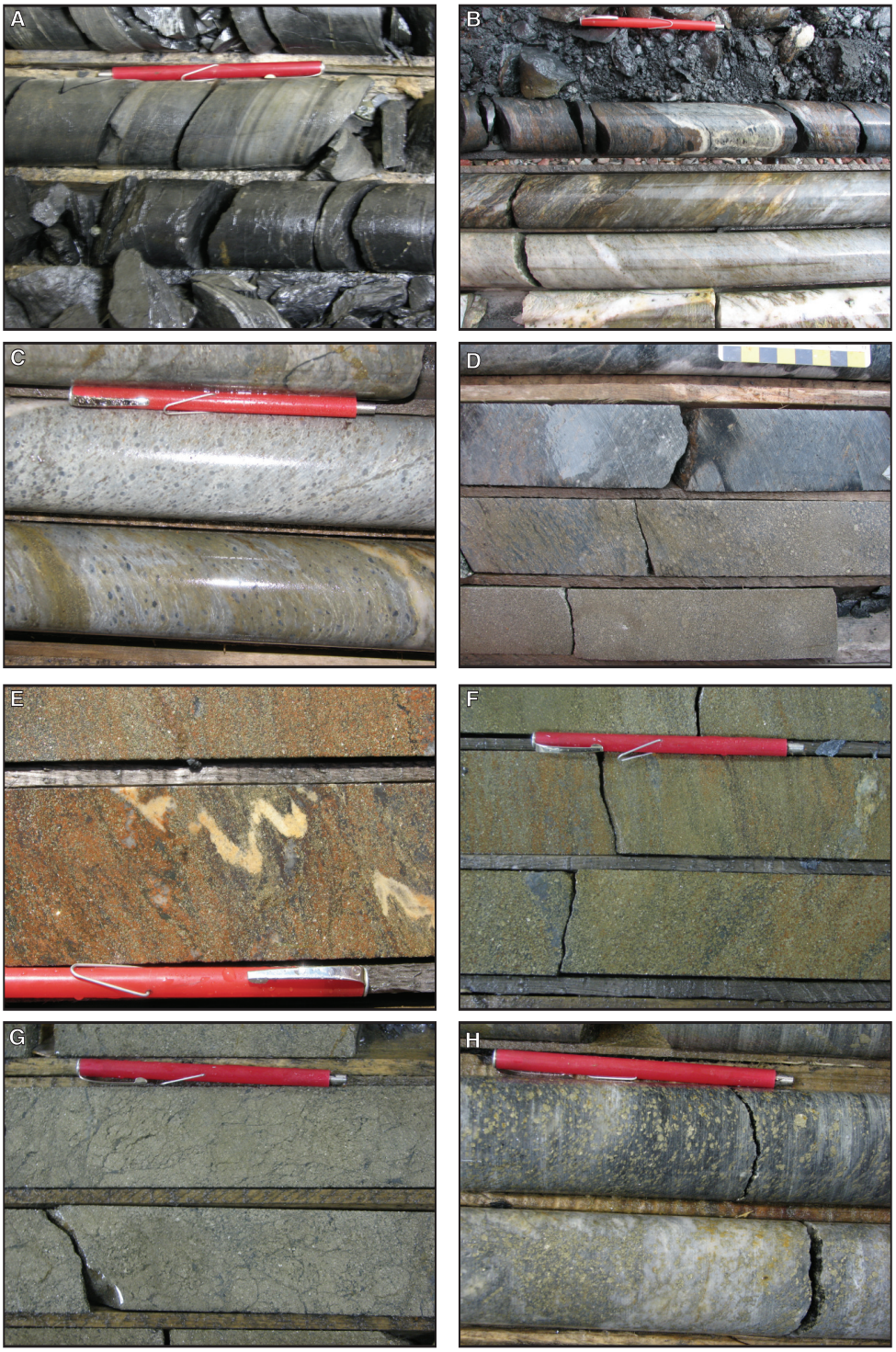

Plate 10. *Photographs of rocks types, mineralization, and alteration at the Tulks East deposit. A. Banded greywacke and black argillite (locally graphitic) (DDH TE-99-04 @ ~185 m); B. contact of graphitic argillite with felsic volcanics (note Tulks East Fault) (DDH TE-99-04 @ ~220 m), C. hangingwall quartz-eye phyric felsic tuff; note intense sericite/pyrite alteration (DDH TE-99-03 @ ~337 m); D. hangingwall felsic volcanics; note intense pyrite/sericite/chlorite alteration (DDH TE-99-04 @ ~234 m); E. Zn-rich massive sulphide; note relict quartz-crystals and post-mineralization folding (DDH TE-99-04 @ ~246 m); F. Cu-rich Tulks East massive sulphide (DDH TE-99-04 @ ~241 m); G. pyritic sulphide keel of the Tulks East A-Zone ore body (DDH TE-99-04 @ ~258 m); and H. intense chlorite/sericite/pyrite alteration of footwall felsic volcanics (DDH TE-99-04 @ ~267 m).*

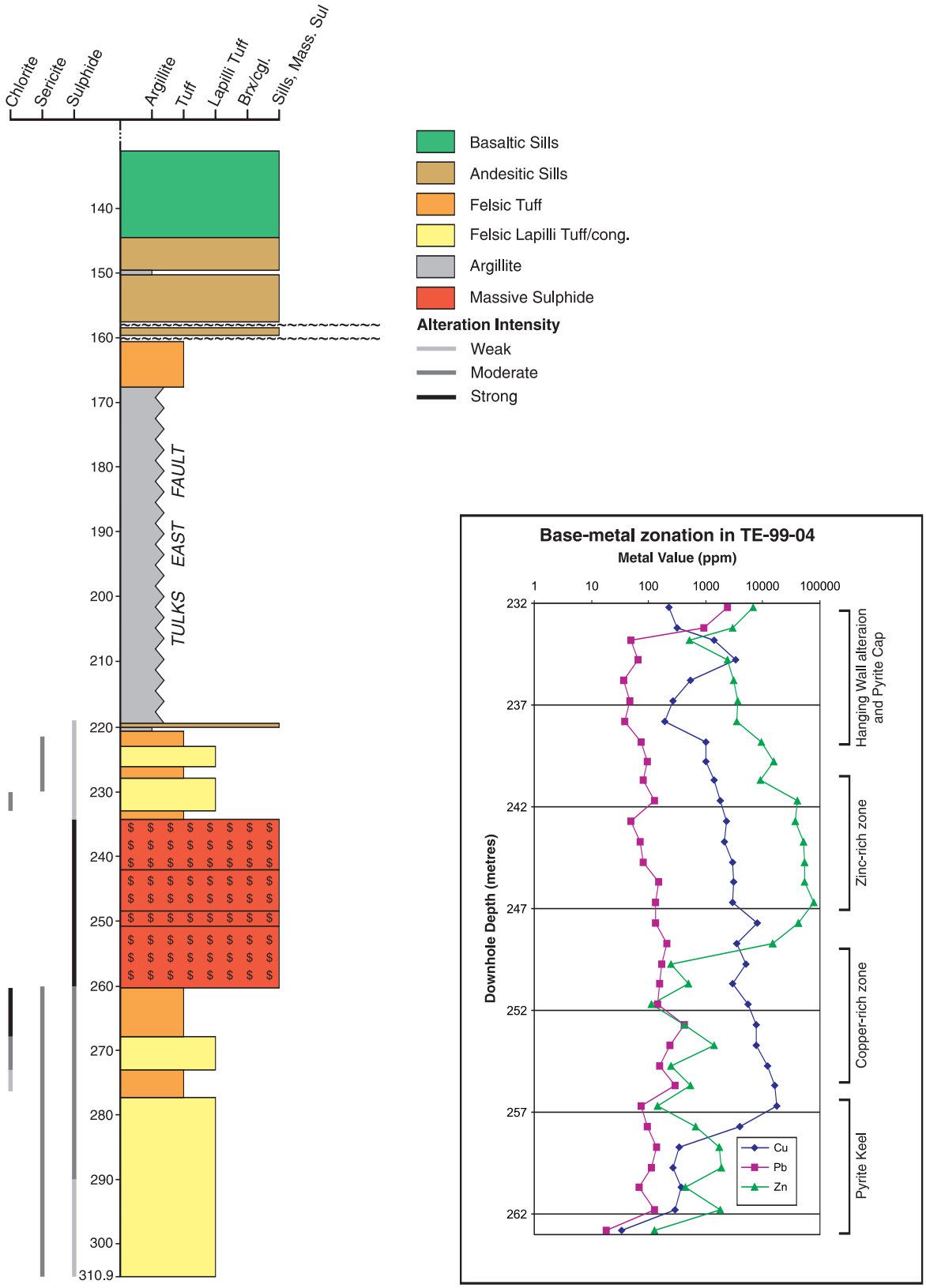

Figure 9. *A. Graphic drill log for DDH TE-99-04 from the Tulks East deposit. The hole intersected the A-Zone massive sulphide lens. Note the presence of alteration in both the footwall and hangingwall and also the metal zonation in the sulphide lens. Graph illustrates base-metal zonations within the massive sulphide lens (Modified from Tallman, 2000).*

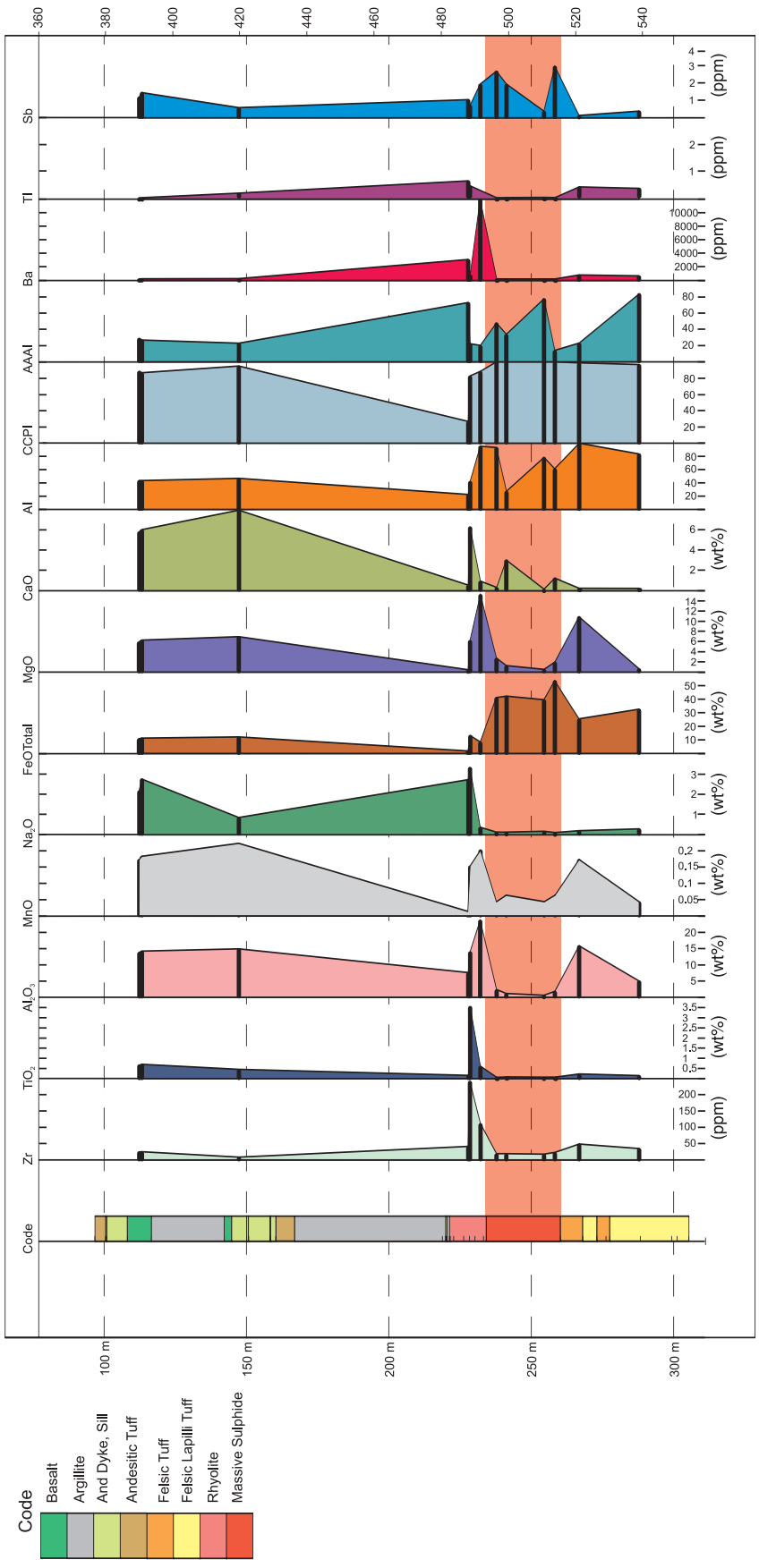

Figure 9. *B. Geochemical strip log for TE-99-04 illustrating elemental changes in relation to the ore horizons.ating elemental variation in relation to the ore horizons.*

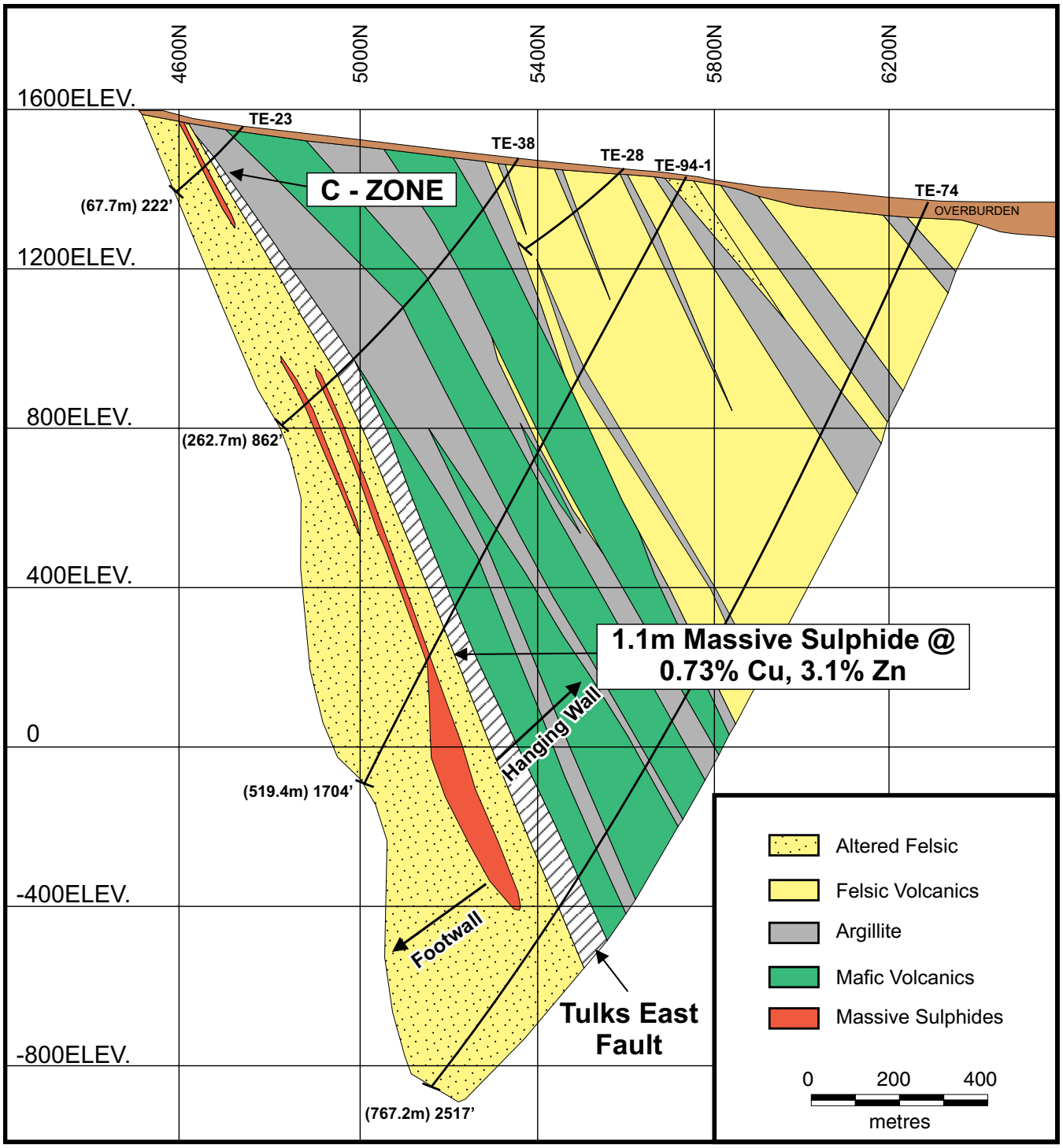

Figure 10. *Cross-section through the Tulks East deposit (from Noranda 1998).*

by the fact that both base-metal contents and the intensity of chloritic alteration increase down-plunge (*e.g.*, to the northeast). For example, DDH TE-05-86, a 100-m step-out from previous drilling, intersected 7 m of 6.2% Zn, 0.4% Cu, 0.3% Pb, 19 g/t Ag, and 0.3 g/t Au (Messina Minerals Inc., Press Release, October 27, 2005). The deeper portions of the A Zone may be more vent proximal. Mineralization within the down-plunge extensions of the A Zone appears to have typical VMS base-metal zonation with a massive pyritic upper blanket close to surface, Zn- and Cu-bearing sulphides in the core of the sulphide lens, and a basal pyritic keel at depth. This pattern is illustrated well by a geochem-

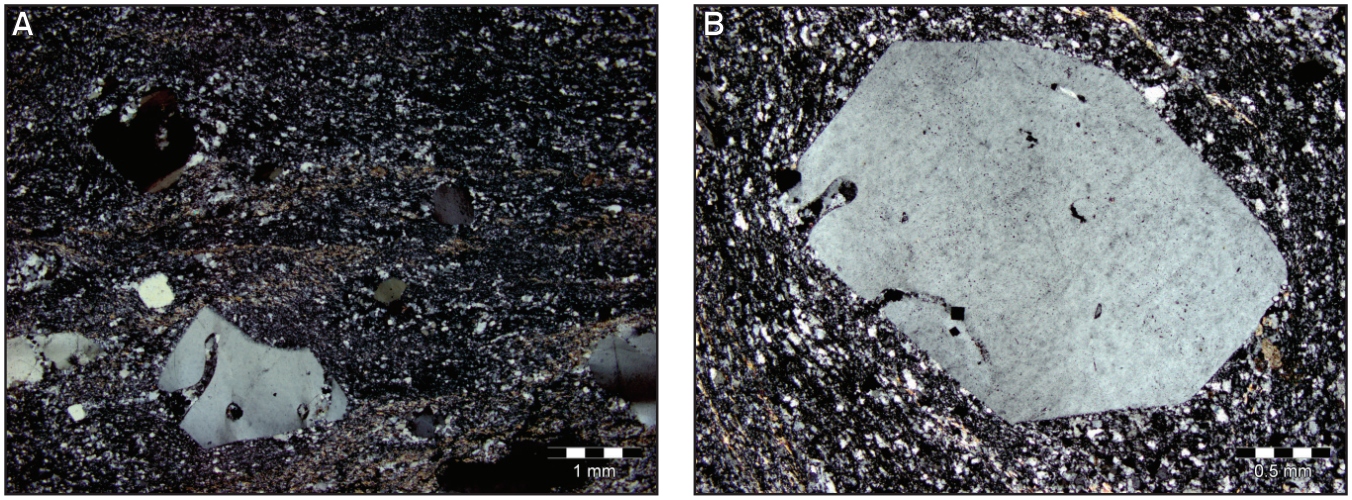

Plate 11. *A and B. Quartz crystals within a fine-grained recrystallized quartz and sericite matrix from a rhyolitic facies at the Tulks East deposit. Note the delicate resorption textures occuring as embayments within the quartz crystals, indicative that the quartz phenocrysts were unstable in the melt prior to its solidification. Both photomicrographs are from JHC-06-022;* see *Appendix 1A for sample location.*

ical profile through the sulphide zone in hole TE-99-04, shown in Figure 9a (after Tallman, 2000).

Alteration

All of the rocks in the vicinity of the Tulks East deposit, as with all rocks in the TVB, experienced regional sub- to greenschist-facies metamorphism. This results in regional, weakly developed, sericite–silica–chlorite alteration assemblages.

The Tulks East deposit is hosted by sericite–silica–pyrite altered felsic volcanic rocks and, locally chlorite–carbonate altered felsic ash- and crystal tuff and lapilli tuff, quartz-phyric rhyolite flows and local basaltic sills. Both the hangingwall and footwall have undergone hydrothermal alteration and contain stringer-style sulphide mineralization, within an alteration envelope that extends approximately 1600 m along strike, 200 m in width, and at least 400 m down dip (McKenzie *et al*., 1993; Noranda, 1998). The presence of intense hydrothermal alteration and sulphide stringers, in both the hangingwall and footwall stratigraphy, suggests a replacement process for mineralization (e.g., Figure 9B, Hinchey, 2007).

The regional hydrothermal alteration defines a penetrative foliation, with sericite and chlorite occurring along the foliation planes. As outcrop around the deposit is limited, and the hangingwall stratigraphy is cut by the Tulks East fault and more mafic rocks, the bulk of the hydrothermal alteration observed is attributed to local alteration associated with the VMS formation. The hangingwall felsic tuffs and rhyolitic rocks contain weak to moderate sericite–chlorite–pyrite alteration with weak silicification. The footwall felsic volcanic rocks commonly display more intense sericite–chlorite–silica–carbonate–pyrite alteration. Zones of alteration with intense black-chlorite and pyrite, as well as zones of intense silica–pyrite alteration, are common in the footwall (*e.g.*, Plate 10H).

Other VMS Occurrences/Prospects

In addition to the above-described massive sulphide deposits, numerous other VMS prospects and occurrences and areas with VMS-style alteration occur throughout the southern TVB (Figure 2). The prospects can be divided into three main types based on the type of mineralization:

Group 1: Coarse-grained, disseminated to semi-massive pyrite with minor base metals associated with chloritized felsic/intermediate (?) volcanic rocks (*e.g.,* Middle Tulks, Al Keats and the Curve Pond prospects).

Group 2: Chalcopyrite and pyrite stringers with anomalous arsenopyrite within chlorite–sericite–silica–pyrite altered felsic (to intermediate?) volcanic rocks (*e.g.,* Tulks West and Mug-up prospects).

Group 3: Massive sulphides (locally base-metal enriched with local anomalous (secondary?) arsenopyrite) associated with exhalative ferruginous sediments (*e.g.*, the main Curve Pond and Dragon Pond prospects).

Group 1

This group includes the Middle Tulks, Al Keats, and a

Plate 12. *Chlorite alteration with semi-massive pyrite at the Middle Tulks VMS showing. Note the variable habit of the pyrite (*e.g., *coarse cubes and fine-grained semi-massive disseminations). Host rock is interpreted to be intermediate volcanic rocks.*

portion of the Curve Pond prospects. The zones of mineralization and alteration consist of intensely chloritized felsic to intermediate volcanic rocks with coarse- (*e.g*, 'Buck-shot type') to fine-grained disseminated pyrite and subordinate base-metal sulphides (Plate 12). Silica–sericite alteration is developed on a local scale.

The Middle Tulks prospect (Figure 2, Plate 12), discovered by Messina Minerals Inc. during 2005, is located between the Tulks East and Tulks Hill deposits. Although predominantly pyritic, selective grab samples have assayed 0.3% Cu, 0.6% Pb, 1.9% Zn, 47 g/t Ag and 0.3 g/t Au (Messina Minerals Inc., Press Release, October 27, 2005). The intense chloritic alteration and disseminated to semi-massive pyrite is identical to that at the Al Keats prospect located to the south. The Al Keats prospect contains abundant interbedded black argillite and greywacke (Plate 1D). Mineralization at this prospect returned grades reaching 4.68% Zn and 1.5% Cu from grab samples, and 0.3% Zn over a 2 m channel (*e.g*., Noranda 1998). The relative location of these prospects along with similarities in alteration and mineralization style suggest that all three may lie on a common horizon; one that may be stratigraphically below that of the Tulks Hill and Tulks East deposits.

Group 2

Prospects within this group include the Tulks West and Mug-up prospects. The Tulks West prospect was discovered by Asarco through follow-up work after the Tulks Hill discovery, whereas the Mug-up prospect was discovered by D. Evans and B. Kean during mapping in 1988. Both prospects

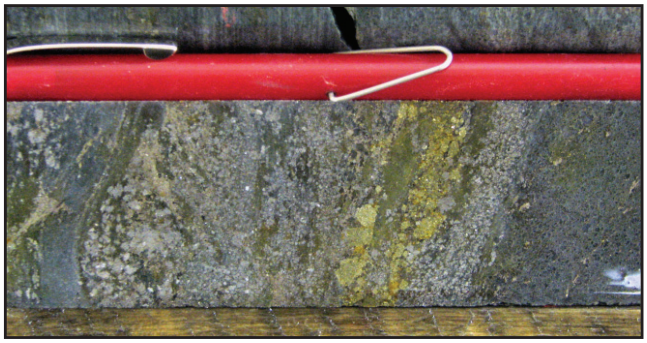

Plate 13. *Stringer of semi-massive arsenopyrite, chalcopyrite, and pyrite cutting felsic-intermediate volcanic rocks of the Tulks West showing (DDH TW-02-01 @ ~91 m). Note that the diamond-drill core is BQ size (~36.5 mm in diameter).*

are predominantly composed of chlorite, sericite, silica, and locally carbonate-altered felsic to intermediate (?) volcanic rocks and associated stringers and disseminations of pyrite, chalcopyrite, arsenopyrite, and local sphalerite and galena (Plate 13). Diamond drilling in the Tulks West area intersected footwall-style stockwork sulphide mineralization and associated minor base metals.

Group 3

Prospects included in this group consist of the 'exhalative-type' Curve Pond and Dragon Pond VMS prospects. Unlike most of the deposits described above, these have ferruginous sedimentary horizons (*i.e.*, iron-formation) associated with massive sulphides (Plate 14). This spatial association likely indicates a genetic link between the two.

The Curve Pond prospect, located southeast of the Boomerang deposit (Figure 2), was discovered in 1990 by BP geologists following detailed mapping and exploration. Iron formation associated with the Curve Pond VMS horizon has been traced, in outcrop and drillcore, for approximately 10 km, and has a minimum recoginizable thickness of a few metres and a maximum thickness of 70 m based on drillcore intersections (Noranda, 1998; Messina Minerals Inc., Press Release, September 18, 2006). At the Curve Pond prospect, iron formation immediately overlies a massive sulphide horizon, which is about 4 m thick (dominated by pyrite with a 10-cm-thick band of zinc-rich sulphides) and 130 m long. Intensely sericite–silica altered quartz-feldspar phyric felsic volcanic rocks comprise the footwall to the massive sulphides. Grab samples by Noranda in 1993 from the main part of the showing returned assays up to 26% Zn and 1.2% Pb (Noranda, 1998). Sulphides vary from massive pyrite ± pyrrhotite to 'layered' pyrite with lesser pyrrhotite, chalcopyrite, sphalerite, and galena (Plate 14).

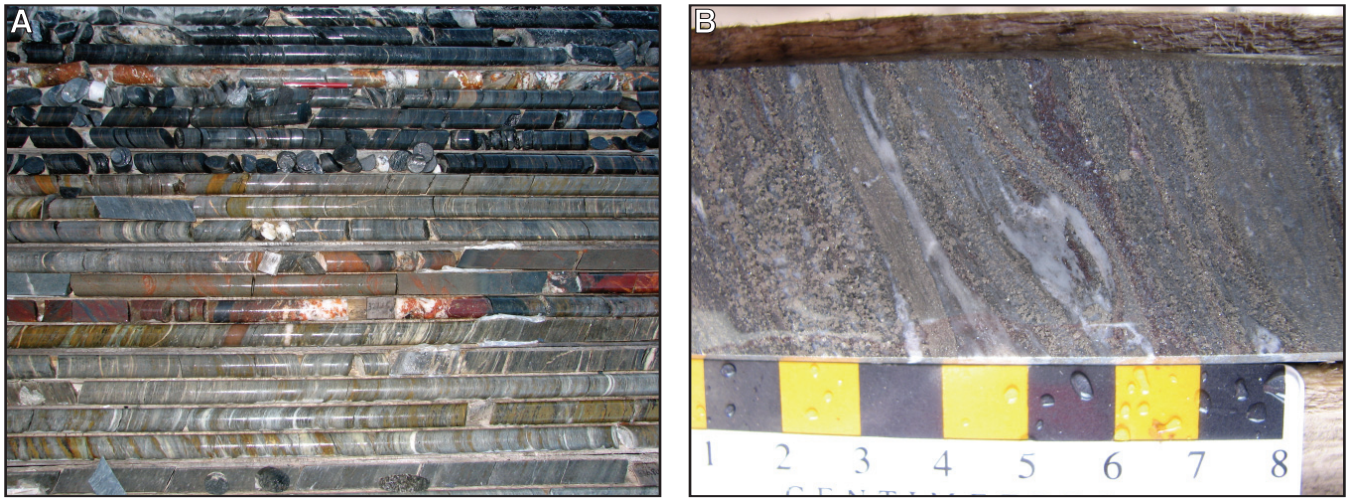

Plate 14. *A. Dragon Pond mineralized horizon; note the change in rock types down-hole from black shales/argillite, into felsic lapilli tuff, into iron-formation, down into sericitized felsic lapilli-tuff (DDH DRP-96-07 @ ~325 m); B. banded massive sulphides (Zn–Pb–Cu) from the Curve Pond showing; note the abundant quartz crystals and fragments in the massive sulphide (DDH CVP-02-02 @ ~38 m); and C. massive pyrite and pyrrhotite at the Curve Pond showing (lower) (DDH CVP-02-01 @ ~32.5 m); note the banded greywacke and chert, which may be a facies of the iron-formation; note that the diamond-drill core is BQ size (~36.5 mm in diameter).*

The Dragon Pond massive sulphide horizon was discovered by diamond drilling by Noranda in 1995. The favourable horizon is sandwiched between sericite–silica–pyrite altered quartz-feldspar felsic volcaniclastic rocks in the footwall and, locally ferruginous, sedimentary rocks (Plate 14). This prospect sits on a horizon that is clearly distinct from that of the Tulks Hill and Tulks East deposits. Although no significant base metals have been recoginized, the large footprint of favourable alteration and the presence of iron formation, suggest exploration potential in this area.

The presence of these mineralized horizons in association with chemical exhalative rocks (iron-formation) at Curve Pond and at Dragon Pond is significant in that the geological environment is analogous to that which hosts massive sulphide deposits of similar age in the Bathurst Mining camp of New Brunswick (Goodfellow and McCutcheon, 2003, and references therein).

GEOLOGY AND VMS MINERALIZATION–NORTHERN TULKS VOLCANIC BELT

LOCAL GEOLOGY

Although all rocks within the northern TVB were initially considered to be part of the TVB by Kean (1977, 1979a, b, 1982, 1983), it was recognized from an early stage that volcanic activity was diachronous, and spanned a time period of at least 498 +6/-4 to 462 +4/-2 Ma (Dunning *et al*., 1987; Evans *et al*., 1990). The relatively young ages from the 'Victoria Bridge Sequence' (Dunning *et al*., 1987), as well as the regional distribution of the graphitic Carodoc shale, provide a clear indication that more than one volcanic group of rocks occurs in the northern TVB, but the lithological similarities make differentiation of these difficult. It was suggested that the variation in ages represents either a major structural or stratigraphic break in the area. Following up on this idea, more recent mapping and geochronological studies by the GSC have revised stratigraphic nomenclature to define a series of generally westward-younging tectonostratigraphic units in the area including the Tulks group (*ca.* 498 Ma), the Sutherlands Pond group (462–457 Ma; Dunning *et al.,* 1987 and Zagorevski *et al.*, 2008), and the Wigwam Brook group (*ca.* 453 Ma; Zagorevski *et al.,* 2003; Rogers *et al.*, 2005; van Staal *et al*., 2005). There may yet be further complications amongst these monotonous rocks. From an exploration perspective, base-metal mineralization can occur within any of these tectonostratigraphic units (*see* http://gis.geosurv.gov.nl.ca/), although it is possible that the styles of mineralization may vary amongst them.

The northern TVB (Figure 3) contains a wide variety of rock types, dominated by felsic, intermediate, and mafic volcanic rocks including ash tuff, lapillistone, agglomerates, massive to flow- banded rhyolite, and rhyolite breccias with local, commonly amygdaloidal, dykes and sills. Sedimentary rocks are also present and include black shale, graphitic argillite, greywacke, and iron formation. The region also contains intrusive bodies, which are generally interpreted to be synvolcanic. The northern TVB has undergone moderate to strong deformation, and sub-greenschist to greenschist-facies metamorphism throughout. Although local-scale structures are commonly observed, the paucity of outcrop impedes identification of regional-scale structures (*see* Discussion below on Daniels Pond). However, geophysical data have aided in the identification of some of the regional structures. Primary textures are usually obliterated by well-developed, bedding-parallel, foliations. Rock units typically strike steeply to the southwest–northeast and dip to the northwest, with a prominent regional foliation defined by the alignment of chlorite and sericite. The belt is transected by late shear zones and faults with variable orientations.

VOLCANOGENIC MASSIVE SULPHIDE DEPOSITS

Volcanogenic massive sulphide mineralization in the northern TVB is characteristically associated with felsic volcanic rocks including ash- and quartz ± feldspar crystal tuff, rhyolite, rhyolitic breccias, volcano-sedimentary debris-flow deposits, with lesser mafic volcanic rocks, hosted within epiclastic sedimentary basin(s). The abundance of locally amygdaloidal bimodal sills, which are broadly synchronous with the volcano-sedimentary sequence, suggests a possible arc-rift or back-arc basin tectonic setting (*see* section on Geochemistry below). Such a setting would likely be highly variable on a local scale, and this is reflected in the varied styles of mineralization (*see* below).

Two important VMS deposits occur within the northern TVB, as well as numerous other prospects and zones of alteration. The most important VMS deposits are the Daniels Pond and Bobbys Pond deposits (Figure 3). Mineralization at these deposits is associated with intense sericite–silica–pyrite alteration and less well-developed chloritic alteration and minor illite and halloysite alteration. The mineralization is thought to have formed in both exhalative as well as subseafloor replacement environments (*see* discussion below).

Daniels Pond Deposit

Location

The Daniels Pond deposit is located on the southeast side of Red Indian Lake in the vicinity of Harbour Round (Figure 3).

Local Geology and Mineralization

The Daniels Pond deposit is hosted by a sequence of intermediate to mafic ash- and crystal- to lapilli tuff affected by sericite–silica–pyrite and minor aluminous (halloysite, illite) alteration, and local chlorite–carbonate alteration (Figures 11, 12 and Plate 15). Intense alteration in the vicinity of the deposit (*see* below) makes identification of the original rock type difficult. Unlike many of the other deposits in the belt, the immediate stratigraphic footwall is dominated by mafic to intermediate volcanic and volcaniclastic rocks, although the surrounding rock types in both the hangingwall and along strike are dominated by felsic volcanic rocks (Figures 11 to 13). The host rocks are steeply dipping, and based on the observed grading in epiclastic

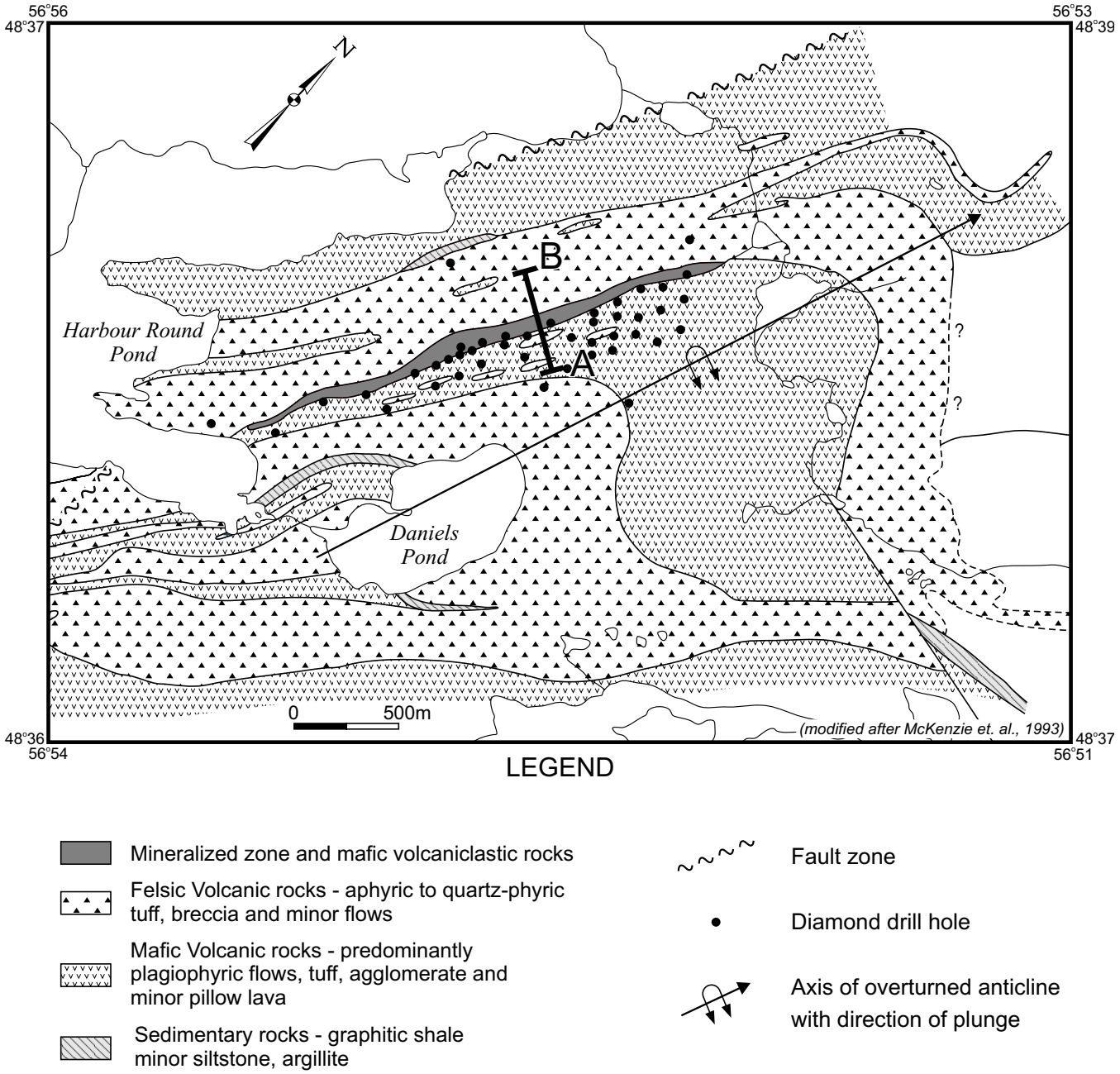

Figure 11. *Geology of the Daniels Pond deposit (from Evans and Kean, 2002; modified after McKenzie* et al.*, 1993).*

rocks, the sequence is interpreted to be overturned to the northwest. The stratigraphic footwall rocks, sitting structurally immediately above the ore horizon, consist of intensely altered intermediate to mafic ash- to lapilli tuff, and intermediate to mafic amygdaloidal sills. The stratigraphic hangingwall (structural footwall) consists of debris flows containing quartz-phyric felsic volcanic, fine-grained argillite, and massive sulphide clasts (Plate 15B). The presence of sulphide clasts within the debris flow may suggest an exhalative origin for much of the mineralization. The remainder of the stratigraphic hangingwall sequence consists of variably altered intermediate to felsic ash, lapilli tuff, and associated epiclastic sedimentary rocks. The proportion of sedimentary rocks (dominantly graphitic argillite and greywacke), as observed in drillcore, increases substantially toward the northeastern portion of the deposit, in the vicinity of a pyrite-rich lens of the deposit.

The mafic to intermediate volcanic and epiclastic host rocks are intensely altered to sericite–silica–carbonate–chlorite–pyrite, and little, if any, of the original minerals are preserved. Locally, relict plagioclase crystals (~0.5 mm) are

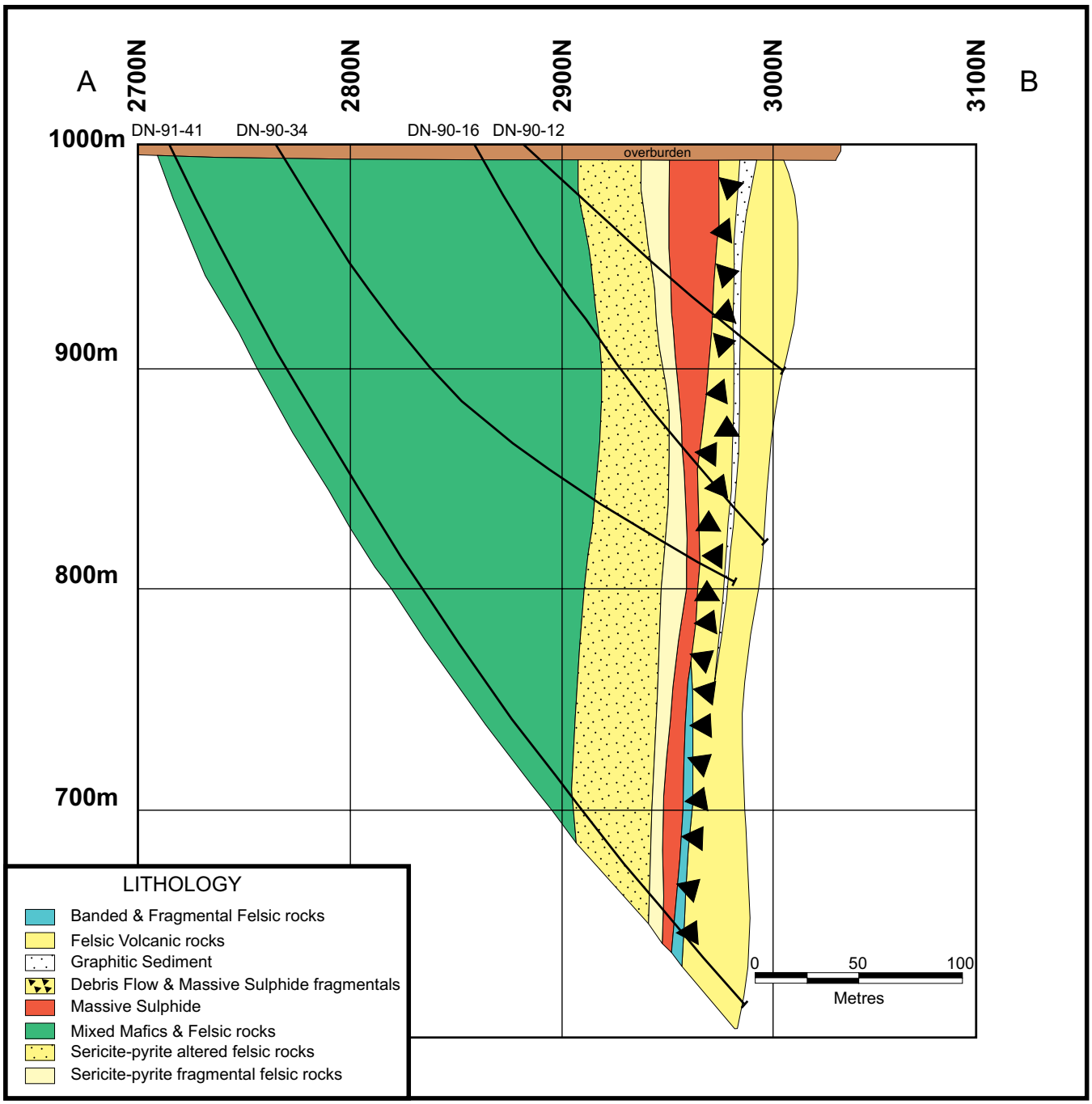

Figure 12. *Cross-section through the Daniels Pond deposit (from Noranda, 1998). Section A–B is located on Figure 11.*

partially preserved, as well as occasional quartz crystals (0.1–0.5 mm; Plate 16), all sitting in a groundmass of fine-grained sericite and microcrystalline quartz. The presence of quartz phenocrysts (0.1–0.3 mm) in some samples (Plate 16D) suggest that the original rock type could have been more felsic or intermediate than mafic; however, geochemical analysis indicates that the bulk of the samples are actually intermediate to mafic in composition (*see* section on Geochemistry below). In some instances, quartz phenocrysts display resorption textures, suggesting that they were unstable in the melt prior to its crystallization. The latter may indicate an andesitic flow mechanism of emplacement rather than a pyroclastic or water-lain emplacement process.

Massive sulphide mineralization at Daniels Pond is contained within two lenses, *i.e.*, a pyrite-dominant, (weakly base-metal-rich) lens to the northeast and a base-metal-

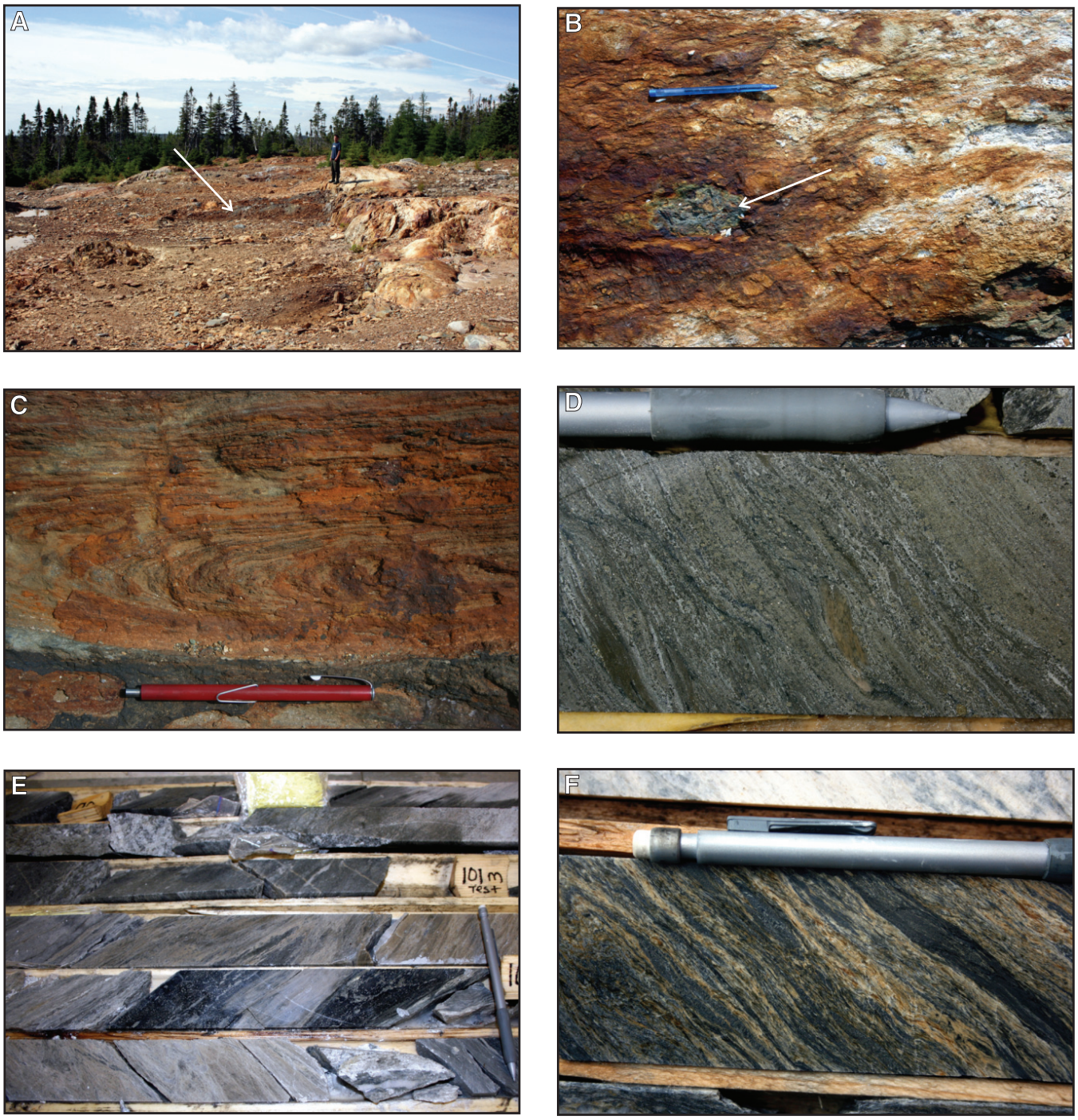

Plate 15. *Photographs of Daniels Pond deposit stratigraphy, alteration, and mineralization, A. Daniels Pond massive sulphide deposit exposed in surface trench; note massive sulphide at the arrow; B. massive sulphide clast (at arrow); C. folded massive sulphides exposed by trenching; D. base-metal-rich massive sulphide; note the altered felsic clasts (DDH DN-02-02 @ ~193 m); E. intense chlorite–clay–aluminous alteration in the immediate FW to the deposit (DDH DN-07-053 @ ~104 m); intense chlorite suggests that the mineralization was vent proximal; and F. intense sericite–clay–aluminous alteration in a stringer zone to the deposit (DDH DN-02-10 @ ~132 m); note that the diamond-drill core is NQ size (~47 mm in diameter).*

Figure 13. *A. Graphic drill log for DDH DN-02-02 from the Daniels Pond deposit illustrating rock types and relations and alteration patterns. Note that stratigraphy is interpreted to be overturned.*

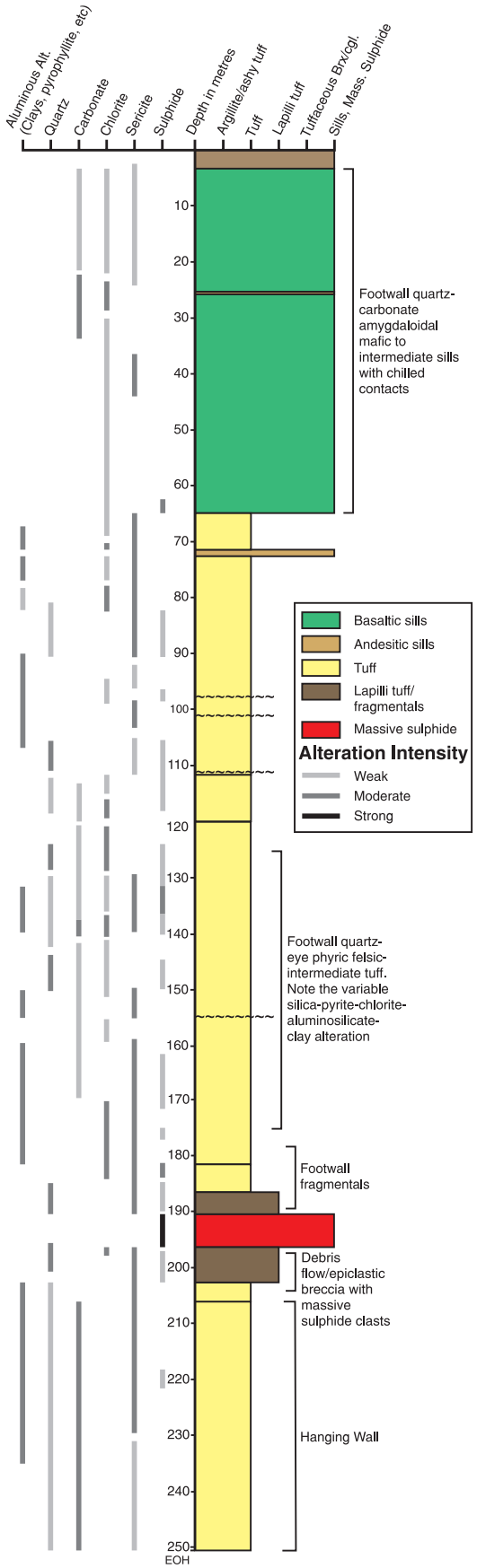

rich lens to the southwest (Royal Roads Corp. website). The massive sulphide lenses are confined to a narrow belt of highly strained rocks trending north-south. The sulphides have been structurally modified (Plate 15C) and show tectonic banding and recrystallized sphalerite, chalcopyrite, galena and pyrite. The base-metal-rich sulphides consist of sphalerite–galena–pyrite±chalcopyrite, in which steeply plunging isoclinal folds are observed (Plate 15C). The presence of coarse-grained pyrite, which overprints banded sulphides, indicates extensive recrystallization. Gangue mineralogy is variable with a mixture of quartz–carbonate±barite distributed throughout the lenses (*see* also McKenzie *et al.*, 1993; Noranda, 1998). The ore in the northern lens is dominated by fine-grained pyrite with fine-scale tectonic (?) banding. Quartz-carbonate veinlets commonly infill cross-cutting fractures and locally contain minor remobilized copper mineralization in the form of chalcopyrite.

The exposures at Daniels Pond provide an illustration of how less compentent material, such as sulphide zones and associated altered rocks, can experience and clearly display intense deformation whereas surrounding, more competent units for the most part hide evidence of such effects. It is also illustrative in that the compositional banding in the Daniels Pond massive sulphides is clearly tectonic, although it would likely be interpreted as primary and perhaps exhalative if seen only in drillcore, where the folding and cross-cutting relationships would be difficult to see.

To date, the deposit contains a NI 43-101 compliant inferred resource of 1.69 million tonnes grading 8.37% Zn, 4.4% Pb, 0.57% Cu, 196.9 g/t Ag, and 0.68 g/t Au (Royal Roads Corp., Press Release, November 7, 2006). More detailed tonnages at various Zn cut-off percentages are given in the report by Webster *et al.* (2008). Additionally, recent deep exploration drilling by Royal Roads Corp. has extended the mineralization (*e.g.*, Royal Roads Corp., Press Release, October 7, 2007). This is supported by DDH DN-07-92A, which intersected 7.9% combined base metals over 2.47 m at 75 m below the currently defined deposit. There is thus potential for expansion of the mineral resource at deeper levels.

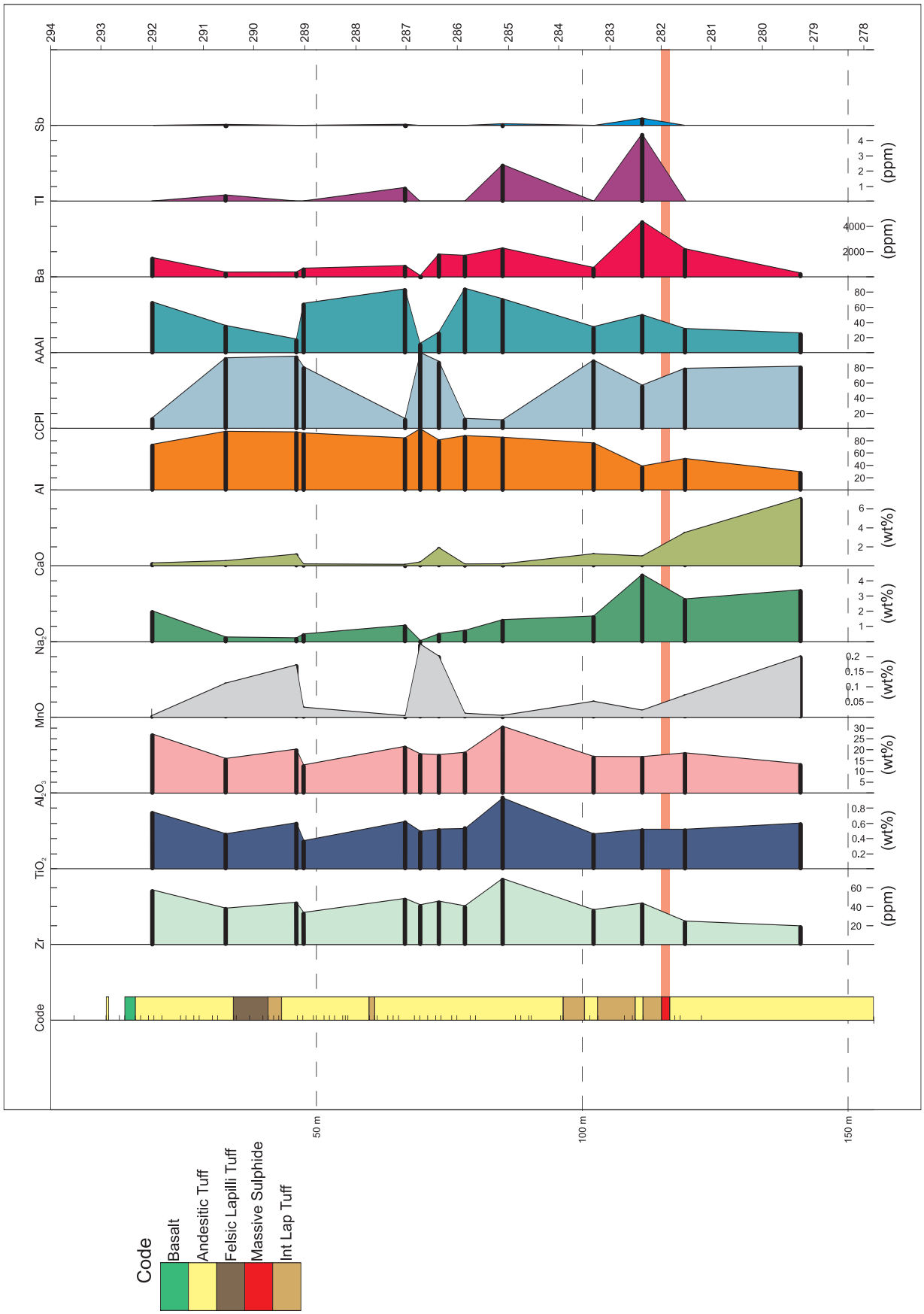

Figure 13. *B. Geochemical strip log for DN-06 illustrating elemental changes in relation to the ore horizons.*

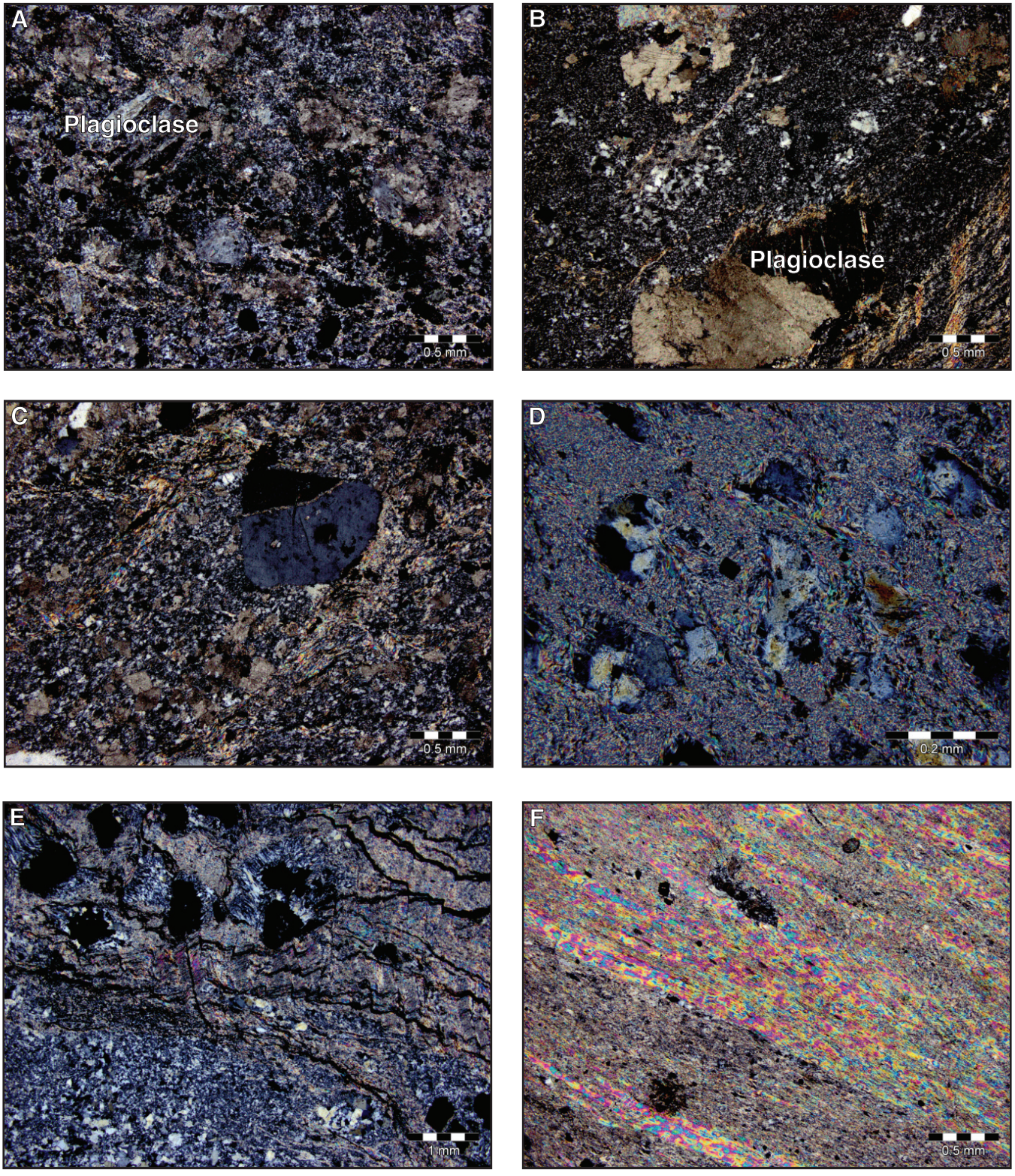

Plate 16. *Photomicrographs of mafic-intermediate host rocks to the Daniels Pond deposit. A–D illustrate relict plagioclase and quartz crystals; and E and F. illustrate very intense sericite–silica ± aluminosilicate alteration. Samples (A) JHC-07-119, B. JHC-07-123, C. JHC-07-142, D. JHC-07-084, and (E and F) JHC-07-096.* See *Appendix 1A for sample location.*

Alteration

In contrast to many of the deposits in the TVB that are associated with large, kilometre-scale, VMS-style alteration systems (*e.g.*, Tulks Hill, Jacks Pond), the Daniels Pond deposit has a relatively small alteration footprint (Figure 3). Alteration is predominantly confined to an area of intensely sheared volcanic rocks in the immediate footwall to the deposit, with minor sericite-carbonate alteration locally present in the hangingwall rocks. Locally, the alteration at the Daniels Pond deposit appears different than that observed at other deposits in the TVB; herein attributed to the local presence of aluminous alteration (*e.g.*, kaolinite group minerals) (*see* below).

Footwall alteration is best developed in intensely sheared intermediate to mafic volcanic tuffs, and consists of variable amounts of sericite, silica, chlorite, carbonate and aluminous alteration, and is associated with pyrite and base-metal stringer sulphide (Plate 16E and F). The preponderance of fine-grained (µm-scale) microcrystalline quartz forming groundmass material with variable amounts of pyrite, and sericite and carbonate alteration replacing plagioclase feldspars impart a dull grey to the intermediate to mafic volcanic rocks. This led to the introduction of the informal term 'grey-pyritic-volcanic' for the altered footwall rocks of the deposit. The use of this term is indicative of the difficulty experienced by numerous geologists in identifying the protolith. Locally, black chlorite, aluminous alteration, ± sericite occurs in the immediate footwall of the deposit, implying a vent proximal acidic mineralizing environment (Plate 15E; *see* discussion below). Local halloysite alteration has been independently identified through the use of visible/infrared spectrometry (J. Hinchey, unpublished data). The proportion and intensity of the aluminous alteration is greater in the area of the base-metal lens then in the area of the pyrite lens.

More regional-scale, less-intense alteration, is recoginized in both the hangingwall and footwall stratigraphy distal to the main mineralized horizon. This alteration is considered to be of regional hydrothermal origin and consists of fine-grained sericite and carbonate.

Bobbys Pond Deposit

Location

The Bobbys Pond deposit (Figure 3) is located on the southeast side of Red Indian Lake, approximately 1 km northeast of Bobbys Pond and approximately 20 km southwest of Millertown.

Local Geology and Mineralization

The Bobbys Pond deposit occurs in a stratigraphic sequence similar to that at the Daniels Pond deposit, but the two cannot be unequivocally correlated. This deposit is hosted by variably altered, bimodal, felsic volcanic sequences, dominated by aphyric to quartz porphyritic rhyolite, rhyolite breccia, felsic ash-, crystal- and lapilli tuff, and intercalated epiclastic sediments (graphitic argillite and greywacke) and minimal mafic volcanic rocks (Figure 14, Plate 17). The preponderance of rhyolite in the sequence distinguishes it from the volcaniclastic-dominated deposits farther south (*e.g.*, Daniels Pond, Tulks East, *etc.*), and may suggest a more vent-proximal environment of formation. Additionally, mafic volcanic rocks are not present in the immediate stratigraphic succession hosting the Bobbys Pond deposit, differentiating it from other deposits in the belt. Strong sericite–carbonate–pyrite–silica alteration and local aluminous alteration are observed in proximity to the sulphide lenses (Figure 14, Plate 17). As with the Daniels Pond stratigraphy, the sequence appears to be overturned. However, locally interpreted fining-upward sequences in drillcore, as well as the presence of alteration both above and below the ore horizon, leave some ambiguity to the direction of stratigraphic tops.

The stratigraphic footwall sequence is interpreted to sit structurally above the ore horizon and is dominated by aphyric to quartz-phyric rhyolite and associated felsic ash- to crystal tuff, lapilli tuff, and related epiclastic sediments. 'Jig-saw-fit' rhyolitic breccias are common in the footwall sequence and result from natural inflation processes associated with emplacement of felsic flows or domes. Similar textures are associated with felsic domes at the Duck Pond deposit (*e.g.*, Squires *et al.*, 2001). It was suggested by Stewart and Beischer (1993) that some of the porphyritic rhyolites may actually be intrusions.

The hangingwall sequence, now structurally below the ore horizon, is dominated by variably altered rhyolite breccias with intercalated felsic ash- and crystal tuff to lapilli tuff, and lesser amounts of siliceous sedimentary rocks. The rocks in both the stratigraphic hangingwall and footwall of the deposit are strongly deformed, and are locally altered to sericite schists.

Petrographically, the felsic volcanic and volcaniclastic host rocks vary from being relatively fresh and unaltered in the hangingwall, where they contain quartz and local feldspar phenocrysts (Plate 18A–C), to intensely sericite–silica–carbonate–pyrite altered rocks in the footwall and in the mineralized horizon. These parts of the sequence

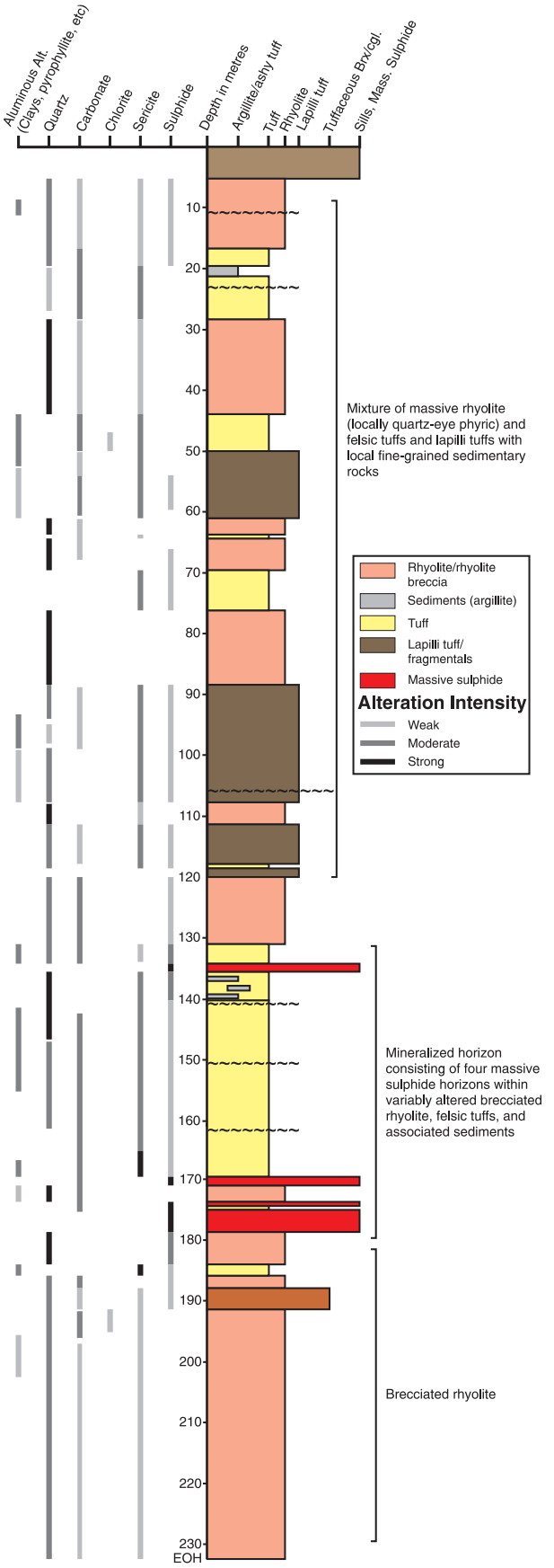

Figure 14. *A. Schematic drillhole stratigraphic column for DDH 77537 from the Bobbys Pond deposit illustrating rock types and relations and alteration patterns. Note that stratigraphy is interpreted to be overturned. Note that the column is not intended to illustrate original stratigraphic order.*

preserve very little of the original minerals (Plate 18D–F). The groundmass or matrix to the phenocrysts is dominated by mixtures of fine-grained (µm scale) sericite and microcrystalline mosaics of quartz. In rare cases, quartz phenocrysts in samples display resorption textures (Plate 18A), suggesting that the quartz phenocrysts were unstable in the the melt prior to its crystallization.

Massive sulphide mineralization occurs in at least four sulphide lenses, within an approximately 100-m-wide zone of moderate to intense alteration. Intense shearing, coupled with the local presence of fault gouge in the immediate vicinity of the mineralization (Plate 17C), imply that the ore horizon 'stratigraphy' may actually represent a series of transposed slices, resulting in repetition of massive sulphide layers and associated alteration. However, some variations in sulphide compositions were observed between the lenses, and there are also subtle contrasts in their host rock types. Such variations could be explained by lateral variations in sulphide lenses, such as demonstrated at Daniels Pond. The suphide lenses vary in thickness from less than 1 m to approximately 10 m, and generally display chemical zoning with a zinc-rich upper portion and a copper-rich lower portion that could be used to informally suggest that stratigraphic tops are up and that the volcanic succession is not overturned. Sulphides are dominated by pyrite with lesser honey-coloured sphalerite, chalcopyrite and galena. Locally, the rhyolite is pervasively replaced by sulphides, suggesting a replacement style of mineralization. Elsewhere, the presence of fine-grained, mineralized siliceous sedimentary rocks in the immediate stratigraphic hangingwall (sitting structurally below the ore horizon) suggests an exhalative style of mineralization.

As currently defined, the Bobbys Pond deposit contains a NI 43-101 compliant indicated resource of 1.1 MT grading 4.61% Zn, 0.86% Cu, 0.44% Pb, 16.56 g/t Ag, and 0.20g/t Au, with an additional inferred resource of 1.2 MT of similar grade (Agnerian, 2008). Mountain Lake Resources Inc. continues to define the resource and to explore for additional mineralization in the area.

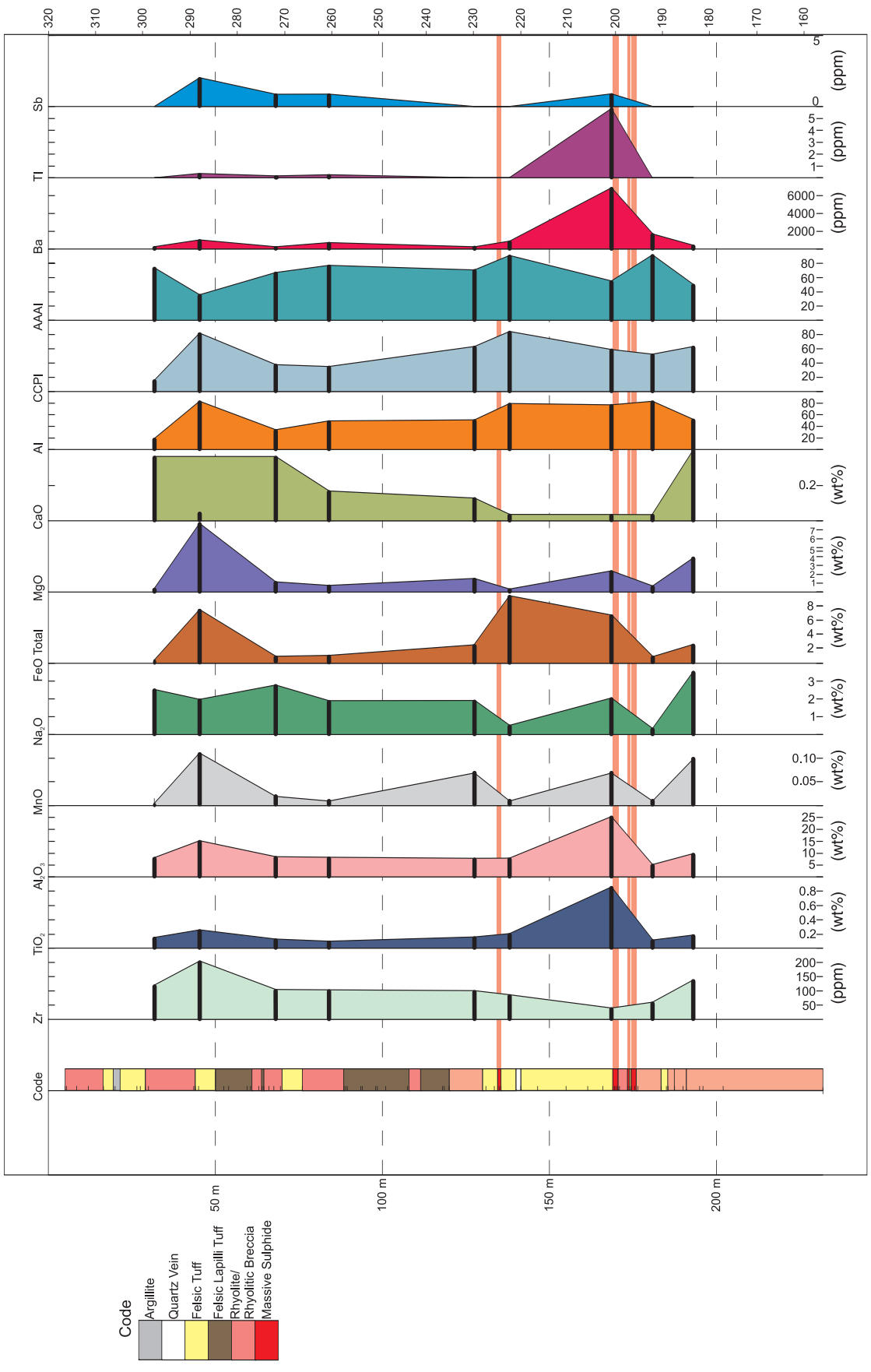

Figure 14. *B. Geochemical strip log for DDH 77537 illustrating elemental changes in relation to the ore horizons.*

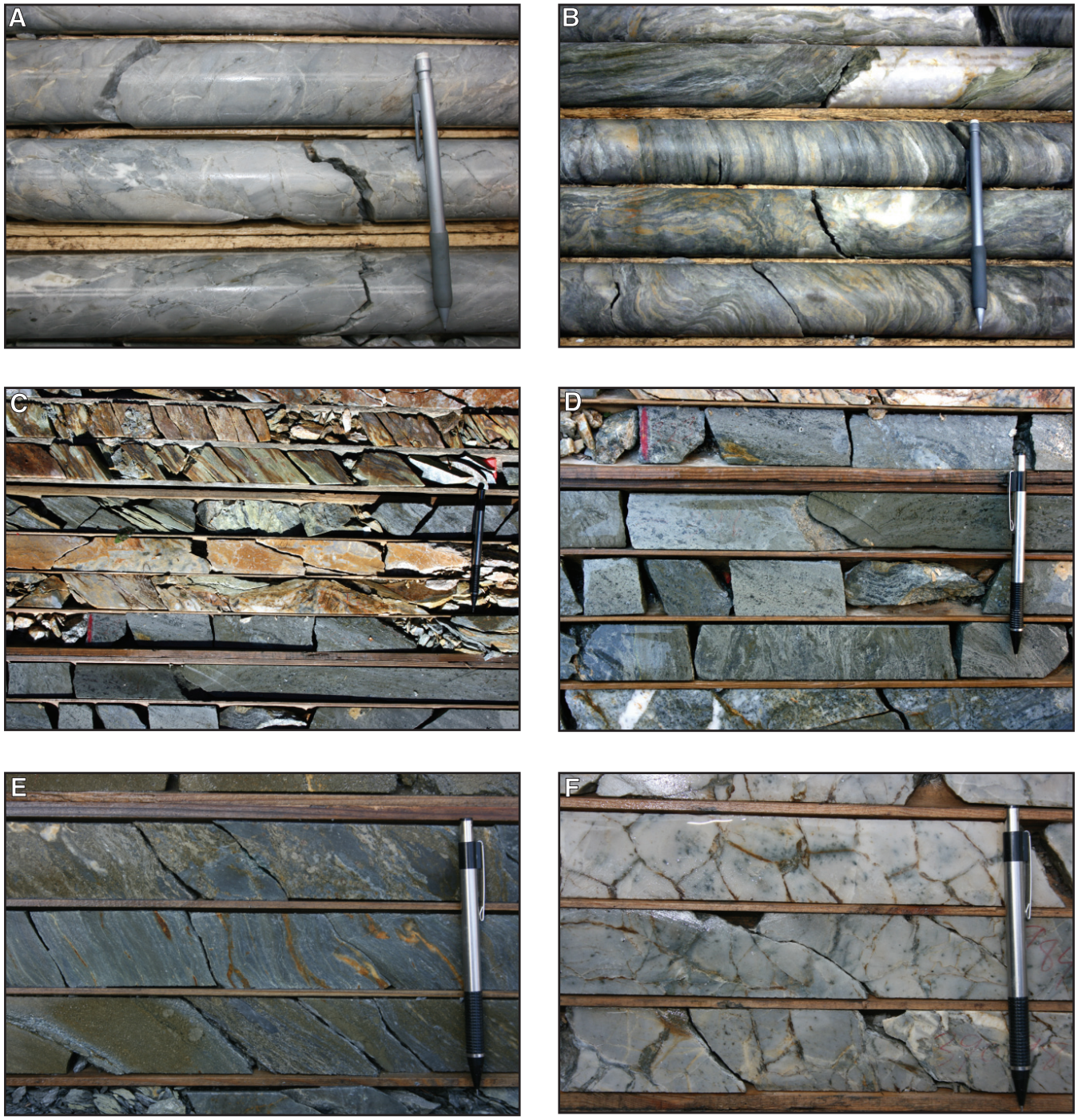

Plate 17. *Photographs of Bobbys Pond deposit stratigraphy, alteration, and mineralization: A. aphyric rhyolite; note the local flow-banding textures (DDH MOA-05-02 @ ~38 m); B. intense sericite–carbonate–aluminous alteration in the FW to the deposit (DDH MOA-05-02 @ ~100 m); C. massive sulphide lenses from the deposit; note the intense carbonate alteration associated with the rhyolitic host in the middle of the photograph (DDH 77537 @ ~175 m); D. base-metal-rich massive sulphide (DDH 77537 @ ~175 m); E. mineralized very fine-grained ashy-tuff to siliceous sediments from the mineralized horizon (DDH 77546 @ ~158 m); and F. jigsaw fit rhyolitic breccia with polygonal clasts indicative of a vent-proximal environment; texture is interpreted to represent the rim of a blocky flow (DDH 77546 @ ~175 m); note that plate A and B are NQ core (~47 mm in diameter) whereas C-F are BQ size (~36.5 mm in diameter).*

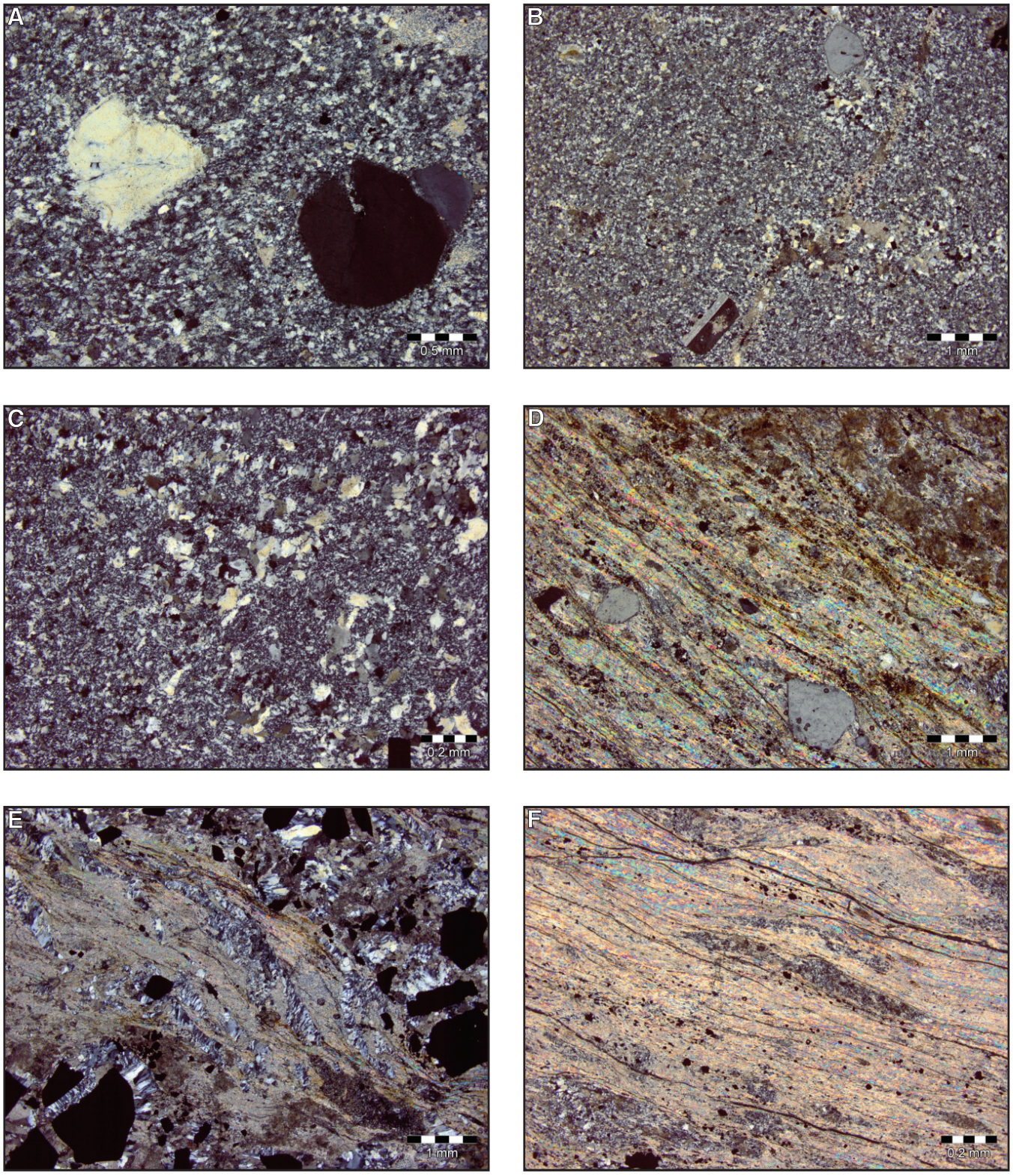

Plate 18. *Photomicrographs of host rocks and alteration, and mineralization at the Bobbys Pond deposit. A, B and C. Quartz and feldspar phyric rhyolite from the hangingwall whereas D, E and F are sericite–silica–carbonate-altered, sheared rhyolite from the footwall. A. JHC-07-255; B. JHC-07-273; C. JHC-07-252; D. JHC-07-268; E. JHC-07-274; F. JHC-07-253.* See *Appendix 1A for sample location.*

Alteration

The alteration observed at the Bobbys Pond deposit, as with the Daniels Pond deposit, represents mostly local hydrothermal alteration associated with the VMS formation. Most of the alteration, and associated sulphide mineralization, occurs within a zone of strong deformation in a zone of strongly altered sericitic schists. As with the Daniels Pond deposit, hydrothermal alteration is localized and there is no well-defined footwall alteration system associated with a typical feeder zone. It appears that the alteration is restricted to the highly deformed zone. The intensity of alteration and its affect on the competency of the footwall rocks likely acted to focus deformation in this region.

Footwall alteration, proximal to massive sulphides, is dominated by silica–sericite–carbonate–pyrite alteration and local chlorite alteration. Carbonate alteration increases significantly in proximity to the massive sulphides as replacement of primary feldspar, and is more intense than that at other deposits elsewhere in the TVB. Hangingwall alteration at Bobbys Pond is weakly defined by variable amounts of albite, chlorite, and carbonate alteration along with ubiquitous silicification.

Other VMS Deposits/Prospects

There are several other VMS prospects, and areas of favourable VMS-style alteration in the northern Tulks Volcanic Belt (Figure 3). These fall into 5 broad groups, *i.e.*,

1) Coarse-grained, disseminated to semi-massive pyrite and lesser base metals associated with felsic to intermediate volcanic rocks with zoned sericite–silica–chlorite alteration (*e.g.,* Jacks Pond deposit, Roebucks Brook prospect).
2) Locally base-metal enriched sulphides associated with ferruginous, siliceous sedimentary rocks interpreted to be of exhalative origin (*e.g.*, Cathys Pond prospect).
3) Felsic volcanic rocks with acidic, aluminous alteration (*e.g.*, pyrophyllite, clays, alunite), native sulphur, topaz, and textures suggestive of a hybrid VMS-epithermal environment. (*e.g.,* Bobbys Pond native sulphur showing and the North Pond prospect).
4) Massive, high-grade sulphide clasts within debris-flow deposits in resedimented volcaniclastic packages of uncertain stratigraphic affinity (*e.g.*, Hungry Hill prospect), and
5) Copper-rich, stringer-style VMS-type mineralization associated with intense black chlorite, carbonate, and quartz alteration (*e.g.*, Victoria Mine).

Group 1

This group is exemplified by the Jacks Pond deposit and the Roebucks Brook prospect (Figure 3). The zones of mineralization and alteration at both are developed in felsic to intermediate volcanic rocks and are manifest by intense sericite–silica–chlorite alteration. Semi-massive to massive, coarse- to fine-grained disseminated pyrite and subordinate base-metal sulphides are associated with this alteration (Plate 19). The local stratigraphy is dominated by quartz-phyric felsic ash- to crystal tuffs, coarse-grained felsic fragmental rocks (*i.e.*, volcaniclastic breccia), abundant graphitic argillite containing fragments of altered volcanic rocks, and minor mafic sills. Based upon the presence of exotic granitic clasts (Plate 20), the coarse-grained volcaniclastic breccias may have developed in association with syn-volcanic faults that exhumed basement (?) or subvolcanic intrusions related to the volcanic pile.

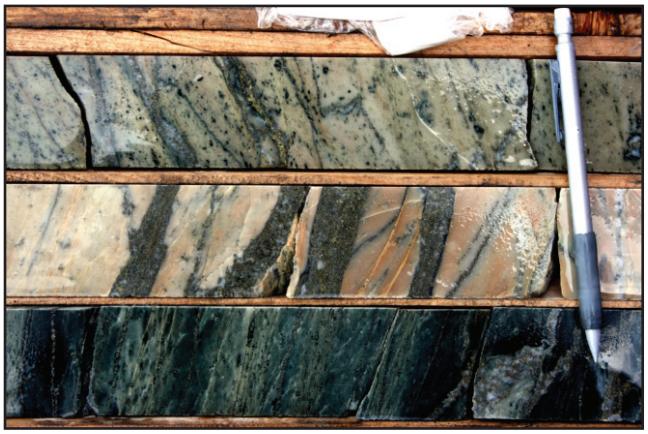

Plate 19. *Variably altered and mineralized felsic tuff from the Jack's Pond deposit (DDH JP-29 @ ~290 m). Note the sericite–carbonate alteration (top) grading to chlorite alteration (bottom). Note that the diamond-drill core is NQ size (~47 mm in diameter).*

The Roebucks Brook prospect (Figure 3) is located between the Tulks East deposit and the Jacks Pond prospect that collectively account for the largest sulphide accumulation and the largest alteration system in the TVB, respectively. Mineralization discovered to date is confined to stringer zones within sericite–silica altered felsic ash- and crystal tuff, but the base-metal-rich nature of the mineralization (*e.g.*, 2.29% Zn over 1.44 m in RB-01-02, Dadson, 2002), along with the general lack of diamond drilling in the vicinity, suggests that the area holds potential for future discoveries.

The Jacks Pond prospect has been interpreted to occur on the same stratigraphic horizon as the Tulks East and Tulks Hill deposits to the south (*e.g.*, Evans and Kean, 1986; McKenzie *et al.*, 1993). The prospect is associated with a very large (2.0 by 0.5 km), alteration envelope at the transition from felsic-dominated volcaniclastic rocks to clastic

Plate 20. *Coarse-grained exotic granitic clasts in volcaniclastic breccia at the Jacks Pond deposit (DDH JP-94-01 @ ~171.5 m). The presence of exotic clasts implies that the breccias were likely derived as fault breccias rather than true volcaniclastic debris-flow breccias. Note that the diamond-drill core is BQ size (~36.5 mm in diameter).*

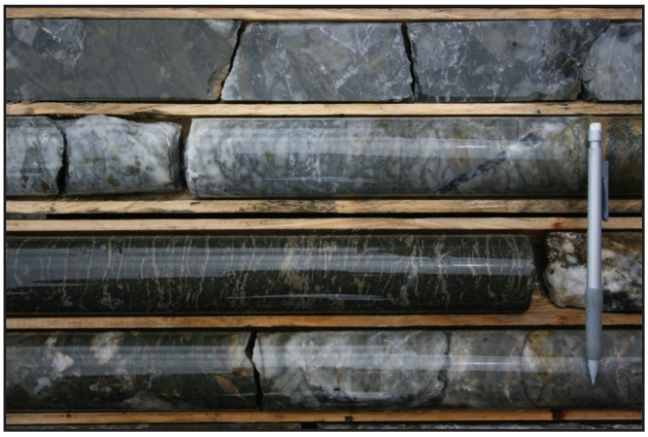

Plate 21. *Exhalative-type mineralization from the Cathys Pond prospect consisting of a silica- and pyrite-rich argillite associated with semi-massive to massive sulphides (DDH JP-30 @ ~65 m). Note the footwall stringer alteration in the top row. Note that the diamond-drill core is NQ size (~47 mm in diameter).*

sedimentary rocks with minor mafic volcanic rocks. The alteration is linked to at least four pyrite-dominant semi-massive to massive sulphide lenses (McKenzie *et al.*, 1993; Noranda, 1998). As elsewhere in the TVB, the Jacks Pond mineralization and alteration is hosted within dominantly felsic volcanic ash and crystal tuff, lapilli tuff, felsic breccia, and local quartz-phyric rhyolite and minor mafic sills. The distribution of sulphides appears to be stratigraphically controlled and, based upon the observed zonation in alteration mineralogy, probably represent an alteration stockwork (*see* discussion in Evans and Kean, 1986, 2002). Alteration is broadly zoned, with an inner discordant core of Mg-rich chlorite–carbonate–sericite–silica alteration enveloped by a more silica–sericite-rich shell (Plate 19). Based on field relationships, and the classic zonation of the alteration package, it is postulated that the Jacks Pond prospect may represent a deep remnant of the hydrothermal conduit system that fed the nearby Cathys Pond exhalative horizon (*e.g.*, *see* Noranda, 1998). Exposure of the Jacks Pond footwall alteration is attributed to contrasts in erosion levels due to faulting and folding during post-VMS deformation.

Group 2

This 'exhalative-type' mineralization is best exemplified by the Cathys Pond prospect (Figure 3). This prospect contrasts with most other deposits and prospects in the TVB in that it is dominated by silica and pyrite-rich argillite horizons containing semi-massive to massive sulphides (Plate 21). The local stratigraphy consists of several conformable to intercalated bodies of sericite-silica altered felsic tuffaceous rocks, massive grey siliceous rocks, and siliceous pyrite-rich argillite. The overall sequence is indicative of a quiescent to low-energy environment typically associated with waning stages of volcanic activity. Based on the relatively weak alteration, and an increase in the proportion of clastic sedimentary rocks, it appears that the area in the northwest portion of the prospect represents a more vent-distal facies compared to that observed on the southern shore of Cathys Pond. Based on the close proximity of the Jacks Pond alteration system to the southern shore of Cathys Pond, this observation provides indirect support for the notion introduced above that the Jacks Pond prospect may represent a deep feeder alteration zone to the exhalative mineralization observed at Cathys Pond.

Group 3

This group includes the Bobbys Pond native sulphur prospect and the North Pond prospect (Plate 22). They consist of felsic volcanic rocks with local acidic and aluminous alteration (*e.g.*, pyrophyllite, clays, and alunite group minerals), native sulphur, topaz, orpiment and possible stibnite. These occurences also exhibit textures suggestive of an epithermal environment, in addition to typical VMS-style mineralization. When viewed in conjunction with the Daniels Pond and Bobbys Pond deposits, which also contain locally acidic, aluminous alteration (*see* above), this hybrid epithermal-VMS style of alteration and mineralization extends over a strike of 4 to 5 km.

The Bobbys Pond native sulphur showing contains abundant argillic to advanced argillic alteration with intense silicification, natroalunite, native sulphur, and topaz on surface, with orpiment and possible stibnite at depth. Topaz was recognized by visible/infrared reflectance spectrometry

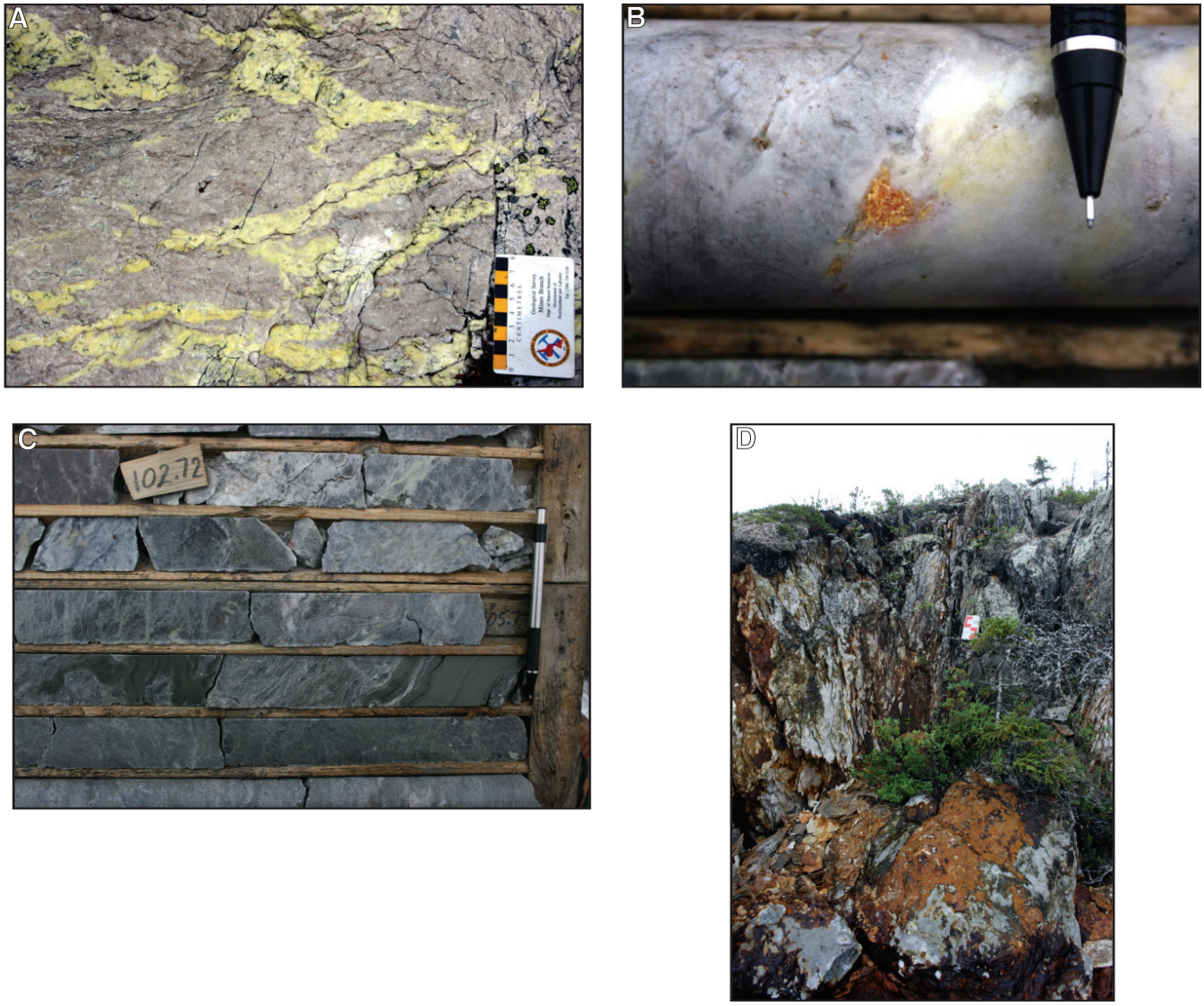

Plate 22. *A. Native sulphur with silica–alunite alteration at the Bobbys Pond native sulphur showing; B. Orpiment crystals associated with the Bobbys Pond native sulphur showing (DDH BP-4 @ ~65 m); C. Native sulphur in association with massive laminated sulphide at Bobbys Pond native sulphur showing (DDH BP-5 @ ~107 m); and D. Massive pyrite mineralization associated with intense silicification and sericite ± alunite alteration at the North Pond prospect.*

methods. The showing typically lacks VMS-style alteration or mineralization, although massive pyrite mineralization is locally developed in drillcore (Plate 22C). As such, the sulphur prospect has historically been viewed as a unique epithermal-style mineralizing event in the TVB, and interpreted to be superimposed on the older VMS mineralization. However, at the nearby North Pond prospect (Plate 22D), intense silicification, alunite, and minor native sulphur occur with VMS-like massive pyrite in silica–sericite-altered felsic ash to crystal tuff. As alunite is not uncommon within weakly metamorphosed VMS-mineralized terrains (*e.g.*, Morne Bossa deposit; stockwork deposits of the green tuff belt in Japan; *see* Hannington *et al.*, 1999 and references therein), the observed field relationships suggest that alunite may have been (meta?) stable within some of the northern TVB prospects, perhaps preserved due to the associated intense silicification. Vuggy quartz textures also point to an 'epithermal-style' of mineralization, as they potentially represent leaching textures derived through the interaction of a highly acidic and oxidized fluid with the host rock at shallow depths. As such, the North Pond prospect may serve as the 'missing-link' connecting the acidic and aluminous alteration observed at the Daniels Pond and Bobbys Pond deposits to the characteristic epithermal-style alteration at the Bobbys Pond sulphur showing. As discussed below, this connection has implications for deposit classification schemes and exploration strategies.

Plate 23. *A. Base-metal-rich sulphide clasts in a heterolithic debris-flow deposit at the Hungry Hill prospect (DDH HH-98-22 @ ~220 m); note that sulphide locally forms stringers and breccia matrix; B. (DDH HH-97-15 @ ~180 m) and C. (DDH HH-97-16 @ ~150 m) sulphides forming the matrix to rhyolitic breccias; and D. semi-massive sulphide (DDH HH-97-16 @ ~150 m); note that the diamond-drill core is NQ size (~47 mm in diameter).*

Group 4

This group includes prospects where high-grade massive sulphide clasts occur in debris-flow deposits, and is exemplified by the Hungry Hill prospect discovered by Celtic Minerals Ltd. in 1996. The assignment of these host rocks in stratigraphic terms is problematic as there are presently two different interpretations. According to the recent mapping conducted by the GSC, the prospect is within the Arenig-Cardoc Wigwam Brook group (Rogers *et al.*, 2005), whereas earlier work placed this area within the northern extremity of the TVB (*e.g.*, Evans and Kean, 2002). The Hungry Hill prospect is located approximately 10 km northeast of the Bobbys Pond deposit, and as with the Bobbys Pond deposit, is hosted by a sequence dominated by massive rhyolite flows, rhyolite breccias, and heterolithic debris-flow volcanic breccias. The latter locally contain massive sulphide clasts (Plate 23A). In addition to this 'transported' style of mineralization, the prospect also contains examples of stringer-type mineralization within massive rhyolite as well as sulphides forming the matrix to rhyolite breccias (Delaney *et al.*, 2001; Plate 23B, C). Such features are reminiscent of textures described from Bobbys Pond. The felsic pyroclastic and volcaniclastic rocks are atypical of the Wigwam Brook group as defined by Rogers *et al.* (2005) suggesting that some re-examination of contacts and stratigraphic assignment in this region is warranted.

Group 5

This group consists of copper-rich VMS-style mineralization associated with intense black chlorite, carbonate, and quartz alteration, and is exemplified by the Victoria Mine and Jig Zone prospects (Figure 3). The stratigraphy in the Victoria Mine area consists of an east–west-striking, north-dipping sequence of volcanic and sedimentary rocks. In general, the stratigraphy can be divided into hangingwall aphyric felsic to intermediate lapilli tuff, intensely altered and mineralized felsic tuffaceous rocks comprising the ore

horizon, and footwall mafic volcanic rocks with associated volcaniclastic sedimentary rocks. The mineralization occurs within altered felsic volcanic rocks or breccias, which are currently included in the Tulks Hill volcanic sequence. The assignment of the host rocks is problematic, because the site lies very close to the proposed stratigraphic boundary between the Tulks and the Sutherlands Pond groups (Rogers *et al.*, 2005). The U–Pb zircon dates from rhyolites in the hangingwall rocks give ages ranging from *ca.* 462 Ma to 457 Ma (Evans *et al.*, 1990; Rogers *et al.*, 2005), which are much younger than the *ca.* 498 Ma inferred age for the TVB (Evans *et al.*, 1990). However, a lithogeochemical survey completed by Celtic Minerals (Greene *et al.*, 2001) suggests that the felsic volcanic rocks that host the mineralization are similar to felsic volcanic rocks elsewhere in the TVB, an interpretation supported by Evans and Kean (2002). Therefore, the mineralization appears to be associated with a north-dipping structure that separates the TVB from younger rocks of the Sutherlands Pond group. One possible explanation for the stratigraphic uncertainty in the area is that the mineralization represents remobilized VMS sulphides (*e.g.*, Desnoyers, 1991) that transcend both groups of rocks. Rocks along the ore horizon consist of strongly schistose, altered dacitic to rhyolitic ash, tuff and tuff breccias. The above-mentioned structure appears to be the locus of intense black chlorite, sericite, carbonate and quartz alteration, with associated disseminated and stringer pyrite–chalcopyrite (Plate 24). Local examples of chaotic quartz–carbonate alteration closely resemble similar alteration at the Duck Pond deposit (Greene *et al.*, 2001). The intense chlorite and carbonate alteration differ from the typical sericite–silica-rich alteration associated with most of the VMS occurrences in the TVB.

The Jig Zone prospect is located approximately 250 m east of the Victoria Mine prospect. Mapping suggests that the massive sulphide is associated with an asymmetrically

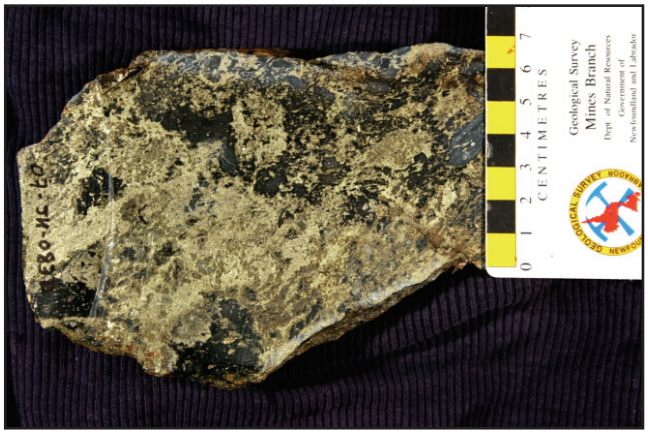

Plate 24. *Chalcopyrite-rich, chloritized felsic pyroclastics from the Victoria Mine prospect. Note that intense carbonate–silica–sericite alteration assemblages are also locally present on the ore horizon.*

folded thrust system, locally termed the Jig Zone fault. However, the exact relationship of the sulphide mineralization to the fault is uncertain. McKenzie *et al.* (1993) suggested that the mineralization and alteration overprint the fault and was synchronous with the accretion of major tectonic blocks. The footwall stratigraphy consists of variably altered felsic volcanic rocks and coarse rhyolite breccias, which most closely resemble the rhyolite breccias at the Hungry Hill prospect. However, the immediate hangingwall stratigraphy consists of pristine, unaltered, green to maroon, felsic to intermediate ash to crystal tuffs. This invites the question of the relative timing of mineralization with respect to thrusting. The plunging massive sulphide lens, although not very well constrained, has been shown to contain economically interesting grades, indicated by a diamond-drill intersection of 11 m having an average grade of 2.9% Cu, 5.7% Zn in Vic-89-02 (*e.g.*, Greene *et al.*, 2001).

GEOCHEMISTRY

INTRODUCTION

A representative suite of all volcanic and volcaniclastic rock types from the TVB were analyzed for major and trace elements using Inductively Coupled Plasma–Emission Spectrometry (ICP-ES) methods outlined in Finch (1998). A smaller subset of samples was analyzed at Acme Analytical Laboratories for trace elements and rare-earth elements (REE) by four-acid digestion, Inductively Coupled Plasma–Mass Spectrometry (ICP-MS) techniques, and for assay *via* INAA. The analytical method used for each element is given in Appendix 1B. Samples were separated into groups based upon their association with the specific VMS deposits described above and, where possible, were further divided into hangingwall and footwall categories to aid in identifying the affects of alteration. The complete geochemical database derived from this project is found in Appendix 1B. Selected chemical ratios for various rock types from each deposit are listed in Table 1 to aid in discussion and comparison. Selected samples were also analyzed for Sm/Nd isotopic compositions (Table 2) by Thermal Ionization Mass Spectrometry (TIMS) techniques at Memorial and Carleton universities.

The samples analyzed in this study cover all rock types and include both altered and unaltered samples. It is very difficult to obtain unaltered material for geochemical analyses, because outcrop is limited, and exploration is naturally focused around areas of mineralization. Most of the samples discussed herein represent diamond-drill core samples.

Samples were selected to study the various rock types associated with each deposit, to compare and contrast the geochemical signatures of the host rocks associated with each deposit, and to study the affects of alteration upon the host rock geochemical signatures. Detailed methods and detection limts are provided in Finch (1998) as well as on Acme Analytical Laboratories website.

ELEMENT MOBILITY CONSIDERATIONS

It is important to account for the effects of element mobility when making inferences about tectonic settings or primary rock type based on geochemistry. As the major rock types in the TVB are felsic-intermediate in composition and volcanic in nature, they are all variably affected by high-temperature alteration. The most common hydrothermal alteration process affecting the felsic-intermediate volcaniclastic rocks of the TVB is replacement of primary feldspar by sericite, effectively resulting in a mass gain of K from hydrothermal fluids and a mass loss of Na and Ca from the rock. Further replacement of feldspar and sericite by chlorite results in a mass gain of Mg ± Fe. Based on the degree of alteration recoginized in the samples collected, it is assumed that Na, K, Ca, Mg, Fe and SiO_2 were mobile during high-temperature alteration; an assumption substantiated by numerous immobile–mobile element plots (not shown). Although other major oxides such as Al_2O_3 and TiO_2, as well as other high-field-strength-elements (HFSE), are commonly assumed to be immobile under most alteration conditions (*e.g.*, Barrett and MacLean, 1999), locally intense carbonate alteration proximal to massive sulphide horizons, suggests that these elements should be also used with caution (*see* Hynes, 1980; Finlow-Bates and Stumpfl, 1981; Jiang *et al.*, 2005; and Pandarinath *et al.*, 2008). The low-field-strength-elements (LFSE) (*e.g.*, Ba, Rb, Cs, Sr) are considered to be mobile under the alteration conditions in this study, and are not used to discriminate rock types. The rare-earth elements (REE), with the exception of Eu (*e.g.*, Sverjensky, 1984; Whitford *et al.*, 1988), are generally considered to be immobile except under extreme hydrothermal alteration conditions, when the light REE (*e.g.*, La, Ce, Pr, Nd) may become mobile (Campbell *et al.*, 1984; MacLean and Barrett, 1993). The coherent behaviour of the middle- (*e.g.*, Sm, Gd, Tb, Dy, Ho) and heavy (*e.g.*, Er, Tm, Yb, Lu) REE in the samples collected suggest that they were immobile, whereas slight variations in light REE concentrations (in particular La) indicate some mobility. The HFSE (*e.g.*, Zr, Hf, Nb, Ta, Y, Th) are immobile in almost all cases (*e.g.*, Barrett and MacLean, 1999; Lentz, 1999). The coherent behaviour of these elements in the dataset suggests that they remained essentially immobile during alteration. It should be noted that the samples analyzed in this study include both volcanic and volcaniclastic rocks; and whereas element immobility can be proven in strictly coherent volcanic facies in the belt, other factors could affect the lithogeochemistry of tuffaceous rocks.

The geochemical data from the five main deposits in the TVB, as well as that of the Pats Pond group (Rogers, 2004; Zagorevski *et al.*, 2007a), are discussed. In addition to ordinary bi-variate plots, discrimination diagrams, and extended trace-element plots, the wholerock geochemical data were also assessed to examine chemical variations associated with hydrothermal alteration. In addition to downhole profiles, samples were also assessed using the alteration box plot (Large *et al.*, 2001). This plot uses two common alteration indexes *viz.*, the Hashimoto Alteration Index (AI) of Ishikawa *et al.* (1976) and the chlorite–carbonate–pyrite index (CCPI) of Large *et al.* (2001) (*see* formula in Table 1). High AI values represent sericite and chlorite alteration

Table 1: Summary of some key major and trace-element ratios for the felsic rocks associated with the VMS deposits in the TVB and the Pats Pond group

BOOMERANG AND DOMINO STRATIGRAPHY

	Felsic Tuff (HW)		Felsic Tuff (FW)		Felsic Lapilli Tuff (HW)		Qtz-fld Tuff (HW)		Qtz-fld Tuff (FW)		Felsic Sill		Felsic Ashy Tuff	
	Average	2 σ	Average	2 σ	Average	2 σ	Average	2 σ	Average	2 σ	Average	2 σ	Average	2 σ
Al	46.21	15.70	59.85	21.60	57.76	10.22	50.65	35.78	55.67	11.43	33.00	8.07	42.61	35.19
CCPI	60.97	9.35	69.64	4.52	55.76	9.09	66.42	23.13	84.63	15.00	44.94	8.28	49.92	17.49
Na/K	16.10	31.64	0.27	0.03	1.33	0.69	8.95	12.15	0.38	0.08	27.39	62.42	9.57	12.78
Zr/Y	2.82	0.75	3.43	0.73	3.67	0.91	2.69	0.14	3.40	0.30	3.73	1.23	5.62	0.63
Zr/Nb	39.66	12.67	29.04	3.47	54.68	15.12	33.45	2.30	39.86	1.52	39.14	6.66	31.04	0.94
Zr/TiO_2	152.65	124.83	156.75	16.14	326.61	217.28	114.50	19.02	193.63	16.82	233.46	140.77	489.33	447.69
Zr/Hf	33.61	2.52	33.92	2.06	38.41	2.88	32.81	0.72	36.51	2.58	35.37	2.20	35.35	0.60
Nb/Y	0.07	0.02	0.11	0.02	0.07	0.03	0.08	0.01	0.09	0.01	0.09	0.03	0.18	0.01
Th/Nb	0.46	0.33	0.41	0.14	0.84	0.46	0.63	0.75	0.31	0.08	0.68	0.40	0.78	0.70
La_N/Yb_N	1.52	0.32	1.83	0.27	2.11	0.37	2.68	1.70	3.50	1.53	2.83	1.63	4.31	1.36
Ce_N/Yb_N	1.49	0.28	1.63	0.25	2.06	0.33	2.38	1.21	3.09	1.59	2.41	1.25	3.60	0.93
La_N/Th_N	1.11	0.55	0.90	0.06	0.84	0.29	1.01	0.50	2.23	0.02	0.96	0.39	0.98	0.54
La_N/Nb_N	3.43	1.22	2.60	0.29	5.80	1.96	5.44	4.22	6.09	2.17	4.72	0.83	4.84	2.22
Zr_N/Sm_N	1.05	0.27	1.41	0.10	1.20	0.29	0.83	0.21	0.97	0.36	1.21	0.22	1.18	0.11
La_N/Sm_N	1.38	0.32	1.89	0.09	1.73	0.23	1.86	0.94	2.22	0.09	2.14	0.69	2.82	0.98
Gd_N/Lu_N	0.97	0.17	0.84	0.06	0.98	0.08	1.03	0.02	1.13	0.51	1.05	0.27	0.94	0.27
Eu/Eu*	0.89	0.10	0.83	0.13	0.88	0.06	1.03	0.12	1.40	0.36	0.90	0.04	0.88	0.10
Nb/Nb*	0.15	0.10	0.09	0.01	0.07	0.04	0.16	0.15	0.11	0.08	0.10	0.10	0.06	0.04
Zr/Zr*	0.28	0.07	0.37	0.04	0.33	0.08	0.23	0.04	0.27	0.09	0.32	0.07	0.36	0.01
Ti/Ti*	0.13	0.05	0.12	0.01	0.04	0.02	0.09	0.01	0.08	0.03	0.10	0.02	0.07	0.06
Nb/Ta	19.64	8.33	13.94	2.58	17.50	5.07	14.75	2.47	10.50	0.71	12.54	4.71	13.08	2.24

TULKS HILL STRATIGRAPHY

	Felsic Tuff (HW)		Felsic Tuff (FW)		Felsic Lapilli Tuff (HW)		Qtz-fld Tuff (HW)		Rhyolite (HW)		Rhyolite (FW)	
	Average	2 σ	Average	2 σ	Average	2 σ	Average	2 σ	Average	2 σ	Average	2 σ
Al	40.10	8.03	57.35	42.44	36.23		46.33		60.90	31.53	63.72	33.48
CCPI	66.84	10.04	78.93	23.81	34.99		27.97		51.12	15.30	60.21	23.24
Na/K	3.67	0.42	9.50	13.32	2.56		1.16		1.82	2.74	3.87	6.31
Zr/Y	-	-	2.22	0.23			2.44		2.14	0.31	2.44	-
Zr/Nb	30.99	7.21	28.35	1.78	36.71		29.21		35.44	7.01	33.91	10.42
Zr/TiO_2	84.59	5.08	460.09	348.97	1512.82		553.00		928.21	535.82	972.40	448.61
Zr/Hf	-	-	34.38	0.96			34.22		31.98	1.58	31.32	-
Nb/Y	-	-	0.08	0.00			0.08		0.06	0.01	0.08	-
Th/Nb	0.69	0.23	0.99	0.57	0.80		0.95		0.92	0.33	0.68	0.43
La_N/Yb_N	-	-	2.39	0.80			1.82		1.48	0.55	1.86	-
Ce_N/Yb_N	-	-	1.93	0.54			1.53		1.31	0.42	1.63	-
La_N/Th_N	-	-	0.63	0.23			0.45		0.65	0.22	0.45	-
La_N/Nb_N	-	-	4.70	1.05			3.59		4.29	0.56	3.94	-
Zr_N/Sm_N	-	-	0.82	0.01			1.15		0.94	0.08	1.02	-
La_N/Sm_N	-	-	2.12	0.36			2.24		1.74	0.34	1.97	-
Gd_N/Lu_N	-	-	0.95	0.11			0.69		0.74	0.13	0.78	-
Eu/Eu*	-	-	0.93	0.23			0.56		0.70	0.15	0.64	-
Nb/Nb*	0.09	0.03	0.04	0.02			0.04		0.06	0.02	0.14	0.14
Zr/Zr*	-	-	0.21	0.00			0.30		0.24	0.02	0.27	-
Ti/Ti*	-	-	0.03	0.02			0.03		0.02	0.01	0.01	-
Nb/Ta	-	-	16.50	-					14.83	1.65	15.00	-

TULKS EAST STRATIGRAPHY

	Felsic Tuff (HW)		Felsic Tuff (FW)		Felsic Lapilli Tuff HW	Felsic Lapilli Tuff FW	Qtz-fld Tuff (HW)		Rhyolite (HW)		Rhyolite (FW)	
	Average	2 σ	Average	2 σ	Average	Average	Average	2 σ	Average	2 σ	Average	2 σ
Al	69.46	31.70	90.06	7.72	46.73	92.29	24.10	17.07	57.58	51.74	92.48	
CCPI	64.89	22.26	89.99	12.59	53.48	82.66	33.76	14.06	56.75	43.73	75.36	
Na/K	1.13	1.78	0.25	0.07	0.96	0.21	9.14	10.39	1.99	2.67	0.19	
Zr/Y	2.23	-	1.99	0.94	1.77	2.52	2.56	1.15	1.15	0.64	1.77	
Zr/Nb	35.53	4.10	168.41	136.58	38.86	56.18	35.68	2.27	42.83	0.36	39.47	
Zr/TiO_2	283.11	125.14	272.70	43.37	201.54	189.16	809.10	477.46	298.49	144.60	346.13	
Zr/Hf	32.34	-	31.81	3.33	30.68	29.37	35.56	2.28	21.64	15.55	30.18	
Nb/Y	0.07	-	0.03	0.02	0.05	0.04	0.07	0.03	0.03	0.01	0.04	
Th/Nb	0.35	0.17	2.69	1.54	0.73	1.05	0.91	0.24	1.01	0.30	0.92	
La_N/Yb_N	1.86	-	0.60	0.53	1.47	1.55	1.53	1.33	1.24	0.15	1.41	
Ce_N/Yb_N	1.66	-	0.56	0.47	1.37	1.62	1.28	0.99	1.17	0.17	1.31	
La_N/Th_N	1.39	-	0.31	0.33	0.85	0.60	0.41	0.06	1.02	0.41	0.64	
La_N/Nb_N	4.50	-	2.96	2.28	5.26	8.10	3.13	1.58	9.27	6.13	5.03	
Zr_N/Sm_N	0.71	-	1.38	0.62	0.68	0.73	1.17	0.04	0.52	0.35	0.65	
La_N/Sm_N	1.63	-	0.78	0.63	1.44	1.33	1.68	0.86	1.37	0.01	1.31	

Gd_N/Lu_N	0.87	-	0.69	0.13	0.89	0.88	0.77	0.19	0.84	0.01	0.87
Eu/Eu*	0.30	-	0.61	0.25	1.04	0.33	0.78	0.19	0.74	0.15	0.29
Nb/Nb*	0.14	0.16	0.02	0.01	0.04	0.07	0.05	0.02	0.03	0.02	0.04
Zr/Zr*	0.19	-	0.28	0.07	0.18	0.20	0.29	0.04	0.13	0.08	0.17
Ti/Ti*	0.05	-	0.05	0.02	0.05	0.06	0.02	0.02	0.03	0.03	0.03
Nb/Ta	-	-	10.25	6.72		-	16.00	-	14.75	14.50	13.00

DANIELS POND STRATIGRAPHY

	Andesite (HW)		Andesite (FW)		Andesite (FW) Extremely altered		Andesite (FW) Immediate FW		Int. Lap. Tuff		Felsic tuff	
	Average	2 σ	Average	2 σ	Average	2 σ	Average	2 σ	Average	2 σ	Average	2 σ
	n=9,2		n=19,6		n=10,4		n=5,5		n=5,1		n=2,0	
AI	47.04	10.77	67.68	25.43	79.37	10.48	46.91	8.71	53.44	14.18	36.49786	0.952406
CCPI	76.24	4.40	73.71	17.96	32.81	32.38	66.83	10.03	62.46	6.20	54.43778	10.79444
Na/K	2.84	3.11	2.17	5.12	0.25	0.09	2.69	0.88	0.41	0.40	1.595775	0.072936
Zr/Y	2.65	0.62	1.99	0.73	10.44	2.90	2.14	0.55	3.63			
Zr/Nb	7.11	5.18	9.01	6.64	29.18	23.05	6.86	1.28	13.34	1.03	45.00369	11.61032
Zr/TiO_2	113.52	133.38	90.89	44.42	76.41	4.23	77.70	12.13	164.24	50.04	418.3901	4.598954
Zr/Hf	38.60	7.69	34.29	3.91	33.16	3.08	34.68	2.51	32.25			
Nb/Y	0.56	0.44	0.23	0.17	0.44	0.18	0.33	0.14	0.25			
Th/Nb	0.19	0.14	0.32	0.14	0.82	0.35	0.21	0.04	0.58			
La_N/Yb_N	1.51	0.29	1.25	0.21	4.20	1.16	1.47	0.11	2.23			
Ce_N/Yb_N	1.30	0.34	1.16	0.18	3.20	0.76	1.28	0.07	1.83			
La_N/Th_N	0.39	0.12	0.49	0.22	0.36	0.10	0.47	0.09	0.31			
La_N/Nb_N	0.15	0.38	1.33	0.74	2.47	1.21	0.84	0.24	1.53			
Zr_N/Sm_N	1.39	0.91	0.84	0.17	2.10	0.47	0.95	0.25	1.35			
La_N/Sm_N	1.84	0.43	1.42	0.31	3.02	0.43	1.74	0.11	2.24			
Gd_N/Lu_N	0.73	0.16	0.77	0.07	0.66	0.15	0.74	0.05	0.76			
Eu/Eu*	0.90	0.16	0.52	0.36	0.48	0.20	1.33	0.48	0.77			
Nb/Nb*	0.32	0.25	0.15	0.08	0.06	0.03	0.20	0.06	0.08			
Zr/Zr*	0.35	0.19	0.22	0.05	0.68	0.17	0.25	0.06	0.37			
Ti/Ti*	0.23	0.14	0.13	0.06	0.46	0.12	0.16	0.02	0.09			
Nb/Ta	-	-	-	-	-	-	-	-	40.00			

BOBBYS POND STRATIGRAPHY

	Felsic Tuff (FW)		Felsic Lapilli Tuff (FW)		Rhyolite (HW)		Rhyolite (FW)		Int. Lap. Tuff	
	Average	2 σ	Average	2 σ	Average	2 σ	Average	2 σ	Average	2 σ
	n=5,2		n=2,1		n=8,4		n=15,8		n=2,0	
AI	72.91	8.64	59.91	23.55	43.46	15.77	40.24	27.69	47.36	5.81
CCPI	74.46	12.92	52.00	9.30	48.76	13.00	40.36	22.00	53.86	11.92
Na/K	0.65	0.39	1.95	1.93	8.72	7.58	30.60	66.34	7.23	5.54
Zr/Y	6.79	3.56	2.98		2.97	0.53	3.03	0.35		
Zr/Nb	16.57	9.99	46.95	12.87	50.80	7.48	53.54	16.12	62.91	22.08
Zr/TiO_2	411.49	268.39	722.29	64.28	754.32	248.14	771.17	157.65	711.59	49.15
Zr/Hf	28.88	5.75	30.36		31.11	1.05	30.14	1.13		
Nb/Y	0.67	0.74	0.05		0.06	0.01	0.06	0.02		
Th/Nb	0.61	0.63	2.14		1.95	0.22	2.04	0.47		
La_N/Yb_N	3.89	1.60	2.01		2.20	0.19	2.24	0.23		
Ce_N/Yb_N	3.32	1.49	1.70		1.85	0.13	1.94	0.18		
La_N/Th_N	0.39	0.06	0.33		0.37	0.06	0.36	0.03		
La_N/Nb_N	1.86	1.76	5.90		6.11	1.33	6.21	1.09		
Zr_N/Sm_N	1.70	0.09	1.22		1.06	0.25	1.15	0.14		
La_N/Sm_N	2.47	0.65	2.03		1.88	0.19	2.07	0.16		
Gd_N/Lu_N	1.02	0.31	0.86		0.91	0.14	0.87	0.07		
Eu/Eu*	0.99	0.84	0.62		0.63	0.05	0.60	0.12		
Nb/Nb*	0.14	0.15	0.02		0.02	0.00	0.02	0.01		
Zr/Zr*	0.49	0.04	0.32		0.29	0.07	0.31	0.04		
Ti/Ti*	0.32	0.41	0.02		0.02	0.01	0.02	0.00		
Nb/Ta	20.48	4.85	9.21		11.34	5.21	9.09	2.78		

AI= Hashimoto index = $100*[(MgO+K_2O)/(MgO+K_2O+Na_2O+CaO)]$ (Ishikawa et al., 1976)

CCPI = chlorite-carbonate-pyrite index = $100*[(MgO+FeO*)/(MgO+FeO*+K_2O+Na_2O)]$ (Large et al., 2001)

$Na/K = Na_2O/K_2O$

$Eu/Eu* = Eu_{pm}/(Gd_{pm}*Sm_{pm})0.5$, $Nb/Nb* = 0.5*Nb_{pm}/(Th_{pm}+La_{pm})$, $Zr/Zr* = 0.5*Zr_{pm}/(Gd_{pm} + Sm_{pm})$, $Ti/Ti* = 0.5*Ti_{pm}/(Gd_{pm} + Sm_{pm})$

pm = primitive mantle normalized

Note that all normalization is to primitive mantle (values after Sun and McDonough, 1989)

Table 2: Sm/Nd isotopic data

Sample	Deposit or Unit	Sm	Nd	$^{147}Sm/^{144}Nd$ (measured)	$^{143}Nd/^{144}Nd$ (measured)	Age (Ma)	$^{143}Nd/^{144}Nd$ initial	eNd CHUR (T)c	Model Age T(DM)***DePaolo
JHC-06-022	Tulks East (TE-99-04)	1.30	4.32	0.1815	0.512737	498	0.512144905	2.90	1434.15
JHC-06-003	Tulks East (TE-94-01)	2.30	8.13	0.1707	0.512712	498	0.512155137	3.10	1171.48
JHC-06-057	Tulks Hill (T-192)	3.59	14.18	0.1529	0.512648	498	0.512149205	2.99	996.05
JHC-06-043	Tulks Hill (T-197)	4.92	19.21	0.1548	0.512656	498	0.512151007	3.02	1006.93
JHC-06-172	Domino (GA-97-05)	6.52	27.86	0.1416	0.512669	491	0.512213572	4.07	803.39
JHC-06-184	Domino (GA-97-05)	2.37	8.59	0.1669	0.512759	491	0.512222199	4.24	934.87
JHC-06-229	Boomerang (GA-04-11)	3.46	10.74	0.1949	0.512902	491	0.512275143	5.27	1137.49
JHC-06-236	Boomerang (GA-04-11)	2.48	9.39	0.1596	0.512786	491	0.512272678	5.22	743.80
JHC-06-239	Boomerang (GA-05-016)	2.59	9.83	0.1592	0.512773	491	0.512260965	4.99	772.93
JHC-06-240	Boomerang (GA-05-079)	4.11	16.52	0.1503	0.512719	491	0.512235590	4.50	793.56
JHC-06-076	Tulks West (TW-12)	3.281	11.23	0.1766	0.512682	498	0.512105890	2.14	1470.63
JHC-06-064	Tulks West (TW-09)	1.006	2.935	0.2073	0.512896	498	0.512219740	4.36	-
JHC-06-143	Curve Pond (CVP-02-01)	14.38	60.40	0.1439	0.512728	498	0.512258565	5.12	705.59
JH-06-064	Dragon Pond Area	1.808	6.274	0.1742	0.512753	498	0.512184720	3.68	1119.23
JHC-06-113	Dragon Pond (DRP-95-01)	1.702	5.699	0.1806	0.512770	498	0.512180841	3.60	1249.70
JHC-07-061	Jacks Pond (JP-94-01)	4.562	18.56	0.1486	0.512625	498	0.512140233	2.81	984.75
JHC-07-114	Daniels Pond (DN-02-02)	1.340	4.454	0.1819	0.512704	498	0.5121106	2.23	1607.84
JHC-07-077	Jacks Pond (JP-97-14)	4.012	17.53	0.1384	0.512612	498	0.512160507	3.21	881.67
JHC-07-273	Bobby's Pond (77547)	4.375	19.75	0.1339	0.512691	498	0.512254187	5.04	688.87
JHC-07-222	Hungry Hill (HH-97-16)	0.662	1.410	0.2839	0.513065	498	0.512138853	2.78	-
JHC-07-142	Daniels Pond (DN-16)	1.12	3.7	0.1831	0.5127	498	0.512102686	2.08	1690.74
JHC-07-255	Bobby's Pond (77544)	1.56	7.12	0.1326	0.512624	498	0.512191428	3.81	799.27
VL02A246b	PP6	2.87	11.22	0.1546	0.512701	488	0.512206803	3.86	892.49
VL02A221	PP4	0.85	3.12	0.1655	0.512777	488	0.51224796	4.66	855.56
VL02A128	PP4	0.63	2.17	0.1766	0.512854	488	0.512289477	5.47	799.11
VL02A202	PP1	2.68	10.14	0.1598	0.512493	488	0.51198218	-0.53	1547.64
VL02A026	PP1	3.30	13.04	0.153	0.512515	488	0.512025917	0.33	1322.16

** T DM = Nd depleted mantle model age - calculated using the Goldstein 143/144 0.513163; and 147/144 of 0.2137
ccalulated using present day chondritic uniform reservoir with 143Nd/144Nd = 0.512638 & 147Sm/144Nd = 0.1967
***TDM Depaolo - calculated using the two stage evolution of DePaolo, 1981
(143/144) is adjusted from the deviation to JNdi-1 Standard (0.512115), mean measured value of the standard gives 0.512135 +- 9 (2sigma StdDev)

products, derived from the breakdown of plagioclase feldspars and volcanic glass; whereas high CCPI values represent chlorite, Fe–Mg carbonate and pyrite alteration typically associated with VMS deposits. Generally, AI indices >70-75 are considered to represent strong alteration. Most of the felsic-intermediate rock types that host the VMS deposits in the TVB are displaced to the right of the 'least altered box' in the alteration box plot of Large *et al.* (2001) (see Figures 22 and 28), with relatively high AI and CCPI, suggesting that they have been strongly affected by hydrothermal alteration. For this reason, emphasis is placed on relatively immobile REE and HFSE in the following discussions. In contrast, the data from the Pats Pond group (Zagorevski *et al.*, 2007a) do not show evidence of strong alteration effects as the focus of that study was to sample for geochemical correlations and tectonic discrimination, with altered rocks being largely avoided. Although not studied in detail in this report, numerous outcrop samples of host rocks, some relatively unaltered, were collected and analyzed as part of this project. All chemical data from such samples are available in Appendix 1B.

SOUTHERN TULKS VOLCANIC BELT

Boomerang–Domino–Hurricane Deposit

Host Rock Geochemistry

Host rocks to the Boomerang–Domino–Hurricane deposit appear to form a continuum from mafic through to felsic compositions; however, the andesitic sills (Figure 15A) have different chemical characteristics and may not be genetically associated with the host rocks to the deposit. Felsic-intermediate host rocks are dominated by quartz-phyric tuff that have average Zr/TiO_2 ratios of 0.015 and 0.016, and average Nb/Y ratios of 0.07 and 0.11 in the hangingwall and footwall, respectively. Quartz–feldspar-crystal tuffs in the hangingwall and footwall have very similar ratios, whereas lapilli tuffs in the hangingwall, ash, and felsic sills have higher Zr/TiO_2 ratios of 0.033, 0.049, and 0.023, respectively (Table 1). The HFSE (Zr, Hf, Y, Nb, Ta) contents of all the felsic to intermediate rocks are low to moderate, characterizing them as volcanic-arc to ocean-ridge type rocks on the Ta *vs*. Yb discrimation diagram (Figure 16A). Primitive-mantle-normalized plots for the felsic-intermediate rocks are characterized by weak to moderate LREE enrichments (refer to the La_N/Sm_N values in Table 1 and Figures 17A, and 18A), relatively flat MREE patterns, and weak to moderate overall REE fractionation. These plots also show weak to moderately negative Nb and Ti anomalies, slightly negative Eu anomalies, and prominent positive Zr and Hf anomalies for the felsic to intermediate ash, crystal- to lapilli tuffs, and some felsic sills (Figures 17A, and 18B). Most of the felsic to intermediate rocks have very low Zr/Y and La/Yb ratios, similar to published values for tholeiitic rocks (Barrett and MacLean, 1999; Table 1). The Sm–Nd isotopic analysis of four samples of felsic to intermediate tuff from the Boomerang and nearby Domino deposits yielded εNd (491 Ma) values from +4.07 to +5.27 (Figure 19, Table 2).

The mafic volcanic rocks from Boomerang are characterized by weak LREE-enriched to flat extended trace-element plots, with values four to ten times that of primitive mantle concentrations, and have profiles that are similar to N-MORB (Figure 20A). All samples have moderately positive Th anomalies and moderately negative Nb anomalies. As such, the samples have island-arc tholeiite signatures. In contrast, samples of the andesitic sills have much higher contents of HFSE and REE, higher degrees of REE fractionation, and have variably moderately to strongly negative Nb and Ti anomalies (Figure 20B). These characteristics suggest a transitional calc-alkaline basalt to island-arc tholeiite affinity (Figure 20B). On a Ti–V discrimination diagram, the mafic volcanic samples plot predominantly within the island-arc tholeiite field but in part overlap the MORB field, whereas the andesitic sills predominantly plot within the alkaline field (Figure 21A), and on a Th–Zr–Nb plot (after Wood, 1980) the mafic volcanic rocks plot predominantly in the arc-basalt field with one sample of the andesitic plotting in the N-MORB field.

Alteration Geochemistry

The Boomerang deposit, like all other deposits studied in this investigation, shows evidence of significant plagioclase destructive alteration coupled with sodium depletion in the footwall, and in the immediate hangingwall. This zone of sodium depletion is commonly associated with increased iron and magnesium related to pyrite and chlorite alteration, increased calcium related to carbonate alteration, and increased barium related to barite alteration (Figure 5B, C).

Chemical and mineralogical changes attributed to hydrothermal alteration at the Boomerang deposit are illustrated in Figure 22A. As illustrated, some of the felsic to intermediate volcanic rocks in proximity to the ore horizon show gains in K_2O, MgO and FeO, and are displaced to the upper right part of the alteration box plot diagram, outside the fields of least altered samples (Figure 22A). This is indicative of sericite–chlorite–carbonate–pyrite alteration. A small subset of felsic to intermediate samples also appear to be trending to the bottom left part of the diagram, *i.e.*, toward the diagenetic albite trend and these are attributed to regional alteration processes.

In addition to major-element variations related to hydrothermal alteration, some of the minor volatile elements

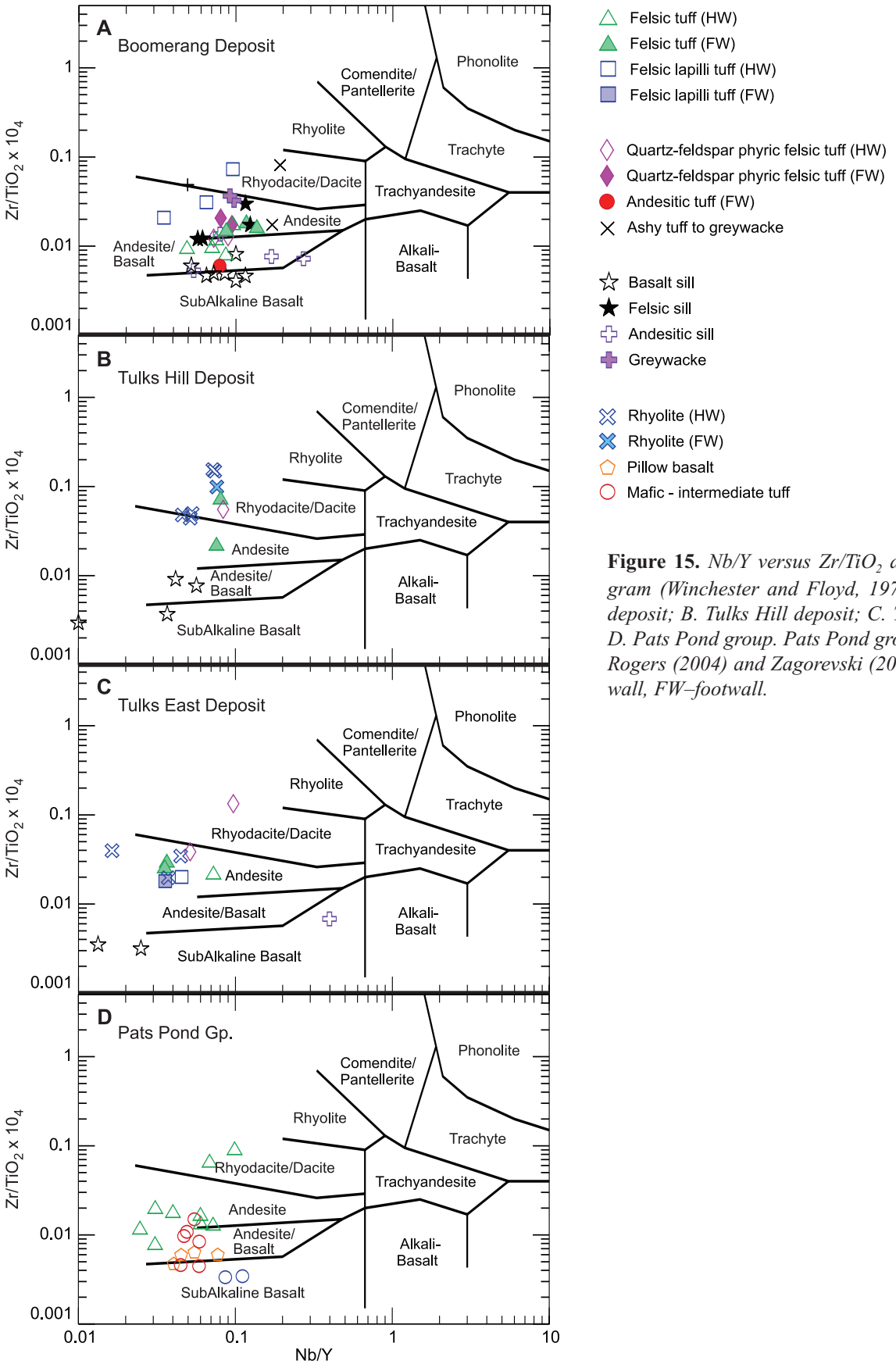

Figure 15. *Nb/Y versus Zr/TiO$_2$ discrimination diagram (Winchester and Floyd, 1977). A. Boomerang deposit; B. Tulks Hill deposit; C. Tulks East deposit; D. Pats Pond group. Pats Pond group chemistry from Rogers (2004) and Zagorevski (2006). HW–hanging-wall, FW–footwall.*

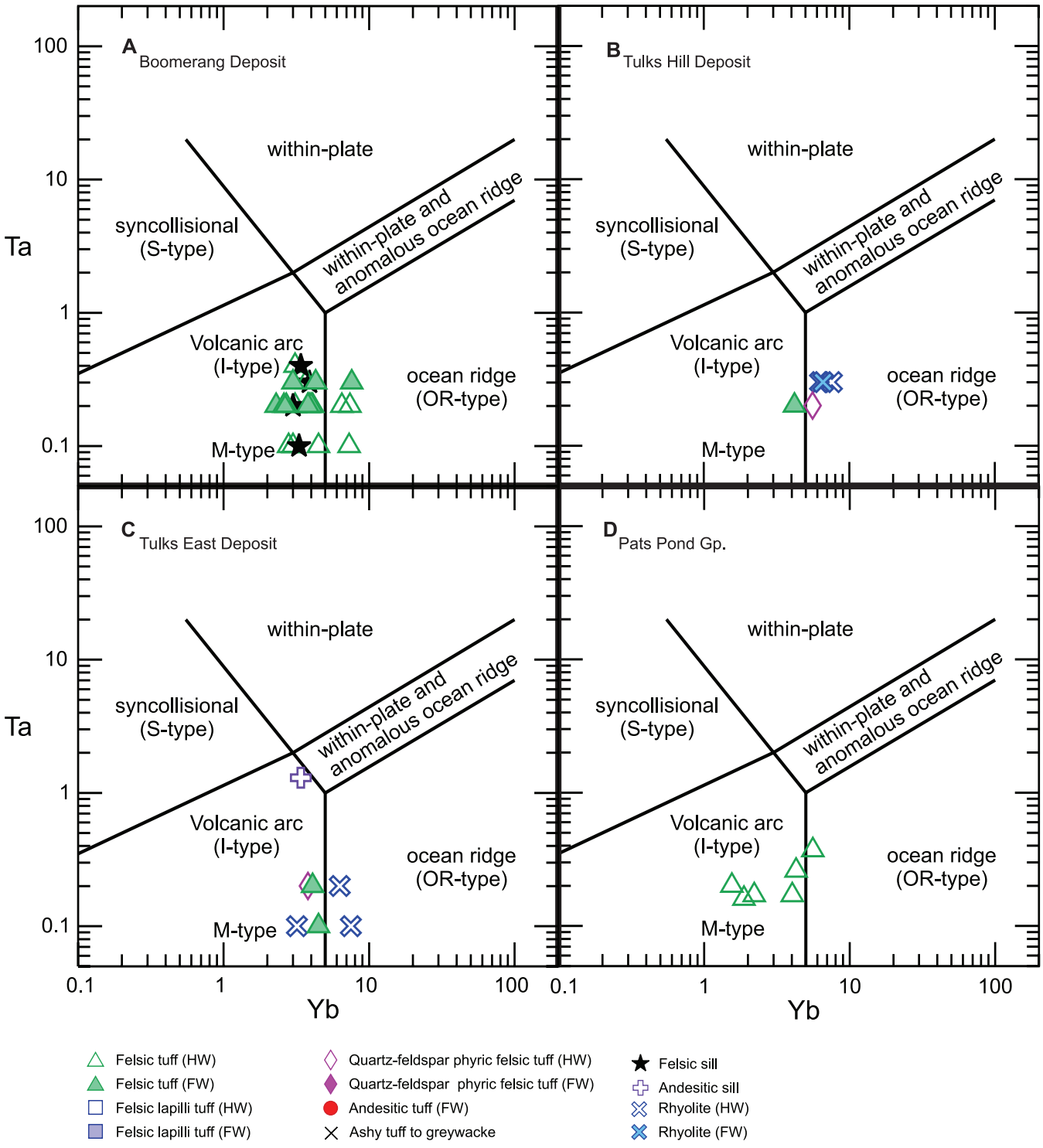

Figure 16. *Yb versus Ta (Pearce* et al.*, 1984) discrimination diagrams for the host felsic volcanic rocks of the three main VMS deposits in the southern TVB and the Pats Pond group: A. Boomerang deposit, B. Tulks Hill deposit, C. Tulks East deposit, D. Pats Pond group. Pats Pond group chemistry from Rogers (2004) and Zagorevski (2006).*

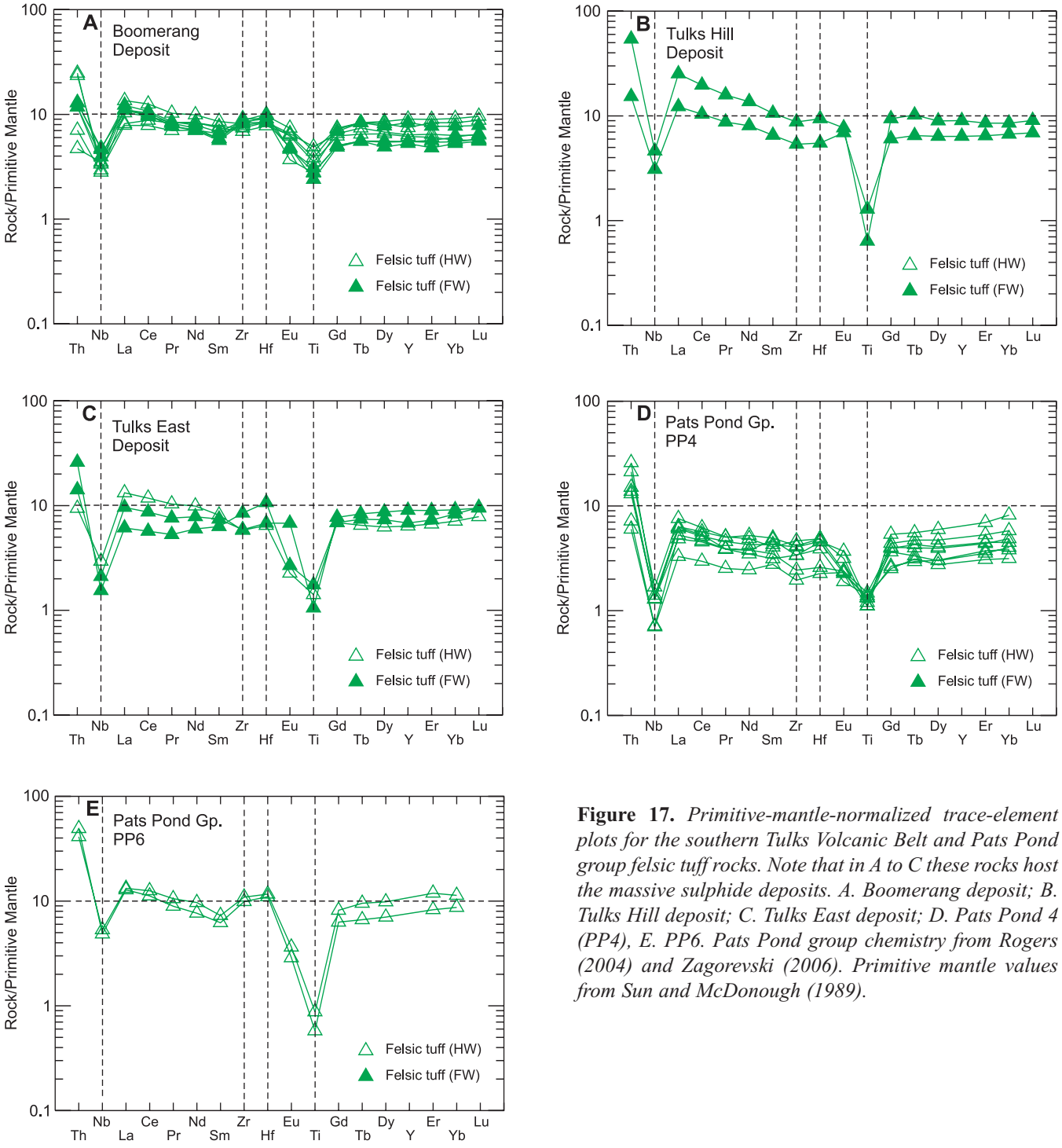

Figure 17. *Primitive-mantle-normalized trace-element plots for the southern Tulks Volcanic Belt and Pats Pond group felsic tuff rocks. Note that in A to C these rocks host the massive sulphide deposits. A. Boomerang deposit; B. Tulks Hill deposit; C. Tulks East deposit; D. Pats Pond 4 (PP4), E. PP6. Pats Pond group chemistry from Rogers (2004) and Zagorevski (2006). Primitive mantle values from Sun and McDonough (1989).*

are also enriched in the rocks immediately surrounding the ore horizons in the hangingwall and footwall. Of note, thallium and antimony occur in enriched haloes around the boomerang ore lens (Figure 5B, C); a zoning similar to many other VMS-mineralized systems (*e.g.*, Rosebery deposit; Large *et al.*, 2001). As shown in Figure 5B and C, the volatile haloes are most strongly developed in the footwall within 20 to 30 m of the sulphide-bearing horizon. Locally, these elements may also form enrichments in the hangingwall as well.

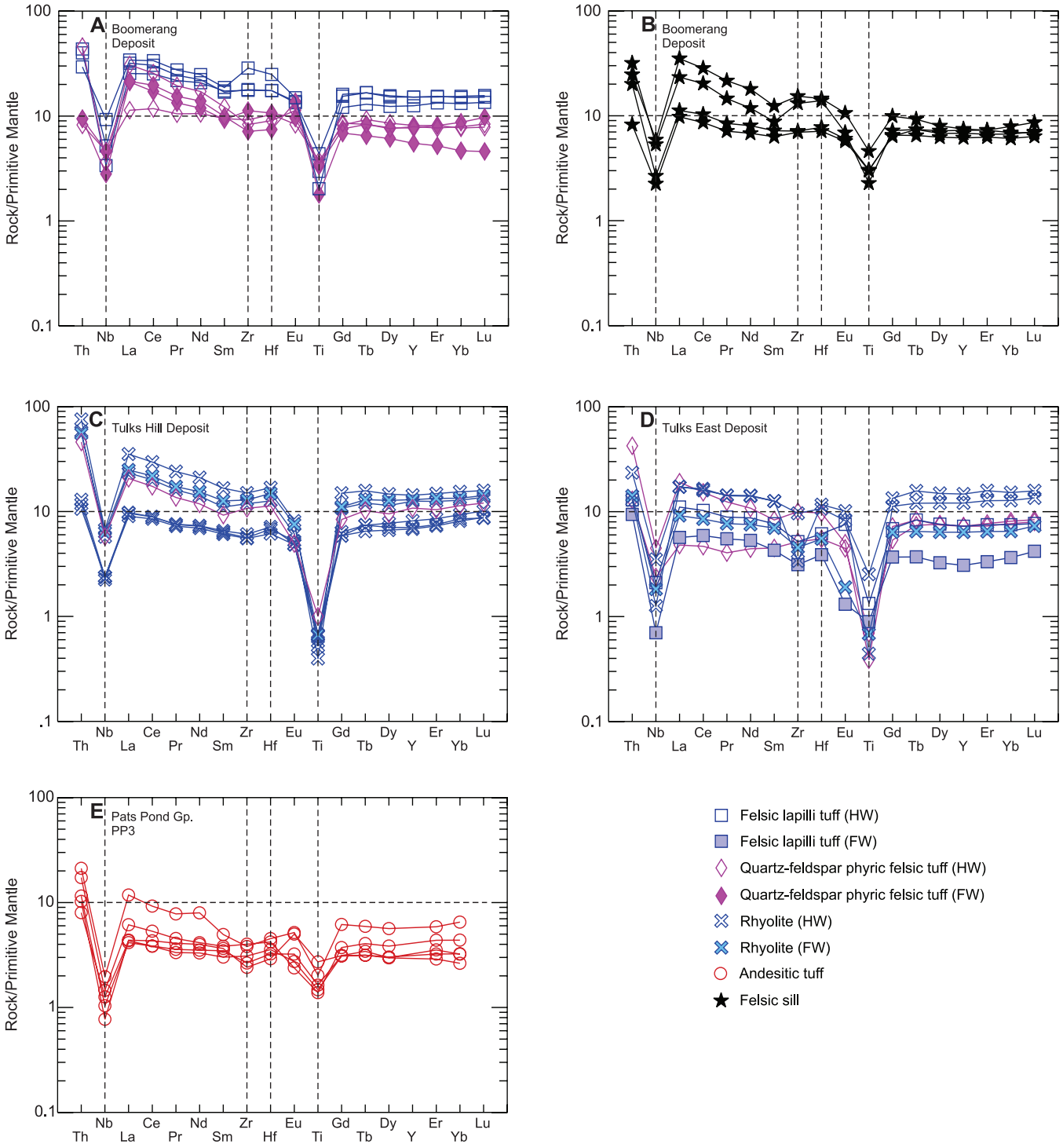

Figure 18. *Primitive-mantle-normalized trace-element plots for other felsic to intermediate rocks from the southern Tulks Volcanic Belt and Pats Pond group. A. Boomerang deposit, B. Boomerang deposit, C. Tulks Hill, D. Tulks East deposit and E. Pats Pond 3 (PP3). Pats Pond group chemistry from Rogers (2004) and Zagorevski (2006). Primitive mantle values from Sun and McDonough (1989).*

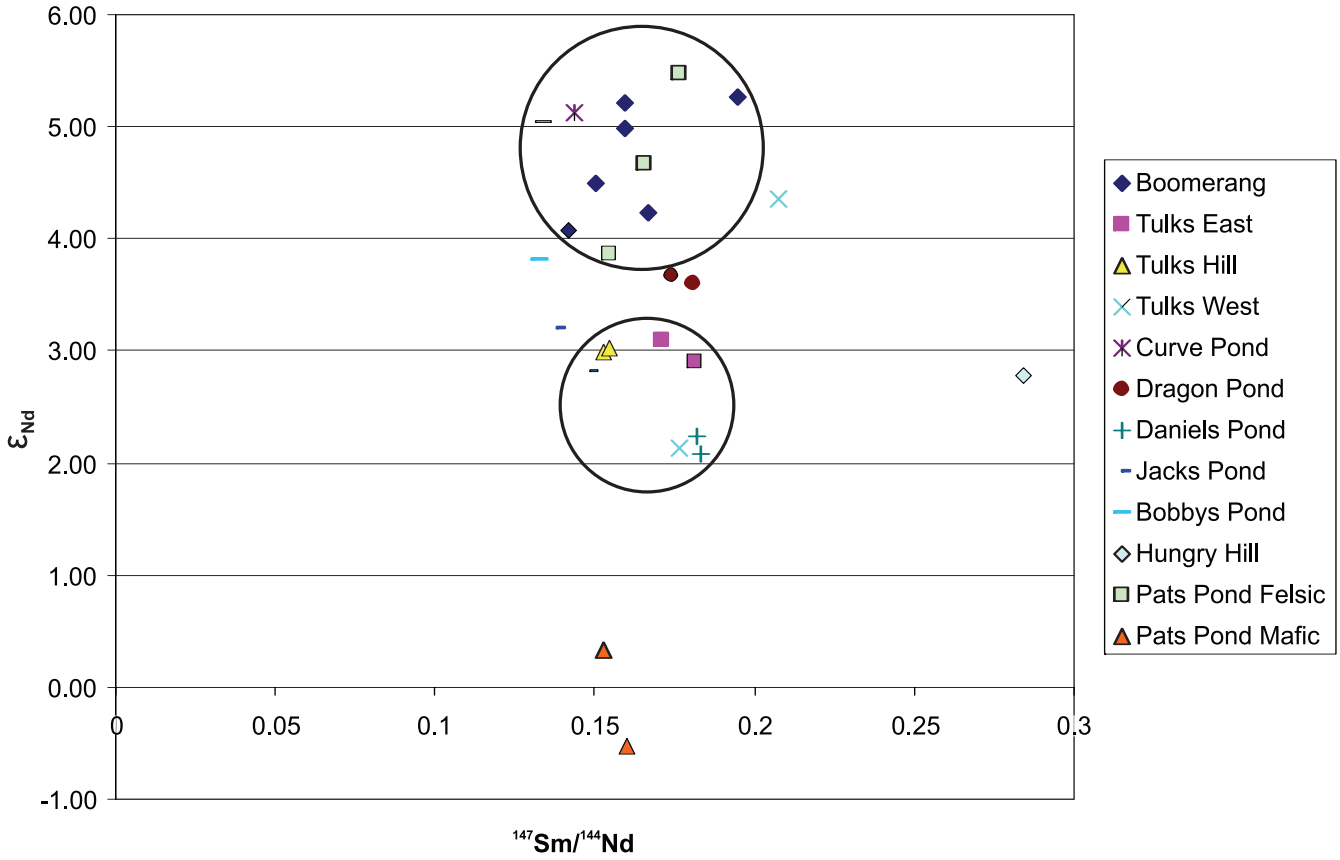

Figure 19. *εNd versus $^{147}Sm/^{144}Nd$ plot illustrating the range of values from rocks hosting VMS deposits and occurrences in the TVB.*

Tulks Hill Deposit

Host Rock Geochemistry

The rocks hosting the Tulks Hill deposit are dominated by quartz-phyric rhyolite, with minor amounts of quartz-phyric crystal tuff, quartz–feldspar-crystal tuff and lapilli tuff. Rhyolites from the hangingwall and footwall have relatively high average Zr/TiO_2 values of 0.0928 and 0.0972, and low to moderate Nb/Y average ratios (0.06 and 0.08), suggestive of a subalkaline affinity (Table 1; Figure 15B). However, there appears to be at least two subgroups of rhyolite *viz.*, a group with relatively low HFSE and REE and a group with relatively higher HFSE and REE (*see* Figures 15B and 18C; not subdivided for the purposes of Table 1). Using this chemical differentiation, the average Zr/TiO_2 ratio of the enriched group is 0.1420 ± 0.0100, significantly higher than the other rhyolite. As there is no way to visually or petrographically distinguish these rocks, they have been combined in one group for comparison purposes. Felsic tuffs, from the hangingwall and footwall, have much lower Zr/TiO_2 ratio averages (0.0084 and 0.0460) compared to the rhyolite, and have similar Nb/Y ratios. Although not analyzed for REEs, a sample of a quartz–feldspar-crystal tuff from the hangingwall of the deposit also has a very high Zr/TiO_2 ratio (0.1512), similar to the subset of rhyolite described above (Figure 15B). The HFSE (*e.g.*, Zr, Hf, Y, Nb, Ta) contents of all the felsic to intermediate rocks are low to moderate, suggesting a volcanic-arc to ocean-ridge-type setting on the Ta *vs.* Yb discrimination diagram (Figure 16B). Primitive-mantle-normalized plots for the felsic-intermediate rocks are characterized by moderate to strong LREE enrichment (*see* the La_N/Sm_N ratios in Table 1 and Figures 17B, and 18C), slight depletion in MREE resulting in slightly concave upward patterns (refer to the Gd_N/Lu_N values in Table 1, and Figures 17B, and 18C), moderate overall REE fractionation, strongly negative Nb and Ti anomalies, slightly negative Eu anomalies, and relatively flat Zr and Hf. Most of the felsic to intermediate rocks have very low Zr/Y and La/Yb values and are similar to published values for tholeiitic rocks (Barrett and MacLean, 1999; Table 1). The Sm–Nd isotopic composition analysis of two samples of felsic tuff yielded εNd (498 Ma) values of +2.99 and +3.02 (Figure 19, Table 2).

Mafic volcanic rocks from Tulks Hill are characterized by weak to moderately fractionated extended trace-element plots, with values four to ten times that of primitive mantle

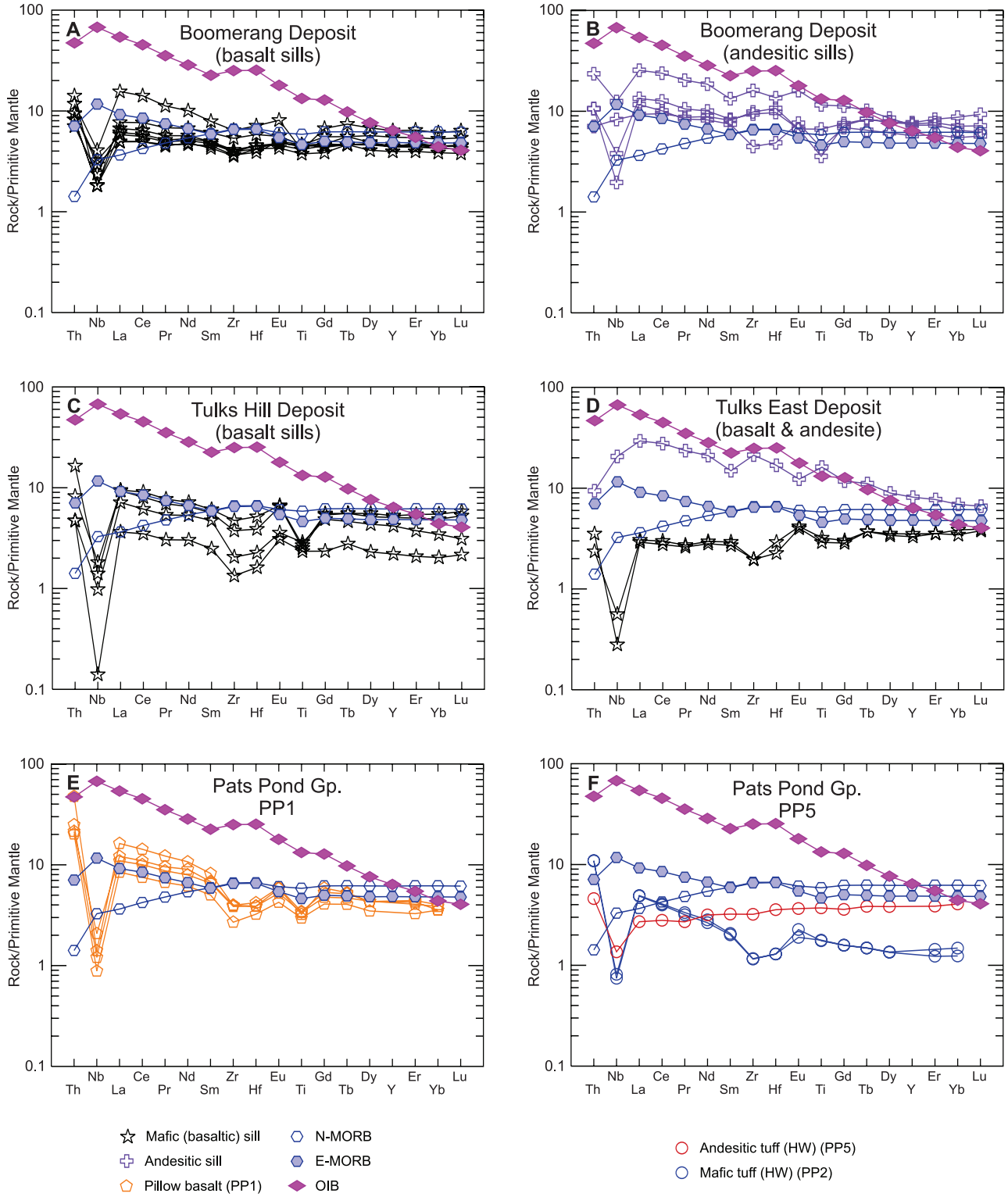

Figure 20. *Primitive-mantle-normalized trace-element plots for mafic to intermediate volcanic rocks of the southern Tulks Volcanic Belt and Pats Pond group rocks. A. Boomerang deposit basaltic sills, B. Boomerang deposit andesitic sills, C. Tulks Hill deposit basaltic sills, D. Tulks East deposit basalt and andesite, E. Pats Pond group (PP) 1 basalt, F. PP2 basalt and mafic tuff and PP5 mafic tuff. Pats Pond group chemistry from Rogers (2004) and Zagorevski (2006). Shown for comparison are N-MORB, E-MORB and OIB. Primitive mantle, N-MORB, E-MORB and OIB values from Sun and McDonough (1989). N-MORB–mid-ocean-ridge basalt, E-MORB–enriched mid-ocean-ridge basalt, OIB–ocean island basalt.*

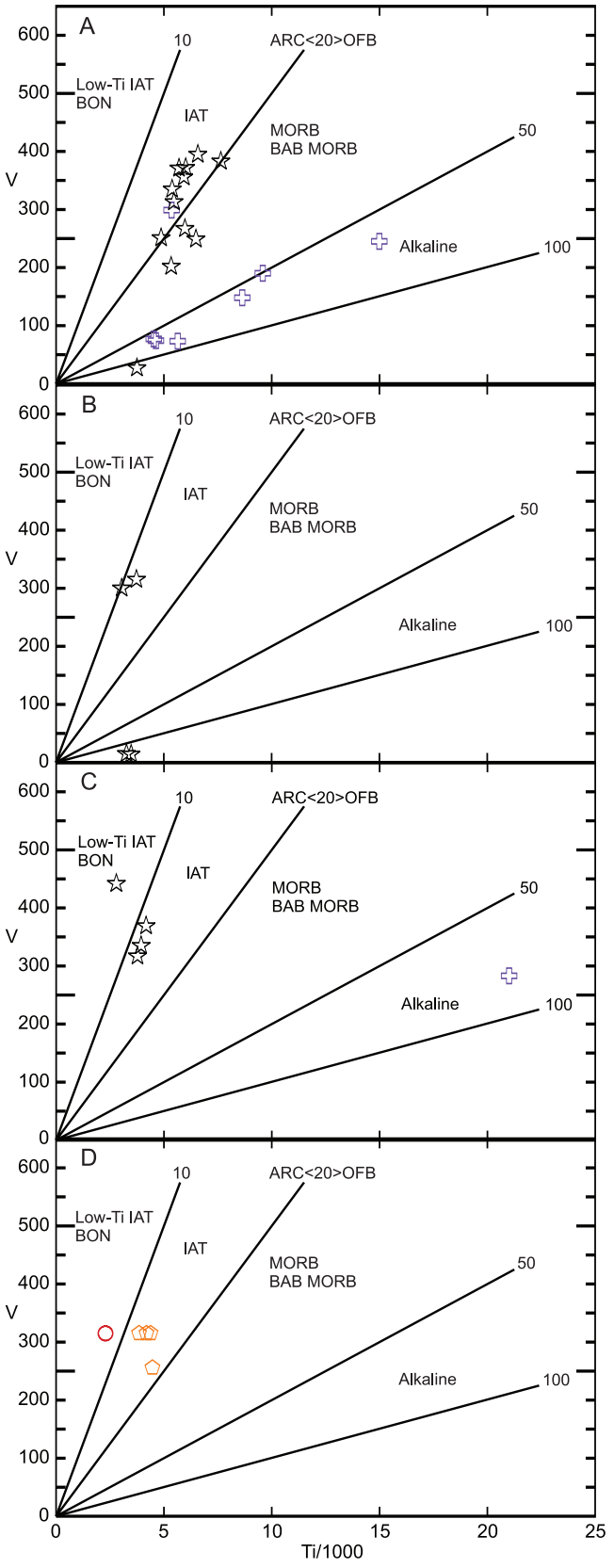

Figure 21. *Ti–V discrimination plot with field boundaries from Shervais (1982) for mafic rocks of the southern TVB and Pats Pond group. Pats Pond group chemistry from Rogers (2004) and Zagorevski (2006). BON–boninite, IAT–island-arc tholeiite, MORB–mid-ocean-ridge basalt, BABB–back-arc-basin basalt. A. Boomerang deposit; B. Tulks Hill deposit; C. Tulks East deposit; and D. Pats Pond group.*

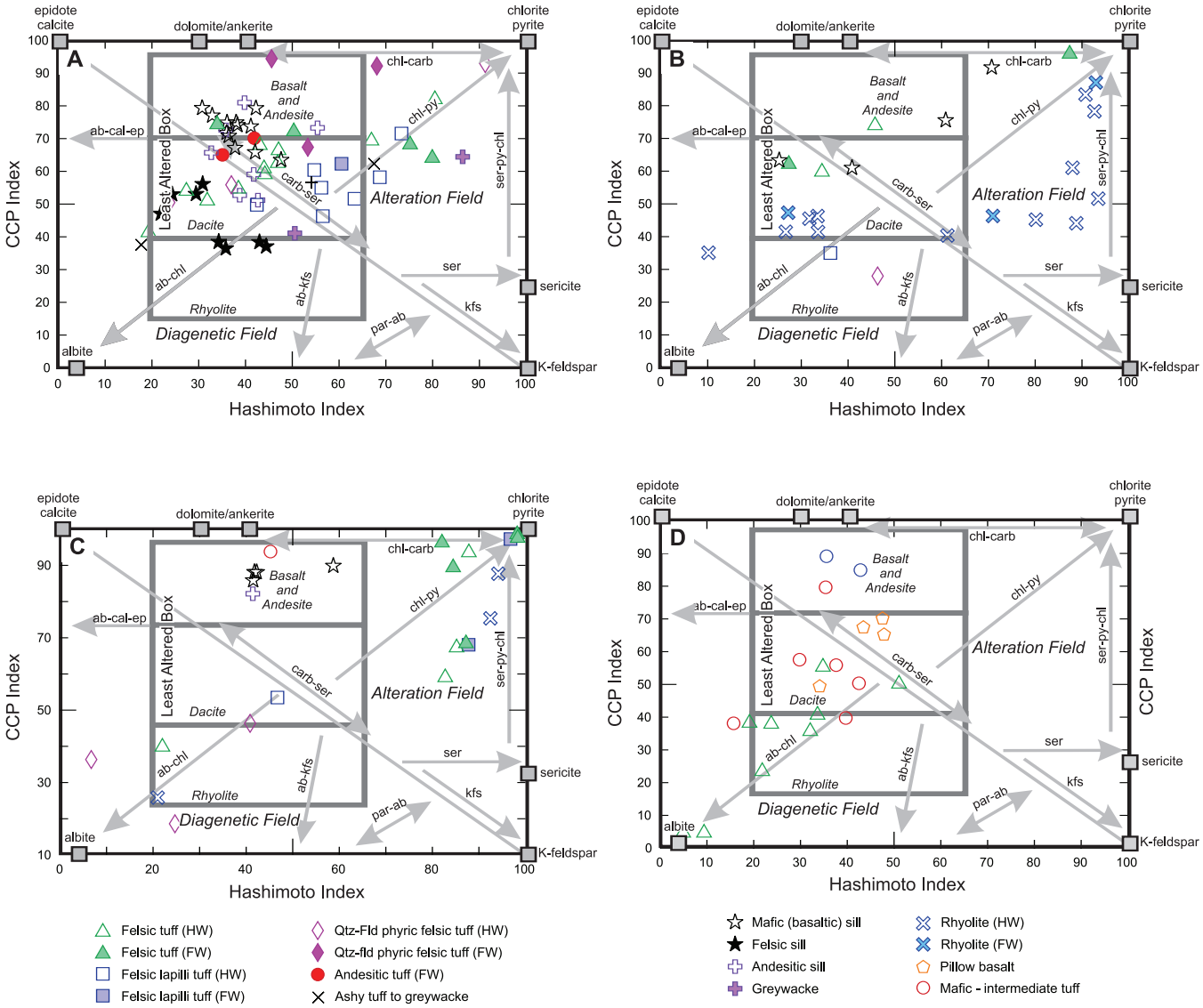

Figure 22. *Alteration box plots of Large* et al. *(2001), with vectors for various alteration minerals and alteration versus diagenetic fields. CCPI–chlorite-carbonate-pyrite index. A. Boomerang deposit, B. Tulks Hill deposit, C. Tulks East deposit, D. Pats Pond group. AI = Hashimoto index = 100*[(MgO+K_2O)/(MgO+K_2O+Na_2O+CaO)] (Ishikawa* et al.*, 1976), CCPI–chlorite-carbonate-pyrite index = 100*[(MgO+FeO*]/(MgO+FeO*+K_2O+Na_2O)] (Large* et al.*, 2001).*

concentrations (Figure 20C). Samples all have a strongly negative Nb anomaly, a strong negative Ti anomaly in two of the four samples, a slightly positive Eu anomaly, and negative Zr and Hf anomalies. Consequently, these samples can be divided into two groups with calc-alkaline basalt or island-arc tholeiite signatures. On a Ti–V discrimination diagram, the two populations are clearly shown, *i.e.*, the two mafic volcanic samples with the island-arc tholeiite signatures plot in the same field, whereas those with calc-alkaline basalt signatures contain very little V and plot toward the bottom of the diagram (Figure 21B). On a Th–Zr–Nb plot (*after* Wood, 1980) all of the mafic volcanic samples plot in the arc-basalt field.

Alteration Geochemistry

The felsic to intermediate volcanic rocks from the Tulks Hill area show evidence of significant plagioclase destruction and sodium depletion in the footwall, and the immediate hangingwall. This zone of sodium depletion is commonly associated with increased iron and magnesium related to pyrite and chlorite formation and increased calcium related to carbonate alteration, as well as increased barium related to barite alteration.

Chemical and mineralogical changes attributed to hydrothermal alteration are illustrated in the alteration box

plot of Large *et al.* (2001; Figure 22B). As illustrated, many of the rhyolite samples plot well to the right of the least altered box, indicative of intense sericite–pyrite–chlorite alteration in both the hangingwall and footwall stratigraphies.

As with the Boomerang deposit, samples from both the hangingwall and footwall show some enrichment in thallium and antimony; however, the degree of enrichment is not to the same level as that at the Boomerang deposit.

Tulks East Deposit

Host Rock Geochemistry

The host rocks to the Tulks East deposit are bimodal. The felsic to intermediate host rocks are divided into crystal tuff, lapilli tuff, and rhyolite. Quartz-phyric crystal tuffs dominate both the hangingwall and footwall sequences, and samples from both have relatively low Zr/TiO_2 (0.0283 and 0.0272) and Nb/Y ratios (0.07 and 0.03), and indicate a subalkaline affinity (Table 1, Figure 15C). Felsic lapilli tuff from the hangingwall and footwall have similar Nb/Y ratios to the crystal tuff, and slightly lower Zr/TiO_2 ratios (0.0201 and 0.0189, respectively), whereas rhyolite from the hangingwall and footwall have similar Zr/TiO_2 but more variable Nb/Y ratios when compared with the crystal tuff. In comparison, quartz–feldspar crystal tuffs from the hangingwall have a distinctly higher Zr/TiO_2 ratio (0.0809) but similar Nb/Y ratios. However, the average is skewed by one sample with a high Zr/TiO_2 ratio. The HFSE (*e.g.*, Zr, Hf, Y, Nb and Ta) contents of all the felsic-intermediate rocks are low to moderate and are indicative of a volcanic-arc to ocean-ridge setting on the Ta *vs.* Yb tectonic discrimination diagram (Figure 16c). Primitive-mantle-normalized plots for the felsic-intermediate rocks (Figures 17C, and 18D), are characterized by weak to moderate LREE enrichments (with the exception of the footwall felsic tuffs that have a slight depletion), as shown by the La_N/Sm_N ratios in Table 1, slight depletions in MREE resulting in a slightly concave upward profile (refer to the Gd_N/Lu_N ratios in Table 1 and Figures 17C, and 18D), slight to moderate overall REE fractionations, strongly negative Nb and Ti anomalies, variably strong negative Eu anomalies, and slightly positive Zr and Hf anomalies. Most of the felsic to intermediate rocks have very low Zr/Y and La/Yb ratios, similar to published values for tholeiitic rocks (Barrett and MacLean, 1999; Table 1). The Sm/Nd isotopic analyses of two samples of felsic tuff yielded εNd (498 Ma) values of +2.90 and +3.10 (Figure 19, Table 2).

The mafic volcanic rocks from Tulks East are characterized by relatively flat, extended trace-element plots, with concentrations that are three to four times that of primitive mantle (Figure 20D). Samples display a strong negative Nb anomaly, a slight positive Eu anomaly, and slightly negative Zr and Hf anomalies. The one sample of an andesitic sill has a unique chemistry with a downward concave, extended trace-element profile, similar to that associated with ocean-island or back-arc-basin basalt. On a Ti–V discrimination diagram, the mafic volcanic rocks plot predominantly in the island-arc tholeiite field, whereas the lone sample of an andesitic sill plots in the alkaline field (Figure 21C). On a Th–Zr–Nb plot (*after* Wood, 1980) the mafic volcanic rocks plot predominantly in the arc-basalt field with the one sample of the andesitic sill plotting at the N-MORB to E-MORB boundary.

Alteration Geochemistry

The Tulks East deposit shows evidence of significant plagioclase destruction and sodium depletion in both the footwall felsic volcanic rocks as well as in the immediate hangingwall felsic volcanic rocks. Sodium depletion is associated with a mass gain of magnesium, and to a lesser extent iron, related to chlorite and pyrite alteration, respectively. Carbonate alteration is fairly minor as indicated by negligible increases in calcium, whereas barium is elevated in the immediate hangingwall relative to the footwall (Figure 9B).

The bulk of the felsic volcanic rocks, both felsic tuff as well as rhyolites, are strongly displaced toward the upper right hand corner of the alteration box plot diagram, outside of the area associated with least altered rock types, indicative of extensive chlorite–pyrite–sericite alteration (Figure 22C). A small subset of felsic to intermediate samples also appear to be trending to the bottom left portion of the diagram, toward the diagenetic albite portion of the diagram, indicative of regional alteration processes.

Volatile element enrichments or haloes, such as antimony and thallium, appear to be more pronounced and developed in the hangingwall felsic volcanic rocks relative to the footwall felsic volcanic rocks (Figure 9B), and are perhaps indicative of the sub-seafloor replacement mechanism for ore formation. Such volatile haloes in hangingwall rocks are not uncommon (*e.g.*, Rosebery and Hellyer deposits, Australia; Large *et al.*, 2001).

Pats Pond Group

The Pats Pond group, as defined by Zagorevski *et al.* (2007a), has been divided into six stratigraphic subunits. For the purposes of this report, the chemistry will be discussed based on rock type, to be consistent with the descriptions of the other deposits herein.

Felsic to intermediate rocks of the Pats Pond group are hosted within the PP4 and PP6 subunits. Subunit PP4 consists of quartz ± feldspar, felsic-intermediate tuffs, and is characterized by relatively low Zr/TiO_2 (0.0139) and Nb/Y (0.05) ratios, placing the samples in the subalkaline andesitic field (Figure 15D). The HFSE (Zr, Hf, Y, Nb, Ta) contents of all the felsic to intermediate rocks are low to moderate, characterizing them as volcanic-arc rocks on the Ta *vs.* Yb tectonic discrimination diagram (Figure 16D). Primitive-mantle-normalized plots for subunit PP4 are characterized by moderate LREE enrichments (refer to the La_N/Sm_N ratios in Table 1 and Figures 17D, and 18E), moderate depletion of MREE, weak overall REE fractionations, moderate to strong negative Nb and Ti anomalies, slightly negative Eu anomalies, and negligibly negative Zr and Hf anomalies (Figure 17D). Subunit PP4 has low Zr/Y and La/Yb values, similar to published values for tholeiitic rocks (Barrett and MacLean, 1999; Table 1). Two Sm–Nd isotopic composition analysis yielded εNd (487 Ma) values of +4.7 and +5.5 (Figure 19, Table 2).

Subunit PP6 consists of high-silica trondhjemitic rhyolite and has much higher Zr/TiO_2 and similar Nb/Y relative to subunit PP4 (Figure 15D). The HFSE (Zr, Hf, Y, Nb, Ta) contents of these rocks are low to moderate, plotting on the boundary of volcanic-arc and ocean-ridge-type rocks on the Ta *vs.* Yb tectonic discrimination diagram (Figure 16D). Primitive-mantle-normalized plots for subunit PP6 are characterized by moderate LREE enrichments (refer to the La_N/Sm_N ratios in Table 1 and Figure 17E), moderate depletion of MREE, weak overall REE fractionations, moderate to strong negative Nb and Ti anomalies, negative Eu anomalies, and prominent positive Zr and Hf anomalies (Figure 17E). A Sm–Nd isotopic composition analysis yielded εNd (487 Ma) of +3.86 (Figure 19, Table 2).

Andesitic tuff of subunit PP3 was used to date the Pats Pond group (Zagorevski *et al.*, 2007a). These rocks consist of feldspar ± quartz, felsic-intermediate tuffs and have very similar chemical characteristics to subunit PP4.

Mafic to intermediate volcanic rocks of the Pats Pond group consist of subunits PP1, PP2 and PP5 of Zagorevski *et al.* (2007a). Subunit PP1 consists of transitional calc-alkaline basaltic andesite to island-arc tholeiite where the mafic volcanic rocks have strong, enriched LREE's, strong Th enrichment, prominent negative Nb anomalies, slight negative Ti anomalies, and negative Zr and Hf anomalies (Figure 20E). Andesitic sills have much higher concentrations of HFSE and REE, display higher degrees of REE fractionation, and have variably moderate to strong negative Nb and Ti anomalies and suggest a transitional calc-alkaline basalt to island-arc tholeiite signature. On a Ti–V discrimination diagram, the mafic volcanic samples plot predominantly within the island-arc tholeiite field (Figure 21D), and on a Th–Zr–Nb plot (*after* Wood, 1980) the mafic volcanics all plot in the arc-basalt field. The Sm–Nd isotopic composition analysis of two samples of subunit PP1 yielded εNd (488Ma) values from +0.33 to -0.53 (Figure 19, Table 2).

Subunit PP2 consists of calc-alkaline basalt and mafic tuffs. This subunit has similar chemistry to subunit PP1, with the exception that it has an overall lower abundance of HFSE and REE and it lacks the negative Ti anomaly (Figure 20F). Subunit PP5 consists of an intermediate to mafic tuff and has chemical characteristics similar to those of the mafic volcanic rocks of the Boomerang deposit. Subunit PP5 has fairly flat to weakly depleted LREE, with overall flat extended trace-element patterns, and values two to three times that of primitive mantle concentrations. The chemical profile parallels that for N-MORB, although with overall lower element concentrations. The unit displays a moderately positive Th anomaly and a moderately negative Nb anomaly, and as such has an island-arc tholeiite signature.

NORTHERN TULKS VOLCANIC BELT

Daniels Pond Deposit

Host Rock Geochemistry

Host rocks at the Daniels Pond deposit are dominanted by intermediate to mafic compositions. As indicated above, the level of alteration has led to confusion and misidentification of many outcrop and drillcore samples, *i.e.*, many samples originally classified as felsic are actually intermediate to mafic in composition. Andesitic to mafic volcanic rocks within the stratigraphy have been divided on the basis of stratigraphic position, petrographic and alteration attributes, and lithogeochemistry, and this has resulted in the identification of four populations, namely:

1) unaltered andesitic tuff in the hangingwall,
2) volumetrically dominant, andesitic tuff in the footwall,
3) relatively unaltered andesitic tuff in the immediate footwall, and
4) intensely altered andesitic tuff in the footwall.

Based upon immobile element systematics (*see* discussion above), it appears that these groups reflect different groups of rocks rather than variations of a single protolith due to alteration processes. There are also minor amounts of intermediate lapilli tuffs, felsic tuffs and mafic sills in the stratigraphy.

The hangingwall andesites are distinguishable from the footwall andesites by their relatively high Zr/TiO_2 (average of 0.0114) and Nb/Y (average of 0.56). In contrast, the typ-

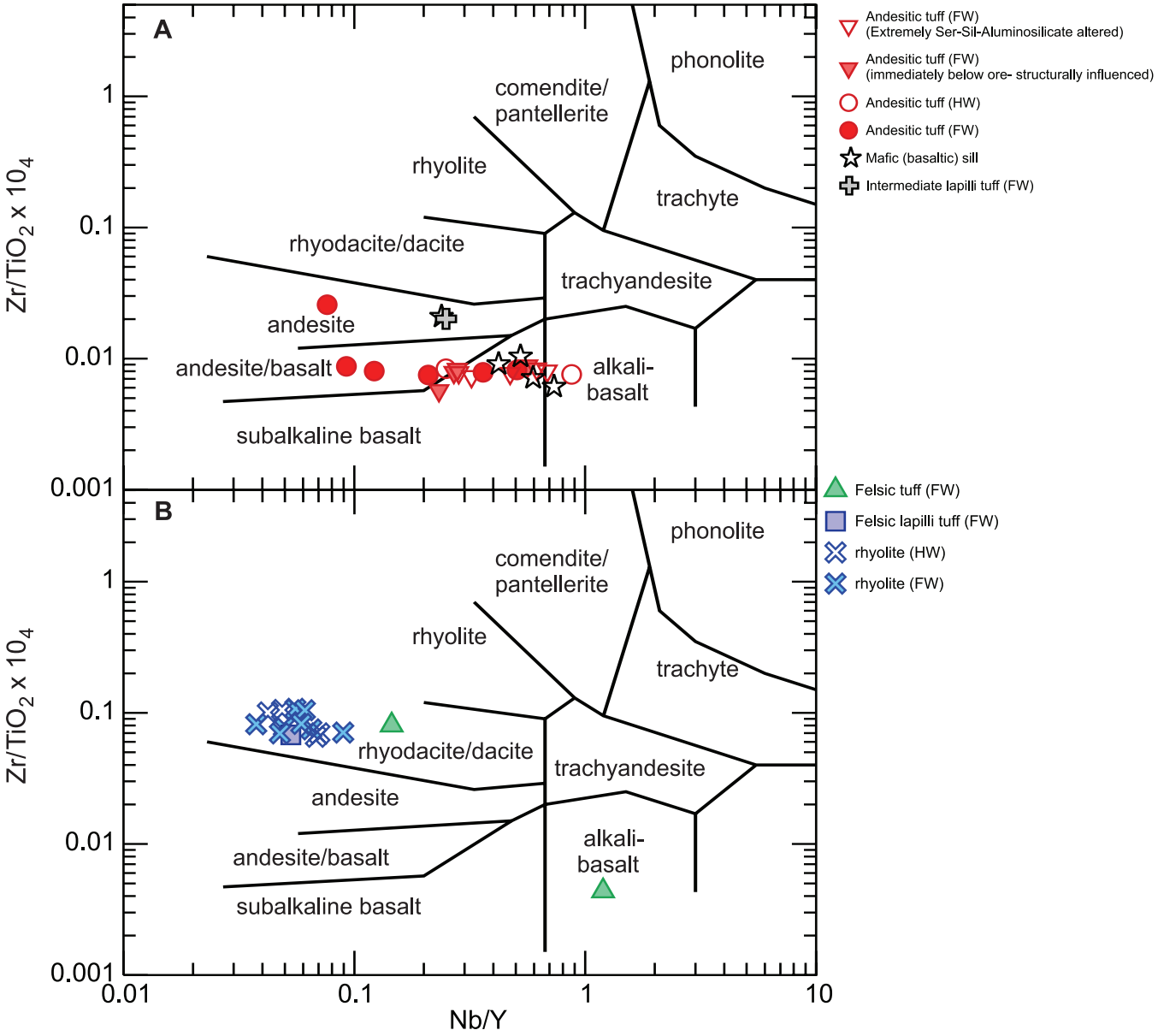

Figure 23. *Nb/Y versus Zr/TiO$_2$ rock type classification diagram (Winchester and Floyd, 1977). A. Daniels Pond deposit; and B. Bobbys Pond deposit. HW–hangingwall, FW–footwall.*

ical footwall andesitic tuff has an average Zr/TiO$_2$ ratio of 0.0091 and a lower average Nb/Y of 0.23. In contrast, the extremely altered andesitic tuff and the andesitic tuff in the immediate footwall have lower average Zr/TiO$_2$ ratios of 0.0076 and 0.0078, respectively, and intermediate average Nb/Y values of 0.44 and 0.33, respectively (Table 1, Figure 23A). In contrast to all other deposits in the TVB that are hosted by more felsic rocks, the andesitic host rocks at the Daniels Pond deposit have lower Zr/TiO$_2$ and higher Nb/Y values. The subordinate intermediate lapilli tuff and felsic ash and crystal tuff within the sequence have Zr/TiO$_2$ and Nb/Y ratios similar to those at the other deposits (Table 1, Figures 15 and 23A). The HFSE (Zr, Hf, Y, Nb, Ta) contents of all the host rocks are low to moderate, and indicate a volcanic-arc to ocean-ridge tectonic setting; see the Ta *vs.* Yb diagram (Figure 24A). Primitive-mantle-normalized plots successfully discriminate amongst the various populations of andesitic tuffaceous rocks described above. The two samples from the hangingwall andesitic tuffs have moderate LREE enrichments (refer to the La$_N$/Sm$_N$ ratios in Table 1 and Figure 25A), relatively flat MREE patterns, with one sample that has positive Zr and Hf anomalies, and one sample that has a moderately negative Ti anomaly (Figure 25A). The volumetrically dominant andesitic tuff from the footwall is characterized by weak to moderate LREE enrichments, as shown by the La$_N$/Sm$_N$ ratios in Table 1, slight

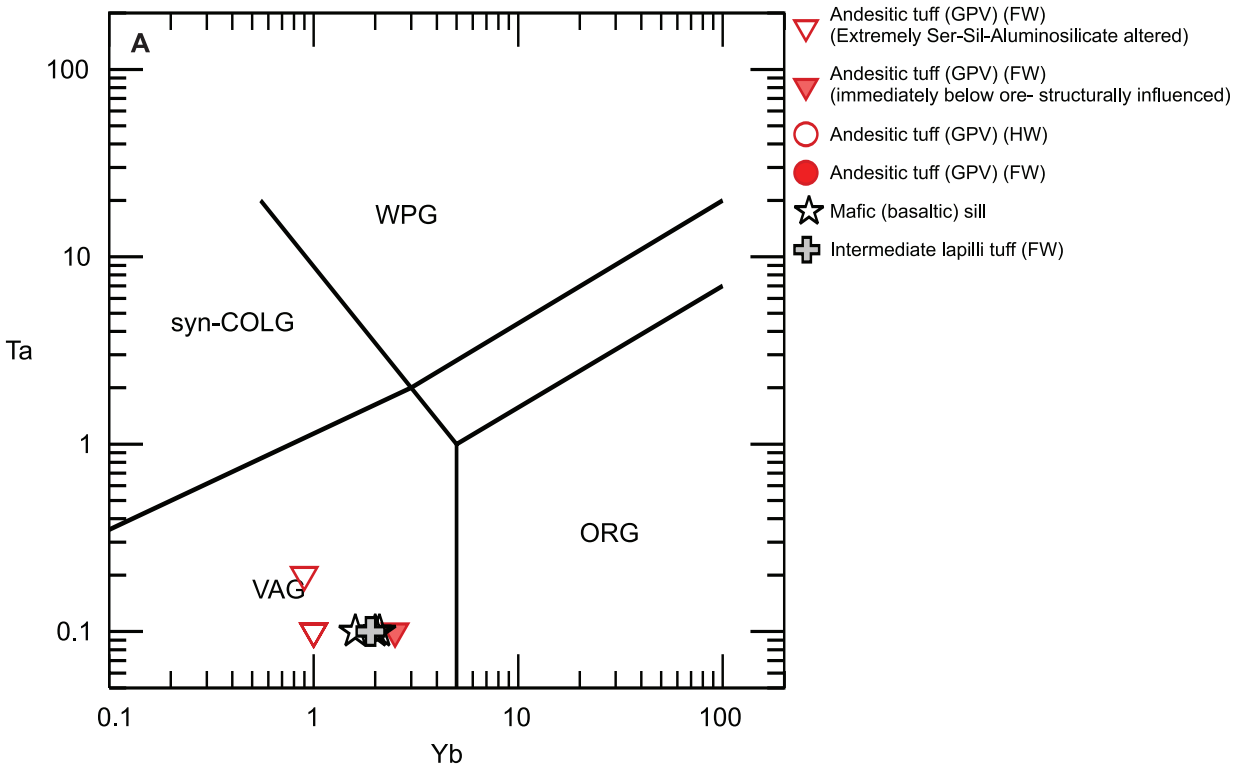

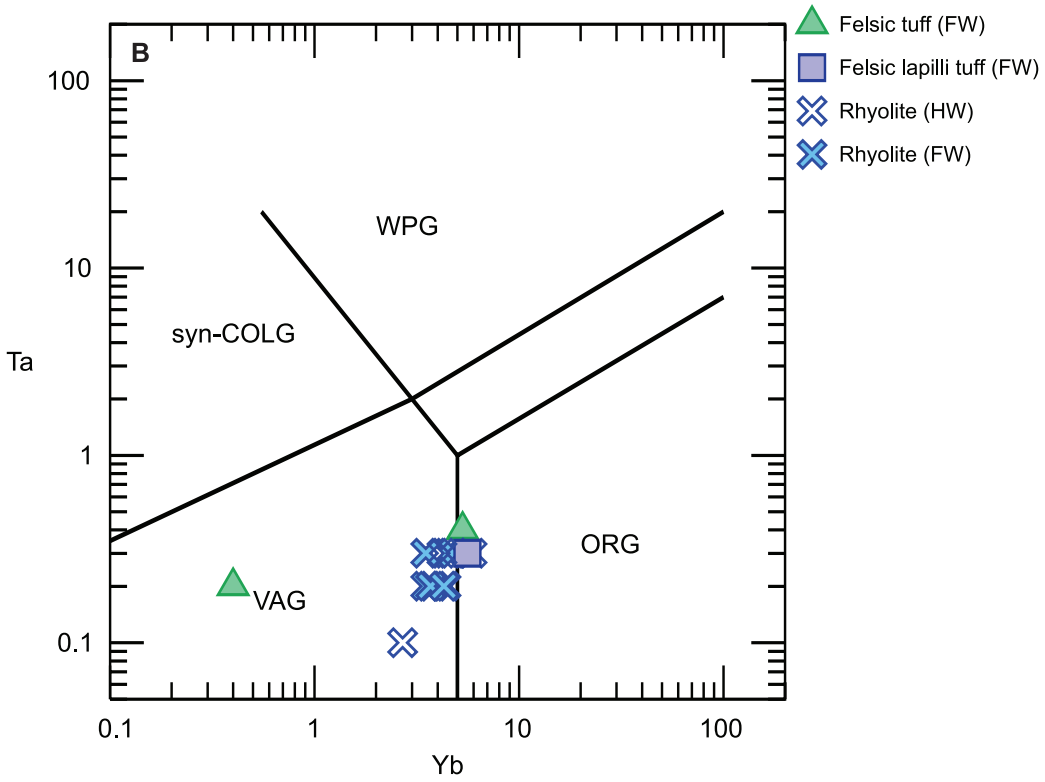

Figure 24. *Yb versus Ta (Pearce* et al.*, 1984) discrimination diagrams for the host felsic volcanic rocks from A. Daniels Pond deposit; and B. Bobbys Pond deposit.*

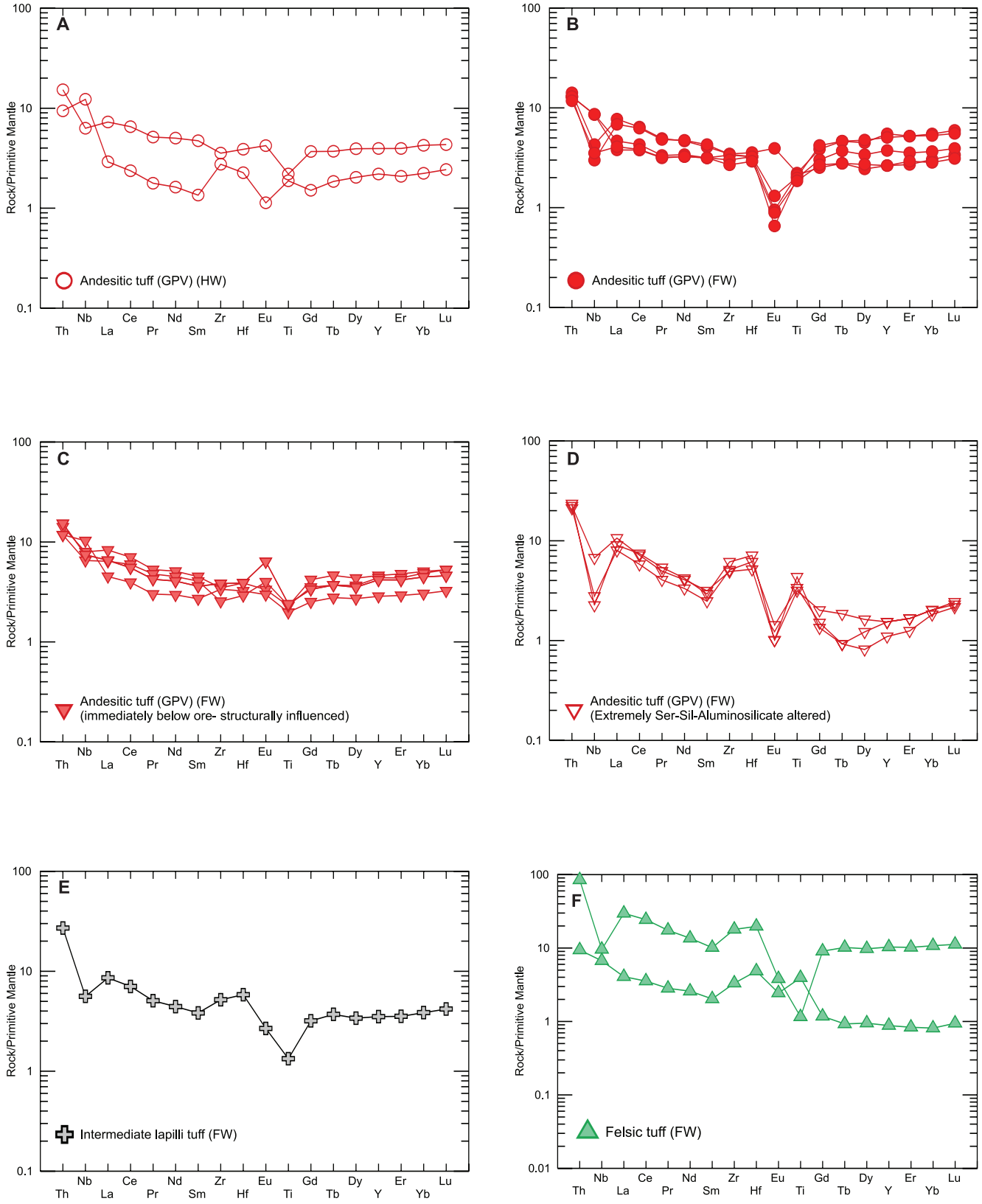

Figure 25. *Primitive-mantle-normalized extended trace-element plots for northern TVB felsic-intermediate rocks. A–E (Daniels Pond), F+G (Bobbys Pond). Normalizing values from Sun and McDonough (1989). HW–hangingwall, FW–footwall.*

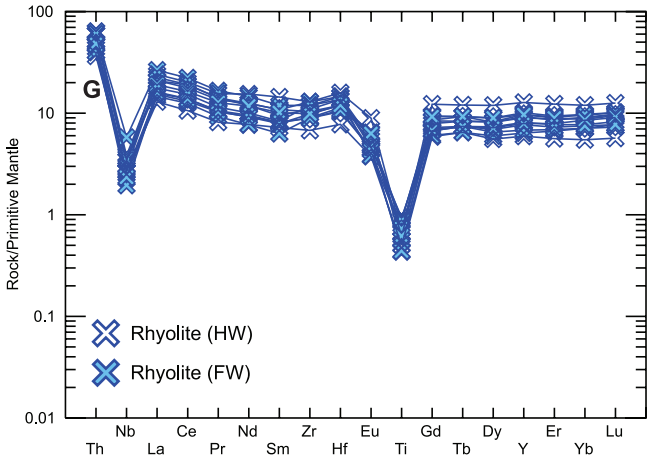

Figure 25 (Continued). *Primitive-mantle-normalized extended trace-element plots for northern TVB felsic-intermediate rocks. A–E (Daniels Pond), F+G (Bobbys Pond). Normalizing values from Sun and McDonough (1989). HW–hangingwall, FW–footwall.*

depletions in MREE resulting in slightly concave upward patterns (refer to the Gd_N/Lu_N ratios in Table 1 and Figure 25B), slight overall REE fractionations, negative Nb and Ti anomalies for all but two samples, and strongly negative Eu anomalies for all but one sample. The andesitic tuffs from immediately below the ore horizon have very similar primitive-mantle-normalized patterns to the dominant andesite except that they lack the prominent negative Nb anomalies, and have flat to positive Eu anomalies (Figure 25C). The variations in Eu anomalies may be attributable to effects of plagioclase fractionation, whereas the variable Nb anomaly most likely reflects a primary compositional variation. In contrast to other andesitic rock units in the footwall, the samples with extreme sericite–silica–aluminosilicate alteration have primitive-mantle-normalized extended trace-element patterns that are distinctly different. Specifically, they have moderate to strong LREE enrichment, as shown by the average La_N/Sm_N ratio of 3.02 in Table 1, slight depletions in MREE causing the slightly concave upward patterns (refer to the Gd_N/Lu_N ratios in Table 1 and Figure 25D), moderate to strong overall REE fractionations, strongly negative Nb and Eu anomalies, and positive Zr, Hf, and Ti anomalies. The intermediate lapilli tuff sample has a primitive-mantle-normalized extended trace-element pattern similar to that of the dominant andesitic tuff described above (Figure 25E). Most of the intermediate rocks have very low Zr/Y and La/Yb ratios, similar to published values for tholeiitic rocks (Barrett and MacLean, 1999; Table 1). The Sm–Nd isotopic composition analysis of two samples of the extremely altered andesitic tuff and the andesitic tuff from the immediate footwall yielded εNd (498 Ma) values of +2.23 and +2.08, respectively (Figure 19, Table 2).

The mafic volcanic rocks from the Daniels Pond deposit show some variation in chemical profiles ranging from weakly fractionated to relatively flat extended trace-element plots with moderately enriched Th and Nb, through to samples with moderate LREE enrichment and weak to moderately negative Nb and Ti anomalies (Figure 26). All of these samples have approximately four to ten times enrichment relative to primitive mantle concentrations. On a Ti–V discrimination diagram, the mafic volcanic samples fall predominantly within the island-arc tholeiite field with a few samples falling into the low Ti island-arc thoellite field (Figure 27). On a Th–Zr–Nb plot (*after* Wood, 1980) the mafic volcanics plot in a range between the arc-basalt field and the ocean island basalt field.

Alteration Geochemistry

The Daniels Pond deposit shows evidence of significant plagioclase destruction and sodium depletion in the footwall of VMS mineraliztion, with little to no alteration (sodium depletion) in the hangingwall (Figure 13). Sodium depletion is commonly associated with increased iron and magnesium related to pyrite and chlorite alteration in the footwall (Figure 13B).

The intermediate volcanic rocks in the hangingwall predominantly plot in the least altered box (Figure 28A). Surprisingly, the andesitic rocks from the immediate footwall (~1-5 m from the massive sulphide) also plot within the field of least altered rocks. In contrast, the typical andesitic rocks that dominate the footwall plot toward the upper right part of the diagram and indicate mixed chlorite–pyrite–sericite alteration. Samples of extremely altered andesite from the footwall plot at the bottom right part of the diagram, and indicate very intense sericite–muscovite–paragonite alteration. This distribution of the rock groups is supported, for the most part, by petrography.The extremely altered footwall rocks, *i.e.*, those with intense sericite–muscovite–paragonite alteration, appear to be disproportionally affected by structural shearing, which imparted a schistosity to these rocks. Given that the massive sulphides locally display evidence of being deformed (*e.g.*, isoclinally folded), it is possible that this alteration signature may be influenced by regional-scale structural and alteration events.

In addition to major-element variations related to VMS-associated hydrothermal alteration, some of the minor volatile elements are also enriched in the rocks immediately surrounding the VMS-bearing horizons. Of note, thallium and antimony are enriched in the rocks immediately around the ore horizon, with the strongest enrichment in the stratigraphic footwall rocks (Figure 13B; note overturned stratigraphy).

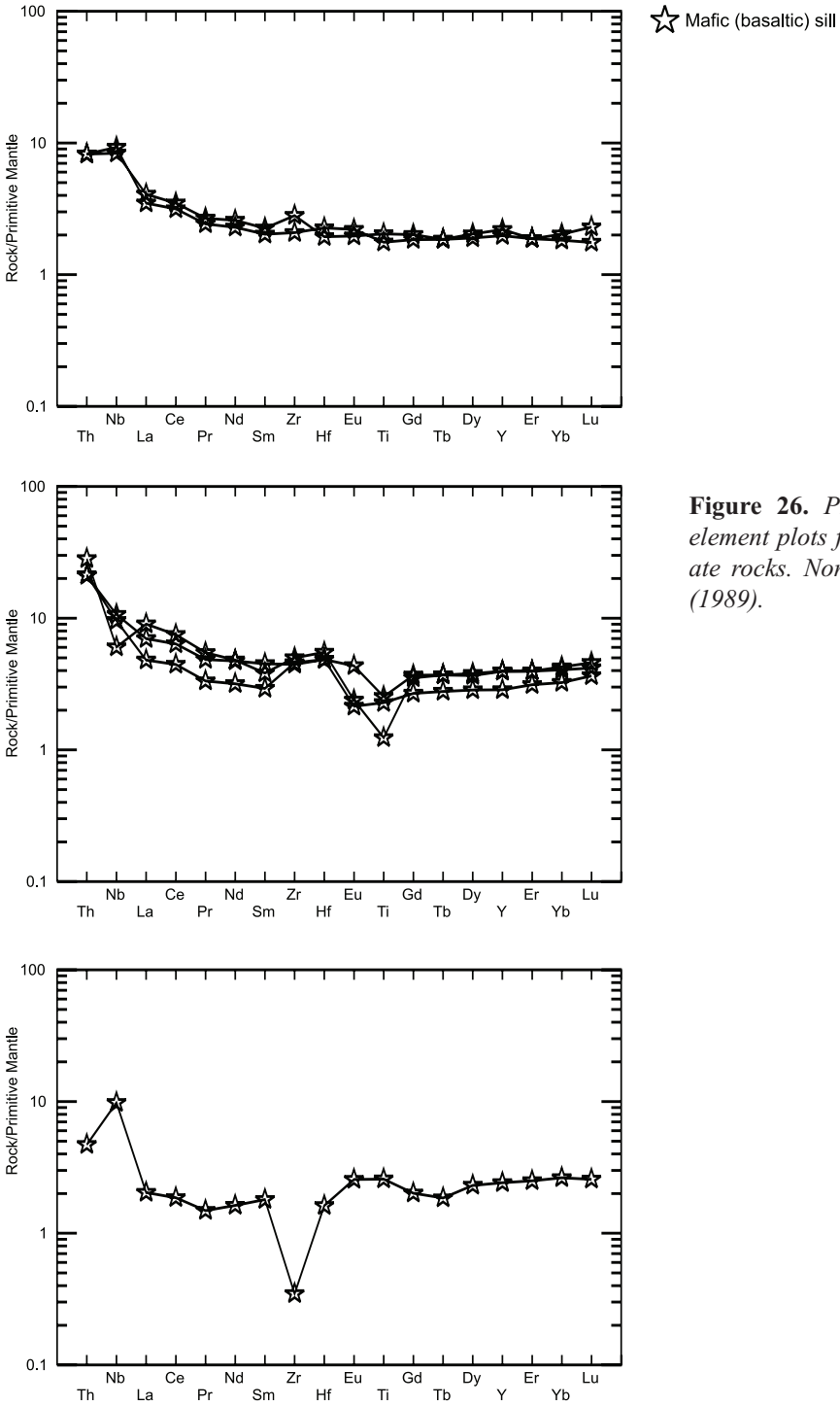

Figure 26. *Primitive-mantle-normalized extended trace-element plots for Daniels Pond deposit mafic to intermediate rocks. Normalizing values from Sun and McDonough (1989).*

Bobbys Pond Deposit

Host Rock Geochemistry

Unlike many of the previously described deposits, the host rocks to the Bobbys Pond deposit are predominantly felsic volcanic and are dominated by massive and coherent rhyolite, with subordinate amounts of tuffaceous rocks. The dominant rhyolitic host rocks from the Bobbys Pond deposit are most similar to those that host the Tulks Hill deposit. All of the felsic rocks at Bobbys Pond, with the exception of the felsic tuff in the footwall, have high Zr/TiO_2 ratios averaging 0.0700 to 0.0775 with Nb/Y averaging 0.05 to 0.06 (Figure 23B). In contrast, the felsic tuff from the footwall has an

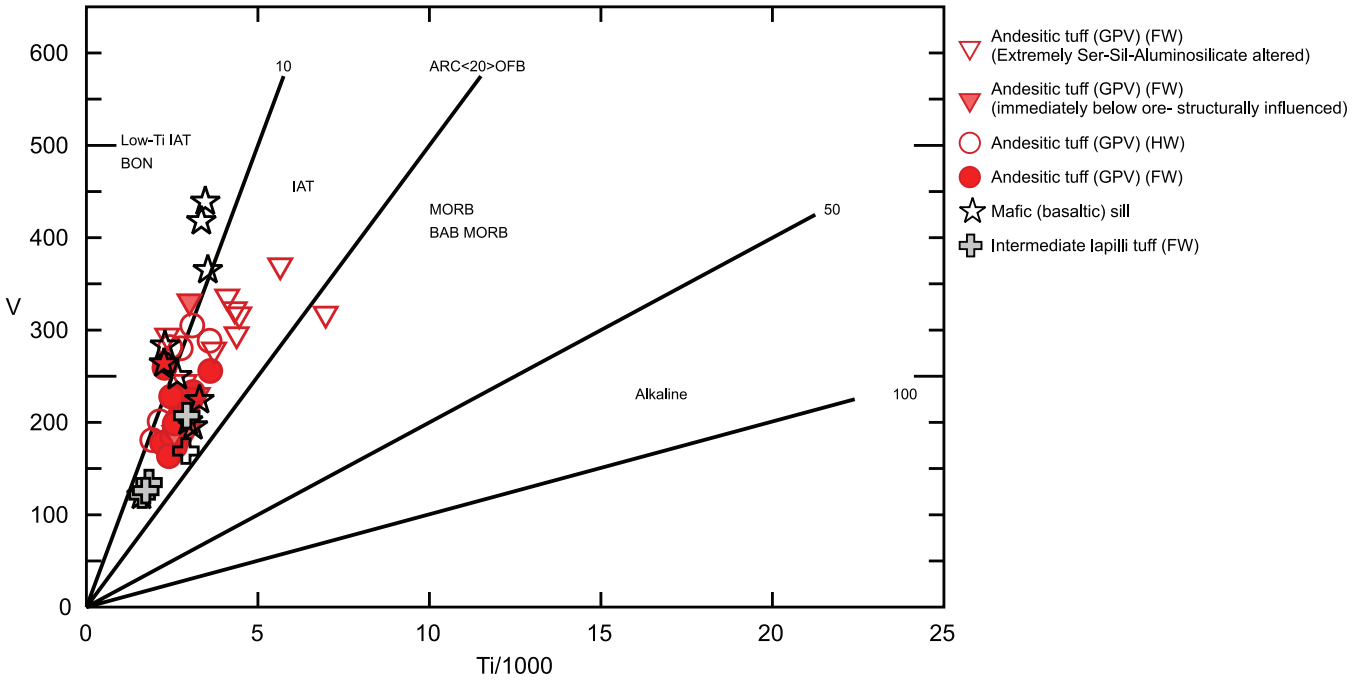

Figure 27. *Ti–V tectonic discrimination diagram from Shervais (1982) for mafic rocks from the Daniels Pond deposit, northern TVB. HW–hangingwall, FW–footwall.*

average Zr/TiO_2 of 0.0411 and an average Nb/Y ratio of 0.67. The HFSE (Zr, Hf, Y, Nb, Ta) contents of all the felsic-intermediate rocks are low to moderate, implying a volcanic-arc to ocean-ridge tectonic setting on the Ta *vs.* Yb diagram (Figure 24B). Primitive-mantle-normalized plots for these rhyolites are characterized by moderate to strong LREE enrichments (refer to the La_N/Sm_N ratios in Table 1 and Figure 25G), slight depletions in the MREE patterns, imparting a slightly concave upwards pattern, moderate REE fractionation, and strongly negative Nb and Ti anomalies (Figure 25G). Most of the rhyolites have relatively low Zr/Y and La/Yb ratios, similar to published values for tholeiitic rocks (Barrett and MacLean, 1999; Table 1). The Sm–Nd isotopic composition analysis of two samples of quartz and feldspar phyric rhyolite from the hangingwall and footwall yielded εNd (498Ma) values of +5.04 and +3.814, respectively (Figure 19, Table 2).

Alteration Geochemistry

The rocks hosting the Bobbys Pond deposit display variably intense, protolith dependant, alteration that is interpreted to result from variable competency, porosity, and permeability between massive flows and tuffaceous rocks. Felsic tuffs from the footwall show evidence of significant plagioclase destruction and replacement by sericite and overall sodium depletion. The sodium depletion in these tuffs is commonly associated with mass addition of iron and magnesium related to pyrite and chlorite alteration, increased calcium related to carbonate alteration, and increased barium related to barite alteration (Figure 14B). In contrast, most of the massive rhyolite, in both the hangingwall and footwall to the massive sulphide horizons, do not show evidence of significant sodium depletion. The exception to this is a small subset of samples from the immediate footwall (within 5 m of VMS) or from between sulphide lenses. As illustrated, the bulk of the felsic tuffaceous rocks, and a subset of the massive rhyolite in the immediate vicinity of the VMS horizon(s) have relatively high-alteration indicies and fall in the upper right part of the alteration box plot diagram, beyond the field of least altered samples (Figure 28B). These samples likely represent mixtures of sericite–chlorite–carbonate–pyrite alteration as supported by petrographic evidence. A small subset of rhyolitic host rocks, all from the footwall of the deposit, plot near the bottom left part of the alteration box plot diagram (Figure 28B), and are indicative of diagenetic albite, a mineralogical observation supported by petrographic examination. The presence of albite in the deeper parts of the footwall suggest Na enrichment, likely due to regional, rather than local, alteration processes. However, it should be noted that the identification of the hangingwall versus footwall stratigraphy at the Bobbys Pond deposit is complicated by structural modifications (*e.g.*, intense shearing, potential repetition of massive sulphide-bearing horizons, and the absence of a well-defined footwall alteration zone. The occurrence of samples with very strong alteration from the same stratigraphic interval that hosts samples with albitization leads to the conclusion

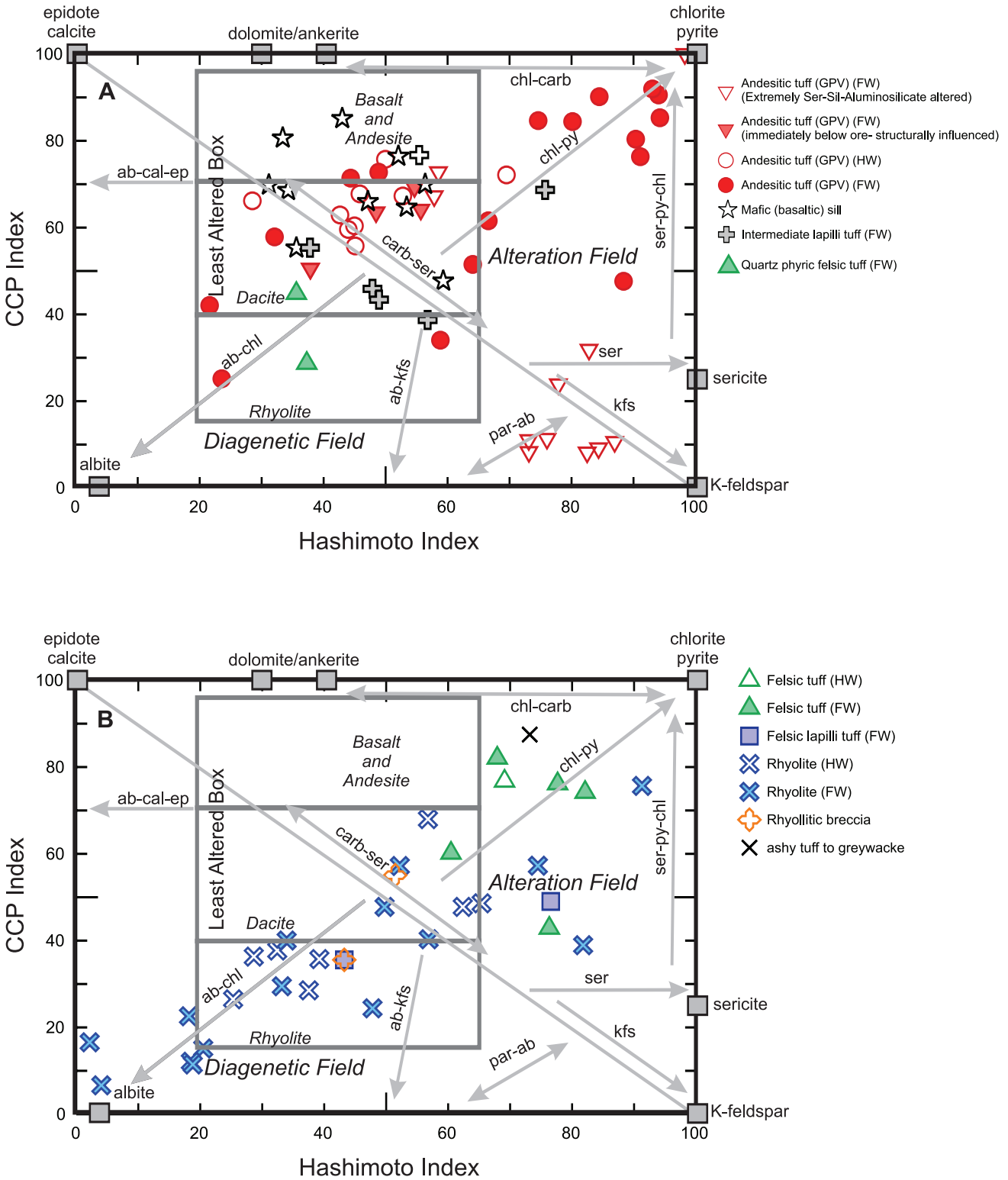

Figure 28. *Alteration box plots for rocks from Daniels Pond and Bobbys Pond deposits with vectors for various alteration minerals and alteration versus diagenetic fields (Large* et al.*, 2001). CCPI–chlorite-carbonate-pyrite index. A. Daniels Pond deposit; and B. Bobbys Pond deposit. HW–hangingwall, FW–footwall.*

that the albitization is occurring in the footwall. As with the other deposits studied, there are minor volatile element haloes (*e.g.*, Sb, Tl, *etc.*) associated with the VMS mineralization at the Bobbys Pond deposit (Figure 14B).

U–Pb GEOCHRONOLOGY

INTRODUCTION

All rocks within the TVB were originally considered to be of similar age based on a U–Pb date of 498 +6/-4 Ma, from a subvolcanic porphyry, located close to the Tulks Hill VMS deposit (Evans *et al*., 1990). However, recent mapping and geochronological studies by the GSC (Rogers *et al.*, 2005; van Staal *et al.*, 2005) have led to a modified interpretation of the TVB to define a series of generally westward-younging sequences of juxtaposed tectonostratigraphic belts, including the Tulks group (*ca.* 498 Ma), the Pats Pond group (*ca.* 488 Ma), the Sutherlands Pond group (*ca.* 462–457 Ma; Dunning *et al.,* 1987; Zagorevski *et al.*, 2008), and the Wigwam Brook group (*ca.* 453 Ma; van Staal *et al*., 2005; Zagorevski *et al*., 2007a). The Wigwam Brook group was dated from a sample of quartz and feldspar crystal tuff immediately south of Pats Pond, whereas the Sutherlands Pond group was dated from a number of localities in the Sutherlands Pond and Victoria River mouth areas in the northern TVB (Dunning *et al.,* 1987; Zagorevski *et al.*, 2008). The age of the Pats Pond group was obtained from a sample of bimodal breccia collected in the Burgeo Highway area, approximately 30 to 35 km southwest of the Boomerang deposit, in a package of rocks physically seperated from the Pats Pond group type section, and the rocks that host the Boomerang deposit. Thus, correlations are not simple, and many assumptions are involved.

Based upon the stratigraphy proposed by the GSC mapping, four of the main VMS occurrences in the TVB (Tulks East, Tulks Hill, Daniels Pond, and Bobbys Pond deposits) are interpreted to occur within the Jacks Pond formation of the Tulks group (van Staal *et al.*, 2005 and Lissenberg *et al.*, 2005), whereas the Boomerang deposit is interpreted to occur within the younger Pats Pond group (Zagorevski *et al.*, 2007a and van Staal *et al.*, 2005).

Geochronological studies were initiated in the TVB as part of this study in an attempt to further characterize the stratigraphy of the belt and constrain the timing of VMS mineralization. Although five samples of felsic tuffs, felsic sills, and rhyolite flows were collected, only two samples contained sufficient zircon for U–Pb age dating. Both samples were from the Boomerang deposit. The U–Pb geochronology analysis was conducted at the Geochronology Laboratory, of the Geological Survey of Canada, as part of a collaborative study with V. McNicoll. The work is discussed by Hinchey and McNicoll (2009).

ANALYTICAL METHODS

All samples selected for geochronological analysis were collected from drillcore. Heavy mineral concentrates were prepared by standard crushing, grinding, Wilfley table, and heavy liquid separation techniques, following which mineral separates were sorted by magnetic susceptibility using a Frantz™ isodynamic separator, all conducted by personnel at the Geochronology Laboratory of the Geological Survey of Canada.

The U–Pb Isotope Dilution-Thermal Ionization Mass Spectrometer (ID-TIMS) analytical methods utilized in this study are outlined in Parrish *et al.* (1987). Multigrain zircon fractions for TIMS analyses comprised between 10 to 25 grains (*see* Table 3) and were very strongly air abraded following the method of Krogh (1982). Details of zircon morphology and quality are summarized in Table 3. Treatment of analytical errors follows procedures outlined in Roddick (1987), with regression analysis modified from York (1969). The U–Pb TIMS analytical results are presented in Table 3, where errors on the ages are reported at the 2σ level, and displayed in a concordia plot (Figure 29A).

The Sensitive High Resolution Ion MicroProbe (SHRIMP II) analyses were conducted using analytical and data reduction procedures described by Stern (1997) and Stern and Amelin (2003). Zircons from the samples and fragments of the GSC laboratory zircon standard (z6266 zircon, with $^{206}Pb/^{238}U$ age = 559 Ma) were cast in an epoxy grain mount (mount IP419), polished with diamond compound to reveal the grain centres, and photographed in transmitted light. The mount was evaporatively coated with 10 nm of high-purity Au, and the internal features of the zircons were characterized with backscattered electrons (BSE) utilizing a scanning electron microscope (SEM). Analyses were conducted using an O^- primary beam projected onto the zircons with an elliptical spot size of 25 μm (in the longest dimension). The count rates of ten isotopes of Zr^+, U^+, Th^+, and Pb^+ in zircon were sequentially measured using a single electron multiplier. Off-line data processing was accomplished using customized GSC software. The SHRIMP II analytical data is presented in Table 4. Common Pb-corrected ratios and ages are reported with 1σ analytical error, which incorporate an external uncertainty of 1.1% in calibrating the standard zircon (*see* Stern and Amelin, 2003). The $^{206}Pb/^{238}U$ ages for the analyses have been corrected for common Pb using both the 204- and 207-methods (Stern,

Table 3: U-Pb TIMS analytical data

Fract.[1]	Description[2]	Wt.	U	Pb[3]	$^{206}Pb/^{204}Pb$[4]	Pb[5]	$^{208}Pb/^{206}Pb$	Isotopic Ratios[6]							Ages (Ma)[8]					
								$^{207}Pb/^{235}U$	±1SE Abs	$^{206}Pb/^{238}U$	±1SE Abs	Corr.[7] Coeff.	$^{207}Pb/^{206}Pb$	±1SE Abs	$^{206}Pb/^{238}U$	±2SE	$^{207}Pb/^{235}U$	±2SE	$^{207}Pb/^{206}Pb$	±2SE	% Disc
		ug	ppm	ppm		pg														
JHC-06-239 (z9127): Ash/lapilli tuff, Boomerang deposit																				
A1 (Z;21)	Co,Clr,fln,fFr,Eu,El, Dia	30	36	3	106	63	0.21	0.70382	0.01320	0.08164	0.00042	0.700	0.06253	0.00097	505.9	5.0	541.1	15.7	692.1	65.1	28.0
A2 (Z;20)	Co,Clr,fln,fFr,Eu,El, Dia	40	57	5	407	29	0.19	0.62881	0.00278	0.07946	0.00012	0.698	0.05739	0.00020	492.9	1.5	495.4	3.5	506.7	15.4	2.8
A3 (Z;21)	Co,Clr,fln,fFr,Eu,El, Dia	41	81	7	372	47	0.18	0.63199	0.00312	0.07989	0.00013	0.709	0.05738	0.00023	495.5	1.6	497.3	3.9	506.0	17.3	2.2
B1 (Z;19)	Br,Clr,fln,fFr,Eu,Pr,Dia	33	59	5	400	25	0.19	0.62987	0.00285	0.07949	0.00013	0.700	0.05747	0.00021	493.1	1.5	496.0	3.6	509.6	15.7	3.4
B2 (Z;25)	Co,Clr,fln,fFr,Eu,Pr,Dia	40	83	7	253	70	0.18	0.63532	0.00430	0.07980	0.00017	0.702	0.05774	0.00032	494.9	2.0	499.4	5.3	520.0	23.9	5.0
C1 (Z;10)	Br,Clr,fln,fFr,Eu,St,Dia	33	64	5	673	16	0.18	0.63209	0.00179	0.07932	0.00011	0.686	0.05779	0.00012	492.1	1.3	497.4	2.2	521.9	9.4	5.9
C2 (Z;15)	Co,Clr,fln,fFr,Eu,St,Dia	60	99	8	266	12	0.17	0.66413	0.00690	0.07993	0.00017	0.530	0.06026	0.00057	495.7	2.0	517.1	8.4	612.9	40.2	19.9

Notes:

[1]Z=zircon. Number in bracket refers to the number of grains in the analysis.

[2]Fraction descriptions: Br=Light Brown, Co=Colourless, Clr=Clear, fFr=Few Fractures, fIn=Few Inclusions, Eu=Euhedral, El=Elongate, Pr=Prismatic, St=Stubby Prism, Dia=Diamagnetic.

[3]Radiogenic Pb

[4]Measured ratio, corrected for spike and fractionation

[5]Total common Pb in analysis corrected for fractionation and spike

[6]Corrected for blank Pb and U and common Pb, errors quoted are 1 sigma absolute; procedural blank values for this study ranged from <0.1- 0.1 pg for U and 1-3 pg for Pb; Pb blank isotopic composition is based on the analysis of procedural blanks; corrections for common Pb were made using Stacey-Kramers compositions

[7]Correlation Coefficient

[8]Corrected for blank and common Pb, errors quoted are 2 sigma in Ma

1997), but there is no significant difference in the results. The data are plotted in concordia diagrams with errors at the 2σ level (Figures 29B and C), using Isoplot v. 3.0 (Ludwig, 2003) to generate the plots. A Concordia age (Ludwig, 1998) is calculated for some of the samples herein. A Concordia age incorporates errors on the decay constants and includes both an evaluation of concordance and an evaluation of equivalence of the data. The calculated Concordia age and errors quoted in the text are at 2σ with decay constant errors included.

RESULTS

Sample JHC-06-239 (z9127)

A sample of intermediate ash to lapilli tuff was collected from diamond drill-core, hole GA-05-016 (interval 345.7–360.1 m). The sample sits directly above the massive sulphide zone at the Boomerang deposit. The sulphide in the deposit replaces this same rock type (Squires *et al.*, 2005; Hinchey, 2007), suggesting that the rock was not completely consolidated at the time of the mineralization and is interpreted to be more or less syn-mineralization in age.

The sample yielded abundant zircon, of fairly good quality, and only minor fractures and inclusions were present in almost all of the grains; zircon morphology ranges from stubby prismatic to elongate. Multigrain zircon fractions were analyzed by ID-TIMS. These data, which were analyzed in four different U–Pb chemistry batches, contain a significant amount of common lead (12–70 pg, Table 3), which is related to inclusions in most of the zircon, as opposed to procedural lead blanks. Some of the zircon analyses are quite discordant (20–28%) and contain inherited components (C2 and A1, not plotted); however, some of the fractions are nearly concordant (Figure 29A, Table 3). A weighted average of the $^{206}Pb/^{238}U$ ages of the most concordant analyses is calculated to be 493.0 ± 2.4 Ma (MSWD=1.8). There is some scatter of the data, which is most likely a result of minor inheritance in these analyses.

Representative zircons from the sample were placed on a grain mount for imaging with a backscatter (BSE) detector on a scanning electron microscope (SEM). Many of the zircons are interpreted to be magmatic in origin, with well-defined oscillatory zoning (Plate 25A). Other grains appear to contain inherited cores and show good core–rim relationships.

The SHRIMP data for this sample define a cluster overlapping concordia (Figure 29B, Table 4) that define an age of 490.6 ± 2.9 Ma (MSWD of concordance and equivalence = 0.72; probability = 0.95; n=22). This calculation utilized

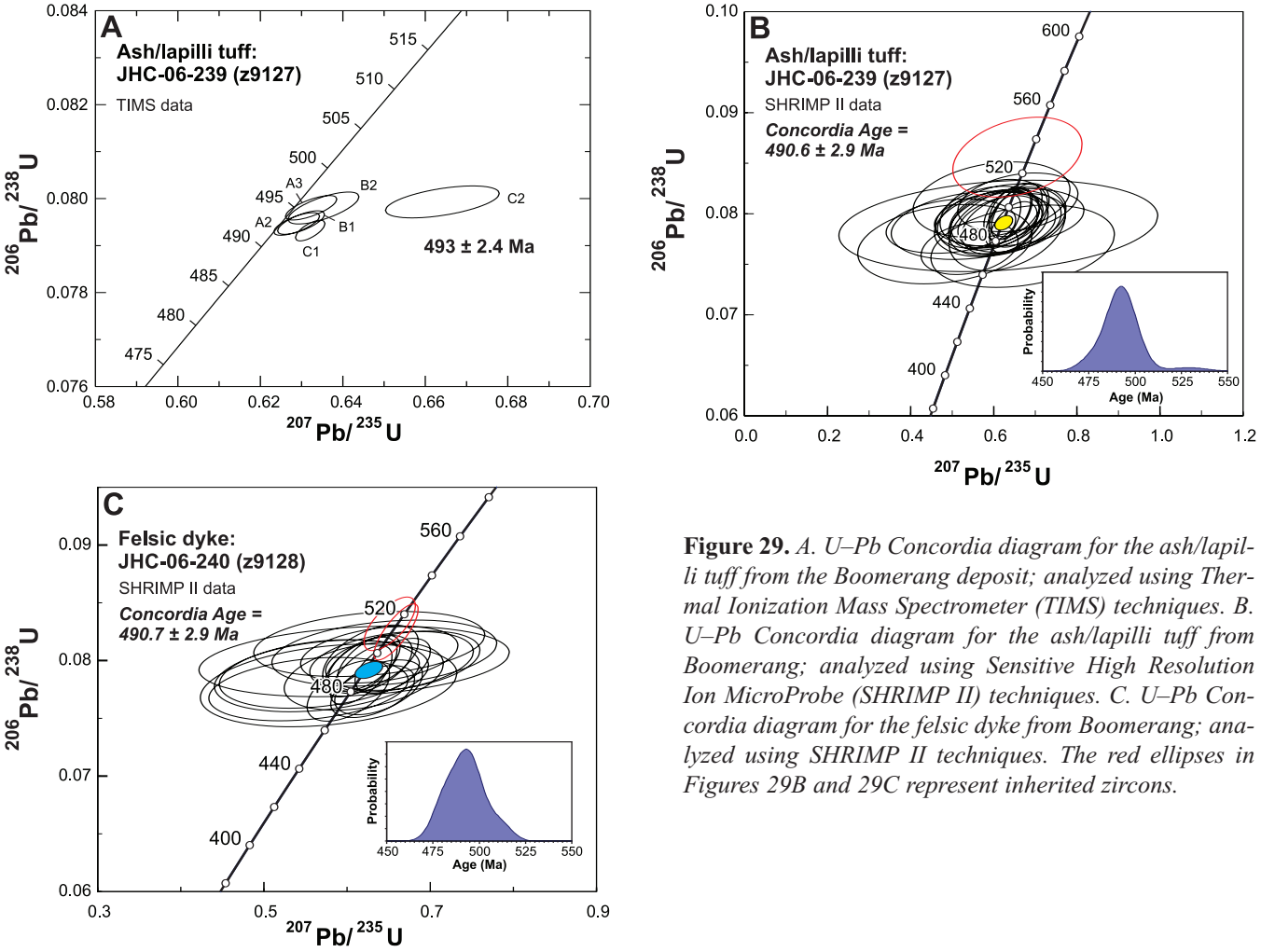

Figure 29. *A. U–Pb Concordia diagram for the ash/lapilli tuff from the Boomerang deposit; analyzed using Thermal Ionization Mass Spectrometer (TIMS) techniques. B. U–Pb Concordia diagram for the ash/lapilli tuff from Boomerang; analyzed using Sensitive High Resolution Ion MicroProbe (SHRIMP II) techniques. C. U–Pb Concordia diagram for the felsic dyke from Boomerang; analyzed using SHRIMP II techniques. The red ellipses in Figures 29B and 29C represent inherited zircons.*

all of the SHRIMP analyses except one, which is highlighted in red on Figure 29B. This older analysis at *ca.* 530 Ma (Table 4) is interpreted to be from an inherited zircon. The date of 491 ± 3 Ma is taken to be the time of crystallization of the zircon in the tuff and constrains the maximum timing of mineralization. Although the sulphides have replaced this host rock, the interval between deposition and mineralization is not considered significant (*e.g.*, *see* Hinchey, 2007).

Sample JHC-06-240 (z9128)

A sample of a felsic dyke was collected from drillhole GA-05-079 (interval 247.1–264.0 m), directly above the sulphide zone at the Boomerang deposit. The sample yielded a very small amount of zircon; not enough material for ID-TIMS analysis, but the zircon retrieved was placed on a grain mount and analyzed using the SHRIMP II. Backscatter SEM images reveal oscillatory-zoned grains that appear magmatic and also grains with possible inherited cores (Plate 25B).

The SHRIMP data define a cluster of data overlapping concordia (Figure 29C, Table 4). A concordia age, utilizing all of the SHRIMP analyses except 2 (*see* below), is calculated to be 490.7 ± 2.9 Ma (MSWD of concordance and equivalence = 0.96; probability = 0.54; n=20). This date of 491 ± 3 Ma is interpreted to reflect the time of crystallization of the felsic dyke and implies that the dyke emplacement was essentially synchronous with the tuffaceous rocks represented by sample JHC-06-239 (z9127).

Two of the analyses are slightly older with ages of *ca.* 510 and 514 Ma (Table 4; highlighted in red on Figure 29C). These zircons are interpreted to be entirely inherited grains in the rock. These inheritance ages are the same as the crystallization ages of volcanic rocks previously dated at the Duck Pond deposit (McNicoll *et al.*, 2008). Given that zircon yield was poor in this sample, there is a possibility that all of the zircon in the felsic dyke is xenocrystic, *i.e.*, inherited from the rocks that the dyke has intruded.

Table 4: U/Pb SHRIMP analytical data

Spot name	U (ppm)	Th (ppm)	Th/U	Pb* (ppm)	^{204}Pb (ppb)	^{204}Pb/^{206}Pb	± ^{204}Pb/^{206}Pb	f(206)^{204}	^{208}Pb/^{206}Pb	± ^{208}Pb/^{206}Pb	^{207}Pb/^{235}U	± ^{207}Pb/^{235}U	^{206}Pb/^{238}U	± ^{206}Pb/^{238}U	Corr Coeff	^{207}Pb/^{206}Pb	± ^{207}Pb/^{206}Pb	Ages (Ma) ^{206}Pb/^{238}U	± ^{206}Pb/^{238}U	^{207}Pb/^{206}Pb	± ^{207}Pb/^{206}Pb
JHC-06-239 (z9127): Ash/lapilli tuff, Boomerang deposit																					
9127-1.1	108	43	0.410	9	2	0.000248	0.000269	0.0043	0.1255	0.0117	0.5851	0.0515	0.0796	0.0013	0.298	0.0533	0.0045	494	7	341	204
9127-2.1	105	44	0.435	9	1	0.000101	0.000225	0.0018	0.1311	0.0130	0.6021	0.0441	0.0794	0.0012	0.327	0.0550	0.0038	492	7	413	164
9127-3.1	109	46	0.438	9	0	0.000010	0.000010	0.0002	0.1409	0.0065	0.6436	0.0200	0.0800	0.0010	0.524	0.0584	0.0016	496	6	544	59
9127-4.1	142	87	0.636	12	3	0.000303	0.000220	0.0052	0.1850	0.0122	0.6078	0.0454	0.0794	0.0012	0.313	0.0555	0.0040	492	7	434	168
9127-6.1	64	35	0.560	5	1	0.000296	0.000429	0.0051	0.1637	0.0180	0.5512	0.0808	0.0788	0.0014	0.241	0.0507	0.0073	489	8	227	301
9127-7.1	134	59	0.456	11	0	0.000010	0.000010	0.0002	0.1609	0.0058	0.6229	0.0175	0.0793	0.0010	0.566	0.0570	0.0013	492	6	491	52
9127-8.1	55	23	0.421	4	0	0.000010	0.000010	0.0002	0.1420	0.0084	0.6326	0.0573	0.0785	0.0017	0.354	0.0585	0.0050	487	10	548	198
9127-9.1	88	49	0.576	7	2	0.000341	0.000248	0.0059	0.1519	0.0181	0.6113	0.0489	0.0790	0.0013	0.322	0.0562	0.0043	490	8	458	179
9127-10.1	122	57	0.484	9	4	0.000494	0.000254	0.0086	0.1313	0.0110	0.5426	0.0478	0.0766	0.0011	0.278	0.0514	0.0044	476	6	258	209
9127-11.1	70	27	0.395	5	3	0.000612	0.000344	0.0106	0.1108	0.0197	0.5747	0.0624	0.0767	0.0012	0.269	0.0544	0.0057	476	7	387	256
9127-12.1	178	88	0.508	15	0	0.000010	0.000010	0.0002	0.1639	0.0050	0.6329	0.0232	0.0800	0.0011	0.470	0.0574	0.0019	496	6	507	73
9127-13.1	98	59	0.626	8	7	0.001009	0.000352	0.0175	0.1630	0.0162	0.4974	0.0638	0.0788	0.0011	0.231	0.0458	0.0058	489	7	0	0
9127-14.1	177	110	0.642	15	0	0.000015	0.000286	0.0003	0.1950	0.0120	0.6436	0.0529	0.0791	0.0012	0.301	0.0590	0.0047	490	7	569	182
9127-15.1	170	116	0.705	15	0	0.000010	0.000010	0.0002	0.2074	0.0066	0.6532	0.0263	0.0804	0.0011	0.444	0.0590	0.0021	498	6	566	81
9127-18.1	73	42	0.597	6	0	0.000010	0.000010	0.0002	0.2046	0.0161	0.6479	0.0232	0.0786	0.0010	0.481	0.0598	0.0019	488	6	595	70
9127-19.1	51	22	0.442	4	0	0.000010	0.000010	0.0002	0.1473	0.0104	0.6605	0.0296	0.0798	0.0013	0.472	0.0600	0.0024	495	8	604	89
9127-20.1	95	35	0.378	8	1	0.000118	0.000362	0.0021	0.1231	0.0159	0.6373	0.0738	0.0796	0.0012	0.247	0.0581	0.0066	494	7	532	269
9127-21.1	102	44	0.450	8	0	0.000050	0.000340	0.0009	0.1408	0.0141	0.6196	0.0631	0.0795	0.0014	0.294	0.0565	0.0056	493	8	474	233
9127-22.1	162	104	0.660	14	3	0.000225	0.000278	0.0039	0.1976	0.0122	0.6005	0.0531	0.0801	0.0013	0.310	0.0544	0.0046	497	8	387	202
9127-23.1	129	51	0.411	11	3	0.000286	0.000252	0.0050	0.1272	0.0110	0.6584	0.0591	0.0811	0.0012	0.284	0.0589	0.0051	503	7	563	201
9127-63.1	146	56	0.394	12	0	0.000031	0.000182	0.0005	0.1189	0.0131	0.6201	0.0393	0.0789	0.0012	0.356	0.0570	0.0034	489	7	493	137
9127-65.1	195	130	0.685	17	3	0.000262	0.000337	0.0046	0.2050	0.0147	0.6094	0.0623	0.0790	0.0013	0.286	0.0559	0.0055	490	8	449	236
9127-25.1	104	65	0.645	10	1	0.000186	0.000275	0.0032	0.1890	0.0125	0.6578	0.0635	0.0856	0.0016	0.315	0.0558	0.0052	529	10	443	220
JHC-06-240 (z9128): Felsic dyke, Boomerang deposit																					
9128-8.1	225	121	0.557	19	0	0.000010	0.000010	0.0002	0.1708	0.0046	0.6261	0.0155	0.0798	0.0010	0.588	0.0569	0.0012	495	6	489	45
9128-9.1	222	123	0.572	18	0	0.000010	0.000010	0.0002	0.1759	0.0067	0.6307	0.0205	0.0772	0.0009	0.475	0.0592	0.0017	480	5	575	64
9128-2.1	229	108	0.487	19	0	0.000010	0.000010	0.0002	0.1583	0.0099	0.6381	0.0216	0.0776	0.0010	0.481	0.0596	0.0018	482	6	590	66
9128-3.1	125	54	0.445	10	3	0.000359	0.000268	0.0062	0.1242	0.0113	0.5538	0.0490	0.0775	0.0011	0.285	0.0519	0.0044	481	7	279	208
9128-4.1	162	71	0.455	13	0	0.000010	0.000010	0.0002	0.1388	0.0051	0.6169	0.0178	0.0794	0.0011	0.566	0.0564	0.0014	492	6	467	54
9128-5.1	137	63	0.474	11	0	0.000010	0.000010	0.0002	0.1514	0.0060	0.6279	0.0206	0.0796	0.0010	0.499	0.0572	0.0016	494	6	500	64
9128-6.1	262	160	0.632	23	1	0.000063	0.000163	0.0011	0.1989	0.0077	0.6389	0.0387	0.0804	0.0010	0.324	0.0576	0.0033	499	6	515	132
9128-10.1	181	103	0.590	15	2	0.000197	0.000392	0.0034	0.1747	0.0165	0.6083	0.0762	0.0798	0.0012	0.246	0.0553	0.0068	495	7	423	299
9128-11.1	290	139	0.494	24	0	0.000010	0.000010	0.0002	0.1527	0.0041	0.6171	0.0151	0.0787	0.0010	0.637	0.0569	0.0011	488	6	487	43
9128-12.1	131	66	0.520	11	0	0.000019	0.000288	0.0003	0.1579	0.0136	0.6447	0.0553	0.0806	0.0012	0.289	0.0581	0.0048	499	7	532	192
9128-13.1	156	68	0.447	12	2	0.000184	0.000176	0.0032	0.1227	0.0102	0.5667	0.0492	0.0788	0.0012	0.297	0.0522	0.0044	489	7	294	203
9128-14.1	136	69	0.524	11	1	0.000120	0.000195	0.0021	0.1533	0.0149	0.6205	0.0391	0.0786	0.0012	0.360	0.0573	0.0034	488	7	502	136
9128-15.1	161	74	0.472	13	0	0.000010	0.000010	0.0002	0.1505	0.0122	0.6552	0.0185	0.0795	0.0010	0.539	0.0598	0.0014	493	6	596	53
9128-17.1	123	56	0.470	10	0	0.000010	0.000010	0.0002	0.1502	0.0081	0.6285	0.0235	0.0801	0.0012	0.498	0.0569	0.0019	497	7	487	74
9128-7.1	298	153	0.529	24	2	0.000095	0.000077	0.0017	0.1587	0.0048	0.6019	0.0202	0.0773	0.0011	0.519	0.0565	0.0016	480	6	470	65
9128-19.1	190	118	0.640	16	1	0.000055	0.000187	0.0010	0.2020	0.0089	0.6537	0.0402	0.0798	0.0011	0.334	0.0594	0.0035	495	6	581	132
9128-3.2	178	79	0.457	14	7	0.000550	0.000279	0.0095	0.1341	0.0126	0.5693	0.0525	0.0786	0.0013	0.294	0.0525	0.0047	488	8	308	216
9128-4.2	408	216	0.546	35	8	0.000290	0.000309	0.0050	0.1588	0.0126	0.6270	0.0567	0.0814	0.0011	0.276	0.0559	0.0049	504	7	449	208
9128-6.2	247	191	0.798	21	9	0.000535	0.000352	0.0093	0.2235	0.0180	0.5780	0.0631	0.0778	0.0015	0.293	0.0539	0.0057	483	9	367	256
9128-8.2	217	143	0.682	19	1	0.000053	0.000170	0.0009	0.2144	0.0094	0.6671	0.0380	0.0799	0.0010	0.347	0.0606	0.0033	496	6	623	120
9128-16.1	968	625	0.667	87	0	0.000006	0.000018	0.0001	0.2068	0.0024	0.6572	0.0108	0.0823	0.0010	0.798	0.0579	0.0006	510	6	527	22
9128-18.1	1204	1015	0.871	113	1	0.000010	0.000010	0.0002	0.2589	0.0056	0.6495	0.0126	0.0830	0.0009	0.676	0.0568	0.0008	514	6	482	32

Notes (see Stern, 1997):

Uncertainties reported at 1s (absolute) and are calculated by numerical propagation of all known sources of error

f206^{204} refers to mole fraction of total ^{206}Pb that is due to common Pb, calculated using the ^{204}Pb-method; common Pb composition used is the surface blank

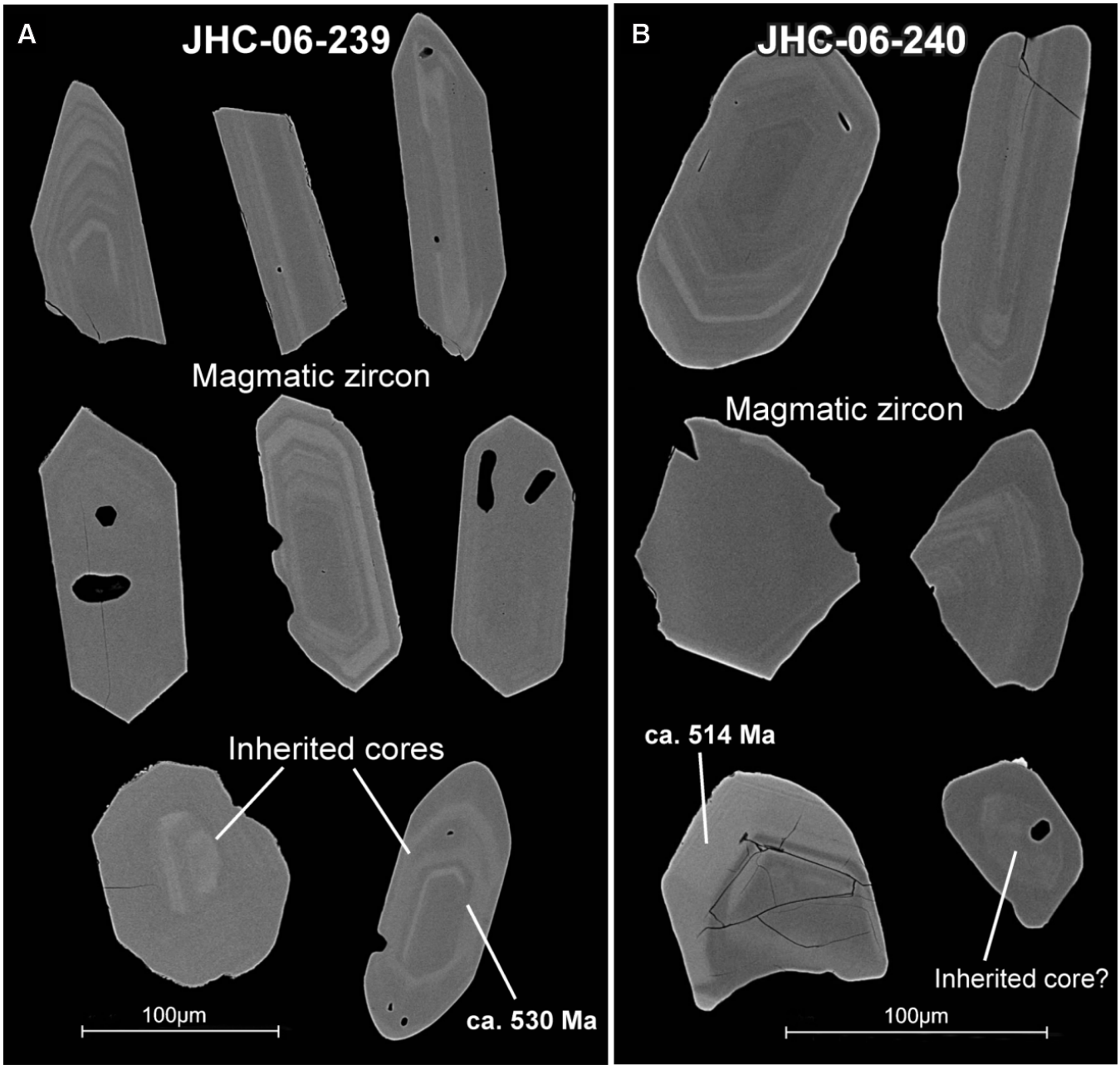

Plate 25. *Representative back-scattered electron images of zircons. A. felsic ash-lapilli tuff from the Boomerang deposit; and B. felsic dyke from the Boomerang deposit.*

DISCUSSION

VMS DEPOSIT CLASSIFICATIONS: SPECTRUM OF DEPOSIT TYPES

Exhalative versus Replacement Ore-Forming Mechanisms

Mechanisms for the formation of VMS deposits are commonly described in terms of two main processes: 1) exhalative or supra-seafloor sulphide accumulation (*e.g.*, chimney-growth process or precipitation from a brine-pool), or 2) sub-seafloor replacement and associated sulphide accumulation (*e.g.*, Doyle and Allen, 2003; Franklin *et al.*, 2005). Both methods of formation are recoginized in the deposits in the TVB. The recognition and understanding of the second process is relatively new and it has implications for the deposits in the TVB, particularly in the southern portion of the belt.

Doyle and Allen (2003) describe three main criteria that are diagnostic of sub-seafloor massive sulphide deposits,

1) the massive sulphides are enclosed within rapidly emplaced volcanic or sedimentary facies (*e.g.,* pyroclastic or tuffaceous rock types, mass-flow deposits),
2) the massive sulphides contain some relicts of the host rocks, and
3) replacement fronts can be recoginized between the massive sulphide and the host rocks.

Other characteristics that may indicate replacement of the host rocks include discordance between mineralization and bedding, and the presence of strong hydrothermal alteration in the hangingwall sequence.

The VMS deposits in the southern portion of the belt, *e.g.*, the Tulks East, Tulks Hill, and Boomerang deposits, display many of these characteristics (*see* Kean and Evans, 1986; Squires *et al.*, 2005; Hinchey, 2007; Squires, 2008). In all cases, hydrothermal fluids permeated favourable horizons in unconsolidated (?), porous, and permeable felsic volcanic and related sedimentary rocks resulting in variable degrees of replacement of the original rock by massive sulphides. The mixing of upwelling hydrothermal fluids with cooler inter-pore fluids and seawater result in the formation of a strata-bound massive sulphide lens, which is enveloped by a halo of hydrothermal alteration (*e.g.*, Gibson, 2005). The three deposits also show evidence of relict host rock types (felsic ash and crystal tuff) within the ore in the form of relict quartz crystals (Plates 3I, 10E), they locally preserve original bedding, and they all display hydrothermal alteration and contain stringer mineralization in both the hangingwall and footwall (Figures 5 and 9, Plates 3–11). In addition, all three deposits contain fine-grained sedimentary rocks either in the mineralized horizon, or directly above it, which may have acted as a physical barrier to fluid migration and trapped the metalliferous fluids in the prospective horizons. Evidence for sub-seafloor replacement processes has also been documented at the Duck Pond deposit (McNicoll *et al.*, 2008), which exhibits similar textures to those outlined above. However, in order for sub-seafloor, replacement-style mineralization to form there must have been upward and outward movement of extremely large volumes of hydrothermal fluids (Franklin *et al.*, 2005 and Doyle and Allen, 2003). Most VMS deposits are associated with rifting of arcs in extensional tectonic regimes, which promotes development of large-scale faults and fractures. Consequently, it is likely that some of the upwelling hydrothermal fluids would reach the seafloor to vent and produce metalliferous exhalative sedimentary rocks. Although evidence of exhalative processes are preserved in the Daniels Pond deposit in the northern TVB, such evidence in the southern TVB is only manifest as exhalative, sulphide-bearing horizons at the Dragon Pond and Curve Pond prospects. The presence of sulphide-bearing (exhalative?) sedimentary rocks in the hangingwall of the Boomerang deposit (Plate 3H) may also represent evidence for the venting of fluids.

In the northern TVB, evidence for possible replacement-style VMS mineralization is observed at the Jacks Pond prospect, and possibly the Bobbys Pond deposit (*see* below; *see* also McKenzie *et al.*, 1993). In both cases it appears that hydrothermal fluids infiltrated favourable horizons in unconsolidated tuffs (Jacks Pond), or heterogenous, variably porous felsic volcanic rocks (Bobbys Pond). This process resulted in variable degrees of replacement of the original host rock by massive sulphides. Both deposits locally retain evidence of primary textures within the ore, *e.g.*, relict quartz crystals, and they display hydrothermal alteration in both the hangingwall and footwall (*e.g.*, Figure 14). In addition, both deposits locally contain fine-grained siliceous sedimentary rocks either within the mineralized horizon (*e.g.*, Bobbys Pond), or stratigraphically above it (*e.g.*, Cathys Pond horizon above the Jacks Pond deposit). Such sedimentary units may have acted as a physical barrier to upward-flowing fluid migration, thereby trapping metalliferous fluids in underlying rocks. The possible genetic link between the Cathys Pond exhalative horizon and the Jacks Pond prospect suggests a large-scale upward migration of hydrothermal fluids. Thus, the system produced mostly replacement-style mineralization at depth, but this was accompanied by exhalative-type mineralization associated with those hydrothermal fluids that did reach the seafloor and vented into the water column. At the Bobbys

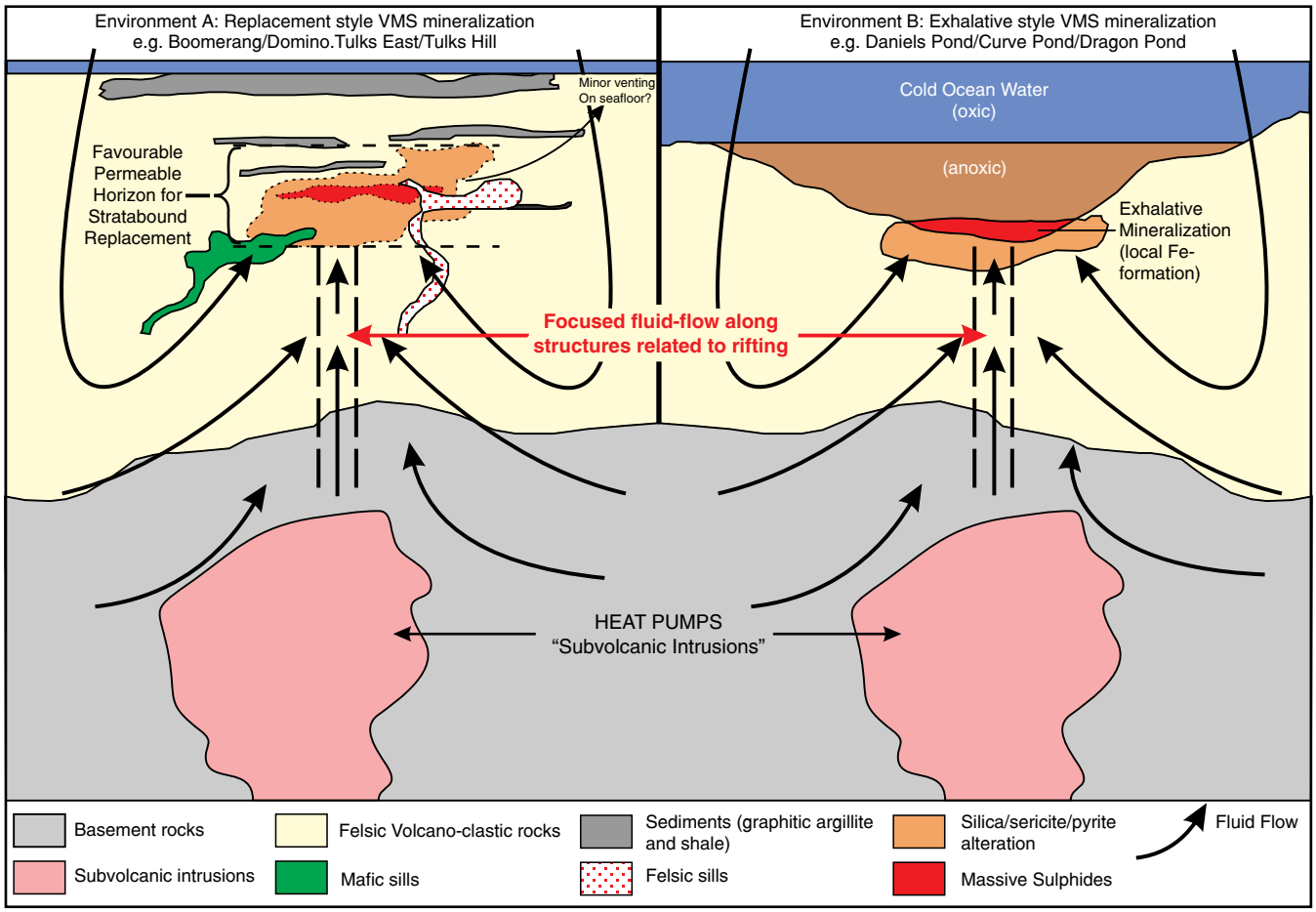

Figure 30. *Schematic diagram illustrating the two types of VMS-forming environments observed in the TVB (replacement versus exhalative). Note that the two environments are commonly interpreted to be related and forming continuums.*

Pond deposit, the occurrences of very fine-grained, sulphide-bearing sedimentary rocks in the immediate hangingwall may represent exhalative mineralization.

The massive sulphide clast-bearing debris-flow breccias in the immediate stratigraphic hangingwall of the Daniels Pond deposit suggest that the mineralization most likely formed through exhalative processes on the seafloor. An alternative explanation would be that the mineralization formed *via* replacement processes and was later tectonically modified *via* either debris-flow volcaniclastic brecciation or fault brecciation along a syn-sedimentary fault.

As such, the TVB contains a spectrum of deposit styles, ranging from exhalative VMS deposits that formed on the seafloor through to replacement-style deposits that formed in the sub-seafloor, and combinations thereof (Figure 30).

Classification of VMS Mineralization

Previous classification schemes of the VMS deposits in the TVB were largely based upon characteristics such as tectonic settings and metal contents (*e.g.*, Swinden 1991, 1996), rather than variations in host rock types or alteration assemblages. Using the recent classification schemes of Barrie and Hannington (1999), Hannington *et al*. (1999) and Galley *et al.* (2007), the VMS deposits in the TVB fit into a number of different classifications.

Southern Tulks Volcanic Belt Deposits

The main deposits in the southern Tulks Volcanic Belt (*e.g.*, Boomerang, Tulks Hill and Tulks East) range from a bimodal felsic to a bimodal siliclastic classification. Generally, the VMS deposits in the southern TVB contain host sequences that are dominated by >50% felsic volcanic rocks and/or 35 to 50% felsic-derived epiclastic rocks, have ~10-15% siliclastic rocks in the host stratigraphic succession, with mafic volcanic and intrusive rocks forming the remainder. However, it should be noted that the deposits may also contain locally abundant siliclastic sedimentary rocks, with proportions on par with felsic and mafic volcanic rocks. As observed in the Tulks deposits, such environments commonly produce Zn-rich ore systems.

The deposits in the southern TVB share some similarities with the Duck Pond and Boundary deposits in the Tally Pond Volcanic Belt to the east, in that they are dominated by replacement-style mineralization (Squires *et al.*, 2001; Squires and Moore, 2004; McNicoll *et al.*, 2010). However, they differ in that the deposits in the Tally Pond Volcanic Belt are associated with felsic volcanic rocks that commonly display coherent flow-banding and form rhyolite domes, whereas deposits in the southern TVB occur in successions dominated by felsic volcaniclastic and sedimentary rocks.

Northern Tulks Volcanic Belt Deposits

Although the major deposits in the northern TVB (*e.g.*, Daniels Pond and Bobbys Pond) have characteristics similar to those of the bimodal felsic type of deposits, they also have some characteristics that are more similar to the hybrid bimodal felsic VMS-high-sulphidation epithermal type deposits (Figure 4). Three lines of evidence for a shallow-water, hybrid VMS-epithermal environment in the northern part of the belt are identified:

1) locally developed acidic aluminosilicate (halloysite–illite–sericite) alteration in the immediate footwall, and locally in the hangingwall (*e.g.*, Daniels Pond and Bobbys Pond deposits),
2) local occurrences of silica–alunite–native sulphur ± pyrite–orpiment–stibnite alteration in the vicinity of the Daniels Pond and Bobbys Pond deposits, and
3) local development of vuggy silica textures in the vicinity of the deposits.

It should be noted that the presence of halloysite (a kaolinite group mineral) has only been tentatively identified in a small number of samples *via* traditional XRD analysis and also using visible-infrared reflectance spectrometry.

Aluminous alteration assemblages have been identified at a number of VMS deposits, in particular from the Kuroko district of Japan, Australian deposits (*e.g.*, Western Tharsis), a small subset of Canadian Deposits (*e.g.*, some deposits in the Doyon Bousquet LaRonde District), and also from active seafloor systems (*e.g.*, *see* Sillitoe *et al.*, 1996; Hannington *et al.*, 1999; Huston and Kamprad, 2001; Dubé *et al.*, 2007; and references therein). The presence of argillic and advanced argillic alteration assemblages indicates that these deposits formed under more oxidized, lower pH, conditions than those typically implied for most VMS deposits in which the hydrothermal fluids are dominated by seawater circulation (*e.g.*, *see* Sillitoe *et al.*, 1996; Hannington *et al.*, 1999). In order for halloysite (a kaolinite group mineral) to be stable in a fluid, the pH of the fluid must be <3.5, *i.e.*, significantly lower that the typical range of 5 to 6 suggested for most VMS-forming fluids (Gifkins *et al.*, 2005). Such low pH fluids could be generated by the introduction of magmatic volatiles into the hydrothermal system. Due to the buffering capacity of potassium-rich sericite and chlorite alteration assemblages within these deposits, this process is likely not applicable to the TVB deposits. Therefore, it is suggested that magmatic fluids played a greater role in VMS hydrothermal systems in the northern TVB, and that fluid boiling may have been locally important. It is also postulated that mineralization formed in a shallow-marine environment, in some respects equivalent to a shallow-submarine version of the typical subaerial, high-sulfidation epithermal deposit environment. This provides a reasonable explanation for characteristics typical of both VMS and epithermal-type deposits (*see* below; Figure 31).

Although the deposits in the northern TVB share many similarities with the deposits in the southern part of the belt (*e.g.*, styles of mineralization, felsic host rocks, *etc.*), the stratigraphy contains a higher proportion of extrusive rhyolitic facies (*e.g.*, blocky rhyolite flows, rhyolite breccias, *etc.*) that are indicative of a more vent-proximal environment (Figure 31). It is also suggested that the northern Tulks deposits likely formed in an area of relatively 'high-standing ground' within the basin, under relatively shallow-water conditions, compared to the deep-water, sediment-dominated distal environment suggested for the southern TVB (Hinchey, 2007). It is also possible that parts of the northern TVB may have been part of an emergent arc environment, although evidence is lacking. From south to north, the TVB, specifically the Jacks Pond formation of the Tulks group, is interpreted to record a transition from a deep-basin, classic VMS environment (*e.g.*, Tulks East, Tulks Hill, and perhaps the Boomerang deposits), to shallower water, vent-proximal bimodal VMS-epithermal-style deposits (*e.g.*, Daniels Pond deposit).

VOLCANIC ENVIRONMENTS AND TECTONIC SETTINGS FOR VMS MINERALIZATION

The VMS deposits of the southern TVB typically occur in thick successions of felsic volcaniclastic rocks intercalated with varying amounts of sedimentary rocks, compared to a more volcanic-dominated environment for the northern TVB. Fining-upward turbiditic sequences are common in the mineralized packages of rocks in the southern TVB whereas felsic-intermediate flows are more commonly associated with the deposits in the northern part of the belt. In both areas, bimodal volcanic sills occur syngenetically with the volcanic, volcaniclastic and sedimentary rocks. Many of the basaltic sills are amygdaloidal at their tops and have chilled lower margins. These relationships suggest that the VMS systems formed in an environment of active volcanism and synchronous sedimentation, most likely within a rifted basin, possibly of back-arc affinity. This interpretation

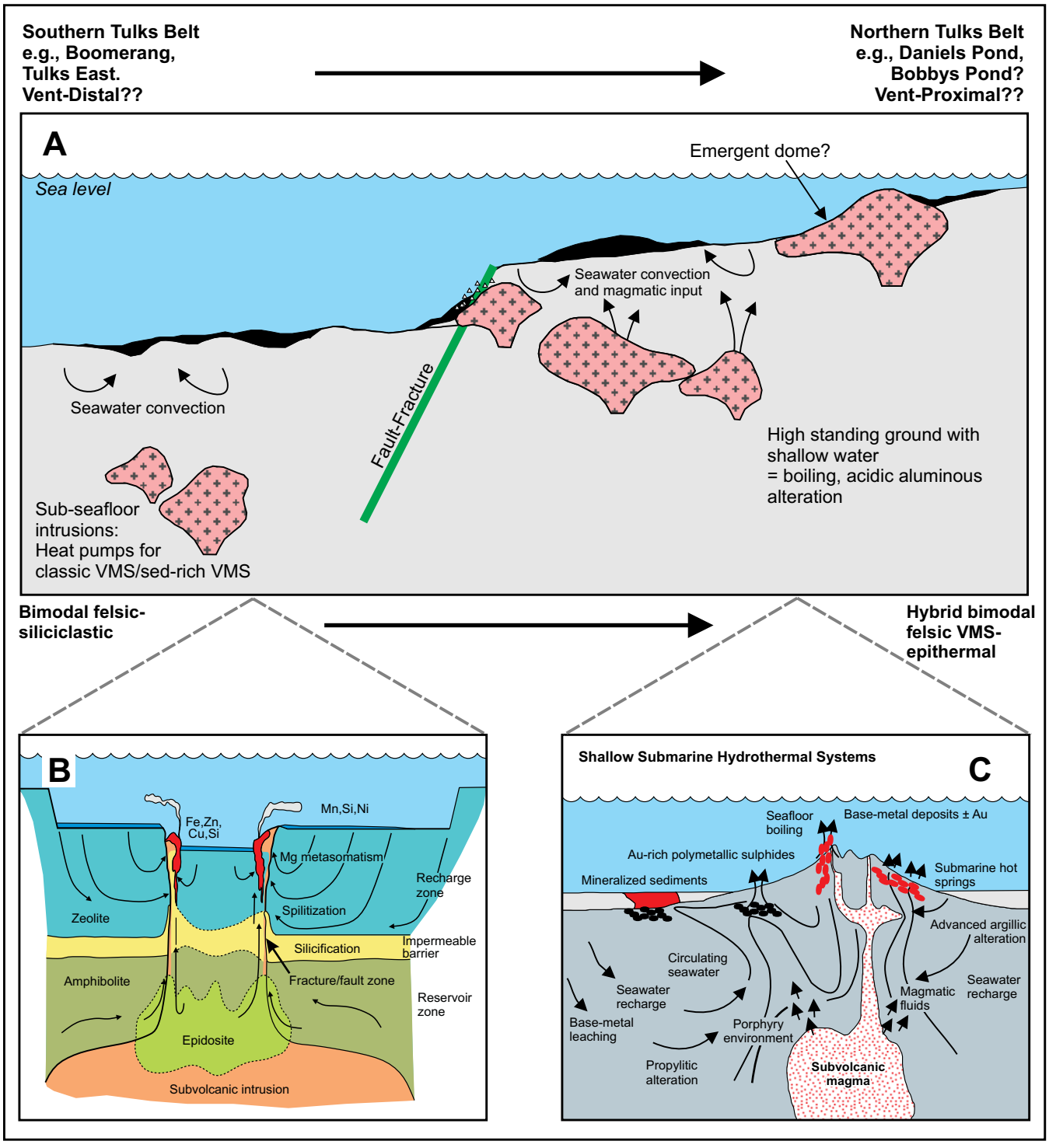

Figure 31. *A) Schematic diagram illustrating the two types of VMS-forming environments in the TVB (after Hannington* et al., *1999) (*e.g.*, deep-water, typical VMS environment suggested for the southern TVB (B) (from Galley, 1993), through to shallower water, VMS–epithermal-type environment suggested for the northern TVB (C) (from Hannington* et al., *1999)).*

is supported through lithogeochemistry conducted as part of this study, as well as previous lithogeochemical investigations in the area (*e.g.*, Swinden *et al.*, 1989; Evans and Kean, 2002 and references therein; Rogers, 2004; Zagorevski *et al.*, 2007a). Although mainly conducted on the mafic volcanic rocks, the early studies of Swinden *et al.* (1989) and Evans and Kean, (2002), were instrumental in documenting the change in chemical signatures that marked the transition

from an active arc to a non-arc or back-arc rift environment. The upper basalts of Swinden *et al*. (1989) have a LREE-enriched trace-element pattern, which, in addition to supporting a non-arc environment, suggests high heat-flow regimes (*see* Figure 13A of Evans and Kean, 2002).

Recent work of Zagorevski *et al.* (2007a) on the area of the southern TVB, as well as the detailed lithogeochemical work associated with this study focusing on areas of VMS mineralization, builds upon the early work and also supports an environment with episodic arc development and rifting (*see* section below on Lithogeochemical Patterns).

This transition from an island-arc (convergent regime) to an arc-rift or back-arc (extensional regime) environment is important as such transitions and extensional environments are considered important for VMS formation. The combination of active progressive rifting and high heat-flow allows conduits to form and focus both upward hydrothermal fluid flux as well as downward seawater recharge into the hydrothermal system (*e.g.,* Lesher *et al*., 1986; Lentz, 1998; Piercey *et al*., 2001). The heat pump for the hydrothermal system may be related to subvolcanic intrusions and/or upwelling asthenospheric mantle in a back-arc rift-environment. Franklin *et al*. (2005) also point out that the bimodal magmatism that accompanies rifting (such as that in the southern TVB) also implies a high geothermal gradient.

LITHOGEOCHEMICAL PATTERNS

The detailed geochemistry presented in this report provides information on the tectonic settings of felsic and mafic volcanic rocks associated with VMS mineral deposits, and also allows comparison of these host sequences.

The relatively low HFSE and REE concentrations of the rocks, coupled with the ubiquitous, yet variably developed, negative Nb and Ti anomalies on primitive-mantle-normalized, extended trace-element plots for the felsic and intermediate rocks are diagnostic of formation in an arc environment (*e.g.*, Pearce and Peate, 1995). In light of the presence of the inherited zircon in geochronological samples from the Boomerang deposit, it could be argued that the negative Nb and Ti anomalies in the felsic rocks could be due to re-melting of older crustal source material with arc parentage that had been previously affected by subduction processes. However, the synchronous mafic rocks of calc-alkaline and island-arc tholeiitic affinity that occur throughout the TVB, suggest an arc environment.

A comparison of the felsic-intermediate host rock lithogeochemical signatures from the five main deposits, as well as for the Pats Pond group, illustrates some subtle but potentially important differences. First, rhyolites from the Tulks Hill and Bobbys Pond deposits have higher Zr/TiO_2 ratios compared to the other areas. However, the variation in the Zr/TiO_2 ratios, especially in the case of the Tulks Hill samples, is predominantly related to lower TiO_2 rather than an increase in Zr concentrations, and this pattern is most likely indicative of greater fractionation in these rhyolites. The rhyolites from these two deposits do have slightly higher concentrations of trace elements, including zirconium, as observed on the primitive-mantle-normalized plots, and may be indicative of a higher temperature of derivation and/or fractionation processes. It should be noted that the felsic tuffs from the Tulks Hill deposit have Zr/TiO_2 ratios similar to those of felsic tuffs and rhyolites from other areas.

Additional chemical variations in the felsic-intermediate volcanic rocks occur in the degree of LREE enrichment and the extent of the negative Nb and Ti anomalies, which appear to be correlated. Samples from the Tulks Hill and Bobbys Pond deposits have greater LREE enrichment and larger and more pronounced negative Nb and Ti anomalies compared to the Boomerang deposit samples, whereas the the Tulks East deposit yielded samples with similar LREE enrichment and similar, but slightly larger, overall negative Nb and Ti anomalies than the Boomerang samples. The Boomerang felsic-intermediate rocks have extended trace-element patterns similar to the PP4 grouping from the Pats Pond group, and positive Zr and Hf anomalies similar to the PP6 grouping.

In contrast to the other deposits, the immediate host rocks at the Daniels Pond deposit are more intermediate to mafic in composition. These samples appear geochemically different than the other host rocks in the belt; they show low Zr/TiO_2 ratios and relatively low concentrations of HFSE and REE. The samples have characteristic U-shaped primitive-mantle-normalized trace-element patterns, and although they vary with the type and intensity of alteration, the overall pattern is remarkably similar to that associated with boninitic magmas.

Mafic volcanic rocks in the TVB vary from transitional calc-alkaline basalts to island-arc tholeiites, with the majority of the rocks characterized by island-arc tholeiitic signatures. The mixtures of calc-alkaline and tholeiitic sequences are best explained by the progressive rifting of predominantly calc-alkaline arcs (*cf.* Zagorevski *et al.*, 2007a). The variations in the chemistry of felsic and intermediate rocks may also reflect this general process.

The last chemical variation that is observed among the five main deposits and the Pats Pond group is differences in εNd of the felsic rocks. The Boomerang deposit and the Pats

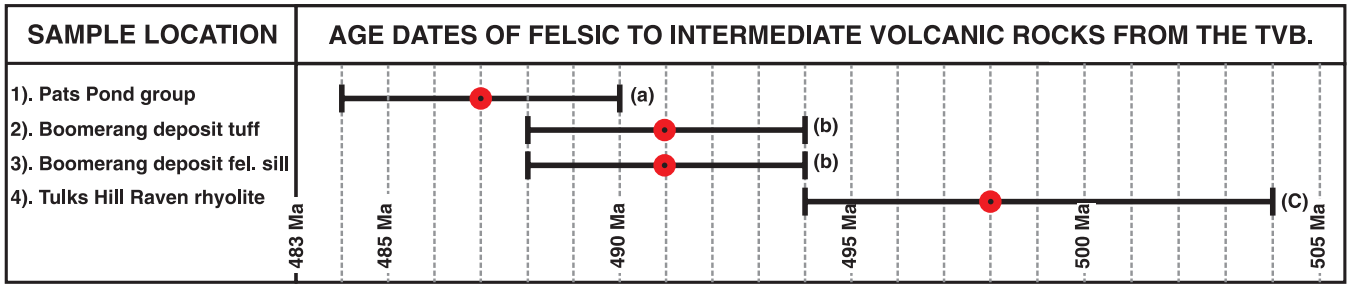

Figure 32. *Comparison of known U–Pb zircon ages from the Tulks Volcanic Belt. Geochronology from: Zagorevski* et al. *(2007a); Hinchey and McNicoll (2009); Evans* et al. *(1990).*

Pond group felsic-intermediate samples, and one sample from the Bobbys Pond deposit have higher εNd (+3.8 to +5.5) compared to those from the Tulks Hill, Tulks East, and Daniels Pond deposits, and a second sample from Bobbys Pond (εNd of around +2 to +3) (Figure 19). Although there is no easy interpretation of these data, the apparent bimodal grouping suggests that the Boomerang area is more similar to the Pats Pond group (and perhaps a portion of the Bobbys Pond stratigraphy) than it is to the Tulks Hill, Tulks East, Daniels Pond, and perhaps the Bobbys Pond areas. However, it should also be noted that felsic to intermediate rocks similar to those hosting the Tulks Hill and Tulks East deposits locally have εNd signatures of +4 to +5.0 (*e.g.*, Rogers, 2004; Table 2); adding to the ambiguity of such data. Therefore, without additional geochronological control, the use of Nd isotopic signatures to correlate rock units in the TVB is questionable.

GEOCHRONOLOGICAL DATA

The U–Pb geochronological data presented in this report was intended to help eludicate the complicated tectonstratigraphy of the TVB, as well as to provide some information on the timing of VMS mineralization within the belt. The area of the recently discovered Boomerang deposit was of particular interest, as it appears to be a zone that has many structural complications (van Staal *et al.*, 2005) (*see* also case study on the Boomerang area stratigraphy below). The data show that the volcanic rocks included within the TVB can be assigned to sequences of at least two ages, *i.e.*, 498 +6/-4 Ma and 491 ± 3 Ma. As a first-order interpretation, this supports the proposal that the TVB is composed of westward-younging volcanic rocks (*e.g.*, van Staal *et al*., 2005; Zagorevski *et al*., 2007a). However, the ages obtained from the Tulks Hill and Boomerang deposits also overlap within error at their respective lower and upper limits, so the results do not preclude the interpretation that volcanism continued over several million years, rather than in discrete pulses. The ages from the Boomerang and Tulks Hill deposits constrain the timing of VMS mineralization and suggest that there was more than one episode of mineralization in this area. This interpretation is supported by the age for the porphyry at Tulks Hill, if this gives a minimum age for mineralization (*see* below). The fact that the age from the felsic sill at the Boomerang deposit is identical to that of the host sequence confirms that bimodal volcanism was synchronous with mineralization, as previously proposed by Hinchey (2007) based on textural relationships. Also, observed zircon inheritance in the sample for the Boomerang deposit implies that these rocks, in part, were developed on a basement of older (Cambrian) rocks that were possibly equivalent to other parts of the VLSG, *e.g.*, the Tally Pond group (*e.g.*, Zagorevski *et al.,* 2007a; McNicoll *et al.*, 2008).

Ages of Volcanism and Mineralization

The identical ages of 491 ± 3 Ma obtained for the felsic tuff that hosts the massive-sulphide mineralization at Boomerang and a crosscutting felsic dyke closely constrain the timing of mineralization. This age is younger than the 498 +6/-4 Ma age obtained from a subvolcanic porphyry at the Tulks Hill deposit (Evans *et al.*, 1990), although their error envelopes do overlap at their respective older and younger limits. However, if the revised age of 496.5 ± 1 Ma for the Tulks Hill porphyry is used (G.R. Dunning, personal communication, 2008), there is no overlap between these ages.

The age of 491 ± 3 Ma obtained for the Boomerang deposit is slightly older than the 488 ± 3 Ma age reported for the Pats Pond group (Zagorevski *et al.*, 2007a). However, these ages overlap extensively at their older and younger limits, respectively (Figure 32).

There is no simple interpretation of these data, but the similarity in ages obtained from both the Boomerang deposit and the Pats Pond group suggests that a link between these areas is more likely than a link between Boomerang and the Tulks deposits. The alternative interpretation is that all of the subdivisions of the VLSG represent nothing more than a long-lived period of volcanism and sedimentation

that extended from *ca.* 498 to *ca.* 488 Ma, a period of some 10 Ma, and that the distinctions between the Tulks group and the Pats Pond group are more semantic than real.

The identical ages obtained for the felsic dyke and the volcaniclastic felsic host tuff at the Boomerang deposit have implications for the environment of VMS mineralization. The occurrence of synchronous sills, both felsic and mafic, is characteristic of extensional regimes with high thermal gradients, such as those in rifted-arc environments. The high heat flow in such settings is key to the establishment of VMS forming hydrothermal convection cells (*e.g.*, Franklin *et al.*, 2005; Galley *et al.*, 2007). A rifted-arc environment is also favoured by the variable chemical signatures of the felsic and mafic rocks at Boomerang, as discussed above.

Zircon Inheritance Patterns

The SHRIMP II data presented herein from the Boomerang deposit indicate zircon inheritance of *ca.* 510 and 514 Ma in the felsic sill sample and inheritance of *ca.* 530 Ma in the felsic tuff sample. The inheritance ages from the felsic sill are similar to the crystallization ages of volcanic rocks previously dated at the Duck Pond deposit, within the Tally Pond group (McNicoll *et al.*, 2008). These data suggest that the host rocks to the Boomerang deposit formed on a substrate represented by these older rocks, rather than being juxtaposed at a later time. The *ca.* 530 Ma inherited zircon from the felsic tuff could represent an older volcanic source. Zagorevski *et al.* (2007a) documented inheritance of *ca.* 560 Ma from the Pats Pond group, whereas Squires and Moore (2004) and McNicoll *et al.* (2008) report inheritance of *ca.* 565 Ma and 573 Ma from zircons within felsic rocks of the Tally Pond group, suggesting that these rocks were built on a Precambrian substrate. Therefore, it appears that the VLSG formed *via* a sequential process of arc magmatism, in which arcs were built on older continental basement, rather than in an ensimatic environment (*cf.* Rogers *et al.*, 2006 and Zagorevski *et al.*, 2007a).

Stratigraphic Compilations and Map-Scale Inconsistencies– A Case Study of the Stratigraphy in the Boomerang Deposit Area

Due to the paucity of outcrop in the TVB, many gaps and uncertainties remain in our understanding of detailed stratigraphic correlations within, and between, facies assemblages. This is particularly important in the area of the Boomerang VMS cluster. Although this study was not focused on producing regional-scale tectonostratigraphic maps of the TVB, it did examine regional-scale correlations of stratigraphy adjacent to the main mineral deposits. Due to the complexities in the area surrounding the Boomerang deposit, a case study of the stratigraphy around that deposit, and the implications of map patterns in that area, was undertaken.

The most recent stratigraphic interpretations in the area suggest that the Boomerang deposit occurs within the *ca*. 487 Ma Pats Pond group, which is *ca.* 11 Ma younger than the Tulks group, which hosts the Tulks East and Tulks Hill deposits (*e.g.*, van Staal *et al.*, 2005; Zagorevski *et al.*, 2007a, b). In addition, the Boomerang host stratigraphy (dated at *ca.* 491 Ma – this study) is interpreted to be structurally bound between two parcels of much younger (*e.g.*, Arenig–Caradoc–Llanvirn) rocks; namely the Dragon Pond formation (Arenig–Caradoc; *ca.* 453 Ma.) and the Victoria River Mouth formation (Llanvirn–Caradoc; *ca.* 457–462 Ma; Figure 33). These assignments have implications in terms of tectonostratigraphic modelling and mineral exploration. The U–Pb site, from which the correlation with the Pats Pond group is drawn, lies about 35 km along strike to the southwest. If the interpretation that the Boomerang deposit sits within a younger package of rocks is correct, it argues against earlier interpretations that VMS mineralization within the southern TVB is hosted by a single volcanic sequence (*e.g.,* Evans *et al.*, 1990; Noranda, 1998). More importantly, if the stratigraphic distribution of units (van Staal *et al.*, 2005; Zagorevski *et al.*, 2007a, b) is correct, then the host to the Boomerang deposit is fault bound by younger rocks. This has implications for exploration as the prospective host rocks to the Boomerang deposit may be cut-off along strike, which would limit exploration potential.

Map Patterns – Potential Structural Models

Before examining the lithogeochemistry of various units in the Boomerang area, it is pertinent to examine the interpreted map patterns and possible explanations. If the map patterns and stratigraphic assignments portrayed by van Staal *et al.* (2005) and Zagorevski *et al.* (2007a, b) are correct, then the structural models for the area would be much more complex than the previously suggested homoclinal models for the TVB, in which all units young to the west (*e.g.*, Evans and Kean, 2002). Based on the map distribution of units there are different structural explainations for the geometry observed. Each model is dependant upon the age inferred for the black shale associated with the units assigned to the Dragon Pond formation. In order to explain the map distibution of units along a section through A-A' on Figure 33, with the *ca.* 491 Ma Boomerang host rocks structurally bound between two blocks of the Dragon Pond formation (ca. 453 Ma) rocks, and with the Victoria River Mouth formation (Llanvirn–Caradoc) and Tulks group rocks (*ca.* 498 Ma) occurring sequentially to the east, there is one possible structural model to fit the interpretation. The age relationships can be explained in terms of a folded thrust model bound by unconformities (Figure 34). In the model,

folding would expose 491 Ma rocks that unconformably underlie younger 453 Ma rocks. Subsequently, all rocks would be thrust eastward upon both younger 462 Ma and older 498 Ma rocks (Figure 34A). This relationship is recognized in diamond-drill core from the Boomerang deposit (Plate 26); although no spatial control or orientation is known. Alternatively, if it is assumed that the sedimentary rocks included in the Dragon Pond formation (van Staal *et al.*, 2005 and Zagorevski *et al.*, 2007a) are of different age, (supported indirectly by geochemistry below) in a generally west-younging sequence, then two structural alternatives could be invoked. The first model would again involve large-scale folding of originally layercake stratigraphy, resulting in variably exposed units (*e.g.*, Plate 27; Figure 34B). The second model involves east-verging large-scale thrust stacks that structurally juxtapose sequentially younger packages of rocks from the west; with the exception of the 462 Ma Victoria River Mouth formation (*see* section on Lithogeochemistry below) (Plate 28; Figure 34C). This latter model is the closest to the original homoclinal models proposed for the belt (Evans and Kean, 2002 and references therein); especially in light of the geochemical evidence given below, which brings into question the validity of the positioning of the eastern panel of the Dragon Pond formation and the Victoria River Mouth formation on Figure 33.

Map Patterns – Geochemical Implications and Inconsistencies

To further assess the geological map pattern in the vicinity of the Boomerang deposit, a lithogeochemical study was designed to compare the chemistry between the two structural panels of Dragon Pond formation (Wigwam Brook group) rocks (Figure 33), interpreted to be 453 Ma, with the surrounding 491 Ma (Pats Pond group (?)) rocks that host the Boomerang deposit, the Tulks group felsic volcanic rocks, and the Wigwam Brook group rocks in the northern TVB. The stratigraphic positioning of the eastern panel of the Dragon Pond formation is very important, because if the interpretation is correct, a large-scale unconformity and/or thrusting must be invoked to juxtapose the 453 Ma rocks with the 491 Ma rocks. The geochemistry of the unit mapped as the Victoria River Mouth formation (Sutherlands Pond group) (van Staal *et al.*, 2005 and Zagorevski *et al.*, 2007a, b) was also investigated and compared with the same unit from the northern part of the TVB where it is distinct with chemistry of E-MORB-like compositions. It should be noted that the distinct chemistry of this unit was recognized by Evans and Kean (2002). Subsequent re-mapping led to the assignment of this unit to the Victoria River Mouth formation by Rogers *et al.* (2005) and van Staal *et al.* (2005). As with the eastern panel of the Dragon Pond formation, if the distribution and assignment of these rocks to the Victoria River Mouth formation in the vicinity of the Boomerang deposit are correct, a large-scale thrust and/or unconformity must be invoked to explain the juxtaposition of rocks of such different ages. In both sceneros above, the apparent positioning of these younger units has direct bearing on the tectonostratigraphic interpretation, which, in turn, has implications for mineral exploration.

In the first case of the Dragon Pond formation (Wigwam Brook group), based upon geochemical samples taken as part of this study as well as by Rogers (2004) and Zagorevski *et al.* (2007a; Figure 35), the eastern mapped panel (Figure 33) is markedly different in terms of geochemistry relative to the western panel. The western panel of the Dragon Pond formation (Figure 35) is characterized by elevated LREE and is indistinguishable from the Wigwam Brook group in the northern TVB (Figure 35). However, the eastern panel of the Dragon Pond formation (van Staal *et al.*, 2005 and Zagorevski *et al.*, 2007a) has a distinct chemistry from the western panel, and appears indistinguishable from rocks of 491 Ma that host the Boomerang deposit as well as 498 Ma rocks of the Tulks group (Figure 35). Of note, the only samples analyzed for geochemistry from the eastern panel of the Dragon Pond formation by Rogers (2004) and Zagorevski *et al.*, (2007a), *e.g.*, samples VL01A344 and VL02A104, are actually classified as being part of the older Pats Pond group chemically (*see* Zagorevski, 2006 and Zagorevski *et al.*, 2007a). As such, due to the difficulty in distinguishing the felsic to intermediate volcanic units in the field and in the absence of supporting evidence to constrain the map patterns, a conclusion of this study is that the eastern portion of the mapped Dragon Pond formation in the Boomerang area is actually composed of *ca.* 491 Ma rocks similar to those that host the Boomerang deposit. Hence, there is no requirement for large-scale unconformaties as proposed by van Staal *et al.* (2005) and Zagorevski *et al.* (2007a).

The Victoria River Mouth formation (Sutherlands Pond group) in the southern TVB of van Staal *et al.* (2005) and Zagorevski *et al.* (2007a, b) (re-named from the Upper Basalts of Evans and Kean, 2002) is defined as tholeiitic pillow basalts with distinct, E-MORB-like chemistry. This group of rocks is interpreted to crop out to the east of the Boomerang deposit and is restricted to a thrust bound slice between the mapped Pats Pond group and the Tulks group (van Staal *et al.*, 2005 and Zagorevski *et al.*, 2007a, b; *see* Figure 33). However, when the extended trace-element profiles for rocks assigned to the Victoria River Mouth formation in the vicinity of the Boomerang deposit are compared to chemical data of Evans and Kean's (2002) Upper Basalts and the Victoria River Mouth formation from the northern TVB, there is a dramatic variance in the chemical profiles (Figure 36). Instead of plotting with E-MORB-like chemistry that defines the rocks in the north, the unit mapped as

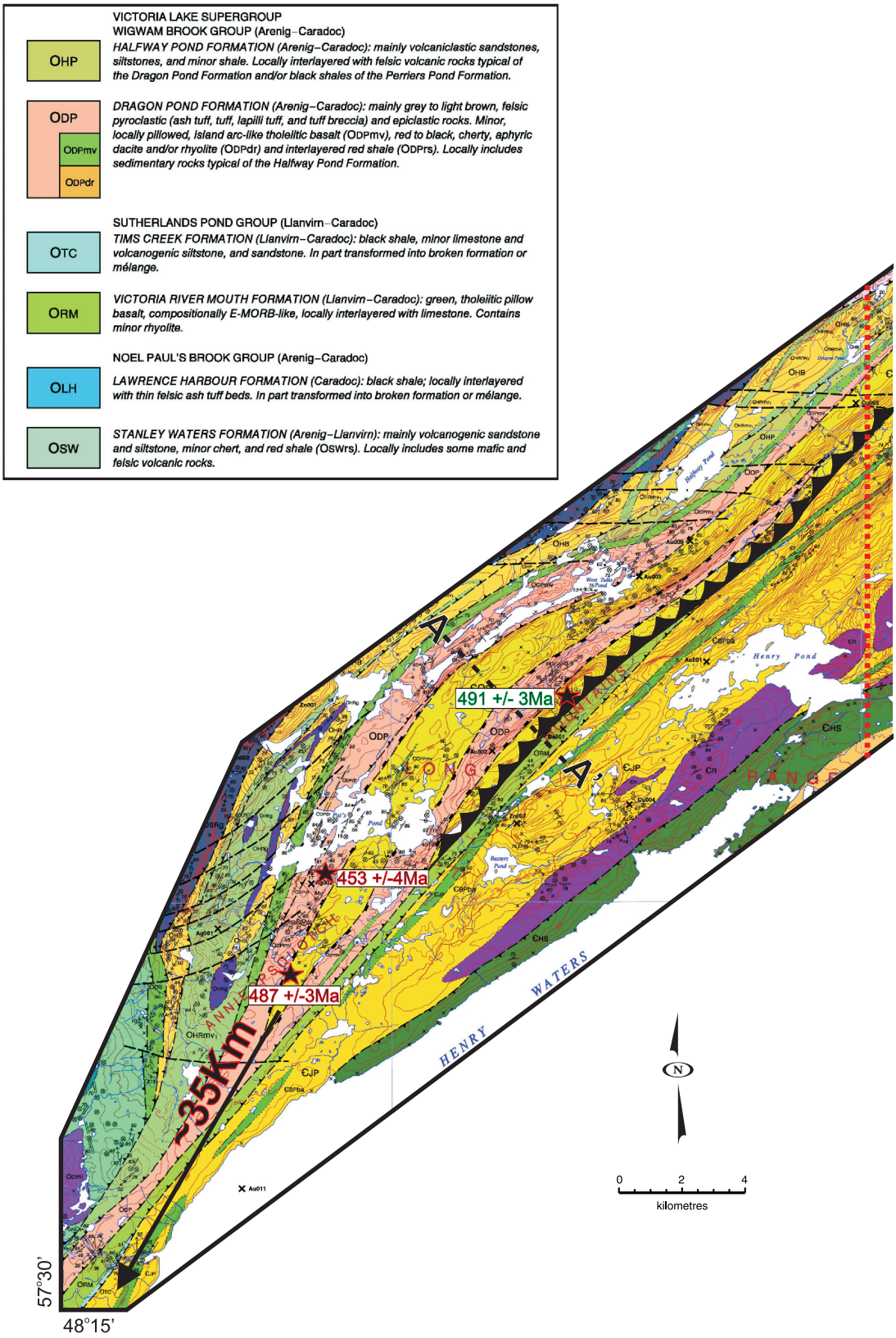

Figure 33. *Geological and stratigraphic relationships in the southern TVB as portrayed by van Staal* et al. *(2005) and Zagorevski* et al. *(2007a). Transect A-A' shown as Figure 34.*

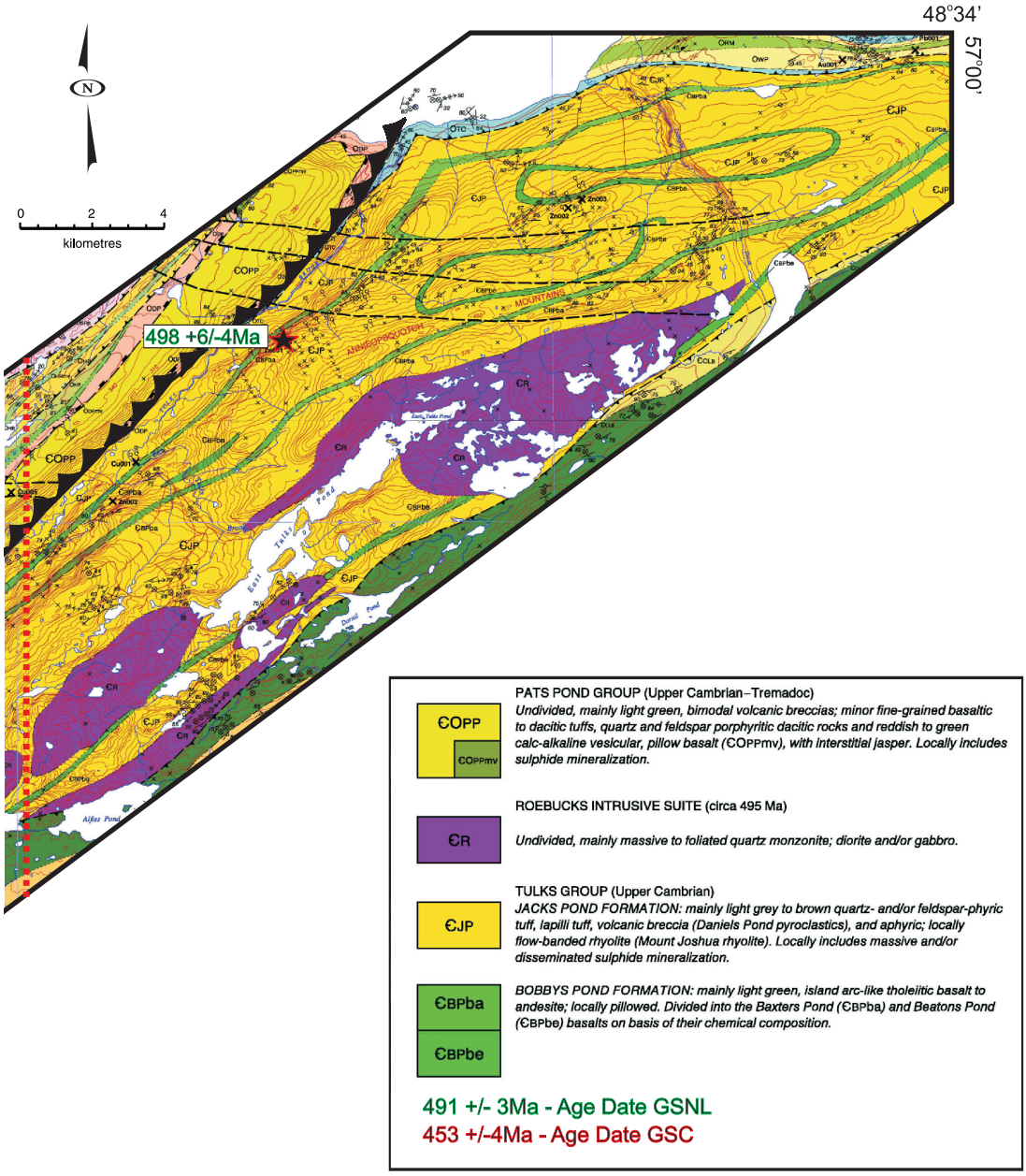

Figure 33 (Continued). *Geological and stratigraphic relationships in the southern TVB as portrayed by van Staal* et al. *(2005) and Zagorevski* et al. *(2007a). Transect A-A' shown as Figure 34.*

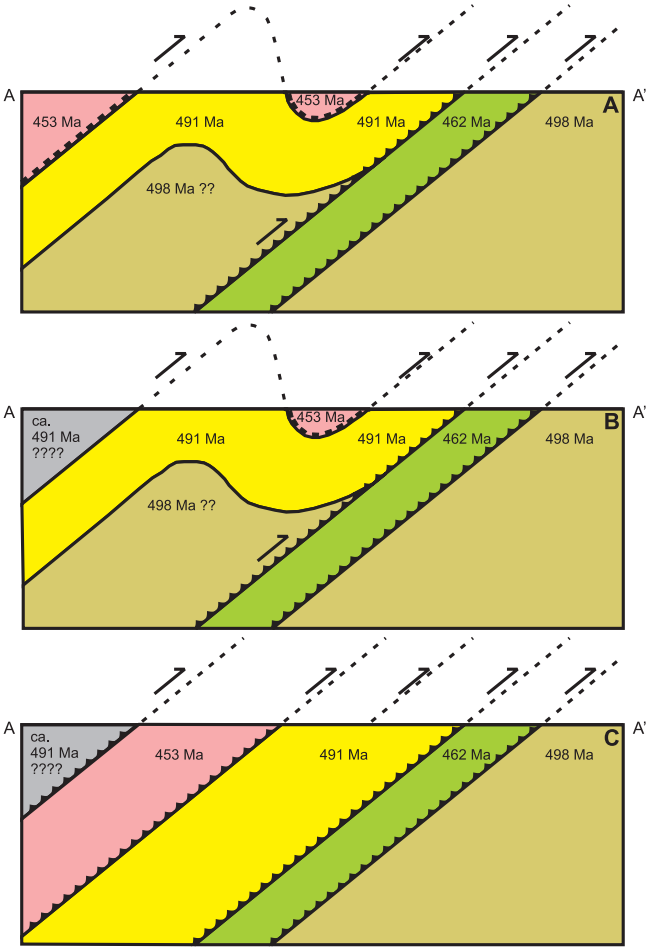

Figure 34. *Structural models illustrating possible explanations of the geology along section A-A' on Figure 33. A. A folded thrust model exposing 491 Ma rocks that unconformably underlie younger 453 Ma rocks; B. A folded thrust model in which the sedimentary rocks included in the Dragon Pond formation (van Staal* et al., *2005 and Zagorevski* et al., *2007a) are of different age; C. Model invoking east-verging large scale thrust stacks that structurally juxtapose sequentially younger packages of rocks from the west (with the exception of the 462 Ma Victoria River Mouth formation).*

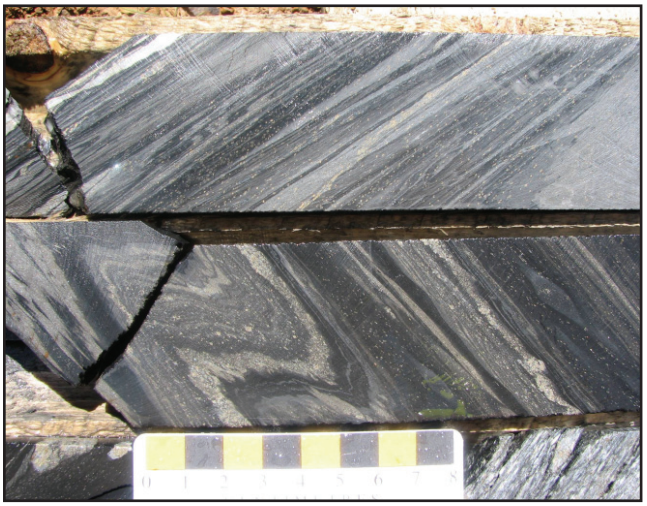

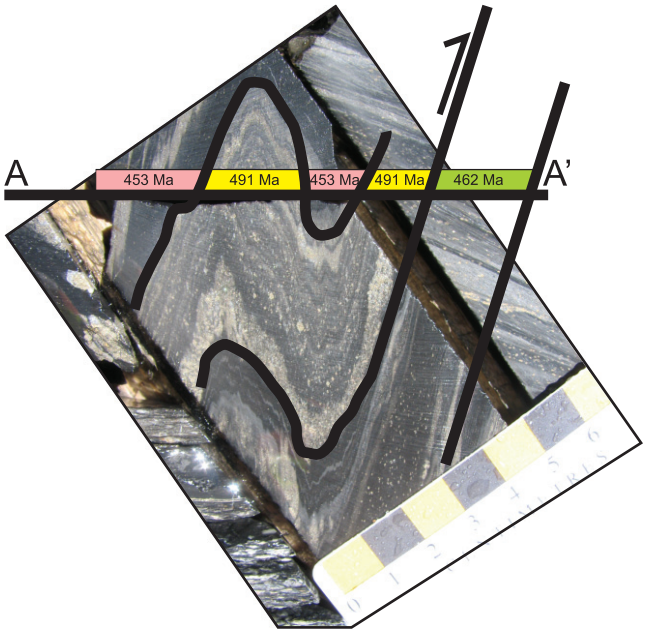

Plate 26. *Folded, mineralized black argillite from the Boomerang deposit representing a potential fold-and-thrust model to explain the map distribution of units along A-A' on Figure 33.*

Victoria River Mouth formation rocks in the Boomerang area plot with distinct negative niobium anomalies and appears very similar to other mafic volcanics of the Pats Pond group and Tulks group (*see* Figures 36, and 37).

A conclusion of this study is that the rocks included as the Victoria River Mouth formation in the vicinity of the Boomerang deposit (*see* Figure 33), do not display the unique E-MORB-like chemistry diagonistic of the Upper Basalts of Evans and Kean (2002) or the Victoria River Mouth formation rocks in the northern TVB of Rogers *et al.* (2006), but rather appear to form part of the older (*ca.* 491–498 Ma) Pats Pond or Tulks group rocks.

If the above lines of evidence are correct, and the eastern panel of the Dragon Pond formation and the panel of the Victoria River Mouth formation do not occur to the east of the Boomerang deposit (Figure 33), then there are implications for tectonostratigraphic modeling for the area. Instead of a series of complex, unconformably and thrust-bound

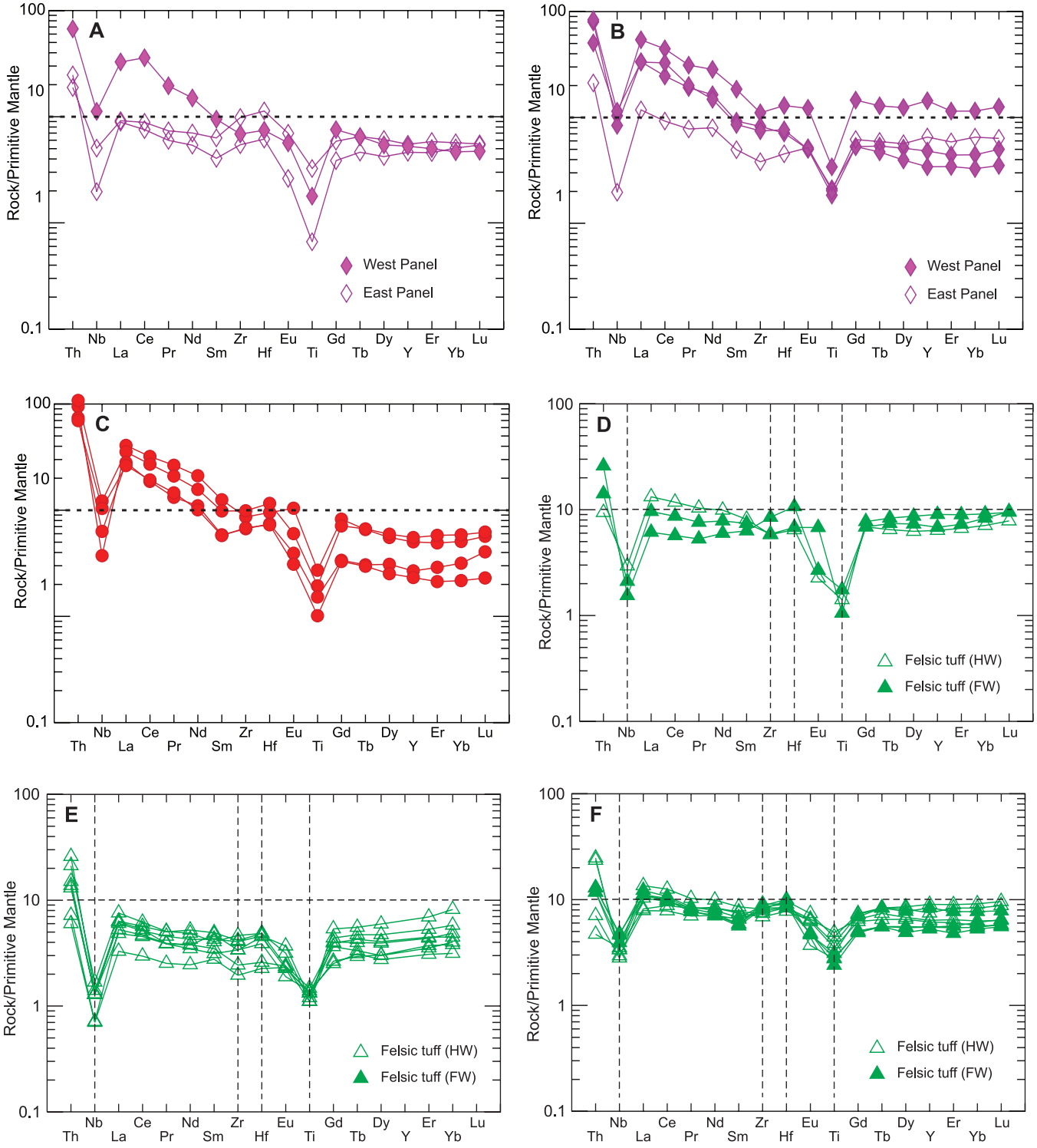

Figure 35. *Comparison of primitive-mantle-normalized trace-element plots for the east and west panels of 'Wigwam Brook' group in the southern TVB with Wigwam Brook group from the northern TVB, Tulks group rocks, and Pats Pond group rocks. A. Wigwam Brook group felsic volcanic rocks from south TVB (this study); B. Wigwam Brook group felsic volcanic rocks from south TVB (Rogers, 2004; Zagorevski* et al.*, 2007a); C. Wigwam Brook group felsic volcanic rocks from north TVB (Rogers, 2004); D. Felsic volcanic rocks from the Tulks East deposit (this study); E. Felsic volcanic rocks from the Pats Pond group (Rogers, 2004; Zagorevski* et al.*, 2007a); F. Felsic volcanic rocks from the Boomerang deposit (this study). HW–hangingwall, FW–footwall.*

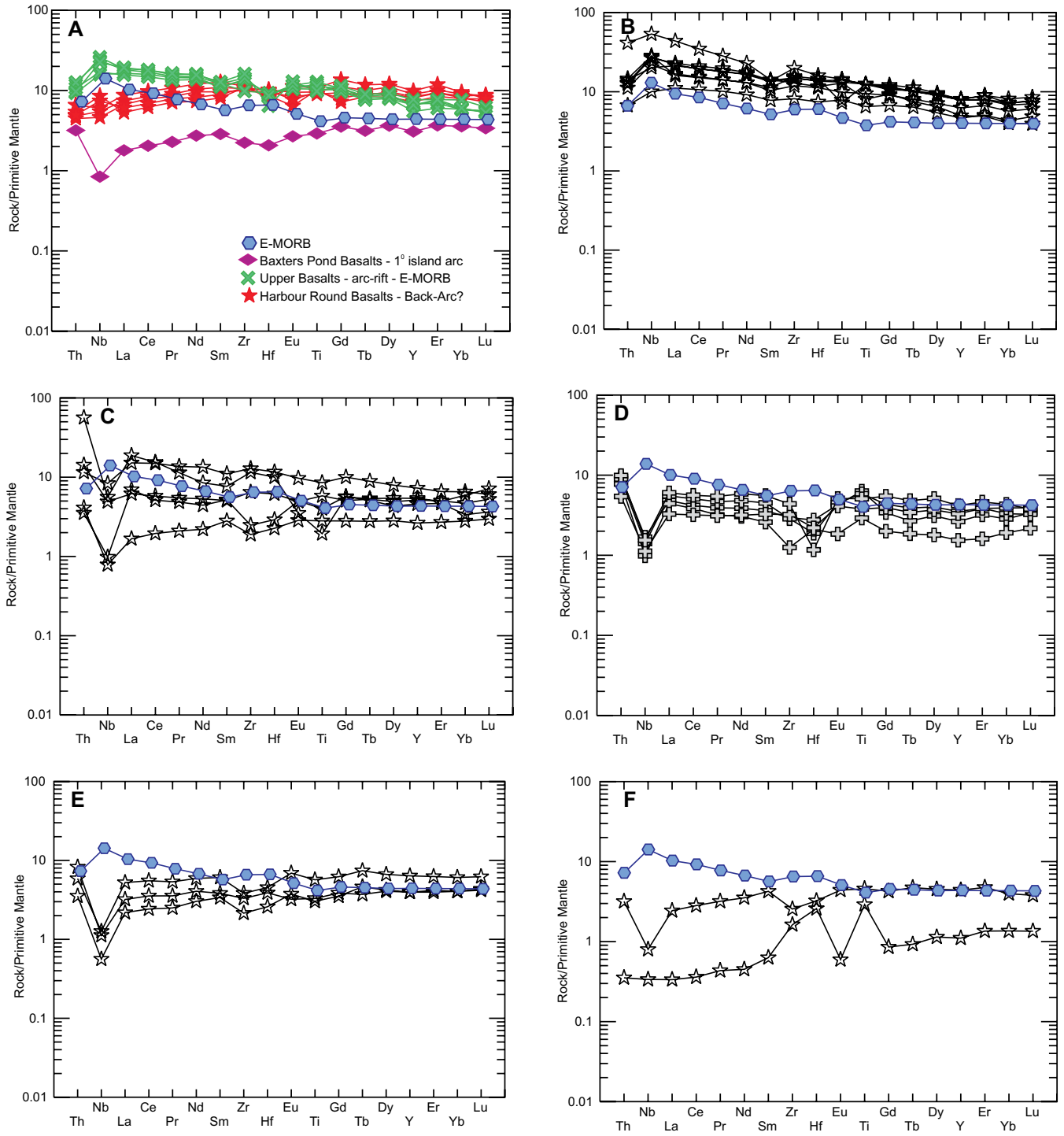

Figure 36. *Comparison of primitive-mantle-normalized trace-element plots for 'Victoria River Mouth formation' rocks in the southern TVB with Victoria River Mouth formation rocks in the northern TVB (*i.e.*, Upper Basalts of Evans and Kean, 2002) and other mafic volcanic rocks in the southern TVB. A. Mafic volcanic rock geochemistry for mafic rocks in the Tulks Valley (Evans and Kean 2002); B. Victoria River Mouth formation (ORM) from the northern TVB (Rogers, 2004); C. Victoria River Mouth formation (ORM) from the southern TVB (Rogers, 2004); D. Tulks Hill Basalts (Evans and Kean, 2002); E. Mafic volcanic rocks from the southern TVB (outcrop samples, this study); F. Mafic volcanic rocks from the southern TVB (Rogers, 2004; Zagorevski* et al.*, 2007a).*

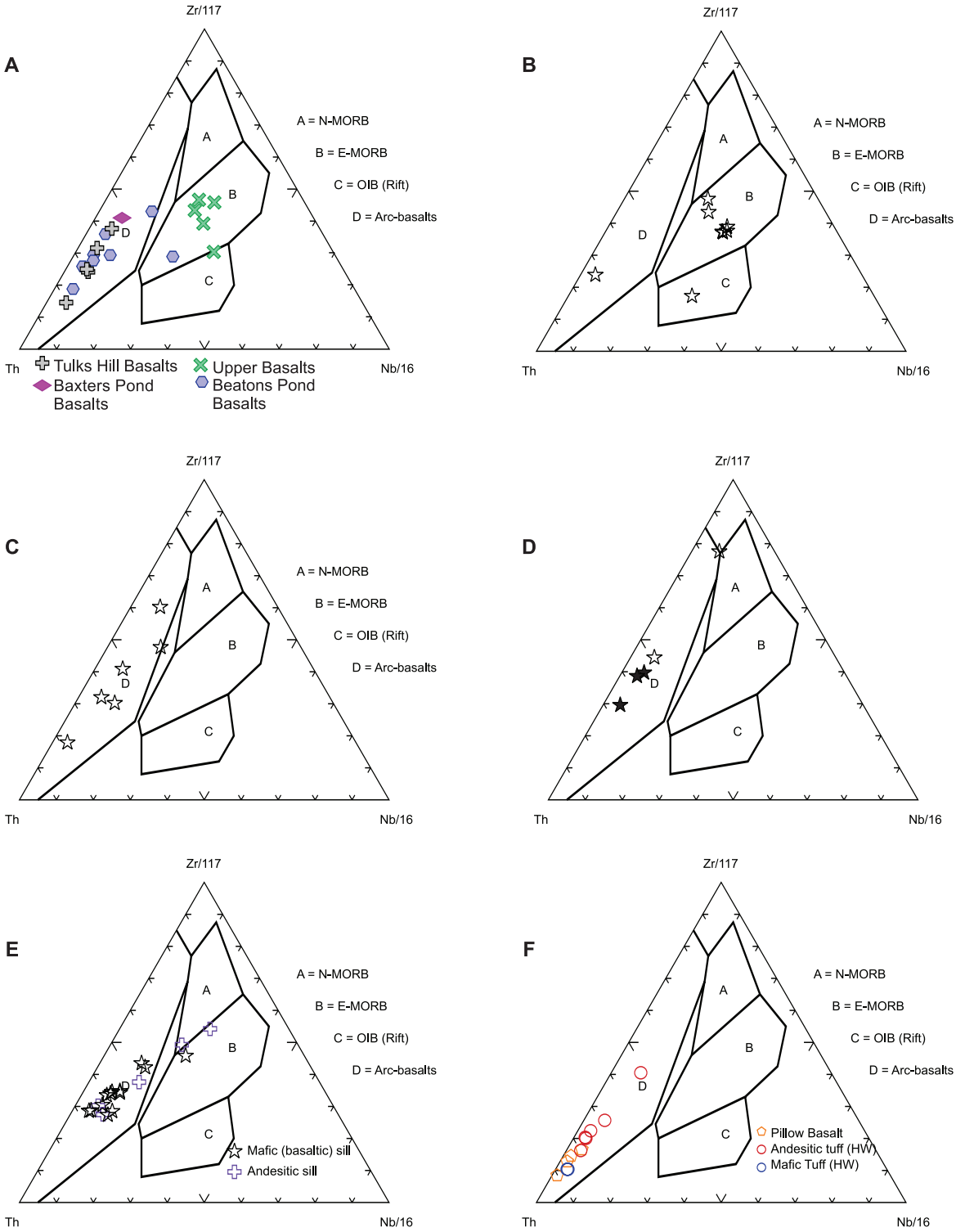

Figure 37. *Comparison of discrimination plots (after Wood, 1980) for 'Victoria River Mouth formation' (ORM) rocks in the southern TVB with Victoria River Mouth formation rocks in the northern TVB (*i.e.*, Upper Basalts of Evans and Kean, 2002) and with other mafic volcanic rocks in the southern TVB. A. Mafic volcanic rock signatures from Evans and Kean (2002); B. Victoria River Mouth formation (ORM) from the northern TVB (Rogers, 2004); C. Victoria River Mouth formation (ORM) from the southern TVB (Rogers 2004); D. Mafic volcanic rock signatures from outcrop as part of this study and from Rogers (2004), Zagorevski* et al. *(2007a); E. Mafic volcanic rock signatures from drillcore samples (this study), and F. mafic volcanic rock signatures from the Pats Pond group (Rogers 2004; Zagorevski* et al.*, 2007a).*

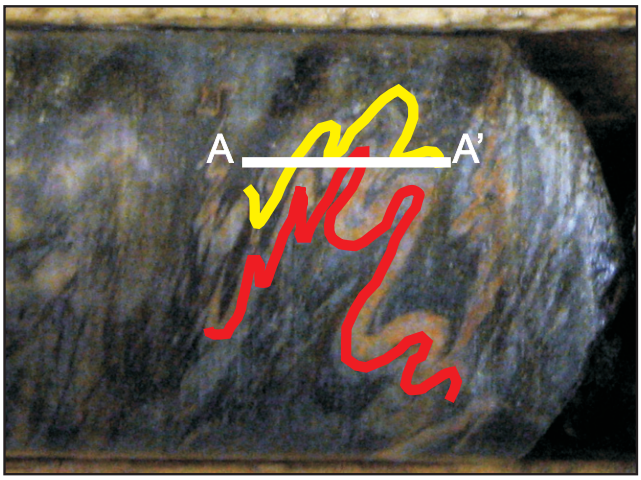

Plate 27. *Z, M and S folds in drillcore from the Tulks West occurrence representing a potential fold and thrust model to explain the map distribution of units along A-A' on Figure 33. Note that the sedimentary unit to the far west on the section are herein interpreted to be ca. 491 Ma versus 453 Ma as interpreted on the map.*

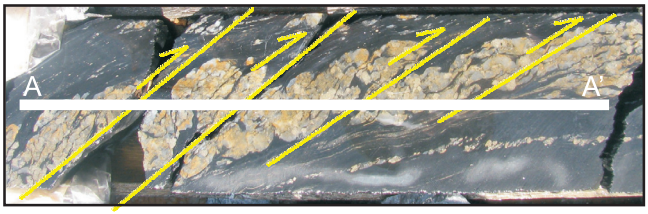

Plate 28. *Thrust-stacked quartz vein in black argillites from the Boomerang deposit representing a possible thrust stack model for the southern TVB to explain the map distribution of units along A-A' on Figure 33. Note that the sedimentary unit to the far west on the section are herein interpreted to be ca. 491 Ma versus 453 Ma as interpreted on the map.*

slivers of various-aged rocks in the southern TVB, the stratigraphy would more closely resemble the homoclinal models with progressively westward-younging sequences of volcanic and volcaniclastic rocks. However, abundant folding and thrusting is recoginized on local scales in drillcore (*see* Plates 26–28), thereby implying that a simple homoclinal model whereby everything becomes progressively younger to the west does not necessarily fit all the observed relationships and evidence.

CONCLUSIONS

Two main types of VMS mineralization occur within the TVB: 1) replacement-style mineralization at the Tulks East, Tulks Hill, Boomerang, and perhaps a portion of the Bobbys Pond deposits, and 2) classic exhalative-style mineralization at the Daniels Pond deposit and the Curve Pond and Dragon Pond prospects. The replacement-style deposits, in particular the Boomerang deposit, display many similarities to deposits such as the Rosebery Deposit in the Cambrian Mount Read Volcanics of Australia. Similarities include the sheet-like replacement style of mineralization, the high Zn–Pb metal content and similar host rocks and alteration styles (*e.g.*, Large *et al.*, 2001). The exhalative-style mineralization has affinities to the world-class deposits of the Bathurst mining camp in New Brunswick (*e.g.,* Goodfellow and McCutcheon, 2003). These similarities include similar ages, bimodal volcanic sedimentary host sequences, and association with regional-scale ferruginous sedimentary rocks (iron formations). Regional geological and geochemical data suggest that most of the VMS mineralization in the TVB developed within an extensional tectonic regime, likely associated with a transition from an active arc to an arc-rift or back-arc environment.

Volcanic lithofacies suggest that there are a number of distinguishable volcanic facies amongst the variable felsic volcanic, pyroclastic and volcaniclastic rocks that host mineralization along the belt. Significantly, there are more vent-proximal rhyolitic facies in the northern part of the belt compared to the volcaniclastic-dominated environments to the south. In contrast to the 'bimodal felsic siliciclastic' dominated deposits in the southern TVB (Hinchey, 2007), the deposits in the northern part of the belt are more akin to 'hybrid VMS-epithermal' style deposits.

New U–Pb zircon data, isotopic data, and geochemical data from volcanic rocks in the TVB of the VLSG are not simple to interpret. In conjunction with previous data, the results suggest that VMS mineralization at the Boomerang deposit is resolvably younger than that at the Tulks Hill deposit. However, the ages are closer to those obtained elsewhere in that part of the unit defined as the Pats Pond group. Subtle lithogeochemical variations, and higher εNd signatures for felsic-intermediate samples from the Boomerang deposit and the Pats Pond group also appear to support this correlation. Inherited zircon of *ca.* 530–510 Ma suggest that the host rocks at the Boomerang deposit, and likely the whole TVB, were deposited upon a substrate of older rocks including material of similar age to the Tally Pond group and, perhaps, also Precambrian basement.

ACKNOWLEDGMENTS

Field work for this project was done with the assistance of Matthew Minnett and Ross Bowers. Many collegues are thanked, including Steve Piercey, Hamish Sandeman, and the geologists of Messina Minerals Inc., Buchans Minerals Corporation (formally Royal Roads Corporation), and Mountain Lake Resources for their interest and helpful discussions on the VLSG and associated VMS deposits. An earlier version of this manuscript benefitted from critical reviews by Andy Kerr and James Walker.

REFERENCES

Agnerian, H.

2008: Technical report on the Bobbys Pond Cu-Zn deposit, Newfoundland and Labrador, Canada. Prepared for Mountain Lake Resources Inc., 110 pages.

Banville, R., Huard, A., Sheppard, D., Woods, G. and Drolet, B.

1998: Assessment report on geological, geochemical, geophysical and diamond drilling exploration for 1997 submission for the Anglo-Newfoundland Development Limited Charter, Reid Lots 227, 229, 234 and 247 and fee simple grants. Volume 1 folio 61 and volume 2 folio 29 in the Victoria Lake-Red Indian Lake areas, central Newfoundland, 10 reports. [012A/1015]

Barbour, D.M. and Thurlow, J.G.

1982: Case histories of two massive sulphide discoveries in central Newfoundland. *In* Prospecting in Areas of Glaciated Terrain. *Edited by* P. Davenport. Canadian Institute of Mining and Metallurgy, pages 300-320.

Barrett, T.J. and MacLean, W.H.
1999: Volcanic sequences, lithogeochemistry and hydrothermal alteration in some bimodal volcanic-associated massive sulfide systems. *In* Volcanic-Associated Massive Sulfide Deposits: Processes and Examples in Modern and Ancient Settings. *Edited by* C.T. Barrie and M.D. Hannington. Reviews in Economic Geology, Society of Economic Geologists, Volume 8, pages 101-127.

Barrie, C.T. and Hannington, M.D.
1999: Classification of volcanogenic-associated massive sulfide deposits based on host-rock composition. *In* Volcanogenic-Associated Massive Sulfide Deposits: Processes and Examples in Modern and Ancient Settings. Reviews in Economic Geology, Society of Economic Geologists, Volume 8, pages 2-12.

Campbell, I.H., Lesher, C.M., Coad, P., Franklin, J.M., Gorton, M.P. and Thurston, P.C.
1984: Rare-earth element mobility in alteration pipes below massive Cu-Zn sulphide deposits. Chemical Geology, Volume 45, pages 181-202.

Dadson, P
2002: Third year and third year supplementary assessment report on geological, geochemical, geophysical and diamond drilling exploration for licences 6565M, 6567M-6570M, 6573M and 6575M on claims in the Jacks Pond to Sutherlands Pond area, central Newfoundland. Assessment file 12A/0935. Kelmet Resources Limited, Royal Roads Corporation and Noranda Incorporated.

Dearin, C.
2006: Technical report on the Tulks South property. Map staked licences: 11924M, 11925M and Reid Lot 228. Red Indian Lake Area, central Newfoundland, Canada. NTS 12A/06 and 12A/11, 158 pages.

Delaney, P., Rice, T., Greene, B.J. and Woods, D.V.
2001: Sixth year assessment report on geophysical and diamond drilling exploration for licence 6166M on claims in the Hungry Hill area, central Newfoundland. Assessment file 12A/0985. Inmet Mining Corporation and Celtic Minerals Limited.

DePaolo, D.J.
1981: Neodymium isotopes in the Colorado Front Range and crust-mangle evolution in the Proterozoic. Nature, Volume 291, pages 193-196.

Desnoyers, D.
1991: Victoria Mine prospect. *In* Metallogenic Framework of Base and Precious Metal Deposits, Central and Western Newfoundland. *Edited by* H.S. Swinden, D.T.W Evans and B.F. Kean. Eighth IAGOD Symposium Field Trip Guidebook. Geological Survey of Canada, Open File 2156, pages 65-67.

Doyle, M.G. and Allen, R.L.
2003: Sub-sea floor replacement in volcanic-hosted massive sulphide deposits. Ore Geology Reviews, Volume 23, pages 183-222.

Dubé, B., Gosselin, P., Hannington, M. and Galley, A.
2007: Gold-rich volcanogenic massive sulphide deposits. *In* Mineral Deposits of Canada: A Synthesis of Major Deposit Types, District Metallogeny, the Evolution of Geological Provinces, and Exploration Methods. *Edited by* W.D. Goodfellow. Geological Association of Canada, Mineral Deposits Division, Special Publication No. 5, pages 141-162.

Dunning, G.R., Kean, B.F., Thurlow, J.G. and Swinden, H.S.
1987: Geochronology of the Buchans, Roberts Arm, and Victoria Lake groups and Mansfield Cove Complex, Newfoundland. Canadian Journal of Earth Sciences, Volume 24, pages 1175-1184.

Evans, D.T.W. and Kean, B.F.
1986: Geology of the Jacks Pond volcanogenic sulphide prospects, Victoria Lake Group, central Newfoundland. *In* Current Research. Newfoundland Department of Mines and Energy, Geological Survey Branch, Report 86-1, pages 59-64.

2002: The Victoria Lake Supergroup, central Newfoundland – its definition, setting and volcanogenic massive sulphide mineralization. Newfoundland Department of Mines and Energy, Geological Survey, Open File NFLD/2790, 68 pages.

Evans, D.T.W., Kean, B.F. and Dunning, G.R.
1990: Geological studies, Victoria Lake Group, central Newfoundland. *In* Current Research. Newfoundland Department of Mines and Energy, Geological Survey Branch, Report 90-1, pages 131-144.

Evans, D.T.W, Kean, B.F. and Jayasinghe, N.R.
1994a: Geology and mineral occurrences of Noel Paul's Brook. Map 94-222. Scale: 1:50 000. Newfoundland Department of Mines and Energy, Geological Survey Branch, Open File 012A/09/0685.

1994b: Geology and mineral occurrences of Badger. Map 94-224. Scale: 1:50 000. Newfoundland Department of Mines and Energy, Geological Survey Branch, Open File 012A/16/0687.

Evans, D.T.W., Kean, B.F. and Mercer, N.L.
1994c: Geology and mineral occurrences of Lake Ambrose. Map 94-223. Scale: 1:50 000. Newfoundland Department of Mines and Energy, Geological Survey Branch, Open File 012A/10/0686. Blueline paper. GS# 012A/10/0686.

Evans, D.T.W. and Wilton, D.H.C.
2000: The Midas Pond gold grospect, Victoria Lake Group, central Newfoundland: A mesothermal quartz vein system with epithermal characteristics. Exploration and Mining Geology, Volume 9, number 1, pages 65-79.

Finch, C.J.
1998: Inductively coupled plasma – emission spectrometry (ICP-ES) at the geochemical laboratory. *In* Current Research. Newfoundland Department of Mines and Energy, Geological Survey Branch, Report 98-1, pages 179-194.

Finlow-Bates, T. and Stumpfl, E.F.
1981: The behaviour of so-called immobile elements in hydrothermally altered rocks associated with volcanogenic submarine-exhalative ore deposits. Mineralium Deposita, Volume 16, pages 319-328.

Franklin, J.M., Gibson, H.L., Jonasson, I.R. and Galley, A.G.
2005: Volcanogenic massive sulfide deposits. *In* 100th Anniversary Volume, 1905-2005. Economic Geology, pages 523-560.

Galley, A.G.
1993: Semi-conformable alteration zones in volcanogenic massive sulphide districts. Journal of Geochemical Exploration, Volume 48, pages 175-200.

Galley, A.G., Hannington, M.D. and Jonasson, I.R.
2007: Volcanogenic massive sulphide deposits. *In* Mineral Deposits of Canada: A Synthesis of Major Deposit Types, District Metallogeny, the Evolution of Geological Provinces, and Exploration Methods. *Edited by* W.D. Goodfellow. Geological Association of Canada, Mineral Deposits Division, Special Publication No. 5, pages 141-162.

Gibson, H.L.
2005: Volcanic-hosted ore deposits. *In* Volcanoes in the Environment. *Edited by* J. Marti and G. Ernst. New York, NY, Cambridge University Press, pages 944-952.

Gifkins, C., Herrmann, W. and Large, R.
2005: Altered Volcanic Rocks: A Guide to Description and Interpretation. Centre for Ore Deposit Research, University of Tasmania, Australia, 275 pages.

Goodfellow, W.D. and McCutcheon, S.R.
2003: Geologic and genetic attributes of volcanic-sediment hosted massive sulphide deposits of the Bathurst Mining Camp, northern New Brunswick – A synthesis. Economic Geology Monograph 11, pages 245-302.

Greene, B.J., Rice, T.G. and Delaney, P.W.
2001: Assessment report on geological, geochemical and trenching exploration for 2000-2001 submission for fee simple grants volume 1 folio 110, volume 2 folio 25 and special volume 2 folio 307 and for first, second and fifth year assessment for licences 6166M, 6710M-6711M, 6743M and 7710M on claims in the Victoria River area, central Newfoundland. Assessment file 12A/0971. Inmet Mining Corporation and Celtic Minerals Limited.

Hannington M.D., Poulsen K.H., Thompson J.F.H. and Sillitoe R.H.
1999: Volcanogenic gold in the massive sulfide environment. *In* Volcanic-Associated Massive Sulfide Deposits: Processes and Examples in Modern and Ancient Settings. *Edited by* C.T. Barrie and M.D. Hannington. Society of Economic Geologists, Littleton, CO, USA, pages 325-356.

Hinchey, J.G.
2007: Volcanogenic massive sulphides of the southern Tulks Volcanic Belt, central Newfoundland: Preliminary findings and overview of styles and environments of mineralization. *In* Current Research. Newfoundland and Labrador Department of Natural Resources, Geological Survey, Report 07-1, pages 117-143.

2008: Volcanogenic massive sulphides of the northern Tulks Volcanic Belt, central Newfoundland: Preliminary findings, overview of deposit reclassifications and mineralizing environments. *In* Current Research. Newfoundland and Labrador Department of Natural Resources, Geological Survey, Report 08-1, pages 151-172.

Hinchey, J.G. and McNicoll, V.
2009: Tectonostratigraphic architecture and VMS mineralization of the southern Tulks Volcanic Belt: New insights from U–Pb geochronology and lithogeochemistry. *In* Current Research. Newfoundland and Labrador Department of Natural Resources, Geological Survey, Report 09-1, pages 13-42.

Huston, D.L. and Kamprad, J.
2001: Zonation of alteration facies at Western Tharsis:

Implications for the genesis of Cu-Au deposits, Mount Lyell Field, Western Tasmania. Economic Geology, Volume 96, pages 1123-1132.

Hynes, A.
1980: Carbonatization and mobility of Ti, Y, and Zr in Ascot Formation metabasalts, SE Québec. Contributions to Mineralogy and Petrology, Volume 75, pages 79-87.

Ishikawa, Y., Sawaguchi, T., Ywaya, S. and Horiuchi, M.
1976: Delineation of prospecting targets for Kuroko deposits based on modes of volcanism of underlying dacite and alteration haloes. Mining Geology, Volume 26, pages 105-117.

Jambor, J.L.
1984: Preliminary report on the mineralogy of the Tulks massive sulphide deposit, Buchans area, Newfoundland. *In* Current Research. Newfoundland Department of Mines and Energy, Mineral Development Division, Report 84-1, page 189.

Jambor, J.L. and Barbour, D.M.
1987: Geology and mineralogy of the Tulks pyritic massive sulphide deposit. *In* Buchans Geology, Newfoundland. *Edited by* R.V. Kirkham. Geological Survey of Canada, Paper 86-24, pages 219-226.

Jiang, S.-Y., Wang, R.-C., Xu, X.-S. and Zhao, K.-D.
2005: Mobility of high field strength elements (HFSE) in magmatic-, metamorphic-, and submarine-hydrothermal systems. Physics and Chemistry of the Earth, Volume 30, pages 1020-1029.

Kean, B.F.
1977: Geology of the Victoria Lake map area (12A/06), Newfoundland. Newfoundland Department of Mines and Energy, Mineral Development Division, Report 77-4, 11 pages.

1979a: Star Lake, Newfoundland. Map 79-001. Scale 1:50,000. Newfoundland Department of Mines and Energy, Mineral Development Division (with descriptive notes).

1979b: Buchans, Newfoundland. Map 79-125. Scale 1:50,000. Newfoundland Department of Mines and Energy, Mineral Development Division (with descriptive notes).

1982: Victoria Lake, Newfoundland. Map 82-009. Scale: 1:50 000. Government of Newfoundland and Labrador, Department of Mines and Energy, Mineral Development Division.

1983: King George IV Lake, Grand Falls district, Newfoundland. Map 82-051. Scale 1:50,000. *In* Geology of the King George IV Lake map area (12A/4). Newfoundland Department of Mines and Energy, Mineral Development Division, Report 83-4, 74 pages.

Kean, B.F., Dean, P.L. and Strong, D.F.
1981: Regional geology of the Central Volcanic Belt of Newfoundland. *In* The Buchans Orebodies: Fifty Years of Geology and Mining. *Edited by* E.A. Swanson, J.G. Thurlow and D.F. Strong. Geological Association of Canada, Special Paper 22, pages 65-78.

Kean, B.F. and Evans, D.T.W
1986: Metallogeny of the Tulks Hill volcanics, Victoria Lake Group, central Newfoundland. *In* Current Research. Newfoundland Department of Mines and Energy, Mineral Development Division, Report 86-1, pages 51-57.

1988: Regional metallogeny of the Victoria Lake Group. *In* Current Research. Newfoundland Department of Mines, Report 88-1, pages 319-330.

Kean, B.F. and Jayasinghe, N.R.
1980: Geology of the Lake Ambrose (12-A/10) – Noel Pauls Brook (12-A/9) map areas, central Newfoundland. Newfoundland Department of Mines and Energy, Mineral Development Division, Report 80-02, 33 pages, 2 maps.

1982: Geology of the Badger map area (12-A/16), Newfoundland. Newfoundland Department of Mines and Energy, Mineral Development Division, Report 81-2, 42 pages.

Kean, B.F. and Mercer, N.L.
1981: Grand Falls map area (2D/13), Newfoundland. Newfoundland Department of Mines and Energy, Mineral Development Division, Map 8199.

Krogh, T.E.
1982: Improved accuracy of U-Pb ages by creation of more concordant systems using an air abrasion technique. Geochimica et Cosmochimica Acta, Volume 46, pages 637-649.

Large, R.R., Gemmell, J.B., Paulick, H. and Huston, D.L.
2001: The alteration box plot: A simple approach to understanding the relationship between alteration mineralogy and lithogeochemistry associated with volcanic-hosted massive sulphide deposits. Economic Geology, Volume 96, pages 957-971.

Lentz, D.R.
1998: Petrogenetic evolution of felsic volcanic sequences associated with Phanerozoic volcanic-hosted massive sulphide systems: The role of extensional geodynamics. Ore Geology Reviews, Volume 12, pages 289-327.

1999: Petrology, geochemistry, and oxygen isotope interpretation of felsic volcanic and related rocks hosting the Brunswick 6 and 12 massive sulphide deposits (Brunswick Belt), Bathurst mining camp, New Brunswick, Canada. Economic Geology, Volume 94, pages 57-86.

Lesher, C.M., Goodwin, A.M., Campbell, I.H. and Gorton, M.P.
1986: Trace element geochemistry of ore-associated and barren felsic metavolcanic rocks in the Superior Province, Canada. Canadian Journal of Earth Sciences, Volume 23, pages 222-237.

Lissenberg, C.J., Zagorevski, A., Rogers, N., van Staal, C.R. and Whalen, J.B.
2005: Geology, Star Lake, Newfoundland and Labrador. Geological Survey of Canada, Open File 1669, scale 1:50 000.

Ludwig, K.R.
1998: On the treatment of concordant uranium-lead ages. Geochimica et Cosmochimica Acta, Volume 62, pages 665-676.

2003: User's manual for Isoplot/Ex rev. 3.00: A Geochronological toolkit for Microsoft Excel, Special Publication, 4, Berkeley Geochronology Center, Berkeley, 70 pages.

MacLean, W.H. and Barrett, T.J.
1993: Lithogeochemical techniques using immobile elements. Journal of Geochemical Exploration, Volume 48, pages 109-133.

McKenzie, C., Desnoyers, D., Barbour, D. and Graves, M.
1993: Contrasting volcanic-hosted massive sulphide styles in the Tulks Belt, central Newfoundland. Exploration and Mining Geology, Volume 2, Number 1, pages 73-84.

McNicoll, V., Squires, G., Kerr, A. and Moore, P.
2010: The Duck Pond and Boundary Cu–Zn deposits, Newfoundland: new insights into ages of host rocks and the timing of VHMS mineralization. Canadian Journal of Earth Sciences, Volume 47, pages 1481-1506.

McNicoll, V.J., Squires, G., Kerr, A. and Moore, P.
2008: Geological and metallogenic implications of new U-Pb zircon geochronological data from the Tally Pond volcanic belt, central Newfoundland. *In* Current Research. Newfoundland and Labrador Department of Natural Resources, Geological Survey, Report 08-1, pages 1-19.

Moore, P.J.
2003: Stratigraphic implications for mineralization: Preliminary findings of a metallogenic investigation of the Tally Pond volcanics, central Newfoundland. *In* Current Research. Newfoundland and Labrador Department of Natural Resources, Geological Survey, Report 03-1, pages 241-257.

Moreton, C.
1984: A geological, geochemical, and structural analysis of the Lower Ordovician Tulks Hill Cu-Zn- (Pb) volcanogenic massive sulphide deposit, central Newfoundland, Canada. M.Sc. thesis, Memorial University of Newfoundland, St. John's, 320 pages.

Noranda Ltd.
1998: Precious and base metal properties available for option in central Newfoundland. Summary Report, ca. 500 pages.

Page, A.M., Lentz, D.R. and Toole, R.M.
2008: Distribution, form, and origin of precious metals in the Boomerang and Domino volcanogenic massive sulfide deposits, Tulks Belt, central Newfoundland. Geological Association of Canada, Abstract Volume 33, page 127.

Pandarinath, K., Dulski, P., Torres-Alvarada, I.S. and Verma, S.P.
2008: Element mobility during the hydrothermal alteration of rhyolitic rocks of the Los Azufres geothermal field, Mexico. Geothermics, Volume 37, pages 53-72.

Parrish, R.R., Roddick, J.C., Loveridge, W.D., and Sullivan, R.W.
1987: Uranium-lead analytical techniques at the Geochronology Labroratory, Geological Survey of Canada. *In* Radiogenic Age and Isotope Studies, Report 1. Geological Survey of Canada Paper 87-2, pages 3-7.

Pearce, J.A. and Peate, D.W.
1995: Tectonic implications of the composition of volcanic arc magmas. Annual Reviews in Earth and Planetary Science, Volume 23, pages 251-285.

Pearce, J.A., Harris, B.W. and Tindle, A.G.
1984: Trace element discrimination diagrams for the tectonic interpretation of granitic rocks. Journal of Petrology, Volume 25, pages 956-983.

Piercey, S.J., Paradis, S., Murphy, D.C. and Mortensen, J.K.
2001: Geochemistry and paleotectonic setting of felsic volcanic rocks in the Finlayson Lake volcanic-hosted massive sulfide (VHMS) district, Yukon, Canada. Economic Geology, Volume 96, pages 1877-1905.

Riley, G.C.
1957: Red Indian Lake (west half), Newfoundland. Geological Survey of Canada, Map 8-1957 (with descriptive notes).

Roddick, J.C.
1987: Generalized numerical error analysis with applications to geochronology and thermodynamics. Geochimica et Cosmochimica Acta, Volume 51, pages 2129-2135.

Rogers, N.
2004: Geochemical Database, Red Indian Line Project, central Newfoundland. Geological Survey of Canada, Open File 4605, 1 CD-ROM.

Rogers, N. and van Staal, C.R.
2002. Towards a Victoria Lake Supergroup: a provisional stratigraphic revision of the Red Indian to Victoria lakes area, central Newfoundland. *In* Current Research. Newfoundland and Labrador Department of Natural Resources, Geological Survey, Report 02-1, pages 185-195.

Rogers, N., van Staal, C.R., McNicoll, V.J., Pollock, J., Zagorevski, A. and Whalen, J.B.
2006: Neoproterozoic and Cambrian arc magmatism along the eastern margin of the Victoria Lake Supergroup: A remnant of Ganderian basement in central Newfoundland? Precambrian Research, Volume 147, pages 320-341.

Rogers, N., van Staal, C.R., McNicoll, V.J., Squires, G.C., Pollock, J. and Zagorevski, A.
2005: Geology, Lake Ambrose and part of Buchans, Newfoundland and Labrador. Geological Survey of Canada, Open File 4544, scale 1: 50 000.

Saunders, P.
1999: Report on the Tulks Property, Newfoundland. Newfoundland and Labrador Geological Survey. Assessment file 12A/11/0883, 1999, 17 pages. J.Tuach Geological Consultants Inc.

Sillitoe, R.L., Hannington, M.D. and Thompson, J.F.H.
1996: High-sulfidation deposits in the volcanogenic massive sulphide environment. Economic Geology, Volume 91, pages 204-212.

Shervais, J.W.
1982: Ti-V plots and the petrogenesis of modern and ophiolitic lavas. Earth and Planetary Science Letters, Volume 59, pages 101-118.

Squires, G.C.
2008: The Boomerang and Duck Pond VMS deposits, Newfoundland: Birth by "raining" or "stewing"? Geological Association of Canada – Newfoundland and Labrador Section Annual Spring Technical Meeting, February, 2008, Program with Abstracts, page 29.

Squires, G.C., Brace, T.D. and Hussey, A.M.
2001: Newfoundland's polymetallic Duck Pond deposit: Earliest Iapetan VMS mineralization, formed within a sub-seafloor, carbonate-rich alteration system. *In* Geology and Mineral Deposits of the Northern Dunnage Zone, Newfoundland Appalachians. *Edited by* D.T.W. Evans and A. Kerr. GAC/MAC Field Trip Guide A2 (Part 1), pages 167-187.

Squires, G.C.S. and Moore, P. J.
2004: Volcanogenic massive sulphide environments of the Tally Pond volcanics and adjacent area: Geological, lithogeochemical and geochronological results. *In* Current Research. Newfoundland and Labrador Department of Natural Resources, Geological Survey, Report 04-1, pages 63-91.

Squires, G., Tallman, P., Sparkes, K., Hyde, D., House, F. and Regular, K.
2005: Messina Minerals' new Boomerang VMS discovery: Preliminary evaluation of a sub-seafloor replacement-style massive sulphide deposit. CIMM Newfoundland Branch Meeting, November, 2005, Program with Abstracts, page 15.

Stern, R.A.
1997: The GSC Sensitive High Resolution Ion Microprobe (SHRIMP): analytical techniques of zircon U-Th-Pb age determinations and performance evaluation. *In* Radiogenic Age and Isotopic Studies, Report 10. *In* Current Research. Geological Survey of Canada, 1997-F, pages 1-31.

Stern, R.A. and Amelin, Y.
2003: Assessment of errors in SIMS zircon U-Pb geochronology using a natural zircon standard and NIST SRM 610 glass. Chemical Geology, Volume 197, pages 111-142.

Stewart, R. and Beischer, G.
1993: The Bobbys Pond base metal sulphide deposit, Victoria property, central Newfoundland. *In* Ore Horizons. *Edited by* A. Hogan and H.S. Swinden. Newfoundland Department of Mines and Energy, Geological Survey Branch, Volume 2, pages 89-100.

Sun, S.-S. and McDonough, W.F.
1989: Chemical and isotopic systematics of oceanic basalts: implications for mantle composition and processes. *In* Magmatism in the Ocean Basins. *Edited by* A.D. Saunders and M.J. Norry. Geological Society, London, Special Publication Number 42, pages 313-345.

Sverjensky, D.A.
1984: Europium redox equilibria in aqueous solutions. Earth and Planetary Science Letters, Volume 67, pages 70-78.

Swinden, H.S.
1990: Regional geology and metallogeny of central Newfoundland. *In* Metallogenic Framework of Base and Precious Metal Deposits, Central and Western Newfoundland. *Edited* by H.S. Swinden, D.T.W. Evans and B.F. Kean. Eight IAGOD Symposium Field Trip Guidebook. Geological Survey of Canada, Open File 2156, pages 1-27.

1991: Paleotectonic settings of volcanogenic massive sulphide deposits in the Dunnage Zone, Newfoundland Appalachians. Canadian Institute of Mining and Metallurgy Bulletin, Volume 84, pages 59-89.

1996: The application of volcanic geochemistry in the metallogeny of volcanic-hosted sulphide deposits in central Newfoundland, *In* Trace Element Geochemistry of Volcanic Rocks: Applications for Massive Sulphide Exploration. *Edited by* D.A. Wyman. Geological Association of Canada, Short Course Notes, Volume 12, pages 329-358.

Swinden, H.S., Jenner, G.A., Kean, B.F. and Evans, D.T.W.
1989: Volcanic rock geochemistry as a guide for massive sulphide exploration in central Newfoundland. *In* Current Research. Newfoundland Department of Mines, Geological Survey Branch, Report 89-1, pages 201-219.

Tallman, P.
2000: Reid Lot 228 Impost Report for 1999: 1978 grid recovery, mapping, drill hole Location, and 1999 diamond drilling part of the Tulks South Property, NTS map sheet 12A/11, central Newfoundland.

2006: Block modeling and grade variance of Messina Minerals' Boomerang massive sulphide deposit, central Newfoundland. Canadian Institute of Mining, Metallurgy and Petroleum, Newfoundland Branch. 53rd Annual Conference and Trade Show, Abstract volume, page 18.

van Staal, C.R., Dewey, J.F., Mac Niocaill, C. and McKerrow, W.S.
1998: The Cambrian - Silurian tectonic evolution of the northern Appalachians and British Caledonides: history of a complex west- and southwest-Pacific type segment of Iapetus. Geological Society, London, Special Publication 143, pages 199-242.

van Staal, C.R., Valverde-Vaquero, P., Zagorevski, A., Rogers, N., Lissenberg, C.J. and McNicoll, V.J.
2005: Geology, Victoria Lake, Newfoundland and Labrador. Geological Survey of Canada, Open File 1667, Scale 1:50,000.

Webster, P.C., Barr, J.F. and Albuquerque, R.C.
2008: Technical report on the Daniels Pond deposit and property holdings of Royal Roads Corp. Red Indian Lake area, Newfoundland, Canada, 96 pages.

Whitford, D.J., Korsch, M.J., Porritt, P.M. and Craven, S.J.
1988: Rare earth element mobility around the volcanogenic polymetallic massive sulphide deposit at Que River, Tasmania, Australia. Chemical Geology, Volume 68, pages 105-119.

Williams, H.
1970: Red Indian Lake (east half), Newfoundland. Geological Survey of Canada, Map 1196A.
1995: Geology of the Appalachian-Caledonian Orogen in Canada and Greenland. Geological Survey of Canada, Geology of Canada: Temporal and Spatial divisions; Chapter 2, pages 21-44.

Williams, H., Colman-Sadd, S.P. and Swinden, H.S.
1988: Tectono-stratigraphic subdivisons of central Newfoundland. *In* Current Research, Part B. Geological Survey of Canada, Paper 88-1B, pages 91-98.

Winchester, J.A. and Floyd, P.A.
1977: Geochemical discrimination of different magma series and their differentiation products using immobile elements. Chemical Geology, Volume 20, pages 325-343.

Wood, D.A.
1980: The application of a Th-Hf-Ta diagram to problems of tectonmagmatic classification and to establishing the nature of crustal contamination of basaltic lavas

of the British Tertiary volcanic province. Earth and Planetary Science Letters, Volume 50, pages 11-30.

York, D.
1969: Least squares fitting of a straight line with correlated errors. Earth and Planetary Science Letters, Volume 5, pages 320-324.

Zagorevski, A.
2006: Tectono-magmatic evolution of peri-Laurentian and peri-Gondwanan arc – backarc complexes along the Red Indian Line, central Newfoundland Appalachians. Unpublished Ph.D. thesis, University of Ottawa, Ottawa, 304 pages.

Zagorevski, A., Rogers, N. and van Staal, C.R.
2003: Tectonostratigraphic relationships in the Lloyds River and Tulks Brook region of central Newfoundland: A geological link between Red Indian and King George IV lakes. *In* Current Research. Newfoundland Department of Mines and Energy, Geological Survey, Report 03-1, pages 167-178.

Zagorevski, A., van Staal, C.R., McNicoll, V. and Rogers, N.
2007a: Upper Cambrian to Upper Ordovician peri-Gondwanan island arc activity in the Victoria Lake Supergroup, Central Newfoundland: Tectonic development of the northern Ganderian margin. American Journal of Science, Volume 307, pages 339-370.

Zagorevski, A., van Staal, C.R., and McNicoll, V.
2007b: Distinct Taconic, Salinic, and Acadian deformation along the Iapetus suture zone, Newfoundland Appalachians. Canadian Journal of Earth Sciences, Volume 44, pages 1567-1585.

Zagorevski, A., van Staal, C.R., McNicoll, V., Rogers, N. and Valverde-Vaquero, P.
2008: Tectonic architecture of an arc-arc collision zone, Newfoundland Appalachians. *In* Formation and Applications of the Sedimentary Record in Arc Collision Zones. *Edited by* A. Draut, P.D. Clift and D.W. Scholl. Geological Society of America, Special Paper 436, pages 309-333.

Appendix 1A: Sample Locations and Brief Descriptions

Hole_ID	From_m	To_m	SampleNum	Property	Descriptn
77537	168.5	168.7	JHC-07-268	Bobbys Pond VMS	Quartz-carbonate-sericite ± pyrophyllite altered felsic tuff. Intensely sheared.
77537	193	193.2	JHC-07-272	Bobbys Pond VMS	Brecciated rhyolite. Silicified throughout and contains carbonate spots throughout.
77537	180.8	181	JHC-07-271	Bobbys Pond VMS	Mineralized rhyolitic breccia with sphalerite-chalcopyrite rich sulphide stringers. Occurs in the immediate footwall.
77537	170.4	170.6	JHC-07-269	Bobbys Pond VMS	Massive base-metal-rich (predominately sphalerite-galena) sulphide.
77537	138	138.2	JHC-07-267	Bobbys Pond VMS	Very fine-grained and silicified felsic tuff with fine-grained sediment. Abundant stringers of pyrite ± sphalerite and galena. Immediate footwall rock.
77537	127.5	127.7	JHC-07-266	Bobbys Pond VMS	Pseudo-brecciated rhyolite.
77537	83.9	84.1	JHC-07-265	Bobbys Pond VMS	Silica-carbonate altered, quartz-eye phyric rhyolite.
77537	68	68.2	JHC-07-264	Bobbys Pond VMS	Very white, bleached and silicified rhyolite.
77537	54.3	54.5	JHC-07-263	Bobbys Pond VMS	Extremely sheared felsic lapilli tuff with cm-scale rhyolitic clasts. Carbonate occurs as overprinting spots.
77537	45.2	45.4	JHC-07-262	Bobbys Pond VMS	Locally schistose, well foliated, altered felsic tuff.
77537	177.9	178.1	JHC-07-270	Bobbys Pond VMS	Massive base-metal-rich (sphalerite-galena) sulphide. Sulphide contains some internal quartz-crystals which may suggest a replacement mineralizing process.
77537	31.7	31.9	JHC-07-261	Bobbys Pond VMS	Very bleached, white, silicifed rhyolite with carbonate spots and disseminations and veinlets of pyrite.
77538	23.3	23.5	JHC-07-278	Bobbys Pond VMS	Quartz-feldspar phyric, altered rhyolite.
77538	166.2	166.4	JHC-07-284	Bobbys Pond VMS	Siliceous, white to light-grey rhyolite.
77538	146.4	146.6	JHC-07-283	Bobbys Pond VMS	Felsic lapilli tuff?
77538	108.1	108.3	JHC-07-282	Bobbys Pond VMS	Felsic lapilli tuff to a rhyolitic breccia. Local pyrite-sphalerite mm-cm scale stringers.
77538	64.5	64.7	JHC-07-281	Bobbys Pond VMS	Silica-sericite-pyrite altered felsic tuff. Intensely sheared.
77538	48.2	48.4	JHC-07-279	Bobbys Pond VMS	Quartz-feldspar phyric, sericite-silica altered rhyolite.
77538	59.4	59.6	JHC-07-280	Bobbys Pond VMS	Bleached massive rhyolite. Carbonate spots and veinlets throughout.
77544	256	256.1	JHC-07-258	Bobbys Pond VMS	Light-grey, massive and silicified rhyolite. Minor pyrite.
77544	261	261.2	JHC-07-259	Bobbys Pond VMS	Light-grey, massive and silicified rhyolite. Minor pyrite.
77544	86	86.2	JHC-07-254	Bobbys Pond VMS	Carbonate-silica-sericite ± pyrophyllite (?) altered rhyolite.
77544	251	251.2	JHC-07-257	Bobbys Pond VMS	Carbonate-silica altered rhyolite as above.
77544	245.1	245.3	JHC-07-256	Bobbys Pond VMS	Carbonate-silica-sericite ± pyrophyllite altered rhyolite. Reddish-brown alteration product with a soapy feeling -- potentially pyrophyllite.
77544	183.2	183.5	JHC-07-255	Bobbys Pond VMS	Massive, silicified and bleached rhyolite with local carbonate alteration and disseminated pyrite.
77544	35	35.2	JHC-07-252	Bobbys Pond VMS	Variably altered, heavily silicified, quartz and feldspar phyric rhyolite. Pyrite is disseminated throughout. Pyrite is commonly associated with chlorite.
77544	77.5	77.6	JHC-07-253	Bobbys Pond VMS	Well-foliated, felsic lapilli tuff. Abundant sericite-carbonate alteration with possible pyrophyllite.
77544	379.5	379.7	JHC-07-260	Bobbys Pond VMS	Light-grey to white rhyolite. Silicified with carbonate spots and minor stringer pyrite throughout.
77546	135	135.2	JHC-07-288	Bobbys Pond VMS	Very sheared, very altered quartz-eye phyric tuff. Intense sericite ± pyrophyllite alteration. Contains pyrite and base-metal rich stringers.
77546	240.3	240.5	JHC-07-293	Bobbys Pond VMS	"Curdy"-textured brecciated rhyolite. Matrix consists of silica-sericite and local chlorite.

Appendix 1A: Sample Locations and Brief Descriptions

Hole_ID	From_m	To_m	SampleNum	Property	Descriptn
77546	33	33.2	JHC-07-285	Bobbys Pond VMS	Massive, light-medium grey, sericite-carbonate altered rhyolite. Carbonate spots occur throughout the unit.
77546	122.2	122.4	JHC-07-287	Bobbys Pond VMS	Quartz-eye phyric rhyolite with sericite and carbonate alteration throughout.
77546	143.7	143.9	JHC-07-289	Bobbys Pond VMS	Quartz porphyritic massive rhyolite with some base-metal-rich sulphide stringers.
77546	156.9	157.1	JHC-07-290	Bobbys Pond VMS	Very fine-grained, quartz-eye phyric felsic tuff with some very fine-grained interbedded siliceous sediment horizons. Exhalative? Local pyrite and sphalerite bands.
77546	197.6	197.9	JHC-07-291	Bobbys Pond VMS	Jig-saw fit rhyolitic breccia. Sericite-chlorite alteration occurs along the fracture surfaces. Minor base-metals (pyrite-sphalerite-galena) along fractures.
77546	216	216.2	JHC-07-292	Bobbys Pond VMS	Quartz-carbonate ± pyrophyllite altered felsic tuff. Sharp contacts with the surrounding rhyolite.
77546	49.6	49.8	JHC-07-286	Bobbys Pond VMS	Extremely sheared and schistose felsic lapilli tuff or rhyolite. Very intense sericite-carbonate alteration.
77547	45.7	45.9	JHC-07-274	Bobbys Pond VMS	Very sheared felsic tuff with intense sericite-carbonate alteration. Pyrite is disseminated throughout. ± pyrophyllite alteration.
77547	60.2	60.4	JHC-07-275	Bobbys Pond VMS	Fine-grained quartz-eye phyric tuff. Intense sericite-silica alteration.
77547	71.9	72.1	JHC-07-276	Bobbys Pond VMS	Silicified rhyolite. Carbonate alteration occurs as overprinting spots. Pyrite occurs as minor disseminations and veinlets throughout.
77547	115	115.2	JHC-07-277	Bobbys Pond VMS	Medium-light grey, silicified rhyolite with small quartz phenocrysts and carbonate spots replacing feldspar.
77547	14.8	15	JHC-07-273	Bobbys Pond VMS	Quartz and feldspar phyric rhyolite. Bleached to a white colour throughout. Base of the unit looks slightly brecciated: a flow (?).
BP-4	155.5	155.7	JHC-07-153	Bobbys Pond Native Sulphur	Green-grey rhyolite. Aphanitic, siliceous with sericite wisps throughout.
BP-4	66.2	66.4	JHC-07-152	Bobbys Pond Native Sulphur	Silica-pyrite-pyrophyllite(?) altered felsic volcanic.
BP-4	53.7	53.9	JHC-07-151	Bobbys Pond Native Sulphur	Silica-sulphur-alunite altered felsic volcanic. Possibly contains pyrophyllite.
BP-4	60	60.2	JHC-07-249	Bobbys Pond Native Sulphur	Pyrite-silica-pyrophyllite(?) altered felsic volcanic rock with alunite. Contains a bright orange mineral interpred to be orpiment.
BP-5	104.1	104.3	JHC-07-251	Bobbys Pond Native Sulphur	Native sulphur-pyrophyllite(?)-silica altered felsic volcanic with laminated and massive pyrite. Contains a grey, fiberous mineral -- stibnite (?).
BP-9	42	42.2	JHC-07-250	Bobbys Pond Native Sulphur	Pyrite-silica-pyrophyllite altered felsic volcanic.
BP-9	96.8	96.9	JHC-07-157	Bobbys Pond Native Sulphur	Silica-pyrophyllite altered felsic tuff.
BP-9	31.3	31.4	JHC-07-154	Bobbys Pond Native Sulphur	Silica-pyrite-native sulphur altered felsic tuff.
BP-9	44.8	45	JHC-07-155	Bobbys Pond Native Sulphur	Silica-pyrite-pyrophyllite altered felsic volcanic.
BP-9	73.2	73.4	JHC-07-156	Bobbys Pond Native Sulphur	Silica-pyrite-pyrophyllite (± alunite?) altered felsic volcanic.
CVP-02-01	32.4	32.6	JHC-06-146	Curve Pond	Massive pyrite with lesser chalcopyrite and pyrrhotite. Tectonically banded.
CVP-02-01	38.6	38.8	JHC-06-147	Curve Pond	Volcaniclastic sediments, banded appearance, exhalative?

Appendix 1A: Sample Locations and Brief Descriptions

Hole_ID	From_m	To_m	SampleNum	Property	Descriptn
CVP-02-01	14.3	14.4	JHC-06-141	Curve Pond	Quartz-phyric felsic tuff. Fines up into fine-grained epiclastic sediments.
CVP-02-01	15.8	16	JHC-06-142	Curve Pond	Massive sulphide-mostly pyrite with minor stringers of chalcopyrite.
CVP-02-01	23.9	24.1	JHC-06-143	Curve Pond	Sericitized/silicified felsic tuff. Locally 3-5% disseminated pyrite. Footwall alteration zone.
CVP-02-01	31.25	31.3	JHC-06-145	Curve Pond	Greywacke/chert. Layered sedimentary rock - exhalative?
CVP-02-01	29.65	29.8	JHC-06-144	Curve Pond	Layered sediment. Siliceous iron-formation - exhalative.
CVP-02-02	33.95	34.15	JHC-06-149	Curve Pond	Intermediate(?) volcanic tuff. Abundant feldspar phenocrysts, sericite alteration with carbonate spots.
CVP-02-02	46.7	46.9	JHC-06-152	Curve Pond	Fine-grained epiclastic sediment.
CVP-02-02	37.7	37.8	JHC-06-151	Curve Pond	Massive sulphide with relict quartz-crystals
CVP-02-02	37.5	37.6	JHC-06-150	Curve Pond	Massive sulphide (pyrite-pyrrhotite-sphalerite). Locally preserved quartz-eyes in the sulphides.
CVP-02-02	20.9	21.05	JHC-06-148	Curve Pond	Coarse-grained felsic tuff. Very silicified, light grey-beige. Quartz-feldpar phyric.
CVP-02-03	56.1	56.15	JHC-06-140	Curve Pond	Quartz vein with minor sphalerite.
CVP-02-03	53.9	54	JHC-06-139	Curve Pond	Potassic altered felsic volcanic (tuff).
CVP-02-03	24.5	24.7	JHC-06-138	Curve Pond	Quartz-feldspar phyric felsic tuff.
DN-02-02	134.7	134.9	JHC-07-113	Daniels Pond	Silica-sericite-pyrite altered intermediate tuff. Base metal stringers (sphalerite-galena) associated with increased chlorite alteration.
DN-02-02	27.6	27.9	JHC-07-107	Daniels Pond	Quartz-carbonate amygdaloidal mafic sill.
DN-02-02	68.5	68.7	JHC-07-108	Daniels Pond	Sericite (± pyrophyllite) altered intermediate tuff. Well foliated. Appears to have relict quartz crystals.
DN-02-02	77.8	77.9	JHC-07-109	Daniels Pond	Chloritized quartz-eye phyric intermediate tuff.
DN-02-02	88	88.2	JHC-07-110	Daniels Pond	Sericite-silica altered felsic-intermediate lapilli tuff with pyrite stringers.
DN-02-02	115.5	115.7	JHC-07-112	Daniels Pond	Silica-sericte-pyrite altered intermediate tuff. Pyrite is associated with intervals that have increased chlorite/carbonate alteration.
DN-02-02	147	147.2	JHC-07-114	Daniels Pond	Silica-sericite-pyrite (± pyrophyllite) altered intermediate tuff.
DN-02-02	167.5	167.8	JHC-07-115	Daniels Pond	Sericite-chlorite (± pyrophyllite/halloysite) altered intermediate tuff.
DN-02-02	187	187.2	JHC-07-116	Daniels Pond	Sericite-chlorite (± pyrophyllite/halloysite) altered intermediate tuff. Contains base-metal-rich (galena) disseminations.
DN-02-02	194.7	194.8	JHC-07-117	Daniels Pond	Semi-massive sulphide (pyrite-galena-sphalerite ± chalcopyrite) with fragments and clasts. Massive ore has internal quartz-crystals.
DN-02-02	195.7	195.9	JHC-07-118	Daniels Pond	Massive sulphide. Base-metal rich.
DN-02-02	201.3	201.5	JHC-07-119	Daniels Pond	Sericite-silica (± pyrophyllite) altered intermediate volcanic. Fragmental from the hangingwall.
DN-02-02	225.5	225.7	JHC-07-120	Daniels Pond	Orange coloured altered intermediate volcanic.
DN-02-02	103.2	103.5	JHC-07-111	Daniels Pond	Sericite (± pyrophyllite/halloysite) altered intermediate tuff.
DN-02-04	236.6	236.8	JHC-07-132	Daniels Pond	Epiclastic breccia from hangingwall (stratigraphic). Dominated by altered quartz-phyric clasts with minor argillite clasts and massive sulphide clasts. Debris flow.
DN-02-04	171.8	172	JHC-07-127	Daniels Pond	Fine-grained green mafic sill. Massive and homogenous. Quartz-filled amygdales throughout.
DN-02-04	200.8	201	JHC-07-128	Daniels Pond	Altered (silica-pyrite) intermediate tuff from below (stratigraphically) the ore-horizon. Stratigraphy is overturned.
DN-02-04	210.8	211	JHC-07-129	Daniels Pond	Altered intermediate volcanic.
DN-02-04	232	232.2	JHC-07-131	Daniels Pond	Epiclastic breccia from hangingwall (stratigraphic). Dominated by altered quartz-phyric clasts with minor argillite clasts and massive sulphide clasts. Debris flow.

Appendix 1A: Sample Locations and Brief Descriptions

Hole_ID	From_m	To_m	SampleNum	Property	Descriptn
DN-02-04	246.2	246.4	JHC-07-133	Daniels Pond	Silica-sericite altered intermediate tuff. Contains disseminated pyrite.
DN-02-04	286	286.2	JHC-07-134	Daniels Pond	Sericite-silica-carbonate altered felsic/intermediate tuff from hangingwall.
DN-02-04	124.1	124.3	JHC-07-126	Daniels Pond	Quartz-eye phyric intermediate tuff.
DN-02-04	96.8	97	JHC-07-125	Daniels Pond	Fine-grained green mafic sill. Locally intense carbonate rhombs replacing feldspars.
DN-02-04	81.5	81.7	JHC-07-124	Daniels Pond	Intermediate lapilli tuff. Rare pyrite fragments. Unit appears to be fining down indicating that the stratigraphy is overturned.
DN-02-04	41.5	41.8	JHC-07-123	Daniels Pond	Silica-pyrite altered intermediate-mafic lithic tuff.
DN-02-04	20.4	20.6	JHC-07-122	Daniels Pond	Quartz-phyric/glomercrystic intermediate-mafic fragmental volcanic with sericite-silica alteration.
DN-02-04	15	15.2	JHC-07-121	Daniels Pond	Quartz-phyric/glomercrystic intermediate-mafic fragmental volcanic with sericite-silica alteration.
DN-02-04	221.3	221.4	JHC-07-130	Daniels Pond	Massive pyrite with some quartz-carbonate stringers with chalcopyrite-galena stringers. Contains quartz-phyric inclusions. Tectonically layered.
DN-02-10	215.3	215.5	JHC-07-086	Daniels Pond	Altered fine-grained sheared volcanic. Intermediate tuff (?).
DN-02-10	47.7	47.9	JHC-07-079	Daniels Pond	Intermediate to mafic sill. Well foliated with abundant chlorite and carbonate alteration. Abundant quartz veinlets throughout.
DN-02-10	65.9	66.1	JHC-07-080	Daniels Pond	Massive looking, fine-grained homogenous green mafic sill with chilled margins and sheared upper contact. Chlorite filled amygdales throughout.
DN-02-10	112	112.2	JHC-07-081	Daniels Pond	Fresh mafic sill.
DN-02-10	123.5	123.7	JHC-07-082	Daniels Pond	Carbonate-chlorite altered mafic sill at the base of the unit. Abundant quartz-carbonate amygdales.
DN-02-10	132.2	132.4	JHC-07-083	Daniels Pond	Intensely sericite altered (± pyrophyllite) mineralized volcanic (chalcopyrite, galena, pyrite). Intermediate-mafic.
DN-02-10	158.1	158.3	JHC-07-084	Daniels Pond	Very altered/sheared tuff with sericite and possibly pyrophyllite. Difficult to determine composition. Chemistry is mafic (basaltic).
DN-02-10	172.1	172.3	JHC-07-085	Daniels Pond	Intensely altered intermediate tuff. Intense sericite ± pyrophyllite alteration with spottly chlorite alteration.
DN-02-10	12.1	12.3	JHC-07-078	Daniels Pond	Mafic to intermediate amygdoloidal sill.
DN-06	32.9	33.1	JHC-07-094	Daniels Pond	Chloritized intermediate-mafic tuff with quartz-eyes. Carbonate replacing feldspar phenocrysts.
DN-06	141.1	141.2	JHC-07-106	Daniels Pond	Chlorite-carbonate altered intermediate-mafic tuff.
DN-06	134.5	134.6	JHC-07-105	Daniels Pond	Deformed intermediate tuff.
DN-06	73	73.2	JHC-07-099	Daniels Pond	Sericite-carbonate-quartz-pyrite altered intermediate-mafic tuff. Pyrite occurs as blebs and stringers. Chaotic carbonate alteration as well.
DN-06	69.5	69.7	JHC-07-098	Daniels Pond	Intensely chloritized tuff with buckshot pyrite (intermediate-mafic). Appears to have relict quartz-feldspar phenocrysts.
DN-06	66.7	66.8	JHC-07-097	Daniels Pond	Sericite-halloysite (± pyrophyllite) altered quartz-eye phyric tuff. Extreme alteration makes identification difficult. Chemistry is mafic.
DN-06	47.5	47.8	JHC-07-096	Daniels Pond	Sericite-silica-pyrite altered tuff. Hard to identify due to alteration.
DN-06	119.3	119.5	JHC-07-104	Daniels Pond	Intensely sheared intermediate tuff. Hangingwall.
DN-06	19.1	19.3	JHC-07-093	Daniels Pond	Sericite-silica altered (± pyrophyllite) tuff. Appears to be quartz-eye phyric. Looks felsic but may be due to intense alteration.
DN-06	111.25	111.45	JHC-07-103	Daniels Pond	Sericite-silica altered intermediate tuff.
DN-06	102.1	102.3	JHC-07-102	Daniels Pond	Chloritized quartz-feldspar phyric intermediate tuff.
DN-06	85	85.2	JHC-07-101	Daniels Pond	Sericite-halloysite altered intermediate tuff. Contains base-metal-rich sulphide stringers.
DN-06	77.9	78.1	JHC-07-100	Daniels Pond	Sericite-silica-pyrite altered intermediate tuff. Contains halloysite.

Appendix 1A: Sample Locations and Brief Descriptions

Hole_ID	From_m	To_m	SampleNum	Property	Descriptn
DN-06	46.2	46.4	JHC-07-095	Daniels Pond	Quartz-feldspar phyric chloritized intermediate tuff. Minor disseminated sulphide. Chlorite alteration overprinted by sericite alteration.
DN-12	142.8	143	JHC-07-150	Daniels Pond	Sheared and silicifed quartz-eye phyric felsic-intermediate tuff.
DN-12	120	120.2	JHC-07-149	Daniels Pond	Argillitic breccia.
DN-16	181.3	181.4	JHC-07-145	Daniels Pond	Mass flow fragmental in immediate stratigraphic hangingwall. Clasts are mostly quartz-phyric volcanics with lesser argillite and massive sulphides.
DN-16	39.6	39.8	JHC-07-135	Daniels Pond	Chlorite-silica altered intermediate tuff. Part of a fining-downward sequence.
DN-16	214.6	214.8	JHC-07-148	Daniels Pond	Sheared, silica-sericite altered fesic-intermediate volcanic.
DN-16	199.15	199.35	JHC-07-147	Daniels Pond	Silica-sericite altered quartz-eye phyric intermediate tuff.
DN-16	185.8	186	JHC-07-146	Daniels Pond	Siliceous fragmental intermediate volcanic.
DN-16	173.7	173.9	JHC-07-144	Daniels Pond	Massive pyrite; recrystallized.
DN-16	163.8	164	JHC-07-143	Daniels Pond	Silica-sericite-pyrite altered quartz-eye phyric intermediate volcanic (tuff).
DN-16	149.8	150	JHC-07-142	Daniels Pond	Silica-carbonate-pyrite altered intermediate tuff. Abundant quartz-eyes.
DN-16	132	132.2	JHC-07-141	Daniels Pond	Quartz-feldspar phyric intermediate tuff.
DN-16	121.1	121.3	JHC-07-140	Daniels Pond	Fine-grained, green mafic sill. Increasing amygdales downhole; stratigraphy is overturned.
DN-16	103.3	103.5	JHC-07-139	Daniels Pond	Chlorite-silica altered intermediate/mafic tuff.
DN-16	88.8	89	JHC-07-138	Daniels Pond	Silica-carbonate altered mafic/intermediate tuff. Quartz-eyes throughout.
DN-16	61.8	62	JHC-07-136	Daniels Pond	Fine-grained, dark-green mafic sill, locally amygdaloidal.
DN-16	82	82.2	JHC-07-137	Daniels Pond	Sericite-silica-pyrite altered intermediate tuff.
DN-5	26.7	26.9	JHC-07-088	Daniels Pond	Silica-carbonate-pyrite altered intermediate tuff. Feldspar phyric (20-30%).
DN-5	42.3	42.4	JHC-07-089	Daniels Pond	Fragmental felsic lapilli tuff with feldspar-phyric clasts.
DN-5	67.5	67.6	JHC-07-092	Daniels Pond	Sericite-carbonate-pyrophyllite(?) Altered tuff.
DN-5	59.35	59.45	JHC-07-091	Daniels Pond	Intermediate tuff. Chemistry is mafic. Pyrite stringer zone.
DN-5	51.5	51.6	JHC-07-090	Daniels Pond	Very fine-grained massive pyrite with minor base metals.
DN-5	20	20.2	JHC-07-087	Daniels Pond	Silicified, feldspar-phyric intermediate tuff. Grades down into more of a lapilli tuff.
DRP-95-01	41.8	42	JHC-06-109	Dragon Pond	Sericitized felsic volcanic from above the iron-formation. Strong sericite alteration.
DRP-95-01	114.1	114.3	JHC-06-115	Dragon Pond	Chloritized quartz-eye phyric felsic volcanic.
DRP-95-01	62.7	62.9	JHC-06-113	Dragon Pond	Quartz and feldspar-phyric intermediate volcanic.
DRP-95-01	46	46.2	JHC-06-111	Dragon Pond	Arsenopyrite-rich iron formation.
DRP-95-01	45	45.3	JHC-06-110	Dragon Pond	Iron formation. Iron-carbonate, hematite, magnetite, pyrrhotite. Associated with a felsic tuff.
DRP-95-01	45.4	45.5	JHC-06-117	Dragon Pond	Massive pyrrhotite.
DRP-95-01	139.9	140.1	JHC-06-116	Dragon Pond	Fragmental felsic volcanic.
DRP-95-01	101.25	101.45	JHC-06-114	Dragon Pond	Sulphide-bearing quartz-phyric felsic volcanic.
DRP-95-01	54.6	54.75	JHC-06-112	Dragon Pond	Sericitized quartz-phyric felsic volcanic (tuff). 5-8% disseminated and veinlets of pyrite. Footwall zone.
DRP-95-02	115.2	115.4	JHC-06-128	Dragon Pond	Sericitized quartz-phyric felsic tuff.
DRP-95-02	86	86.2	JHC-06-127	Dragon Pond	Chloritized quartz-eye phyric felsic tuff.
DRP-95-02	78.2	78.4	JHC-06-126	Dragon Pond	Sericitized and heavily pyritized quartz-phyric felsic volcanic (tuff).
DRP-95-04	106.5	106.75	JHC-06-125	Dragon Pond	Silicified quartz-phyric felsic volcanic (tuff).
DRP-95-04	101.5	101.7	JHC-06-124	Dragon Pond	Sericitized quartz-phyric felsic volcanic (tuff).
DRP-95-04	97.1	97.4	JHC-06-123	Dragon Pond	Mafic volcanic. Medium-green, fine-medium grained. Well-defined chilled margins, Sill/dyke.
DRP-95-04	94.3	94.5	JHC-06-122	Dragon Pond	Sericitized/pyritized felsic tuff.

Appendix 1A: Sample Locations and Brief Descriptions

Hole_ID	From_m	To_m	SampleNum	Property	Descriptn
DRP-95-04	85.2	85.4	JHC-06-121	Dragon Pond	Quartz-phyric felsic tuff. Chlorite-sericite alteration, local disseminated pyrite.
DRP-95-04	72.2	72.4	JHC-06-120	Dragon Pond	Sericitized quartz-phyric felsic volcanic. Disseminated/veinlet pyrite.
DRP-95-04	70.2	70.4	JHC-06-119	Dragon Pond	Ferrogenous sediment.
DRP-95-04	68.6	68.85	JHC-06-118	Dragon Pond	Quartz-phyric felsic tuff. Sericite alteration. Has small rip-ups of black argillite.
DRP-96-07	15.6	15.8	JHC-06-094	Dragon Pond	Black argillite/phyllite.
DRP-96-07	229.7	229.9	JHC-06-096	Dragon Pond	Silicified phyllite.
DRP-96-07	338.8	339	JHC-06-099	Dragon Pond	Quartz and feldspar crystal tuff. Quartz-carbonate veining throughout. Minor disseminated pyrrhotite.
DRP-96-07	18.2	18.35	JHC-06-095	Dragon Pond	Quartz-phyric felsic tuff. Abundant sericite alteration. Minor pyrite and pyrrhotite.
DRP-96-07	322.2	322.35	JHC-06-097	Dragon Pond	Quartz-phyric felsic tuff. Sericite alteration, minor disseminated pyrite and pyrrhotite.
DRP-96-07	326.4	326.6	JHC-06-098	Dragon Pond	Iron formation. Iron-carbonate, hematite, magnetite, pyrrhotite. Associated with a felsic tuff.
DRP-96-07	351	351.2	JHC-06-100	Dragon Pond	Quartz and feldspar-phyric felsic volcanic. Disseminated pyrite and pyrrhotite.
DRP-96-07	368.1	368.25	JHC-06-101	Dragon Pond	Quartz-phyric felsic tuff. Sericite alteration.
DRP-96-07	386.5	386.8	JHC-06-102	Dragon Pond	Quartz-phyric felsic tuff. Sericite alteration.
GA-04-11	161.1	161.4	JHC-06-229	Boomerang	Felsic ash. Ash-crystal tuff with local "rhyolitic" fragments. Local argillic horizons.
GA-04-11	84.1	84.35	JHC-06-226	Boomerang	Felsic lapilli tuff. Clasts are felsic QFP and siltstone. Sericite and chlorite matrix. Very minor sulphide.
GA-04-11	44.9	45.1	JHC-06-225	Boomerang	Felsic ash. Base is sharp and is defined by the appearance of quartz and feldspar crystals.
GA-04-11	317.3	317.45	JHC-06-237	Boomerang	Felsic ash.
GA-04-11	309.1	309.3	JHC-06-236	Boomerang	Felsic ash in immediate footwall. Abundant semi-massive to massive sulphide (pyrite + sphalerite) stringers and intense sericite alteration with local chlorite alteration.
GA-04-11	265.5	265.65	JHC-06-235	Boomerang	Felsic lapilli tuff with sulphide stringers composed of massive pyrite and minor galena and sphalerite. Sericite alteration.
GA-04-11	254.7	254.9	JHC-06-234	Boomerang	Felsic sill with chilled margins. Light pink-beige, quartz veining throughout. Banded appearance due to sericite along foliations.
GA-04-11	240.5	240.7	JHC-06-233	Boomerang	Silicifed ash. Fine-grained, grey, primary bedding.
GA-04-11	201	201.2	JHC-06-230	Boomerang	Mafic sill. Light-green and homogeneous, very few amygdales. Basal contact intrudes and cuts laminations in an ash.
GA-04-11	235	235.2	JHC-06-232	Boomerang	Felsic lapilli tuff with 10-20 cm argillite horizons.
GA-04-11	149.2	149.4	JHC-06-228	Boomerang	Basaltic sill. Medium green, medium grained with local amygdales toward the base. Chilled margins but no contact brecciation suggesting a sill.
GA-04-11	10	10.2	JHC-06-222	Boomerang	Very fine-grained, dark-grey layered siltstone/cherty horizon. Local argillite horizons.
GA-04-11	25	25.2	JHC-06-223	Boomerang	Felsic lapilli tuff - conglomerate. Clasts are flattened and stretched, mostly quartz-feldspar rich clasts with some argillite rip-ups and cherty clasts.
GA-04-11	36.9	37.2	JHC-06-224	Boomerang	Polylithic conglomerate, clast supported. Local grey chert clasts and rhyolitic clasts. Some clasts have alteration rims.
GA-04-11	95.6	95.8	JHC-06-227	Boomerang	Felsic ash to crystal tuff.

Appendix 1A: Sample Locations and Brief Descriptions

Hole_ID	From_m	To_m	SampleNum	Property	Descriptn
GA-04-11	227.5	227.8	JHC-06-231	Boomerang	Mafic sill. Medium-green basalt with local iron-carbonate and silicification throughout.
GA-05-016	323.7	338.8	JHC-06-238	Boomerang	Felsic crystal tuff. Sericitized feldspar-phyric, crystal to lapilli tuff. Contains minor sulphide.
GA-05-016	345.7	360.1	JHC-06-239	Boomerang	Felsic crystal tuff. Intensely sericitized and chloritized. From immediately above ore, ore replaces this unit. Has intercalated black shale. Geochronology sample. 491 ± 3 Ma.
GA-05-079	247.1	264	JHC-06-240	Boomerang	Felsic dyke. From above the ore horizon. Geochronology sample. Moderately to strongly foliated, 491 ± 3 Ma
GA-05-21	504.4	504.7	JHC-06-219	Boomerang	Felsic lapilli tuff about 15 m above ore.
GA-05-21	22.4	22.65	JHC-06-190	Boomerang	Felsic lapilli tuff. Chlorite alteration gives a pseudo-breccia texture.
GA-05-21	319.2	319.4	JHC-06-209	Boomerang	Basaltic sill. Medium-green, massive and amygdaloidal. Amygdales are filled with calcite/carbonate.
GA-05-21	410	410.2	JHC-06-214	Boomerang	Beige to light-brown amygdaloidal basaltic sill.
GA-05-21	453.7	453.85	JHC-06-216	Boomerang	Felsic sill. Fine-grained with 1-2% quartz-feldspar phenocrysts. Locally amygdaloidal.
GA-05-21	558.2	558.5	JHC-06-221	Boomerang	Felsic ash. Fine-grained, very sheared. Moderate sericite alteration. Disseminated to stringer pyrite. Crenulated cleavage.
GA-05-21	57.2	57.4	JHC-06-194	Boomerang	Fine-grained grey-green felsic tuff with argillite wisps along foliations.
GA-05-21	287	287.25	JHC-06-207	Boomerang	Fine-grained felsic ash to crystal tuff with sections of intense chlorite alteration along small fault zones.
GA-05-21	252.9	253.1	JHC-06-205	Boomerang	Basaltic sill. Amygdaloidal (filled with calcite). Shearing at top and bottom, no contact breccias. High-level sill.
GA-05-21	233.1	233.3	JHC-06-204	Boomerang	Greywacke. Very fine-grained, homogeneous with local wisps of argillite.
GA-05-21	221.3	221.55	JHC-06-202	Boomerang	Quartz and feldspar-phyric felsic tuff with local argillite rip-up clasts.
GA-05-21	211	211.2	JHC-06-201	Boomerang	Ash to felsic crystal tuff. Locally preserved grey bedded sediments with local argillite horizons. Minor pyrite along bedding planes.
GA-05-21	196.7	196.95	JHC-06-200	Boomerang	Ash to felsic crystal tuff. Locally preserved grey bedded sediments with local argillite horizons. Minor pyrite along bedding planes.
GA-05-21	180.8	181	JHC-06-199	Boomerang	Felsic sandy tuff with locally preserved bedding. Intense chlorite and iron-carbonate alteration.
GA-05-21	67.3	67.45	JHC-06-195	Boomerang	Amygdaloidal basaltic sill, carbonate filled amygdales.
GA-05-21	129.4	129.8	JHC-06-197	Boomerang	Felsic sill, quartz and feldspar-phyric, abundant chlorite alteration locally dominating matrix.
GA-05-21	358.6	358.85	JHC-06-211	Boomerang	Felsic sill. Minor quartz and feldspar phenocrysts. Only slightly foliated, slightly bleached at the bottom contact.
GA-05-21	48	48.2	JHC-06-192	Boomerang	Quartz-phyric felsic tuff, minor sericite-chlorite alteration, minor pyrite disseminations.
GA-05-21	29.4	29.6	JHC-06-191	Boomerang	Ash tuff. Local quartz crystals, local wisps of argillite.
GA-05-21	527.3	527.5	JHC-06-220	Boomerang	Felsic sill. Massive with 10-15% quartz and feldspar phenocrysts. Sharp contacts.
GA-05-21	54.2	54.4	JHC-06-193	Boomerang	Felsic lapillistone with cm-scale flattened clasts, monolithic felsic clasts. Minor pyrite. Sericite and chlorite alteration in matrix.
GA-05-21	98.8	99.08	JHC-06-196	Boomerang	Felsic conglomerate/lapillistone. Dominated by quartz-feldspar rich clasts, matrix supported, lozenge shaped clasts.
GA-05-21	223.1	223.4	JHC-06-203	Boomerang	Lapilli tuff to conglomerate. Matrix supported.
GA-05-21	330.9	331.1	JHC-06-210	Boomerang	Sheared argillite with underlying massive pyrrhotite. Exhalitive horizon?
GA-05-21	153.3	153.5	JHC-06-198	Boomerang	Quartz and feldspar-phyric, massive, light grey-beige felsic sill.

Appendix 1A: Sample Locations and Brief Descriptions

Hole_ID	From_m	To_m	SampleNum	Property	Descriptn
GA-05-21	372.5	372.8	JHC-06-212	Boomerang	Interbedded ash tuff and graphitic argillite/siltstone. Fine bedding preserved.
GA-05-21	489.6	489.8	JHC-06-218	Boomerang	Mafic sill. Dark-green to medium brown. Amygdaloidal. Sharp contacts.
GA-05-21	297.6	297.8	JHC-06-208	Boomerang	Feldspar and quartz-phyric felsic sill. Contacts are sharp, increased foliation at the base. Base is chilled/bleached.
GA-05-21	393.1	393.2	JHC-06-213	Boomerang	Black chloritic and graphitic argillite. Quartz-veining throughout.
GA-05-21	422.1	422.35	JHC-06-215	Boomerang	Fine-grained felsic tuff with argillite clasts. Quartz-feldspar phyric.
GA-05-21	464.1	464.3	JHC-06-217	Boomerang	Very fine-grained grey cherty siltstone.
GA-05-21	267.1	267.35	JHC-06-206	Boomerang	Basaltic sill. Amygdaloidal (filled with calcite). No contact breccias. High-level sill.
GA-96-4	59.6	59.8	JHC-06-244	Boomerang	Mafic tuff?
GA-97-05	73.9	74.1	JHC-06-153	Domino	Basaltic sill. Looks synvolcanic due to interfingered lower contact.
GA-97-05	573.5	573.7	JHC-06-185	Domino	Mineralized quartz and feldspar-rich felsic lapilli tuff. Local rhyolite/cherty clasts. Local arsenopyrite, sphalerite and abundant pyrite. Immediate footwall to Domino.
GA-97-05	294.4	294.6	JHC-06-164	Domino	Basaltic sill. Amygdules filled mostly with quartz, chlorite, epidote, calcite. High-level basaltic sill.
GA-97-05	252.2	252.4	JHC-06-162	Domino	Ash tuff.
GA-97-05	170.6	170.8	JHC-06-158	Domino	Felsic sill. Irregular lower contact with volcaniclastic sediments whereby the contact is wavy and alteration goes 1-2 cm into sediments. Syn-sedimentary dyke.
GA-97-05	200.8	201	JHC-06-161	Domino	Felsic lapilli tuff.
GA-97-05	290.2	290.4	JHC-06-163	Domino	Basaltic sill. Amygdules filled mostly with quartz, chlorite, epidote, calcite. High-level basaltic sill.
GA-97-05	574	574.2	JHC-06-184	Domino	Mineralized quartz and feldspar-rich felsic lapilli tuff. Local rhyolite/cherty clasts. Local arsenopyrite, sphalerite and abundant pyrite. Immediate footwall to Domino.
GA-97-05	198.2	198.4	JHC-06-160	Domino	Felsic lapilli tuff.
GA-97-05	162.5	162.7	JHC-06-157	Domino	Andesitic dyke with irregular contact.
GA-97-05	191	191.2	JHC-06-159	Domino	Felsic lapilli tuff. Clast suported with flatted to lozenge shaped clasts, locally copper mineralized clasts.
GA-97-05	108.35	108.5	JHC-06-155	Domino	Felsic sill.
GA-97-05	220.7	220.9	JHC-06-165	Domino	Lapillistone/pyroclastic breccia. Foot of turbidite- angular matrix supported coarse flow. Fragments of aphyric rhyolite, grey QFP, grey chert. Local sulphide stringers.
GA-97-05	103.1	103.3	JHC-06-156	Domino	Andesitic dyke with sharp margins.
GA-97-05	352.9	353.1	JHC-06-169	Domino	Mafic sill, amygdaloidal, local chlorite spots.
GA-97-05	464.5	464.7	JHC-06-175	Domino	Andesitic sill. Feldspar porphyry with quartz amygdales. Iron-carbonate alteration spots.
GA-97-05	491.4	491.6	JHC-06-176	Domino	Quartz and feldspar felsic sill. Patchy iron-carbonate alteration.
GA-97-05	506.5	506.7	JHC-06-177	Domino	Felsic lapilli tuff, feldspar and quartz phenocrysts, grey cherty clasts, matrix supported.
GA-97-05	81.6	81.8	JHC-06-154	Domino	Felsic sill.
GA-97-05	566.8	567	JHC-06-183	Domino	Quartz and feldspar-rich felsic lapilli tuff. Local rhyolite/cherty clasts. Local arsenopyrite, sphalerite and abundant pyrite. Immediate footwall to Domino.
GA-97-05	508.2	508.4	JHC-06-178	Domino	Andesitic sill. Minor pyrite, well-preserved chilled margins.

Appendix 1A: Sample Locations and Brief Descriptions

Hole_ID	From_m	To_m	SampleNum	Property	Descriptn
GA-97-05	441	441.2	JHC-06-173	Domino	Andesitic sill. Feldspar porphyry with quartz amygdales. Iron-carbonate alteration spots.
GA-97-05	423.6	423.8	JHC-06-172	Domino	Felsic tuff.
GA-97-05	364	364.2	JHC-06-170	Domino	Mafic sill, amygdaloidal, local chlorite spots.
GA-97-05	446.7	446.9	JHC-06-174	Domino	Andesitic sill. Feldspar porphyry with quartz amygdales. Iron-carbonate alteration spots.
GA-97-05	338.5	338.7	JHC-06-167	Domino	Andesitic sill with plagioclase phenocrysts. Disseminated pyrite and minor stringers of pyrite-pyrrhotite.
GA-97-05	315.4	315.6	JHC-06-166	Domino	Mafic sill. Good chilled margins, medium-grained with a salt and pepper texture, almost diabase. Local pyrite nodules.
GA-97-05	623	623.2	JHC-06-187	Domino	Felsic lapilli tuff. Quartz-feldspar phyric with local clasts. Strong sericite alteration and pyrite stringers.
GA-97-05	605	605.2	JHC-06-186	Domino	Felsic lapilli tuff. Quartz and feldspar-phyric with local clasts. Strong sericite alteration and local pyrite stringers.
GA-97-05	345	345.2	JHC-06-168	Domino	Quartz-feldspar phyric lapillistone. Clast supported with angular fragments.
GA-97-05	531.7	531.9	JHC-06-179	Domino	Felsic lapilli tuff, quartz-feldspar phenocrysts, moderate to intense sericite and pyrite alteration with heavy sericite bands.
GA-97-05	535.9	536.3	JHC-06-180	Domino	Pyritized felsic tuff from hangingwall.
GA-97-05	548.2	548.5	JHC-06-181	Domino	Fine-grained ash tuff with abundant pyrite.
GA-97-05	554.5	554.65	JHC-06-182	Domino	Quartz and feldspar felsic tuff, intense sericite and pyrite alteration. Immediate hangingwall.
GA-97-05	399.4	399.6	JHC-06-171	Domino	Felsic tuff with white-grey feldspar-rich lapilli size fragments, rip-up clasts of argillite, crystal-rich.
GP-02-038	63.5	63.7	JHC-06-108	Midas Pond	Mafic volcanic with a banded appearance.
GP-02-038	54.9	55.15	JHC-06-105	Midas Pond	Intermediate volcanic hosting quartz-carbonate veining and disseminated/vein pyrite (5-20%).
GP-02-038	57.8	58.1	JHC-06-107	Midas Pond	Quartz-carbonate veins crosscutting felsic volcanics.
GP-02-038	19.85	20.1	JHC-06-103	Midas Pond	Very sericitized felsic volcanic (tuff). Strongly foliated.
GP-02-038	43.7	43.9	JHC-06-104	Midas Pond	Sericitized/silicified felsic volcanic (tuff).
GP-02-038	57	57.3	JHC-06-106	Midas Pond	Quartz-carbonate veins crosscutting felsic volcanics.
GP-02-039	100.25	100.45	JHC-06-133	Midas Pond	Coarse-grained altered (silica-sericite) felsic tuff with 2-3 % disseminated pyrite.
GP-02-039	90.9	91.2	JHC-06-131	Midas Pond	Mottled looking, pyrite-rich, silicified felsic tuff - Mineralized Zone.
GP-02-039	20	20.2	JHC-06-129	Midas Pond	Mafic dyke.
GP-02-039	77.9	80.05	JHC-06-130	Midas Pond	Pyrite-rich, sericite-silica altered felsic tuff.
GP-02-039	96.5	96.7	JHC-06-132	Midas Pond	Banded mafic with quartz-veining.
GP-93-01	86	86.4	JHC-06-241	Glitter Pond	Quartz-phyric felsic tuff.
GP-93-01	93.7	93.9	JHC-06-242	Glitter Pond	Mafic dyke.
GP-93-01	192	192.2	JHC-06-243	Glitter Pond	Felsic lapilli tuff.
GS-2	4	4.2	JHC-06-134	Curve Pond	Quartz and feldspar-phyric felsic tuff. Silicified throughout with less than 1% disseminated pyrite.
GS-2	34.5	34.7	JHC-06-137	Curve Pond	Felsic tuff from footwall. Mixed unit with tuffaceous material mixed with volcaniclastic sediments.
GS-2	24.7	24.9	JHC-06-136	Curve Pond	Massive sulphide with bedding and sphalerite and chalcopyrite-rich zones.
GS-2	13.6	13.65	JHC-06-135	Curve Pond	Iron formation(?). Siliceous.
HH-96-12	146	146.2	JHC-07-248	Hungry Hill	Litharenite. Has a fine-grained, quartz-eye phyric tuffaceous appearance.

Appendix 1A: Sample Locations and Brief Descriptions

Hole_ID	From_m	To_m	SampleNum	Property	Descriptn
HH-96-12	132.5	132.7	JHC-07-247	Hungry Hill	Heterolitic breccia with quartz-eye phyric, chloritized clasts and quartz crystals in the matrix.
HH-96-12	42.3	42.5	JHC-07-246	Hungry Hill	Massive and homogeneous dark-green to grey quartz-eye phyric rhyolite.
HH-97-16	12	12.2	JHC-07-219	Hungry Hill	Quartz-eye phyric felsic-intermediate tuff.
HH-97-16	288.4	288.6	JHC-07-229	Hungry Hill	Intermediate-mafic lapilli tuff.
HH-97-16	257	257.2	JHC-07-228	Hungry Hill	Very coarse-grained siliceous, non-mineralized fragmental. Most of the fragments are quartz-phyric tuff/rhyolite.
HH-97-16	216	216.2	JHC-07-227	Hungry Hill	Mineralized, very coarse-grained fragmental debris flow with pyrite-sphalerite-chalcopyrite wisps and clasts. Increased sulphide with increased chlorite-carbonate alteration.
HH-97-16	194.2	194.4	JHC-07-226	Hungry Hill	Quartz-eye phyric felsic tuff with stringer sulphides. Local small fragments.
HH-97-16	178.5	178.7	JHC-07-225	Hungry Hill	Heterolitic debris-flow breccia with interstitial to wispy pyrite and chalcopyrite in the matrix.
HH-97-16	165.2	165.3	JHC-07-224	Hungry Hill	Massive to semi-massive sphalerite-pyrite with minor chalcopyrite within a heterolitic fragmental. Mostly massive pyrite with wisps of sphalerite.
HH-97-16	149.5	149.7	JHC-07-223	Hungry Hill	Stringer sphalerite-chalcopyrite in a quartz-phyric rhyolite.
HH-97-16	123.6	123.8	JHC-07-222	Hungry Hill	Massive quartz-eye phyric rhyolite.
HH-97-16	33.4	33.6	JHC-07-220	Hungry Hill	Mafic sill with carbonate filled amygdales.
HH-97-16	51.3	51.5	JHC-07-221	Hungry Hill	Quartz-eye phyric, chlorite specked rhyolite.
HH-98-18	112.2	112.4	JHC-07-231	Hungry Hill	Massive, quartz-carbonate amygdaloidal mafic sill. Locally displays hyaloclastic breccia textures with quartz-carbonate filling in the fractures.
HH-98-18	159.5	159.7	JHC-07-232	Hungry Hill	Rhyolitic breccia. Most clasts are composed of rhyolite. Chlorite-carbonate-sericite occurs in the matrix.
HH-98-18	263.4	263.6	JHC-07-233	Hungry Hill	Quartz-eye phyric rhyolite with chlorite spots (alteration after feldspar crystals). See a slight increase in pyrite content toward the base of the unit.
HH-98-18	333.5	333.7	JHC-07-235	Hungry Hill	Litharenite. Medium dark-grey rock with a greywacke/sedimentary matrix containing rounded clasts of felsic volcanics and argillite.
HH-98-18	286	286.2	JHC-07-234	Hungry Hill	Light-grey-green polylithic rhyolitic breccia with chlorite/sulphide stringers.
HH-98-18	101.5	101.7	JHC-07-230	Hungry Hill	Massive, light grey-green, quartz-eye phyric rhyolite. Silica-sericite alteration throughout. Local chlorite alteration.
HH-98-22	220.6	220.7	JHC-07-239	Hungry Hill	Heterolithic breccia typical of Hungry Hill stratigraphy.
HH-98-22	395	395.2	JHC-07-244	Hungry Hill	Spherulitic mafic flow/sill?
HH-98-22	296.7	296.9	JHC-07-240	Hungry Hill	Polylithic breccia. Dominated by quartz-eye phyric clasts, disseminated pyrite in the matrix.
HH-98-22	219.4	219.6	JHC-07-238	Hungry Hill	Heterolithic breccia with base-metal-rich massive sulphide clasts. Clasts of rhyolite, mafic volcanic and argillite. Poorly sorted, clast supported.
HH-98-22	190	190.2	JHC-07-237	Hungry Hill	Light-brown litharenite.
HH-98-22	131.2	131.4	JHC-07-236	Hungry Hill	Light green-grey, quartz-eye phyric rhyolite. Moderate silicification throuhgout.
HH-98-22	376.5	376.7	JHC-07-243	Hungry Hill	Polylithic breccia with rhyolite, argillite and massive-pyrite clasts. Unit contains some sections of greywacke/siltstone laminations.
HH-98-22	316	316.2	JHC-07-242	Hungry Hill	Massive rhyolite. Quartz-phyric throughtout with chlorite and sericite spots.
HH-98-22	411.2	411.4	JHC-07-245	Hungry Hill	Massive, medium-green, aphyric and carbonate amygdaloidal basalt.
HH-98-22	305.6	305.75	JHC-07-241	Hungry Hill	Mineralized and brecciated rhyolite with abundant black chlorite alteration and pyrite ± chalcopyrite.

Appendix 1A: Sample Locations and Brief Descriptions

Hole_ID	From_m	To_m	SampleNum	Property	Descriptn
JP-29	27	27.2	JHC-07-024	Jacks Pond	Intensely silicified, with minor sericite, altered felsic ash to crystall tuff.
JP-29	131.1	131.3	JHC-07-031	Jacks Pond	Sericite-pyrite altered felsic tuff.
JP-29	217.7	217.9	JHC-07-035	Jacks Pond	Sericite-silica altered felsic tuff with quartz-carbonate veins.
JP-29	198	198.2	JHC-07-034	Jacks Pond	Silica-sericite-chlorite altered felsic tuff with disseminated pyrite.
JP-29	166.5	166.7	JHC-07-033	Jacks Pond	Mafic sill. Chilled contacts. Carbonate spots replacing feldspar?
JP-29	143.5	143.7	JHC-07-032	Jacks Pond	Weakly chlorite-pyrite altered felsic tuff.
JP-29	122	122.2	JHC-07-030	Jacks Pond	Sericite-chlorite altered felsic tuff.
JP-29	93.6	93.8	JHC-07-029	Jacks Pond	Silica-sericite altered felsic tuff with minor sulphide stringers.
JP-29	85	85.2	JHC-07-028	Jacks Pond	Silicified felsic tuff.
JP-29	65.2	65.4	JHC-07-027	Jacks Pond	Chlorite-sericite altered felsic ash to crystal tuff.
JP-29	36.3	36.5	JHC-07-025	Jacks Pond	Sericite-silica-pyrite altered felsic ash to crystal tuff.
JP-29	13.75	13.95	JHC-07-023	Jacks Pond	Felsic ash to crystal tuff. Intensely altered with sericite-silica-disseminated pyrite alteration.
JP-29	227	227.2	JHC-07-036	Jacks Pond	Silica-sericte-chlorite-pyrite altered felsic tuff.
JP-29	304	304.4	JHC-07-041	Jacks Pond	Carbonate-pyrite altered felsic tuff. Pink colouration due to carbonate. Pyrite stringers.
JP-29	44.9	45.1	JHC-07-026	Jacks Pond	Sericite-silica-pyrite altered felsic ash to crystal tuff.
JP-29	282.2	282.4	JHC-07-038	Jacks Pond	Mineralized felsic tuff with chlorite-sulphide (pyrite-galena +/- sphalerite) and quartz-carbonate veins.
JP-29	296.9	297.1	JHC-07-040	Jacks Pond	Sericite altered felsic tuff with pyrite stringers and disseminations.
JP-29	329.1	329.2	JHC-07-042	Jacks Pond	Fold/thrust/kink banding terminated by small slips.Evidence for thrusting.
JP-29	340.9	341.1	JHC-07-043	Jacks Pond	Sphalerite-galena mineralized vein in intensely sericitized felsic tuff.
JP-29	268.5	268.7	JHC-07-037	Jacks Pond	Chlorite-pyrite altered felsic tuff with sphalerite ± galena.
JP-29	292	292.4	JHC-07-039	Jacks Pond	Sericite-silica altered felsic tuff with chlorite spots.
JP-30	6	6.2	JHC-07-063	Jacks Pond	Mafic amygdaloidal dyke. Chilled margins. Quartz filled amygdales.
JP-30	16.8	17	JHC-07-064	Jacks Pond	Intensely silicified quartz-eye phyric felsic tuff.
JP-30	19.5	19.7	JHC-07-065	Jacks Pond	Quartz-feldspar porphyritic felsic sill. Upper contact is gradational, lower contact is chilled.
JP-30	31	31.3	JHC-07-066	Jacks Pond	Very silicified felsic volcanic with cm-scale pyrite stringers.
JP-30	65.53	65.73	JHC-07-067	Jacks Pond	Intercalated silicified felsic tuff with fine-grained silicified pyritiferous mudstone. Pyrite srtingers throughout.
JP-38	112.4	112.6	JHC-07-049	Jacks Pond	Silica-sericite-pyrite altered felsic tuff.
JP-38	192.2	192.4	JHC-07-053	Jacks Pond	Silica-sericite-chlorite altered felsic tuff.
JP-38	170.6	170.8	JHC-07-052	Jacks Pond	Chlorite-sericite altered felsic tuff below semi-massive pyrite.
JP-38	157.25	157.5	JHC-07-050	Jacks Pond	Chlorite-sulphide altered felsic tuff. Immediately above a semi-massive sulphide horizon.
JP-38	98.45	98.65	JHC-07-048	Jacks Pond	Diabase dyke/sill. Chilled contacts, increased magnetite toward the centre.
JP-38	67.5	67.7	JHC-07-047	Jacks Pond	Sericite altered felsic tuff.
JP-38	62.5	62.7	JHC-07-046	Jacks Pond	Sericite-silica altered felsic volcanic with circular alteration patterns. Pillowed rhyolite?
JP-38	45.7	45.9	JHC-07-045	Jacks Pond	Silica-sericite altered felsic tuff.
JP-38	23.45	23.65	JHC-07-044	Jacks Pond	Sericite-silica altered felsic tuff with mm-scale pyrite stringers.
JP-38	160	160.1	JHC-07-051	Jacks Pond	Semi-massive pyrite. Minor chalcopyrite in quartz veins. Underlain by chlorite stockwork.
JP-94-01	174.4	174.6	JHC-07-059	Jacks Pond	Coarse-grained fragmental with chlorite and quartz-eyes in the matrix. Looks like a mass flow breccia? or a fault breccia? Contains granitic clasts. Hydrothermal chlorite.

Appendix 1A: Sample Locations and Brief Descriptions

Hole_ID	From_m	To_m	SampleNum	Property	Descriptn
JP-94-01	347.5	347.7	JHC-07-062	Jacks Pond	Silicified fine-grained felsic volcanic? Rhyolitic flow?
JP-94-01	167	167.2	JHC-07-058	Jacks Pond	Chlorite altered quartz-eye phyric ash to crystal felsic tuff. Abundant carbonate spots.
JP-94-01	117.7	118	JHC-07-057	Jacks Pond	Coarse-grained volcanilclastic breccia with grey siliceous fragments.
JP-94-01	109.3	109.5	JHC-07-056	Jacks Pond	Fragmental felsic lapilli tuff. Very sericitic matrix with relict quartz-eyes.
JP-94-01	55.3	55.5	JHC-07-055	Jacks Pond	Silicified brecciated rhyolite. Pyrite occurs in matrix.
JP-94-01	17.7	17.9	JHC-07-054	Jacks Pond	Fine-grained, grey, aphyric massive rhyolite. Silicified.
JP-94-01	171.6	171.8	JHC-07-061	Jacks Pond	Granitic clast in breccia. Perhaps part of Roebucks intrusive? Suggests that unit is a fault breccia rather than mass flow.
JP-94-01	288.1	288.3	JHC-07-060	Jacks Pond	Chlorite-sericiite altered ash to crystal felsic tuff.
JP-94-07	102.3	102.5	JHC-07-071	Cathys Pond	Quartz-feldspar pyhric, massive looking felsic volcanic. Disseminated pyrite.
JP-94-07	112.7	112.8	JHC-07-072	Cathys Pond	Fine-grained pyritic mud with coarse-grained pyrite associated with exhalitive argillite.
JP-94-07	78.7	78.9	JHC-07-070	Cathys Pond	Sericite-silica altered felsic tuff. Quartz and feldspar phyric. Carbonate spots throughout.
JP-94-07	72.8	73	JHC-07-069	Cathys Pond	Sericite altered felsic lapilli tuff with abundant cm-scale fine-grained sericitized clasts. Abundant mm-scale quartz-eyes in the matrix.
JP-94-07	44.9	45	JHC-07-068	Cathys Pond	Silica-sericite altered quartz-eye phyric felsic tuff.
JP-94-07	129.8	130	JHC-07-073	Cathys Pond	Fine-grained quartz and feldspar phyric, sericite and silica altered, felsic tuff.
JP-95-09(30A)	90.8	91	JHC-07-074	Cathys Pond	Intercalated fine-grained pyritiferous mudstone with fine-grained exhalitive silica.
JP-95-09(30A)	105.6	105.8	JHC-07-075	Cathys Pond	Chlorite altered felsic tuff from below the exhalitive horizon with the pyriteferous muds.
JP-97-14	183.5	183.7	JHC-07-076	Jacks Pond	Massive and homogeneous quartz-phyric felsic volcanic. Massive rhyolitic sill or possibly a flow.
JP-97-14	294	307	JHC-07-077	Jacks Pond	Quartz-feldspar phyric altered felsic tuff. Abundant sericite alteration. Unit looks rhyolitic in places.
MOA-05-02	119.5	119.7	JHC-07-185	Bobbys Pond VMS	Altered lapilli tuff.
MOA-05-02	122.3	122.5	JHC-07-186	Bobbys Pond VMS	Altered lapilli tuff.
RB-01-02	105.4	105.6	JHC-07-020	Roebucks Brook	Intermediate ash to crystal tuff with minor quartz-phyric clasts.
RB-01-02	95.2	95.4	JHC-07-019	Roebucks Brook	Pseudo-fragmental.
RB-01-02	82.5	82.7	JHC-07-018	Roebucks Brook	Quartz-sericite-sulphide altered quartz-phyric felsic tuff. Significant amount of stringers of base-metals (sphalerite-chalcopyrite-pyrite +/- galena).
RB-01-02	163.4	163.6	JHC-07-022	Roebucks Brook	Mafic ash to crystal tuff.
RB-01-02	133.2	133.4	JHC-07-021	Roebucks Brook	Quartz-phyric intermediate tuff. Chaotic carbonate veining.
RB-01-02	64.4	64.6	JHC-07-017	Roebucks Brook	Plagioclase phyric mafic dyke, fairly homogeneous.
RB-01-02	52.8	53	JHC-07-016	Roebucks Brook	Fine-grained ash to mafic crystal tuff. Sill(?).
RB-01-02	43.6	43.8	JHC-07-015	Roebucks Brook	Fine-grained, quartz-phyric intermediate tuff.
RB-01-02	26.4	26.6	JHC-07-014	Roebucks Brook	Graphitic argillite with fine-grained felsic volcanic clasts. Disseminated pyrite throughout.
RB-01-02	19.4	19.6	JHC-07-013	Roebucks Brook	Silicified fine-grained greywacke/siltstone.
RB-01-02	15.7	15.9	JHC-07-012	Roebucks Brook	Felsic lapilli tuff with argillite clasts.
RB-01-02	14.8	15	JHC-07-011	Roebucks Brook	Graphitic argillite with abundant felsic tuff fragments. Sedimentary breccia.
RB-96-01	32.6	32.8	JHC-07-001	Roebucks Brook	Graphitic argillite to ash. Disseminations and veinlets of pyrite throughout.

Appendix 1A: Sample Locations and Brief Descriptions

Hole_ID	From_m	To_m	SampleNum	Property	Descriptn
RB-96-01	75.7	75.9	JHC-07-003	Roebucks Brook	Basaltic sill. Abundant chlorite spots and carbonate veining. Sharp upper and lower contacts.
RB-96-01	87.5	87.7	JHC-07-004	Roebucks Brook	Feldspar-phyric mafic dyke. Carbonate veinlets throughout.
RB-96-01	110.8	110.9	JHC-07-005	Roebucks Brook	Quartz-eye phyric felsic tuff with base-metal stringers (mostly sphalerite). Intense silica-sericite alteration. Local chalcopyrite.
RB-96-01	149.2	149.4	JHC-07-010	Roebucks Brook	Fine-grained green mafic ash to crystal tuff. Chaotic carbonate veining throughout.
RB-96-01	128	128.2	JHC-07-007	Roebucks Brook	Felsic crystal-lapilli tuff. Fining upward sequence.
RB-96-01	129.7	129.9	JHC-07-008	Roebucks Brook	Felsic lapilli tuff, base of a fining upward sequence.
RB-96-01	141.8	141.9	JHC-07-009	Roebucks Brook	Argillite-rich felsic fragmental. Siliceous clasts, minor pyrite and pyrrhotite disseminated throughout.
RB-96-01	117.1	117.3	JHC-07-006	Roebucks Brook	Silica-sericite altered quartz-eye phyric felsic tuff with base-metal stringers.
RB-96-01	68.8	69	JHC-07-002	Roebucks Brook	Chloritized felsic ash to crystal tuff.
SU-01-01	122.1	122.3	JHC-07-162	Sutherlands Pond	Silica-chlorite-carbonate altered intermediate lapilli tuff.
SU-01-01	180.3	180.5	JHC-07-163	Sutherlands Pond	Chlorite-carbonate altered felsic lapilli tuff.
SU-01-01	229.9	230.1	JHC-07-164	Sutherlands Pond	Coarse-grained, rhyolitic breccia. Grey siliceous rhyolitic fragments within a black chloritic matrix.
SU-01-01	237.8	238	JHC-07-165	Sutherlands Pond	Silicified felsic tuff.
SU-01-01	266.8	267	JHC-07-166	Sutherlands Pond	Fine-grained grey-green felsic tuff. Chlorite alteration.
SU-01-01	298.6	298.8	JHC-07-167	Sutherlands Pond	Rhyolitic breccia. Dark green chloritic matrix. Some sections contain base-metal sulphides in the matrix (pyrite-galena-sphalerite ± chalcopyrite).
SU-01-01	96.9	97.1	JHC-07-160	Sutherlands Pond	Feldspar phyric intermediate tuff. Unit is fining downward.
SU-01-01	107	107.2	JHC-07-161	Sutherlands Pond	Carbonate-green mica altered intermediate tuff.
SU-01-01	24.7	24.9	JHC-07-158	Sutherlands Pond	Aphyric rhyolite.
SU-01-01	58.6	58.8	JHC-07-159	Sutherlands Pond	Felsic framental. Spherulititc devitrified rhyolite?
SU-01-01	367.9	368.1	JHC-07-168	Sutherlands Pond	Chlorite altered, massive grey-green rhyolite.
T-192	69.7	69.9	JHC-06-060	Tulks Hill	Mafic volcanic. Medium grey-green, foliated, fine-grained, sill or flow?
T-192	36.5	36.7	JHC-06-059	Tulks Hill	Mafic volcanic. Medium grey-green, foliated, fine-grained, sill or flow?
T-192	28.9	29.1	JHC-06-058	Tulks Hill	Massive banded (tectonically) sulphide. Host is a quartz-feldspar fragmental. Sulphides consist of pyrite with lesser chalcopyrite and sphalerite.
T-192	17.5	17.7	JHC-06-057	Tulks Hill	Quartz and feldspar-phyric felsic volcanic, silicified.
T-192	7.6	7.8	JHC-06-056	Tulks Hill	Fine-grained vitric felsic tuff.
T-194	16.7	17	JHC-06-068	Middle Tulks	Plagioclase phyric intermediate/mafic volcanic. Quartz amygdaloidal toward the base of the unit.
T-194	47.4	47.6	JHC-06-069	Middle Tulks	Fine-grained intermediate volcanic. Possibly a bleached mafic dyke. Massive.
T-194	70.5	70.8	JHC-06-070	Middle Tulks	Felsic tuff, lapilli rich. Silicified throughout. Minor chalcopyrite.
T-197	49.9	50.1	JHC-06-043	Tulks Hill	Quartz and feldspar phenocrystic rhyolite? Possibly a crystal tuff? Silicified throughout with local sericite alteration.
T-197	36.2	36.5	JHC-06-042	Tulks Hill	Very silicified quartz-phyric rhyolite. Below the stockwork zone.
T-197	30.5	30.7	JHC-06-041	Tulks Hill	Disseminated/stringer pyrite in rhyolite. Quartz-phyric rhyolite - stockwork zone. Siicification with local sericite alteration.
T-202	70.4	70.6	JHC-06-047	Tulks Hill	Sericitized/silicified felsic volcanic.
T-202	88.5	88.7	JHC-06-049	Tulks Hill	Mineralized quartz-phyric felsic fragmental. Fragments are quartz-phyric rhyolite.

Appendix 1A: Sample Locations and Brief Descriptions

Hole_ID	From_m	To_m	SampleNum	Property	Descriptn
T-202	60.3	60.6	JHC-06-046	Tulks Hill	Felsic lapilli tuff with quartz-phyric lapilli.
T-202	45.1	45.2	JHC-06-045	Tulks Hill	Chloritized quartz-eye phyric felsic volcanic.
T-202	27.9	28	JHC-06-044	Tulks Hill	Quartz-eye phyric rhyolite from the hangingwall.
T-202	96.9	97.1	JHC-06-050	Tulks Hill	Chloritized felsic volcanic (rhyolite?).
T-202	74	74.3	JHC-06-048	Tulks Hill	Pyritized quartz-phyric felsic tuff. From the mineralized horizon.
T-205	7.47	7.68	JHC-06-031	Tulks Hill	Rhyolite. Very silicified. Minor pyrite mineralization.
T-205	56.4	56.6	JHC-06-034	Tulks Hill	Mafic volcanic. Very sharp contacts indicate a dyke.
T-205	49.4	49.7	JHC-06-033	Tulks Hill	Rhyolite. Silica-chlorite altered.
T-205	37.7	37.9	JHC-06-032	Tulks Hill	Rhyolite. Sericite-silica altered, quartz-eye phyric.
T-205	65.8	66	JHC-06-035	Tulks Hill	Felsic lapilli tuff.
T-205	75.8	76.1	JHC-06-036	Tulks Hill	Mafic volcanic. Fine-grained, non-magnetic dyke. Penetrative foliation. Sharp upper and lower contacts. Amygdaloidal (quartz-feldspar).
T-205	89.9	90.1	JHC-06-037	Tulks Hill	Sericitized/silicified rhyolite. Quartz-eye phyric, minor disseminated pyrite.
T-205	109.6	109.7	JHC-06-038	Tulks Hill	Rhyolitic stockwork with minor pyrite. Silica-sericite alteration.
T-205	189.9	190.1	JHC-06-040	Tulks Hill	Rhyolite. Quartz phenocrysts and minor black (chlorite?) spots throughout.
T-205	169.3	169.5	JHC-06-039	Tulks Hill	Silicified/sericitzed rhyolite. Minor chlorite alteration. Light grey-green in colour, well foliated.
T-212	147.2	147.4	JHC-06-054	Tulks Hill	Quartz-phyric felsic tuff. Heavy sericite alteration. Local pyrite and pyrrhotite stringers/veinlets.
T-212	169.1	169.3	JHC-06-055	Tulks Hill	Silicified black sediment (argillite).
T-212	136.3	136.5	JHC-06-053	Tulks Hill	Chloritized quartz-eye phyric felsic volcanic (rhyolite?).
T-212	108.2	108.5	JHC-06-052	Tulks Hill	Chloritized quartz-eye phyric rhyolite.
T-212	52.2	52.3	JHC-06-051	Tulks Hill	Quartz-phyric rhyolite.
TE-94-01	398.7	399.2	JHC-06-003	Tulks East	Felsic lapilli tuff. Abundant blue quartz eyes (10%). Abundant stringer sulphides. Stockwork above ore.
TE-94-01	338.2	338.3	JHC-06-002	Tulks East	Mafic volcanic with carbonate alteration. Beige in colour. Very massive and dyke/sill like. Sheared basal contact.
TE-94-01	491.7	492	JHC-06-008	Tulks East	Rhyolite. Massive, quartz eye phyric rhyolitic flow? Very sharp upper contact with a tuff. Contains stringer pyrite and pyrrohite.
TE-94-01	419	419.2	JHC-06-005	Tulks East	Felsic lapilli tuff. Intense sericite and chlorite alteration. Monolithic fragments with blue quartz eyes. Disseminated and wispy pyrite and sphalerite.
TE-94-01	271.6	271.75	JHC-06-001	Tulks East	Mafic volcanic, massive, no pillows, looks like diabase in places. Chlorite alteration throughout, local pyrite.
TE-94-01	413.9	141	JHC-06-004	Tulks East	Massive pyritic ore. C-Zone. Minor chalcopyrite and sphalerite bands. Ore is recrystallized with coarse crystalline pyrite. 10% silica matrix.
TE-94-01	460.6	460.75	JHC-06-007	Tulks East	Felsic tuff. Blue quartz eyes throughout and massive. Very sharp contact with the above tuff. Alternatively a rhyolitic flow?
TE-94-01	387.9	388.1	JHC-06-061	Tulks Hill	Contact of graphitic argillite and felsic tuff at Tulks East.
TE-94-01	456.6	456.7	JHC-06-006	Tulks East	Felsic lapilli tuff. Stockwork to the ore zone. Strongly foliated. Alteration is dominated by sericite. Abundant pyrite and siliceous stringers.
TE-99-03	345.8	346	JHC-06-012	Tulks East	Sericitized felsic tuff, hangingwall.
TE-99-03	379.9	380.1	JHC-06-018	Tulks East	Chloritized felsic tuff from below ore zone.
TE-99-03	378	378.3	JHC-06-017	Tulks East	Quartz eye phyric felsic tuff with stringer pyrite. Pyrite occurs as coarse dessiminations as well as massive equigranular recrystallized pyrite.

Appendix 1A: Sample Locations and Brief Descriptions

Hole_ID	From_m	To_m	SampleNum	Property	Descriptn
TE-99-03	370.6	370.8	JHC-06-015	Tulks East	Sericitized felsic tuff. Directly below the A-Zone sulphides. Contains minor pyrite srtingers.
TE-99-03	364.65	364.8	JHC-06-013	Tulks East	Massive pyrite ore with minor sphalerite. A-Zone mineralization.
TE-99-03	344.6	344.8	JHC-06-011	Tulks East	Chloritized/sericitized felsic tuff, hangingwall.
TE-99-03	343.3	343.5	JHC-06-010	Tulks East	Pyrite ± galena? Vein in quartz-phyric felsic tuff.
TE-99-03	334.7	334.9	JHC-06-009	Tulks East	Quartz-phyric felsic tuff. Heavy sericite alteration. Local pyrite and pyrrhotite stringers/veinlets.
TE-99-03	376.5	376.8	JHC-06-016	Tulks East	Altered felsic tuff. Extreme deformation of the lapilli, which have been stretched and folded.
TE-99-03	354.6	354.8	JHC-06-014	Tulks East	Massive pyrite ore. A-Zone mineralization.
TE-99-04	237.5	237.65	JHC-06-024	Tulks East	Massive sulphide (pyrite). A-Zone ore.
TE-99-04	241	241.15	JHC-06-025	Tulks East	Massive sulphide with sphalerite. A-Zone ore.
TE-99-04	278.3	278.5	JHC-06-029	Tulks East	Sericitized felsic lapilli tuff. Footwall stockwork .
TE-99-04	228.2	228.4	JHC-06-188	Tulks East	Andesitic dyke.
TE-99-04	287.5	287.7	JHC-06-030	Tulks East	Buckshot pyrite in felsic lapilli tuff. Footwall to ore.
TE-99-04	266.5	266.7	JHC-06-028	Tulks East	Chloritied/pyritized felsic tuff. Stockwork with up to 30% pyrite.
TE-99-04	258	258.2	JHC-06-027	Tulks East	Massive sulphide (pyrite). A-Zone ore.
TE-99-04	112	112.2	JHC-06-019	Tulks East	Fine-grained mafic volcanic. Locally amygdaloidal (filled with carbonate and chlorite). Sharp upper contact but cannot observe the lower. Sill?
TE-99-04	227.5	227.7	JHC-06-022	Tulks East	Rhyolite. Quartz-phyric throughout. Strongly foliated. 10-15% quartz phenocrysts (resorbed). Silicified with minor chlorite alteration at base above the A-Zone.
TE-99-04	147	147.2	JHC-06-021	Tulks East	Andesitic (intermediate) tuff. Light brown to beige. Carbonate alteration throughout with lesser chlorite, silica and pyrite.
TE-99-04	254.2	254.35	JHC-06-026	Tulks East	Massive sulphide with chalcopyrite. A-Zone ore.
TE-99-04	113	113.2	JHC-06-020	Tulks East	Fine-grained mafic volcanic. Locally amygdaloidal (filled with carbonate and chlorite). Sharp upper contact but cannot observe the lower contact. Sill?
TE-99-04	231.8	232	JHC-06-023	Tulks East	Rhyolite. Same as JHC-06-022 but more chlorite alteration. Immediately above the A-Zone sulphide lens.
TW-02-01	90.9	91.1	JHC-06-092	Tulks West	Arsenopyrite-pyrrhotite-chalcopyrite veinlet in quartz-eye phyric felsic volcanics (tuff)
TW-02-01	44.65	44.8	JHC-06-090	Tulks West	Medium to dark-green quartz-phyric crystal tuff - andesite? Chlorite and carbonate alteration.
TW-02-01	93.5	93.7	JHC-06-093	Tulks West	Pyrite/arsenopyrite veinlet in quartz-eye phyric felsic tuff.
TW-02-01	54.6	54.75	JHC-06-091	Tulks West	Chloritized quartz-eye phyric felsic volcanic
TW-09	88	88.2	JHC-06-066	Tulks West	Ash tuff (intermediate?). Sericite alteration.
TW-09	96.3	96.5	JHC-06-067	Tulks West	Silicifed lithic tuff (felsic to intermediate) 3-5 % pyrite-pyrrhotite-chalcopyrite veinlets in cleavage/foliation planes.
TW-09	40.8	41	JHC-06-062	Tulks West	Quartz and plagioclase phyric intermediate volcanic flow/sill. Moderately foliated.
TW-09	53.7	53.8	JHC-06-064	Tulks West	Plagioclase phyric intermediate volcanic.
TW-09	46.4	46.5	JHC-06-063	Tulks West	Quartz phyric felsic tuff.
TW-09	78.1	78.3	JHC-06-065	Tulks West	Felsic volcanic. Quartz-phyric. Tuff or a rhyolite.
TW-10	9.2	9.4	JHC-06-084	Tulks West	Intermediate tuff.
TW-10	74.4	74.6	JHC-06-089	Tulks West	Mafic volcanic. Feldspar-phyric mafic sill.
TW-10	27.4	27.7	JHC-06-085	Tulks West	Intermediate tuff. Light-brown, quartz-feldspar phyric. Intense carbonate alteration.

Appendix 1A: Sample Locations and Brief Descriptions

Hole_ID	From_m	To_m	SampleNum	Property	Descriptn
TW-10	31.6	31.7	JHC-06-086	Tulks West	Intermediate volcanic. Light to medium-grey, quartz-phyric.
TW-10	49.3	49.6	JHC-06-088	Tulks West	Intermediate-mafic volcanic with stringer base metals. Difficult to tell if mafic or intermediate. Amygdaloidal throughout. Chilled margins - Basaltic sill.
TW-10	47.6	47.7	JHC-06-087	Tulks West	Intermediate volcanic with stringer base metals. Difficult to tell if mafic or intermediate. Amygdaloidal throughout. Chilled margins - Basaltic sill.
TW-11	61.7	61.8	JHC-06-081	Tulks West	Altered mafic-intermediate volcanic. Coarse pyrite-silica-carbonate vein. Chlorite alteration.
TW-11	60.9	61.1	JHC-06-080	Tulks West	Amygdlaoidal mafic-intermediate volcanic. Chlorite alteration.
TW-11	53.6	53.8	JHC-06-079	Tulks West	Chlorite altered mafic-intermediate volcanic. Locally amygdaloidal (dolomite filling). Very chloritized.
TW-11	69.4	69.6	JHC-06-083	Tulks West	Heavily pyritized intermediate volcanic. Minor chalcopyrite and pyrrhotite.
TW-11	45.7	45.9	JHC-06-077	Tulks West	Quartz and feldspar-phyric felsic volcanic. Looks like a silicified rhyolite. Maybe pseudo-fragmental.
TW-11	46.9	47.1	JHC-06-078	Tulks West	Quartz and feldspar-phyric felsic volcanic. Massive rhyolite.
TW-11	62.9	63	JHC-06-082	Tulks West	Intermediate volcanic. Light to medium-grey, quartz-phyric.
TW-12	67.9	68.1	JHC-06-072	Tulks West	Altered felsic tuff. Chlorite alteration with lesser sericite and carbonate. Finely dessiminated pyrrhotite and chalcopyrite.
TW-12	104.2	104.5	JHC-06-073	Tulks West	Quartz-phyric felsic volcanic - Rhyolite? Local sericite-silica-iron carbonate alteration.
TW-12	119.4	119.7	JHC-06-074	Tulks West	Stringer chalcopyrite/pyrrhotite in quartz-eye phyric felsic volcanic (Rhyolite?).
TW-12	129.5	129.7	JHC-06-075	Tulks West	Felsic tuff. Beginning of the unit looks tuffaceous but the base looks more massive?
TW-12	144.4	144.6	JHC-06-076	Tulks West	Felsic tuff. Beginning of the unit looks tuffaceous but the base looks more massive?
TW-12	54.6	54.8	JHC-06-071	Tulks West	Sericite/silica altered felsic volcanic. Fine-grained, medium brown.
V-94-01	164.8	165	JHC-07-173	Victoria Mine	Intermediate lapilli tuff.
V-94-01	387.8	388	JHC-07-184	Victoria Mine	Silica-chlorite altered felsic lapilli tuff. Chlorite-carbonate alteration with pyrite in addition to pyrite as clasts.
V-94-01	325.5	325.7	JHC-07-182	Victoria Mine	Carbonate-silica altered intermediate tuff.
V-94-01	310.2	310.4	JHC-07-181	Victoria Mine	Feldspar-phyric, fine-grained mafic dyke/sill.
V-94-01	273	273.2	JHC-07-180	Victoria Mine	Chlorite-carbonate altered intermediate? lapilli tuff. Extreme chlorite alteration.
V-94-01	271.8	272	JHC-07-179	Victoria Mine	Silica-chlorite altered intermediate lapilli tuff with blebby/buckshot pyrite. Minor chalcopyrite. Fragmental. Chlorite in matrix. Appears brecciated.
V-94-01	263.7	263.9	JHC-07-178	Victoria Mine	Chlorite-carbonate-pyrite altered tuff with disseminated/blebby and veinlets of pyrite.
V-94-01	248	248.2	JHC-07-177	Victoria Mine	Chlorite-carbonate altered felsic tuff. 5-7% disseminated pyrite. Chaotic quartz-carbonate alteration. Intense chlorite alteration.
V-94-01	243.4	243.6	JHC-07-176	Victoria Mine	Chlorite-carbonate altered felsic tuff?. 5-7% disseminated pyrite. Extreme chlorite alteration.
V-94-01	371.2	371.4	JHC-07-183	Victoria Mine	Silica-carbonate altered felsic fragmental. Grey siliceous clasts.
V-94-01	215.8	216	JHC-07-174	Victoria Mine	Intermediate tuff.
V-94-01	226.8	227	JHC-07-175	Victoria Mine	Quartz-eye phyric felsic tuff to lapilli-tuff. Unit locally has 10-15% disseminated pyrite. Has sericite-silica alteration.

Appendix 1A: Sample Locations and Brief Descriptions

Hole_ID	From_m	To_m	SampleNum	Property	Descriptn
V-94-01	20.2	20.4	JHC-07-169	Victoria Mine	Green-mauve intermediate fragmental volcanic. Fragments comprise ~ 60% of unit and are composed of hematized fragments, siliceous felsic fragments, pumaceous fragments.
V-94-01	72.2	72.4	JHC-07-170	Victoria Mine	Fine-grained intermediate tuff with siliceous alteration.
V-94-01	83.4	83.6	JHC-07-171	Victoria Mine	Silicifed intermediate-felsic tuff.
V-94-01	137.7	137.9	JHC-07-172	Victoria Mine	Chlorite-carbonate altered intermediate tuff.
VIC-01-02	26.8	27	JHC-07-215	Victoria Mine	Mafic tuff. Dark green with a few quartz-eyes.
VIC-01-02	155.6	155.8	JHC-07-218	Victoria Mine	Silicifed graphitic argillite breccia. Abundant disaggregated quartz veins.
VIC-01-02	123	123.2	JHC-07-217	Victoria Mine	Massive and homogenous mafic sill.
VIC-01-02	41.2	41.4	JHC-07-216	Victoria Mine	Chlorite altered quartz-phyric felsic tuff with significant chalcopyrite occuring in pyrite-chalcopyrite veinlets.
VIC-88-01	24.1	24.3	JHC-07-203	Jig Zone	Heterolithic hematite-carbonate altered felsic lithic tuff (intermediate-mafic). Disseminated/blebby pyrite and sphalerite.
VIC-88-01	111.3	111.5	JHC-07-210	Jig Zone	Heterolitic sericite-silica-pyrite altered lithic wacke. Poorly sorted, clasts of grey siliceous rhyolite, black argillite, sediments.
VIC-88-01	91.7	91.9	JHC-07-209	Jig Zone	Very fine-grained pyritiferous mud/siltstone.
VIC-88-01	62.5	62.8	JHC-07-208	Jig Zone	Silica-sericite-pyrite altered quartz-eye phyric felsic tuff to lapilli tuff.
VIC-88-01	34.3	34.4	JHC-07-207	Jig Zone	Sericite-pyrite altered quartz-phyric tuff.
VIC-88-01	24.2	24.3	JHC-07-206	Jig Zone	Fine-grained argillite, pyriteferous.
VIC-88-01	17.4	17.5	JHC-07-205	Jig Zone	Chaotic silica-carbonate-chlorite altered tuff with sphalerite veins.
VIC-88-01	13.4	13.5	JHC-07-204	Jig Zone	Heterolitic breccia.
VIC-88-04	36	36.2	JHC-07-213	Jig Zone	Quartz-feldspar phyric felsic tuff.
VIC-88-04	29.7	29.9	JHC-07-212	Jig Zone	Heterolithic lapilli tuff to a fragmental. Cm-scale angular fragments varying from grey aphyric siliceous clasts, to quartz-phyric clasts, to jasper.
VIC-88-04	10.9	11.1	JHC-07-211	Jig Zone	Chlorite-carbonate altered mafic tuff-lapilli tuff. Minor hematitic fragments.
VIC-88-04	42	42.2	JHC-07-214	Jig Zone	Pyritiferous argillite.
VIC-89-01	76.2	76.3	JHC-07-200	Victoria Mine	Quartz-eye phyric intermediate fragmental with pyriteferous mud as matrix. Local chaotic carbonate alteration.
VIC-89-01	9.9	10.1	JHC-07-196	Victoria Mine	Intermediate tuff.
VIC-89-01	40.8	41	JHC-07-197	Victoria Mine	Hematite-chlorite-carbonate altered intermediate lapilli tuff.
VIC-89-01	108.2	108.4	JHC-07-202	Victoria Mine	Quartz-rich lithic fragmental rock with disseminated sphalerite throughout.
VIC-89-01	60.5	60.6	JHC-07-199	Victoria Mine	Chaotic quartz-carbonate alteration in an intermediate fragmental rock with a pyriteferous mud matrix.
VIC-89-01	81.3	81.4	JHC-07-201	Victoria Mine	Quartz-rich lithic tuff with pyrite-base metal stringers.
VIC-89-01	56.6	56.8	JHC-07-198	Victoria Mine	Chlorite-sericite altered quartz-eye phyric intermediate tuff.
VIC-90-02	198.6	198.8	JHC-07-195	Victoria Mine	Grey siliceous tuff. Contains sericite-silica-pyrite alteration.
VIC-90-02	180.3	180.5	JHC-07-194	Victoria Mine	Carbonate altered, quartz-eye phyric lapilli tuff.
VIC-90-02	168.3	168.5	JHC-07-193	Victoria Mine	Carbonate-chlorite altered quartz-phyric intermediate tuff. Abundant overprinting pink carbonate.
VIC-90-02	135.5	135.65	JHC-07-192	Victoria Mine	Quartz-crystal, heterolithic lapilli tuff. Contains black very fine-grained sedimentary clasts as well as jasper clasts.
VIC-90-02	103.7	103.9	JHC-07-191	Victoria Mine	Quartz-eye phyric, locally almost lapilli tuff, with abundant red hematized fragments.
VIC-90-02	86.6	86.8	JHC-07-190	Victoria Mine	Chlorite-altered mafic tuff with siliceous zones. Unit is fining downward.
VIC-90-02	58.5	58.7	JHC-07-189	Victoria Mine	Quartz-eye phyric intermediate tuff with abundant maroon fragments.
VIC-90-02	32.3	32.5	JHC-07-188	Victoria Mine	Massive rhyolite with silicification.
VIC-90-02	14.1	14.3	JHC-07-187	Victoria Mine	Intermediate tuff with weak chlorite-carbonate alteration.

APPENDIX 1B

Legend

GS = Geological Survey Labs
AL = Acme Analytical Labs
GS Major and GS Trace = Analysis via Inductively Coupled Plasma–Emission Spectrometry (methods outlined by Finch (1998))
GS BPD = Basic partial dilution via HNO_3 with analysis via ICP-OES.
AL Trace = Analysis via Inductively Coupled Plasma–Emission Spectrometry after total dissolution by a ithium metaborate/tetraborate fusion and dilute nitric digestion at Acme Analytical Labs
AL 4B2Std = Analysis via Inductively Coupled Mass Spectrometry following the dissolution as in AL Trace at Acme Analytical Labs
LOI = Losson ignition, by gravimetric analysis
Total = Total of majors including LOI etc.
$Eu/Eu^* = Eu_{pm}/(Gd_{pm}*Sm_{pm})0.5$, $Nb/Nb = 0.5*Nb_{pm}/(Th_{pm}+La_{pm})$, $Zr/Zr^* = 0.5*Zr_{pm}/(Gd_{pm} + Sm_{pm})$, $Ti/Ti^* = 0.5*Ti_{pm}/(Gd_{pm} + Sm_{pm})$
All normalizing values from Sun and McDonough, 1989–Primitive Mantle
-99 = not analyzed

Appendix 1B: Lithogeochemistry data table for samples analyzed from TVB

SampleNumber	Property	SiO2	Al2O3	Fe2O3	FeO	FeOTotal	MgO	CaO	Na2O	K2O	TiO2	MnO	P2O5	Zr	Ba	LOI	Total
Units		%	%	%	%	%	%	%	%	%	%	%	%	%	%	%	%
Analytical Method		GS Major	GS Major	GS Major	GS Major	GS Major	GS Major	GS Major	GS Major	GS Major	GS Major	GS Major	GS Major	GS Major	GS Major	GS Major	GS Major
JHC-06-001	Tulks East	54.7	14.24	2.1	8.53	10.63	5.66	5.84	2.13	0.06	0.696	0.16	0.064	22	99	3.29	98.41
JHC-06-002	Tulks East	45.31	16.07	0.59	11.96	12.55	8.38	3.64	2.3	0.07	0.466	0.2	0.022	4	76	7.85	98.19
JHC-06-003	Tulks East	68.64	12.04	1.3	2.36	3.66	1.67	2.32	2.28	2.36	0.289	0.08	0.062	58	3582	6.06	99.48
JHC-06-005	Tulks East	68.08	8.51	1.82	5.75	7.58	7.95	0.19	0.09	0.35	0.194	0.12	0.051	35	2785	5.76	98.87
JHC-06-006	Tulks East	72.44	12.33	0.63	5.51	6.14	1.04	0.1	0.45	2.92	0.298	0.03	0.067	59	4317	4.28	100.7
JHC-06-008	Tulks East	77.62	10.22	1.07	2.5	3.57	2.84	0.04	0.33	1.77	0.148	0.05	0.025	51	804	2.78	99.41
JHC-06-009	Tulks East	78.36	9.97	0.99	1.73	2.71	0.18	0.4	3.45	0.91	0.114	0.01	0.041	53	4303	2.03	98.17
JHC-06-010	Tulks East	39.46	6.21	6.36	20.74	27.1	0.28	0.07	0.21	1.7	0.141	0.02	0.011	35	2170	22.9	98.11
JHC-06-011	Tulks East	48.59	24.47	1.78	4.63	6.41	6.26	0.27	1.61	4.57	0.571	0.16	0.131	117	5692	5.42	98.97
JHC-06-012	Tulks East	75.1	12.41	1.46	2.85	4.31	0.96	0.11	0.71	2.95	0.306	0.02	0.056	65	8027	3.48	100.42
JHC-06-013	Tulks East	39.1	0.36	6.06	26.75	32.81	0	0.06	0.08	0	0.002	0.02	0.003	9	3231	20.24	92.65
JHC-06-014	Tulks East	3.42	0.7	6.19	40.31	46.5	1.14	8.85	0.26	0.02	0.013	0.16	0.118	11	21	29.1	90.28
JHC-06-015	Tulks East	71.54	14.04	0.94	3.14	4.08	2.37	0.06	0.63	2.35	0.228	0.05	0.033	66	3114	2.94	98.67
JHC-06-017	Tulks East	55.8	8.71	2.07	16.11	18.18	1.1	0.16	0.39	1.91	0.179	0.04	0.053	40	1273	11.42	99.72
JHC-06-018	Tulks East	25.59	20.22	3.14	18.3	21.44	15.75	0.14	0.15	0.42	0.38	0.23	0.069	95	993	11.01	97.43
JHC-06-019	Tulks East	53.68	13.7	1.94	7.99	9.93	5.74	5.73	2.12	0	0.629	0.17	0.064	22	17	5.56	98.21
JHC-06-020	Tulks East	52.45	14.08	2.19	8.23	10.42	6.14	5.94	2.72	0.01	0.658	0.18	0.063	21	47	4.52	98.1
JHC-06-021	Tulks East	44.37	14.8	0.62	10.63	11.25	6.76	7.83	0.81	0.38	0.395	0.22	0.019	5	92	4.53	92.55
JHC-06-022	Tulks East	85.14	7.41	0.36	0.67	1.03	0.14	0.43	2.67	0.69	0.096	0.01	0.045	38	2927	1.27	98.92
JHC-06-023	Tulks East	38.51	23.57	0.31	7.21	7.51	15.05	0.8	0.31	2.87	0.549	0.21	0.125	108	11815	8.2	98.51
JHC-06-024	Tulks East	24.42	2.07	4.92	35.7	40.62	2.52	0.18	0.05	0	0	0.04	0.014	15	8	24.35	98.22
JHC-06-025	Tulks East	19.83	0.92	6.36	35.17	41.53	1.03	2.93	0.06	0	0	0.06	0.048	15	16	22.14	88.55
JHC-06-026	Tulks East	10.99	0.35	5.07	33.84	38.91	0.25	0.02	0.06	0	0.001	0.04	0.01	14	3	29.02	83.41
JHC-06-027	Tulks East	4.39	1.59	11.44	41.71	53.15	1.77	1.15	0.06	0.03	0.002	0.06	0.29	19	21	31.07	98.21
JHC-06-028	Tulks East	30.14	15.78	4.79	19.82	24.61	10.72	0.06	0.14	0.77	0.172	0.17	0.023	46	637	13.31	98.09
JHC-06-030	Tulks East	37.52	4.86	4.84	27.14	31.97	0.46	0.08	0.24	1.04	0.096	0.04	0.021	32	513	18.93	98.29
JHC-06-031	Tulks Hill	80.7	9.17	0.47	0.93	1.4	1.11	0.39	0.14	3.05	0.084	0.02	0.015	117	4202	2.41	98.48
JHC-06-032	Tulks Hill	82.38	7.59	0.94	1.36	2.3	0.32	0	0.18	2.27	0.068	0	0.011	108	1205	2.54	97.83
JHC-06-033	Tulks Hill	80.3	9.26	0.56	1.72	2.28	2.15	0.19	0.43	2.4	0.086	0.06	0.016	133	1007	2.46	99.83
JHC-06-034	Tulks Hill	39.05	16.72	1	13.79	14.78	10.8	3.23	1.56	0.76	0.623	0.22	0.053	23	100	8.55	97.88
JHC-06-035	Tulks Hill	79.48	9.35	0.24	1.21	1.45	0.92	0.63	3.17	1.24	0.085	0.04	0.01	128	168	1.74	98.25
JHC-06-036	Tulks Hill	38.49	14.17	1.23	7.47	8.71	7.07	7.45	0.24	4.88	0.508	0.35	0.051	15	592	13.62	96.36
JHC-06-037	Tulks Hill	73.97	11.53	0.61	2.59	3.2	0.98	1.42	3.65	1.38	0.125	0.05	0.019	62	284	2.23	98.84
JHC-06-038	Tulks Hill	64.12	9.45	6.42	6.19	12.6	0.79	0.02	0.3	2.37	0.092	0.03	0.007	127	2739	8.22	98.68
JHC-06-039	Tulks Hill	68.12	13.36	0.51	3.97	4.47	4.89	0.43	0.16	2.45	0.113	0.21	0.012	168	896	3.68	98.32
JHC-06-040	Tulks Hill	74.55	12.42	0.98	2.32	3.29	0.85	0.62	4.75	1.1	0.142	0.07	0.024	68	178	1.3	99.38
JHC-06-041	Tulks Hill	39.74	12.65	13.95	11.31	25.25	0.94	0.13	0.22	3.68	0.096	0.04	0.021	135	5445	15.09	99.12
JHC-06-042	Tulks Hill	73.99	12.15	0.63	2.73	3.36	1.48	0.2	4.96	0.44	0.131	0.04	0.021	68	534	1.48	98.56
JHC-06-043	Tulks Hill	69.85	13.02	0.36	1.52	1.88	2.1	0.86	1.34	3.28	0.146	0.03	0.017	144	317	3.02	95.71
JHC-06-044	Tulks Hill	71.09	11.52	1.1	1.82	2.92	0.38	3.07	5.52	0.59	0.143	0.07	0.029	63	84	2.57	98.11
JHC-06-045	Tulks Hill	56.87	14.88	1.91	7.59	9.5	4.06	2.41	3.69	1.09	0.624	0.13	0.152	51	82	4.48	98.72
JHC-06-047	Tulks Hill	70.22	12.83	0.66	1.19	1.86	2.13	1.2	0.42	4.42	0.186	0.03	0.028	124	1090	3.73	97.18
JHC-06-048	Tulks Hill	45.48	7.33	2.12	18.27	20.39	3.44	0.56	0.08	0.97	0.138	0.1	0.17	98	1339	10.96	91.65
JHC-06-050	Tulks Hill	69.31	11.52	0.84	4.96	5.79	1.99	1.4	4.51	0.24	0.279	0.11	0.066	60	22	2.93	98.71

Appendix 1B: Lithogeochemistry data table for samples analyzed from TVB

SampleNumber	Property	SiO2	Al2O3	Fe2O3	FeO	FeOTotal	MgO	CaO	Na2O	K2O	TiO2	MnO	P2O5	Zr	Ba	LOI	Total
Units		%	%	%	%	%	%	%	%	%	%	%	%	%	%	%	%
Analytical Method		GS Major	GS Major	GS Major	GS Major	GS Major	GS Major	GS Major	GS Major	GS Major	GS Major	GS Major	GS Major	GS Major	GS Major	GS Major	GS Major
JHC-06-051	Tulks Hill	73.37	11.89	0.98	2.61	3.59	0.87	0.95	4.46	1.86	0.164	0.06	0.03	52	179	1.28	98.83
JHC-06-052	Tulks Hill	72.59	12.68	1.07	2.83	3.9	0.82	1.83	3.58	1.9	0.25	0.07	0.056	55	206	2.21	100.19
JHC-06-053	Tulks Hill	61.01	15.18	1.03	5.63	6.67	2.69	2.5	5.04	1.27	0.558	0.08	0.153	49	154	3.34	99.11
JHC-06-054	Tulks Hill	68.91	14.51	0.54	1.38	1.92	2.1	1.18	2.4	3.55	0.138	0.02	0.018	156	330	3.46	98.36
JHC-06-057	Tulks Hill	74.67	12.37	0.71	0.87	1.58	0.6	0.68	3.01	2.59	0.217	0.02	0.06	120	784	2.08	97.97
JHC-06-059	Tulks Hill	63.62	13.92	1.74	4.38	6.12	1.82	2.93	2.89	2.19	0.546	0.12	0.168	42	296	4.35	99.17
JHC-06-060	Tulks Hill	60.77	14.6	1.25	5.69	6.94	1.79	3.39	4.26	0.8	0.582	0.15	0.165	53	122	4.26	98.35
JHC-06-062	Tulks West	43.02	14.99	1.39	9.04	10.43	8.24	6.09	3.58	0.03	0.733	0.17	0.064	26	3	9.16	97.5
JHC-06-063	Tulks West	41.91	14.55	1.18	8.19	9.37	8.1	7.84	3.5	0.03	0.96	0.19	0.095	27	3	9.92	97.39
JHC-06-064	Tulks West	42.44	13.64	0.58	9.41	9.99	9.58	6.14	2.61	0.06	0.86	0.3	0.073	21	5	12.46	99.19
JHC-06-068	Middle Tulks	48.75	14.76	1.94	9.06	11	9.23	2.5	2.27	0.28	1.043	0.15	0.083	38	27	6.99	98.06
JHC-06-069	Middle Tulks	50.78	14.26	1.45	9.61	11.06	6.41	4.12	2.93	0.03	0.988	0.22	0.097	39	2	6.52	98.48
JHC-06-070	Middle Tulks	47.02	17.42	0.8	11.78	12.58	10.12	0.27	2.95	0.05	1	0.23	0.075	32	51	5.68	98.71
JHC-06-071	Tulks West	47.45	16.01	0.93	8.28	9.21	4.99	4.92	5.13	0.21	0.704	0.26	0.061	21	47	9.36	99.22
JHC-06-072	Tulks West	43.78	21.08	0.99	12.14	13.13	5.66	1.95	2.61	1.71	1.323	0.17	0.114	46	274	6.02	98.9
JHC-06-073	Tulks West	70.22	13.7	0.65	5.29	5.94	3.86	0.02	0.43	1.73	0.158	0.03	0.014	150	966	3.32	100.03
JHC-06-074	Tulks West	33.51	17.91	4.72	21.29	26.01	7.52	0.13	0.51	0.3	0.383	0.23	0.071	214	283	6.94	95.87
JHC-06-075	Tulks West	67.47	13.07	1.11	6.48	7.6	2.13	0.77	0.96	1.6	0.34	0.06	0.043	155	972	3.14	97.89
JHC-06-076	Tulks West	56.22	19.27	0.5	3.95	4.45	3.3	3.06	1.37	3.01	0.621	0.1	0.174	193	1123	7.11	99.12
JHC-06-077	Tulks West	69.02	10.66	1.26	2.21	3.47	2.11	3.56	4.29	0.65	0.209	0.19	0.025	103	324	6.11	100.29
JHC-06-078	Tulks West	75.31	10.02	0.67	1.11	1.78	1.1	1.88	4.19	0.59	0.191	0.11	0.026	100	378	3.46	98.77
JHC-06-079	Baxters Pond Alteration Zone	35.02	16.8	0.64	8.32	8.96	16.21	4.49	1.6	0.02	0.812	0.99	0.127	15	3	12.93	98.88
JHC-06-082	Tulks West	43.15	14.15	1.03	8.39	9.42	10.1	5.08	3.21	0.02	0.65	0.43	0.058	13	4	8.74	95.94
JHC-06-083	Tulks West	10.85	2.29	0.29	41.41	41.7	3.78	5.06	0.07	0.03	0.09	0.5	0.223	25	13	23.07	92.24
JHC-06-086	Tulks West	72.01	12.23	0.52	4.23	4.74	0.68	1.62	3.23	0.93	0.278	0.07	0.057	80	168	2.29	98.61
JHC-06-087	Tulks West	51.29	15.19	3.65	5.61	9.26	1.09	2.05	6.63	0.47	0.876	0.13	0.146	48	246	5.97	93.1
JHC-06-088	Tulks West	43.32	16.89	1.05	9.5	10.55	4.16	6.39	5.37	0.19	1.047	0.43	0.122	54	50	9.42	98.95
JHC-06-089	Tulks West	47.95	15.15	2.68	6.95	9.63	9.87	6.66	3.4	0.03	0.765	0.16	0.067	33	192	6.19	100.65
JHC-06-091	Tulks West	60.06	15.52	1.02	7.06	8.09	3.85	1.45	4.01	0.89	0.616	0.14	0.109	53	845	3.28	98.79
JHC-06-092	Tulks West	26.57	17.08	8.58	21.03	29.62	0.72	0.38	0.36	4.35	0.541	0.06	0.113	58	1351	18.35	98.15
JHC-06-095	Dragon Pond	71.84	12.59	0.64	2.5	3.14	1.19	1.33	3.74	1.55	0.405	0.05	0.056	145	665	2.47	98.63
JHC-06-097	Dragon Pond	55.42	16.55	1.56	2.54	4.09	1.5	4.26	0.07	5.82	0.352	0.03	0.077	38	381	5.1	93.55
JHC-06-098	Dragon Pond	41.24	14	0.94	11.28	12.21	5.56	6.59	4.05	0.52	3.527	0.19	0.611	254	107	8.88	98.64
JHC-06-100	Dragon Pond	56.71	16.38	3.51	5.44	8.95	2.9	3.53	6.54	0.18	0.368	0.07	0.051	32	28	5.01	100.69
JHC-06-101	Dragon Pond	55.1	12.51	1.64	5.54	7.18	2.83	5.79	1.5	1.62	0.268	0.15	0.041	29	255	8.59	96.19
JHC-06-102	Dragon Pond	60.53	13.46	3.15	4.8	7.94	4.28	0.86	2.74	1.98	0.269	0.21	0.043	36	246	6.05	98.91
JHC-06-103	Midas Pond	78.88	14.44	0.06	0.13	0.19	0.04	0.19	2.43	0.45	0.293	0	0.105	223	80	2.2	99.22
JHC-06-104	Midas Pond	70.37	13.93	0.79	1.44	2.24	2.16	1.2	3.64	0.9	0.542	0.02	0.103	116	277	3.49	98.58
JHC-06-105	Midas Pond	53.17	13.86	1.6	10.99	12.58	5.42	1.58	2.52	0.26	1.151	0.08	0.096	89	45	6.63	98.56
JHC-06-108	Midas Pond	59.35	13.26	0.86	6.64	7.5	4.56	2.59	3.09	0.24	1.122	0.08	0.21	102	37	5.79	98.54
JHC-06-109	Dragon Pond	40.98	12.45	3.43	6.38	9.81	2.14	11.32	1.5	3.06	0.512	0.11	0.149	28	327	10.65	93.38
JHC-06-111	Dragon Pond	44.7	0.86	6.2	25.39	31.59	0.71	2.45	0.07	0.11	0.03	0.08	0.109	19	3	16.1	96.81
JHC-06-112	Dragon Pond	54.19	15.27	5.23	4.32	9.55	0.74	3.42	2.17	3.3	0.321	0.05	0.103	30	241	9.38	98.97

Appendix 1B: Lithogeochemistry data table for samples analyzed from TVB

SampleNumber	Property	SiO2	Al2O3	Fe2O3	FeO	FeOTotal	MgO	CaO	Na2O	K2O	TiO2	MnO	P2O5	Zr	Ba	LOI	Total
Units		%	%	%	%	%	%	%	%	%	%	%	%	%	%	%	%
Analytical Method		GS Major	GS Major	GS Major	GS Major	GS Major	GS Major	GS Major	GS Major	GS Major	GS Major	GS Major	GS Major	GS Major	GS Major	GS Major	GS Major
JHC-06-113	Dragon Pond	60.19	15.06	0.24	6.64	6.88	3.18	4.9	2.12	0.88	0.315	0.09	0.051	35	329	4.25	98.66
JHC-06-115	Dragon Pond	57.89	14.67	3.93	4.56	8.48	5.99	0.11	1.29	0.88	0.298	0.04	0.042	41	228	8.08	98.27
JHC-06-118	Dragon Pond	57.88	15.35	2.3	3.37	5.67	2.28	2.97	0.12	4.56	0.335	0.05	0.141	50	383	5.64	95.38
JHC-06-120	Dragon Pond	48.64	12.92	11.15	6	17.15	0.62	1.51	0.13	4.47	0.284	0.02	0.369	31	303	11.47	98.24
JHC-06-121	Dragon Pond	57.61	15.72	6.15	2.42	8.57	2.43	0.95	0.28	5.6	0.324	0.04	0.118	41	500	7.05	98.96
JHC-06-122	Dragon Pond	52.85	15.81	7.99	2.57	10.56	2.26	2.54	0.96	5	0.347	0.05	0.077	38	526	8.34	99.08
JHC-06-123	Dragon Pond	41.29	15.23	2.88	10.66	13.55	6.6	7.77	3.05	0.08	3.712	0.24	0.608	255	44	5.13	98.45
JHC-06-124	Dragon Pond	55.37	15.16	5.27	2.85	8.12	1.24	4.09	1.21	4.21	0.322	0.1	0.044	39	560	7.07	97.25
JHC-06-125	Dragon Pond	59.21	13.79	2.79	5.13	7.92	4.99	2.64	1.92	1.45	0.289	0.33	0.042	28	242	5.1	98.24
JHC-06-126	Dragon Pond	55.4	13.58	5.89	2.38	8.27	3.21	3.13	1.73	2.67	0.269	0.06	0.044	36	520	10.09	98.71
JHC-06-127	Dragon Pond	58.18	14.17	1.18	6.38	7.56	2.42	5.71	3.44	1.42	0.275	0.1	0.032	37	331	5.93	99.93
JHC-06-128	Dragon Pond	54.5	12.62	2.78	2.68	5.46	2.36	8.21	1.23	4.78	0.239	0.12	0.039	30	373	7.36	97.21
JHC-06-130	Midas Pond	71.54	13.08	0.84	1.43	2.27	1.63	1.32	4.26	0.74	0.518	0.02	0.115	111	320	3.65	99.14
JHC-06-131	Midas Pond	73.37	11.96	1.05	1.67	2.72	1.36	0.74	5.42	0.12	0.38	0.02	0.066	118	26	2.45	98.62
JHC-06-133	Midas Pond	71.73	13.15	0.93	1.57	2.5	1.17	1.69	4.56	0.53	0.349	0.03	0.088	174	112	4.12	99.93
JHC-06-134	Curve Pond	76.72	12.85	0.09	1.57	1.66	0.3	0.22	3.73	1.48	0.228	0.02	0.044	148	1445	1.59	99.04
JHC-06-135	Curve Pond	55.68	18.97	1.45	6.19	7.64	2.98	0.24	0.54	4.81	0.806	0.24	0.149	179	4902	7.34	100.07
JHC-06-141	Curve Pond	67.8	13.14	1.04	7.62	8.66	2.05	0.08	1.23	1.49	0.201	0.18	0.033	149	6123	3.71	99.43
JHC-06-142	Curve Pond	5.89	0.37	0.08	47.73	47.81	0.05	0.07	0.1	0.07	0.001	0.22	0.003	16	36	33.19	93.08
JHC-06-143	Curve Pond	74.08	15.27	0.43	0.59	1.02	0.33	0.12	5.2	1.49	0.282	0.01	0.049	549	2773	1.3	99.16
JHC-06-145	Curve Pond	29.66	7.85	0.03	20.27	20.3	2.37	8.31	0.71	0.32	0.357	5.47	0.491	59	251	18.62	96.7
JHC-06-146	Curve Pond	18.78	0.22	7.41	40.84	48.25	0.18	0.9	0.05	0.09	0.007	0.17	0.006	17	23	27.54	96.19
JHC-06-147	Curve Pond	40.87	11.6	0.37	16.2	16.56	3.59	5.03	1.03	0.78	0.524	1.98	0.202	106	492	11.27	95.23
JHC-06-148	Curve Pond	67.74	18.47	0.74	0.82	1.56	0.93	0.48	8.64	0.49	0.554	0.05	0.076	420	2107	1.26	100.26
JHC-06-149	Curve Pond	55.68	13.85	1.07	8.91	9.98	8.06	1.69	2.1	0.07	0.649	0.4	0.053	31	65	5.29	98.79
JHC-06-150	Curve Pond	12.19	0.37	5.36	32.12	37.48	0.2	8.51	0.06	0.06	0.015	0.77	0.029	14	41	23.73	83.42
JHC-06-153	Boomerang/Domino	48.64	16.98	0.99	9.9	10.88	5.5	3.76	5.38	0.1	0.898	0.17	0.091	44	40	6.13	99.64
JHC-06-154	Boomerang/Domino	67.04	15.59	1.42	1.91	3.33	1.02	0.8	4.33	3.07	0.494	0.02	0.111	147	649	2.59	98.38
JHC-06-156	Boomerang/Domino	45.19	15.24	0.57	8	8.57	6.5	6	2.02	3.48	1.599	0.2	0.388	172	498	8.19	98.26
JHC-06-157	Boomerang/Domino	55.79	14.66	2.5	3.58	6.07	2.24	4.92	4.04	3.43	0.941	0.2	0.188	50	597	5.78	98.28
JHC-06-158	Boomerang/Domino	71.03	12.74	0.96	1.44	2.4	1.14	2.96	3.64	2.54	0.395	0.12	0.078	126	566	3.18	100.21
JHC-06-162	Boomerang/Domino	76.55	10.77	0.42	1.61	2.03	1.06	1.27	4.88	0.26	0.173	0.06	0.032	140	46	1.65	98.92
JHC-06-164	Boomerang/Domino	52.93	18.23	0.56	6.63	7.19	5.21	2.49	5.7	0.74	0.89	0.17	0.13	72	230	4.26	98.68
JHC-06-166	Boomerang/Domino	51.39	16.44	2.82	6.49	9.31	4.59	4.29	4.9	0.57	1.082	0.24	0.101	55	115	4.7	98.32
JHC-06-167	Boomerang/Domino	53.94	14.62	3.92	6.74	10.66	4.04	2.26	5.34	0.2	1.441	0.17	0.238	110	32	4.68	98.32
JHC-06-169	Boomerang/Domino	51	18.35	1.24	8.38	9.63	4.05	2.08	5.9	0.8	1.097	0.19	0.089	45	381	5.45	99.58
JHC-06-170	Boomerang/Domino	50.34	16.65	2.42	8.66	11.08	5.36	4.63	5.08	0.66	0.951	0.18	0.078	44	244	3.08	99.04
JHC-06-171	Boomerang/Domino	69.16	13.8	1.1	2.86	3.96	2.93	0.84	1.89	3.06	0.446	0.08	0.065	187	475	3.19	99.73
JHC-06-172	Boomerang/Domino	69.04	14.39	1.59	1.87	3.46	1.87	1.26	2.79	3.39	0.644	0.05	0.131	200	381	2.83	100.06
JHC-06-173	Boomerang/Domino	59.78	17.61	0.71	5.08	5.79	3.96	1.3	5.71	1.06	0.756	0.11	0.148	102	237	3.55	100.34
JHC-06-174	Boomerang/Domino	62.6	17.43	0.75	3.88	4.63	2.98	1.38	5.29	1.98	0.773	0.11	0.149	105	538	3.1	100.84
JHC-06-175	Boomerang/Domino	52.81	17.04	2.96	6.32	9.28	4.38	3.16	6.72	0.42	0.894	0.15	0.105	46	67	3.85	99.5
JHC-06-176	Boomerang/Domino	59.36	18.22	0.71	4.88	5.6	2.58	1.68	7.69	0.33	0.808	0.09	0.158	103	105	3.37	100.42
JHC-06-177	Boomerang/Domino	67.95	14.45	1.51	2.34	3.85	2.17	0.94	4.35	1.73	0.476	0.08	0.077	170	346	2.4	98.49

Appendix 1B: Lithogeochemistry data table for samples analyzed from TVB

SampleNumber	Property	SiO2	Al2O3	Fe2O3	FeO	FeOTotal	MgO	CaO	Na2O	K2O	TiO2	MnO	P2O5	Zr	Ba	LOI	Total
Units		%	%	%	%	%	%	%	%	%	%	%	%	%	%	%	%
Analytical Method		GS Major	GS Major	GS Major	GS Major	GS Major	GS Major	GS Major	GS Major	GS Major	GS Major	GS Major	GS Major	GS Major	GS Major	GS Major	GS Major
JHC-06-178	Boomerang/Domino	46.19	15.52	1.1	9.8	10.91	6.44	6.17	3.88	0.2	2.501	0.19	0.497	180	53	5.09	98.68
JHC-06-179	Boomerang/Domino	58.88	18.07	2.27	4.4	6.67	5.08	0.52	2.22	2.46	0.947	0.07	0.186	197	449	4.83	99.93
JHC-06-180	Boomerang/Domino	54.67	18.42	3.65	4.69	8.34	1.27	0.53	4.2	2.47	0.839	0.02	0.145	109	656	6.63	98.06
JHC-06-181	Boomerang/Domino	56.57	21.01	3.09	4.09	7.18	1.08	0.36	1.74	3.26	0.809	0.02	0.144	140	2559	6.72	99.36
JHC-06-182	Boomerang/Domino	52.18	17.76	3.12	4.24	7.36	2.05	3.09	1.44	3.12	0.725	0.12	0.133	126	2282	8.8	97.25
JHC-06-183	Boomerang/Domino	36.41	24.21	2.37	4.35	6.72	3.4	4.52	1.03	5.1	0.918	0.14	0.136	162	15497	12.07	95.15
JHC-06-184	Boomerang/Domino	19.14	10.11	4.2	17.82	22.02	5.38	7.39	0.45	1.19	0.388	0.2	0.139	80	8505	19.24	87.62
JHC-06-185	Boomerang/Domino	27.05	16.99	5.37	11.22	16.59	7.47	3.75	0.49	1.56	0.639	0.1	0.149	128	12261	15.89	91.92
JHC-06-188	Tulks East	40.35	13.87	6.19	6.32	12.51	5.98	6.21	3.28	0.74	3.504	0.15	0.544	238	643	8.14	95.98
JHC-06-190	Boomerang/Domino	60.63	16.61	1.31	5.1	6.41	3.42	1.03	3.9	2.54	0.924	0.09	0.08	87	660	2.92	99.11
JHC-06-191	Boomerang/Domino	65.4	14.88	0.6	3.36	3.96	1.09	2.78	6.14	1.04	0.835	0.08	0.208	77	341	2.41	99.2
JHC-06-192	Boomerang/Domino	51.79	17.97	1.11	6.06	7.17	6.09	2.19	5.75	0.97	0.963	0.15	0.088	91	223	4.53	98.32
JHC-06-194	Boomerang/Domino	62.5	14.77	1.82	4.17	5.99	1.99	1.97	4.54	2.09	0.797	0.12	0.13	74	396	3.37	98.72
JHC-06-197	Boomerang/Domino	72.24	14.99	0.23	1.75	1.98	2.07	0.13	4.83	1.67	0.325	0.01	0.043	169	251	1.83	100.31
JHC-06-198	Boomerang/Domino	30.51	18.67	0.65	10.96	11.61	19.14	0.43	1.48	0.85	0.759	0.1	0.137	93	62	13.38	98.28
JHC-06-199	Boomerang/Domino	66.19	13.62	1.56	2.6	4.17	1.57	1.91	4.22	1.29	0.597	0.12	0.106	68	553	4.09	97.88
JHC-06-200	Boomerang/Domino	53.53	19.35	2.95	4.93	7.89	6.2	0.22	3.97	2.28	0.965	0.06	0.146	74	262	4.77	99.38
JHC-06-201	Boomerang/Domino	51.68	20.02	1.12	6.45	7.57	3.9	2.92	5.04	2.35	1.062	0.11	0.138	83	244	5.3	100.8
JHC-06-202	Boomerang/Domino	55.2	17.58	0.73	5.37	6.1	2.79	3.82	4.78	2.25	0.787	0.11	0.062	73	221	4.89	98.98
JHC-06-204	Boomerang/Domino	65.89	17.32	1.36	1.8	3.17	2.12	0.17	4.72	2.87	0.496	0.02	0.095	161	281	2.58	99.45
JHC-06-205	Boomerang/Domino	50.12	16.37	0.83	9.44	10.27	5.61	2.99	5.4	0.26	0.989	0.18	0.079	46	82	5.76	99.08
JHC-06-207	Boomerang/Domino	67.04	14.47	0.35	3.88	4.23	4.98	0.2	5.49	0.05	0.624	0.04	0.111	74	16	2.75	100.42
JHC-06-209	Boomerang/Domino	67.03	14.52	0.31	4.15	4.46	5.1	0.22	5.45	0.05	0.626	0.04	0.11	75	17	2.71	100.78
JHC-06-210	Boomerang/Domino	67.73	12.75	1.91	3.59	5.5	2.51	0.93	0.13	4.29	0.352	0.04	0.07	129	724	3.22	97.56
JHC-06-211	Boomerang/Domino	63.34	14.85	0.5	4.2	4.7	1.85	1.4	6.89	0.47	0.65	0.15	0.111	75	236	3.48	98.37
JHC-06-214	Boomerang/Domino	47.43	16.54	0.98	10.19	11.18	5.89	3.83	4.36	0.1	1.275	0.24	0.131	71	29	6.67	98.78
JHC-06-216	Boomerang/Domino	65.94	14.97	0.83	3.95	4.78	2.38	1.12	5.82	0.51	0.651	0.11	0.112	78	318	2.53	99.37
JHC-06-218	Boomerang/Domino	47.52	15.79	1.38	9.24	10.62	5.06	5.74	4.65	0.03	0.997	0.2	0.1	60	29	7.19	98.92
JHC-06-219	Boomerang/Domino	61.45	18.72	1.51	2.45	3.96	3.38	0.88	3.61	2.4	0.44	0.04	0.087	321	1504	3.93	98.89
JHC-06-220	Boomerang/Domino	53.5	23.03	0.67	4.27	4.94	0.66	1.26	5.89	3.07	0.848	0.02	0.16	169	632	5.45	99.3
JHC-06-221	Boomerang/Domino	65.43	13.67	0.53	4.71	5.23	2.26	0.98	0.69	2.81	0.52	0.03	0.111	93	464	5.81	98.08
JHC-06-225	Boomerang/Domino	56.67	16.25	1.69	5.42	7.11	4.84	2.79	4.77	0.87	0.763	0.12	0.087	88	125	4.3	99.17
JHC-06-226	Boomerang/Domino	62.74	17.72	1.72	2.47	4.19	3.31	1.48	2.86	4.17	0.524	0.05	0.076	137	547	3.59	100.7
JHC-06-227	Boomerang/Domino	52.07	18.15	0.93	8.82	9.75	5.27	1.43	6.18	0.22	1.188	0.13	0.095	63	76	3.54	98.99
JHC-06-228	Boomerang/Domino	48.74	16.55	4.17	7.24	11.4	4.75	8.08	3.72	0.49	1.003	0.18	0.076	41	388	3.52	99.31
JHC-06-229	Boomerang/Domino	51.89	17.89	0.48	8.11	8.59	4.57	2.76	6.6	0.48	1.114	0.14	0.118	67	286	4.08	99.13
JHC-06-230	Boomerang/Domino	50.34	17.41	2.63	7.86	10.48	5.5	4.6	5.29	0.07	0.912	0.15	0.078	42	55	3.07	98.78
JHC-06-231	Boomerang/Domino	48.08	16.11	0.72	7.91	8.63	4.6	4.54	4.73	0.72	0.813	0.24	0.077	40	203	8.68	98.1
JHC-06-233	Boomerang/Domino	66.13	14.71	0.29	4.16	4.46	2.52	1.03	5.86	0.08	0.616	0.09	0.106	73	25	2.69	98.76
JHC-06-234	Boomerang/Domino	58.79	14.35	0.11	4.64	4.75	1.59	3.75	4.55	1.08	0.997	0.11	0.351	172	347	7.42	98.25
JHC-06-235	Boomerang/Domino	37.07	16.55	5.78	13.43	19.21	1.2	0.28	0.89	3.62	0.598	0.03	0.129	102	620	13.19	92.75
JHC-06-236	Boomerang/Domino	64.21	15.54	2.07	4.26	6.33	1	0.28	0.81	3.31	0.607	0.01	0.098	96	1052	5.9	98.56
JHC-06-237	Boomerang/Domino	43	10.71	1.04	2.82	3.87	4.79	13.02	0.72	2.28	0.416	0.64	0.074	60	472	14.42	93.94
JHC-06-238	Boomerang/Domino	65.84	14.99	1.44	2.55	4	2.55	1.1	2.88	2.14	0.436	0.07	0.061	212	495	6.36	100.43

Appendix 1B: Lithogeochemistry data table for samples analyzed from TVB

SampleNumber	Property	SiO2	Al2O3	Fe2O3	FeO	FeOTotal	MgO	CaO	Na2O	K2O	TiO2	MnO	P2O5	Zr	Ba	LOI	Total
Units		%	%	%	%	%	%	%	%	%	%	%	%	%	%	%	%
Analytical Method		GS Major	GS Major	GS Major	GS Major	GS Major	GS Major	GS Major	GS Major	GS Major	GS Major	GS Major	GS Major	GS Major	GS Major	GS Major	GS Major
JHC-06-239	Boomerang/Domino	40.42	15.8	1.49	5.4	6.88	4.65	7.17	0.92	3.54	0.672	0.38	0.119	98	1250	13.63	94.79
JHC-06-240	Boomerang/Domino	66.32	15.51	0.7	4.26	4.96	2.91	0.47	6.12	0.03	0.661	0.05	0.115	80	29	2.27	99.89
JHC-06-242	Baxters Pond Alteration Zone	40.51	14.22	1.51	10.85	12.36	7.47	7.9	2.27	0.04	1.838	0.23	0.245	100	26	10.27	98.55
JHC-06-243	Baxters Pond Alteration Zone	67.53	14.62	1.58	2.66	4.23	2.15	1.47	3.74	1.59	0.364	0.15	0.094	91	301	3.25	99.2
JHC-06-244	Baxters Pond Alteration Zone	50.23	16.77	3.1	7.24	10.35	7.12	2.09	5.55	0.11	0.904	0.16	0.077	38	28	5.57	99.74
JHC-07-002	Roebucks Brook	45.71	15.09	0.83	4.72	6.07	1.68	12.13	2.24	2.86	0.55	0.11	0.205	122	1637	12.06	98.71
JHC-07-003	Roebucks Brook	40.95	15.58	2.39	13.26	17.13	7.82	7.41	2.2	0.05	2.383	0.26	0.383	159	56	4.23	98.39
JHC-07-004	Roebucks Brook	45.76	19.22	3.43	5.67	9.73	3.48	12.41	1.17	0.69	0.71	0.11	0.096	58	259	5.26	98.65
JHC-07-006	Roebucks Brook	77.53	10.18	1.61	0.84	2.46	2.59	0.28	2.25	1.44	0.135	0.06	0.044	73	752	2.66	99.64
JHC-07-007	Roebucks Brook	46.15	12.62	0.99	7.09	8.87	4.3	12.06	2.91	0.06	1.474	0.15	0.249	94	47	10.3	99.13
JHC-07-009	Roebucks Brook	58.9	17.5	2.49	4.43	7.42	3.43	1.76	0.23	4.24	0.57	0.09	0.177	139	2036	4.43	98.75
JHC-07-010	Roebucks Brook	45.39	14.8	1.87	12.18	15.41	6.65	7.38	2.94	0.31	2.042	0.23	0.358	147	501	3.65	99.17
JHC-07-013	Roebucks Brook	79.9	8.11	2.71	1.16	3.87	1.78	0.43	0.69	1.23	0.36	0.12	0.082	68	340	2.32	98.88
JHC-07-015	Roebucks Brook	41.08	13.91	0.79	12.67	14.87	6.75	7.81	0.66	0.53	2.013	0.21	0.346	138	77	9.67	97.85
JHC-07-016	Roebucks Brook	44.05	14.79	2.71	12.03	16.08	6.96	6.64	2.3	0.01	2.056	0.21	0.344	138	23	5.64	99.08
JHC-07-017	Roebucks Brook	46.8	17.62	2.44	7.48	10.76	4.23	11.45	1.1	0.18	0.63	0.09	0.161	58	97	5.78	98.81
JHC-07-018	Roebucks Brook	66.74	13.45	3.76	1.88	5.64	0.6	0.2	0.34	3.6	0.214	0.01	0.056	89	4719	5.11	95.95
JHC-07-019	Roebucks Brook	70.23	15.03	2.07	1.17	3.24	1.31	0.18	1.21	3.6	0.168	0.03	0.035	113	2565	3.58	98.61
JHC-07-020	Roebucks Brook	40.13	13.7	2.15	7.93	10.97	5.93	14.82	1.48	0	1.542	0.17	0.2	84	9	9.21	98.14
JHC-07-021	Roebucks Brook	42.5	15.13	4.12	10.58	15.87	6.92	8.48	1.82	0.02	2.072	0.24	0.351	144	33	5.25	98.65
JHC-07-022	Roebucks Brook	45.22	13.39	1.74	11.79	14.83	7.3	4.63	1.11	1.35	1.977	0.14	0.397	304	475	7.79	98.14
JHC-07-023	Jacks Pond	71.63	12.88	1.33	0.83	2.15	1.18	1.06	2.69	2.82	0.341	0.03	0.059	153	452	3.26	98.1
JHC-07-024	Jacks Pond	76.99	12.8	1.11	0.82	1.93	0.16	0.05	5.63	1.08	0.078	0.03	0.023	728	173	1.56	100.36
JHC-07-025	Jacks Pond	69.69	11.02	2.07	1.17	3.24	1.89	2.36	2.37	2.42	0.279	0.11	0.07	125	375	4.63	98.09
JHC-07-026	Jacks Pond	73.79	12.25	1.12	0.71	1.83	1.18	1.24	3.33	2.26	0.312	0.06	0.072	138	385	3.13	99.44
JHC-07-027	Jacks Pond	62.66	11.15	2.06	0.66	2.72	12.48	0.98	0.05	0.78	0.291	0.09	0.063	128	146	6.78	98.06
JHC-07-028	Jacks Pond	70.29	12.76	1.14	0.53	1.66	5.48	0.31	0.24	2.85	0.333	0.04	0.073	146	459	4.04	98.09
JHC-07-029	Jacks Pond	58.02	14.15	1.21	5.02	6.79	7.16	0.2	0.12	3.04	0.365	0.08	0.081	162	501	7.39	97.39
JHC-07-030	Jacks Pond	66.6	11.66	1.8	0.65	2.45	10.82	0.12	0.06	1.35	0.26	0.12	0.049	180	299	5.33	98.81
JHC-07-031	Jacks Pond	69.33	12.85	1.84	0.87	2.7	4.45	0.11	0.14	3.16	0.325	0.06	0.068	137	788	3.89	97.08
JHC-07-032	Jacks Pond	59.34	12.55	2.67	0.8	3.47	15.06	0.23	0.21	0.34	0.322	0.17	0.068	135	115	6.92	98.68
JHC-07-033	Jacks Pond	45.92	13.83	4.78	6.76	12.29	5.93	8.6	2.8	0.02	2.264	0.22	0.266	170	309	6.76	98.9
JHC-07-034	Jacks Pond	65.7	11.74	2.54	1.03	3.57	8.51	0.71	1.16	1.18	0.29	0.16	0.061	145	737	5	98.09
JHC-07-035	Jacks Pond	63.02	6.01	1.27	0.47	1.74	0.94	0.58	0.12	1.72	0.167	0.03	0.044	69	107241	3.55	77.94
JHC-07-036	Jacks Pond	72.82	10.53	3.02	1.39	4.41	2.61	0.28	0.39	2.55	0.255	0.05	0.058	132	6607	4.12	98.08
JHC-07-037	Jacks Pond	69.96	12.61	0.98	3.54	4.91	3.36	0.25	0.65	2.63	0.301	0.13	0.065	156	7716	3.54	98.38
JHC-07-039	Jacks Pond	73.95	9.91	1.13	4.06	5.64	0.94	0.3	0.23	2.75	0.207	0.05	0.048	130	5935	4.06	98.08
JHC-07-040	Jacks Pond	76.34	10.7	0.49	3.54	4.42	0.53	0.03	0.14	3.19	0.238	0.01	0.048	140	4109	3.54	99.18
JHC-07-041	Jacks Pond	77.77	9.42	0.79	3.85	5.07	0.59	0.03	0.15	2.76	0.202	0.01	0.045	127	3044	3.85	99.9
JHC-07-043	Jacks Pond	82.64	9.3	0.91	0.46	1.37	0.7	0.09	0.13	2.84	0.198	0.02	0.038	129	3050	2.22	99.55
JHC-07-044	Jacks Pond	74.18	11.19	1.1	0.54	1.64	5.13	0.24	1.65	1.66	0.282	0.04	0.066	123	268	3.25	99.31

Appendix 1B: Lithogeochemistry data table for samples analyzed from TVB

SampleNumber	Property	SiO2	Al2O3	Fe2O3	FeO	FeOTotal	MgO	CaO	Na2O	K2O	TiO2	MnO	P2O5	Zr	Ba	LOI	Total
Units		%	%	%	%	%	%	%	%	%	%	%	%	%	%	%	%
Analytical Method		GS Major	GS Major	GS Major	GS Major	GS Major	GS Major	GS Major	GS Major	GS Major	GS Major	GS Major	GS Major	GS Major	GS Major	GS Major	GS Major
JHC-07-045	Jacks Pond	68.01	11.94	2.33	1.08	3.41	6.78	0.33	1.79	1.46	0.293	0.09	0.067	142	327	4.73	98.9
JHC-07-047	Jacks Pond	68.93	11.19	1.99	0.8	2.79	9.61	0.3	1.37	0.76	0.238	0.11	0.055	146	267	4.95	100.3
JHC-07-048	Jacks Pond	45.63	13.25	2.39	8.25	11.55	5.53	9.06	2.93	0.08	2.169	0.2	0.252	157	43	8.25	98.91
JHC-07-049	Jacks Pond	72.87	11.4	1.33	0.58	1.92	5.64	0.21	0.12	2.41	0.243	0.11	0.038	150	820	3.78	98.75
JHC-07-050	Jacks Pond	53.12	12.38	6.07	1.6	7.67	15.52	0.75	0.04	0.1	0.267	0.18	0.037	161	102	8.09	98.17
JHC-07-052	Jacks Pond	38.2	17.08	3.13	9.74	13.95	18.75	0.11	0.01	0	0.492	0.45	0.099	248	13	9.74	98.89
JHC-07-053	Jacks Pond	71.54	11.6	2.69	1.24	3.93	3.39	0.31	0.18	2.81	0.282	0.09	0.067	138	2285	3.9	98.08
JHC-07-054	Jacks Pond	77.63	11.73	0.76	0.49	1.25	0.26	0.25	3.66	1.88	0.325	0	0.093	140	1165	1.56	98.64
JHC-07-060	Jacks Pond	67.01	15.38	0.42	3.18	3.95	3.55	0.2	1.34	3.6	0.376	0.03	0.089	194	538	3.18	98.7
JHC-07-061	Jacks Pond	73.99	12.11	0.24	1.96	2.42	0.88	1.16	5.64	0.67	0.282	0.05	0.083	164	141	1.96	99.24
JHC-07-062	Jacks Pond	79.29	10.46	0.62	1.1	1.84	0.89	0.22	5.36	0.17	0.213	0.03	0.045	127	37	1.1	99.61
JHC-07-063	Jacks Pond	37.42	12.32	8.07	3.43	11.5	3.26	10.04	0.11	4.28	1.723	0.28	0.387	220	1032	14.27	95.58
JHC-07-064	Jacks Pond	75.52	12.64	0.95	0.57	1.51	0.65	0.22	1.4	3.54	0.313	0.01	0.081	142	1385	2.23	98.12
JHC-07-065	Jacks Pond	61.67	17.46	2.27	1.57	3.84	2.53	0.49	1.23	5.78	0.409	0.03	0.086	198	991	4.74	98.27
JHC-07-066	Jacks Pond	47.61	7.24	8.87	14.2	24.65	2.47	0.41	0.52	1.4	0.097	0.17	0.065	43	209	14.2	98.82
JHC-07-070	Cathys Pond	61.75	17.34	1.73	1.17	2.9	2.24	1.66	1.06	5.78	0.412	0.04	0.088	193	779	5.48	98.75
JHC-07-073	Cathys Pond	61.09	18.84	1.88	1.28	3.17	1.66	0.49	0.22	6.73	0.453	0.02	0.14	203	2056	4.14	96.94
JHC-07-075	Cathys Pond	61.41	17.09	2.54	1.52	4.06	3.66	0.83	2.38	3.4	0.412	0.04	0.087	185	1247	4.85	98.22
JHC-07-076	Jacks Pond	76.31	11.26	0.83	0.51	1.34	2.55	0.28	3.35	1.71	0.282	0.02	0.074	127	248	2.24	99.41
JHC-07-077	Jacks Pond	70.53	12.9	1.41	0.94	2.35	2.24	0.16	3.23	2.93	0.329	0.03	0.074	139	394	3.73	98.5
JHC-07-078	Daniels Pond	53.74	16.31	3.07	6.68	10.49	2.62	5.03	0.05	3.94	0.443	0.13	0.065	31	155	6.68	99.5
JHC-07-079	Daniels Pond	54.74	16.56	1.41	6.7	8.85	3.37	2.68	2.7	2.8	0.518	0.05	0.014	46	201	6.7	98.97
JHC-07-080	Daniels Pond	49.28	13.58	5.6	7.81	14.29	5.32	4.84	2.26	0.04	0.578	0.2	0.043	19	11	7.81	98.23
JHC-07-081	Daniels Pond	50.4	13.08	5.2	7.47	13.5	4.48	6.12	2.85	0.02	0.559	0.21	0.044	4	30	7.47	98.75
JHC-07-082	Daniels Pond	44.48	14.76	8.68	3.14	11.82	3.23	7.55	1.77	0.99	0.591	0.19	0.046	0	202	13.27	98.69
JHC-07-083	Daniels Pond	41.04	25.15	3.92	2.42	6.34	0.98	0.41	1.08	6.2	0.686	0.01	0.079	55	3408	9.29	91.25
JHC-07-084	Daniels Pond	61.2	24.84	0.31	0.21	0.52	0.65	0.13	1.67	5.05	0.731	0	0.08	57	892	3.82	98.69
JHC-07-085	Daniels Pond	72.46	14.7	0.83	0.42	1.24	2.94	0.21	0.58	3.11	0.44	0.02	0.109	38	661	3.16	98.98
JHC-07-086	Daniels Pond	46.34	16.71	4.35	2.18	6.53	4.32	6.03	2.49	2.67	0.459	0.12	0.204	45	6561	11.07	96.95
JHC-07-087	Daniels Pond	60.78	14.67	3.09	1.92	5.01	2.53	4.31	5.85	0.27	0.431	0.09	0.232	34	67	5.89	100.08
JHC-07-088	Daniels Pond	66.33	16.21	1.84	1.37	3.21	1.12	1.74	6.11	1.3	0.481	0.03	0.271	39	293	2.92	99.73
JHC-07-091	Daniels Pond	53.14	14.89	7.34	7.16	15.3	3.25	0.59	4.17	0.78	0.407	0.04	0.058	31	2255	7.16	99.79
JHC-07-093	Daniels Pond	59.08	26.88	0.16	0.11	0.26	0.78	0.23	1.97	5.21	0.744	0	0.108	57	1517	4.04	99.3
JHC-07-094	Daniels Pond	55.92	15.59	1.66	6.03	8.36	9.7	0.44	0.26	1.38	0.461	0.11	0.099	38	354	6.03	98.36
JHC-07-095	Daniels Pond	37.99	19.88	5.94	1.72	7.67	16.84	1.17	0.19	1.44	0.602	0.17	0.058	44	361	9.36	95.37
JHC-07-096	Daniels Pond	62.92	12.64	1.23	6.31	8.24	3.02	0.08	0.45	2.44	0.368	0.03	0.051	33	648	6.31	96.55
JHC-07-097	Daniels Pond	67.45	21.21	0.26	0.16	0.42	0.35	0.05	1.03	4.72	0.621	0	0.025	48	885	3.24	99.12
JHC-07-098	Daniels Pond	24.28	17.77	5.37	13.99	20.91	18.85	0.32	0.01	0	0.492	0.24	0.075	41	3	13.99	96.92
JHC-07-099	Daniels Pond	28.22	17.39	3.81	15.35	20.87	5.78	1.81	0.47	3.43	0.518	0.2	0.043	45	1790	15.35	94.08
JHC-07-100	Daniels Pond	70.77	18.47	0.08	0.05	0.13	0.58	0.1	0.68	4.65	0.542	0.01	0.016	40	1675	2.95	98.9
JHC-07-101	Daniels Pond	52.93	30.41	0.12	0.09	0.21	0.78	0.11	1.39	7.29	0.943	0	0.066	69	2270	4.27	98.39
JHC-07-102	Daniels Pond	49.45	16.54	6.28	6.77	13.8	7.4	1.19	1.64	0.93	0.461	0.05	0.059	36	714	6.77	98.3
JHC-07-103	Daniels Pond	59.51	16.4	1.02	6.16	7.86	0.8	0.95	4.37	2.44	0.52	0.02	0.096	43	4416	6.16	99.14
JHC-07-104	Daniels Pond	49.32	18.24	0.64	8.14	9.68	4.8	3.43	2.76	1.38	0.515	0.07	0.094	24	2214	8.14	98.42

Appendix 1B: Lithogeochemistry data table for samples analyzed from TVB

SampleNumber	Property	SiO2	Al2O3	Fe2O3	FeO	FeOTotal	MgO	CaO	Na2O	K2O	TiO2	MnO	P2O5	Zr	Ba	LOI	Total
Units		%	%	%	%	%	%	%	%	%	%	%	%	%	%	%	%
Analytical Method		GS Major	GS Major	GS Major	GS Major	GS Major	GS Major	GS Major	GS Major	GS Major	GS Major	GS Major	GS Major	GS Major	GS Major	GS Major	GS Major
JHC-07-106	Daniels Pond	47.06	13.16	8	3.34	11.34	3.84	7.1	3.35	0.33	0.599	0.2	0.114	19	315	11.62	98.73
JHC-07-107	Daniels Pond	60.49	12.75	3.83	1.86	5.69	1.87	3.93	0.09	4	0.268	0.09	0.064	56	169	6.47	95.71
JHC-07-108	Daniels Pond	64.93	13.48	1.13	0.59	1.71	1.68	3.95	0.18	4.22	0.419	0.05	0.089	43	159	5.59	96.31
JHC-07-109	Daniels Pond	53.39	16.76	4.84	5.59	11.06	7.87	0.42	0.19	2.13	0.49	0.02	0.096	45	65	5.59	98.02
JHC-07-110	Daniels Pond	55.99	16.44	3.1	1.65	4.75	1.57	4.01	0.6	4.49	0.488	0.04	0.069	38	297	6.32	94.76
JHC-07-111	Daniels Pond	46.3	36.46	0.16	0.14	0.3	0.74	0.14	2.7	7	1.164	0	0.082	92	1064	5.19	100.07
JHC-07-112	Daniels Pond	40.06	14.65	0.38	11.85	13.55	9.16	1.62	0.41	1.89	0.431	0.49	0.063	32	370	11.85	94.17
JHC-07-113	Daniels Pond	59.25	14.72	1.48	6.73	8.96	5.01	0.09	0.67	2.19	0.43	0.15	0.077	34	436	6.73	98.28
JHC-07-114	Daniels Pond	68.28	13.77	2.24	1.19	3.43	3.47	0.4	2.57	1.83	0.402	0.09	0.093	30	374	4.64	98.98
JHC-07-115	Daniels Pond	58.02	24.57	0.76	0.5	1.26	1.63	0.5	1.47	5.33	0.722	0.04	0.205	52	2161	5.01	98.78
JHC-07-116	Daniels Pond	61.38	15.44	3.43	4.59	8.53	3.91	0.39	3.62	1.14	0.497	0.03	0.137	39	2198	4.59	99.67
JHC-07-119	Daniels Pond	53.05	16.31	5.05	2.48	7.52	4.31	3.53	3.44	1.17	0.476	0.05	0.118	40	1402	9.01	98.99
JHC-07-120	Daniels Pond	49.84	10.87	6.45	2.9	9.36	4.03	6.01	2.1	1.99	0.321	0.17	0.056	21	467	13.64	98.38
JHC-07-121	Daniels Pond	61.41	12.51	3.39	1.66	5.04	1.8	4.11	1.1	2.98	0.271	0.15	0.06	50	329	5.74	95.17
JHC-07-122	Daniels Pond	63.22	14.01	0.5	4.7	5.72	1.48	3.7	2.62	2.37	0.304	0.11	0.066	57	256	4.7	98.29
JHC-07-123	Daniels Pond	60.21	13.28	4.11	2.06	6.18	1.27	3.79	1.02	3.33	0.289	0.11	0.067	58	392	5.66	95.19
JHC-07-124	Daniels Pond	63.14	14.6	0.85	5.15	6.57	2.99	1.5	0.49	3.23	0.32	0.03	0.065	54	443	5.15	98.08
JHC-07-125	Daniels Pond	53.72	17.26	5.92	5.14	11.62	5.21	1.26	4.98	0.35	0.55	0.06	0.051	50	140	5.14	100.21
JHC-07-126	Daniels Pond	45.67	13.94	5.79	2.63	8.42	3.42	7.37	2.95	1.46	0.38	0.18	0.056	20	169	14.61	98.46
JHC-07-127	Daniels Pond	51.3	15.25	2.85	7.27	10.92	7.68	2.48	4.6	0.01	0.383	0.18	0.037	23	15	7.27	100.11
JHC-07-128	Daniels Pond	55.09	14.92	4.2	6.51	11.43	4.6	1.18	3.67	1.25	0.428	0.06	0.066	38	356	6.51	99.2
JHC-07-129	Daniels Pond	71.87	12.02	2.12	0.93	3.06	1.19	2.26	1.61	0.98	0.268	0.04	0.063	113	938	4.64	98
JHC-07-133	Daniels Pond	54.95	15.62	0.83	8.92	10.75	2.53	1.95	1.6	1.88	0.484	0.04	0.127	41	3645	8.92	98.85
JHC-07-134	Daniels Pond	49.29	12.53	5.58	2.67	8.25	4.37	5.29	2.56	2.05	0.357	0.17	0.059	29	452	13.64	98.57
JHC-07-135	Daniels Pond	69.29	13.46	0.81	3.76	4.98	2.61	1.01	1.53	2.45	0.224	0.05	0.052	58	276	3.76	99.41
JHC-07-136	Daniels Pond	57.3	16.69	6.56	3.86	10.85	3.48	1.16	5.65	0.28	0.495	0.06	0.045	51	133	3.86	99.87
JHC-07-137	Daniels Pond	48.99	14.46	1.86	10.56	13.59	1.33	2.98	0.65	3.8	0.393	0.15	0.066	28	358	10.56	96.98
JHC-07-138	Daniels Pond	46.93	15.76	7.57	3.41	10.98	5.37	1.6	3.14	1.14	0.478	0.09	0.026	40	176	13.08	98.61
JHC-07-139	Daniels Pond	52.24	15.91	2.31	7.36	10.48	5.15	3.1	3.51	1.17	0.413	0.09	0.046	37	140	7.36	99.48
JHC-07-140	Daniels Pond	51.35	14.94	1.27	7.31	9.39	3.85	5.64	3.96	1.16	0.377	0.17	0.055	25	130	7.31	98.19
JHC-07-141	Daniels Pond	46.64	13.72	7.52	2.84	10.36	4.52	7.08	1.02	1.93	0.384	0.2	0.056	25	124	12.09	98.01
JHC-07-142	Daniels Pond	47.67	18.44	5.38	2.76	8.14	6.47	3.87	4.19	1.11	0.502	0.09	0.215	29	283	7.47	98.18
JHC-07-143	Daniels Pond	70.07	16.33	1.74	0.86	2.6	0.63	1.27	2.23	1.44	0.392	0.02	0.077	163	1442	4.42	99.48
JHC-07-147	Daniels Pond	56.03	14.39	6.8	2.8	9.61	3.45	2.63	1.68	1.37	0.445	0.07	0.104	34	2206	9.63	99.42
JHC-07-150	Daniels Pond	73.44	10.22	1.7	4.79	7.02	0.82	0.04	0.88	1.29	0.223	0.01	0.042	104	648	4.79	98.78
JHC-07-151	Bobbys Pond Native Sulphur	69.98	12.19	0.2	0.09	0.29	0.08	0	1.53	0.99	0.251	0	0.086	54	281	13.67	99.07
JHC-07-152	Bobbys Pond Native Sulphur	70.45	16.07	4.1	1.25	5.35	0.1	0.02	0.06	0	0.351	0	0.107	68	313	6.12	98.63
JHC-07-153	Bobbys Pond Native Sulphur	72.73	10.53	2.82	1.38	4.2	2.43	0.76	2.99	0.43	0.247	0.11	0.087	59	246	4.99	99.5
JHC-07-156	Bobbys Pond Native Sulphur	70.75	14.82	3.55	1.67	5.21	0.14	0.04	1.94	1.27	0.333	0	0.103	65	336	5.07	99.67
JHC-07-158	Sutherlands Pond	70.97	14.25	0.92	2.5	3.7	0.61	0.85	2.14	3.83	0.301	0.08	0.117	105	840	2.5	99.34

Appendix 1B: Lithogeochemistry data table for samples analyzed from TVB

SampleNumber	Property	SiO2	Al2O3	Fe2O3	FeO	FeOTotal	MgO	CaO	Na2O	K2O	TiO2	MnO	P2O5	Zr	Ba	LOI	Total
Units		%	%	%	%	%	%	%	%	%	%	%	%	%	%	%	%
Analytical Method		GS Major	GS Major	GS Major	GS Major	GS Major	GS Major	GS Major	GS Major	GS Major	GS Major	GS Major	GS Major	GS Major	GS Major	GS Major	GS Major
JHC-07-160	Sutherlands Pond	53.36	14.58	3.44	6.95	11.16	5.72	4.5	1.89	1.37	0.524	0.17	0.088	33	262	6.95	100.31
JHC-07-162	Sutherlands Pond	53.37	13.42	5.66	2.58	8.24	2.85	7.96	2.29	1.7	0.478	0.26	0.196	40	796	8.89	99.66
JHC-07-163	Sutherlands Pond	71.74	12.26	2.48	2.62	5.39	1.79	0.49	1.88	2.31	0.304	0.14	0.104	50	1537	2.62	99.03
JHC-07-165	Sutherlands Pond	77.97	9.73	1.69	2.08	4	1.84	0.18	1.17	1.92	0.233	0.05	0.089	46	1272	2.08	99.27
JHC-07-166	Sutherlands Pond	75.49	11.38	1.21	2.44	3.92	2.41	0.44	2.28	1.79	0.272	0.14	0.099	53	1046	2.44	100.65
JHC-07-167	Sutherlands Pond	39.62	18.22	0.08	8.22	9.22	7.82	2.69	3.33	1.97	0.511	0.94	0.12	75	718	8.22	92.66
JHC-07-168	Sutherlands Pond	67.89	13.81	3.72	2.85	6.89	3.19	0.42	3.71	1.21	0.404	0.2	0.094	46	429	2.85	100.69
JHC-07-170	Victoria Mine	54.52	15.25	1.06	7.16	9.01	3.38	5.71	3.24	1.05	0.621	0.14	0.225	85	244	7.16	100.3
JHC-07-171	Victoria Mine	74.84	13.63	0.81	0.5	1.31	0.4	1.45	2.99	2.15	0.364	0.02	0.077	311	258	3.19	100.43
JHC-07-172	Victoria Mine	58.2	13.5	3.15	6.15	9.98	3.2	4.44	2.26	1.2	0.504	0.22	0.106	33	357	6.15	99.76
JHC-07-173	Victoria Mine	49.34	15.55	0.29	8.2	9.41	3.46	7.76	5.56	0.3	0.44	0.15	0.102	22	54	8.2	100.27
JHC-07-174	Victoria Mine	55.11	20.88	1.91	4.12	6.49	2.42	2.57	5.11	2.77	1.212	0.05	0.05	32	178	4.12	100.77
JHC-07-175	Victoria Mine	52.53	17.72	3.52	8.39	12.85	1.8	0.08	3.51	2.98	0.737	0.02	0.017	39	173	8.39	100.62
JHC-07-176	Victoria Mine	35.1	14.41	0.33	11.57	13.19	22.05	1.67	0.08	0	0.619	0.1	0.139	43	0	11.57	98.92
JHC-07-180	Victoria Mine	22.14	15.85	10.81	15.35	27.86	16.05	0.22	0.02	0	0.618	0.21	0.086	44	15	15.35	98.41
JHC-07-181	Victoria Mine	60.7	14.73	0.5	5.86	7.01	3.88	2.31	2.28	0.78	1.149	0.19	0.366	227	149	5.86	99.24
JHC-07-182	Victoria Mine	55.84	13.75	6.22	2.69	8.91	5.85	0.43	3.06	0.38	0.267	0.51	0.034	11	76	10.11	99.14
JHC-07-184	Victoria Mine	47.6	18.72	3.15	7.34	11.3	9.18	0.41	3.96	0.76	0.362	0.24	0.051	24	135	7.34	99.93
JHC-07-187	Victoria Mine	56.88	14.97	4.95	2.37	7.31	2.72	5.96	2.36	1.81	0.631	0.1	0.233	114	244	7.29	100.25
JHC-07-188	Victoria Mine	72.14	14.58	0.04	2.07	2.34	0.39	1.49	6.72	0.76	0.363	0.07	0.072	293	159	2.08	101.01
JHC-07-190	Victoria Mine	64.55	13.73	6.48	3.47	10.34	3.79	0.49	2.25	1.07	0.514	0.12	0.14	35	335	3.47	100.45
JHC-07-191	Victoria Mine	60.61	15.2	1.64	4.8	6.97	2.17	4.12	5.93	0.51	0.371	0.1	0.112	9	109	4.8	100.89
JHC-07-193	Victoria Mine	38.33	13.6	6.19	2.55	8.74	3.62	16.08	3.4	0.71	0.778	0.18	0.047	30	85	15.26	100.75
JHC-07-194	Victoria Mine	35.13	12.35	6.64	2.56	9.21	4.58	16.27	2.97	0.81	0.71	0.23	0.051	18	126	18.05	100.36
JHC-07-195	Victoria Mine	69.43	8.83	5.01	1.97	6.98	3.15	1.4	1.35	0.55	0.207	0.19	0.057	15	84	6.55	98.68
JHC-07-196	Victoria Mine	60.7	15.95	0.89	4.94	6.38	4.18	1.83	3.08	2.93	0.527	0.09	0.253	96	718	4.94	100.87
JHC-07-198	Victoria Mine	69.68	11.77	4.04	1.72	5.76	1.64	3.82	1.33	1.15	0.301	0.09	0.129	36	199	5.28	100.96
JHC-07-207	Jig Zone	68.44	11.98	1.07	5.12	6.76	3.16	0.63	2.99	0.74	0.36	0.09	0.073	33	102	5.12	100.34
JHC-07-208	Jig Zone	67.28	13.99	0.18	5.24	6.01	3.63	0.62	2.31	1.11	0.413	0.07	0.085	58	208	5.24	100.77
JHC-07-211	Jig Zone	50.16	16.62	8.46	5.63	14.72	5.86	1.67	3.36	0.69	1.003	0.08	0.094	24	72	5.63	99.9
JHC-07-213	Jig Zone	66.86	13.48	2.17	3.69	6.28	2.08	1.46	3.84	1.28	0.341	0.05	0.069	28	193	3.69	99.44
JHC-07-215	Victoria Mine	59.37	13.93	5.74	4.53	10.77	3.13	2.14	4.9	0.12	0.539	0.17	0.119	29	57	4.53	99.7
JHC-07-216	Victoria Mine	25.22	12.17	16.33	15.15	33.16	10.42	0.6	0.1	0	0.439	0.16	0.115	40	2	15.15	97.51
JHC-07-217	Victoria Mine	43.46	17.81	8.85	4.76	14.14	7.42	5.39	3.7	0.14	2.218	0.21	0.314	138	91	4.76	99.57
JHC-07-219	Hungry Hill	64.93	14.14	1.33	5.26	7.18	2.64	1.09	0.42	3.22	0.256	0.21	0.055	22	270	5.26	99.39
JHC-07-220	Hungry Hill	51.48	17.19	6.51	5.7	12.85	7.99	1.15	3.11	0.77	0.547	0.13	0.048	18	99	5.7	100.98
JHC-07-221	Hungry Hill	68.94	12.14	2.65	4.61	7.77	2.45	0.2	1.44	1.96	0.226	0.06	0.051	23	207	4.61	99.86
JHC-07-222	Hungry Hill	67.76	13.02	2.71	4.14	7.31	4.77	0.13	1.78	0.89	0.239	0.2	0.055	21	61	4.14	100.3
JHC-07-226	Hungry Hill	76.23	10.1	3.19	1.48	4.67	0.52	0.06	0.49	2.26	0.184	0.01	0.042	17	426	4.23	98.8
JHC-07-229	Hungry Hill	68.38	12.8	2.78	3.43	6.59	3.09	1.29	3.71	0.58	0.262	0.15	0.065	32	74	3.43	100.36
JHC-07-230	Hungry Hill	66.07	14.19	1.98	3.81	6.22	1.71	1.42	3.6	2.41	0.268	0.05	0.056	17	236	3.81	99.79
JHC-07-231	Hungry Hill	61.58	14.1	5.46	4.58	10.55	4.57	0.37	2.48	1.43	0.464	0.09	0.043	29	125	4.58	100.25
JHC-07-233	Hungry Hill	66.61	13.85	3.57	3.77	7.76	3.16	0.33	3.28	0.82	0.262	0.19	0.044	19	98	3.8	100.11
JHC-07-236	Hungry Hill	72.03	12.67	1.57	2.8	4.68	2.64	0.89	3.3	0.91	0.137	0.06	0.059	30	83	2.8	100.18

Appendix 1B: Lithogeochemistry data table for samples analyzed from TVB

SampleNumber	Property	SiO2	Al2O3	Fe2O3	FeO	FeOTotal	MgO	CaO	Na2O	K2O	TiO2	MnO	P2O5	Zr	Ba	LOI	Total
Units		%	%	%	%	%	%	%	%	%	%	%	%	%	%	%	%
Analytical Method		GS Major	GS Major	GS Major	GS Major	GS Major	GS Major	GS Major	GS Major	GS Major	GS Major	GS Major	GS Major	GS Major	GS Major	GS Major	GS Major
JHC-07-242	Hungry Hill	67.41	14.68	2.45	3.65	6.51	3.85	0.43	2.26	1.24	0.272	0.2	0.056	23	118	3.65	100.55
JHC-07-245	Hungry Hill	55.63	14.73	7.24	3.58	11.22	6.2	2.82	5.98	0.07	0.455	0.15	0.051	13	37	3.58	100.91
JHC-07-246	Hungry Hill	71.67	13.09	2.42	1.4	3.82	0.95	2.02	2.13	2.76	0.136	0.04	0.059	28	218	3.5	100.16
JHC-07-248	Hungry Hill	69.83	13.29	2.33	2.75	5.38	1.96	0.66	3.19	2.12	0.228	0.06	0.059	23	157	2.75	99.52
JHC-07-252	Bobby's Pond VMS	81.38	10.25	0.29	0.2	0.49	0.21	0.31	5.75	0.04	0.158	0	0.033	122	39	1.04	99.69
JHC-07-254	Bobby's Pond VMS	77.31	10.42	1.03	0.53	1.56	1.84	0.11	2.25	1.27	0.191	0.04	0.03	131	572	3.85	98.87
JHC-07-255	Bobby's Pond VMS	84.51	8.42	0.31	0.15	0.45	0.33	0.11	2.39	0.31	0.094	0	0.021	100	133	1.62	98.27
JHC-07-256	Bobby's Pond VMS	73.29	10.73	1.41	0.69	2.1	3.78	0.95	2.9	0.44	0.194	0.05	0.04	145	311	6.53	101
JHC-07-259	Bobby's Pond VMS	82.92	8.22	0.86	0.43	1.29	1.44	0.56	2.89	0.21	0.089	0.02	0.039	95	165	3.11	100.79
JHC-07-260	Bobby's Pond VMS	76.13	10.56	1.4	0.77	2.17	1.58	0.72	3.24	0.98	0.225	0.09	0.04	103	594	3.71	99.46
JHC-07-261	Bobby's Pond VMS	85.87	7.98	0.11	0.06	0.17	0.33	0.36	2.51	0.32	0.147	0	0.021	117	193	1.59	99.32
JHC-07-262	Bobby's Pond VMS	52.85	14.99	5.23	2.22	7.45	7.67	0.05	1.94	1.5	0.251	0.11	0.026	201	965	13.19	100.04
JHC-07-264	Bobby's Pond VMS	82.51	8.26	0.51	0.26	0.77	1.08	0.36	2.75	0.46	0.124	0.02	0.026	101	201	2.52	98.88
JHC-07-265	Bobby's Pond VMS	83.46	8.09	0.59	0.3	0.89	0.68	0.17	1.86	1.17	0.096	0.01	0.024	100	651	2.14	98.58
JHC-07-266	Bobby's Pond VMS	82.24	7.55	1.66	0.77	2.43	1.44	0.13	1.88	0.54	0.156	0.07	0.023	97	240	3.03	99.47
JHC-07-267	Bobby's Pond VMS	72.58	7.67	2.57	6.18	9.44	0.26	0.04	0.48	1.54	0.2	0.01	0.058	83	822	6.18	98.45
JHC-07-268	Bobby's Pond VMS	50.74	25.1	4.17	2.48	6.65	2.29	0.04	2.02	4.34	0.855	0.07	0.022	37	6812	8.51	100.62
JHC-07-271	Bobby's Pond VMS	89.92	5.03	0.53	0.23	0.76	0.59	0.04	0.31	0.97	0.115	0.01	0.048	57	1634	1.73	99.51
JHC-07-272	Bobby's Pond VMS	74.92	9.57	1.62	0.84	2.47	3.82	0.4	3.49	0.31	0.183	0.1	0.026	136	373	5.51	100.79
JHC-07-273	Bobby's Pond VMS	82.07	9.77	0.5	0.27	0.78	1.22	0.4	2.96	0.8	0.111	0.06	0.016	116	482	2.79	100.97
JHC-07-275	Bobby's Pond VMS	72.88	11.95	0.07	4.6	5.18	0.38	0.08	1.41	1.9	0.286	0	0.074	114	1550	4.6	98.74
JHC-07-276	Bobby's Pond VMS	66.42	9.47	2.79	1.16	3.95	6.49	0.06	0.72	1.74	0.189	0.14	0.043	134	978	9.8	99.02
JHC-07-277	Bobby's Pond VMS	66.28	17.58	0.24	1.86	2.31	0.19	0.18	10.27	0.04	0.315	0.01	0.046	227	40	1.89	99.09
JHC-07-278	Bobby's Pond VMS	82.7	8.43	0.74	0.33	1.07	1.45	0.08	1.23	0.72	0.18	0.06	0.068	98	381	3.25	99.24
JHC-07-279	Bobby's Pond VMS	72.55	10.54	0.8	0.5	1.3	2.62	1.86	5.24	0.23	0.19	0.11	0.048	107	163	5.28	99.98
JHC-07-280	Bobby's Pond VMS	74.79	12.35	0.92	0.42	1.34	2.08	0.04	1.61	1.03	0.144	0.09	0.018	145	695	4.81	98.28
JHC-07-281	Bobby's Pond VMS	64.45	7.66	3.17	8.66	12.79	0.36	0.24	0.59	1.39	0.194	0.01	0.226	77	839	8.66	96.57
JHC-07-282	Bobby's Pond VMS	73.9	11.81	1.18	0.64	1.81	1.67	0.25	3.22	0.97	0.229	0.07	0.027	155	425	3.76	97.72
JHC-07-283	Bobby's Pond VMS	73.9	11.81	1.18	0.64	1.81	1.67	0.25	3.22	0.97	0.229	0.07	0.027	155	425	4.04	98.01
JHC-07-284	Bobby's Pond VMS	85.7	8.69	0.23	0.13	0.35	0.37	0.28	3.4	0.48	0.158	0.01	0.028	110	213	1.33	100.8
JHC-07-285	Bobby's Pond VMS	78.6	9.25	1.42	0.78	2.2	1.94	0.76	3.71	0.37	0.134	0.06	0.026	110	297	3.9	100.96
JHC-07-286	Bobby's Pond VMS	64.51	17.07	1.92	0.98	2.89	3.09	0.2	1.56	2.67	0.301	0.03	0.034	231	1750	6.76	99.11
JHC-07-287	Bobby's Pond VMS	81.3	8.52	0.34	0.2	0.54	1.16	1.25	4.56	0.13	0.095	0.01	0.023	91	79	2.6	100.19
JHC-07-289	Bobby's Pond VMS	78.63	9.17	1.73	0.76	2.49	1.95	0.12	0.96	1.2	0.167	0.08	0.055	102	559	4.43	99.24
JHC-07-290	Bobby's Pond VMS	64.79	5.6	4.73	9.93	15.75	0.97	0.5	0.31	1.25	0.217	0.05	0.016	18	765	9.93	99.39
JHC-07-291	Bobby's Pond VMS	80.5	10.54	0.67	0.39	1.06	1.2	0.28	4.13	0.29	0.204	0.05	0.037	134	259	2.45	100.75
JHC-07-292	Bobby's Pond VMS	52.75	9.86	7.02	2.98	10	8.43	0.64	3.23	0.22	0.787	0.26	0.286	52	167	14.44	100.9
JHC-07-293	Bobby's Pond VMS	78.54	6.38	1.26	0.55	1.81	4	1.28	1.93	0.21	0.109	0.09	0.029	76	103	5.99	100.38

Appendix 1B: Lithogeochemistry data table for samples analyzed from TVB

SampleNumber	Li	Cd	V	Cr	Co	Ni	Cu	Zn	Ga	Ge	As	Te	Se	Rb	Sr	Y	Nb	Mo	Ag	In	Sn	Sb	Cs
Units	ppm	ppm	ppm	ppm	ppm	ppm	ppm	ppm	ppm	ppm	ppm	ppm	ppm	ppm	ppm	ppm	ppm	ppm	ppm	ppm	ppm	ppm	ppm
Analytical Method	GS Trace	AL Trace	AL Trace	AL Trace	AL Trace	AL Trace	AL Trace	GS Trace	AL Trace	AL 4b2std	AL Trace	AL Trace	AL Trace	AL Trace	AL Trace	AL 4b2std	AL Trace	AL Trace	AL GS BPD	AL 4b2std	AL 4b2std	AL Trace	AL Trace
JHC-06-001	13	<d.L.	369	120	34.5	51.9	137	90.8	16.1	2	0.3	0.6	<d.L.	<d.L.	158	16	0.4	<d.L.	<d.L.	-99	<d.L.	1.8	-99
JHC-06-002	38.2	<d.L.	442	39	52.8	24.4	90	114.8	16.4	-99	56.2	0.2	0.8	0.6	61.7	-99	<d.L.	<d.L.	<d.L.	-99	-99	-99	-99
JHC-06-003	7.2	<d.L.	18	1	4.1	1.2	7.4	62.9	12.4	-99	184	0.2	<d.L.	34.4	69.4	33	1.5	3.4	0.1	-99	1	1.9	1.04
JHC-06-005	18.2	37.6	8	1.9	3	0.8	1040	5758	17.9	-99	31.8	1.1	4.6	5.8	7.7	14	0.5	3.7	2.2	0.5	4	0.4	0.11
JHC-06-006	6.8	9.3	13	1.2	3.5	0.6	312	2524.9	14	-99	5930	2.9	6.5	31.4	32.2	-99	1.4	2.8	1.9	-99	-99	42.6	0.44
JHC-06-008	7.4	<d.L.	2	3.2	1.2	<d.L.	9.3	56.1	14.3	-99	18	0.5	2.8	23.1	21.7	29	1.3	3.6	<d.L.	-99	2	0.1	0.26
JHC-06-009	2.5	<d.L.	2	2.8	1.3	1.4	12.9	14.1	8.7	-99	60.6	<d.L.	3.6	11.6	36.1	-99	1.4	7.7	0.2	-99	-99	1.2	0.18
JHC-06-010	3.2	0.5	7	1.4	2.1	<d.L.	43.6	234.9	7	-99	10000	4.5	6.2	25.3	8.1	-99	<d.L.	59.6	5.3	-99	-99	500	0.35
JHC-06-011	27.8	0.3	23	4	6.2	<d.L.	51.3	216.8	26.2	-99	66.3	0.4	0.9	14.4	58.1	-99	3.1	2	0.2	-99	-99	3.3	0.49
JHC-06-012	6.6	3.1	22	0.8	3.3	<d.L.	78.2	901.6	16	-99	2420	2.3	<d.L.	45	31.5	29	2.1	8.2	0.2	-99	9	15.9	0.57
JHC-06-013	<d.L.	78	<d.L.	1.6	1.5	<d.L.	3320	9377.4	5.9	-99	820	49.6	6	0.8	1.8	-99	<d.L.	52.6	9.8	-99	-99	9.5	0.3
JHC-06-014	2.4	45.3	20	1.8	0.9	8.4	2720	6248.8	10	-99	1730	34.1	12.3	0.9	54.1	-99	<d.L.	7.4	14.3	-99	-99	18.5	0.06
JHC-06-015	10.1	<d.L.	1	1.9	0.8	<d.L.	34.4	111	15.4	-99	2.4	0.8	<d.L.	26.8	76.4	41	1.5	1.4	<d.L.	-99	2	0.8	0.28
JHC-06-017	3.7	0.4	15	1.5	3.7	0.6	20.7	67.9	13.3	-99	73.1	3.7	16.3	27.1	22.8	-99	0.1	43.2	0.6	-99	-99	0.4	0.23
JHC-06-018	43.6	<d.L.	3	2.8	3.7	<d.L.	65.6	207.7	31.8	-99	90.1	1.4	2.7	5	9.5	31	1.1	16.1	0.4	-99	<d.L.	0.4	0.09
JHC-06-019	12.3	<d.L.	317	119	32.8	52	75.8	85.5	15.6	2	2.9	0.3	1.6	<d.L.	122	15	0.2	0.2	<d.L.	-99	<d.L.	1.4	0.06
JHC-06-020	12.6	<d.L.	335	120	34.7	53.4	57.3	86.1	16.1	-99	2.7	0.4	1.7	<d.L.	113	-99	0.3	0.1	<d.L.	-99	-99	1.7	-99
JHC-06-021	39.2	<d.L.	423	35.6	39.3	21.3	117	97.7	15.2	3	10.9	0.5	0.7	4.2	161	5	<d.L.	<d.L.	<d.L.	-99	<d.L.	0.8	0.12
JHC-06-022	3.1	0.5	25	1.7	1.6	3.7	5.3	74.3	6.4	1	100	<d.L.	1.3	10.5	29.3	55	0.9	10.6	0.2	0.3	13	1.3	0.19
JHC-06-023	50.8	5.7	25	1.7	6.5	1.1	18.7	1550.9	29.1	1	15.1	8.4	3.8	44	24.1	67	2.5	4.1	3.2	0.2	14	2.2	0.7
JHC-06-024	6	18.6	15	1.7	1.5	0.7	267	2314.6	11.3	-99	2010	18	6.6	<d.L.	3.3	-99	<d.L.	20.7	2.5	-99	-99	3	-99
JHC-06-025	0.9	257	5	1.5	0.1	2.2	1860	12752.5	15	-99	347	496	77.7	<d.L.	31.3	-99	<d.L.	40.6	8.7	-99	-99	2.2	0.08
JHC-06-026	0.2	1	2	1.8	0.5	1.1	10000	140.1	2.5	-99	988	70.9	31.7	<d.L.	1.6	-99	<d.L.	11.9	15.2	-99	-99	0.6	-99
JHC-06-027	3.9	13.5	8	2.8	46.3	2.2	335	1471.4	5.7	-99	1230	37	13.9	0.3	11.3	-99	<d.L.	36.3	2.2	-99	-99	3.3	-99
JHC-06-028	27.4	<d.L.	18	2	7	0.7	7.6	204.1	36	-99	50.3	1.9	8.8	13.2	10.7	35	0.3	59.6	0.5	-99	<d.L.	0.3	0.45
JHC-06-030	1.5	0.4	12	2.7	41.2	1.1	49.4	42.9	9.1	-99	123	14.2	21.2	15.1	12.5	-99	0.2	48	1.3	-99	-99	0.6	0.23
JHC-06-031	8.9	0.2	2	1.5	0.4	<d.L.	19.9	42.5	12.4	-99	20	0.3	0.8	59.9	12.4	-99	3.5	3.6	0.4	-99	-99	2.2	0.75
JHC-06-032	2.5	7.1	2	1.3	<d.L.	<d.L.	367	1113	12.7	-99	83.2	0.2	4	48.3	10.4	-99	2.9	59.1	3.4	-99	-99	8.6	0.34
JHC-06-033	6.6	<d.L.	<d.L.	1.2	<d.L.	<d.L.	19.8	94.4	12.8	-99	15.8	0.1	2.9	50.3	10.4	57	4.1	1.7	<d.L.	-99	1	0.6	0.52
JHC-06-034	27.2	0.1	315	96	46.2	81.6	49.9	402	23.5	2	9.6	0.2	4.6	4.9	48.1	19	0.7	0.1	0.1	-99	<d.L.	0.2	0.09
JHC-06-035	3.4	<d.L.	3	2.7	0.2	0.9	6.4	36.4	12.4	-99	2.1	0.1	0.8	11.7	31.9	-99	3.5	2.7	<d.L.	-99	-99	0.1	0.17
JHC-06-036	15.9	0.2	300	92.2	36.5	63.9	62.5	107.2	15.2	2	5.5	0.3	<d.L.	53.1	139	10	0.1	<d.L.	<d.L.	-99	<d.L.	0.2	1.99
JHC-06-037	3.4	<d.L.	<d.L.	1.4	1.2	1	2.9	39.2	13.2	-99	3.9	0.2	1.2	7.5	39.8	32	1.7	0.5	<d.L.	-99	<d.L.	0.2	0.19
JHC-06-038	3.5	0.6	15	1.8	0.7	1.1	35.8	405.4	24.2	-99	41.1	<d.L.	0.7	44.3	19.4	-99	2.4	23.8	10.8	-99	-99	10.3	0.87
JHC-06-039	16.2	1	<d.L.	3.4	0.3	2.2	8.7	407.8	21.6	-99	1.3	0.2	2.4	35.3	13.7	65	4.8	4.9	0.2	-99	2	0.3	0.59
JHC-06-040	3.8	<d.L.	<d.L.	1.7	0.6	0.6	1.6	89.4	14	1	0.8	0.1	<d.L.	5.7	38.6	37	1.7	0.5	<d.L.	-99	<d.L.	0.1	0.41
JHC-06-041	9.8	3.8	8	1.8	0.2	2.2	55.1	1723.6	20.1	-99	115	0.1	7	58.3	6.7	-99	5.5	7.5	14.7	-99	-99	22.3	1.09
JHC-06-042	5.3	<d.L.	1	1	0.6	<d.L.	35.2	121.1	12.8	-99	6.6	<d.L.	4.2	2.1	34.2	-99	1.5	0.1	<d.L.	-99	-99	0.6	0.11
JHC-06-043	5.4	<d.L.	7	1.8	1.3	1	3.2	82.8	16.5	1	5.4	0.2	3.5	29.4	47.4	59	4.5	<d.L.	<d.L.	-99	1	0.3	0.89
JHC-06-044	2.1	<d.L.	2	1.5	2	0.9	10.6	37	12	-99	2	0.1	0.6	3	66	31	1.6	2.7	<d.L.	-99	1	0.1	0.1
JHC-06-045	13.6	<d.L.	107	3.2	16.4	1.4	16.2	114.3	16.6	-99	3.3	0.1	3.4	9.7	74.6	-99	1.4	<d.L.	<d.L.	-99	-99	0.2	0.2
JHC-06-047	11.4	0.2	6	1.7	1.1	0.8	4.7	85.7	15.6	-99	1.8	0.2	3.2	45.6	37.5	-99	3.5	<d.L.	<d.L.	-99	-99	0.4	1.62
JHC-06-048	7.3	170	157	14.9	13.6	36.8	5960	10956.5	21.4	2	154	2.5	20.8	13.2	15.3	41	3.3	16.5	47.9	2.5	33	7.1	0.38
JHC-06-050	5.6	2.7	<d.L.	2.3	2.6	0.7	3.5	197.4	14.4	1	1.3	<d.L.	<d.L.	0.9	32.8	29	2.2	0.2	<d.L.	-99	1	-99	-99

Appendix 1B: Lithogeochemistry data table for samples analyzed from TVB

SampleNumber	Li	Cd	V	Cr	Co	Ni	Cu	Zn	Ga	Ge	As	Te	Se	Rb	Sr	Y	Nb	Mo	Ag	In	Sn	Sb	Cs
Units	ppm	ppm	ppm	ppm	ppm	ppm	ppm	ppm	ppm	ppm	ppm	ppm	ppm	ppm	ppm	ppm	ppm	ppm	ppm	ppm	ppm	ppm	ppm
Analytical Method	GS Trace	AL Trace	AL Trace	AL Trace	AL Trace	AL Trace	AL Trace	GS Trace	AL Trace	AL 4b2std	AL Trace	AL Trace	AL Trace	AL Trace	AL Trace	AL 4b2std	AL Trace	AL Trace	AL GS BPD	AL 4b2std	AL 4b2std	AL Trace	AL Trace
JHC-06-051	5.2	<d.L.	<d.L.	2.7	0.8	<d.L.	1.7	93.3	14.8	-99	1.7	<d.L.	<d.L.	10.7	34.9	-99	1.8	0.5	<d.L.	-99	-99	0.2	1.82
JHC-06-052	4.1	<d.L.	1	3.1	1.5	<d.L.	<d.L.	84.1	17.2	-99	1.4	0.1	1.1	16.3	40.2	-99	2	0.5	<d.L.	-99	-99	-99	0.66
JHC-06-053	9.8	<d.L.	42	3.4	8.9	1.2	0.4	96.3	16.4	-99	1.9	0.2	<d.L.	9	68.8	-99	1.9	0.3	<d.L.	-99	-99	0.1	1.08
JHC-06-054	13.5	<d.L.	6	1.5	1.5	2	6.7	58.6	16.9	-99	2.5	<d.L.	<d.L.	32.8	34.2	-99	5.8	<d.L.	<d.L.	-99	-99	0.3	1.25
JHC-06-057	3.2	<d.L.	9	2.1	0.7	<d.L.	3.2	44.9	14	-99	1.6	0.2	0.2	31.1	57.5	49	4.1	<d.L.	<d.L.	-99	<d.L.	0.3	0.61
JHC-06-059	7.5	0.3	15	1.8	7.1	0.6	<d.L.	164.2	15.7	1	2	0.3	3.8	13.4	77.4	23	1.3	<d.L.	<d.L.	-99	<d.L.	0.4	0.42
JHC-06-060	10.1	0.2	14	3.6	7.8	1.4	0.4	122.2	17.7	-99	1.9	0.1	3.4	6.1	62.4	24	1	0.2	0.1	-99	<d.L.	0.2	0.18
JHC-06-062	11.3	<d.L.	327	31.6	48.6	35.9	105	78.3	16.4	1	3.7	0.4	0.5	1.3	143	15	0.5	<d.L.	<d.L.	-99	<d.L.	0.3	0.21
JHC-06-063	13.9	<d.L.	348	120	54.4	90	59.2	82	17.2	-99	33.7	0.3	2.3	0.4	140	-99	0.3	0.2	<d.L.	-99	-99	0.3	0.1
JHC-06-064	16.9	<d.L.	292	143	44.6	109	36.2	101.4	14.8	1	56.2	0.3	<d.L.	<d.L.	104	16	0.2	<d.L.	<d.L.	-99	<d.L.	0.1	-99
JHC-06-068	16.3	0.3	414	28	40.7	16.4	92.3	207.9	19.1	-99	<d.L.	0.2	<d.L.	6.4	57.8	27	0.9	<d.L.	0.2	-99	<d.L.	0.5	0.5
JHC-06-069	11.3	<d.L.	387	2.1	43	3.1	25.6	116.2	19.9	-99	25.8	0.2	2	<d.L.	56.2	19	0.5	0.3	<d.L.	-99	<d.L.	0.1	-99
JHC-06-070	12.2	0.3	390	19.8	24	12.3	1250	204.2	20.3	-99	1.9	0.1	<d.L.	0.3	43.1	-99	0.8	0.1	0.3	-99	-99	0.4	0.05
JHC-06-071	12.2	<d.L.	238	17.1	17.6	12.3	<d.L.	87.1	15.6	-99	1	0.2	<d.L.	1.6	66.8	-99	0.5	0.6	0.1	-99	-99	-99	0.09
JHC-06-072	18.5	<d.L.	439	11.2	36.7	13.7	58.4	85.9	31.5	-99	1.3	0.4	<d.L.	15	61.9	-99	1.3	0.7	<d.L.	-99	-99	0.4	0.23
JHC-06-073	12.3	<d.L.	3	2.9	15.4	<d.L.	99.9	51.7	13.6	-99	1	0.2	<d.L.	20.5	26.1	41	4.2	12.6	<d.L.	-99	1	-99	0.26
JHC-06-074	21.6	6	7	2	64.7	1	10000	287.6	22.4	1	1.2	2.4	17.8	2.9	11.9	59	4.5	3.1	8.4	1	1	0.3	0.09
JHC-06-075	9.3	<d.L.	4	2	12	0.8	47.2	68.6	13.9	-99	1.1	0.8	0.5	20	31.6	-99	4.7	0.8	<d.L.	-99	-99	-99	0.29
JHC-06-076	10.1	0.1	156	4.8	9	29.3	10.7	50.5	24.8	-99	5.5	0.4	1.2	16.3	101	53	5.6	18.1	<d.L.	-99	<d.L.	0.6	0.4
JHC-06-077	2.5	1.6	48	18.1	8.2	14.2	57.7	154.2	10.9	-99	4.6	0.3	1.3	9.5	74.2	-99	3	1.6	0.2	-99	-99	0.2	0.22
JHC-06-078	1.5	<d.L.	37	10.6	6.7	8.5	86.2	19.5	10.1	-99	2.9	<d.L.	2	8.1	55.4	-99	3.1	1.3	<d.L.	-99	-99	-99	0.21
JHC-06-079	30.6	0.2	327	165	41.8	124	1	394	15.8	-99	30.7	0.8	2.3	<d.L.	43.1	-99	0.6	1.2	0.6	-99	-99	-99	-99
JHC-06-082	19.3	0.2	267	184	39.3	107	98.4	127.1	14.4	-99	7	0.2	<d.L.	<d.L.	60.2	12	0.5	0.3	0.2	-99	<d.L.	0.2	-99
JHC-06-083	5.4	1.3	171	19.4	201	187	2010	95.5	3.3	-99	112	2.5	47.4	0.6	43	-99	1.6	23.2	3.1	-99	-99	0.7	-99
JHC-06-086	5.2	<d.L.	-99	2.5	1.9	<d.L.	1.3	122.4	16.9	1	1.9	0.1	0.8	11.2	57.1	36	2.8	0.8	<d.L.	-99	<d.L.	0.1	0.2
JHC-06-087	0.8	161	101	90.4	55.2	46.6	2530	12865.5	7.9	-99	35.6	3.9	44.2	0.6	59.6	-99	0.7	11.6	7.8	-99	-99	5.3	0.05
JHC-06-088	15.5	0.4	284	146	39.4	66	45.4	364.6	18.9	-99	1.2	0.4	0.2	2.1	93.3	20	1	0.6	0.2	-99	<d.L.	0.1	0.06
JHC-06-089	9.5	<d.L.	284	234	47.3	153	14	76.9	14.7	2	1.9	0.5	<d.L.	<d.L.	254	18	0.6	0.3	<d.L.	-99	<d.L.	0.5	0.11
JHC-06-091	9.8	<d.L.	99	2.2	13.9	<d.L.	<d.L.	79.5	19	-99	10	<d.L.	<d.L.	5.4	68.4	-99	2.1	0.2	<d.L.	-99	-99	1.7	0.26
JHC-06-092	3.2	8.4	85	1.8	100	<d.L.	4230	166.5	21.5	-99	10000	7.9	23.6	37.7	14.5	-99	1	4.3	48.9	-99	-99	123	0.72
JHC-06-095	8.6	<d.L.	76	35.6	9.3	15.7	17	42	13.3	-99	55.2	<d.L.	1.4	42.3	167	-99	7	0.3	<d.L.	-99	-99	0.6	1.18
JHC-06-097	20.4	0.1	221	19.4	6.6	7.6	39.3	68.8	15.6	-99	13.1	<d.L.	1.2	54.7	143	14	1	<d.L.	<d.L.	-99	<d.L.	2.2	1.76
JHC-06-098	26.6	0.1	275	53.4	44.4	71.1	14.3	125.4	21.6	1	74.6	0.2	0.2	5.5	290	38	16.3	1.6	<d.L.	-99	2	3.4	0.36
JHC-06-100	15.4	<d.L.	241	12.4	29.5	12.7	123	75.3	15.9	-99	33.7	0.8	5.8	0.8	99.7	17	1	0.6	<d.L.	-99	<d.L.	3.6	0.05
JHC-06-101	16.6	<d.L.	174	7.2	24.7	11.3	163	77.4	12.5	-99	135	1.3	4	16.7	82.6	-99	0.6	0.8	0.3	-99	-99	1.5	0.7
JHC-06-102	9.8	0.3	192	12.3	22.9	9.3	166	136	12.9	-99	119	4.9	2.4	11.3	55.1	-99	0.8	0.9	0.6	-99	-99	1.5	0.49
JHC-06-103	13.2	<d.L.	31	3	0.6	<d.L.	<d.L.	6.5	6.2	-99	5.5	0.2	<d.L.	5.1	111	-99	3.8	1.7	<d.L.	-99	-99	0.2	0.68
JHC-06-104	6.8	<d.L.	24	2.6	2.9	<d.L.	<d.L.	14.5	16.8	-99	6.3	0.2	<d.L.	4.2	66.6	-99	3.6	10.3	<d.L.	-99	-99	0.2	0.48
JHC-06-105	14.9	<d.L.	298	13.4	15.7	6.2	<d.L.	127.3	22.6	-99	6	1.4	0.5	2.1	90.5	-99	1.7	1.9	0.1	-99	-99	0.8	0.11
JHC-06-108	10.3	<d.L.	254	10	9	5	<d.L.	83.8	19.8	-99	4.5	<d.L.	<d.L.	2.2	107	-99	2	0.9	<d.L.	-99	-99	1	0.12
JHC-06-109	9.4	0.1	161	9.4	14.9	10.6	20.8	75.7	14.1	1	23.3	0.2	<d.L.	52.2	286	16	0.6	0.4	0.2	-99	<d.L.	1.1	1.47
JHC-06-111	1.3	<d.L.	153	11	71	137	53.6	67.4	2.4	-99	10000	0.5	5.3	0.2	48	-99	0.7	4.8	0.6	-99	-99	28.7	0.05
JHC-06-112	5.5	0.4	236	10.5	36.2	19.1	140	166.6	18.5	-99	462	1.6	13.1	22.1	44.9	17	0.6	2.3	0.3	-99	<d.L.	5.8	0.76

Appendix 1B: Lithogeochemistry data table for samples analyzed from TVB

SampleNumber	Li	Cd	V	Cr	Co	Ni	Cu	Zn	Ga	Ge	As	Te	Se	Rb	Sr	Y	Nb	Mo	Ag	In	Sn	Sb	Cs
Units	ppm	ppm	ppm	ppm	ppm	ppm	ppm	ppm	ppm	ppm	ppm	ppm	ppm	ppm	ppm	ppm	ppm	ppm	ppm	ppm	ppm	ppm	ppm
Analytical Method	GS Trace	AL Trace	AL Trace	AL Trace	AL Trace	AL Trace	AL Trace	GS Trace	AL Trace	AL 4b2std	AL Trace	AL Trace	AL Trace	AL Trace	AL Trace	AL 4b2std	AL Trace	AL Trace	AL GS BPD	AL 4b2std	AL 4b2std	AL Trace	AL Trace
JHC-06-113	18.4	<d.L.	205	15.7	24.1	11.8	122	112	14.1	-99	75.1	0.5	2.2	7.3	122	17	0.8	0.6	<d.L.	-99	<d.L.	4.7	0.4
JHC-06-115	21.5	<d.L.	206	11.4	22.4	7.7	114	54.7	14.9	-99	110	3.1	16.1	7.5	66.1	-99	0.9	2	0.1	-99	-99	10.3	0.32
JHC-06-118	19.1	<d.L.	125	9.9	11	9.8	41	92.2	15.8	2	19.6	0.2	<d.L.	72.7	87.3	25	1.2	0.3	<d.L.	-99	<d.L.	2.2	1.99
JHC-06-120	10.9	<d.L.	355	11.3	47.1	49.3	56.4	49.7	12.8	-99	463	<d.L.	2.7	45.3	19.7	35	0.6	33.6	0.4	-99	<d.L.	17.9	1.02
JHC-06-121	34.6	<d.L.	224	9.8	44.5	22.1	179	51.7	14.2	-99	589	0.2	1.8	34.9	14.9	24	0.7	3.1	0.7	-99	<d.L.	13.8	1.42
JHC-06-122	24.5	1.5	246	8.4	39.5	19.8	136	352.7	15.8	-99	316	0.7	4.9	34.9	37.7	-99	0.9	3.7	0.9	-99	-99	38.4	1.76
JHC-06-123	21.7	<d.L.	291	56	47.7	74.8	<d.L.	133.6	22.4	1	15.1	0.2	0.4	<d.L.	450	39	17.2	1.4	0.1	-99	2	6.8	0.4
JHC-06-124	10.6	0.9	245	9.6	25	21.7	135	206.5	16.6	-99	511	1.4	8.3	31	64.5	-99	1.1	6.6	0.9	-99	-99	17.8	1.1
JHC-06-125	30.4	0.2	224	9.9	24.2	14.1	119	146.5	13.4	-99	88.8	0.4	1.1	5.4	89.5	-99	0.7	0.7	0.4	-99	-99	2.4	0.29
JHC-06-126	7.6	0.5	205	10.5	23.5	9.4	127	157.1	12.5	-99	193	3.4	8.2	17.1	52.5	-99	0.9	0.8	0.4	-99	-99	3.3	0.55
JHC-06-127	10.5	<d.L.	226	22.9	19.1	8.3	50.6	62	13.5	-99	19.4	<d.L.	2.9	7.6	191	-99	1.1	0.2	0.1	-99	-99	4.5	0.33
JHC-06-128	17.5	0.2	205	18.2	24.9	9.5	47.2	101.3	11.6	-99	40.8	0.9	5.7	37.3	121	-99	0.8	0.8	0.2	-99	-99	1.5	1.36
JHC-06-130	4.6	<d.L.	32	2.8	3.6	0.6	3.7	41.9	13.8	-99	3.7	0.2	2.8	4	66.3	-99	2.1	0.2	<d.L.	-99	-99	0.2	0.24
JHC-06-131	3	<d.L.	22	3.3	3.4	0.6	2.7	22.5	12.7	-99	3.9	0.3	0.3	<d.L.	36.4	16	1.9	3.6	<d.L.	-99	<d.L.	0.2	-99
JHC-06-133	3.4	<d.L.	55	4.7	5.4	2.2	3.8	17.1	7.5	-99	5.4	0.6	<d.L.	3	104	-99	3.1	2.4	<d.L.	-99	-99	0.9	0.29
JHC-06-134	1	<d.L.	13	2.6	2.1	<d.L.	<d.L.	32	15.4	-99	1	<d.L.	<d.L.	21.5	41.1	24	5.2	1.4	<d.L.	-99	<d.L.	0.1	0.24
JHC-06-135	4.7	<d.L.	111	54.2	21.7	69.9	26.5	86.2	26.8	2	8.6	<d.L.	<d.L.	45.7	29.9	36	11.3	0.3	0.1	-99	3	0.4	0.8
JHC-06-141	9.1	<d.L.	11	2	1.8	0.7	1.6	95.9	21.8	3	2.3	<d.L.	1.1	17.5	27.2	31	5.4	1.6	0.1	-99	3	0.1	0.28
JHC-06-142	0.4	2.2	8	1.9	500	15.3	4670	569.6	19.5	-99	450	2.1	33.8	<d.L.	9	-99	0.1	221	2.6	-99	-99	28.3	-99
JHC-06-143	1	0.1	9	4	2	5.3	3.5	22.3	23.1	-99	11.1	0.1	0.8	22.7	30.3	210	9	4.6	<d.L.	-99	<d.L.	0.2	0.22
JHC-06-145	8	<d.L.	77	37.1	78.7	68.7	53.2	76.1	12.2	2	50.8	0.3	0.8	11.6	92.4	41	7	1.7	3.4	-99	2	0.8	0.26
JHC-06-146	0.6	38.2	<d.L.	2.6	261	17.2	3540	5062.9	2.6	-99	516	2.3	13.8	0.7	8	-99	<d.L.	60	6.6	-99	-99	17.6	-99
JHC-06-147	10.3	0.2	132	46.6	97.2	105	105	117.3	18.8	2	125	0.5	1.8	19.6	95.4	43	10.7	3.7	1.6	-99	2	0.3	0.26
JHC-06-148	1.8	<d.L.	4	2.9	3.4	3.9	<d.L.	34.1	21.7	-99	6	<d.L.	1.5	0.7	62.8	102	8.6	2	<d.L.	-99	2	0.2	0.06
JHC-06-149	20.7	<d.L.	223	493	48.4	211	60.2	93.2	16.2	1	67.2	<d.L.	1.4	0.3	28.5	18	0.8	0.3	0.3	-99	<d.L.	0.3	0.08
JHC-06-150	<d.L.	123	12	2.6	300	14.2	7840	16038.7	11.9	-99	753	2.8	59.1	1.5	50.5	-99	0.4	7.6	19.5	-99	-99	36.8	0.1
JHC-06-153	10.8	<d.L.	335	10.8	34.6	6.6	45.2	139.5	20.1	1	2.6	<d.L.	<d.L.	0.4	88.7	20	1.7	0.2	<d.L.	-99	<d.L.	0.3	-99
JHC-06-154	7.6	0.4	59	4	3.7	8.2	<d.L.	84	16.6	-99	31.4	<d.L.	0.8	18.1	22.7	33	3.8	6.7	0.1	-99	<d.L.	1.4	0.44
JHC-06-156	15.3	<d.L.	190	126	36.5	97.4	8.1	172.5	15.1	-99	46.5	<d.L.	<d.L.	77.7	103	-99	7.6	0.9	0.3	-99	-99	1	2.58
JHC-06-157	6	1.1	73	1.6	7.6	1	5.9	423.5	16.9	-99	11.8	0.2	<d.L.	21.5	73.4	26	1.4	0.3	0.3	-99	<d.L.	2	1.61
JHC-06-158	8.1	0.1	22	1.9	2.7	0.8	4.5	48.2	12.1	-99	4.1	<d.L.	0.9	21	48.1	-99	3.6	0.9	<d.L.	-99	-99	0.6	0.79
JHC-06-162	2.3	<d.L.	11	1.5	1.2	6.5	3.5	35.5	7.8	-99	1.2	<d.L.	<d.L.	1	40.8	23	4.4	1.3	<d.L.	-99	<d.L.	0.8	0.05
JHC-06-164	9.6	0.1	202	11.4	22.1	9.2	62.8	98.8	19	-99	3.6	0.2	<d.L.	6	147	29	2.9	0.4	0.4	-99	<d.L.	0.5	0.2
JHC-06-166	14.7	0.2	249	8.6	30	6.5	30.5	103.4	18.8	-99	8.6	0.2	<d.L.	1.4	83.6	-99	2.3	1.7	0.2	-99	-99	0.5	0.07
JHC-06-167	10.7	0.2	148	1.3	24.3	2.8	102	124.5	21.3	-99	1.4	<d.L.	0.9	1	57.6	35	5.9	1.2	0.3	-99	<d.L.	0.2	-99
JHC-06-169	10.7	<d.L.	395	11.9	29.5	6.6	16.8	106.1	19.1	-99	20.5	<d.L.	<d.L.	0.9	44	-99	1.6	0.2	<d.L.	-99	-99	0.4	0.1
JHC-06-170	10.1	0.3	371	10.8	35.3	7.7	39.1	96.9	19.4	2	2.2	0.1	0.7	8.1	272	20	2.3	0.5	<d.L.	-99	<d.L.	1.5	0.89
JHC-06-171	8.5	0.3	18	2.6	2.1	0.8	1.7	114.5	19.9	-99	2.5	<d.L.	<d.L.	29.7	22.5	-99	2.5	0.3	<d.L.	-99	-99	1.6	0.31
JHC-06-172	8.3	0.2	26	2.9	2.7	1.2	<d.L.	48.2	20.5	-99	2.3	<d.L.	1.8	30.6	27	57	3.7	1.1	<d.L.	-99	1	0.6	0.39
JHC-06-173	8.7	0.1	77	1.9	9.5	1	<d.L.	93.6	19.5	-99	7.2	<d.L.	0.5	4.8	51.7	-99	2.9	0.5	<d.L.	-99	-99	1.4	0.16
JHC-06-174	7.6	<d.L.	74	1.3	6.9	1.1	<d.L.	74.5	18.6	-99	1.1	<d.L.	<d.L.	5.4	39.2	34	2.7	0.3	<d.L.	-99	<d.L.	0.3	0.21
JHC-06-175	10.8	<d.L.	299	7	27.2	5.7	47.9	91.6	18.4	-99	1.8	<d.L.	1.1	2.3	102	-99	1.3	0.1	<d.L.	-99	-99	0.4	0.44
JHC-06-176	7.1	<d.L.	77	1.1	9.3	0.7	10.6	79.9	17.5	1	5.9	<d.L.	1.1	0	71.5	37	3.3	0.2	<d.L.	-99	<d.L.	0.4	-99
JHC-06-177	8.8	0.4	27	2.8	2.7	1	0.7	126.1	19.5	-99	5.9	<d.L.	<d.L.	17.1	65.6	-99	3.2	0.7	<d.L.	-99	-99	0.8	0.32

Appendix 1B: Lithogeochemistry data table for samples analyzed from TVB

SampleNumber	Li	Cd	V	Cr	Co	Ni	Cu	Zn	Ga	Ge	As	Te	Se	Rb	Sr	Y	Nb	Mo	Ag	In	Sn	Sb	Cs
Units	ppm	ppm	ppm	ppm	ppm	ppm	ppm	ppm	ppm	ppm	ppm	ppm	ppm	ppm	ppm	ppm	ppm	ppm	ppm	ppm	ppm	ppm	ppm
Analytical Method	GS Trace	AL Trace	AL Trace	AL Trace	AL Trace	AL Trace	AL Trace	GS Trace	AL Trace	AL 4b2std	AL Trace	AL Trace	AL Trace	AL Trace	AL Trace	AL 4b2std	AL Trace	AL Trace	AL GS BPD	AL 4b2std	AL 4b2std	AL Trace	AL Trace
JHC-06-178	12.6	0.2	245	77.9	39.4	77.7	18.8	111.5	19	2	13.1	0.4	0.1	3.9	177	33	8.9	0.8	<d.L.	-99	1	3.2	0.48
JHC-06-179	21.5	0.2	32	2.5	4.4	0.8	1.1	98.7	22.2	-99	24.1	<d.L.	0.1	34.4	46	69	2.4	1.9	0.1	-99	1	1.1	0.44
JHC-06-180	7.2	0.2	173	1.7	17.5	4.5	20.4	56.4	19	-99	107	<d.L.	2.4	14.4	48.7	-99	3.5	1.7	0.4	-99	-99	3.8	0.6
JHC-06-181	12.8	0.3	131	1.2	15.9	1.8	7.7	82.4	21.6	1	42.6	<d.L.	0.4	39.8	77.8	27	4.6	1.8	0.4	-99	<d.L.	4.5	0.58
JHC-06-182	9.3	1.7	106	1	14.5	1.5	75.2	423	17.4	1	90	<d.L.	<d.L.	24.8	65.9	35	3.3	2.2	1.4	-99	1	7.5	0.48
JHC-06-183	7.5	43.3	164	2.3	12.3	8.2	60	5335.9	25	-99	117	1.2	1.9	41.9	16	-99	5.7	17	14.4	-99	-99	20	0.81
JHC-06-184	7.5	317	66	0.8	33.7	4.4	2950	14570.6	15.4	1	371	3.1	8.5	23.9	37.3	25	2	12.8	32.4	2.9	3	338	0.32
JHC-06-185	24.9	130	115	1	31.7	3.7	859	9638	27.8	-99	9790	4.2	6.4	23.3	20.3	-99	3.1	12.9	22.8	-99	-99	29.6	0.44
JHC-06-188	24.9	0.6	283	33.8	43.1	56	60.8	186.1	19.4	1	5.4	0.3	2.5	2.1	130	37	14.7	1.4	0.2	-99	1	0.9	0.14
JHC-06-190	10.2	0.1	29	2.5	6.4	<d.L.	<d.L.	121.2	18.4	-99	2.5	<d.L.	0.1	30.3	29.4	-99	1.6	<d.L.	<d.L.	-99	-99	0.3	0.49
JHC-06-191	4.4	<d.L.	35	1.1	5.3	0.7	<d.L.	103.5	16.7	-99	106	<d.L.	1.1	4.1	47.1	41	2	0.1	<d.L.	-99	<d.L.	0.6	0.17
JHC-06-192	15.7	<d.L.	37	1.1	7.4	<d.L.	<d.L.	151.1	18.6	-99	29.7	<d.L.	<d.L.	10	40.5	34	2.4	2.1	0.3	-99	<d.L.	3.1	0.2
JHC-06-194	7	0.4	30	1.4	6.7	0.6	8.6	143.9	16.3	-99	18.5	<d.L.	1.6	8.2	33.9	-99	1.7	1.2	0.2	-99	-99	2.4	0.33
JHC-06-197	5.2	<d.L.	38	1.4	2.1	0.7	<d.L.	25.1	12.3	-99	10.5	<d.L.	0.8	6	29.1	-99	3.9	1.5	<d.L.	-99	-99	0.5	0.22
JHC-06-198	26.4	<d.L.	95	1.4	7.5	2	9.2	103.3	29.7	1	4.3	0.3	0.3	14.7	25.9	36	2.6	2.6	<d.L.	-99	1	0.2	0.51
JHC-06-199	2.8	0.5	19	1	3.2	<d.L.	17.2	96.5	14.1	-99	10.9	<d.L.	0.7	9.7	44.8	-99	1.8	0.8	<d.L.	-99	-99	0.7	0.21
JHC-06-200	10.9	<d.L.	212	10.3	23.2	8.6	2.2	74.9	20.9	-99	24	0.2	2.2	8.4	27.6	-99	2.3	1.5	0.1	-99	-99	3.2	0.36
JHC-06-201	10.6	<d.L.	225	12.3	19.2	9	17.1	91.6	21.1	1	11.2	<d.L.	0.7	6.7	57.6	29	2.5	0.2	<d.L.	-99	<d.L.	0.2	0.46
JHC-06-202	7.5	<d.L.	134	4.6	23.4	6.9	39.3	86	16.1	-99	13.2	0.2	<d.L.	9.4	63.5	-99	2.2	2.3	<d.L.	-99	-99	0.6	0.35
JHC-06-204	6.2	<d.L.	58	2.6	5.4	2.5	12.5	26.2	16.7	-99	29	0.1	0.1	13	28	38	3.7	3.6	<d.L.	-99	1	0.6	0.46
JHC-06-205	12.2	<d.L.	356	10.4	31.4	6.7	22.3	96	17.7	2	9.5	<d.L.	0.3	4.7	159	20	1.3	0.3	<d.L.	-99	<d.L.	-99	0.5
JHC-06-207	9.3	<d.L.	27	1.3	3.2	<d.L.	<d.L.	34.4	14.4	-99	8.3	0.4	0.3	<d.L.	34.2	-99	2.3	0.4	<d.L.	-99	-99	0.3	-99
JHC-06-209	9.5	<d.L.	27	1.1	3.9	0.7	<d.L.	34.9	15.1	-99	29	0.3	1.4	2.4	35.6	-99	2.3	0.4	<d.L.	-99	-99	0.3	0.2
JHC-06-210	9.4	0.1	48	4.9	5.8	4.5	21.6	50.1	14.4	-99	6.6	<d.L.	2.3	39.6	10.8	36	3.3	3.4	<d.L.	-99	<d.L.	0.4	0.46
JHC-06-211	5.3	0.2	19	1	3.3	<d.L.	<d.L.	95.5	15.8	-99	2.1	<d.L.	<d.L.	0.3	57	-99	2	0.2	<d.L.	-99	-99	0.1	0.08
JHC-06-214	15.3	0.1	383	10.7	37.4	11.7	30.3	103.3	20.1	-99	34.4	<d.L.	0.5	<d.L.	111	-99	1.7	<d.L.	<d.L.	-99	-99	-99	-99
JHC-06-216	6.8	<d.L.	16	1.7	3.4	<d.L.	<d.L.	85.9	16.3	1	1.8	<d.L.	0.5	0.7	70.3	28	1.6	0.2	<d.L.	-99	<d.L.	-99	0.13
JHC-06-218	9.3	0.1	267	21.6	34.5	16.9	42.5	96.4	18.1	2	3.2	<d.L.	1.8	<d.L.	192	25	1.3	0.6	<d.L.	-99	<d.L.	0.2	0.08
JHC-06-219	16.6	0.7	22	6.5	2.4	2.1	2.4	127.5	25.1	1	9.2	<d.L.	0.9	12.1	69	69	6.6	0.6	<d.L.	-99	2	0.9	0.48
JHC-06-220	4.1	0.8	162	1.8	21.5	11.1	5.2	85.8	28.6	-99	109	<d.L.	0.9	13.3	48.2	-99	6.4	8.9	0.6	-99	-99	8.7	0.46
JHC-06-221	8.8	1.4	83	0.8	9.4	0.9	19.2	281	13.6	-99	1100	0.1	0.5	31	27.7	24	2.8	1.5	2.4	-99	<d.L.	29.3	0.56
JHC-06-225	15	0.4	166	3.1	18	2.5	20.3	81.2	16.6	-99	21.3	<d.L.	<d.L.	14.9	76.9	28	2.1	0.3	<d.L.	-99	<d.L.	0.3	0.19
JHC-06-226	13.9	0.5	61	3.2	6.2	2.7	5.9	65.2	19.4	-99	16.1	<d.L.	1.7	25.9	36.3	-99	3.8	2.1	<d.L.	-99	-99	0.9	0.43
JHC-06-227	8.8	0.4	223	2.9	22	3	18	108.9	22.4	-99	18.3	<d.L.	2.6	0.9	40.7	-99	2.3	0.6	<d.L.	-99	-99	0.4	-99
JHC-06-228	10.3	0.3	372	3.6	31	5.8	43.8	93.2	19.3	2	16.7	0.4	<d.L.	7.4	407	21	2.1	0.6	<d.L.	-99	<d.L.	3.2	0.6
JHC-06-229	12.3	0.4	186	3.6	19.1	3.4	35.1	100.9	19.9	1	12.7	<d.L.	0.3	1.7	93.2	33	2.6	0.7	<d.L.	-99	<d.L.	1	0.26
JHC-06-230	9.8	0.3	313	6.9	28.4	5.8	46.2	89.9	17.8	-99	8.6	0.3	1.8	0.3	202	-99	1.3	0.2	<d.L.	-99	-99	0.6	0.07
JHC-06-231	16.1	<d.L.	251	6.5	22.9	4.3	49	86.6	16.6	1	22.3	<d.L.	0.2	13	92.8	18	1.3	0.2	<d.L.	-99	<d.L.	0.2	0.1
JHC-06-233	12.2	0.4	16	0.6	3.5	0.6	<d.L.	79.2	15.7	-99	47.8	<d.L.	0.6	<d.L.	45.6	-99	2.2	0.2	<d.L.	-99	-99	0.5	-99
JHC-06-234	4.2	0.2	60	0.6	8	1.5	<d.L.	78.1	17.9	1	16.1	<d.L.	2.4	9.7	149	34	4.2	1.2	<d.L.	-99	2	0.9	0.25
JHC-06-235	9.9	122	113	0.7	14.9	1.5	539	11090.9	31.5	1	352	7.7	9.4	65.2	35.6	25	2.4	12.6	11.6	0.2	2	30.2	1.29
JHC-06-236	5.9	1.3	106	1	12	1.8	15.2	300.2	16.3	-99	120	<d.L.	2.3	46.7	27.6	25	3.4	0.6	0.5	-99	2	7.6	0.8
JHC-06-237	5.8	0.1	75	1.3	7.9	3.4	6.5	42.9	11.8	-99	61.9	0.5	0.9	37.5	68.7	-99	2.4	0.5	0.8	-99	-99	4.1	0.61
JHC-06-238	10.5	0.4	15	2.1	1.7	1.2	1.4	134.1	22	-99	11	<d.L.	1.1	14.4	49.7	69	3.4	1	<d.L.	-99	1	1.3	0.42

Appendix 1B: Lithogeochemistry data table for samples analyzed from TVB

SampleNumber	Li	Cd	V	Cr	Co	Ni	Cu	Zn	Ga	Ge	As	Te	Se	Rb	Sr	Y	Nb	Mo	Ag	In	Sn	Sb	Cs
Units	ppm	ppm	ppm	ppm	ppm	ppm	ppm	ppm	ppm	ppm	ppm	ppm	ppm	ppm	ppm	ppm	ppm	ppm	ppm	ppm	ppm	ppm	ppm
Analytical Method	GS Trace	AL Trace	AL Trace	AL Trace	AL Trace	AL Trace	AL Trace	GS Trace	AL Trace	AL 4b2std	AL Trace	AL Trace	AL Trace	AL Trace	AL Trace	AL 4b2std	AL Trace	AL Trace	AL GS BPD	AL 4b2std	AL 4b2std	AL Trace	AL Trace
JHC-06-239	8.3	5.5	117	2.6	14.3	5	116	1121.9	20.9	1	176	1.2	2.3	40.3	76	38	3.3	2.6	3.2	-99	7	10.9	0.89
JHC-06-240	8.3	<d.L.	21	1.9	3.3	<d.L.	<d.L.	67.5	17.4	-99	2.1	0.2	4.9	<d.L.	80.1	31	1.9	<d.L.	<d.L.	-99	<d.L.	0.3	-99
JHC-06-242	13.7	0.2	286	121	57.9	111	18.2	149	18.9	-99	<d.L.	0.3	<d.L.	1.4	256	-99	6.6	0.4	<d.L.	-99	-99	2.1	1.34
JHC-06-243	2.5	<d.L.	53	2.5	5.8	1	95.3	104	14.2	-99	15.1	0.8	1.5	21.5	50.2	-99	2.3	1.9	0.2	-99	-99	0.9	0.64
JHC-06-244	8.6	<d.L.	327	7.6	28.4	5.9	55.9	102	17.5	-99	<d.L.	0.3	0.9	5.2	129	-99	1	<d.L.	<d.L.	-99	-99	0.1	1.02
JHC-07-002	20.9	<d.L.	66	9.2	12.6	1.5	5	75.2	-99	-99	15.3	-99	-99	71.8	217.6	-99	8	<d.L.	<d.L.	-99	-99	-99	-99
JHC-07-003	28	0.4	420	75.6	64.1	62.8	29.8	136.2	26	1	12.6	-99	-99	11.2	238.6	39	22.2	<d.L.	<d.L.	<d.L.	1	4.3	<d.L.
JHC-07-004	20.7	0.1	273	41.8	26.5	9	59.5	76.3	-99	-99	9.7	-99	-99	21.8	553.1	-99	7.8	<d.L.	<d.L.	-99	-99	-99	-99
JHC-07-006	17.5	<d.L.	3	2.1	2.4	<d.L.	9	53.9	14	<d.L.	74.1	-99	-99	19.5	53.4	46	2.5	<d.L.	0.3	<d.L.	1	5.1	0.8
JHC-07-007	24	0.3	238	146.3	42.6	58.7	23	73.3	-99	-99	18.9	-99	-99	7.1	247.9	-99	15.1	<d.L.	<d.L.	-99	-99	-99	-99
JHC-07-009	20.1	<d.L.	62	11.2	16.1	2	26	125.2	-99	-99	15.3	-99	-99	96.5	43.7	-99	23.9	<d.L.	<d.L.	-99	-99	-99	-99
JHC-07-010	14.5	0.2	355	64.9	56.7	48.9	64.5	167.3	23	1	7.8	-99	-99	15.3	318.7	36	19.8	<d.L.	<d.L.	<d.L.	1	2.9	<d.L.
JHC-07-013	24.3	<d.L.	51	51.2	32.4	34.9	28.3	58.5	-99	-99	55.8	-99	-99	43.3	47.4	-99	7	<d.L.	<d.L.	-99	-99	-99	-99
JHC-07-015	78.5	0.4	341	58.6	44.9	52	38.4	118.5	-99	-99	2.4	-99	-99	27	399.2	-99	13.1	<d.L.	<d.L.	-99	-99	-99	-99
JHC-07-016	28.2	0.4	372	64.4	59	55.3	47.4	128.1	-99	-99	9	-99	-99	14.5	303.6	-99	19.7	<d.L.	<d.L.	-99	-99	-99	-99
JHC-07-017	28.3	0.3	267	36.7	26.8	10.3	81.5	81.6	-99	-99	17.2	-99	-99	10	456.5	-99	8.3	<d.L.	<d.L.	-99	-99	-99	-99
JHC-07-018	6.2	46.2	2	1.1	3.4	<d.L.	448.1	9281.9	20	<d.L.	399.3	-99	-99	36.8	55.2	53	4.8	6.6	0.7	<d.L.	1	10.9	1.8
JHC-07-019	11.8	3.7	<d.L.	7.3	2.2	<d.L.	45.3	1688.8	-99	-99	629.4	-99	-99	40.3	78.9	-99	4.1	2	3.7	-99	-99	-99	-99
JHC-07-020	15.3	0.5	244	72.3	49.6	53.1	44.5	85.1	-99	-99	17.6	-99	-99	11.4	380.4	-99	14.8	<d.L.	<d.L.	-99	-99	-99	-99
JHC-07-021	15.2	0.4	359	64.9	58	47	30.7	123.7	-99	-99	4.5	-99	-99	9.4	354.1	-99	19.6	<d.L.	<d.L.	-99	-99	-99	-99
JHC-07-022	20.4	0.2	255	29.9	38.3	21.9	38.5	138.9	-99	-99	2.5	-99	-99	33.3	93.4	-99	17.8	<d.L.	<d.L.	-99	-99	-99	-99
JHC-07-023	1.3	<d.L.	2	1.9	4	<d.L.	3.5	19.9	-99	-99	68.2	-99	-99	45	33.2	-99	4.4	2.7	0.4	-99	-99	-99	-99
JHC-07-024	0.5	11.7	1	2.1	<d.L.	<d.L.	7.9	816.3	42	2	6.5	-99	-99	24.5	29.6	235	99.1	<d.L.	<d.L.	<d.L.	22	<d.L.	<d.L.
JHC-07-025	1.6	0.2	3	2	3.6	<d.L.	11.5	50.3	-99	-99	68	-99	-99	44.6	53.7	-99	4.6	1.7	0.4	-99	-99	-99	-99
JHC-07-026	1.5	<d.L.	<d.L.	1.4	3.7	<d.L.	2.7	32.5	-99	-99	34.4	-99	-99	37	29.4	-99	4.6	1.4	0.3	-99	-99	-99	-99
JHC-07-027	22.6	0.1	6	2	2.4	<d.L.	6.8	129.7	-99	-99	15.8	-99	-99	22.9	15.1	-99	3	1.3	0.3	-99	-99	-99	-99
JHC-07-028	10.3	<d.L.	<d.L.	1.9	3.6	<d.L.	6.1	100.9	-99	-99	12.8	-99	-99	59.7	18.9	-99	4.4	1.9	0.3	-99	-99	-99	-99
JHC-07-029	13	9.4	5	1.4	2.5	<d.L.	136.2	2809.4	-99	-99	88.3	-99	-99	68.3	12.3	-99	6.8	4.2	2.6	-99	-99	-99	-99
JHC-07-030	19.3	<d.L.	<d.L.	1.5	2.2	<d.L.	8.1	168.7	17	<d.L.	17	-99	-99	35.9	6.4	53	3.7	1.6	0.3	<d.L.	2	1.1	<d.L.
JHC-07-031	8.1	6.5	7	2.6	3.3	<d.L.	13.3	1399.9	-99	-99	19.1	-99	-99	70	10.7	-99	4.2	2.6	0.4	-99	-99	-99	-99
JHC-07-032	26	0.7	6	1.6	1.7	<d.L.	4.2	557	-99	-99	8	-99	-99	14.8	6.6	-99	2.8	<d.L.	0.4	-99	-99	-99	-99
JHC-07-033	7.1	0.3	313	116.7	46	21.5	48.9	103.8	22	1	11.1	-99	-99	13	255.2	43	11.9	<d.L.	<d.L.	<d.L.	1	4	<d.L.
JHC-07-034	13.2	<d.L.	<d.L.	1.5	2.6	<d.L.	3.6	138.9	-99	-99	14.2	-99	-99	27.8	31	-99	4.5	2.6	0.4	-99	-99	-99	-99
JHC-07-035	1.5	16.3	4	1.1	<d.L.	<d.L.	70.5	1036.2	-99	-99	18	-99	-99	33.6	536.3	-99	2.3	3.8	0.5	-99	-99	-99	-99
JHC-07-036	4.7	0.5	1	1.7	2.8	<d.L.	3.3	71.4	15	<d.L.	19.2	-99	-99	53.2	15.5	38	4.2	2.5	0.2	<d.L.	1	<d.L.	0.6
JHC-07-037	5.8	0.1	3	1.4	4.2	<d.L.	1.3	72.1	-99	-99	10.4	-99	-99	47.4	20.8	-99	5.1	1.7	0.3	-99	-99	-99	-99
JHC-07-039	1.8	0.3	<d.L.	1.2	14	<d.L.	2462.2	82.1	-99	-99	26.8	-99	-99	49.6	14.7	-99	4.8	4.1	1.1	-99	-99	-99	-99
JHC-07-040	1.1	0.2	1	1.4	8.5	<d.L.	408.1	46	-99	-99	35	-99	-99	53.6	15.1	-99	4.8	2.1	0.4	-99	-99	-99	-99
JHC-07-041	1.4	0.2	1	1.1	3.4	<d.L.	310.5	44.8	-99	-99	77.3	-99	-99	44.4	13	-99	4.5	2	0.4	-99	-99	-99	-99
JHC-07-043	1.9	1.5	6	1.4	1.8	<d.L.	96.2	215.4	-99	-99	39.9	-99	-99	50.1	9.9	-99	2.7	11.7	1.1	-99	-99	-99	-99
JHC-07-044	9.8	<d.L.	1	1.5	3	<d.L.	1.8	33.6	13	<d.L.	21.8	-99	-99	33.6	14.5	27	3.4	1.5	0.3	<d.L.	5	0.8	<d.L.

Appendix 1B: Lithogeochemistry data table for samples analyzed from TVB

SampleNumber	Li	Cd	V	Cr	Co	Ni	Cu	Zn	Ga	Ge	As	Te	Se	Rb	Sr	Y	Nb	Mo	Ag	In	Sn	Sb	Cs
Units	ppm	ppm	ppm	ppm	ppm	ppm	ppm	ppm	ppm	ppm	ppm	ppm	ppm	ppm	ppm	ppm	ppm	ppm	ppm	ppm	ppm	ppm	ppm
Analytical Method	GS Trace	AL Trace	AL Trace	AL Trace	AL Trace	AL Trace	AL Trace	GS Trace	AL Trace	AL 4b2std	AL Trace	AL Trace	AL Trace	AL Trace	AL Trace	AL 4b2std	AL Trace	AL Trace	AL GS BPD	AL 4b2std	AL 4b2std	AL Trace	AL Trace
JHC-07-045	12.7	3.1	3	1.6	2.7	<d.L.	34.7	821.7	-99	-99	37.3	-99	-99	27.7	15.2	-99	4.8	1.4	0.7	-99	-99	-99	-99
JHC-07-047	18.3	<d.L.	<d.L.	2.2	2	<d.L.	8	75.6	-99	-99	21.3	-99	-99	17.7	11.9	-99	4	<d.L.	<d.L.	-99	-99	-99	-99
JHC-07-048	11.2	0.3	308	115.7	46.2	19.5	44	90.9	23	2	19.5	-99	-99	9.3	201.5	43	11.8	<d.L.	0.3	<d.L.	2	3.8	<d.L.
JHC-07-049	9.6	1.9	<d.L.	1.4	2	<d.L.	59.2	651.2	-99	-99	34.8	-99	-99	44.9	11.1	-99	3.2	1.4	0.2	-99	-99	-99	-99
JHC-07-050	30.3	0.2	<d.L.	9.2	3.3	<d.L.	21.9	228	-99	-99	31.9	-99	-99	7.7	11.2	-99	5.2	3.1	0.3	-99	-99	-99	-99
JHC-07-052	44.5	1.4	7	1.5	5.3	<d.L.	943.7	947.7	-99	-99	28.3	-99	-99	9.3	3.4	-99	10.9	4.9	0.9	-99	-99	-99	-99
JHC-07-053	7.7	6.8	<d.L.	1.6	2.2	<d.L.	186.9	1566	-99	-99	17.3	-99	-99	48.9	15.6	-99	4.8	3.2	0.3	-99	-99	-99	-99
JHC-07-054	1.4	<d.L.	6	1.3	3.3	<d.L.	2.7	19.1	20	<d.L.	9	-99	-99	23.6	48.3	47	3.7	4.6	0.5	<d.L.	2	1.1	<d.L.
JHC-07-060	12.6	<d.L.	<d.L.	1.5	2.7	<d.L.	<d.L.	175.9	-99	-99	2.8	-99	-99	76.5	30.3	-99	4.5	9.1	<d.L.	-99	-99	-99	-99
JHC-07-061	2.4	<d.L.	5	3.5	2.9	<d.L.	6.6	32.4	15	<d.L.	47.9	-99	-99	13.2	125.4	52	3.3	<d.L.	0.3	<d.L.	<d.L.	<d.L.	<d.L.
JHC-07-062	3.1	<d.L.	<d.L.	1.3	3.3	<d.L.	<d.L.	45	10	<d.L.	2.3	-99	-99	<d.L.	67.2	38	2.3	<d.L.	0.2	<d.L.	<d.L.	<d.L.	<d.L.
JHC-07-063	10.7	0.7	226	87.9	43.1	41.1	52.4	125.7	20	2	95.5	-99	-99	79.1	169.7	36	13.1	<d.L.	0.5	<d.L.	<d.L.	<d.L.	1
JHC-07-064	3.6	0.1	24	2.2	5.2	<d.L.	6.7	27.5	-99	-99	25.5	-99	-99	46.6	17.1	-99	3.1	1.6	0.4	-99	-99	-99	-99
JHC-07-065	12.2	<d.L.	17	3.2	5.9	<d.L.	1.8	92.9	24	1	13	-99	-99	111.1	27.6	49	5.2	<d.L.	0.2	<d.L.	2	1.2	1.5
JHC-07-066	6.6	0.8	40	4	7	11.4	67.9	181.4	-99	-99	48.1	-99	-99	28.7	38.6	-99	14.7	<d.L.	0.9	-99	-99	-99	-99
JHC-07-070	9.7	<d.L.	9	2.6	4.3	<d.L.	1.1	72.3	-99	-99	6.4	-99	-99	113.2	41	-99	4.9	<d.L.	<d.L.	-99	-99	-99	-99
JHC-07-073	5.9	1.4	21	2.7	10	4.8	4.5	130.3	25	1	29.8	-99	-99	111.4	19.4	48	5.3	3.8	0.2	<d.L.	2	<d.L.	1.1
JHC-07-075	18	<d.L.	<d.L.	2.4	4	<d.L.	3.9	98.4	-99	-99	4	-99	-99	65.8	52.1	-99	4.6	<d.L.	0.2	-99	-99	-99	-99
JHC-07-076	6.5	<d.L.	2	1.6	3.1	<d.L.	<d.L.	66.4	-99	-99	5.8	-99	-99	19.8	32.7	-99	2.7	<d.L.	0.1	-99	-99	-99	-99
JHC-07-077	6.1	<d.L.	<d.L.	1.5	3.7	<d.L.	<d.L.	45.6	17	<d.L.	7.5	-99	-99	28.7	25	43	3.6	2	<d.L.	<d.L.	1	1.5	0.5
JHC-07-078	19.1	0.3	250	11.1	18.2	<d.L.	65.1	90.9	16	1	8.8	-99	-99	34.2	66.8	10	6	<d.L.	<d.L.	<d.L.	<d.L.	4.2	1
JHC-07-079	18.5	0.3	196	2.2	21.6	<d.L.	55.4	105.3	-99	-99	3.5	-99	-99	33.9	55.9	-99	5.3	<d.L.	<d.L.	-99	-99	-99	-99
JHC-07-080	37.2	0.5	439	14.9	33.4	1.3	115	102.7	-99	-99	2.8	-99	-99	8.1	79.8	-99	7.9	<d.L.	<d.L.	-99	-99	-99	-99
JHC-07-081	26	0.5	418	13.6	30.6	<d.L.	132.9	104.7	16	1	4.5	-99	-99	10.4	128.7	11	7	<d.L.	<d.L.	<d.L.	2	2.7	<d.L.
JHC-07-082	20.1	0.3	365	13.7	28.6	4.6	135.9	85.8	-99	-99	13.4	-99	-99	14.6	183.3	-99	6.5	<d.L.	<d.L.	-99	-99	-99	-99
JHC-07-083	7.4	155.9	336	4.6	39.3	6.2	1723.9	12251.8	19	<d.L.	32913	-99	-99	73.3	83.7	7	4.8	74.4	655.7	<d.L.	1	> 200	2
JHC-07-084	11	<d.L.	295	3.8	5.6	<d.L.	<d.L.	21.8	11	<d.L.	34.1	-99	-99	56.4	130.5	7	2	2.9	0.4	<d.L.	<d.L.	5.4	2
JHC-07-085	21.9	<d.L.	202	3	5.5	<d.L.	<d.L.	37.6	12	<d.L.	11.3	-99	-99	37.3	51.9	23	2.1	<d.L.	<d.L.	<d.L.	<d.L.	2.1	1.1
JHC-07-086	14.3	0.5	280	7.2	22.9	1.7	83.9	180.9	-99	-99	53.2	-99	-99	34.4	147.9	-99	4	5.2	1.1	-99	-99	-99	-99
JHC-07-087	14.8	0.6	174	2.5	27.1	<d.L.	77	254.2	-99	-99	45.2	-99	-99	7.5	98.4	-99	3.6	1.5	<d.L.	-99	-99	-99	-99
JHC-07-088	5.6	0.2	204	2.9	16.6	<d.L.	63.9	118.1	17	<d.L.	35.6	-99	-99	13.8	82.3	25	3.1	<d.L.	<d.L.	<d.L.	<d.L.	1	<d.L.
JHC-07-091	20.9	1.4	281	14.2	61	16.3	154.1	537.2	16	1	676.3	-99	-99	11.3	32.4	10	8.8	<d.L.	3.7	<d.L.	2	6.3	<d.L.
JHC-07-093	14	<d.L.	317	5.5	7.5	<d.L.	<d.L.	34.2	-99	-99	17.7	-99	-99	57.6	151.4	-99	2.4	2.4	1.5	-99	-99	-99	-99
JHC-07-094	65.1	<d.L.	203	3	29.1	1.2	126.7	48.8	19	<d.L.	96.3	-99	-99	17.9	23.7	12	6.1	<d.L.	<d.L.	<d.L.	<d.L.	<d.L.	0.5
JHC-07-095	100.3	30.7	256	4	34.6	<d.L.	194.2	4614.7	-99	-99	114.1	-99	-99	21.3	33.6	-99	4.8	3.6	12	-99	-99	-99	-99
JHC-07-096	21.4	34.9	178	2.7	50.6	<d.L.	536.4	4618.5	-99	-99	7764	-99	-99	27.3	34.5	-99	5.6	3.2	14.3	-99	-99	-99	-99
JHC-07-097	4.2	<d.L.	279	3.4	4.9	<d.L.	<d.L.	13.8	15	<d.L.	17.6	-99	-99	41.7	65.7	4	1.9	1.3	0.1	<d.L.	<d.L.	<d.L.	1.7
JHC-07-098	98.7	1	215	3.1	46.1	2	32.9	658.6	-99	-99	424.9	-99	-99	7.5	6.4	-99	11.9	<d.L.	1	-99	-99	-99	-99
JHC-07-099	29.2	23.1	233	3.7	27.8	28.7	1536.3	8949.8	-99	-99	1214	-99	-99	43.6	59.8	-99	15.8	2.9	54.6	-99	-99	-99	-99
JHC-07-100	4	7.3	229	3.8	4.5	<d.L.	205.4	2388.3	-99	-99	54.8	-99	-99	49.2	55.9	-99	1.7	3.4	9.6	-99	-99	-99	-99
JHC-07-101	10	<d.L.	370	4.6	5.6	<d.L.	<d.L.	16.1	17	<d.L.	6.5	-99	-99	78.7	118	5	1.6	3.1	<d.L.	<d.L.	<d.L.	<d.L.	2.4
JHC-07-102	56.4	0.5	211	3.2	16.6	1.7	36.6	248.3	-99	-99	72.6	-99	-99	12	51.4	-99	8.1	6.1	<d.L.	-99	-99	-99	-99
JHC-07-103	3	1.2	219	2.4	22.9	1.7	39.8	204.2	17	<d.L.	61.2	-99	-99	25.6	50.2	19	5.3	2.1	0.2	<d.L.	1	4.9	0.7
JHC-07-104	34.9	0.9	305	50.9	27.8	6.7	104	599.5	-99	-99	81.8	-99	-99	17.1	142.6	-99	5.5	3.6	<d.L.	-99	-99	-99	-99

Appendix 1B: Lithogeochemistry data table for samples analyzed from TVB

SampleNumber	Li	Cd	V	Cr	Co	Ni	Cu	Zn	Ga	Ge	As	Te	Se	Rb	Sr	Y	Nb	Mo	Ag	In	Sn	Sb	Cs
Units	ppm	ppm	ppm	ppm	ppm	ppm	ppm	ppm	ppm	ppm	ppm	ppm	ppm	ppm	ppm	ppm	ppm	ppm	ppm	ppm	ppm	ppm	ppm
Analytical Method	GS Trace	AL Trace	AL Trace	AL Trace	AL Trace	AL Trace	AL Trace	GS Trace	AL Trace	AL 4b2std	AL Trace	AL Trace	AL Trace	AL Trace	AL Trace	AL 4b2std	AL Trace	AL Trace	AL GS BPD	AL 4b2std	AL 4b2std	AL Trace	AL Trace
JHC-07-106	26.2	0.4	288	28.1	27.5	3.4	167.6	141.8	-99	-99	7	-99	-99	8.3	174.2	-99	6.7	<d.L.	<d.L.	-99	-99	-99	-99
JHC-07-107	8.6	0.1	120	6.5	13.9	<d.L.	21.8	61.8	13	1	10.3	-99	-99	31.4	74.3	18	4.3	<d.L.	0.2	<d.L.	<d.L.	1.7	1
JHC-07-108	5	0.1	184	2.3	4.7	<d.L.	<d.L.	15.3	-99	-99	46.9	-99	-99	35.8	58.7	-99	1.5	1.8	0.2	-99	-99	-99	-99
JHC-07-109	64	0.2	213	2.8	42	<d.L.	92.6	18	-99	-99	82	-99	-99	19.5	16.7	-99	6.8	<d.L.	<d.L.	-99	-99	-99	-99
JHC-07-110	8.4	0.5	207	2.7	23.9	<d.L.	<d.L.	15.1	-99	-99	890.9	-99	-99	42	87.1	-99	2.9	<d.L.	0.2	-99	-99	-99	-99
JHC-07-111	20.8	<d.L.	317	4	4	<d.L.	<d.L.	15.9	-99	-99	6.1	-99	-99	63.3	222.1	-99	1.2	2.2	<d.L.	-99	-99	-99	-99
JHC-07-112	49.7	56.4	194	2	24.7	<d.L.	925.1	8974.6	-99	-99	639.6	-99	-99	23.8	46.1	-99	8	4.6	26.3	-99	-99	-99	-99
JHC-07-113	30.6	0.5	199	2.5	34	<d.L.	282.5	197.3	17	<d.L.	142.9	-99	-99	27.8	51	17	6.1	<d.L.	0.4	<d.L.	<d.L.	<d.L.	0.8
JHC-07-114	17	0.3	163	2.2	13.8	<d.L.	5.3	164.6	10	<d.L.	40.1	-99	-99	19.9	51.3	12	2.5	<d.L.	<d.L.	<d.L.	<d.L.	1.4	0.6
JHC-07-115	12.1	<d.L.	322	3.7	9.4	<d.L.	<d.L.	39.6	-99	-99	22.1	-99	-99	60.8	146.2	-99	1	1.9	0.2	-99	-99	-99	-99
JHC-07-116	29.1	0.4	191	2	31.3	<d.L.	135	204.5	16	1	124.8	-99	-99	11.7	57.1	21	5.7	2.5	<d.L.	<d.L.	1	<d.L.	<d.L.
JHC-07-119	26.4	5	215	3.7	17.7	<d.L.	105.4	1176.6	16	<d.L.	80.2	-99	-99	13.1	171.1	18	4.5	1.5	0.7	<d.L.	<d.L.	6.2	0.7
JHC-07-120	5.1	<d.L.	181	9	14.5	<d.L.	20.5	119	-99	-99	5.9	-99	-99	28.9	109.5	-99	6	<d.L.	0.3	-99	-99	-99	-99
JHC-07-121	5.6	1.7	121	6.9	12.8	<d.L.	44.2	322.8	-99	-99	41.1	-99	-99	28.4	57.6	-99	3.8	<d.L.	1.1	-99	-99	-99	-99
JHC-07-122	10.6	<d.L.	135	8.4	13.3	<d.L.	45.7	69.4	-99	-99	20.7	-99	-99	25.3	58.8	-99	4.1	<d.L.	0.1	-99	-99	-99	-99
JHC-07-123	3.1	0.7	126	7.7	17.6	<d.L.	57.3	143.7	13	<d.L.	43.9	-99	-99	33.5	71	16	4	3.1	1	0.3	<d.L.	<d.L.	1
JHC-07-124	17.6	<d.L.	<d.L.	1.4	2.1	<d.L.	6	180.9	-99	-99	6.4	-99	-99	59.6	33.6	-99	4.6	<d.L.	0.1	-99	-99	-99	-99
JHC-07-125	32.6	0.2	224	2.9	23.1	<d.L.	100.6	101.9	19	<d.L.	4.6	-99	-99	5.9	46.2	18	7.6	<d.L.	<d.L.	<d.L.	<d.L.	1.4	<d.L.
JHC-07-126	13.2	0.3	259	13.3	21.9	3.9	63.3	72.8	-99	-99	3.6	-99	-99	25.1	94.9	-99	5.3	<d.L.	0.4	-99	-99	-99	-99
JHC-07-127	24.2	0.4	283	28.3	25.9	5.1	100.2	105.8	15	1	3.1	-99	-99	2.5	60.1	9	6.6	<d.L.	<d.L.	<d.L.	<d.L.	1.7	<d.L.
JHC-07-128	20.4	0.3	188	2.4	17.7	<d.L.	70.9	110	14	<d.L.	62.5	-99	-99	13.3	44.4	13	7.3	<d.L.	<d.L.	<d.L.	<d.L.	<d.L.	<d.L.
JHC-07-129	14.6	0.1	<d.L.	1.2	1.9	<d.L.	3.4	75	-99	-99	20.5	-99	-99	13.4	136.9	-99	3.1	<d.L.	0.4	-99	-99	-99	-99
JHC-07-133	20.2	<d.L.	169	1.8	20.5	16.1	104.9	143.1	-99	-99	75.6	-99	-99	21.2	163.2	-99	9.3	<d.L.	1.4	-99	-99	-99	-99
JHC-07-134	6.5	<d.L.	201	10.5	18.2	<d.L.	82.5	62.1	-99	-99	14.1	-99	-99	26.8	129.6	-99	5.5	<d.L.	0.4	-99	-99	-99	-99
JHC-07-135	15.6	<d.L.	<d.L.	1.2	1.4	<d.L.	4	163.3	20	1	4.4	-99	-99	44.3	31.2	52	4	<d.L.	0.2	<d.L.	<d.L.	<d.L.	1
JHC-07-136	21.6	0.2	201	2.7	21.3	<d.L.	56.3	105	18	<d.L.	6.7	-99	-99	7.7	43.9	13	6.8	<d.L.	<d.L.	<d.L.	<d.L.	1.2	<d.L.
JHC-07-137	4.3	0.2	294	15.2	33.2	8.9	170.5	60	-99	-99	106.3	-99	-99	52.1	46.1	-99	8.8	<d.L.	1.5	-99	-99	-99	-99
JHC-07-138	19.8	0.2	244	10.9	20.8	2.9	34.1	93.3	16	<d.L.	6	-99	-99	21.3	67.3	11	6.8	<d.L.	0.3	<d.L.	<d.L.	1.8	0.5
JHC-07-139	29.3	0.2	228	19.9	24.6	3.9	49.7	89.2	-99	-99	3.9	-99	-99	25	54.1	-99	6.6	<d.L.	<d.L.	-99	-99	-99	-99
JHC-07-140	21.1	0.2	264	26.4	23.1	5.1	92.6	72.6	-99	-99	10	-99	-99	15.4	82.8	-99	5.9	<d.L.	0.2	-99	-99	-99	-99
JHC-07-141	21.2	0.4	263	13	23.5	5.6	104.3	204.8	-99	-99	9.8	-99	-99	27.7	102	-99	6.5	<d.L.	0.5	-99	-99	-99	-99
JHC-07-142	27.3	0.2	331	18	36.5	7.3	83.5	166.1	18	<d.L.	32.3	-99	-99	19.4	102.3	20	4.7	<d.L.	<d.L.	<d.L.	<d.L.	<d.L.	0.6
JHC-07-143	19.2	0.1	6	1.4	2.5	<d.L.	5.5	67.2	-99	-99	58.1	-99	-99	15.3	174.7	-99	3.1	1.1	0.5	-99	-99	-99	-99
JHC-07-147	21.3	0.5	229	5	19.6	<d.L.	124.7	128.8	-99	-99	54.6	-99	-99	19.1	155.5	-99	5.9	<d.L.	3.1	-99	-99	-99	-99
JHC-07-150	13.8	<d.L.	<d.L.	1.1	1.5	<d.L.	168.2	42.8	-99	-99	154.7	-99	-99	16.2	51.2	-99	5.5	<d.L.	0.1	-99	-99	-99	-99
JHC-07-151	0.3	<d.L.	19	8.6	<d.L.	<d.L.	12.2	5.9	2	<d.L.	14	-99	-99	<d.L.	523.6	2	<d.L.	1.8	<d.L.	<d.L.	2	1.7	<d.L.
JHC-07-152	0.8	<d.L.	43	27.6	16	5	130.8	15.4	18	<d.L.	108.2	-99	-99	<d.L.	390.7	23	4.1	<d.L.	0.2	<d.L.	2	<d.L.	<d.L.
JHC-07-153	10.4	<d.L.	29	2.1	5.8	<d.L.	37.1	117.6	12	<d.L.	15.9	-99	-99	6.1	61.5	17	3.3	<d.L.	0.3	<d.L.	<d.L.	<d.L.	<d.L.
JHC-07-156	7.8	<d.L.	44	3.2	7.1	<d.L.	16.4	15.4	17	<d.L.	12.4	-99	-99	12.4	125.9	33	4.1	<d.L.	<d.L.	<d.L.	<d.L.	<d.L.	0.7
JHC-07-158	3.9	<d.L.	38	3.1	5.6	<d.L.	28.7	53.4	-99	-99	5.8	-99	-99	96.5	49.8	-99	4.7	1.1	0.1	-99	-99	-99	-99

Appendix 1B: Lithogeochemistry data table for samples analyzed from TVB

SampleNumber	Li	Cd	V	Cr	Co	Ni	Cu	Zn	Ga	Ge	As	Te	Se	Rb	Sr	Y	Nb	Mo	Ag	In	Sn	Sb	Cs
Units	ppm	ppm	ppm	ppm	ppm	ppm	ppm	ppm	ppm	ppm	ppm	ppm	ppm	ppm	ppm	ppm	ppm	ppm	ppm	ppm	ppm	ppm	ppm
Analytical Method	GS Trace	AL Trace	AL Trace	AL Trace	AL Trace	AL Trace	AL Trace	GS Trace	AL Trace	AL 4b2std	AL Trace	AL Trace	AL Trace	AL Trace	AL Trace	AL 4b2std	AL Trace	AL Trace	AL GS BPD	AL 4b2std	AL 4b2std	AL Trace	AL Trace
JHC-07-160	35.6	0.1	244	15.2	23.2	1.3	10	110.3	17	<d.L.	3.4	-99	-99	34.1	104.7	17	7.5	<d.L.	<d.L.	<d.L.	<d.L.	1.2	1.5
JHC-07-162	23.9	<d.L.	30	3	12.3	<d.L.	3.3	105.9	-99	-99	2.2	-99	-99	36.3	133.9	-99	5.4	<d.L.	0.6	-99	-99	-99	-99
JHC-07-163	11	<d.L.	13	2.2	8.1	<d.L.	14	208.1	-99	-99	4.1	-99	-99	36.4	49.1	-99	4.1	<d.L.	0.2	-99	-99	-99	-99
JHC-07-165	10.4	<d.L.	<d.L.	1.3	6.2	<d.L.	<d.L.	132.7	10	<d.L.	4.7	-99	-99	26.1	23.7	17	3.7	<d.L.	<d.L.	<d.L.	<d.L.	<d.L.	1
JHC-07-166	11.9	<d.L.	19	2.4	5.8	<d.L.	<d.L.	194.8	13	<d.L.	3.6	-99	-99	29.2	32.9	16	3.5	<d.L.	0.2	<d.L.	<d.L.	<d.L.	1.1
JHC-07-167	31.7	115.5	127	6.4	20.9	<d.L.	1417.8	15404.7	-99	-99	14.4	-99	-99	30.9	72.8	-99	5.2	18.3	2.1	-99	-99	-99	-99
JHC-07-168	14.4	<d.L.	100	5.7	8.3	<d.L.	4	186.4	14	<d.L.	13.6	-99	-99	23.7	51.2	25	5.3	<d.L.	0.2	<d.L.	<d.L.	<d.L.	0.9
JHC-07-170	46.3	0.3	235	36.3	23.3	5.2	35.7	93.9	-99	-99	5.5	-99	-99	29.3	173.1	-99	7.8	<d.L.	<d.L.	-99	-99	-99	-99
JHC-07-171	6.3	<d.L.	8	1.7	3.1	<d.L.	<d.L.	36.1	19	1	27.7	-99	-99	51.3	113	44	7.9	20.4	0.1	<d.L.	2	3.4	2.7
JHC-07-172	27.8	0.2	159	3.1	19	<d.L.	37.9	113.6	-99	-99	4.3	-99	-99	26.3	104.1	-99	6.6	<d.L.	0.3	-99	-99	-99	-99
JHC-07-173	21.9	0.4	148	27.1	17.8	2.6	20.3	117.2	-99	-99	5.2	-99	-99	10.7	155.6	-99	6.1	<d.L.	<d.L.	-99	-99	-99	-99
JHC-07-174	20.2	0.2	619	45.6	33.7	10	6.4	95.9	26	<d.L.	10.6	-99	-99	54.5	134.4	16	5.9	<d.L.	<d.L.	<d.L.	<d.L.	13.6	2.5
JHC-07-175	16.1	0.6	242	3.7	25	<d.L.	27.7	152.5	20	<d.L.	93.2	-99	-99	37.3	48.2	28	8	6.5	0.3	<d.L.	<d.L.	<d.L.	2.2
JHC-07-176	29.2	0.3	199	2.9	29	<d.L.	32.6	208.4	-99	-99	58.8	-99	-99	6.2	40.7	-99	7.1	<d.L.	0.5	-99	-99	-99	-99
JHC-07-180	110.3	0.6	230	2.4	22.1	1.2	10001	379.5	-99	-99	117.4	-99	-99	8.8	9.3	-99	15.1	14	1.8	-99	-99	-99	-99
JHC-07-181	41.2	0.2	93	1.6	17.7	<d.L.	10.8	92.1	21	1	15.1	-99	-99	14.2	116.6	33	12.1	<d.L.	0.2	<d.L.	4	<d.L.	1
JHC-07-182	31.2	0.3	181	19.9	16.2	1.7	31.3	141.9	-99	-99	65.8	-99	-99	12.4	86.4	-99	5.4	<d.L.	0.7	-99	-99	-99	-99
JHC-07-184	84.2	0.4	230	31.6	26.3	6.1	47.8	247.9	-99	-99	153.3	-99	-99	16.2	66	-99	6.5	<d.L.	<d.L.	-99	-99	-99	-99
JHC-07-187	34	0.2	172	24.7	17.3	<d.L.	<d.L.	98.9	18	1	3.7	-99	-99	52.2	122.9	20	6.5	<d.L.	0.1	<d.L.	1	<d.L.	1.8
JHC-07-188	5.6	<d.L.	0	1.2	3	<d.L.	9.8	73.5	19	1	4.3	-99	-99	18.2	136.9	36	10.4	<d.L.	0.1	<d.L.	18	<d.L.	0.7
JHC-07-190	36.1	<d.L.	172	3.5	21.4	<d.L.	35	107.8	-99	-99	3.3	-99	-99	21.4	56	-99	6.6	<d.L.	<d.L.	-99	-99	-99	-99
JHC-07-191	17.6	0.3	75	5.5	12	<d.L.	15.5	82.2	18	<d.L.	3.3	-99	-99	10.1	142.5	15	4	<d.L.	<d.L.	<d.L.	<d.L.	1.6	0.5
JHC-07-193	35.3	0.3	354	29.5	30.6	5.1	<d.L.	92.3	-99	-99	3.1	-99	-99	14.6	158	-99	5.6	<d.L.	<d.L.	-99	-99	-99	-99
JHC-07-194	33	0.2	343	27.1	28.9	<d.L.	14.8	81.8	-99	-99	2.8	-99	-99	16	169.3	-99	5.5	<d.L.	<d.L.	-99	-99	-99	-99
JHC-07-195	22.1	0.2	65	7.1	11.9	<d.L.	9.6	87.3	-99	-99	74	-99	-99	8.2	79.5	-99	4.3	<d.L.	0.3	-99	-99	-99	-99
JHC-07-196	19.3	<d.L.	81	3.4	11.1	<d.L.	<d.L.	73.9	18	2	9.1	-99	-99	84.8	91.9	24	6	<d.L.	<d.L.	<d.L.	1	2.6	2.8
JHC-07-198	26.5	0.1	29	1.9	7.5	<d.L.	34.2	81.3	13	1	4.1	-99	-99	20.4	110.4	23	4.3	<d.L.	0.2	<d.L.	<d.L.	1.7	1.1
JHC-07-207	27.1	9.6	74	8.5	12.6	<d.L.	171.2	1673.4	13	<d.L.	209.3	-99	-99	11.7	59	23	4.7	3	0.7	0.4	1	2.2	0.9
JHC-07-208	36.5	1.7	94	8.4	11	1.2	304.7	328.1	-99	-99	131.5	-99	-99	19	73.5	-99	4.1	2.5	0.7	-99	-99	-99	-99
JHC-07-211	39.2	0.5	513	35.5	47.4	5.1	32.3	144.7	-99	-99	3.4	-99	-99	19.6	57.5	-99	9.4	<d.L.	<d.L.	-99	-99	-99	-99
JHC-07-213	16.2	<d.L.	129	11.3	10.5	<d.L.	3.7	83.1	-99	-99	2.4	-99	-99	26.2	72.6	-99	4.1	<d.L.	<d.L.	-99	-99	-99	-99
JHC-07-215	20.9	0.2	185	3.2	21.6	<d.L.	35.7	109.3	16	1	5.5	-99	-99	7.2	141.1	17	6.5	<d.L.	<d.L.	<d.L.	<d.L.	0.8	<d.L.
JHC-07-216	64.5	0.7	202	3.1	15.3	<d.L.	16290	280.1	-99	-99	75.1	-99	-99	8.4	9.4	-99	19.3	<d.L.	3	-99	-99	-99	-99
JHC-07-217	40.1	0.3	341	48.8	59.5	41.8	57.2	109.3	23	1	12.8	-99	-99	13.1	261.6	35	21.8	<d.L.	<d.L.	<d.L.	1	5.6	0.9
JHC-07-219	12.4	6.6	91	2.2	14.5	<d.L.	95	1718	16	<d.L.	11.2	-99	-99	31.1	24.4	14	4.9	<d.L.	0.5	0.5	1	<d.L.	1.9
JHC-07-220	39.5	0.3	414	110.3	46.7	25.9	119.1	109.1	18	<d.L.	64	-99	-99	16	70.9	6	8.2	<d.L.	<d.L.	<d.L.	<d.L.	2.6	1.1
JHC-07-221	14.2	0.2	81	2	13.5	<d.L.	114.2	44.6	-99	-99	44.6	-99	-99	22.5	21.8	-99	5.4	<d.L.	0.4	-99	-99	-99	-99
JHC-07-222	23.2	0.2	87	2.1	16	<d.L.	141	115.2	14	<d.L.	56.5	-99	-99	12.6	44.8	14	5.2	2.9	0.4	<d.L.	<d.L.	<d.L.	0.6
JHC-07-226	3.9	<d.L.	76	1.9	10.3	<d.L.	32	13.1	-99	-99	72.4	-99	-99	19.8	48.9	-99	3.5	2.4	0.3	-99	-99	-99	-99
JHC-07-229	14.1	0.2	69	17.7	11.3	1.8	69.9	137	13	<d.L.	27.8	-99	-99	8.8	52.9	21	4.6	<d.L.	0.2	<d.L.	<d.L.	<d.L.	<d.L.
JHC-07-230	7.8	<d.L.	96	2.1	14	<d.L.	13.4	69.6	16	<d.L.	13.7	-99	-99	28.9	69.8	14	4.4	<d.L.	<d.L.	<d.L.	<d.L.	0.7	1.1
JHC-07-231	22.7	0.7	291	59	34.9	13.3	121	97.5	17	<d.L.	1086	-99	-99	16.3	40.1	18	7.5	<d.L.	0.2	<d.L.	<d.L.	20.7	0.6
JHC-07-233	13.8	0.4	92	2.4	14.9	<d.L.	30.9	164.1	-99	-99	30.7	-99	-99	8.7	74.1	-99	5.2	<d.L.	<d.L.	-99	-99	-99	-99
JHC-07-236	15.9	0.1	6	1.2	4.7	<d.L.	12.8	67.6	13	1	5.8	-99	-99	12	43.5	20	3.5	<d.L.	<d.L.	<d.L.	1	2.3	<d.L.

Appendix 1B: Lithogeochemistry data table for samples analyzed from TVB

SampleNumber	Li	Cd	V	Cr	Co	Ni	Cu	Zn	Ga	Ge	As	Te	Se	Rb	Sr	Y	Nb	Mo	Ag	In	Sn	Sb	Cs
Units	ppm	ppm	ppm	ppm	ppm	ppm	ppm	ppm	ppm	ppm	ppm	ppm	ppm	ppm	ppm	ppm	ppm	ppm	ppm	ppm	ppm	ppm	ppm
Analytical Method	GS Trace	AL Trace	AL Trace	AL Trace	AL Trace	AL Trace	AL Trace	GS Trace	AL Trace	AL 4b2std	AL Trace	AL Trace	AL Trace	AL Trace	AL Trace	AL 4b2std	AL Trace	AL Trace	AL GS BPD	AL 4b2std	AL 4b2std	AL Trace	AL Trace
JHC-07-242	18.6	0.2	95	2.4	15.3	<d.L.	19.6	135.3	-99	-99	28.8	-99	-99	17.9	62.3	-99	4.8	<d.L.	<d.L.	-99	-99	-99	-99
JHC-07-245	8	0.3	289	36	35	11	117.2	89.8	16	1	3.2	-99	-99	6.1	83.6	12	6.8	<d.L.	<d.L.	<d.L.	<d.L.	1.5	<d.L.
JHC-07-246	6.1	<d.L.	5	1.3	4	<d.L.	<d.L.	51.5	-99	-99	2	-99	-99	28.6	46.8	-99	3.2	<d.L.	<d.L.	-99	-99	-99	-99
JHC-07-248	9.5	0.5	37	9.2	8.6	<d.L.	46.8	209.2	-99	-99	8.6	-99	-99	18.2	50	-99	4.5	<d.L.	<d.L.	-99	-99	-99	-99
JHC-07-252	0.4	<d.L.	2	1.3	2.1	<d.L.	3.1	12.4	8	<d.L.	29.6	-99	-99	<d.L.	60.5	44	2.2	1.5	0.3	<d.L.	1	2.9	<d.L.
JHC-07-254	6.7	<d.L.	<d.L.	1.2	1.2	<d.L.	<d.L.	19.4	-99	-99	3.1	-99	-99	15.7	79.6	-99	2.2	<d.L.	<d.L.	-99	-99	-99	-99
JHC-07-255	5.6	<d.L.	<d.L.	1	1.8	<d.L.	1.1	8.3	9	<d.L.	4.7	-99	-99	3.3	70.3	29	1.6	<d.L.	0.2	<d.L.	<d.L.	2	<d.L.
JHC-07-256	9	<d.L.	4	1.4	1.4	<d.L.	<d.L.	37.7	12	1	5.7	-99	-99	5.9	132.8	42	2.7	<d.L.	<d.L.	<d.L.	1	<d.L.	<d.L.
JHC-07-259	3.6	<d.L.	1	1.3	1.8	<d.L.	3.9	21.9	-99	-99	17.1	-99	-99	2.3	80.4	-99	2.1	<d.L.	<d.L.	-99	-99	-99	-99
JHC-07-260	6	<d.L.	<d.L.	1.1	2.2	<d.L.	2	74	-99	-99	15.4	-99	-99	12.4	73.9	-99	2.2	1.1	0.2	-99	-99	-99	-99
JHC-07-261	4.7	<d.L.	<d.L.	1.1	<d.L.	<d.L.	<d.L.	6.8	-99	-99	5.6	-99	-99	<d.L.	79.4	-99	1.6	1	<d.L.	-99	-99	-99	-99
JHC-07-262	13.3	<d.L.	<d.L.	1.4	2.7	<d.L.	1.6	61.9	14	<d.L.	4.8	-99	-99	20.7	109.9	47	6.8	<d.L.	<d.L.	<d.L.	2	1.9	0.9
JHC-07-264	3.9	<d.L.	<d.L.	1.1	<d.L.	<d.L.	<d.L.	18.9	8	<d.L.	5.4	-99	-99	7.6	64.2	37	1.4	2.8	<d.L.	<d.L.	2	<d.L.	<d.L.
JHC-07-265	3.5	<d.L.	<d.L.	1	<d.L.	<d.L.	1.4	12.5	13	<d.L.	27	-99	-99	9.7	47.2	31	1.9	1	<d.L.	<d.L.	1	<d.L.	<d.L.
JHC-07-266	6.4	0.1	13	1.4	3	<d.L.	17.7	150.1	-99	-99	7.7	-99	-99	4	49.3	-99	3.6	1.2	0.1	-99	-99	-99	-99
JHC-07-267	3.3	1.9	22	1.6	1.7	<d.L.	2180.1	486.7	-99	-99	180	-99	-99	19.6	29.5	-99	7.1	19	2.8	-99	-99	-99	-99
JHC-07-268	16.7	0.3	484	147	36.9	15.8	67.9	76.9	28	3	72.8	-99	-99	67.1	111.8	4	4.8	1.6	3	<d.L.	<d.L.	<d.L.	1.1
JHC-07-271	3.1	2.4	14	17.8	2	<d.L.	344.1	781.8	-99	-99	31.1	-99	-99	10.8	26.4	-99	1.3	13.9	4.8	-99	-99	-99	-99
JHC-07-272	8.2	<d.L.	6	2	2.5	<d.L.	<d.L.	68.4	-99	-99	4.2	-99	-99	5.6	80.3	-99	2.9	1.5	<d.L.	-99	-99	-99	-99
JHC-07-273	4.8	<d.L.	<d.L.	1.1	<d.L.	<d.L.	1.2	21.9	13	<d.L.	22.1	-99	-99	12.8	68.7	41	2	1.4	0.3	<d.L.	2	0.8	<d.L.
JHC-07-275	8.2	0.2	17	2.7	2.2	1.6	32.3	36.8	-99	-99	110	-99	-99	27.5	70.7	-99	4.6	38.1	1.2	-99	-99	-99	-99
JHC-07-276	7.1	<d.L.	5	2.2	2.2	<d.L.	2.1	79.9	14	<d.L.	6.6	-99	-99	29.9	61.1	46	4.1	5.8	0.2	<d.L.	2	<d.L.	0.7
JHC-07-277	0.3	0.1	1	1.6	7.9	<d.L.	11.8	12.2	-99	-99	203.6	-99	-99	<d.L.	106.1	-99	3	5.3	1	-99	-99	-99	-99
JHC-07-278	7.6	<d.L.	4	3.4	1.6	<d.L.	4.9	63.2	-99	-99	6.3	-99	-99	7.6	63.4	-99	2.2	8.5	<d.L.	-99	-99	-99	-99
JHC-07-279	2	3.1	7	6.1	2.7	<d.L.	5.8	683.1	-99	-99	9.4	-99	-99	4.4	96	-99	1.9	1.1	0.3	-99	-99	-99	-99
JHC-07-280	11.2	<d.L.	<d.L.	<d.L.	<d.L.	<d.L.	<d.L.	109.9	18	<d.L.	8.5	-99	-99	13.3	81.3	58	2.4	1.2	0.2	<d.L.	1	<d.L.	0.9
JHC-07-281	4.7	64.3	16	<d.L.	1.6	3.2	1455.1	10165.3	-99	-99	985.1	-99	-99	19.6	37.2	-99	8.7	57.8	7.5	-99	-99	-99	-99
JHC-07-282	7.6	10	<d.L.	1.2	<d.L.	<d.L.	527.4	3087.9	-99	-99	199.8	-99	-99	19	61.1	-99	2	2.6	1	-99	-99	-99	-99
JHC-07-283	6.7	<d.L.	<d.L.	125.6	2	53.8	1.9	46.7	15	<d.L.	4.7	-99	-99	15.3	112.7	52	2.8	13.9	<d.L.	<d.L.	1	1.1	<d.L.
JHC-07-284	2.4	<d.L.	<d.L.	1.2	<d.L.	<d.L.	1	10.7	8	<d.L.	22	-99	-99	3.2	73.1	35	1.7	<d.L.	<d.L.	<d.L.	<d.L.	0.7	<d.L.
JHC-07-285	6	<d.L.	<d.L.	<d.L.	2.2	<d.L.	1.1	30.8	8	<d.L.	10.6	-99	-99	<d.L.	91.3	44	2.6	5.7	0.1	<d.L.	<d.L.	<d.L.	<d.L.
JHC-07-286	11.8	<d.L.	<d.L.	1.9	3.4	<d.L.	<d.L.	35.9	-99	-99	10	-99	-99	33.5	108	-99	6.1	<d.L.	<d.L.	-99	-99	-99	-99
JHC-07-287	0.9	<d.L.	<d.L.	1.2	<d.L.	<d.L.	<d.L.	12.8	-99	-99	5.6	-99	-99	<d.L.	85.2	-99	1.6	<d.L.	<d.L.	-99	-99	-99	-99
JHC-07-289	7	<d.L.	1	1.6	2.6	<d.L.	356.3	68.3	-99	-99	6.3	-99	-99	16.2	52.3	-99	3.9	<d.L.	0.2	-99	-99	-99	-99
JHC-07-290	2.1	1.1	94	123.2	15.6	34.2	3046.7	147.2	-99	-99	464.4	-99	-99	10.9	22.5	-99	9.9	29.1	2	-99	-99	-99	-99
JHC-07-291	5	<d.L.	<d.L.	1.2	1.5	<d.L.	1.8	25.1	11	<d.L.	8.2	-99	-99	4.1	83.3	36	2.5	1.8	<d.L.	<d.L.	<d.L.	1.3	<d.L.
JHC-07-292	6.8	0.3	80	2.2	11.2	<d.L.	384.9	175.3	-99	-99	28	-99	-99	8.7	102.3	-99	7.1	<d.L.	0.3	-99	-99	-99	-99
JHC-07-293	7.8	<d.L.	5	1.5	1.8	<d.L.	<d.L.	45.8	8	<d.L.	4.5	-99	-99	2.4	129.8	27	1.9	1.6	0.1	<d.L.	<d.L.	1.5	<d.L.

Appendix 1B: Lithogeochemistry data table for samples analyzed from TVB

SampleNumber	La	Ce	Pr	Nd	Sm	Eu	Gd	Tb	Dy	Ho	Er	Tm	Yb	Lu	Hf	Ta	W	Tl	Pb	Bi	Th	U
Units	ppm	ppm	ppm	ppm	ppm	ppm	ppm	ppm	ppm	ppm	ppm	ppm	ppm	ppm	ppm	ppm	ppm	ppm	ppm	ppm	ppm	ppm
Analytical Method	AL 4b2std	AL 4b2std	AL 4b2std	AL 4b2std	AL 4b2std	AL 4b2std	AL 4b2std	AL 4b2std	AL 4b2std	AL 4b2std	AL 4b2std	AL 4b2std	AL 4b2std	AL 4b2std	AL 4b2std	AL 4b2std	AL Trace	AL Trace	AL Trace	AL Trace	AL Trace	AL Trace
JHC-06-001	2.1	5.3	0.75	4.0	1.3	0.70	1.8	0.4	2.6	0.6	1.7	0.28	1.9	0.29	0.9	<d.L.	0.3	<d.L.	3	<d.L.	0.2	0.2
JHC-06-002	-99	-99	-99	-99	-99	-99	-99	-99	-99	-99	-99	-99	-99	-99	-99	-99	0.4	<d.L.	2	<d.L.	<d.L.	<d.L.
JHC-06-003	7.6	18.2	2.45	11.8	3.4	1.27	4.1	0.9	5.6	1.2	3.6	0.56	3.7	0.57	1.9	<d.L.	1.2	1.05	16	<d.L.	1.1	1
JHC-06-005	3.9	10.5	1.52	7.2	1.9	0.22	2.2	0.4	2.4	0.5	1.6	0.26	1.8	0.31	1.2	<d.L.	0.7	0.18	3	<d.L.	0.8	1.5
JHC-06-006	-99	-99	-99	-99	-99	-99	-99	-99	-99	-99	-99	-99	-99	-99	-99	-99	1.5	0.98	362	0.08	0.7	0.7
JHC-06-008	6.3	15.1	2.12	10.2	3.1	0.32	3.8	0.7	4.7	1.0	3.1	0.48	3.2	0.54	1.7	0.1	0.6	0.22	6	0.07	1.2	0.4
JHC-06-009	-99	-99	-99	-99	-99	-99	-99	-99	-99	-99	-99	-99	-99	-99	-99	-99	1.1	1.61	12	0.24	0.7	7.2
JHC-06-010	-99	-99	-99	-99	-99	-99	-99	-99	-99	-99	-99	-99	-99	-99	-99	-99	1.7	1.46	786	0.04	0.2	0.3
JHC-06-011	-99	-99	-99	-99	-99	-99	-99	-99	-99	-99	-99	-99	-99	-99	-99	-99	4.1	3	28	0.04	0.5	0.6
JHC-06-012	9.1	20.9	2.86	13.4	3.6	0.38	4.1	0.7	4.6	1.0	3.2	0.51	3.5	0.58	2.0	<d.L.	4.4	2.15	45	0.05	0.8	2.1
JHC-06-013	-99	-99	-99	-99	-99	-99	-99	-99	-99	-99	-99	-99	-99	-99	-99	-99	0.2	<d.L.	1950	0.05	<d.L.	1.3
JHC-06-014	-99	-99	-99	-99	-99	-99	-99	-99	-99	-99	-99	-99	-99	-99	-99	-99	0.3	0.2	1290	0.05	0.1	1.3
JHC-06-015	6.6	15.4	2.10	10.6	3.3	1.14	4.6	0.9	6.4	1.4	4.3	0.68	4.5	0.70	2.1	0.1	1.1	1.16	8	<d.L.	1.2	0.9
JHC-06-017	-99	-99	-99	-99	-99	-99	-99	-99	-99	-99	-99	-99	-99	-99	-99	-99	0.9	0.22	43	2.39	0.5	0.8
JHC-06-018	4.2	10.1	1.46	8.1	2.8	0.45	4.1	0.8	5.4	1.1	3.5	0.58	4.1	0.71	3.3	0.2	0.9	0.09	8	0.3	2.2	1.7
JHC-06-019	2.0	4.9	0.72	3.8	1.2	0.67	1.7	0.4	2.5	0.5	1.7	0.26	1.7	0.28	0.7	-99	0.3	<d.L.	3	<d.L.	0.3	0.2
JHC-06-020	-99	-99	-99	-99	-99	-99	-99	-99	-99	-99	-99	-99	-99	-99	-99	-99	0.4	<d.L.	2	<d.L.	0.2	0.2
JHC-06-021	0.4	0.8	0.12	0.7	0.3	0.26	0.5	0.1	0.8	0.2	0.6	0.10	0.7	0.11	0.2	<d.L.	0.6	0.15	4	<d.L.	<d.L.	<d.L.
JHC-06-022	11.8	29.3	3.91	19.0	5.6	1.70	6.7	1.3	8.9	1.9	6.1	0.95	6.3	1.00	3.6	0.2	1	0.63	29	<d.L.	1.1	6.3
JHC-06-023	11.9	28.3	3.95	19.3	5.6	1.38	8.0	1.7	11.0	2.4	7.6	1.14	7.5	1.17	3.3	0.1	3.4	2.57	1300	0.08	2	1.2
JHC-06-024	-99	-99	-99	-99	-99	-99	-99	-99	-99	-99	-99	-99	-99	-99	-99	-99	0.3	<d.L.	132	4.32	<d.L.	0.5
JHC-06-025	-99	-99	-99	-99	-99	-99	-99	-99	-99	-99	-99	-99	-99	-99	-99	-99	0.5	<d.L.	777	1.17	<d.L.	3.6
JHC-06-026	-99	-99	-99	-99	-99	-99	-99	-99	-99	-99	-99	-99	-99	-99	-99	-99	<d.L.	<d.L.	36	2.65	<d.L.	0.5
JHC-06-027	-99	-99	-99	-99	-99	-99	-99	-99	-99	-99	-99	-99	-99	-99	-99	-99	0.3	<d.L.	120	6.45	<d.L.	14.3
JHC-06-028	0.1	0.5	0.10	0.9	0.9	0.27	2.7	0.8	5.8	1.3	4.0	0.62	4.0	0.61	1.3	<d.L.	0.9	0.39	14	0.54	0.8	1.2
JHC-06-030	-99	-99	-99	-99	-99	-99	-99	-99	-99	-99	-99	-99	-99	-99	-99	-99	0.5	0.34	24	6.46	0.6	0.3
JHC-06-031	-99	-99	-99	-99	-99	-99	-99	-99	-99	-99	-99	-99	-99	-99	-99	-99	1.4	1.79	89	0.09	4.7	1.5
JHC-06-032	-99	-99	-99	-99	-99	-99	-99	-99	-99	-99	-99	-99	-99	-99	-99	-99	0.9	0.73	1160	0.08	4.1	1.4
JHC-06-033	16.0	35.5	4.43	19.0	4.9	1.03	6.4	1.3	8.4	1.8	6.0	0.94	6.3	1.01	3.9	0.3	0.9	0.41	6	0.03	4.9	1.3
JHC-06-034	4.9	10.9	1.48	7.2	2.1	0.60	2.9	0.5	3.2	0.6	1.8	0.27	1.7	0.23	0.7	<d.L.	2.2	0.06	5	<d.L.	0.4	0.1
JHC-06-035	-99	-99	-99	-99	-99	-99	-99	-99	-99	-99	-99	-99	-99	-99	-99	-99	0.7	0.07	4	<d.L.	2.8	1.2
JHC-06-036	2.5	6.2	0.84	4.1	1.1	0.52	1.4	0.3	1.7	0.3	1.0	0.16	1.0	0.16	0.5	<d.L.	1.4	0.51	3	<d.L.	0.4	0.1
JHC-06-037	6.2	15.1	2.00	9.4	2.7	0.81	3.5	0.8	5.2	1.1	3.6	0.60	4.2	0.64	1.9	<d.L.	0.7	0.14	5	0.06	1.1	0.5
JHC-06-038	-99	-99	-99	-99	-99	-99	-99	-99	-99	-99	-99	-99	-99	-99	-99	-99	3.3	3.38	1220	0.22	1.7	3.2
JHC-06-039	24.2	52.5	6.63	28.5	7.4	1.36	8.9	1.7	10.8	2.3	7.1	1.16	7.6	1.17	5.2	0.3	1.3	0.31	416	0.12	6.4	2.7
JHC-06-040	6.7	15.8	2.09	9.9	2.9	0.82	3.8	0.8	5.7	1.2	4.1	0.68	4.6	0.75	2.2	<d.L.	0.5	<d.L.	2	<d.L.	0.9	0.3
JHC-06-041	-99	-99	-99	-99	-99	-99	-99	-99	-99	-99	-99	-99	-99	-99	-99	-99	3.7	6.4	2050	0.31	1.1	3
JHC-06-042	-99	-99	-99	-99	-99	-99	-99	-99	-99	-99	-99	-99	-99	-99	-99	-99	1.2	0.53	5	0.03	1.2	0.6
JHC-06-043	17.1	38.7	4.76	20.9	5.6	1.27	6.6	1.4	9.4	2.1	6.4	0.99	6.6	1.05	4.6	0.3	0.7	0.71	9	0.03	4.7	1.9
JHC-06-044	6.6	15.8	2.07	9.8	2.8	0.88	3.5	0.7	4.9	1.1	3.5	0.58	4.0	0.65	2.1	<d.L.	0.5	<d.L.	4	0.09	1	0.5
JHC-06-045	-99	-99	-99	-99	-99	-99	-99	-99	-99	-99	-99	-99	-99	-99	-99	-99	0.5	<d.L.	4	<d.L.	1.2	0.4
JHC-06-047	-99	-99	-99	-99	-99	-99	-99	-99	-99	-99	-99	-99	-99	-99	-99	-99	0.9	1.34	8	<d.L.	3.5	1.1
JHC-06-048	17.3	34.9	4.37	18.5	4.7	1.29	5.6	1.1	6.6	1.3	4.1	0.65	4.2	0.67	2.9	0.2	0.4	1.36	5000	32.3	4.6	3
JHC-06-050	8.4	18.4	2.41	10.9	2.9	1.16	3.6	0.7	4.7	1.0	3.1	0.50	3.3	0.51	1.7	<d.L.	0.3	<d.L.	29	0.09	1.3	0.4

Appendix 1B: Lithogeochemistry data table for samples analyzed from TVB

SampleNumber	La	Ce	Pr	Nd	Sm	Eu	Gd	Tb	Dy	Ho	Er	Tm	Yb	Lu	Hf	Ta	W	Tl	Pb	Bi	Th	U
Units	ppm	ppm	ppm	ppm	ppm	ppm	ppm	ppm	ppm	ppm	ppm	ppm	ppm	ppm	ppm	ppm	ppm	ppm	ppm	ppm	ppm	ppm
Analytical Method	AL 4b2std	AL 4b2std	AL 4b2std	AL 4b2std	AL 4b2std	AL 4b2std	AL 4b2std	AL 4b2std	AL 4b2std	AL 4b2std	AL 4b2std	AL 4b2std	AL 4b2std	AL 4b2std	AL 4b2std	AL 4b2std	AL Trace	AL Trace	AL Trace	AL Trace	AL Trace	AL Trace
JHC-06-051	-99	-99	-99	-99	-99	-99	-99	-99	-99	-99	-99	-99	-99	-99	-99	-99	0.1	0.09	10	0.05	1.1	0.3
JHC-06-052	-99	-99	-99	-99	-99	-99	-99	-99	-99	-99	-99	-99	-99	-99	-99	-99	0.5	0.1	5	0.03	1.3	0.4
JHC-06-053	-99	-99	-99	-99	-99	-99	-99	-99	-99	-99	-99	-99	-99	-99	-99	-99	1.2	0.11	6	0.04	1	0.3
JHC-06-054	-99	-99	-99	-99	-99	-99	-99	-99	-99	-99	-99	-99	-99	-99	-99	-99	1	0.31	16	0.1	5.4	1.6
JHC-06-057	14.2	30.8	3.75	16.0	4.1	0.83	5.0	1.1	7.0	1.5	5.0	0.82	5.6	0.89	3.5	0.2	0.9	1.13	5	<d.L.	3.9	0.9
JHC-06-059	6.4	14.3	1.91	8.8	2.5	1.09	3.2	0.6	3.8	0.8	2.4	0.37	2.4	0.39	1.2	<d.L.	0.5	0.44	5	<d.L.	0.7	0.2
JHC-06-060	6.5	16.1	2.13	9.7	2.7	1.12	3.3	0.6	4.1	0.8	2.6	0.41	2.7	0.43	1.6	<d.L.	1	0.06	4	<d.L.	1.4	0.4
JHC-06-062	3.8	8.5	1.14	5.4	1.6	0.69	1.9	0.4	2.5	0.5	1.6	0.24	1.6	0.23	0.8	<d.L.	0.2	<d.L.	4	<d.L.	0.7	0.2
JHC-06-063	-99	-99	-99	-99	-99	-99	-99	-99	-99	-99	-99	-99	-99	-99	-99	-99	0.7	<d.L.	4	0.03	0.4	0.3
JHC-06-064	3.1	8.0	1.17	6.0	1.9	0.79	2.3	0.4	2.7	0.5	1.7	0.25	1.6	0.24	0.8	<d.L.	0.4	<d.L.	2	<d.L.	0.4	0.3
JHC-06-068	2.2	5.1	0.71	3.9	1.4	0.65	2.8	0.6	4.4	0.9	2.7	0.41	2.5	0.35	1.2	<d.L.	1.3	<d.L.	100	0.02	0.7	0.7
JHC-06-069	3.6	9.1	1.26	6.1	1.9	0.92	2.4	0.5	3.3	0.7	2.1	0.32	2.2	0.33	1.2	<d.L.	0.9	<d.L.	3	<d.L.	0.7	0.3
JHC-06-070	-99	-99	-99	-99	-99	-99	-99	-99	-99	-99	-99	-99	-99	-99	-99	-99	1.4	<d.L.	3	0.18	14.2	0.6
JHC-06-071	-99	-99	-99	-99	-99	-99	-99	-99	-99	-99	-99	-99	-99	-99	-99	-99	1.9	<d.L.	6	0.11	2.1	0.4
JHC-06-072	-99	-99	-99	-99	-99	-99	-99	-99	-99	-99	-99	-99	-99	-99	-99	-99	4.1	0.09	5	0.55	1.7	0.7
JHC-06-073	12.5	27.9	3.34	14.3	3.5	0.45	4.4	0.9	6.1	1.4	4.8	0.80	5.5	0.90	4.9	0.4	1	0.12	4	0.3	4.9	1.5
JHC-06-074	20.3	43.7	5.27	21.9	5.3	0.55	6.5	1.3	8.8	2.0	6.4	1.05	7.2	1.20	6.6	0.4	1.2	<d.L.	24	1.95	7	3.2
JHC-06-075	-99	-99	-99	-99	-99	-99	-99	-99	-99	-99	-99	-99	-99	-99	-99	-99	1.2	0.14	9	1.06	8.5	2.8
JHC-06-076	27.4	60.1	6.97	29.0	6.9	1.76	7.1	1.4	9.2	1.9	5.8	0.92	5.9	0.89	6.0	0.4	1.1	0.28	12	0.26	6.4	15.7
JHC-06-077	-99	-99	-99	-99	-99	-99	-99	-99	-99	-99	-99	-99	-99	-99	-99	-99	0.4	0.09	7	0.27	3.2	1.2
JHC-06-078	-99	-99	-99	-99	-99	-99	-99	-99	-99	-99	-99	-99	-99	-99	-99	-99	0.3	0.08	4	0.15	3.3	1
JHC-06-079	-99	-99	-99	-99	-99	-99	-99	-99	-99	-99	-99	-99	-99	-99	-99	-99	0.7	<d.L.	30	0.61	0.4	1.6
JHC-06-082	2.1	5.0	0.68	3.5	1.1	0.51	1.6	0.3	2.0	0.4	1.3	0.20	1.3	0.19	0.6	<d.L.	0.8	<d.L.	5	0.14	0.7	0.2
JHC-06-083	-99	-99	-99	-99	-99	-99	-99	-99	-99	-99	-99	-99	-99	-99	-99	-99	0.3	<d.L.	53	13.6	1.7	5.3
JHC-06-086	9.5	21.5	2.66	11.7	3.3	1.18	4.6	0.9	6.2	1.3	4.1	0.65	4.2	0.64	2.5	0.1	0.1	0.08	6	0.35	2.8	1.3
JHC-06-087	-99	-99	-99	-99	-99	-99	-99	-99	-99	-99	-99	-99	-99	-99	-99	-99	2.4	0.06	5000	11.3	0.6	1.4
JHC-06-088	5.2	14.1	1.97	9.5	2.7	0.91	3.0	0.5	3.4	0.7	2.2	0.33	2.2	0.35	1.7	<d.L.	1.3	<d.L.	33	0.43	1.1	0.6
JHC-06-089	3.4	8.7	1.21	6.0	1.8	0.74	2.4	0.5	3.0	0.6	1.9	0.28	1.8	0.28	1.1	<d.L.	0.1	<d.L.	8	0.17	0.8	0.3
JHC-06-091	-99	-99	-99	-99	-99	-99	-99	-99	-99	-99	-99	-99	-99	-99	-99	-99	1.2	0.14	4	0.15	1.5	0.9
JHC-06-092	-99	-99	-99	-99	-99	-99	-99	-99	-99	-99	-99	-99	-99	-99	-99	-99	10.5	0.75	881	969	0.6	0.8
JHC-06-095	-99	-99	-99	-99	-99	-99	-99	-99	-99	-99	-99	-99	-99	-99	-99	-99	0.7	0.31	5	0.42	10	2.4
JHC-06-097	3.5	8.8	1.12	5.3	1.5	0.35	1.8	0.4	2.4	0.5	1.5	0.21	1.4	0.21	1.3	<d.L.	1	1.17	3	0.33	1.4	0.6
JHC-06-098	20.8	53.1	7.06	31.1	7.2	2.86	7.2	1.2	7.0	1.3	3.8	0.54	3.5	0.51	5.3	1.4	<d.L.	0.18	16	0.26	1.1	0.3
JHC-06-100	2.9	7.0	0.91	4.3	1.2	0.33	1.7	0.4	2.5	0.5	1.8	0.29	2.0	0.32	1.0	<d.L.	0.3	<d.L.	4	0.28	1.1	0.4
JHC-06-101	-99	-99	-99	-99	-99	-99	-99	-99	-99	-99	-99	-99	-99	-99	-99	-99	0.6	0.27	12	0.38	0.7	0.6
JHC-06-102	-99	-99	-99	-99	-99	-99	-99	-99	-99	-99	-99	-99	-99	-99	-99	-99	0.7	0.12	28	0.44	0.7	0.7
JHC-06-103	-99	-99	-99	-99	-99	-99	-99	-99	-99	-99	-99	-99	-99	-99	-99	-99	0.3	<d.L.	5	0.19	2	0.6
JHC-06-104	-99	-99	-99	-99	-99	-99	-99	-99	-99	-99	-99	-99	-99	-99	-99	-99	0.7	0.1	5	0.22	2.7	0.8
JHC-06-105	-99	-99	-99	-99	-99	-99	-99	-99	-99	-99	-99	-99	-99	-99	-99	-99	9.2	<d.L.	6	0.66	1.6	0.5
JHC-06-108	-99	-99	-99	-99	-99	-99	-99	-99	-99	-99	-99	-99	-99	-99	-99	-99	11.7	<d.L.	6	0.14	1.7	0.4
JHC-06-109	5.2	11.7	1.35	6.0	1.7	0.73	1.9	0.4	2.4	0.5	1.7	0.26	1.8	0.30	1.0	<d.L.	3.2	0.86	9	0.22	1.1	0.4
JHC-06-111	-99	-99	-99	-99	-99	-99	-99	-99	-99	-99	-99	-99	-99	-99	-99	-99	0.1	<d.L.	9	0.43	0.6	1.7
JHC-06-112	3.7	8.4	1.03	4.9	1.4	0.46	2.0	0.4	2.6	0.6	1.9	0.30	2.0	0.32	0.8	<d.L.	0.7	0.51	27	0.2	0.8	1.7

Appendix 1B: Lithogeochemistry data table for samples analyzed from TVB

SampleNumber	La	Ce	Pr	Nd	Sm	Eu	Gd	Tb	Dy	Ho	Er	Tm	Yb	Lu	Hf	Ta	W	Tl	Pb	Bi	Th	U
Units	ppm	ppm	ppm	ppm	ppm	ppm	ppm	ppm	ppm	ppm	ppm	ppm	ppm	ppm	ppm	ppm	ppm	ppm	ppm	ppm	ppm	ppm
Analytical Method	AL 4b2std	AL 4b2std	AL 4b2std	AL 4b2std	AL 4b2std	AL 4b2std	AL 4b2std	AL 4b2std	AL 4b2std	AL 4b2std	AL 4b2std	AL 4b2std	AL 4b2std	AL 4b2std	AL 4b2std	AL 4b2std	AL Trace	AL Trace	AL Trace	AL Trace	AL Trace	AL Trace
JHC-06-113	4.0	9.1	1.13	5.2	1.5	0.48	1.9	0.4	2.6	0.6	1.8	0.30	2.0	0.32	1.1	<d.L.	0.5	0.29	6	0.1	1.1	0.5
JHC-06-115	-99	-99	-99	-99	-99	-99	-99	-99	-99	-99	-99	-99	-99	-99	-99	-99	0.5	0.14	15	0.41	1.2	0.5
JHC-06-118	6.4	15.0	1.67	7.7	2.2	0.74	3.1	0.6	4.1	0.9	2.7	0.44	3.0	0.47	1.6	<d.L.	1.3	2.31	4	0.11	1.8	2.8
JHC-06-120	7.9	12.7	1.48	6.6	1.8	0.43	2.7	0.6	4.0	1.0	3.3	0.55	3.7	0.61	0.9	<d.L.	2	5.47	23	0.11	0.7	23.7
JHC-06-121	3.1	7.0	0.90	4.3	1.3	0.46	2.0	0.4	3.2	0.7	2.5	0.42	3.0	0.50	1.3	<d.L.	2.6	1.4	59	0.11	0.6	3.1
JHC-06-122	-99	-99	-99	-99	-99	-99	-99	-99	-99	-99	-99	-99	-99	-99	-99	-99	2.6	1.46	65	0.15	0.7	1.2
JHC-06-123	20.9	52.5	7.03	30.9	7.1	2.95	7.3	1.2	7.1	1.4	3.9	0.56	3.5	0.53	5.5	1.4	<d.L.	0.11	9	0.03	1	0.3
JHC-06-124	-99	-99	-99	-99	-99	-99	-99	-99	-99	-99	-99	-99	-99	-99	-99	-99	1.9	1.77	39	0.13	0.6	3.4
JHC-06-125	-99	-99	-99	-99	-99	-99	-99	-99	-99	-99	-99	-99	-99	-99	-99	-99	0.8	0.44	27	<d.L.	0.7	0.4
JHC-06-126	-99	-99	-99	-99	-99	-99	-99	-99	-99	-99	-99	-99	-99	-99	-99	-99	0.6	0.36	19	0.05	0.7	0.5
JHC-06-127	-99	-99	-99	-99	-99	-99	-99	-99	-99	-99	-99	-99	-99	-99	-99	-99	0.3	0.13	4	0.43	1.5	0.2
JHC-06-128	-99	-99	-99	-99	-99	-99	-99	-99	-99	-99	-99	-99	-99	-99	-99	-99	0.4	0.13	5	0.62	1.1	0.6
JHC-06-130	-99	-99	-99	-99	-99	-99	-99	-99	-99	-99	-99	-99	-99	-99	-99	-99	0.1	<d.L.	8	0.43	3.2	0.9
JHC-06-131	4.4	10.1	1.22	5.3	1.4	0.41	1.9	0.4	2.5	0.6	1.8	0.30	2.1	0.36	3.4	0.2	0.5	<d.L.	4	0.31	1.9	0.3
JHC-06-133	-99	-99	-99	-99	-99	-99	-99	-99	-99	-99	-99	-99	-99	-99	-99	-99	1.2	<d.L.	6	0.4	2.8	0.6
JHC-06-134	15.7	33.1	3.68	14.1	3.0	0.50	2.9	0.6	3.6	0.8	2.5	0.43	3.1	0.52	3.7	0.4	0.2	0.22	6	0.26	5.2	1.7
JHC-06-135	42.1	131.0	9.97	37.4	7.0	1.71	6.1	1.1	6.2	1.2	3.9	0.61	4.1	0.62	5.1	0.9	7.3	0.82	5	0.23	4.3	1.4
JHC-06-141	20.1	43.2	4.44	16.5	3.4	0.52	3.3	0.7	4.6	1.0	3.5	0.58	4.1	0.70	4.3	0.6	1.4	2.08	3	0.26	6.1	2.3
JHC-06-142	-99	-99	-99	-99	-99	-99	-99	-99	-99	-99	-99	-99	-99	-99	-99	-99	0.9	0.34	240	16.1	<d.L.	0.4
JHC-06-143	53.9	122.0	14.20	56.0	14.0	2.23	17.9	4.3	29.5	6.4	21.3	3.45	22.5	3.62	14.1	0.5	2.6	0.21	5	0.56	5.5	0.5
JHC-06-145	64.3	269.0	14.30	54.4	10.9	2.61	10.5	1.7	9.1	1.7	5.0	0.70	4.3	0.60	2.4	0.5	3.2	0.09	24	0.81	7.2	1
JHC-06-146	-99	-99	-99	-99	-99	-99	-99	-99	-99	-99	-99	-99	-99	-99	-99	-99	1.7	2.51	479	25.8	0.2	0.3
JHC-06-147	64.6	282.0	15.10	57.2	11.0	2.70	9.3	1.5	8.3	1.5	4.5	0.65	4.2	0.61	3.7	0.7	1.2	0.15	47	1.16	9.8	1.2
JHC-06-148	45.7	105.0	12.50	53.0	12.8	2.52	14.9	2.8	17.7	3.7	11.3	1.71	11.0	1.63	10.5	0.6	1.2	<d.L.	8	0.38	2.7	0.2
JHC-06-149	2.2	6.5	0.79	4.5	1.8	0.82	2.9	0.7	4.1	0.7	1.9	0.27	1.6	0.22	1.0	<d.L.	0.9	<d.L.	26	0.25	0.5	0.1
JHC-06-150	-99	-99	-99	-99	-99	-99	-99	-99	-99	-99	-99	-99	-99	-99	-99	-99	1.4	4.71	5000	23.3	0.3	1
JHC-06-153	4.6	11.4	1.57	7.7	2.2	0.77	2.7	0.5	3.5	0.7	2.2	0.34	2.2	0.34	1.4	<d.L.	0.2	<d.L.	3	0.14	0.6	0.2
JHC-06-154	16.0	36.0	4.02	16.0	3.9	1.16	4.3	0.8	5.3	1.1	3.5	0.57	3.9	0.64	4.3	0.3	0.4	0.12	8	0.26	2.7	2.5
JHC-06-156	-99	-99	-99	-99	-99	-99	-99	-99	-99	-99	-99	-99	-99	-99	-99	-99	1	0.97	9	0.19	3.4	0.9
JHC-06-157	8.0	17.9	2.31	11.1	3.3	1.28	4.1	0.7	4.5	0.9	2.8	0.41	2.7	0.42	1.5	<d.L.	0.8	0.43	85	0.29	0.9	0.2
JHC-06-158	-99	-99	-99	-99	-99	-99	-99	-99	-99	-99	-99	-99	-99	-99	-99	-99	0.5	0.24	7	0.28	4.8	1.2
JHC-06-162	27.2	56.7	6.32	25.1	5.0	1.37	3.9	0.6	3.3	0.8	3.0	0.50	3.7	0.64	3.9	0.3	1.4	<d.L.	3	0.25	5.6	1.9
JHC-06-164	10.7	25.1	3.09	13.6	3.5	1.36	4.0	0.8	5.0	1.0	3.1	0.47	3.0	0.47	2.2	0.1	0.6	<d.L.	4	0.25	1	0.3
JHC-06-166	-99	-99	-99	-99	-99	-99	-99	-99	-99	-99	-99	-99	-99	-99	-99	-99	0.5	<d.L.	7	0.27	0.5	0.4
JHC-06-167	6.4	16.8	2.40	12.0	3.6	1.12	4.5	0.9	5.8	1.2	4.0	0.64	4.3	0.69	3.3	0.4	1	<d.L.	5	0.27	0.6	0.5
JHC-06-169	-99	-99	-99	-99	-99	-99	-99	-99	-99	-99	-99	-99	-99	-99	-99	-99	0.4	<d.L.	6	0.25	0.4	0.1
JHC-06-170	4.0	9.9	1.36	6.9	2.1	0.82	2.8	0.5	3.4	0.7	2.1	0.32	2.1	0.31	1.3	<d.L.	0.4	0.13	5	0.24	0.8	0.2
JHC-06-171	-99	-99	-99	-99	-99	-99	-99	-99	-99	-99	-99	-99	-99	-99	-99	-99	0.4	0.23	9	0.32	3.1	1
JHC-06-172	21.9	54.0	6.75	30.1	7.5	2.25	7.2	1.4	9.1	2.0	6.4	1.00	6.5	1.00	5.4	0.2	0.5	0.25	6	0.3	3.4	1.2
JHC-06-173	-99	-99	-99	-99	-99	-99	-99	-99	-99	-99	-99	-99	-99	-99	-99	-99	0.7	0.05	3	0.28	1.4	0.5
JHC-06-174	9.2	22.4	2.91	13.6	3.7	1.12	4.3	0.9	5.7	1.2	3.7	0.55	3.5	0.53	3.0	0.2	0.6	<d.L.	2	0.24	0.9	0.2
JHC-06-175	-99	-99	-99	-99	-99	-99	-99	-99	-99	-99	-99	-99	-99	-99	-99	-99	0.2	0.07	8	0.29	0.3	0.1
JHC-06-176	7.8	20.9	2.90	14.3	4.2	1.40	4.9	1.0	6.3	1.3	3.9	0.59	3.8	0.58	3.2	0.2	0.7	<d.L.	2	0.24	0.7	0.2
JHC-06-177	-99	-99	-99	-99	-99	-99	-99	-99	-99	-99	-99	-99	-99	-99	-99	-99	0.3	0.14	8	0.27	1.9	0.7

Appendix 1B: Lithogeochemistry data table for samples analyzed from TVB

SampleNumber	La	Ce	Pr	Nd	Sm	Eu	Gd	Tb	Dy	Ho	Er	Tm	Yb	Lu	Hf	Ta	W	Tl	Pb	Bi	Th	U
Units	ppm	ppm	ppm	ppm	ppm	ppm	ppm	ppm	ppm	ppm	ppm	ppm	ppm	ppm	ppm	ppm	ppm	ppm	ppm	ppm	ppm	ppm
Analytical Method	AL 4b2std	AL 4b2std	AL 4b2std	AL 4b2std	AL 4b2std	AL 4b2std	AL 4b2std	AL 4b2std	AL 4b2std	AL 4b2std	AL 4b2std	AL 4b2std	AL 4b2std	AL 4b2std	AL 4b2std	AL 4b2std	AL Trace	AL Trace	AL Trace	AL Trace	AL Trace	AL Trace
JHC-06-178	17.5	42.3	5.61	25.1	5.9	2.69	6.7	1.1	6.3	1.2	3.5	0.51	3.2	0.46	4.2	0.6	0.4	0.07	6	0.21	2	0.5
JHC-06-179	17.5	44.7	6.01	28.1	7.7	2.31	9.6	1.8	11.5	2.4	7.4	1.12	7.4	1.12	5.4	0.2	0.5	1.4	13	0.32	3.7	1.5
JHC-06-180	-99	-99	-99	-99	-99	-99	-99	-99	-99	-99	-99	-99	-99	-99	-99	-99	0.6	2.38	14	0.23	0.9	1
JHC-06-181	14.5	32.9	3.99	17.1	4.4	1.16	4.4	0.8	5.1	1.0	3.1	0.48	3.1	0.48	4.0	0.4	1	4.1	31	0.27	1.3	1.4
JHC-06-182	14.5	30.4	3.69	16.1	4.1	1.61	4.5	0.9	5.7	1.2	3.9	0.62	4.3	0.72	3.3	0.3	1.2	3.18	109	1.11	0.8	0.8
JHC-06-183	-99	-99	-99	-99	-99	-99	-99	-99	-99	-99	-99	-99	-99	-99	-99	-99	4.1	11.1	4980	0.39	0.4	6.2
JHC-06-184	14.7	34.9	4.26	18.8	4.4	2.30	4.1	0.7	4.5	0.9	2.5	0.37	2.3	0.34	2.3	0.2	3.1	5.26	4050	19.5	0.8	5.8
JHC-06-185	-99	-99	-99	-99	-99	-99	-99	-99	-99	-99	-99	-99	-99	-99	-99	-99	4.1	7.29	5000	35.6	0.9	4.7
JHC-06-188	20.2	49.1	6.50	28.5	6.6	2.06	7.0	1.2	6.6	1.3	3.7	0.54	3.4	0.49	5.2	1.3	6.7	0.45	10	0.27	0.8	0.2
JHC-06-190	-99	-99	-99	-99	-99	-99	-99	-99	-99	-99	-99	-99	-99	-99	-99	-99	0.3	0.66	16	0.13	1.9	0.6
JHC-06-191	7.1	17.1	2.29	11.3	3.3	1.07	4.3	0.9	6.3	1.4	4.3	0.69	4.5	0.71	2.4	0.1	0.3	0.11	3	0.15	0.6	0.2
JHC-06-192	9.3	22.3	2.83	13.4	3.8	1.24	4.4	0.9	6.0	1.3	4.0	0.62	4.1	0.65	3.0	0.2	0.6	0.48	6	0.12	2	0.7
JHC-06-194	-99	-99	-99	-99	-99	-99	-99	-99	-99	-99	-99	-99	-99	-99	-99	-99	0.4	0.11	16	0.15	0.6	0.2
JHC-06-197	-99	-99	-99	-99	-99	-99	-99	-99	-99	-99	-99	-99	-99	-99	-99	-99	0.8	0.19	7	0.1	4.3	1.9
JHC-06-198	21.1	45.4	5.36	23.2	5.4	1.90	5.1	0.9	5.6	1.2	3.7	0.58	3.9	0.62	2.8	0.2	1.2	0.11	3	0.26	3.9	1.1
JHC-06-199	-99	-99	-99	-99	-99	-99	-99	-99	-99	-99	-99	-99	-99	-99	-99	-99	0.3	0.08	20	0.09	1	0.3
JHC-06-200	-99	-99	-99	-99	-99	-99	-99	-99	-99	-99	-99	-99	-99	-99	-99	-99	0.7	0.2	7	0.18	0.4	0.4
JHC-06-201	5.6	15.6	2.28	11.3	3.4	1.10	3.9	0.8	5.0	1.0	3.1	0.47	3.1	0.47	2.6	0.2	0.3	0.08	3	0.08	0.4	0.1
JHC-06-202	-99	-99	-99	-99	-99	-99	-99	-99	-99	-99	-99	-99	-99	-99	-99	-99	0.5	0.08	6	0.16	0.4	0.4
JHC-06-204	10.4	23.9	3.15	14.8	4.2	0.81	5.0	1.0	6.0	1.3	4.2	0.67	4.5	0.72	4.7	0.3	0.5	0.28	4	0.22	1.8	1.4
JHC-06-205	4.2	10.4	1.42	7.2	2.2	0.80	2.8	0.6	3.6	0.7	2.3	0.34	2.2	0.33	1.4	<d.L.	0	0.07	2	0.04	0.7	0.2
JHC-06-207	-99	-99	-99	-99	-99	-99	-99	-99	-99	-99	-99	-99	-99	-99	-99	-99	1	<d.L.	2	0.06	0.7	0.6
JHC-06-209	-99	-99	-99	-99	-99	-99	-99	-99	-99	-99	-99	-99	-99	-99	-99	-99	1.2	<d.L.	2	0.12	1.1	0.7
JHC-06-210	7.3	20.9	2.74	12.7	3.6	0.84	4.1	0.9	5.5	1.1	3.6	0.59	4.0	0.64	3.7	0.2	0.3	0.41	3	0.09	2.9	1.9
JHC-06-211	-99	-99	-99	-99	-99	-99	-99	-99	-99	-99	-99	-99	-99	-99	-99	-99	0.2	<d.L.	5	0.04	0.6	0.2
JHC-06-214	-99	-99	-99	-99	-99	-99	-99	-99	-99	-99	-99	-99	-99	-99	-99	-99	0.3	<d.L.	2	0.03	1.4	0.5
JHC-06-216	6.7	15.3	1.97	9.2	2.8	0.96	3.9	0.7	4.6	1.0	3.0	0.46	3.0	0.47	2.2	0.2	0.1	<d.L.	2	0.02	0.7	0.2
JHC-06-218	5.3	13.6	1.88	9.1	2.7	0.94	3.3	0.6	4.2	0.9	2.6	0.39	2.6	0.40	1.8	<d.L.	0.1	<d.L.	3	0.02	1.2	0.4
JHC-06-219	23.5	59.8	7.58	33.6	8.3	2.51	9.2	1.8	11.2	2.3	7.3	1.14	7.6	1.16	7.7	0.3	0.2	3.13	7	0.42	2.5	1.7
JHC-06-220	-99	-99	-99	-99	-99	-99	-99	-99	-99	-99	-99	-99	-99	-99	-99	-99	3.1	11.6	14	0.36	1.2	2.9
JHC-06-221	7.7	17.6	2.12	9.5	2.5	0.81	2.9	0.6	3.6	0.7	2.3	0.38	2.6	0.41	2.6	0.2	2.5	2.29	99	0.39	1	0.5
JHC-06-225	5.4	13.9	1.93	9.6	2.9	1.04	3.7	0.7	4.8	1.0	2.9	0.44	2.8	0.42	2.6	0.1	0.3	0.21	2	0.3	2.1	0.7
JHC-06-226	-99	-99	-99	-99	-99	-99	-99	-99	-99	-99	-99	-99	-99	-99	-99	-99	0.7	0.42	7	0.33	1.7	1.1
JHC-06-227	-99	-99	-99	-99	-99	-99	-99	-99	-99	-99	-99	-99	-99	-99	-99	-99	0.4	0.07	2	0.24	0.5	0.3
JHC-06-228	3.4	8.8	1.28	6.3	2.0	0.84	2.6	0.5	3.4	0.7	2.1	0.33	2.2	0.33	1.2	<d.L.	0.6	0.11	5	0.2	0.8	0.2
JHC-06-229	5.7	15.4	2.16	11.5	3.7	1.26	4.5	0.9	5.6	1.1	3.3	0.48	3.0	0.44	2.0	0.1	0.5	0.1	3	0.16	0.4	0.3
JHC-06-230	-99	-99	-99	-99	-99	-99	-99	-99	-99	-99	-99	-99	-99	-99	-99	-99	0.3	0.08	2	0.12	0.6	0.2
JHC-06-231	3.4	8.8	1.24	6.5	1.9	0.72	2.3	0.5	3.0	0.6	1.9	0.29	1.9	0.28	1.3	<d.L.	0.3	0.39	2	0.12	0.7	0.1
JHC-06-233	-99	-99	-99	-99	-99	-99	-99	-99	-99	-99	-99	-99	-99	-99	-99	-99	0.6	0.09	3	0.07	0.4	0.3
JHC-06-234	24.1	50.3	5.95	24.3	5.5	1.78	5.9	1.0	5.9	1.2	3.5	0.52	3.4	0.51	4.5	0.4	1.6	1.05	8	0.1	2.1	0.7
JHC-06-235	7.6	18.3	2.27	10.0	2.6	0.62	3.0	0.6	4.0	0.8	2.6	0.41	2.7	0.43	2.8	0.2	6.7	18.6	5000	0.94	1	1.4
JHC-06-236	7.5	17.4	2.14	9.6	2.6	0.80	3.0	0.6	4.1	0.9	2.7	0.44	3.0	0.48	2.8	0.3	2.2	7.17	630	0.19	1.1	1
JHC-06-237	-99	-99	-99	-99	-99	-99	-99	-99	-99	-99	-99	-99	-99	-99	-99	-99	1.9	4.16	11	0.05	1.5	1
JHC-06-238	18.8	47.4	6.23	28.7	7.8	2.37	8.7	1.7	11.2	2.3	7.2	1.10	7.3	1.14	5.7	0.1	0.3	1.33	8	0.13	2.2	1.1

Appendix 1B: Lithogeochemistry data table for samples analyzed from TVB

SampleNumber	La	Ce	Pr	Nd	Sm	Eu	Gd	Tb	Dy	Ho	Er	Tm	Yb	Lu	Hf	Ta	W	Tl	Pb	Bi	Th	U
Units	ppm	ppm	ppm	ppm	ppm	ppm	ppm	ppm	ppm	ppm	ppm	ppm	ppm	ppm	ppm	ppm	ppm	ppm	ppm	ppm	ppm	ppm
Analytical Method	AL 4b2std	AL 4b2std	AL 4b2std	AL 4b2std	AL 4b2std	AL 4b2std	AL 4b2std	AL 4b2std	AL 4b2std	AL 4b2std	AL 4b2std	AL 4b2std	AL 4b2std	AL 4b2std	AL 4b2std	AL 4b2std	AL Trace	AL Trace	AL Trace	AL Trace	AL Trace	AL Trace
JHC-06-239	8.4	19.0	2.35	10.7	3.0	0.78	4.1	0.9	5.7	1.2	3.7	0.58	3.8	0.58	3.1	0.2	3	8.36	1060	0.47	1.1	1.2
JHC-06-240	7.7	18.3	2.33	10.9	3.2	1.01	3.8	0.8	5.0	1.0	3.2	0.50	3.3	0.52	2.4	0.1	0.5	<d.L.	1	<d.L.	1.7	0.6
JHC-06-242	-99	-99	-99	-99	-99	-99	-99	-99	-99	-99	-99	-99	-99	-99	-99	-99	0.3	<d.L.	10	<d.L.	0.6	0.1
JHC-06-243	-99	-99	-99	-99	-99	-99	-99	-99	-99	-99	-99	-99	-99	-99	-99	-99	1.2	0.19	20	0.62	1.1	0.4
JHC-06-244	-99	-99	-99	-99	-99	-99	-99	-99	-99	-99	-99	-99	-99	-99	-99	-99	0.5	<d.L.	2	<d.L.	0.5	0.2
JHC-07-002	-99	-99	-99	-99	-99	-99	-99	-99	-99	-99	-99	-99	-99	-99	-99	-99	-99	<d.L.	5	-99	-99	-99
JHC-07-003	12.2	29.9	4.53	20.2	5.3	1.95	6.5	1.1	6.8	1.4	3.9	0.57	3.6	0.54	3.9	0.9	-99	<d.L.	<d.L.	<d.L.	1.1	0.3
JHC-07-004	-99	-99	-99	-99	-99	-99	-99	-99	-99	-99	-99	-99	-99	-99	-99	-99	-99	-99	12	-99	-99	-99
JHC-07-006	4.0	10.0	1.51	8.0	2.6	0.69	4.1	0.9	6.5	1.5	4.7	0.74	5.1	0.79	2.6	<d.L.	-99	0.7	27	<d.L.	1.9	0.8
JHC-07-007	-99	-99	-99	-99	-99	-99	-99	-99	-99	-99	-99	-99	-99	-99	-99	-99	-99	-99	<d.L.	-99	-99	-99
JHC-07-009	-99	-99	-99	-99	-99	-99	-99	-99	-99	-99	-99	-99	-99	-99	-99	-99	-99	-99	18	-99	-99	-99
JHC-07-010	11.0	26.7	4.05	18.0	4.7	1.64	5.7	1.0	6.1	1.2	3.4	0.50	3.2	0.48	3.7	0.8	-99	<d.L.	2	-99	1.2	0.3
JHC-07-013	-99	-99	-99	-99	-99	-99	-99	-99	-99	-99	-99	-99	-99	-99	-99	-99	-99	-99	7	-99	-99	-99
JHC-07-015	-99	-99	-99	-99	-99	-99	-99	-99	-99	-99	-99	-99	-99	-99	-99	-99	-99	-99	1	-99	-99	-99
JHC-07-016	-99	-99	-99	-99	-99	-99	-99	-99	-99	-99	-99	-99	-99	-99	-99	-99	-99	-99	1	-99	-99	-99
JHC-07-017	-99	-99	-99	-99	-99	-99	-99	-99	-99	-99	-99	-99	-99	-99	-99	-99	-99	-99	8	-99	-99	-99
JHC-07-018	9.2	20.8	2.66	14.5	4.8	1.35	6.6	1.3	8.4	1.9	5.9	0.93	6.2	0.98	3.3	0.1	2	2	12248	-99	2.5	1.2
JHC-07-019	-99	-99	-99	-99	-99	-99	-99	-99	-99	-99	-99	-99	-99	-99	-99	-99	-99	-99	1305	-99	-99	-99
JHC-07-020	-99	-99	-99	-99	-99	-99	-99	-99	-99	-99	-99	-99	-99	-99	-99	-99	-99	-99	2	-99	-99	-99
JHC-07-021	-99	-99	-99	-99	-99	-99	-99	-99	-99	-99	-99	-99	-99	-99	-99	-99	-99	-99	<d.L.	-99	-99	-99
JHC-07-022	-99	-99	-99	-99	-99	-99	-99	-99	-99	-99	-99	-99	-99	-99	-99	-99	-99	-99	2	-99	-99	-99
JHC-07-023	-99	-99	-99	-99	-99	-99	-99	-99	-99	-99	-99	-99	-99	-99	-99	-99	-99	-99	21	-99	-99	-99
JHC-07-024	30.3	76.5	9.49	48.1	15.3	1.08	21.0	4.8	34.2	7.4	24.0	3.89	24.8	3.46	29.6	11.5	4	0.3	157	-99	27.2	7.7
JHC-07-025	-99	-99	-99	-99	-99	-99	-99	-99	-99	-99	-99	-99	-99	-99	-99	-99	-99	-99	49	-99	-99	-99
JHC-07-026	-99	-99	-99	-99	-99	-99	-99	-99	-99	-99	-99	-99	-99	-99	-99	-99	-99	-99	14	-99	-99	-99
JHC-07-027	-99	-99	-99	-99	-99	-99	-99	-99	-99	-99	-99	-99	-99	-99	-99	-99	-99	-99	10	-99	-99	-99
JHC-07-028	-99	-99	-99	-99	-99	-99	-99	-99	-99	-99	-99	-99	-99	-99	-99	-99	-99	-99	27	-99	-99	-99
JHC-07-029	-99	-99	-99	-99	-99	-99	-99	-99	-99	-99	-99	-99	-99	-99	-99	-99	-99	-99	4136	-99	-99	-99
JHC-07-030	15.6	33.5	3.82	15.9	4.6	1.24	5.5	1.1	7.6	1.7	5.4	0.86	5.8	0.92	5.5	0.3	1	0.3	36	-99	9.6	2.4
JHC-07-031	-99	-99	-99	-99	-99	-99	-99	-99	-99	-99	-99	-99	-99	-99	-99	-99	-99	-99	383	-99	-99	-99
JHC-07-032	-99	-99	-99	-99	-99	-99	-99	-99	-99	-99	-99	-99	-99	-99	-99	-99	-99	-99	114	-99	-99	-99
JHC-07-033	11.2	29.0	3.90	18.7	5.8	1.99	7.0	1.3	7.7	1.6	4.6	0.65	4.1	0.60	4.6	0.4	-99	<d.L.	5	-99	1.6	0.6
JHC-07-034	-99	-99	-99	-99	-99	-99	-99	-99	-99	-99	-99	-99	-99	-99	-99	-99	-99	-99	27	-99	-99	-99
JHC-07-035	-99	-99	-99	-99	-99	-99	-99	-99	-99	-99	-99	-99	-99	-99	-99	-99	-99	-99	254	-99	-99	-99
JHC-07-036	19.7	39.8	4.34	17.4	4.6	0.78	4.9	0.9	6.1	1.3	4.1	0.65	4.3	0.65	3.8	0.3	-99	0.7	9	-99	6.5	1.7
JHC-07-037	-99	-99	-99	-99	-99	-99	-99	-99	-99	-99	-99	-99	-99	-99	-99	-99	-99	-99	13	-99	-99	-99
JHC-07-039	-99	-99	-99	-99	-99	-99	-99	-99	-99	-99	-99	-99	-99	-99	-99	-99	-99	-99	51	-99	-99	-99
JHC-07-040	-99	-99	-99	-99	-99	-99	-99	-99	-99	-99	-99	-99	-99	-99	-99	-99	-99	-99	41	-99	-99	-99
JHC-07-041	-99	-99	-99	-99	-99	-99	-99	-99	-99	-99	-99	-99	-99	-99	-99	-99	-99	-99	27	-99	-99	-99
JHC-07-043	-99	-99	-99	-99	-99	-99	-99	-99	-99	-99	-99	-99	-99	-99	-99	-99	-99	-99	2009	-99	-99	-99
JHC-07-044	15.1	31.3	3.42	13.6	3.6	0.85	3.8	0.7	4.3	0.9	3.0	0.49	3.3	0.52	3.5	0.3	1	0.5	8	-99	6.6	1.8

Appendix 1B: Lithogeochemistry data table for samples analyzed from TVB

SampleNumber	La	Ce	Pr	Nd	Sm	Eu	Gd	Tb	Dy	Ho	Er	Tm	Yb	Lu	Hf	Ta	W	Tl	Pb	Bi	Th	U
Units	ppm	ppm	ppm	ppm	ppm	ppm	ppm	ppm	ppm	ppm	ppm	ppm	ppm	ppm	ppm	ppm	ppm	ppm	ppm	ppm	ppm	ppm
Analytical Method	AL 4b2std	AL 4b2std	AL 4b2std	AL 4b2std	AL 4b2std	AL 4b2std	AL 4b2std	AL 4b2std	AL 4b2std	AL 4b2std	AL 4b2std	AL 4b2std	AL 4b2std	AL 4b2std	AL 4b2std	AL 4b2std	AL Trace	AL Trace	AL Trace	AL Trace	AL Trace	AL Trace
JHC-07-045	-99	-99	-99	-99	-99	-99	-99	-99	-99	-99	-99	-99	-99	-99	-99	-99	-99	-99	165	-99	-99	-99
JHC-07-047	-99	-99	-99	-99	-99	-99	-99	-99	-99	-99	-99	-99	-99	-99	-99	-99	-99	-99	12	-99	-99	-99
JHC-07-048	11.0	28.5	3.88	18.6	5.9	2.14	6.8	1.3	7.7	1.5	4.5	0.64	4.0	0.59	4.5	0.4	-99	<d.L.	13	-99	1.6	0.6
JHC-07-049	-99	-99	-99	-99	-99	-99	-99	-99	-99	-99	-99	-99	-99	-99	-99	-99	-99	-99	290	-99	-99	-99
JHC-07-050	-99	-99	-99	-99	-99	-99	-99	-99	-99	-99	-99	-99	-99	-99	-99	-99	-99	-99	20	-99	-99	-99
JHC-07-052	-99	-99	-99	-99	-99	-99	-99	-99	-99	-99	-99	-99	-99	-99	-99	-99	-99	-99	76	-99	-99	-99
JHC-07-053	-99	-99	-99	-99	-99	-99	-99	-99	-99	-99	-99	-99	-99	-99	-99	-99	-99	-99	20	-99	-99	-99
JHC-07-054	19.6	41.0	4.58	18.7	5.1	1.17	5.7	1.1	7.1	1.6	4.9	0.77	5.1	0.79	4.2	0.3	1	0.7	9	-99	7.4	3.7
JHC-07-060	-99	-99	-99	-99	-99	-99	-99	-99	-99	-99	-99	-99	-99	-99	-99	-99	-99	-99	13	-99	-99	-99
JHC-07-061	17.9	37.9	4.42	18.6	5.3	1.19	6.3	1.2	8.0	1.7	5.6	0.89	5.8	0.91	4.5	0.2	-99	<d.L.	1	-99	7.2	1.8
JHC-07-062	15.3	30.2	3.42	15.6	4.4	0.86	4.7	0.9	5.9	1.3	3.9	0.60	4.0	0.62	3.5	0.2	-99	<d.L.	2	-99	6.1	1.6
JHC-07-063	15.4	34.9	4.41	19.9	5.5	2.20	6.0	1.0	6.1	1.2	3.6	0.52	3.2	0.47	5.1	0.9	2	1.1	5	-99	1.4	0.5
JHC-07-064	-99	-99	-99	-99	-99	-99	-99	-99	-99	-99	-99	-99	-99	-99	-99	-99	-99	-99	52	-99	-99	-99
JHC-07-065	24.7	52.0	5.97	24.8	6.7	1.64	7.4	1.3	8.3	1.8	5.6	0.88	5.8	0.88	6.0	0.4	1	2.5	9	-99	9.5	3.3
JHC-07-066	-99	-99	-99	-99	-99	-99	-99	-99	-99	-99	-99	-99	-99	-99	-99	-99	-99	-99	41	-99	-99	-99
JHC-07-070	-99	-99	-99	-99	-99	-99	-99	-99	-99	-99	-99	-99	-99	-99	-99	-99	-99	-99	7	-99	-99	-99
JHC-07-073	20.4	45.4	5.37	24.8	6.8	1.59	8.1	1.5	9.1	1.8	5.3	0.78	4.9	0.71	6.3	0.4	1	3.5	11	-99	9.8	7
JHC-07-075	-99	-99	-99	-99	-99	-99	-99	-99	-99	-99	-99	-99	-99	-99	-99	-99	-99	-99	6	-99	-99	-99
JHC-07-076	-99	-99	-99	-99	-99	-99	-99	-99	-99	-99	-99	-99	-99	-99	-99	-99	-99	-99	3	-99	-99	-99
JHC-07-077	19.5	40.3	4.49	18.7	4.8	1.14	5.5	1.0	6.6	1.4	4.4	0.68	4.4	0.70	4.4	0.4	-99	0.3	10	-99	8.1	2
JHC-07-078	2.8	6.2	0.74	3.5	1.0	0.33	1.2	0.2	1.5	0.3	0.9	0.14	0.9	0.13	0.6	<d.L.	-99	0.2	3	-99	0.7	0.5
JHC-07-079	-99	-99	-99	-99	-99	-99	-99	-99	-99	-99	-99	-99	-99	-99	-99	-99	-99	-99	<d.L.	-99	-99	-99
JHC-07-080	-99	-99	-99	-99	-99	-99	-99	-99	-99	-99	-99	-99	-99	-99	-99	-99	-99	-99	4	-99	-99	-99
JHC-07-081	1.4	3.3	0.41	2.2	0.8	0.43	1.2	0.2	1.7	0.4	1.2	0.19	1.3	0.19	0.5	<d.L.	-99	<d.L.	6	-99	0.4	0.2
JHC-07-082	-99	-99	-99	-99	-99	-99	-99	-99	-99	-99	-99	-99	-99	-99	-99	-99	-99	-99	2	-99	-99	-99
JHC-07-083	7.3	12.7	1.37	5.5	1.4	0.17	1.2	0.2	1.2	0.2	0.8	0.15	1.0	0.17	1.6	0.1	2	1.9	16839	9.8	1.9	10.5
JHC-07-084	5.5	10.3	1.12	4.5	1.1	0.24	0.9	0.1	0.9	0.2	0.8	0.14	1.0	0.18	1.9	0.1	3	1.5	<d.L.	0.7	1.8	1.3
JHC-07-085	4.7	11.1	1.33	6.4	1.9	0.22	2.5	0.5	3.5	0.8	2.5	0.39	2.6	0.41	1.0	<d.L.	2	0.9	1	-99	1.1	0.7
JHC-07-086	-99	-99	-99	-99	-99	-99	-99	-99	-99	-99	-99	-99	-99	-99	-99	-99	-99	-99	157	-99	-99	-99
JHC-07-087	-99	-99	-99	-99	-99	-99	-99	-99	-99	-99	-99	-99	-99	-99	-99	-99	-99	-99	6	-99	-99	-99
JHC-07-088	5.3	11.4	1.36	6.3	1.8	0.66	2.3	0.5	3.3	0.7	2.5	0.41	2.7	0.44	1.1	<d.L.	-99	0.7	1	-99	1.2	3.3
JHC-07-091	2.0	4.2	0.49	2.2	0.6	0.19	0.9	0.2	1.5	0.3	1.0	0.17	1.1	0.18	0.7	<d.L.	-99	1.2	1358	0.5	0.8	1.6
JHC-07-093	-99	-99	-99	-99	-99	-99	-99	-99	-99	-99	-99	-99	-99	-99	-99	-99	-99	-99	13	-99	-99	-99
JHC-07-094	2.6	6.7	0.87	4.4	1.4	0.16	1.5	0.3	1.8	0.4	1.3	0.21	1.5	0.25	1.0	<d.L.	-99	0.4	5	1.2	1.1	0.8
JHC-07-095	-99	-99	-99	-99	-99	-99	-99	-99	-99	-99	-99	-99	-99	-99	-99	-99	-99	-99	3380	-99	-99	-99
JHC-07-096	-99	-99	-99	-99	-99	-99	-99	-99	-99	-99	-99	-99	-99	-99	-99	-99	-99	-99	1859	-99	-99	-99
JHC-07-097	2.6	5.9	0.69	2.9	0.7	0.00	0.5	0.0	0.4	0.1	0.4	0.08	0.7	0.12	1.3	<d.L.	-99	0.9	3	0.4	1.4	1
JHC-07-098	-99	-99	-99	-99	-99	-99	-99	-99	-99	-99	-99	-99	-99	-99	-99	-99	-99	-99	622	-99	-99	-99
JHC-07-099	-99	-99	-99	-99	-99	-99	-99	-99	-99	-99	-99	-99	-99	-99	-99	-99	-99	-99	5515	-99	-99	-99
JHC-07-100	-99	-99	-99	-99	-99	-99	-99	-99	-99	-99	-99	-99	-99	-99	-99	-99	-99	-99	1239	-99	-99	-99
JHC-07-101	6.2	13.2	1.49	5.7	1.3	0.17	0.8	0.1	0.6	0.1	0.6	0.11	0.9	0.16	2.2	0.2	-99	2.4	<d.L.	-99	2	1
JHC-07-102	-99	-99	-99	-99	-99	-99	-99	-99	-99	-99	-99	-99	-99	-99	-99	-99	-99	-99	9	-99	-99	-99
JHC-07-103	4.5	9.8	1.17	5.5	1.6	1.07	2.0	0.4	2.6	0.6	2.0	0.33	2.2	0.34	1.2	<d.L.	-99	4.4	28	-99	1.3	1.5
JHC-07-104	-99	-99	-99	-99	-99	-99	-99	-99	-99	-99	-99	-99	-99	-99	-99	-99	-99	-99	59	-99	-99	-99

Appendix 1B: Lithogeochemistry data table for samples analyzed from TVB

SampleNumber	La	Ce	Pr	Nd	Sm	Eu	Gd	Tb	Dy	Ho	Er	Tm	Yb	Lu	Hf	Ta	W	Tl	Pb	Bi	Th	U
Units	ppm	ppm	ppm	ppm	ppm	ppm	ppm	ppm	ppm	ppm	ppm	ppm	ppm	ppm	ppm	ppm	ppm	ppm	ppm	ppm	ppm	ppm
Analytical Method	AL 4b2std	AL 4b2std	AL 4b2std	AL 4b2std	AL 4b2std	AL 4b2std	AL 4b2std	AL 4b2std	AL 4b2std	AL 4b2std	AL 4b2std	AL 4b2std	AL 4b2std	AL 4b2std	AL 4b2std	AL 4b2std	AL Trace	AL Trace	AL Trace	AL Trace	AL Trace	AL Trace
JHC-07-106	-99	-99	-99	-99	-99	-99	-99	-99	-99	-99	-99	-99	-99	-99	-99	-99	-99	-99	24	-99	-99	-99
JHC-07-107	6.2	13.3	1.51	6.5	1.7	0.40	2.1	0.4	2.7	0.6	1.9	0.32	2.1	0.34	1.7	0.1	-99	0.4	4	-99	2.4	1.4
JHC-07-108	-99	-99	-99	-99	-99	-99	-99	-99	-99	-99	-99	-99	-99	-99	-99	-99	-99	-99	<d.L.	-99	-99	-99
JHC-07-109	-99	-99	-99	-99	-99	-99	-99	-99	-99	-99	-99	-99	-99	-99	-99	-99	-99	-99	<d.L.	-99	-99	-99
JHC-07-110	-99	-99	-99	-99	-99	-99	-99	-99	-99	-99	-99	-99	-99	-99	-99	-99	-99	-99	9	-99	-99	-99
JHC-07-111	-99	-99	-99	-99	-99	-99	-99	-99	-99	-99	-99	-99	-99	-99	-99	-99	-99	-99	<d.L.	-99	-99	-99
JHC-07-112	-99	-99	-99	-99	-99	-99	-99	-99	-99	-99	-99	-99	-99	-99	-99	-99	-99	-99	12245	-99	-99	-99
JHC-07-113	3.2	7.6	0.92	4.6	1.4	0.11	1.8	0.4	2.5	0.6	1.7	0.28	1.8	0.29	1.0	<d.L.	2	0.6	41	-99	1.1	0.6
JHC-07-114	2.8	6.8	0.88	4.4	1.4	0.15	1.6	0.3	2.0	0.4	1.4	0.21	1.4	0.23	0.9	<d.L.	2	0.5	108	-99	1	0.6
JHC-07-115	-99	-99	-99	-99	-99	-99	-99	-99	-99	-99	-99	-99	-99	-99	-99	-99	-99	-99	17	-99	-99	-99
JHC-07-116	5.7	12.5	1.46	6.9	2.0	0.56	2.5	0.5	3.2	0.7	2.3	0.36	2.5	0.39	1.2	0.1	-99	1.6	11	-99	1.2	3.5
JHC-07-119	5.0	11.6	1.42	6.8	2.1	0.71	2.2	0.4	2.9	0.6	1.9	0.31	2.1	0.32	1.2	<d.L.	-99	0.9	336	-99	1.3	1.9
JHC-07-120	-99	-99	-99	-99	-99	-99	-99	-99	-99	-99	-99	-99	-99	-99	-99	-99	-99	-99	12	-99	-99	-99
JHC-07-121	-99	-99	-99	-99	-99	-99	-99	-99	-99	-99	-99	-99	-99	-99	-99	-99	-99	-99	33	-99	-99	-99
JHC-07-122	-99	-99	-99	-99	-99	-99	-99	-99	-99	-99	-99	-99	-99	-99	-99	-99	-99	-99	4	-99	-99	-99
JHC-07-123	5.9	12.5	1.40	6.0	1.7	0.45	1.9	0.4	2.5	0.5	1.7	0.28	1.9	0.31	1.8	0.1	-99	0.3	24	-99	2.3	1.1
JHC-07-124	-99	-99	-99	-99	-99	-99	-99	-99	-99	-99	-99	-99	-99	-99	-99	-99	-99	-99	<d.L.	-99	-99	-99
JHC-07-125	4.8	11.3	1.34	6.4	2.0	0.73	2.2	0.4	2.8	0.6	1.9	0.30	2.0	0.31	1.5	0.1	-99	<d.L.	<d.L.	-99	1.8	0.9
JHC-07-126	-99	-99	-99	-99	-99	-99	-99	-99	-99	-99	-99	-99	-99	-99	-99	-99	-99	-99	2	-99	-99	-99
JHC-07-127	2.4	5.6	0.67	3.1	0.9	0.37	1.1	0.2	1.4	0.3	0.9	0.15	1.0	0.17	0.7	<d.L.	-99	<d.L.	1	-99	0.7	0.4
JHC-07-128	3.1	7.0	0.83	4.0	1.2	0.50	1.5	0.3	2.0	0.5	1.4	0.22	1.5	0.24	1.0	<d.L.	-99	0.5	23	-99	1	0.5
JHC-07-129	-99	-99	-99	-99	-99	-99	-99	-99	-99	-99	-99	-99	-99	-99	-99	-99	-99	-99	9	-99	-99	-99
JHC-07-133	-99	-99	-99	-99	-99	-99	-99	-99	-99	-99	-99	-99	-99	-99	-99	-99	-99	-99	55	-99	-99	-99
JHC-07-134	-99	-99	-99	-99	-99	-99	-99	-99	-99	-99	-99	-99	-99	-99	-99	-99	-99	-99	3	-99	-99	-99
JHC-07-135	6.6	16.4	2.19	11.9	4.1	1.57	5.8	1.2	8.1	1.8	5.7	0.87	5.6	0.87	2.1	<d.L.	-99	0.3	1	-99	0.9	0.5
JHC-07-136	3.3	7.9	0.92	4.3	1.3	0.36	1.6	0.3	2.1	0.5	1.5	0.23	1.6	0.27	1.5	0.1	-99	0.1	1	-99	1.8	1.6
JHC-07-137	-99	-99	-99	-99	-99	-99	-99	-99	-99	-99	-99	-99	-99	-99	-99	-99	-99	-99	14	-99	-99	-99
JHC-07-138	2.4	5.6	0.64	3.0	0.9	0.39	1.2	0.2	1.7	0.4	1.2	0.19	1.3	0.20	1.1	<d.L.	-99	0.1	2	-99	1.2	0.7
JHC-07-139	-99	-99	-99	-99	-99	-99	-99	-99	-99	-99	-99	-99	-99	-99	-99	-99	-99	-99	<d.L.	-99	-99	-99
JHC-07-140	-99	-99	-99	-99	-99	-99	-99	-99	-99	-99	-99	-99	-99	-99	-99	-99	-99	-99	3	-99	-99	-99
JHC-07-141	-99	-99	-99	-99	-99	-99	-99	-99	-99	-99	-99	-99	-99	-99	-99	-99	-99	-99	24	-99	-99	-99
JHC-07-142	4.4	10.6	1.32	6.1	1.8	0.67	2.1	0.4	2.7	0.6	2.1	0.35	2.4	0.39	0.9	<d.L.	-99	0.4	3	-99	1	1.6
JHC-07-143	-99	-99	-99	-99	-99	-99	-99	-99	-99	-99	-99	-99	-99	-99	-99	-99	-99	-99	8	-99	-99	-99
JHC-07-147	-99	-99	-99	-99	-99	-99	-99	-99	-99	-99	-99	-99	-99	-99	-99	-99	-99	-99	14	-99	-99	-99
JHC-07-150	-99	-99	-99	-99	-99	-99	-99	-99	-99	-99	-99	-99	-99	-99	-99	-99	-99	-99	23	-99	-99	-99
JHC-07-151	11.0	22.4	2.38	8.3	1.8	0.40	0.6	0.0	0.3	0.0	0.4	0.08	0.7	0.13	1.8	<d.L.	1	<d.L.	5	-99	3.6	0.8
JHC-07-152	13.8	32.0	3.47	14.6	3.9	0.84	3.0	0.5	3.3	0.7	2.5	0.43	3.0	0.50	2.3	<d.L.	1	<d.L.	17	-99	3.8	2.2
JHC-07-153	10.7	22.7	2.56	10.9	2.7	0.52	2.3	0.4	2.5	0.6	1.9	0.31	2.1	0.34	2.0	<d.L.	-99	<d.L.	14	-99	3.4	1.7
JHC-07-156	12.6	26.2	2.96	13.1	3.7	0.88	4.1	0.7	4.9	1.1	3.3	0.51	3.2	0.50	2.2	<d.L.	2	<d.L.	4	-99	3.6	1.7
JHC-07-158	-99	-99	-99	-99	-99	-99	-99	-99	-99	-99	-99	-99	-99	-99	-99	-99	-99	-99	7	-99	-99	-99

Appendix 1B: Lithogeochemistry data table for samples analyzed from TVB

SampleNumber	La	Ce	Pr	Nd	Sm	Eu	Gd	Tb	Dy	Ho	Er	Tm	Yb	Lu	Hf	Ta	W	Tl	Pb	Bi	Th	U
Units	ppm	ppm	ppm	ppm	ppm	ppm	ppm	ppm	ppm	ppm	ppm	ppm	ppm	ppm	ppm	ppm	ppm	ppm	ppm	ppm	ppm	ppm
Analytical Method	AL 4b2std	AL 4b2std	AL 4b2std	AL 4b2std	AL 4b2std	AL 4b2std	AL 4b2std	AL 4b2std	AL 4b2std	AL 4b2std	AL 4b2std	AL 4b2std	AL 4b2std	AL 4b2std	AL 4b2std	AL 4b2std	AL Trace	AL Trace	AL Trace	AL Trace	AL Trace	AL Trace
JHC-07-160	6.2	12.8	1.48	6.6	1.9	0.61	2.0	0.4	2.5	0.6	1.7	0.27	1.8	0.29	0.9	<d.L.	-99	0.2	1	-99	1.3	0.6
JHC-07-162	-99	-99	-99	-99	-99	-99	-99	-99	-99	-99	-99	-99	-99	-99	-99	-99	-99	-99	3	-99	-99	-99
JHC-07-163	-99	-99	-99	-99	-99	-99	-99	-99	-99	-99	-99	-99	-99	-99	-99	-99	-99	-99	7	-99	-99	-99
JHC-07-165	6.9	15.2	1.74	7.6	2.1	0.47	2.1	0.4	2.4	0.6	1.8	0.30	2.0	0.32	1.5	<d.L.	-99	0.2	4	-99	2.3	1
JHC-07-166	7.4	16.1	1.85	8.1	2.3	0.53	2.1	0.4	2.4	0.5	1.8	0.29	1.9	0.32	1.7	<d.L.	-99	0.2	3	-99	2.4	1.3
JHC-07-167	-99	-99	-99	-99	-99	-99	-99	-99	-99	-99	-99	-99	-99	-99	-99	-99	-99	-99	206	-99	-99	-99
JHC-07-168	5.1	11.4	1.37	6.7	2.1	0.56	2.6	0.5	3.5	0.8	2.5	0.39	2.6	0.42	1.7	<d.L.	1	0.2	2	-99	1.8	1.4
JHC-07-170	-99	-99	-99	-99	-99	-99	-99	-99	-99	-99	-99	-99	-99	-99	-99	-99	-99	-99	11	-99	-99	-99
JHC-07-171	29.1	59.2	6.44	25.5	6.0	1.36	6.0	1.1	6.8	1.4	4.4	0.70	4.6	0.73	7.8	1.5	-99	0.5	9	-99	9.1	2.6
JHC-07-172	-99	-99	-99	-99	-99	-99	-99	-99	-99	-99	-99	-99	-99	-99	-99	-99	-99	-99	10	-99	-99	-99
JHC-07-173	-99	-99	-99	-99	-99	-99	-99	-99	-99	-99	-99	-99	-99	-99	-99	-99	-99	-99	4	-99	-99	-99
JHC-07-174	3.5	8.9	1.19	6.4	2.1	0.82	2.3	0.4	2.5	0.5	1.5	0.21	1.3	0.19	1.1	<d.L.	-99	0.6	1	-99	1.2	4.1
JHC-07-175	6.0	13.5	1.60	7.7	2.4	0.83	2.9	0.6	3.9	0.9	2.7	0.42	2.9	0.46	1.5	<d.L.	4	0.5	8	-99	1.4	1.3
JHC-07-176	-99	-99	-99	-99	-99	-99	-99	-99	-99	-99	-99	-99	-99	-99	-99	-99	-99	-99	37	-99	-99	-99
JHC-07-180	-99	-99	-99	-99	-99	-99	-99	-99	-99	-99	-99	-99	-99	-99	-99	-99	-99	-99	42	-99	-99	-99
JHC-07-181	22.1	48.0	5.46	22.9	5.7	1.91	5.5	0.9	5.5	1.1	3.3	0.49	3.1	0.48	5.5	0.9	3	0.2	5	1.1	4.2	1.2
JHC-07-182	-99	-99	-99	-99	-99	-99	-99	-99	-99	-99	-99	-99	-99	-99	-99	-99	-99	-99	9	-99	-99	-99
JHC-07-184	-99	-99	-99	-99	-99	-99	-99	-99	-99	-99	-99	-99	-99	-99	-99	-99	-99	-99	6	-99	-99	-99
JHC-07-187	25.0	49.8	5.29	19.9	4.6	1.21	3.8	0.6	3.2	0.6	1.9	0.28	1.8	0.27	3.1	0.2	-99	0.4	2	-99	9.1	3.4
JHC-07-188	27.4	58.5	6.52	26.8	6.2	1.56	5.7	1.0	5.7	1.2	3.6	0.57	3.7	0.56	7.0	1.1	1	0.1	2	0.5	6.5	1.9
JHC-07-190	-99	-99	-99	-99	-99	-99	-99	-99	-99	-99	-99	-99	-99	-99	-99	-99	-99	-99	2	-99	-99	-99
JHC-07-191	3.6	8.0	0.97	4.7	1.4	0.53	1.7	0.3	2.3	0.5	1.6	0.26	1.7	0.28	0.9	<d.L.	-99	<d.L.	<d.L.	-99	1	0.7
JHC-07-193	-99	-99	-99	-99	-99	-99	-99	-99	-99	-99	-99	-99	-99	-99	-99	-99	-99	-99	2	-99	-99	-99
JHC-07-194	-99	-99	-99	-99	-99	-99	-99	-99	-99	-99	-99	-99	-99	-99	-99	-99	-99	-99	3	-99	-99	-99
JHC-07-195	-99	-99	-99	-99	-99	-99	-99	-99	-99	-99	-99	-99	-99	-99	-99	-99	-99	-99	14	-99	-99	-99
JHC-07-196	24.7	49.0	5.24	20.2	4.8	1.28	4.2	0.6	3.7	0.8	2.4	0.37	2.4	0.39	2.9	0.2	-99	0.6	<d.L.	-99	8.8	3.1
JHC-07-198	5.0	10.8	1.29	6.1	1.9	0.56	2.4	0.5	3.3	0.7	2.4	0.38	2.5	0.39	1.3	<d.L.	-99	0.3	6	-99	1.6	1.3
JHC-07-207	4.2	10.2	1.27	6.3	2.0	0.79	2.6	0.5	3.5	0.8	2.4	0.38	2.5	0.40	1.7	<d.L.	2	0.5	37	-99	1.2	1.2
JHC-07-208	-99	-99	-99	-99	-99	-99	-99	-99	-99	-99	-99	-99	-99	-99	-99	-99	-99	-99	30	-99	-99	-99
JHC-07-211	-99	-99	-99	-99	-99	-99	-99	-99	-99	-99	-99	-99	-99	-99	-99	-99	-99	-99	<d.L.	-99	-99	-99
JHC-07-213	-99	-99	-99	-99	-99	-99	-99	-99	-99	-99	-99	-99	-99	-99	-99	-99	-99	-99	<d.L.	-99	-99	-99
JHC-07-215	4.0	8.9	1.06	5.0	1.6	0.49	1.9	0.4	2.6	0.6	1.9	0.29	1.9	0.30	1.0	<d.L.	-99	<d.L.	<d.L.	-99	1.2	0.7
JHC-07-216	-99	-99	-99	-99	-99	-99	-99	-99	-99	-99	-99	-99	-99	-99	-99	-99	-99	-99	22	-99	-99	-99
JHC-07-217	13.6	31.3	3.97	18.5	5.3	1.95	5.6	1.0	6.0	1.2	3.5	0.50	3.2	0.47	3.6	1.1	-99	<d.L.	<d.L.	-99	1.2	0.4
JHC-07-219	1.9	4.5	0.56	2.9	1.0	0.37	1.3	0.3	2.0	0.5	1.5	0.24	1.7	0.27	0.7	<d.L.	-99	0.2	9	-99	0.4	0.3
JHC-07-220	0.7	1.7	0.23	1.4	0.6	0.42	0.8	0.2	1.1	0.2	0.7	0.12	0.8	0.12	0.5	<d.L.	4	0.1	<d.L.	-99	0.2	0.3
JHC-07-221	-99	-99	-99	-99	-99	-99	-99	-99	-99	-99	-99	-99	-99	-99	-99	-99	-99	-99	9	-99	-99	-99
JHC-07-222	0.7	1.8	0.24	1.5	0.6	0.24	1.1	0.2	1.9	0.5	1.5	0.24	1.6	0.27	0.5	<d.L.	-99	0.2	11	-99	0.3	0.2
JHC-07-226	-99	-99	-99	-99	-99	-99	-99	-99	-99	-99	-99	-99	-99	-99	-99	-99	-99	-99	15	-99	-99	-99
JHC-07-229	2.8	6.7	0.81	4.2	1.4	0.38	2.0	0.4	3.1	0.7	2.3	0.38	2.6	0.41	0.9	<d.L.	-99	<d.L.	4	-99	0.7	0.4
JHC-07-230	1.4	3.3	0.43	2.5	0.9	0.31	1.4	0.3	2.1	0.5	1.6	0.24	1.6	0.28	0.6	<d.L.	-99	0.2	<d.L.	-99	0.4	0.2
JHC-07-231	1.8	4.4	0.59	3.3	1.2	0.65	1.7	0.4	2.7	0.6	1.9	0.29	2.0	0.31	0.9	<d.L.	3	0.2	16	-99	0.4	0.5
JHC-07-233	-99	-99	-99	-99	-99	-99	-99	-99	-99	-99	-99	-99	-99	-99	-99	-99	-99	-99	6	-99	-99	-99
JHC-07-236	1.9	4.6	0.60	3.4	1.2	0.31	1.8	0.4	2.9	0.7	2.2	0.36	2.5	0.41	0.9	<d.L.	-99	0.1	<d.L.	-99	0.5	0.4

Appendix 1B: Lithogeochemistry data table for samples analyzed from TVB

SampleNumber	La	Ce	Pr	Nd	Sm	Eu	Gd	Tb	Dy	Ho	Er	Tm	Yb	Lu	Hf	Ta	W	Tl	Pb	Bi	Th	U
Units	ppm	ppm	ppm	ppm	ppm	ppm	ppm	ppm	ppm	ppm	ppm	ppm	ppm	ppm	ppm	ppm	ppm	ppm	ppm	ppm	ppm	ppm
Analytical Method	AL 4b2std	AL 4b2std	AL 4b2std	AL 4b2std	AL 4b2std	AL 4b2std	AL 4b2std	AL 4b2std	AL 4b2std	AL 4b2std	AL 4b2std	AL 4b2std	AL 4b2std	AL 4b2std	AL 4b2std	AL 4b2std	AL Trace	AL Trace	AL Trace	AL Trace	AL Trace	AL Trace
JHC-07-242	-99	-99	-99	-99	-99	-99	-99	-99	-99	-99	-99	-99	-99	-99	-99	-99	-99	-99	1	-99	-99	-99
JHC-07-245	0.9	2.4	0.35	2.2	0.9	0.30	1.3	0.3	1.9	0.4	1.3	0.20	1.3	0.21	0.5	<d.L.	-99	<d.L.	<d.L.	-99	0.3	0.2
JHC-07-246	-99	-99	-99	-99	-99	-99	-99	-99	-99	-99	-99	-99	-99	-99	-99	-99	-99	-99	<d.L.	-99	-99	-99
JHC-07-248	-99	-99	-99	-99	-99	-99	-99	-99	-99	-99	-99	-99	-99	-99	-99	-99	-99	-99	2	-99	-99	-99
JHC-07-252	14.3	33.7	3.90	16.1	4.2	0.64	4.7	0.9	6.1	1.4	4.4	0.70	4.7	0.75	4.2	0.3	6	<d.L.	14	-99	5.1	1.6
JHC-07-254	-99	-99	-99	-99	-99	-99	-99	-99	-99	-99	-99	-99	-99	-99	-99	-99	-99	-99	2	-99	-99	-99
JHC-07-255	10.0	22.2	2.56	10.4	2.8	0.74	3.5	0.7	4.4	1.0	3.2	0.52	3.5	0.57	3.2	0.2	-99	0.1	4	-99	3.4	2.3
JHC-07-256	15.4	33.9	3.91	16.9	4.8	0.92	5.1	1.0	6.0	1.3	4.1	0.66	4.5	0.72	4.5	0.3	-99	0.7	2	-99	5.4	1.5
JHC-07-259	-99	-99	-99	-99	-99	-99	-99	-99	-99	-99	-99	-99	-99	-99	-99	-99	-99	-99	7	-99	-99	-99
JHC-07-260	-99	-99	-99	-99	-99	-99	-99	-99	-99	-99	-99	-99	-99	-99	-99	-99	-99	-99	4	-99	-99	-99
JHC-07-261	-99	-99	-99	-99	-99	-99	-99	-99	-99	-99	-99	-99	-99	-99	-99	-99	-99	-99	4	-99	-99	-99
JHC-07-262	20.4	43.2	4.81	18.4	4.5	0.64	5.4	1.1	7.2	1.6	4.9	0.79	5.3	0.83	6.1	0.4	-99	0.3	<d.L.	-99	7.2	1.8
JHC-07-264	10.8	24.5	2.92	12.9	3.6	1.00	4.3	0.8	5.4	1.2	3.7	0.57	3.8	0.61	3.5	0.2	1	0.1	3	7.2	3.7	1.1
JHC-07-265	10.5	23.3	2.83	12.5	3.6	0.74	4.0	0.8	4.8	1.0	3.3	0.52	3.5	0.54	3.3	0.3	1	0.2	5	-99	3.4	1
JHC-07-266	-99	-99	-99	-99	-99	-99	-99	-99	-99	-99	-99	-99	-99	-99	-99	-99	-99	-99	14	-99	-99	-99
JHC-07-267	-99	-99	-99	-99	-99	-99	-99	-99	-99	-99	-99	-99	-99	-99	-99	-99	-99	-99	28	-99	-99	-99
JHC-07-268	2.8	6.3	0.78	3.5	0.9	0.41	0.7	0.1	0.7	0.1	0.4	0.06	0.4	0.07	1.5	0.2	4	5.8	19	-99	0.8	2.3
JHC-07-271	-99	-99	-99	-99	-99	-99	-99	-99	-99	-99	-99	-99	-99	-99	-99	-99	-99	-99	174	-99	-99	-99
JHC-07-272	-99	-99	-99	-99	-99	-99	-99	-99	-99	-99	-99	-99	-99	-99	-99	-99	-99	-99	3	-99	-99	-99
JHC-07-273	14.4	31.5	3.74	16.9	4.8	1.08	5.0	0.9	6.0	1.3	4.2	0.66	4.4	0.72	3.7	0.2	-99	0.5	9	-99	4	1.2
JHC-07-275	-99	-99	-99	-99	-99	-99	-99	-99	-99	-99	-99	-99	-99	-99	-99	-99	-99	-99	176	-99	-99	-99
JHC-07-276	18.2	39.4	4.58	19.9	5.3	0.81	5.6	1.0	6.6	1.5	4.5	0.70	4.8	0.75	4.5	0.3	-99	0.9	19	-99	5.4	1.4
JHC-07-277	-99	-99	-99	-99	-99	-99	-99	-99	-99	-99	-99	-99	-99	-99	-99	-99	-99	-99	19	-99	-99	-99
JHC-07-278	-99	-99	-99	-99	-99	-99	-99	-99	-99	-99	-99	-99	-99	-99	-99	-99	-99	-99	7	-99	-99	-99
JHC-07-279	-99	-99	-99	-99	-99	-99	-99	-99	-99	-99	-99	-99	-99	-99	-99	-99	-99	-99	14	-99	-99	-99
JHC-07-280	16.5	35.9	4.30	20.9	6.4	1.50	7.3	1.3	8.8	1.9	5.9	0.89	5.9	0.93	4.9	0.3	-99	1.5	1	-99	5.1	1.9
JHC-07-281	-99	-99	-99	-99	-99	-99	-99	-99	-99	-99	-99	-99	-99	-99	-99	-99	-99	-99	161	-99	-99	-99
JHC-07-282	-99	-99	-99	-99	-99	-99	-99	-99	-99	-99	-99	-99	-99	-99	-99	-99	-99	-99	3306	-99	-99	-99
JHC-07-283	15.7	34.2	3.97	17.9	5.0	1.11	6.1	1.2	7.8	1.7	5.3	0.83	5.6	0.88	5.1	0.3	-99	0.3	3	1.1	5.9	1.6
JHC-07-284	11.1	24.6	2.86	12.4	3.5	0.72	4.1	0.8	5.1	1.1	3.5	0.55	3.7	0.57	3.7	0.2	-99	0.1	6	-99	4.2	1.4
JHC-07-285	13.1	28.9	3.50	15.9	4.5	1.06	5.5	1.0	6.6	1.4	4.3	0.66	4.3	0.70	3.7	0.2	-99	0.1	8	-99	4.1	1.2
JHC-07-286	-99	-99	-99	-99	-99	-99	-99	-99	-99	-99	-99	-99	-99	-99	-99	-99	-99	-99	<d.L.	-99	-99	-99
JHC-07-287	-99	-99	-99	-99	-99	-99	-99	-99	-99	-99	-99	-99	-99	-99	-99	-99	-99	-99	4	-99	-99	-99
JHC-07-289	-99	-99	-99	-99	-99	-99	-99	-99	-99	-99	-99	-99	-99	-99	-99	-99	-99	-99	3	-99	-99	-99
JHC-07-290	-99	-99	-99	-99	-99	-99	-99	-99	-99	-99	-99	-99	-99	-99	-99	-99	-99	-99	39	-99	-99	-99
JHC-07-291	12.1	27.2	3.16	13.6	3.7	0.78	4.0	0.8	5.3	1.2	3.8	0.61	4.2	0.67	4.2	0.3	-99	0.3	3	-99	5.1	1.3
JHC-07-292	-99	-99	-99	-99	-99	-99	-99	-99	-99	-99	-99	-99	-99	-99	-99	-99	-99	-99	7	-99	-99	-99
JHC-07-293	8.9	18.8	2.25	10.5	3.2	0.63	3.6	0.7	4.1	0.9	2.7	0.42	2.7	0.42	2.4	0.1	-99	0.1	5	-99	3.1	1

Appendix 1B: Lithogeochemistry data table for samples analyzed from TVB

SampleNumber	Au	Mn	P	Sc	AI	CCPI	AAAI	Na/K	Zr/Y
Units	ppb	ppm	ppm	ppm					
Analytical Method	INAA	GS Trace	GS Trace	GS Trace					
JHC-06-001	-99	1202	276	45.3	42	88	29	36.92	1.4
JHC-06-002	-99	1512	103	61.6	59	90	24	33.94	
JHC-06-003	-99	655	262	16.5	47	53	52	0.96	1.8
JHC-06-005	-99	945	213	10.9	97	97	45	0.25	2.5
JHC-06-006	-99	232	295	17.9	88	68	82	0.16	
JHC-06-008	-99	461	99	19.6	92	75	71	0.19	1.8
JHC-06-009	-99	68	195	10.8	22	40	66	3.79	
JHC-06-010	3250	159	44	7.4	88	93	88	0.12	
JHC-06-011	-99	1211	572	32.4	85	67	37	0.35	
JHC-06-012	-99	161	254	17.9	83	59	81	0.24	2.2
JHC-06-013	479	175	6	0.8	0	100	97		
JHC-06-014	547	1104	511	2.3	11	99	3	11.59	
JHC-06-015	-99	381	152	24.8	87	68	70	0.27	1.6
JHC-06-017	19	299	220	14.8	84	89	77	0.20	
JHC-06-018	-99	1701	332	12	98	98	14	0.35	3.1
JHC-06-019	-99	1277	264	42.5	42	88	28		1.5
JHC-06-020	-99	1362	276	45.4	42	86	26	258.14	
JHC-06-021	-99	1630	92	57.8	45	94	22	2.13	0.9
JHC-06-022	-99	48	203	8.9	21	26	72	3.88	0.7
JHC-06-023	-99	1567	546	20.9	94	88	19	0.11	1.6
JHC-06-024	222	252	45	1.3	92	100	47		
JHC-06-025	146	442	202	1.1	26	100	33		
JHC-06-026	379	299	16	1.5	77	100	77		
JHC-06-027	118	410	1124	1.9	60	100	13	2.25	
JHC-06-028	7	1268	89	16.3	98	98	22	0.18	1.3
JHC-06-030	40	320	76	7.3	82	96	83	0.24	
JHC-06-031	-99	166	46	7.7	89	44	83	0.05	
JHC-06-032	-99	26	22	8.7	93	52	94	0.08	
JHC-06-033	-99	527	31	9.4	88	61	74	0.18	2.3
JHC-06-034	-99	1595	223	47.2	71	92	20	2.06	1.2
JHC-06-035	-99	336	19	9.3	36	35	63	2.56	
JHC-06-036	-99	2662	233	45.9	61	76	21	0.05	1.5
JHC-06-037	-99	366	78	20.8	32	45	55	2.65	1.9
JHC-06-038	-99	233	35	9.4	91	83	85	0.13	
JHC-06-039	-99	1695	36	13.5	93	78	55	0.06	2.6
JHC-06-040	-99	527	97	21.7	27	41	54	4.31	1.8
JHC-06-041	176	302	68	12.8	93	87	76	0.06	
JHC-06-042	-99	336	85	21.2	27	47	53	11.15	
JHC-06-043	-99	266	58	14	71	46	62	0.41	2.4
JHC-06-044	-99	558	116	19.4	10	35	44	9.31	2.0
JHC-06-045	-99	964	649	27.1	46	74	36	3.38	
JHC-06-047	-99	238	101	10.8	80	45	65	0.09	
JHC-06-048	433	815	736	9.2	87	96	53	0.08	2.4
JHC-06-050	-99	803	286	20.6	27	62	47	18.92	2.1

Appendix 1B: Lithogeochemistry data table for samples analyzed from TVB

SampleNumber	Au	Mn	P	Sc	AI	CCPI	AAAI	Na/K	Zr/Y
Units	ppb	ppm	ppm	ppm					
Analytical Method	INAA	GS Trace	GS Trace	GS Trace					
JHC-06-051	-99	476	122	19.4	34	41	54	2.39	
JHC-06-052	-99	507	257	22.6	33	46	54	1.88	
JHC-06-053	-99	618	678	24.1	34	60	37	3.97	
JHC-06-054	-99	184	61	13.6	61	40	55	0.67	
JHC-06-057	-99	138	267	9.2	46	28	64	1.16	2.4
JHC-06-059	-99	914	799	23.6	41	61	45	1.32	1.8
JHC-06-060	-99	1151	783	23.8	25	63	39	5.30	2.2
JHC-06-062	-99	1258	289	40.9	46	84	19	108.63	1.7
JHC-06-063	-99	1401	418	37.9	42	83	18	102.29	
JHC-06-064	-99	2171	324	36.9	52	88	19	46.47	1.3
JHC-06-068	-99	1101	370	40.3	67	89	26	8.09	1.4
JHC-06-069	-99	1585	416	40.6	48	86	27	87.26	2.0
JHC-06-070	-99	1700	360	39.3	76	88	26	53.69	
JHC-06-071	-99	1849	281	32.7	34	73	24	24.97	
JHC-06-072	-99	1262	516	46.4	62	81	30	1.52	
JHC-06-073	-99	266	59	8.9	92	82	62	0.25	3.7
JHC-06-074	89	1754	181	18.2	93	98	29	1.71	3.6
JHC-06-075	-99	499	193	14.2	68	79	64	0.60	
JHC-06-076	-99	759	832	21.2	59	64	42	0.46	3.6
JHC-06-077	-99	1456	120	12.5	26	53	41	6.63	
JHC-06-078	-99	916	131	10.9	22	38	51	7.12	
JHC-06-079	-99	-99	-99	-99	73	94	14	67.53	
JHC-06-082	-99	3170	269	41.2	55	86	19	167.33	1.1
JHC-06-083	23	3476	962	4.3	43	100	11	2.29	
JHC-06-086	-99	532	243	20	25	57	57	3.47	2.2
JHC-06-087	26	931	256	32.1	15	59	34	14.04	
JHC-06-088	-99	3111	529	38.1	27	73	21	27.75	2.7
JHC-06-089	-99	1155	273	40.1	50	85	19	102.92	1.8
JHC-06-091	-99	1046	505	37.7	46	71	39	4.52	
JHC-06-092	855	445	459	26.8	87	87	65	0.08	
JHC-06-095	-99	397	256	12	35	45	53	2.41	
JHC-06-097	-99	268	372	38	63	49	49	0.01	2.7
JHC-06-098	-99	1393	2605	29	36	80	20	7.76	6.7
JHC-06-100	-99	512	236	40.5	23	64	30	37.18	1.9
JHC-06-101	-99	1172	181	35.1	38	76	35	0.93	
JHC-06-102	-99	1653	182	39.5	63	72	43	1.38	
JHC-06-103	-99	7	487	3.4	16	7	75	5.38	
JHC-06-104	-99	137	423	10.8	39	49	50	4.07	
JHC-06-105	-99	559	394	38.6	58	87	36	9.78	
JHC-06-108	3	578	938	31.4	46	78	37	13.05	
JHC-06-109	-99	856	642	31.1	29	72	22	0.49	1.7
JHC-06-111	627	578	452	30.8	25	99	58	0.59	
JHC-06-112	-99	416	430	41.7	42	65	46	0.66	1.7

Appendix 1B: Lithogeochemistry data table for samples analyzed from TVB

SampleNumber	Au	Mn	P	Sc	AI	CCPI	AAAI	Na/K	Zr/Y
Units	ppb	ppm	ppm	ppm					
Analytical Method	INAA	GS Trace	GS Trace	GS Trace					
JHC-06-113	-99	637	200	36.9	37	77	37	2.41	2.0
JHC-06-115	19	311	169	40.9	83	87	44	1.46	
JHC-06-118	-99	450	646	29.6	69	63	52	0.03	2.0
JHC-06-120	10	158	1607	44.2	76	79	68	0.03	0.9
JHC-06-121	-99	320	488	42.7	87	65	61	0.05	1.7
JHC-06-122	127	406	330	42.1	67	68	48	0.19	
JHC-06-123	-99	1626	2541	30.8	38	87	19	38.44	6.5
JHC-06-124	-99	808	182	42	51	63	46	0.29	
JHC-06-125	-99	2496	197	35.5	59	79	38	1.32	
JHC-06-126	-99	459	190	39	55	72	41	0.65	
JHC-06-127	-99	713	138	36.8	30	67	33	2.42	
JHC-06-128	-99	907	169	36.6	43	57	32	0.26	
JHC-06-130	2	181	460	12.3	30	44	50	5.74	
JHC-06-131	-99	170	291	8.9	19	42	49	43.78	7.4
JHC-06-133	18	264	353	10.7	21	42	49	8.62	
JHC-06-134	-99	201	206	6.1	31	27	64	2.52	6.1
JHC-06-135	-99	1919	644	22.3	91	67	60	0.11	5.0
JHC-06-141	-99	1399	135	5.2	73	80	67	0.83	4.8
JHC-06-142	306	1534	6	1.4	41	100	73	1.39	
JHC-06-143	-99	121	133	3.4	25	17	57	3.50	2.6
JHC-06-145	-99	34365	1970	11.6	23	96	21	2.25	1.4
JHC-06-146	448	1150	17	1.2	22	100	63	0.54	
JHC-06-147	-99	14034	818	16.7	42	92	30	1.32	2.5
JHC-06-148	-99	418	303	7.4	13	21	40	17.75	4.1
JHC-06-149	-99	2823	186	37.2	68	89	32	31.65	1.7
JHC-06-150	228	6355	97	1.4	3	100	12	0.97	
JHC-06-153	-99	1275	398	36.8	38	75	25	52.65	2.2
JHC-06-154	-99	158	498	12.4	44	37	52	1.41	4.5
JHC-06-156	-99	1537	1670	25.7	55	73	24	0.58	
JHC-06-157	-99	1518	842	16.2	39	53	33	1.18	1.9
JHC-06-158	-99	964	340	9.1	36	36	48	1.43	
JHC-06-162	-99	435	141	11	18	38	51	18.61	6.1
JHC-06-164	-99	1232	547	22.6	42	66	28	7.75	2.5
JHC-06-166	-99	1704	418	31.5	36	72	27	8.55	
JHC-06-167	-99	1204	1012	31.7	36	73	32	27.01	3.1
JHC-06-169	-99	1459	383	41.6	38	67	30	7.40	
JHC-06-170	-99	1322	341	41.1	38	74	25	7.66	2.2
JHC-06-171	-99	583	282	15.6	69	58	55	0.62	
JHC-06-172	-99	389	570	17.1	57	46	54	0.82	3.5
JHC-06-173	-99	799	659	20.1	42	59	35	5.37	
JHC-06-174	-99	797	663	20.7	43	51	39	2.68	3.1
JHC-06-175	-99	1147	476	35.6	33	66	27	16.03	
JHC-06-176	-99	708	681	20.9	24	50	33	22.98	2.8
JHC-06-177	-99	649	345	16	42	50	48	2.52	

Appendix 1B: Lithogeochemistry data table for samples analyzed from TVB

SampleNumber	Au	Mn	P	Sc	AI	CCPI	AAAI	Na/K	Zr/Y
Units	ppb	ppm	ppm	ppm					
Analytical Method	INAA	GS Trace	GS Trace	GS Trace					
JHC-06-178	-99	1362	2131	31.2	40	81	22	19.12	5.5
JHC-06-179	-99	522	814	24	73	72	43	0.90	2.9
JHC-06-180	23	155	651	24.1	44	59	48	1.70	
JHC-06-181	-99	182	649	20.8	67	62	64	0.53	5.2
JHC-06-182	-99	912	580	19.6	53	67	44	0.46	3.6
JHC-06-183	107	1087	611	21.9	61	62	29	0.20	
JHC-06-184	338	1572	279	8.8	46	94	13	0.38	3.2
JHC-06-185	225	749	670	17.7	68	92	19	0.31	
JHC-06-188	-99	1105	2360	29.1	41	82	21	4.44	6.4
JHC-06-190	-99	668	354	30	55	60	42	1.54	
JHC-06-191	-99	638	950	25.4	19	41	40	5.91	1.9
JHC-06-192	-99	1116	381	32.1	47	66	27	5.91	2.7
JHC-06-194	-99	891	549	27.9	38	55	42	2.17	
JHC-06-197	-99	83	195	9.3	43	38	51	2.89	
JHC-06-198	-99	690	580	12.1	91	93	13	1.74	2.6
JHC-06-199	-99	918	474	21.3	32	51	46	3.26	
JHC-06-200	-99	452	642	24.9	67	69	34	1.74	
JHC-06-201	-99	826	602	25.5	44	61	30	2.15	2.8
JHC-06-202	-99	860	285	19.8	37	56	33	2.12	
JHC-06-204	-99	176	423	15.8	51	41	48	1.64	4.2
JHC-06-205	-99	1372	349	42.4	41	74	26	20.37	2.3
JHC-06-207	-99	294	474	19.8	47	62	39	114.83	
JHC-06-209	-99	307	460	19.8	48	63	38	101.98	
JHC-06-210	-99	358	316	12.3	86	64	65	0.03	3.6
JHC-06-211	-99	1202	486	22.9	22	47	38	14.54	
JHC-06-214	-99	1762	567	37.7	42	79	25	42.98	
JHC-06-216	-99	819	489	23	29	53	41	11.35	2.8
JHC-06-218	-99	1418	421	34.7	33	77	24	180.68	2.4
JHC-06-219	-99	339	351	14.9	56	55	44	1.51	4.7
JHC-06-220	-99	165	693	26.7	34	38	41	1.92	
JHC-06-221	398	238	480	14.5	75	68	62	0.25	3.9
JHC-06-225	-99	879	342	26.8	43	68	31	5.45	3.2
JHC-06-226	-99	381	316	14.8	63	52	45	0.69	
JHC-06-227	-99	934	401	33.6	42	70	29	27.88	
JHC-06-228	-99	1331	324	42.6	31	79	23	7.61	2.0
JHC-06-229	-99	1010	490	27	35	65	27	13.63	2.0
JHC-06-230	-99	1112	347	36.4	36	75	25	71.08	
JHC-06-231	-99	1750	341	32.2	36	71	26	6.58	2.2
JHC-06-233	-99	693	468	19	27	54	41	69.90	
JHC-06-234	-99	880	1591	13.3	24	53	37	4.22	5.1
JHC-06-235	216	187	550	16.6	80	82	61	0.24	4.1
JHC-06-236	9	103	464	19.1	80	64	76	0.24	3.8
JHC-06-237	-99	4916	330	13.2	34	74	19	0.32	
JHC-06-238	-99	528	251	17.1	54	57	50	1.34	3.1

Appendix 1B: Lithogeochemistry data table for samples analyzed from TVB

SampleNumber	Au	Mn	P	Sc	AI	CCPI	AAAI	Na/K	Zr/Y
Units	ppb	ppm	ppm	ppm					
Analytical Method	INAA	GS Trace	GS Trace	GS Trace					
JHC-06-239	-99	2909	518	20.5	50	72	24	0.26	2.6
JHC-06-240	-99	403	499	20.3	31	56	41	181.40	2.6
JHC-06-242	-99	-99	-99	-99	42	90	19	55.12	
JHC-06-243	-99	-99	-99	-99	42	54	48	2.35	
JHC-06-244	-99	-99	-99	-99	49	76	25	50.83	
JHC-07-002	-99	774	808	21	24	60	22	0.78	
JHC-07-003	-99	1771	1514	45.9	45	92	19	42.53	4.1
JHC-07-004	-99	778	365	32.7	24	88	21	1.69	
JHC-07-006	-99	489	123	12	61	58	60	1.57	1.6
JHC-07-007	-99	1028	986	30.4	23	82	19	50.36	
JHC-07-009	-99	700	734	22.4	79	71	52	0.06	
JHC-07-010	-99	1590	1317	40.6	40	87	21	9.37	4.1
JHC-07-013	-99	901	286	14.5	73	75	73	0.56	
JHC-07-015	-99	1499	1346	37.8	46	95	21	1.24	
JHC-07-016	-99	1446	1337	40.7	44	91	22	192.96	
JHC-07-017	-99	660	595	29.8	26	92	22	5.96	
JHC-07-018	82	106	185	19.9	89	61	85	0.09	1.7
JHC-07-019	27	208	98	20.8	78	49	72	0.34	
JHC-07-020	-99	1175	837	31.9	27	92	15		
JHC-07-021	-99	1601	1341	39.9	40	93	20	96.47	
JHC-07-022	-99	1011	1509	36.6	60	90	26	0.82	
JHC-07-023	-99	188	191	10.2	52	38	59	0.95	
JHC-07-024	-99	268	12	0.4	18	24	57	5.24	3.1
JHC-07-025	-99	812	228	9	48	52	51	0.98	
JHC-07-026	-99	425	241	10	43	35	56	1.47	
JHC-07-027	-99	688	196	8.8	93	95	32	0.06	
JHC-07-028	-99	317	254	10	94	70	54	0.08	
JHC-07-029	17	612	276	11.8	97	82	44	0.04	
JHC-07-030	-99	874	134	12	99	90	38	0.04	3.4
JHC-07-031	-99	458	227	11.2	97	68	60	0.04	
JHC-07-032	-99	1239	244	7.5	97	97	28	0.61	
JHC-07-033	-99	1437	960	43.6	34	87	21	169.30	3.9
JHC-07-034	3	1154	192	11.4	84	84	39	0.98	
JHC-07-035	-99	277	124	5.3	79	59	79	0.07	
JHC-07-036	5	416	168	11.5	88	71	69	0.15	3.5
JHC-07-037	-99	995	204	12.9	87	72	62	0.25	
JHC-07-039	-99	350	116	10.1	87	69	83	0.08	
JHC-07-040	-99	72	131	11	96	60	92	0.04	
JHC-07-041	-99	107	122	9.7	95	66	91	0.05	
JHC-07-043	-99	144	91	8.9	94	41	90	0.05	
JHC-07-044	-99	286	224	7.9	78	67	51	0.99	4.6

Appendix 1B: Lithogeochemistry data table for samples analyzed from TVB

SampleNumber	Au	Mn	P	Sc	AI	CCPI	AAAI	Na/K	Zr/Y
Units	ppb	ppm	ppm	ppm					
Analytical Method	INAA	GS Trace	GS Trace	GS Trace					
JHC-07-045	-99	684	224	11.5	80	76	43	1.22	
JHC-07-047	-99	820	168	9	86	85	38	1.80	
JHC-07-048	-99	1385	953	42.5	32	85	21	36.83	3.6
JHC-07-049	7	797	97	10.5	96	75	55	0.05	
JHC-07-050	-99	1288	96	8.5	95	99	25	0.38	
JHC-07-052	-99	3028	341	11.8	99	100	17		
JHC-07-053	-99	664	214	12.5	93	71	65	0.06	
JHC-07-054	-99	28	345	12.1	35	21	65	1.95	3.0
JHC-07-060	-99	203	310	15.3	82	60	57	0.37	
JHC-07-061	-99	366	279	12.6	19	34	49	8.48	3.1
JHC-07-062	-99	236	126	7	16	33	55	31.93	3.3
JHC-07-063	-99	1936	1512	33.4	43	77	22	0.03	6.1
JHC-07-064	-99	60	291	12.3	72	30	77	0.40	
JHC-07-065	-99	219	310	15	83	48	59	0.21	4.0
JHC-07-066	22	1233	237	5.9	81	93	58	0.38	
JHC-07-070	-99	269	316	14.9	75	43	55	0.18	
JHC-07-073	-99	138	524	16.2	92	41	72	0.03	4.2
JHC-07-075	-99	281	313	14.3	69	57	47	0.70	
JHC-07-076	-99	155	267	10.2	54	43	55	1.96	
JHC-07-077	-99	215	278	10.2	60	43	56	1.10	3.2
JHC-07-078	-99	964	256	37.4	56	77	41	0.01	3.1
JHC-07-079	-99	397	14	41.4	53	69	38	0.97	
JHC-07-080	-99	1342	136	66.6	43	90	28	56.97	
JHC-07-081	-99	1424	154	63.7	33	86	27	136.49	0.4
JHC-07-082	-99	1359	163	51.6	31	85	26	1.79	
JHC-07-083	-99	111	279	49	83	50	62	0.17	7.9
JHC-07-084	-99	13	327	37.9	76	15	71	0.33	8.2
JHC-07-085	-99	186	411	45.9	88	53	66	0.19	1.7
JHC-07-086	-99	872	857	45.2	45	68	27	0.93	
JHC-07-087	-99	668	966	34.6	22	55	32	21.41	
JHC-07-088	-99	220	1145	42	24	37	42	4.71	1.5
JHC-07-091	-99	281	205	41.2	46	79	40	5.32	3.1
JHC-07-093	-99	32	433	36.5	73	13	66	0.38	
JHC-07-094	-99	834	374	38.1	94	92	35	0.19	3.1
JHC-07-095	-99	969	253	39	93	94	17	0.13	
JHC-07-096	-99	226	165	34.2	91	80	64	0.18	
JHC-07-097	-99	12	52	42.8	83	12	83	0.22	12.0
JHC-07-098	48	1642	278	31	98	100	11		
JHC-07-099	260	1594	123	48.3	80	87	26	0.14	
JHC-07-100	-99	50	9	33.6	87	12	84	0.15	
JHC-07-101	-99	12	253	50.3	84	10	70	0.19	13.8
JHC-07-102	-99	386	191	39.5	75	89	33	1.76	
JHC-07-103	-99	150	378	44	38	56	49	1.79	2.3
JHC-07-104	-99	487	334	47.3	50	78	31	2.00	

Appendix 1B: Lithogeochemistry data table for samples analyzed from TVB

SampleNumber	Au	Mn	P	Sc	AI	CCPI	AAAI	Na/K	Zr/Y
Units	ppb	ppm	ppm	ppm					
Analytical Method	INAA	GS Trace	GS Trace	GS Trace					
JHC-07-106	-99	1387	432	44.9	29	81	25	10.19	
JHC-07-107	-99	669	207	24.6	59	65	51	0.02	3.1
JHC-07-108	-99	349	329	37.2	59	44	53	0.04	
JHC-07-109	-99	179	343	40.3	94	89	39	0.09	
JHC-07-110	-99	316	228	47.6	57	55	48	0.13	
JHC-07-111	-99	6	298	32.3	73	10	56	0.39	
JHC-07-112	51	3392	252	40.4	84	91	26	0.22	
JHC-07-113	-99	1112	263	37.4	90	83	51	0.31	2.0
JHC-07-114	24	696	328	33.5	64	61	51	1.41	2.5
JHC-07-115	-99	338	834	47.5	78	30	62	0.28	
JHC-07-116	-99	243	521	39.9	56	72	44	3.18	1.9
JHC-07-119	-99	353	454	41.8	44	72	32	2.94	2.2
JHC-07-120	-99	1191	174	33.8	43	77	29	1.05	
JHC-07-121	-99	1112	191	26.2	48	63	47	0.37	
JHC-07-122	-99	810	219	27.7	38	59	45	1.11	
JHC-07-123	-99	797	190	26.8	49	63	50	0.30	3.6
JHC-07-124	-99	255	208	36.6	76	72	56	0.15	
JHC-07-125	-99	456	147	46.9	47	76	32	14.07	2.8
JHC-07-126	-99	1307	181	41.2	32	73	25	2.02	
JHC-07-127	-99	1276	98	45.8	52	80	26	407.94	2.6
JHC-07-128	-99	405	203	37.6	55	77	37	2.94	2.9
JHC-07-129	-99	277	207	19.8	36	62	59	1.65	
JHC-07-133	-99	352	490	44.2	55	79	47	0.85	
JHC-07-134	-99	1187	186	37.2	45	73	29	1.25	
JHC-07-135	-99	355	149	25.8	67	66	57	0.62	1.1
JHC-07-136	-99	432	125	40.7	36	71	36	19.82	3.9
JHC-07-137	35	1110	215	45.8	59	77	50	0.17	
JHC-07-138	-99	629	46	44.1	58	79	32	2.76	3.6
JHC-07-139	-99	628	124	40.8	49	77	31	3.00	
JHC-07-140	-99	1152	167	44.7	34	72	28	3.43	
JHC-07-141	-99	1386	167	40.1	44	83	27	0.53	
JHC-07-142	-99	678	845	52.1	48	73	25	3.76	1.4
JHC-07-143	-99	187	249	21.1	37	47	63	1.54	
JHC-07-147	-99	536	376	41.3	53	81	42	1.23	
JHC-07-150	-99	63	105	17.8	70	78	81	0.69	
JHC-07-151	-99	3	303	6.9	41	13	81	1.54	27.2
JHC-07-152	-99	28	235	16.8	54	99	98		2.9
JHC-07-153	-99	812	301	14.5	43	66	54	6.95	3.5
JHC-07-156	-99	34	353	20.3	42	63	77	1.53	2.0
JHC-07-158	-99	620	456	15.6	60	42	66	0.56	

Appendix 1B: Lithogeochemistry data table for samples analyzed from TVB

SampleNumber	Au	Mn	P	Sc	AI	CCPI	AAAI	Na/K	Zr/Y
Units	ppb	ppm	ppm	ppm					
Analytical Method	INAA	GS Trace	GS Trace	GS Trace					
JHC-07-160	-99	1186	293	35	53	84	31	1.38	1.9
JHC-07-162	-99	1851	758	26.6	31	74	29	1.35	
JHC-07-163	-99	1070	394	18	63	63	63	0.82	
JHC-07-165	-99	380	314	11.7	74	65	71	0.61	2.7
JHC-07-166	-99	1014	365	17.5	61	61	60	1.27	3.3
JHC-07-167	-99	6168	422	33.8	62	76	22	1.69	
JHC-07-168	-99	1479	340	25.8	52	67	48	3.06	1.8
JHC-07-170	-99	1002	871	36.5	33	74	31	3.10	
JHC-07-171	-99	177	242	7.7	37	25	61	1.39	7.1
JHC-07-172	-99	1557	380	43	40	79	37	1.87	
JHC-07-173	-99	1062	354	38.9	22	69	23	18.39	
JHC-07-174	-99	374	164	70.5	40	53	35	1.85	2.0
JHC-07-175	-99	134	27	45.9	57	69	49	1.18	1.4
JHC-07-176	-99	683	479	11.5	93	100	13		
JHC-07-180	-99	1480	260	20.3	99	100	12		
JHC-07-181	-99	1356	1490	16.6	50	78	42	2.94	6.9
JHC-07-182	-99	3594	105	38.4	64	81	37	8.01	
JHC-07-184	-99	1673	140	49.8	69	81	26	5.18	
JHC-07-187	-99	683	857	25.9	35	71	34	1.30	5.7
JHC-07-188	-99	555	305	8	12	27	46	8.86	8.1
JHC-07-190	-99	845	488	41.4	64	81	50	2.11	
JHC-07-191	-99	722	452	29.1	21	59	33	11.65	0.6
JHC-07-193	-99	1235	132	45.6	18	75	14	4.79	
JHC-07-194	-99	1588	155	42.2	22	78	13	3.66	
JHC-07-195	13	1376	201	14.9	57	84	54	2.46	
JHC-07-196	-99	706	966	23.6	59	64	40	1.05	4.0
JHC-07-198	-99	671	435	22.9	35	75	51	1.16	1.6
JHC-07-207	48	670	260	22.5	52	73	50	4.03	1.5
JHC-07-208	36	545	266	29	62	74	51	2.09	
JHC-07-211	-99	581	339	56.1	57	84	32	4.84	
JHC-07-213	-99	428	240	36.4	39	62	48	3.00	
JHC-07-215	-99	1213	438	45.4	32	73	37	41.77	1.7
JHC-07-216	-99	1124	323	26.6	94	100	18		
JHC-07-217	-99	1471	1195	40.4	45	85	21	25.98	4.0
JHC-07-219	-99	1564	171	33.3	80	73	61	0.13	1.6
JHC-07-220	-99	915	129	51.3	67	84	30	4.03	3.1
JHC-07-221	-99	489	154	27	73	75	63	0.73	
JHC-07-222	-99	1439	160	29	75	82	50	2.00	1.5
JHC-07-226	-99	90	117	26.5	83	65	88	0.22	
JHC-07-229	-99	1067	206	30.9	42	69	46	6.37	1.5
JHC-07-230	-99	414	188	35.3	45	57	50	1.49	1.2
JHC-07-231	-99	693	113	40.3	68	79	45	1.73	1.6
JHC-07-233	-99	1385	171	33.5	52	73	50	4.00	
JHC-07-236	-99	444	188	19.5	46	64	51	3.65	1.5

Appendix 1B: Lithogeochemistry data table for samples analyzed from TVB

SampleNumber	Au	Mn	P	Sc	AI	CCPI	AAAI	Na/K	Zr/Y
Units	ppb	ppm	ppm	ppm					
Analytical Method	INAA	GS Trace	GS Trace	GS Trace					
JHC-07-242	-99	1449	182	33.1	65	75	51	1.82	
JHC-07-245	-99	1042	173	50.7	42	74	27	82.72	1.1
JHC-07-246	-99	298	203	20.9	47	49	58	0.77	
JHC-07-248	-99	452	206	31.8	51	58	55	1.51	
JHC-07-252	-99	47	71	5.7	4	11	56	132.45	2.8
JHC-07-254	-99	322	61	9.1	57	49	65	1.77	
JHC-07-255	-99	60	32	8.1	20	23	75	7.62	3.5
JHC-07-256	-99	378	93	9.4	52	64	49	6.64	3.5
JHC-07-259	-99	195	96	7.6	32	47	63	13.67	
JHC-07-260	-99	671	145	10.8	39	47	58	3.30	
JHC-07-261	-99	46	72	5.2	18	15	73	7.84	
JHC-07-262	-99	842	37	10.9	82	81	35	1.29	4.3
JHC-07-264	-99	154	47	7.8	33	37	66	5.93	2.7
JHC-07-265	-99	111	35	11.2	48	34	76	1.58	3.2
JHC-07-266	-99	518	88	5.4	50	62	70	3.47	
JHC-07-267	-99	57	175	8.2	78	83	90	0.31	
JHC-07-268	-99	505	36	71.4	76	58	54	0.46	9.3
JHC-07-271	123	108	157	4.9	82	51	91	0.32	
JHC-07-272	-99	717	96	8.2	51	62	49	11.15	
JHC-07-273	-99	444	42	13.4	38	35	64	3.72	2.8
JHC-07-275	-99	50	252	11.4	60	63	80	0.74	
JHC-07-276	-99	1049	106	8.2	91	81	48	0.41	2.9
JHC-07-277	-99	82	172	6.4	2	19	38	237.72	
JHC-07-278	-99	472	223	5.2	62	56	75	1.71	
JHC-07-279	-99	838	153	6	29	42	43	22.67	
JHC-07-280	-99	691	45	14.5	65	56	67	1.56	2.5
JHC-07-281	203	104	870	6.6	68	87	84	0.42	
JHC-07-282	-99	629	73	6.3	43	45	59	3.31	
JHC-07-283	-99	526	105	9.9	43	45	59	3.31	3.0
JHC-07-284	-99	78	61	6.5	19	16	68	7.07	3.1
JHC-07-285	-99	462	42	7.4	34	50	55	10.14	2.5
JHC-07-286	-99	253	33	13.2	77	59	57	0.58	
JHC-07-287	-99	84	48	5.7	18	27	54	35.17	
JHC-07-289	-99	657	180	6.6	74	67	72	0.80	
JHC-07-290	-99	417	6	14	73	91	78	0.25	
JHC-07-291	-99	381	96	7.2	25	34	59	14.07	3.7
JHC-07-292	-99	1796	1106	27.8	69	84	30	14.40	
JHC-07-293	-99	664	76	9.2	57	73	52	9.09	2.8

Appendix 1B: Lithogeochemistry data table for samples analyzed from TVB

SampleNumber Units Analytical Method	Zr/Nb	Zr/TiO2	Zr/Hf	Nb/Y	104*Ga/Al	Th/Nb	Sc/Nb	Ti/Sc	Zr/Sc	LaN/YbN	CeN/YbN	LaN/ThN	LaN/NbN	ZrN/SmN	Eu/Eu*	Nb/Nb*	Zr/Zr*	Ti/Ti*	Nb/TA
JHC-06-001	55.1	31.6	24.5	0.03	117.5	0.5	113.27	92.09	0.49	0.8	0.8	1.3	5.4	0.67	1.40	0.05	0.17	0.27	
JHC-06-002		8.4			106.1			45.35	0.06										
JHC-06-003	38.9	201.5	30.7	0.05	107.1	0.7	11.01	104.93	3.53	1.5	1.4	0.8	5.3	0.68	1.04	0.04	0.18	0.05	
JHC-06-005	70.5	181.3	29.4	0.04	218.7	1.6	21.71	107.34	3.25	1.6	1.6	0.6	8.1	0.73	0.33	0.02	0.20	0.06	
JHC-06-006	41.9	197.0			118.1	0.5	12.77	99.73	3.28							0.12			
JHC-06-008	39.5	346.1	30.2	0.04	145.5	0.9	15.05	45.39	2.62	1.4	1.3	0.6	5.0	0.65	0.29	0.04	0.17	0.03	13.00
JHC-06-009	38.2	468.6			90.8	0.5	7.68	63.56	4.97							0.12			
JHC-06-010		248.0			117.1			114.68	4.75							0.00			
JHC-06-011	37.6	204.3			111.4	0.2	10.44	105.64	3.6							0.37			
JHC-06-012	30.8	211.5	32.3	0.07	134.1	0.4	8.54	102.24	3.61	1.9	1.7	1.4	4.5	0.71	0.30	0.06	0.19	0.05	
JHC-06-013		5459.7			1722.4			13.45	12.25										
JHC-06-014		839.6			1489.4			32.82	4.6										
JHC-06-015	43.8	287.9	31.3	0.04	114	0.8	16.51	55.17	2.65	1.1	1.0	0.7	4.6	0.79	0.90	0.04	0.19	0.03	15.00
JHC-06-017	396.6	221.9			158.9	5.0	147.71	72.54	2.69							0.01			
JHC-06-018	86.4	249.8	28.8	0.04	163.6	2.0	10.88	190.35	7.93	0.7	0.7	0.2	4.0	1.34	0.41	0.02	0.32	0.07	5.50
JHC-06-019	108.8	34.6	31.1	0.01	118.4	1.5	212.55	88.62	0.51	0.8	0.8	0.8	10.4	0.72	1.44	0.02	0.17	0.26	
JHC-06-020	71.3	32.5			119	0.7	151.41	86.76	0.47							0.09			
JHC-06-021		11.6	23.0	0.00	106.8			40.99	0.08	0.4	0.3			0.61	2.06	0.00	0.14	0.60	
JHC-06-022	42.6	400.7	10.6	0.02	89.9	1.2	9.85	64.61	4.32	1.3	1.3	1.3	13.6	0.27	0.85	0.02	0.07	0.01	4.50
JHC-06-023	43.1	196.2	32.6	0.04	128.4	0.8	8.35	157.63	5.16	1.1	1.0	0.7	4.9	0.76	0.63	0.04	0.18	0.05	25.00
JHC-06-024					568.3			0	12.03										
JHC-06-025					1692.8			0	13.77										
JHC-06-026		12950.5			737.9			4.23	9.14										
JHC-06-027		12518.1			371.7			4.83	10.09										
JHC-06-028	153.3	266.8	35.4	0.01	237.3	2.7	54.38	63.31	2.82	0.0	0.0	0.0	0.3	2.02	0.53	0.02	0.31	0.06	
JHC-06-030	162.0	337.1			194.8	3.0	36.38	79.17	4.45							0.02			
JHC-06-031	33.4	1384.4			140.6	1.3	2.21	65.35	15.1							0.04			
JHC-06-032	37.2	1584.1			173.9	1.4	2.99	47	12.42							0.04			
JHC-06-033	32.4	1550.6	34.0	0.07	143.7	1.2	2.30	54.37	14.07	1.8	1.6	0.4	4.1	1.07	0.56	0.04	0.27	0.01	13.67
JHC-06-034	33.4	37.5	33.4	0.04	146.1	0.6	67.48	79	0.49	2.1	1.8	1.5	7.3	0.44	0.74	0.04	0.11	0.15	
JHC-06-035	36.7	1512.8			137.9	0.8	2.66	54.62	13.79							0.07			
JHC-06-036	147.3	29.0	29.5	0.01	111.6	4.0	459.48	66.28	0.32	1.8	1.7	0.8	25.9	0.53	1.28	0.01	0.14	0.24	
JHC-06-037	36.5	496.5	32.6	0.05	119.1	0.6	12.22	36.02	2.98	1.1	1.0	0.7	3.8	0.91	0.81	0.05	0.23	0.02	
JHC-06-038	52.9	1385.4			266.4	0.7	3.90	58.76	13.58							0.08			
JHC-06-039	35.1	1483.3	32.4	0.07	168.1	1.3	2.81	50.48	12.49	2.3	1.9	0.5	5.2	0.90	0.51	0.03	0.24	0.01	16.00
JHC-06-040	39.8	475.4	30.8	0.05	117.3	0.5	12.78	39.27	3.11	1.0	1.0	0.9	4.1	0.92	0.76	0.06	0.23	0.03	
JHC-06-041	24.6	1414.4			165.2	0.2	2.33	44.73	10.56							0.30			
JHC-06-042	45.1	517.4			109.6	0.8	14.11	37.05	3.2							0.07			
JHC-06-043	32.0	985.4	31.3	0.08	131.8	1.0	3.11	62.57	10.29	1.9	1.6	0.4	3.9	1.02	0.64	0.04	0.27	0.01	15.00
JHC-06-044	39.5	441.7	30.1	0.05	108.3	0.6	12.11	44.22	3.26	1.2	1.1	0.8	4.3	0.89	0.86	0.05	0.23	0.03	
JHC-06-045	36.1	81.0			116	0.9	19.33	138.1	1.87							0.07			
JHC-06-047	35.4	667.1			126.4	1.0	3.10	102.59	11.42							0.06			
JHC-06-048	29.6	706.8	33.7	0.08	303.5	1.4	2.80	89.66	10.58	3.0	2.3	0.5	5.4	0.82	0.77	0.03	0.22	0.02	16.50
JHC-06-050	27.1	213.3	35.1	0.08	129.9	0.6	9.38	81.17	2.89	1.8	1.5	0.8	4.0	0.81	1.10	0.06	0.21	0.05	

Appendix 1B: Lithogeochemistry data table for samples analyzed from TVB

SampleNumber Units Analytical Method	Zr/Nb	Zr/TiO2	Zr/Hf	Nb/Y	104*Ga/Al	Th/Nb	Sc/Nb	Ti/Sc	Zr/Sc	LaN/YbN	CeN/YbN	LaN/ThN	LaN/NbN	ZrN/SmN	Eu/Eu*	Nb/Nb*	Zr/Zr*	Ti/Ti*	Nb/TA
JHC-06-051	28.9	318.0			129.5	0.6	10.76	50.7	2.69							0.10			
JHC-06-052	27.3	218.1			141	0.7	11.28	66.43	2.42							0.09			
JHC-06-053	25.9	88.2			112.3	0.5	12.69	138.65	2.04							0.11			
JHC-06-054	27.0	1133.8			121.1	0.9	2.34	60.9	11.52							0.06			
JHC-06-057	29.2	553.0	34.2	0.08	117.7	1.0	2.23	141.72	13.08	1.8	1.5	0.4	3.6	1.15	0.56	0.04	0.30	0.03	20.50
JHC-06-059	32.6	77.7	35.4	0.06	117.3	0.5	18.14	138.81	1.8	1.9	1.7	1.1	5.1	0.67	1.18	0.05	0.17	0.11	
JHC-06-060	52.9	90.9	33.0	0.04	126.1	1.4	23.80	146.46	2.22	1.7	1.7	0.6	6.7	0.77	1.15	0.03	0.20	0.12	
JHC-06-062	52.3	35.7	32.7	0.03	113.8	1.4	81.84	107.34	0.64	1.7	1.5	0.7	7.9	0.65	1.21	0.03	0.17	0.25	
JHC-06-063	90.0	28.1			122.9	1.3	126.35	151.85	0.71							0.04			
JHC-06-064	106.9	24.9	26.7	0.01	112.8	2.0	184.54	139.58	0.58	1.4	1.4	0.9	16.1	0.44	1.16	0.02	0.12	0.24	
JHC-06-068	42.0	36.2	31.5	0.03	134.6	0.8	44.79	155.11	0.94	0.6	0.6	0.4	2.5	1.07	1.01	0.05	0.21	0.31	
JHC-06-069	77.3	39.1	32.2	0.03	145.1	1.4	81.20	145.87	0.95	1.2	1.1	0.6	7.5	0.80	1.32	0.03	0.21	0.27	
JHC-06-070	39.9	31.9			121.2	17.8	49.09	152.56	0.81							0.00			
JHC-06-071	42.0	29.8			101.4	4.2	65.32	129.25	0.64							0.01			
JHC-06-072	35.8	35.1			155.4	1.3	35.71	170.83	1							0.05			
JHC-06-073	35.7	947.7	30.6	0.10	103.2	1.2	2.13	106.03	16.77	1.6	1.4	0.3	3.1	1.69	0.35	0.04	0.44	0.02	10.50
JHC-06-074	47.6	560.2	32.5	0.08	130.1	1.6	4.05	125.72	11.75	2.0	1.7	0.4	4.7	1.60	0.29	0.03	0.42	0.04	11.25
JHC-06-075	33.0	456.4			110.6	1.8	3.02	143.69	10.94							0.03			
JHC-06-076	34.4	310.5	32.1	0.11	133.9	1.1	3.79	175.32	9.08	3.3	2.8	0.5	5.1	1.11	0.77	0.03	0.31	0.05	14.00
JHC-06-077	34.3	492.0			106.4	1.1	4.16	100.25	8.23							0.06			
JHC-06-078	32.3	523.9			104.8	1.1	3.52	104.89	9.17							0.06			
JHC-06-079	24.6	18.2			97.8	0.7	0.00									0.09			
JHC-06-082	26.7	20.5	22.2	0.04	105.8	1.4	82.42	94.52	0.32	1.2	1.1	0.4	4.4	0.48	1.18	0.03	0.12	0.29	
JHC-06-083	15.7	279.1			150.1	1.1	2.69	125.79	5.86							0.06			
JHC-06-086	28.7	289.3	32.1	0.08	143.7	1.0	7.15	83.14	4.01	1.6	1.4	0.4	3.5	0.96	0.93	0.04	0.24	0.04	28.00
JHC-06-087	68.5	54.8			54.1	0.9	45.83	163.61	1.5							0.07			
JHC-06-088	53.8	51.4	31.6	0.05	116.4	1.1	38.07	164.89	1.41	1.7	1.8	0.6	5.4	0.79	0.98	0.03	0.22	0.22	
JHC-06-089	55.0	43.2	30.0	0.03	100.9	1.3	66.76	114.42	0.82	1.4	1.3	0.5	5.9	0.72	1.09	0.03	0.18	0.22	
JHC-06-091	25.1	85.7			127.3	0.7	17.95	97.94	1.4							0.08			
JHC-06-092	57.5	106.4			130.9	0.6	26.83	120.75	2.14							0.10			
JHC-06-095	20.8	358.6			109.9	1.4	1.71	202.43	12.11							0.04			
JHC-06-097	37.5	106.4	28.9	0.07	98	1.4	38.01	55.57	0.99	1.8	1.7	0.3	3.6	0.99	0.65	0.03	0.26	0.13	
JHC-06-098	15.6	71.9	47.9	0.43	160.5	0.1	1.78	727.68	8.73	4.3	4.2	2.3	1.3	1.39	1.22	0.26	0.40	0.29	11.64
JHC-06-100	31.6	85.9	31.6	0.06	100.9	1.1	40.46	54.52	0.78	1.0	1.0	0.3	3.0	1.04	0.71	0.04	0.25	0.15	
JHC-06-101	48.0	107.4			104	1.2	58.46	45.81	0.82							0.05			
JHC-06-102	45.4	135.2			99.7	0.9	49.32	40.83	0.92							0.07			
JHC-06-103	58.7	760.8			44.7	0.5	0.89	517.51	65.7							0.11			
JHC-06-104	32.3	214.8			125.4	0.8	2.99	301.5	10.81							0.08			
JHC-06-105	52.3	77.3			169.6	0.9	22.70	178.78	2.3							0.06			
JHC-06-108	51.2	91.3			155.3	0.9	15.72	213.84	3.26							0.07			
JHC-06-109	46.2	54.1	27.7	0.04	117.8	1.8	51.80	98.72	0.89	2.1	1.8	0.6	9.0	0.64	1.24	0.02	0.18	0.17	
JHC-06-111	27.5	647.3			289.1	0.9	44.02	5.79	0.63							0.07			
JHC-06-112	49.2	92.1	36.9	0.04	126	1.3	69.55	46.07	0.71	1.3	1.2	0.6	6.4	0.83	0.84	0.03	0.20	0.11	

Appendix 1B: Lithogeochemistry data table for samples analyzed from TVB

SampleNumber Units Analytical Method	Zr/Nb	Zr/TiO2	Zr/Hf	Nb/Y	104*Ga/Al	Th/Nb	Sc/Nb	Ti/Sc	Zr/Sc	LaN/YbN	CeN/YbN	LaN/ThN	LaN/NbN	ZrN/SmN	Eu/Eu*	Nb/Nb*	Zr/Zr*	Ti/Ti*	Nb/TA
JHC-06-113	43.3	109.9	31.5	0.05	97.4	1.4	46.11	51.19	0.94	1.4	1.3	0.4	5.2	0.91	0.87	0.03	0.24	0.11	
JHC-06-115	45.6	137.9			105.6	1.3	45.48	43.56	1							0.04			
JHC-06-118	41.6	149.0	31.2	0.05	107	1.5	24.66	67.83	1.69	1.5	1.4	0.4	5.5	0.90	0.87	0.03	0.22	0.08	
JHC-06-120	51.2	108.3	34.1	0.02	103.1	1.2	73.74	38.4	0.69	1.5	1.0	1.4	13.7	0.67	0.60	0.02	0.16	0.08	
JHC-06-121	58.1	125.6	31.3	0.03	93.9	0.9	61.06	45.39	0.95	0.7	0.6	0.6	4.6	1.24	0.87	0.04	0.29	0.12	
JHC-06-122	42.7	110.8			103.9	0.8	46.83	49.34	0.91							0.08			
JHC-06-123	14.8	68.7	46.3	0.44	152.9	0.1	1.79	721.9	8.27	4.3	4.2	2.6	1.3	1.42	1.25	0.28	0.40	0.30	12.29
JHC-06-124	35.9	122.5			113.9	0.5	38.16	45.98	0.94							0.11			
JHC-06-125	40.1	97.2			101.1	1.0	50.66	48.79	0.79							0.06			
JHC-06-126	40.4	134.9			95.7	0.8	43.39	41.33	0.93							0.08			
JHC-06-127	33.7	134.7			99.1	1.4	33.45	44.86	1.01							0.04			
JHC-06-128	37.3	124.9			95.6	1.4	45.75	39.13	0.82							0.04			
JHC-06-130	52.9	214.4			109.7	1.5	5.87	252.27	9.02							0.04			
JHC-06-131	62.3	311.5	34.8	0.12	110.5	1.0	4.66	256.87	13.35	1.5	1.3	0.3	2.4	3.34	0.77	0.05	0.83	0.14	9.50
JHC-06-133	56.1	498.7			59.3	0.9	3.44	196.04	16.31							0.07			
JHC-06-134	28.4	646.3	39.9	0.22	124.6	1.0	1.17	225.3	24.3	3.6	3.0	0.4	3.1	1.94	0.52	0.04	0.57	0.05	13.00
JHC-06-135	15.8	221.7	35.0	0.31	147	0.4	1.98	216.29	8	7.4	8.9	1.2	3.9	1.01	0.80	0.07	0.31	0.07	12.56
JHC-06-141	27.6	742.8	34.7	0.17	172.5	1.1	0.97	229.31	28.42	3.5	2.9	0.4	3.9	1.73	0.48	0.04	0.50	0.04	9.00
JHC-06-142	158.4	14834.8			5442.8	0.0	14.34	4.46	11.05										
JHC-06-143	61.0	1946.4	39.0	0.04	157.3	0.6	0.38	492.86	160.07	1.7	1.5	1.2	6.2	1.55	0.43	0.04	0.40	0.01	18.00
JHC-06-145	8.4	165.5	24.6	0.17	161.6	1.0	1.66	184.09	5.08	10.7	17.4	1.1	9.5	0.21	0.75	0.03	0.06	0.02	14.00
JHC-06-146		2547.0			1212.9			32.87	13.97							0.00			
JHC-06-147	9.9	202.7	28.7	0.25	168.6	0.9	1.56	188.06	6.36	11.0	18.7	0.8	6.3	0.38	0.82	0.04	0.12	0.03	15.29
JHC-06-148	48.8	757.1	40.0	0.08	122.2	0.3	0.86	448.98	56.72	3.0	2.7	2.1	5.5	1.30	0.56	0.06	0.35	0.02	14.33
JHC-06-149	38.8	47.9	31.1	0.04	121.7	0.6	46.44	104.65	0.84	1.0	1.1	0.5	2.9	0.68	1.10	0.06	0.16	0.17	
JHC-06-150	34.5	916.2			3324.8	0.8	3.62	62.38	9.54							0.08			
JHC-06-153	25.6	48.5	31.1	0.09	123.1	0.4	21.66	146.09	1.18	1.5	1.4	0.9	2.8	0.78	0.97	0.09	0.20	0.22	
JHC-06-154	38.7	297.8	34.2	0.12	110.8	0.7	3.26	238.69	11.86	2.9	2.6	0.7	4.4	1.49	0.87	0.05	0.41	0.07	12.67
JHC-06-156	22.6	107.4			103	0.4	3.38	373.21	6.69							0.13			
JHC-06-157	35.9	53.4	33.5	0.05	119.9	0.6	11.55	348.81	3.11	2.1	1.8	1.1	5.9	0.60	1.07	0.04	0.16	0.15	
JHC-06-158	35.1	319.6			98.8	1.3	2.54	259.2	13.82							0.04			
JHC-06-162	31.7	805.9	35.8	0.19	75.3	1.3	2.49	94.61	12.72	5.3	4.3	0.6	6.4	1.10	0.95	0.03	0.35	0.02	14.67
JHC-06-164	24.9	81.0	32.8	0.10	108.4	0.3	7.79	236.27	3.19	2.6	2.3	1.3	3.8	0.81	1.11	0.07	0.22	0.14	29.00
JHC-06-166	24.1	51.2			118.9	0.2	13.71	205.69	1.76							0.27			
JHC-06-167	18.6	76.1	33.2	0.17	151.5	0.1	5.38	272.2	3.46	1.1	1.1	1.3	1.1	1.20	0.85	0.25	0.31	0.21	14.75
JHC-06-169	28.4	41.5			108.3	0.3	25.99	158.04	1.09							0.24			
JHC-06-170	19.2	46.5	34.1	0.12	121.2	0.3	17.88	138.65	1.08	1.4	1.3	0.6	1.8	0.83	1.04	0.11	0.21	0.23	
JHC-06-171	74.9	419.8			150	1.2	6.25	171.01	11.98							0.05			
JHC-06-172	53.9	309.8	37.0	0.06	148.2	0.9	4.61	226.26	11.7	2.4	2.3	0.8	6.1	1.05	0.94	0.04	0.31	0.05	18.50
JHC-06-173	35.0	134.4			115.2	0.5	6.93	225.33	5.05							0.12			
JHC-06-174	38.9	135.8	35.0	0.08	111	0.3	7.66	224.09	5.08	1.9	1.8	1.3	3.5	1.12	0.86	0.08	0.30	0.11	13.50
JHC-06-175	35.7	52.0			112.3	0.2	27.35	150.64	1.31							0.26			
JHC-06-176	31.3	127.9	32.3	0.09	99.9	0.2	6.34	231.32	4.94	1.5	1.5	1.4	2.5	0.97	0.94	0.12	0.26	0.11	16.50
JHC-06-177	53.0	356.0			140.3	0.6	5.01	178.06	10.58							0.10			

Appendix 1B: Lithogeochemistry data table for samples analyzed from TVB

SampleNumber Units Analytical Method	Zr/Nb	Zr/TiO2	Zr/Hf	Nb/Y	104*Ga/Al	Th/Nb	Sc/Nb	Ti/Sc	Zr/Sc	LaN/YbN	CeN/YbN	LaN/ThN	LaN/NbN	ZrN/SmN	Eu/Eu*	Nb/Nb*	Zr/Zr*	Ti/Ti*	Nb/TA
JHC-06-178	20.3	72.1	43.0	0.27	127.3	0.2	3.50	481.03	5.79	3.9	3.7	1.1	2.0	1.21	1.31	0.13	0.33	0.24	14.83
JHC-06-179	82.2	208.4	36.5	0.03	127.8	1.5	9.99	236.64	8.23	1.7	1.7	0.6	7.6	1.01	0.82	0.02	0.26	0.07	12.00
JHC-06-180	31.0	129.4			107.3	0.3	6.90	208.28	4.5							0.23			
JHC-06-181	30.4	172.8	34.9	0.17	106.9	0.3	4.52	232.87	6.71	3.4	2.9	1.4	3.3	1.26	0.81	0.09	0.36	0.11	11.50
JHC-06-182	38.3	174.4	38.3	0.09	101.9	0.2	5.93	221.96	6.46	2.4	2.0	2.2	4.6	1.22	1.15	0.08	0.34	0.10	11.00
JHC-06-183	28.3	175.9			107.4	0.1	3.85	250.7	7.36							0.85			
JHC-06-184	39.9	205.8	34.7	0.08	158.4	0.4	4.41	263.58	9.05	4.6	4.2	2.2	7.6	0.72	1.66	0.05	0.21	0.05	10.00
JHC-06-185	41.4	200.7			170.2	0.3	5.71	216.54	7.25							0.20			
JHC-06-188	16.2	68.0	45.8	0.40	145.5	0.1	1.98	722.69	8.2	4.3	4.0	3.1	1.4	1.43	0.93	0.26	0.40	0.30	11.31
JHC-06-190	54.1	93.7			115.2	1.2	18.75	184.64	2.89							0.05			
JHC-06-191	38.5	92.1	32.1	0.05	116.7	0.3	12.69	197.2	3.03	1.1	1.1	1.4	3.7	0.92	0.87	0.08	0.23	0.13	20.00
JHC-06-192	37.9	94.4	30.3	0.07	107.7	0.8	13.36	179.88	2.83	1.6	1.5	0.6	4.0	0.95	0.93	0.05	0.25	0.14	12.00
JHC-06-194	43.6	93.0			114.8	0.4	16.40	171.26	2.66							0.17			
JHC-06-197	43.4	521.4			85.4	1.1	2.38	210.05	18.28							0.05			
JHC-06-198	35.9	122.9	33.3	0.07	165.5	1.5	4.65	376.83	7.73	3.9	3.2	0.7	8.4	0.68	1.11	0.02	0.20	0.08	13.00
JHC-06-199	37.6	113.3			107.6	0.6	11.82	168.25	3.18							0.11			
JHC-06-200	32.3	77.0			112.3	0.2	10.84	232.11	2.98							0.34			
JHC-06-201	33.1	77.8	31.8	0.09	109.6	0.2	10.18	249.95	3.25	1.3	1.4	1.7	2.3	0.96	0.92	0.14	0.26	0.17	12.50
JHC-06-202	33.2	92.7			95.2	0.2	8.98	238.53	3.69							0.33			
JHC-06-204	43.6	325.3	34.4	0.10	100.3	0.5	4.27	188.11	10.21	1.7	1.5	0.7	2.9	1.52	0.54	0.07	0.40	0.06	12.33
JHC-06-205	35.5	46.6	32.9	0.07	112.4	0.5	32.61	139.79	1.09	1.4	1.3	0.7	3.4	0.83	0.99	0.06	0.21	0.24	
JHC-06-207	32.2	118.6			103.5	0.3	8.59	189.27	3.75							0.20			
JHC-06-209	32.4	119.2			108.1	0.5	8.60	189.47	3.77							0.12			
JHC-06-210	39.0	365.7	34.8	0.09	117.4	0.9	3.72	171.79	10.48	1.3	1.5	0.3	2.3	1.41	0.67	0.05	0.38	0.05	16.50
JHC-06-211	37.5	115.3			110.6	0.3	11.43	170.28	3.28							0.20			
JHC-06-214	41.6	55.5			126.4	0.8	22.15	202.95	1.88							0.07			
JHC-06-216	49.0	120.6	35.7	0.06	113.2	0.4	14.38	169.48	3.41	1.6	1.4	1.2	4.3	1.11	0.89	0.06	0.27	0.12	8.00
JHC-06-218	46.3	60.4	33.5	0.05	119.2	0.9	26.73	171.92	1.73	1.5	1.5	0.5	4.2	0.88	0.96	0.04	0.23	0.20	
JHC-06-219	48.7	729.8	41.7	0.10	139.5	0.4	2.26	176.61	21.51	2.2	2.2	1.2	3.7	1.53	0.88	0.07	0.42	0.03	22.00
JHC-06-220	26.4	199.2			129.2	0.2	4.17	190.6	6.33							0.32			
JHC-06-221	33.3	179.2	35.8	0.12	103.5	0.4	5.17	215.31	6.44	2.1	1.9	0.9	2.9	1.47	0.92	0.09	0.40	0.11	14.00
JHC-06-225	42.1	115.7	34.0	0.08	106.2	1.0	12.74	170.97	3.3	1.4	1.4	0.3	2.7	1.20	0.97	0.05	0.31	0.14	21.00
JHC-06-226	36.1	262.0			113.9	0.4	3.88	212.59	9.29							0.13			
JHC-06-227	27.3	52.9			128.3	0.2	14.59	212.14	1.87							0.27			
JHC-06-228	19.7	41.3	34.6	0.10	121.3	0.4	20.26	141.29	0.97	1.1	1.1	0.5	1.7	0.82	1.13	0.10	0.21	0.26	
JHC-06-229	25.7	60.0	33.4	0.08	115.7	0.2	10.38	247.43	2.48	1.4	1.4	1.7	2.3	0.71	0.95	0.14	0.19	0.16	26.00
JHC-06-230	32.7	46.5			106.3	0.5	28.03	150.04	1.17							0.13			
JHC-06-231	31.0	49.5	31.0	0.07	107.2	0.5	24.75	151.53	1.25	1.3	1.3	0.6	2.7	0.84	1.05	0.07	0.22	0.23	
JHC-06-233	33.4	119.1			111	0.2	8.63	194.64	3.87							0.33			
JHC-06-234	41.1	172.9	38.3	0.12	129.7	0.5	3.17	449.49	12.97	5.1	4.1	1.4	6.0	1.24	0.96	0.05	0.35	0.10	10.50
JHC-06-235	42.6	171.2	36.5	0.10	197.9	0.4	6.92	215.68	6.16	2.0	1.9	0.9	3.3	1.56	0.68	0.07	0.42	0.13	12.00
JHC-06-236	28.2	157.8	34.2	0.14	109.1	0.3	5.63	189.95	5	1.8	1.6	0.8	2.3	1.46	0.88	0.10	0.39	0.13	11.33
JHC-06-237	24.9	143.7			114.6	0.6	5.52	188.36	4.52							0.09			
JHC-06-238	62.3	485.9	37.2	0.05	152.7	0.6	5.03	152.74	12.38	1.8	1.8	1.0	5.7	1.07	0.88	0.04	0.29	0.03	34.00

Appendix 1B: Lithogeochemistry data table for samples analyzed from TVB

SampleNumber Units Analytical Method	Zr/Nb	Zr/TiO2	Zr/Hf	Nb/Y	104*Ga/Al	Th/Nb	Sc/Nb	Ti/Sc	Zr/Sc	LaN/YbN	CeN/YbN	LaN/ThN	LaN/NbN	ZrN/SmN	Eu/Eu*	Nb/Nb*	Zr/Zr*	Ti/Ti*	Nb/TA
JHC-06-239	29.8	146.3	31.7	0.09	137.5	0.3	6.22	196.4	4.8	1.6	1.4	0.9	2.6	1.30	0.68	0.09	0.32	0.11	16.50
JHC-06-240	42.0	120.8	33.3	0.06	116.6	0.9	10.71	194.75	3.93	1.7	1.5	0.6	4.2	0.99	0.89	0.04	0.26	0.11	19.00
JHC-06-242	15.1	54.3			138.3	0.1	0.00									0.65			
JHC-06-243	39.4	249.2			101	0.5	0.00									0.12			
JHC-06-244	38.4	42.5			108.5	0.5	0.00									0.12			
JHC-07-002	15.3	222.0				0.0	2.63	157.09	5.82										
JHC-07-003	7.2	66.9	40.8	0.57	173.6	0.0	2.07	311.31	3.47	2.4	2.3	1.4	0.6	1.19	1.02	0.50	0.31	0.24	24.66
JHC-07-004	7.4	81.6				0.0	4.16	130.2	1.77										
JHC-07-006	29.4	539.9	28.1	0.05	143	0.8	4.86	67.26	6.06	0.6	0.5	0.3	1.7	1.11	0.65	0.06	0.26	0.02	
JHC-07-007	6.2	63.6				0.0	2.01	290.59	3.08										
JHC-07-009	5.8	243.0				0.0	0.94	152.57	6.19										
JHC-07-010	7.4	71.8	39.6	0.55	161.6	0.1	2.05	301.08	3.61	2.5	2.3	1.1	0.6	1.23	0.97	0.46	0.32	0.23	24.81
JHC-07-013	9.8	190.5				0.0	2.08	148.48	4.72										
JHC-07-015	10.5	68.3				0.0	2.89	318.96	3.64										
JHC-07-016	7.0	66.9				0.0	2.07	302.73	3.38										
JHC-07-017	7.0	91.9				0.0	3.61	126.74	1.94										
JHC-07-018	18.7	417.4	27.0	0.09	154.7	0.5	4.17	64.32	4.48	1.1	0.9	0.5	2.0	0.74	0.73	0.08	0.18	0.02	47.78
JHC-07-019	27.3	670.2				0.0	5.03	48.53	5.43										
JHC-07-020	5.7	54.4				0.0	2.15	289.38	2.63										
JHC-07-021	7.3	69.5				0.0	2.03	311.11	3.61										
JHC-07-022	17.1	153.7				0.0	2.05	323.85	8.31										
JHC-07-023	34.6	450.4				0.0	2.30	199.96	15.03										
JHC-07-024	7.3	9305.8	24.6	0.42	341.2	0.3	0.00	1172.14	1820.1	0.9	0.9	0.1	0.3	1.88	0.18	0.19	0.47	0.00	8.62
JHC-07-025	27.2	447.5				0.0	1.96	185.97	13.89										
JHC-07-026	29.6	441.0				0.0	2.15	187.22	13.78										
JHC-07-027	42.8	440.8				0.0	2.92	199.46	14.67										
JHC-07-028	33.3	438.2				0.0	2.27	200.72	14.67										
JHC-07-029	23.8	443.8				0.0	1.74	184.59	13.67										
JHC-07-030	48.9	690.9	32.6	0.07	151.6	2.6	3.27	129.69	14.95	1.9	1.6	0.2	4.4	1.54	0.75	0.02	0.41	0.03	12.24
JHC-07-031	32.5	422.0				0.0	2.64	174.27	12.27										
JHC-07-032	48.0	420.9				0.0	2.66	256.87	18.04										
JHC-07-033	14.2	74.9	36.9	0.28	165.4	0.1	3.65	310.93	3.89	2.0	2.0	0.9	1.0	1.16	0.96	0.24	0.31	0.21	29.84
JHC-07-034	32.4	499.3				0.0	2.55	152.95	12.74										
JHC-07-035	30.2	414.0				0.0	2.32	188.11	12.99										
JHC-07-036	31.2	516.6	34.6	0.11	148.1	1.5	2.72	133.24	11.48	3.3	2.6	0.4	4.8	1.13	0.50	0.03	0.32	0.03	14.06
JHC-07-037	30.4	518.1				0.0	2.52	139.94	12.1										
JHC-07-039	27.1	626.1				0.0	2.11	122.93	12.84										
JHC-07-040	29.4	588.2				0.0	2.31	129.56	12.72										
JHC-07-041	28.2	629.2				0.0	2.15	125.28	13.15										
JHC-07-043	48.0	651.1				0.0	3.31	133.28	14.48										
JHC-07-044	36.2	436.1	35.1	0.13	120.9	1.9	2.32	214.9	15.64	3.3	2.6	0.3	4.6	1.35	0.70	0.02	0.38	0.04	11.31

Appendix 1B: Lithogeochemistry data table for samples analyzed from TVB

SampleNumber Units Analytical Method	Zr/Nb	Zr/TiO2	Zr/Hf	Nb/Y	104*Ga/Al	Th/Nb	Sc/Nb	Ti/Sc	Zr/Sc	LaN/YbN	CeN/YbN	LaN/ThN	LaN/NbN	ZrN/SmN	Eu/Eu*	Nb/Nb*	Zr/Zr*	Ti/Ti*	Nb/TA
JHC-07-045	29.4	485.3				0.0	2.38	152.23	12.33										
JHC-07-047	36.9	613.3				0.0	2.27	158.71	16.24										
JHC-07-048	13.3	72.3	34.9	0.27	180.5	0.1	3.60	305.5	3.69	2.0	2.0	0.8	1.0	1.05	1.03	0.24	0.28	0.20	29.55
JHC-07-049	46.3	616.5				0.0	3.23	139.38	14.34										
JHC-07-050	30.9	602.7				0.0	1.63	188.25	18.93										
JHC-07-052	22.7	503.5				0.0	1.08	249.07	20.93										
JHC-07-053	29.0	491.4				0.0	2.63	134.79	11.05										
JHC-07-054	37.3	429.3	33.2	0.08	177.3	2.0	3.23	161.03	11.53	2.8	2.2	0.3	5.4	1.08	0.66	0.02	0.30	0.04	12.47
JHC-07-060	43.3	515.0				0.0	3.42	147.25	12.65										
JHC-07-061	48.9	580.0	36.3	0.06	128.8	2.2	3.75	134.6	13.03	2.2	1.8	0.3	5.5	1.22	0.63	0.02	0.32	0.03	16.74
JHC-07-062	56.3	596.6	36.3	0.06	99.4	2.7	3.08	183.69	18.29	2.7	2.1	0.3	7.0	1.14	0.58	0.02	0.32	0.03	11.29
JHC-07-063	16.8	127.6	43.1	0.36	168.8	0.1	2.55	308.71	6.57	3.5	3.0	1.3	1.2	1.58	1.17	0.24	0.44	0.18	14.55
JHC-07-064	45.1	451.5				0.0	3.92	152.75	11.51										
JHC-07-065	38.3	484.3	33.0	0.11	142.9	1.8	2.90	163.39	13.2	3.1	2.5	0.3	5.0	1.17	0.71	0.02	0.32	0.03	12.93
JHC-07-066	2.9	446.0				0.0	0.40	99.21	7.38										
JHC-07-070	39.3	468.4				0.0	3.04	165.21	12.91										
JHC-07-073	38.3	448.5	32.2	0.11	138	1.8	3.05	167.44	12.53	3.0	2.6	0.3	4.0	1.18	0.66	0.03	0.31	0.04	13.27
JHC-07-075	39.8	448.3				0.0	3.09	172.42	12.9										
JHC-07-076	46.1	448.5				0.0	3.71	166.09	12.43										
JHC-07-077	38.9	422.5	31.6	0.08	137	2.3	2.87	192.55	13.57	3.2	2.5	0.3	5.7	1.15	0.68	0.02	0.31	0.04	8.93
JHC-07-078	5.3	71.1	52.5	0.60	102	0.1	6.28	70.99	0.84	2.2	1.9	0.5	0.5	1.24	0.92	0.34	0.33	0.24	
JHC-07-079	8.6	88.7				0.0	7.75	74.98	1.11										
JHC-07-080	2.4	33.0				0.0	8.44	52.07	0.29										
JHC-07-081	0.6	7.0	7.8	0.64	127.2	0.1	9.11	52.55	0.06	0.8	0.7	0.4	0.2	0.19	1.34	0.72	0.05	0.34	
JHC-07-082	0.0	0.0				0.0	7.98	68.58	0										
JHC-07-083	11.5	80.4	34.4	0.69	78.6	0.4	10.20	83.9	1.13	5.2	3.5	0.5	1.6	1.56	0.40	0.10	0.48	0.31	48.01
JHC-07-084	28.8	78.1	30.1	0.28	46	0.9	19.07	115.74	1.51	3.9	2.9	0.4	2.9	2.05	0.74	0.05	0.64	0.42	19.85
JHC-07-085	18.0	87.1	38.3	0.09	84.9	0.5	21.58	57.34	0.83	1.3	1.2	0.5	2.3	0.80	0.31	0.08	0.20	0.12	
JHC-07-086	11.2	98.1				0.0	11.27	60.82	1										
JHC-07-087	9.3	77.8				0.0	9.60	74.75	0.97										
JHC-07-088	12.7	80.3	35.1	0.12	109	0.4	13.74	68.76	0.92	1.4	1.2	0.5	1.8	0.85	0.99	0.10	0.22	0.14	
JHC-07-091	3.5	75.7	44.0	0.88	111.7	0.1	4.71	59.21	0.75	1.3	1.1	0.3	0.2	2.03	0.79	0.50	0.48	0.33	
JHC-07-093	23.8	76.1				0.0	15.36	122.1	1.55										
JHC-07-094	6.2	81.8	37.7	0.51	126.8	0.2	6.26	72.56	0.99	1.2	1.2	0.3	0.4	1.06	0.34	0.25	0.30	0.19	
JHC-07-095	9.3	73.8				0.0	8.13	92.49	1.14										
JHC-07-096	6.0	90.8				0.0	6.14	64.5	0.98										
JHC-07-097	25.3	77.2	36.9	0.47	73.5	0.7	22.60	86.94	1.12	2.7	2.3	0.2	1.4	2.71	0.00	0.07	0.89	0.59	
JHC-07-098	3.5	84.2				0.0	2.60	95.26	1.34										
JHC-07-099	2.8	87.0				0.0	3.05	64.28	0.93										
JHC-07-100	24.2	73.8				0.0	20.33	96.72	1.19										
JHC-07-101	42.7	73.0	31.3	0.32	58.1	1.2	31.20	112.38	1.37	4.9	4.1	0.4	4.0	2.09	0.51	0.03	0.72	0.51	8.06
JHC-07-102	4.5	78.9				0.0	4.87	69.96	0.92										
JHC-07-103	8.1	82.7	35.8	0.28	107.8	0.2	8.27	70.86	0.98	1.5	1.2	0.4	0.9	1.06	1.83	0.17	0.28	0.17	
JHC-07-104	4.4	46.5				0.0	8.61	65.28	0.51										

Appendix 1B: Lithogeochemistry data table for samples analyzed from TVB

SampleNumber Units Analytical Method	Zr/Nb	Zr/TiO2	Zr/Hf	Nb/Y	104*Ga/Al	Th/Nb	Sc/Nb	Ti/Sc	Zr/Sc	LaN/YbN	CeN/YbN	LaN/ThN	LaN/NbN	ZrN/SmN	Eu/Eu*	Nb/Nb*	Zr/Zr*	Ti/Ti*	Nb/TA
JHC-07-106	2.8	31.5				0.0	6.68	79.94	0.42										
JHC-07-107	13.0	208.8	32.9	0.24	106	0.6	5.72	65.21	2.27	2.1	1.8	0.3	1.5	1.30	0.65	0.08	0.34	0.08	43.03
JHC-07-108	28.7	103.4				0.0	24.63	67.54	1.16										
JHC-07-109	6.6	91.2				0.0	5.94	72.89	1.11										
JHC-07-110	13.0	76.9				0.0	16.49	61.49	0.79										
JHC-07-111	78.4	78.8				0.0	27.56	216.14	2.84										
JHC-07-112	4.1	75.3				0.0	5.06	63.87	0.8										
JHC-07-113	5.5	78.4	33.7	0.36	120.1	0.2	6.09	68.86	0.9	1.3	1.2	0.4	0.5	0.95	0.21	0.24	0.24	0.16	
JHC-07-114	12.0	74.9	33.4	0.21	75.5	0.4	13.34	71.9	0.9	1.4	1.3	0.3	1.2	0.85	0.31	0.11	0.23	0.16	
JHC-07-115	50.6	72.3				0.0	46.07	91.08	1.1										
JHC-07-116	6.9	78.5	32.5	0.27	107.7	0.2	7.02	74.63	0.98	1.6	1.4	0.6	1.0	0.77	0.77	0.18	0.20	0.13	56.79
JHC-07-119	8.9	83.5	33.2	0.25	102	0.3	9.29	68.37	0.95	1.7	1.5	0.5	1.2	0.75	1.01	0.14	0.21	0.13	
JHC-07-120	3.5	64.4				0.0	5.66	56.91	0.61										
JHC-07-121	13.4	185.4				0.0	6.98	61.95	1.92										
JHC-07-122	14.0	188.2				0.0	6.77	65.82	2.07										
JHC-07-123	14.5	200.7	32.2	0.25	101.8	0.6	6.69	64.74	2.17	2.2	1.8	0.3	1.5	1.35	0.77	0.08	0.37	0.09	40.00
JHC-07-124	11.8	170.0				0.0	7.95	52.45	1.49										
JHC-07-125	6.6	90.8	33.3	0.42	114.5	0.2	6.17	70.27	1.06	1.7	1.6	0.3	0.7	0.99	1.07	0.19	0.27	0.15	76.00
JHC-07-126	3.7	52.2				0.0	7.76	55.34	0.48										
JHC-07-127	3.5	61.0	33.4	0.73	102.3	0.1	6.93	50.07	0.51	1.7	1.6	0.4	0.4	1.03	1.14	0.39	0.27	0.23	
JHC-07-128	5.1	87.9	37.6	0.57	97.6	0.1	5.12	68.32	1	1.5	1.3	0.4	0.4	1.24	1.14	0.32	0.32	0.19	
JHC-07-129	36.8	421.6				0.0	6.44	81.21	5.71										
JHC-07-133	4.4	84.8				0.0	4.74	65.7	0.93										
JHC-07-134	5.3	81.4				0.0	6.79	57.45	0.78										
JHC-07-135	14.5	257.5	27.5	0.08	154.5	0.2	6.48	52.09	2.24	0.8	0.8	0.9	1.7	0.56	0.99	0.14	0.14	0.03	
JHC-07-136	7.5	103.7	34.2	0.53	112.2	0.3	5.96	72.84	1.26	1.5	1.4	0.2	0.5	1.56	0.76	0.18	0.41	0.20	68.26
JHC-07-137	3.1	70.2				0.0	5.18	51.43	0.6										
JHC-07-138	5.9	83.4	36.3	0.62	105.6	0.2	6.50	64.9	0.9	1.3	1.2	0.2	0.4	1.75	1.15	0.27	0.44	0.27	
JHC-07-139	5.5	89.3				0.0	6.15	60.54	0.9										
JHC-07-140	4.3	67.3				0.0	7.53	50.58	0.57										
JHC-07-141	3.8	65.5				0.0	6.14	57.3	0.63										
JHC-07-142	6.1	56.8	31.7	0.23	101.5	0.2	11.20	57.68	0.55	1.3	1.2	0.5	1.0	0.63	1.06	0.18	0.17	0.15	
JHC-07-143	53.2	415.1				0.0	6.92	111.03	7.69										
JHC-07-147	5.6	75.4				0.0	6.95	64.55	0.81										
JHC-07-150	18.8	465.1				0.0	3.23	75.14	5.83										
JHC-07-151		216.0	30.2	0.00	17.1			217.77	7.85	11.3	8.9	0.4		1.19	1.18	0.00	0.48	0.11	
JHC-07-152	16.6	193.2	29.5	0.18	116.5	0.9	4.13	125.07	4.03	3.3	3.0	0.4	3.5	0.69	0.75	0.04	0.22	0.06	
JHC-07-153	17.6	237.9	29.3	0.20	118.5	1.0	4.34	102.17	4.06	3.7	3.0	0.4	3.3	0.86	0.64	0.04	0.26	0.06	
JHC-07-156	15.9	196.5	29.8	0.12	119.3	0.9	4.92	98.44	3.23	2.8	2.3	0.4	3.2	0.70	0.69	0.05	0.19	0.05	
JHC-07-158	22.6	350.8				0.0	3.33	115.71	6.77										

Appendix 1B: Lithogeochemistry data table for samples analyzed from TVB

SampleNumber Units Analytical Method	Zr/Nb	Zr/TiO2	Zr/Hf	Nb/Y	104*Ga/Al	Th/Nb	Sc/Nb	Ti/Sc	Zr/Sc	LaN/YbN	CeN/YbN	LaN/ThN	LaN/NbN	ZrN/SmN	Eu/Eu*	Nb/Nb*	Zr/Zr*	Ti/Ti*	Nb/TA
JHC-07-160	4.4	62.6	36.5	0.44	121.3	0.2	4.65	89.8	0.94	2.5	2.0	0.6	0.9	0.68	0.96	0.22	0.19	0.16	
JHC-07-162	7.4	83.5				0.0	4.94	107.45	1.5										
JHC-07-163	12.1	162.8				0.0	4.38	101.38	2.75										
JHC-07-165	12.4	198.8	30.9	0.22	106.9	0.6	3.14	119.45	3.96	2.5	2.1	0.4	1.9	0.87	0.69	0.07	0.25	0.07	
JHC-07-166	14.9	193.4	30.9	0.22	118.8	0.7	4.98	93.07	3	2.8	2.4	0.4	2.2	0.90	0.74	0.06	0.27	0.07	
JHC-07-167	14.3	146.2				0.0	6.47	90.73	2.21										
JHC-07-168	8.8	114.4	27.2	0.21	105.4	0.3	4.90	93.95	1.79	1.4	1.2	0.3	1.0	0.87	0.73	0.13	0.23	0.10	
JHC-07-170	11.0	137.3				0.0	4.70	101.78	2.33										
JHC-07-171	39.4	855.8	39.9	0.18	145	1.2	0.97	283.13	40.43	4.5	3.6	0.4	3.8	2.05	0.69	0.04	0.59	0.04	5.27
JHC-07-172	5.0	65.6				0.0	6.52	70.32	0.77										
JHC-07-173	3.6	49.0				0.0	6.41	67.87	0.55										
JHC-07-174	5.4	26.3	29.0	0.37	129.5	0.2	12.01	102.96	0.45	1.9	1.9	0.4	0.6	0.60	1.14	0.21	0.17	0.33	
JHC-07-175	4.8	52.8	25.9	0.29	117.4	0.2	5.73	96.15	0.85	1.5	1.3	0.5	0.8	0.64	0.96	0.22	0.17	0.17	
JHC-07-176	6.0	69.2				0.0	1.62	321.65	3.71										
JHC-07-180	2.9	71.6				0.0	1.35	182.01	2.17										
JHC-07-181	18.8	197.4	41.2	0.37	148.3	0.3	1.37	415.47	13.68	5.1	4.3	0.6	1.9	1.57	1.04	0.10	0.46	0.12	13.43
JHC-07-182	2.0	41.6				0.0	7.05	41.64	0.29										
JHC-07-184	3.6	65.2				0.0	7.66	43.56	0.47										
JHC-07-187	17.6	181.0	36.9	0.32	125.1	1.4	3.99	146.05	4.41	10.0	7.7	0.3	4.0	0.98	0.89	0.03	0.30	0.09	32.48
JHC-07-188	28.0	805.7	41.8	0.29	135.5	0.6	0.77	272.08	36.58	5.3	4.4	0.5	2.7	1.87	0.80	0.06	0.56	0.04	9.50
JHC-07-190	5.3	68.7				0.0	6.24	74.47	0.85										
JHC-07-191	2.3	24.9	10.3	0.27	123.2	0.3	7.28	76.51	0.32	1.5	1.3	0.4	0.9	0.26	1.05	0.16	0.07	0.14	
JHC-07-193	5.3	37.9				0.0	8.20	102.21	0.65										
JHC-07-194	3.2	24.7				0.0	7.64	100.73	0.42										
JHC-07-195	3.6	74.3				0.0	3.50	83.05	1.03										
JHC-07-196	15.9	182.4	33.2	0.25	117.3	1.5	3.91	133.68	4.07	7.4	5.7	0.3	4.2	0.79	0.87	0.03	0.24	0.07	30.20
JHC-07-198	8.4	120.1	27.8	0.19	114.9	0.4	5.32	78.57	1.57	1.4	1.2	0.4	1.2	0.75	0.80	0.12	0.19	0.08	
JHC-07-207	7.1	92.8	19.7	0.20	112.9	0.3	4.80	95.82	1.48	1.2	1.1	0.4	0.9	0.66	1.06	0.16	0.17	0.09	
JHC-07-208	14.1	140.9				0.0	7.02	85.2	2										
JHC-07-211	2.5	23.7				0.0	5.97	107.11	0.42										
JHC-07-213	6.7	81.8				0.0	8.80	56.21	0.77										
JHC-07-215	4.5	54.2	29.2	0.38	119.5	0.2	6.94	71.16	0.64	1.5	1.3	0.4	0.6	0.72	0.86	0.23	0.19	0.18	
JHC-07-216	2.1	91.6				0.0	1.38	98.89	1.51										
JHC-07-217	6.3	62.4	38.4	0.62	134.3	0.1	1.85	329.21	3.43	3.0	2.7	1.4	0.6	1.03	1.10	0.45	0.29	0.24	19.86
JHC-07-219	4.5	87.0	31.8	0.35	117.7	0.1	6.76	46.16	0.67	0.8	0.7	0.6	0.4	0.88	0.99	0.46	0.22	0.13	
JHC-07-220	2.2	33.7	36.8	1.37	108.9	0.0	6.27	63.8	0.36	0.6	0.6	0.4	0.1	1.21	1.86	1.70	0.31	0.47	
JHC-07-221	4.3	103.3				0.0	4.96	50.17	0.86										
JHC-07-222	4.0	87.9	42.1	0.37	111.9	0.1	5.55	49.42	0.72	0.3	0.3	0.3	0.1	1.39	0.90	0.80	0.29	0.17	
JHC-07-226	4.9	94.4				0.0	7.50	41.65	0.66										
JHC-07-229	6.8	120.6	35.2	0.22	105.6	0.2	6.66	50.89	1.02	0.8	0.7	0.5	0.6	0.89	0.70	0.26	0.22	0.09	
JHC-07-230	3.9	62.8	28.1	0.31	117.3	0.1	8.08	45.54	0.48	0.6	0.6	0.4	0.3	0.74	0.85	0.45	0.17	0.14	
JHC-07-231	3.9	63.1	32.5	0.41	125.4	0.1	5.40	68.99	0.73	0.6	0.6	0.6	0.3	0.96	1.39	0.71	0.24	0.19	
JHC-07-233	3.7	74.3				0.0	6.42	46.87	0.58										
JHC-07-236	8.6	219.1	33.3	0.17	106.7	0.1	5.61	42.05	1.54	0.5	0.5	0.5	0.6	0.99	0.65	0.28	0.23	0.06	

Appendix 1B: Lithogeochemistry data table for samples analyzed from TVB

SampleNumber Units Analytical Method	Zr/Nb	Zr/TiO2	Zr/Hf	Nb/Y	104*Ga/Al	Th/Nb	Sc/Nb	Ti/Sc	Zr/Sc	LaN/YbN	CeN/YbN	LaN/ThN	LaN/NbN	ZrN/SmN	Eu/Eu*	Nb/Nb*	Zr/Zr*	Ti/Ti*	Nb/TA
JHC-07-242	4.8	85.1				0.0	6.89	49.19	0.7										
JHC-07-245	1.9	29.3	26.7	0.57	113	0.0	7.40	53.85	0.26	0.5	0.5	0.4	0.1	0.59	0.85	0.99	0.14	0.25	
JHC-07-246	8.9	205.6				0.0	6.62	39.12	1.34										
JHC-07-248	5.0	99.3				0.0	7.05	43.08	0.71										
JHC-07-252	56.1	773.3	29.1	0.05	81.1	2.3	2.63	165.51	21.36	2.2	2.0	0.3	6.8	1.15	0.44	0.02	0.31	0.02	7.27
JHC-07-254	59.2	688.8				0.0	4.09	125.97	14.48										
JHC-07-255	62.3	1071.3	31.4	0.06	111.2	2.1	5.01	69.54	12.43	2.0	1.8	0.4	6.4	1.42	0.72	0.02	0.37	0.02	8.06
JHC-07-256	53.0	746.1	32.2	0.07	116.3	2.0	3.43	123.89	15.42	2.5	2.1	0.3	5.8	1.19	0.57	0.02	0.33	0.02	9.12
JHC-07-259	45.7	1065.0				0.0	3.64	70.62	12.55										
JHC-07-260	46.8	457.8				0.0	4.89	125.28	9.57										
JHC-07-261	75.0	796.7				0.0	3.33	169.43	22.52										
JHC-07-262	29.5	801.9	32.9	0.15	97.1	1.1	1.60	137.97	18.46	2.8	2.3	0.3	3.1	1.77	0.40	0.04	0.47	0.03	17.06
JHC-07-264	72.7	816.5	28.9	0.04	100.8	2.7	5.61	95.15	12.96	2.0	1.8	0.4	8.1	1.11	0.78	0.02	0.29	0.02	6.95
JHC-07-265	52.8	1045.2	30.3	0.06	167.2	1.8	5.93	51.05	8.9	2.2	1.8	0.4	5.8	1.10	0.60	0.02	0.30	0.01	6.31
JHC-07-266	27.1	622.8				0.0	1.50	173.49	18.03										
JHC-07-267	11.7	415.4				0.0	1.15	146.97	10.19										
JHC-07-268	7.8	43.6	24.8	1.20	116	0.2	14.92	71.76	0.52	5.0	4.4	0.4	0.6	1.64	1.58	0.25	0.52	0.62	23.91
JHC-07-271	45.5	498.0				0.0	3.91	140	11.63										
JHC-07-272	47.3	746.3				0.0	2.83	134.04	16.69										
JHC-07-273	58.2	1050.6	31.4	0.05	138.4	2.0	6.70	49.54	8.68	2.3	2.0	0.4	7.5	0.96	0.68	0.02	0.27	0.01	9.98
JHC-07-275	25.1	398.8				0.0	2.50	150.85	10.04										
JHC-07-276	32.4	705.6	29.7	0.09	153.8	1.3	1.99	138.62	16.32	2.7	2.3	0.4	4.6	1.00	0.46	0.03	0.28	0.02	13.73
JHC-07-277	74.8	720.3				0.0	2.11	294.8	35.43										
JHC-07-278	44.4	542.3				0.0	2.39	205.54	18.6										
JHC-07-279	57.6	560.8				0.0	3.24	190.1	17.79										
JHC-07-280	59.2	1006.0	29.6	0.04	151.6	2.1	5.92	59.64	10.01	2.0	1.7	0.4	7.0	0.90	0.67	0.02	0.24	0.01	8.16
JHC-07-281	8.8	397.8				0.0	0.76	175.58	11.65										
JHC-07-282	78.5	676.8				0.0	3.19	217.76	24.59										
JHC-07-283	56.0	676.8	30.4	0.05	132.1	2.1	3.57	139.13	15.71	2.0	1.7	0.3	5.9	1.22	0.62	0.02	0.32	0.02	9.21
JHC-07-284	65.9	695.4	29.7	0.05	95.7	2.5	3.91	145.1	16.84	2.2	1.8	0.3	6.9	1.24	0.58	0.02	0.33	0.02	8.34
JHC-07-285	42.5	823.6	29.8	0.06	89.9	1.6	2.84	108.95	14.97	2.2	1.9	0.4	5.2	0.97	0.65	0.03	0.25	0.02	12.98
JHC-07-286	37.8	767.7				0.0	2.16	136.93	17.54										
JHC-07-287	57.4	955.8				0.0	3.59	100.11	15.97										
JHC-07-289	26.3	608.1				0.0	1.71	151.57	15.38										
JHC-07-290	1.8	84.2				0.0	1.42	92.63	1.3										
JHC-07-291	54.6	655.9	31.9	0.07	108.5	2.1	2.92	170.8	18.69	2.1	1.8	0.3	5.1	1.43	0.62	0.02	0.40	0.03	8.18
JHC-07-292	7.3	66.2				0.0	3.91	169.46	1.87										
JHC-07-293	39.8	696.3	31.6	0.07	130.5	1.6	4.81	71.15	8.27	2.4	1.9	0.4	4.8	0.94	0.57	0.03	0.26	0.02	19.06

Appendix 1C: Location Information for Diamond Drill Holes Referred to in the Text

Hole_ID	UTMEast	UTMNorth	Elev_m	AZIMUTH	DIP	Depth_m	NTS_map
77537	515080	5390250	320	317	-45	231.9	12A/10
77538	515990	5390090	279	317	-45	191.1	12A/10
77544	515180	5390210	326	317	-45	403.6	12A/10
77546	515100	5390170	322	317	-45	277.1	12A/10
77547	514990	5390090	313	317	-45	154.6	12A/10
77557	514990	5390000	314	317	-45	152.4	12A/10
BP-4	518460	5388650	222	315	-50	107.89	12A/10
CVP-02-01	475070	5361899	363	146	-45	45.7	12A/06
CVP-02-02	475101	5361934	366	146	-45	49.7	12A/06
CVP-02-03	475133	5361992	368	146	-45	78.9	12A/06
DN-02-02	507587	5385489	288	320	-60	250.9	12A/10
DN-02-04	507298	5386079	277	320	-60	323	12A/10
DN-02-10	507601	5385559	289	320	-60	250	12A/10
DN-06	507542.65	5385610.02	294	323	-60	154.84	12A/10
DN-12	507850.95	5386181.72	286	320	-45	156.97	12A/10
DN-16	507874.11	5386151.62	286	320	-60	113.08	12A/10
DRP-95-01	480199.3	5371061.12	217	140	-50	149.4	12A/06
DRP-95-02	479005.8	5369982.08	246	140	-50	121	12A/06
DRP-95-04	480772.6	5371625.88	223	140	-50	146.3	12A/06
DRP-96-07	480050	5371150	220	140	-70	403.86	12A/06
GA-97-05	473800	5364250	360	142	-75	628	12A/06
GS-2	475110	5362050	325	150	-43	58.83	12A/06
HH-96-12	525130	5395440	228	140	-48	201	12A/10
HH-97-16	525140	5395720	227	140	-55	351.7	12A/10
HH-98-18	525100	5395770	230	140	-50	343	12A/10
JP-29	501325.94	5379511.6	368	332	-65	374.9	12A/10
JP-30	501185.62	5379935.61	350	332	-45	88.39	12A/10
JP-38	501303.2	5379672.15	360	332	-55	242.93	12A/10
JP-94-01	501161.8	5379920	261	332	-55	401.1	12A/10
JP-94-07	501534.7	5380248.82	268	332	-46	145.5	12A/10
JP-95-09(30A)	501140	5379950	261	332	-45	294.4	12A/10
JP-97-14	501354.4	5379278.77	364	332	-65	368	12A/10
RB-01-02	497929	5378983	249	140	-45	166.16	12A/11
RB-96-01	498000	5379100	238	150	-52	162.15	12A/11
SU-01-01	518949.13	5397362.04	221	142	-62.5	401.12	12A/10
T-192	486500	5374200	300	152	-45	76.2	12A/11
T-194	487500	5374180	356	152	-45	76.2	12A/11
T-197	485890	5373790	334	152	-45	76.2	12A/11
T-202	486540	5374300	293	152	-45	106.68	12A/11
T-205	485800	5373890	309	152	-50	213.36	12A/11
T-212	486500	5374390	283	152	-55	223.72	12A/11
TE-94-01	490496	5376247	281	152	-64	519.6	12A/11
TE-99-03	490257	5376112	283	152	-58	407	12A/11
TE-99-04	490302	5376039	295	152	-58	310.9	12A/11
TW-09	482170	5371060	219	152	-45	100.58	12A/06
TW-10	482230	5370710	235	152	-45	76.2	12A/06
TW-11	482060	5371040	219	152	-45	76.2	12A/06
TW-12	482140	5371130	219	154	-45	146.3	12A/06
VIC-01-02	521049.25	5398135.69	212	142	-60	203	12A/10
VIC-88-01	522251.69	5398191.07	231	225	-45	128.7	12A/10
VIC-88-04	522337.42	5398148.45	230	225	-45	56.4	12A/10
VIC-89-01	522209.43	5398290.55	231	135	-45	112.17	12A/10
VIC-90-02	522082.76	5398444.97	211	100	-90	209.4	12A/10
GA-04-11	473508	5364284	377.8	140	-60	327	12A/06
GA-05-21	473418	5364397	335.5	141	-61	611.4	12A/06